ERDC/CHL TR-13-15

US Army Corps
of Engineers®
Engineer Research and
Development Center

ERDC
INNOVATIVE SOLUTIONS
for a safer, better world

West Bay Sediment Diversion Effects

Jeremy Sharp, Charlie Little, Gary Brown, Thad Pratt,
Ronnie Heath, Lisa Hubbard, Freddie Pinkard, Keith Martin,
Nathan Clifton, David Perkey, and Naveen Ganesh

November 2013

Coastal and Hydraulics Laboratory

The US Army Engineer Research and Development Center (ERDC) solves the nation's toughest engineering and environmental challenges. ERDC develops innovative solutions in civil and military engineering, geospatial sciences, water resources, and environmental sciences for the Army, the Department of Defense, civilian agencies, and our nation's public good. Find out more at www.erdc.usace.army.mil.

To search for other technical reports published by ERDC, visit the ERDC online library at http://acwc.sdp.sirsi.net/client/default.

ERDC/CHL TR-13-15
November 2013

West Bay Sediment Diversion Effects

Jeremy Sharp, Charlie Little, Gary Brown, Thad Pratt,
Ronnie Heath, Lisa Hubbard, Freddie Pinkard,
Keith Martin, Nathan Clifton, David Perkey, and Naveen Ganesh

Coastal and Hydraulics Laboratory
US Army Engineer Research and Development Center
3909 Halls Ferry Road
Vicksburg, MS 39180-6199

Final report

Prepared for US Army Corps of Engineers New Orleans District
New Orleans, LA

Abstract

An investigation is required to examine whether or not the West Bay Sediment Diversion (WBSD) is inducing shoaling in the Pilottown Anchorage Area (PAA) and in the navigation channel of the Mississippi River. Flow Diversions have the potential to induce shoaling (a sandbank or sand bar in the bed of a body of water) in the river channels from which water is being withdrawn (Letter et al. 2008). Thus, they can significantly reduce the sediment transport capacity of the main-stem river thereby inducing shoaling. The actual impact on shoaling is dependent upon a number of factors including the amount of water and sediment being diverted and the characteristics of the sediment being transported in the river. Diverting increasing amounts of water generally increases the potential for shoaling within the river, but the amount of water and sediment diverted is not necessarily linearly related. The objectives of this study are to understand the sediment transport processes in the Mississippi River in the vicinity of the WBSD and what, if any, impact the WBSD has on these processes.

Contents

Figures and Tables

Figures

Tables

Preface

The US Army Engineer Research and Development Center (ERDC), Coastal and Hydraulics Laboratory (CHL) conducted the West Bay Sediment Division study from April 2009 to December 2012, under the direct supervision of William Martin and José Sanchez, Director CHL, Bruce A. Ebersole and Ty V. Wamsley, Chief, Flood and Storm Protection Division, Lisa Hubbard and Loren L. Wehmeyer, Chief, River Engineering, Pat McKinney, Chief, Field Data Collection and Analysis Branch, Robert McAdory, Chief, Estuarine Engineering Branch. Thad Pratt was the field data collection project manager and Lisa Hubbard and Charlie D. Little the overall project managers. John Bull, William Butler, Chris Callegan, John Kirklin, Pat McKinney, David Perky, and Terry Waller performed the field work. William Butler, Chris Callegan, David Perky, and Naveen Ganesh processed and analyzed the data. Michael Tubman wrote the data collection report. Charlie Little was the lead on the geomorphic assessment, assisted by Peggy Hoffman and Deborah Cooper. Freddie Pinkard, Ronnie Heath, and Jeremy Sharp led the 1-dimensional modeling effort assisted by Nathan Clifton and Deborah Cooper. Gary Brown led the multi-dimensional effort assisted by Keith Martin, Phu Luong and Ben Brown. The following lists the authors by chapters: Chapter 1 was written by Lisa Hubbard, Charlie Little, and Jeremy Sharp; Chapter 2 was written by Thad Pratt and David Perky; Chapter 3 was written by Charlie Little; Chapter 4 was written by Jeremy Sharp, Ronnie Heath, and Nathan Clifton; Chapter 5 was written by Gary Brown and Keith Martin; and Chapter 6 was written by Charlie Little, Gary Brown, Ronnie Heath, and Jeremy Sharp.

The authors gratefully acknowledge the contribution of Rick Broussard of the US Army Corps of Engineers (USACE), New Orleans District, Engineering Division, Civil Branch, as author of the historic events timeline report. The comprehensive events chronology prepared by Broussard was an invaluable resource in developing a thorough understanding of the history of the study area from a river engineering perspective. His contributions were essential to accurately interpretate and evaluate the results of this study and are greatly appreciated.

During the time of the study, COL Gary E. Johnston, COL Kevin J. Wilson, and COL Jeffrey R. Eckstein were Commander and Executive Director of the ERDC. Dr. Jeffery P. Holland was the Director.

Executive Summary – West Bay Sediment Diversion Study

An investigation is required to examine whether or not the West Bay Sediment Diversion (WBSD) is inducing shoaling in the Pilottown Anchorage Area (PAA) and in the navigation channel of the Mississippi River. Flow Diversions have the potential to induce shoaling (a sandbank or sand bar in the bed of a body of water) in the river channels from which water is being withdrawn (Letter et al. 2008). The actual impact on shoaling is dependent upon a number of factors including the amount of water and sediment being diverted and the characteristics of the sediment being transported in the river. Diverting increasing amounts of water generally increases the potential for shoaling within the river, but the amount of water and sediment diverted is not necessarily linearly related. For example, water withdrawal might not lead to significant induced shoaling for the types of sediment being transported until a point is reached when water withdrawal reaches a threshold level at which induced shoaling might become substantial.

The objectives of this study are to understand the sediment transport processes in the Mississippi River in the vicinity of the WBSD and what, if any, impact the WBSD has on these processes. The study involves several components, which are designed to evaluate how the river responds to diversions and specifically, response to the WBSD. The study tasks include a comprehensive flow and sediment field data collection effort; a geomorphic assessment of the entire lower Mississippi River south of Belle Chase, LA; a 50-year regional scale modeling effort for the entire lower Mississippi River from Vicksburg, MS downstream to and including Southwest Pass. Models applied include an enhanced version of an existing 1-dimentional (1D) HEC-6T regional model (MBH 2009), a 2-dimensional (2D) depth-averaged Adaptive Hydraulic model (AdH) coupled to the sediment transport library (SEDLIB), and a multi-day, high flow simulation conducted with the 3-dimensional (3D) CH3D-SED sediment transport model.

The study revealed the general patterns of sand transport in the study area. The loss of water through each of the five major diversions (Fort St. Philips, Grand Pass, Baptiste Collette, WBSD, and Cubits Gap) upstream of Head of Passes (HOP), together with the increase in river width that begins upstream of the WBSD, results in a loss of sediment transport capacity. This

induces deposition of a large percentage of the sandy sediment carried by the river. The magnitude and spatial distribution of this deposition is influenced primarily by two factors; the inflowing discharge hydrograph and the available sediment supply. During moderate discharge years, significant amounts of sand are stored in the channel upstream of the WBSD, with a relatively small volume of sediment reaching the study site. During high discharge years, the sediment can be mobilized and redistributed to the PAA and adjacent navigation channel, resulting in a larger volume of deposition. However, if the high discharge event occurs during a year with limited upstream in-channel sediment storage (i.e. if a high discharge event in the previous year has scoured the channel of available sediment) the discharge can become sediment starved, and some erosion of the face of the point bar/lateral bar in the PAA may occur.

Analysis of field data has shown that as much as 45 percent of the measured water discharge at River Mile (RM) 12.1 is captured by Grand Pass, Baptiste Collette, WBSD, Cubits Gap, and various other small cuts. These cuts capture sediment loads that are approximately proportional to this water discharge volume. The sediment associated with both suspended sediment and bed sediment sampling consists of clay, silts, and sand up to the medium sand size class. The bed material gradations are variable, but the deposit in the PAA has been found to consist primarily of fine sand. Approximately 9 percent of the total discharge of the Mississippi river leaves through the cut at Fort St. Philips, which is upstream from Venice. This was measured for one flow condition of approximately 930,000 cubic feet per second (cfs) on the main river. The percentage may be reduced with lower discharges because the cut contains shallow areas that would not convey discharge during lower discharges. Cubits Gap drops to about 13 percent during low discharge conditions from 19 percent during medium to high discharge conditions. The bed load measurement taken from March 31 to April 1, 2010 shows a net depositional region between River Mile (RM) 8.5 and RM 4.0. This measurement supports the geomorphic analysis that indicates a growing point bar in that region of the river.

The geomorphic assessment indicates that the PAA footprint rests along the face of a lateral bar. This lateral bar has been building for many years previous to the establishment of the WBSD. The growth of the point bar is likely associated with several factors, including the deepening of Grand Pass and Baptiste Collette in the late 1970s, deepening of the navigation project that occurred in 1987, and the construction of WBSD.

The combined modeling analyses (1D, 2D, and 3D) indicate that the WBSD is responsible for approximately 21 +/- 10 percent of the deposition in the combined dredging footprint of the PAA and the adjacent navigation channel. This percentage remains somewhat consistent among all analysis efforts, including many different discharge and sediment loading conditions. These estimates are based on current conditions where approximately 7 percent of the RM 12.1 discharge is diverted through the WBSD. Note that measurements have indicated that the percentage of discharge captured by the WBSD has increased since it opened in 2003. Any future increases will likely influence the impact of the diversion on downstream shoaling.

The percent of sediment deposition associated with each dredge footprint (the PAA and the adjacent navigation channel) is more uncertain than the combined result. The location of the PAA footprint along the face of the point bar means that any adjustment of the cross-section resulting from changing discharge and/or sediment flux conditions is reflected strongly in the volume of dredging in the PAA. Hence, although the impact of the WBSD on the combined PAA and adjacent navigation channel footprint is fairly consistent, the partitioning between these footprints can vary dramatically with changing river discharge and sediment transport scenarios.

Modeling results indicate that the percent of deposition due to the WBSD in the PAA footprint is 25 +/- 15 percent, and 20 +/- 15 percent in the adjacent navigation channel footprint. These variations are observed on an inter-annual time-scale. The uncertainty associated with this percentage is high, and will require more study to quantify the induced percentage more precisely. A suitable set of discharge and sediment conditions, for a predefined time frame, will have to be determined to quantify the percentage as a function of these conditions.

Model simulations were conducted to simulate the long term equilibrium morphology of the river. These simulations indicate that the long term trend of deposition in the PAA is likely to continue either with or without the WBSD in place. The WBSD will induce more deposition in the right descending bank shoal, but the spatial extent of the deposition in the PAA will be nearly identical either with or without the diversion. The presence of the WBSD increases the deposition in the adjacent navigation channel, but this increased deposition is almost entirely offset by a decrease in deposition in Southwest Pass (the effect of the WBSD shifts this quantity of sediment deposition further upstream in the channel). Hence, the

percent difference in shoaling due to the WBSD is associated with a morphologic trend toward the formation of a shallower right descending bank point bar and an upstream shift in channel deposition. The long term spatial extent of shoaling potential in the PAA is largely unaffected by the presence of the WBSD.

1 Introduction

Purpose

The Coastal Wetlands Planning, Protection, and Restoration Act (CWPPRA), West Bay Sediment Diversion (WBSD) Project (MR-03), is located on the right descending bank of the Mississippi River in Plaquemines Parish, LA, at River Mile (RM) 4.7 above Head of Passes (HOP). This effort was focused on determining if the WBSD induces shoaling in the Pilottown Anchorage Area (PAA) and navigation channel, and if so, the percentage of shoaling being caused by the WBSD and the percentage being caused by "natural" effects such as other passes, dredging, or unknown causes.

Study area

The West Bay Subdelta Complex is one of the six subdelta complexes of the modern Mississippi River Birdfoot Delta identified by Coleman and Gagliano (1964). This subdelta originated around 1838 during a flood stage as a break in the natural Mississippi River levee just below Venice, LA known as "The Jump" (Andrus 2007). By the mid 1900s the subdelta had entered into the natural deterioration phase of its life cycle (Andrus 2007). During this phase the marsh underwent erosion and subsidence as inputs of fresh water, nutrients, and sediment decreased.

To address the decline of the West Bay Subdelta Complex, CWPPRA submitted the WBSD Project (MR-03) to Congress in November 1991 as part of the annual Priority Project List. The project was approved for planning, design, and construction funding sponsored by the Louisiana Department of Natural Resources (LDNR) and the US Army Corps of Engineers (USACE). The project was designed to restore and maintain approximately 9,831 acres of fresh water to intermediate fresh water marsh in the West Bay area by diverting fresh water and sediment from the Mississippi River over the 20-year project life from 2003 through 2023 (Figure 1.1). The diversion benefits were based on construction of a 50, 000 cubic feet per second (cfs) conveyance channel at the 50 percent duration stage of the Mississippi River at Venice, and construction of sediment retention enhancement devices (SREDS) in the receiving area. The project included the excavation of an uncontrolled diversion channel through the west bank of the Mississippi River at River Mile (RM) 4.7

(Figure 1.2). Construction was completed in November 2003 to deliver the design discharge of 20,000 cfs at the 50 percent duration stage of the Mississippi River at Venice, making the WBSD the largest constructed sediment diversion in Louisiana. The diversion channel was initially constructed using a hydraulic cutterhead dredge with a pipeline transport system (Figure 1.3) as a 25-foot-deep channel 195-ft-wide. It was intended for the project to be mechanically enlarged after two to three years so that a discharge capacity of 50,000 cfs at the 50 percent duration stage of the Mississippi River at Venice would be reached, if it was determined that the channel would not capture the thalweg of the Mississippi River. The enlargement of the conveyance channel has not occurred and the SREDS have not been constructed. It appears that the initial target discharge of 20,000 cfs was not reached as measured discharge data from 2004 and 2005 showed a discharge for the diversion of 14,000 cfs at the 50 percent duration stage. However, the diversion did grow over time and according to measured discharge data in 2007 and 2008 the capacity of the diversion had almost doubled to 27,000 cfs at the 50 percent duration stage. Andrus (2007) gives a more detailed account of the development of the study area and the design of WBSD itself.

Figure 1.1. WBSD Project Area location.

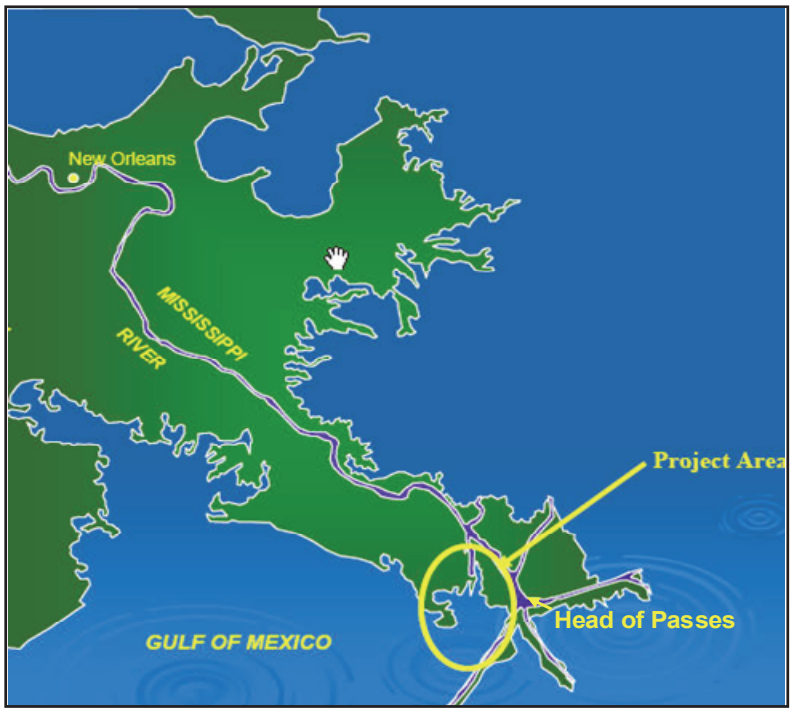

Figure 1.2. Satellite image of Project Area including WBSD, PAA, and West Bay.

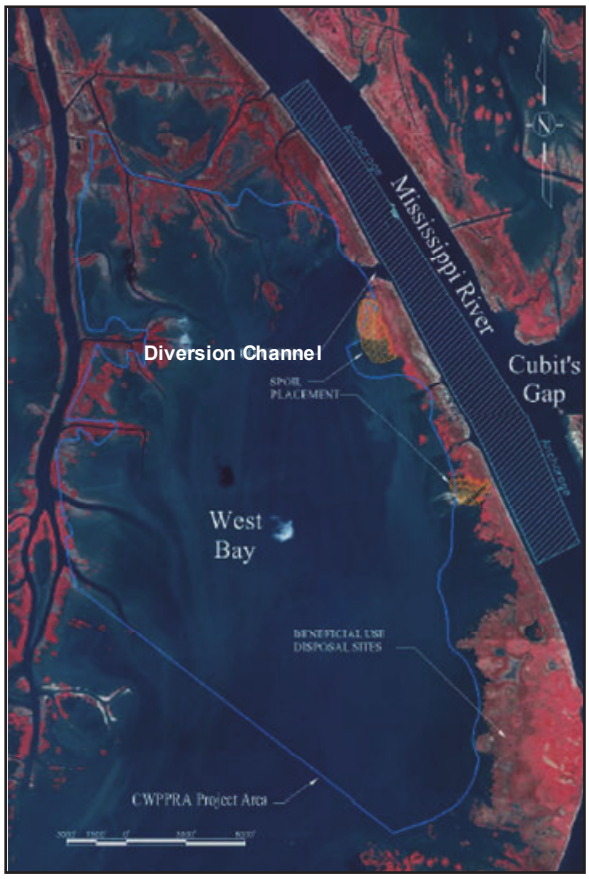

Figure 1.3. WBSD channel under construction.

The local and Federal sponsors recognized that a potential consequence of the WBSD was shoaling in the main navigation channel of the Mississippi River and the adjacent PAA. The PAA is a US Coast Guard designated safe harbor outside of the federally maintained navigation channel. It is the first federally authorized deep-draft anchorage but is used by both shallow and deep-draft vessels traveling on the Lower Mississippi River. It is located along the right descending bank (Figure 1.2). The PAA extends from river mile 1.5 to 6.7. After thorough negotiations with the navigation industry, an agreement for maintaining the PAA was developed and executed. The Cost Sharing Agreement states:

> "Included as a Project feature is the maintenance of the outermost (eastern) 250-ft-wide strip of the PAA and the entire width of the adjoining access area between this strip of the PAA and the Mississippi River navigation channel. Advanced maintenance of the PAA shall be undertaken to account for the anticipated shoaling induced by the Project. Below the conveyance channel, the anchorage and access areas shall be maintained at the depths existing at the time the Phase One interim conveyance channel is constructed. Above the cut, three 45-ft deep by 1,500-ft long anchorage berths shall be constructed and/or maintained."

The project is responsible for this channel maintenance as a direct project cost throughout the project life, which ends in 2023 unless a new project cost sharing agreement is negotiated and signed by the State of Louisiana and the Corps of Engineers.

Approach

The ERDC prepared a workplan that included four primary tasks. Those tasks included are as follows:

- a comprehensive data collection program
- a detailed geomorphic assessment
- 1D modeling
- Multi-dimensional modelings of the West Bay reach.

The data collection program included channel geometry, discharge, suspended sediment, bed material and salinity. The geomorphic assessment included geometric data analysis, gauge and discharge data analysis, dredge records analysis, sediment data analysis, and events timeline analysis. The

1D sediment routing modeling provides the opportunity for evaluating long term channel changes and delivery of sediments at a regional spatial scale and provides boundary condition input for multi-dimensional modeling. The 1-D modeling effort was undertaken using the HEC-6T Sediment in Stream Networks software (MBH 2009) a proprietary software owned by MBH Software, Inc. of Clinton, Mississippi and is an enhanced version of the Corps' HEC-6 program (USACE 1993). The multi-dimensional modeling task conducted simulations using both the Adaptive Hydraulic Model (AdH), a 2D model and Curvilinear Hydrodynamics in 3 Dimensions (CH3D) to simulate the effects of the WBSD on shoaling in the navigation channel and PAA.

Each of the tasks developed for the WBSD workplan (data collection, geomorphic assessment, 1D modeling, and multi-dimentional modeling) have their individual strengths and limitations. The overall strategy behind the workplan was to utilize all available tools such that the limitations of any one tool did not inhibit the success of the overall effort.

2 Data Collection

Purpose of Data Collection

The work plan called for field data collection to serve as the foundation for increasing the usefulness of additional modeling efforts. The new data improves the defining of boundary conditions for 1D and multi-dimensional models. Field data are essential for describing the ratio of diversion sediment to river sediment, which is required information for the 1D model. Also, the data are essential in calibrating and verifying the numerical model results.

As specified in the work plan, the deliverables of the field data collection effort are as follows:

- A bathymetric base map of the Mississippi River channel in the vicinity of the diversion entrance channel and through the diversion entrance channel into West Bay to the extent that water depths in the Bay allow.
- Current speeds and directions across transects of the Mississippi River in the vicinity of the diversion, and across the diversion entrance, as well as acoustic backscatter intensity measurements across the same transects.
- Suspended sediment concentrations and suspended sediment types (percent sand and fines) at horizontal and vertical sample locations along the Acoustic Doppler Current Profiler (ADCP) transect.
- Optical backscatter and salinity measurements along the ADCP transect.
- Bottom-sediment types and grain-size distributions at selected locations in the Mississippi River and West Bay, and samples for additional analyses at the same locations.

Design of the Data Collection Program

Several issues impact how surveys should be conducted in this reach of the lower Mississippi River. The first involves the possibility of a salt-water wedge, which can enter the River at discharges below 300,000 cfs (Soileau et al. 1989). Recent observational studies have shown the wedge is an effective sediment trap for fine particulates in the Mississippi River channel adjacent to the WBSD channel (Galler and Allison 2008). However, there

are very limited observations of sediment transport in this reach of the Mississippi River. The workplan calls for water current measurements to provide salinity profiling to detect the presence of the wedge, and suspended sediment concentration.

A second factor is the limited availability of detailed bathymetry information. To provide this information, the workplan called for a multi-beam bathymetric survey in the Mississippi River in the vicinity of the WBSD entrance channel, and through the diversion entrance channel into West Bay to the extent that water depths in the Bay allow. During planning for the field work, following the development of the workplan, it was decided that a previously conducted muti-beam survey that extended about 2.25 miles south of the diversion channel, about 0.5 miles north of the channel, and through the diversion channel entrance into West Bay (to the extent that water depths in the Bay allowed), provided sufficient data to fulfill the purposes of the work plan.

A third limitation is the absence of diverse data from nearby monitoring stations, since most only collect river stage. The nearest real-time active monitoring station that collects stage and discharge is at Belle Chasse (RM75.5), but the station record only extends to December 2007. Long-term monitoring data were unavailable below the station at Tarbert Landing (RM306.2), immediately below the Old River control structure. Given what has recently been learned about sediment storage and remobilization processes in the lower river due to a reduction in water surface slope in lower discharges, which extends upstream to the approximate tidal limit (at about Baton Rouge), predicting suspended sediment concentrations in the river at the diversion entrance is imprecise. This set of processes, and the likelihood that suspended sediment concentrations differ significantly from those measure at even Belle Chasse, mean a single integrated survey of suspended sediments and currents (combined with historical monitoring data) is unlikely to answer the objectives. Further, while bed load measurements have recently been made in the lower river using modern techniques (Nittrouer et al. 2008), none of these measurements have been made at monitoring stations like Belle Chasse, making estimation of the bed load component of sediment transport at West Bay difficult. Several measurements of sediment transport are necessary to answer the objectives. Sediment fluxes do not co-vary linearly with water discharge in the river adjacent to the diversion. Thus the work plan calls for six surveys within a single flood year.

Instrumentation

The bathymetric survey was conducted using an interferometric (phase measuring) swath sonar. The swath system (Geo-Acoustics 250 kHz) measures both bathymetry and seabed acoustic backscatter from a hull mounted transducer, providing co-registered depth soundings and side scan sonar information in water depths ranging from 1.64 to 328 ft. In contrast to fixed-angle algorithms utilized by beam-forming multi-beams, interferometric swath systems determine angle and travel time for every sampling interval (~50 ms). Measuring angles from phase shifts at rapid sampling intervals provide a denser number of soundings at the outer ranges resulting in a wide horizontal swath (approximately 8-10 times water depth) in shallow water and resolution of three-dimensional features ranging in size from inches to miles. Coupled with GPS, during the survey, an Applanix POSMV IMU system measured the inertial position of the vessel along with its angular orientation. These measurements are typically acquired at a rate of up to 200 Hz. Each trajectory measurement is described by 7 parameters. They are 3 position coordinates, typically latitude, longitude and elevation relative to some datum, 3 angular coordinates, roll, pitch, heading, and a time stamp. These 7 parameters completely describe the vessel position and orientation at each sample time.

The current and acoustic backscatter surveys were conducted using a vessel mounted broadband Acoustic Doppler Current Profilers (ADCP) manufactured by RD Instruments, Inc. (RDI). The first current measurements, made on March 10 and 11, 2009 were made using a 1200 kHz ADCP. However, it was discovered that because of the high degree of turbulence in the area, a 600 kHz system would produce better statistical reliability and a 600 kHz system was used for all subsequent current surveys. During data collection, the ADCP is capable of measuring vessel velocity, water velocity, water temperature, bottom bathymetry, and acoustic backscatter. The measurement of the velocity of the vessel over the bottom allows the current velocity data to be corrected for the movement of the survey vessel. However, if there is sufficient sediment transport down-river at the bottom, the ADCP measurements of the velocity of the survey vessel over the bottom will contain some inaccuracies that will introduce errors in the calculated current velocities. These can be removed by using a GPS to measure the velocity of the survey vessel. The surveys included a GPS system to measure the vessels speed and track (i.e., ship track). The GPS system also provided required heading information to the ADCP system.

All water samples were collected in clean 1 L HDPE plastic bottles. At each collection point, a five depth profile at approximately 1 ft below surface, 25 percent water depth, 50 percent water depth, 75 percent water depth, and 1 ft above bottom was collected. A P-6 isokinetic sampler was lowered to each target depth and opened for 30-50 seconds, depending upon discharge conditions. Sample bottles were filled to 50-75 percent full to ensure that over filling and flushing of sediment from the bottle did not occur. Water flows below 2.0 ft/s were found to be insufficient to purge the air from within the P-6 sampler and fill the bottle. Therefore, a water pump was used to fill the sample bottles when average flows were below 2.0 ft/s. In these instances a water hose was attached to a 100 lb weight and lowered to each target depth. Sufficient time was allowed to flush the water line before filling a bottle from a specified depth. After collection, samples were stored upright in a cooler and transported back to the lab for analysis.

During the suspended sediment sampling and current survey conducted on May 29 and 30, July 21 and 22 and September 23 and 24, 2009, measurements were made using an optical backscatter device (OBS). The OBS is an optical sensor for measuring turbidity by detecting infra-red light scattered from suspended matter. The OBS-3A manufactured by D&A Instruments also records depth, temperature, and salinity along with the backscatter data. During the surveys, the OBS and the P-61 sampler were connected to give concurrent suspended sediment samples and OBS data. On July 3, 2009, CTD casts were made using a YSI 600 XLM sensor.

Bottom sediments were obtained using a push-core type sampler. The sampler consists of a 1.5-in.-diameter PVC pipe, 18 in. in length (Figure 2.1). Attached to this is a smaller section of pipe with a valve attached at the upper end. The purpose of the valve is to create a reduced pressure holding the sample in the larger diameter pipe. The samples were then brought to the surface and classified by visual inspection or transported back to ERDC for more detailed analysis. The push-core sampling method is only good for water depths less than 15 ft in materials that have high clay/silt content. At the deeper and sandier locations, bottom samples were taken using a drag bucket. The bucket was dragged along the bottom by a rope, and the weight of a chain attached to the open end of the bucket forced it to dig into the bed and fill the bucket with a bottom sample.

Figure 2.1. Push-core sampler.

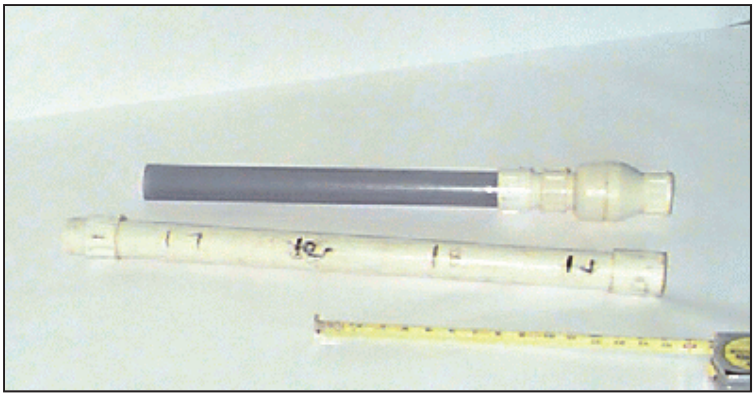

Survey and Sample Locations

The coverage of the multi-beam survey is shown in Figure 2.2. It extends from about 2 miles north of the diversion channel to about 2.25 miles south of the diversion channel. It also extends into West Bay to the extent allowed by the water depths in the Bay.

Figure 2.2. Multi-beam survey coverage.

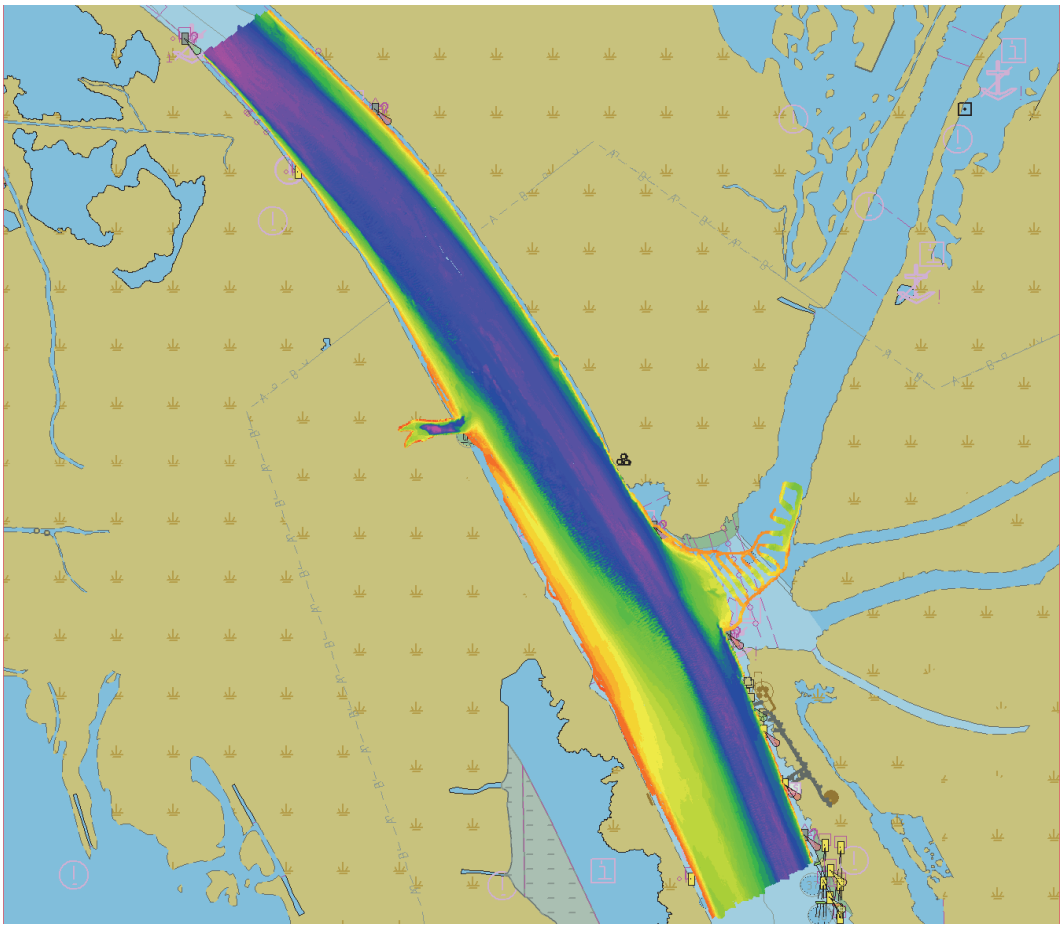

ADCP surveys were conducted in an area extending from the Venice, Louisiana area, RM 12.1, to just south of Cubits Gap, RM 2.6 (Figure 2.3). The locations of the survey transect lines are shown in Figures 2.4 through 2.19. In the figures, with the exception of Figure 2.5 that shows the general locations of the areas surveyed on April 22 and 23, ADCP survey transect numbers are given on each survey line. The ADCP surveys were conducted on March 10 and 11, 2009 (Figure 2.4), April 22 and 23, 2009 (Figures 2.5-2.9), May 5 and 6, 2009 (Figure 2.10), May 29 and 30, 2009, (Figures 2.11 and 2.12), June 16 and 17, 2009 (Figures 2.13 and 2.14), July 21 and 22, 2009 (Figures 2.15 and 2.16) and September 23 and 24, 2009 (Figures 2.17 and 2.18).

Figure 2.3. ADCP survey area.

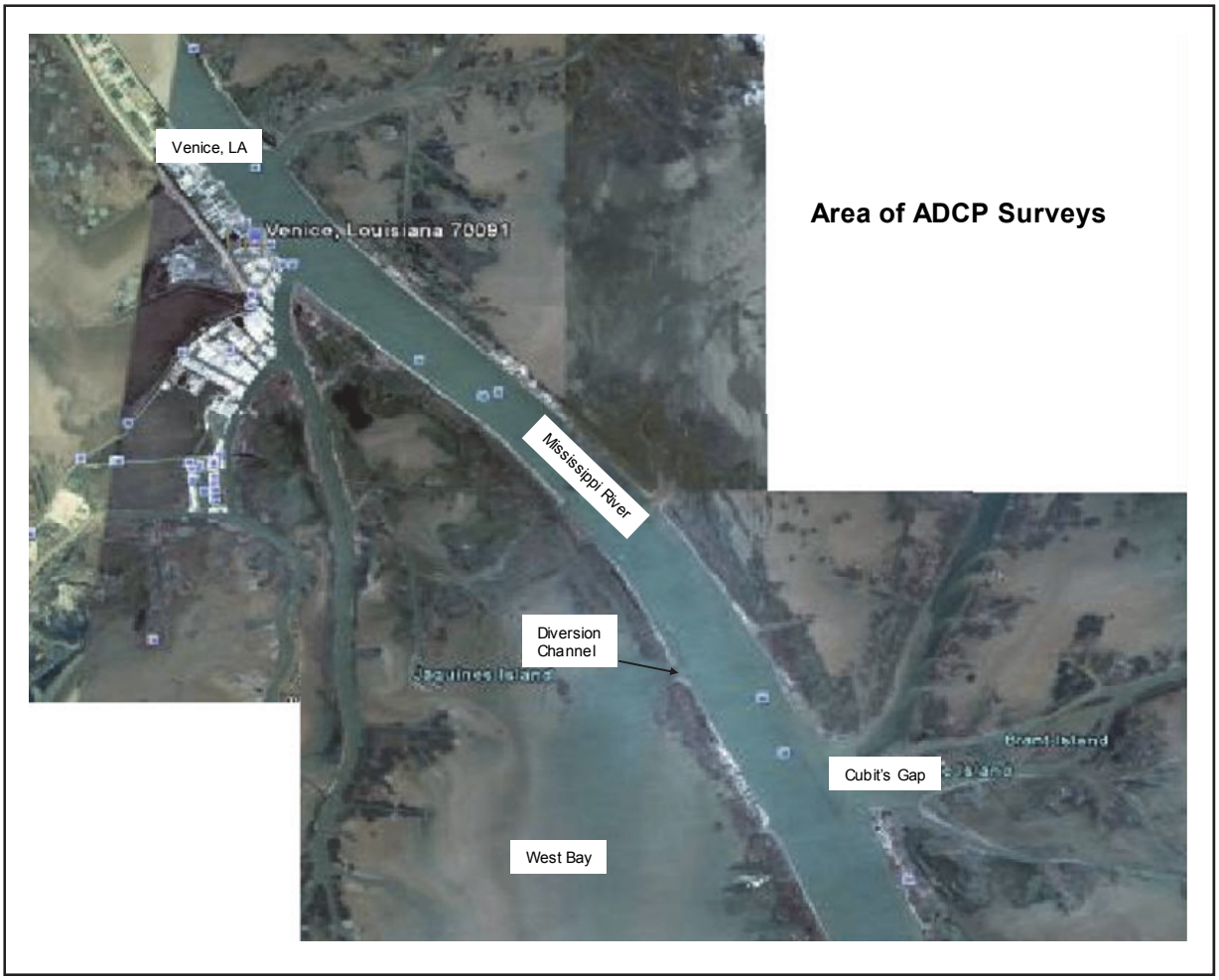

Figure 2.4. ADCP survey transects on March 10 and 11, 2009.

March 10-11, 2009

Figure 2.5. Transect areas during the ADCP survey on April 22 and 23, 2009.

Area 1 – April 22-23, 2009

Area 2 – April 22-23, 2009

Area 3 – April 22-23, 2009

Area 4 – April 22-23, 2009

Figure 2.6 ADCP survey transects on April 23, 2009 in Area 1.

Area 1 – April 22-23, 2009

Figure 2.7. ADCP survey transects on April 22 and 23, 2009 in Area 2.

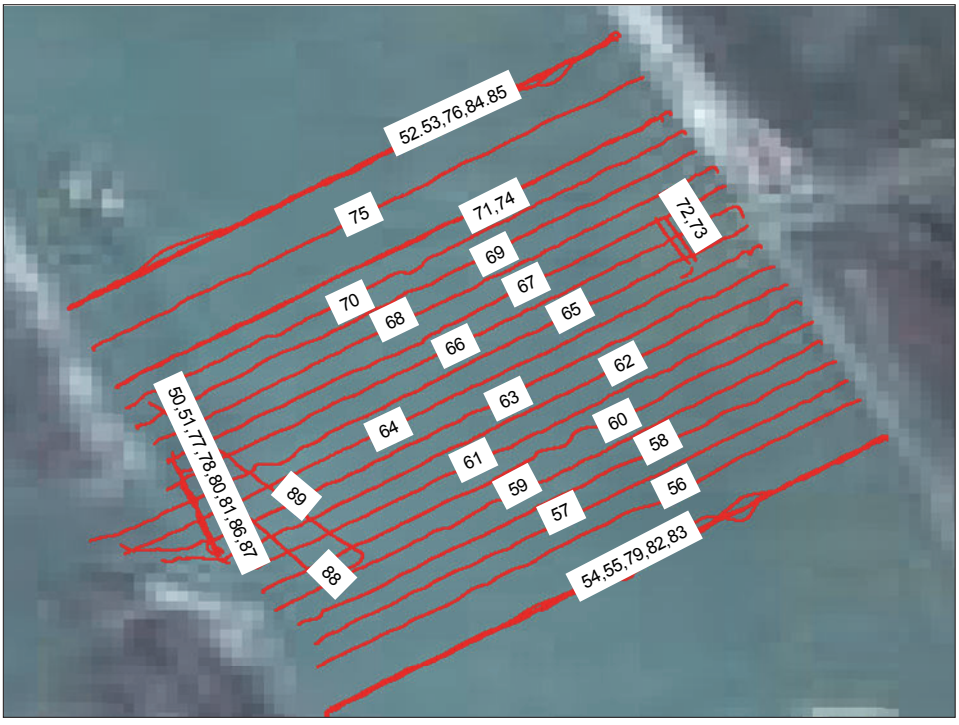

Area 2 – April 22-23, 2009

Figure 2.8. ADCP survey transects on April 22, 2009 in Area 3.

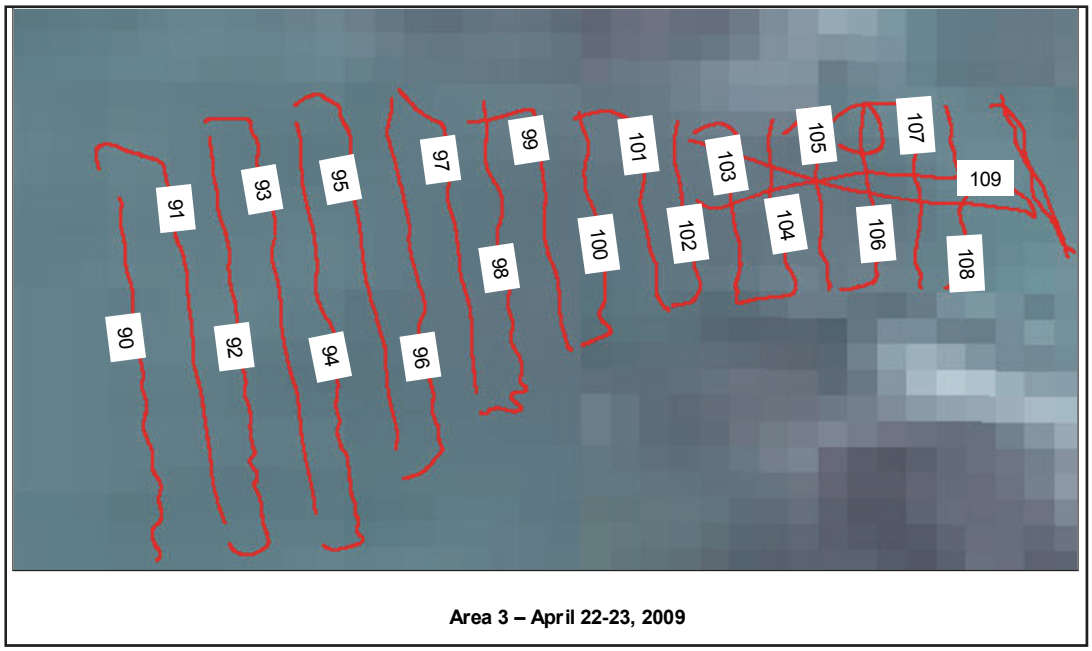

Figure 2.9. ADCP survey transects on April 23, 2009 in Area 4.

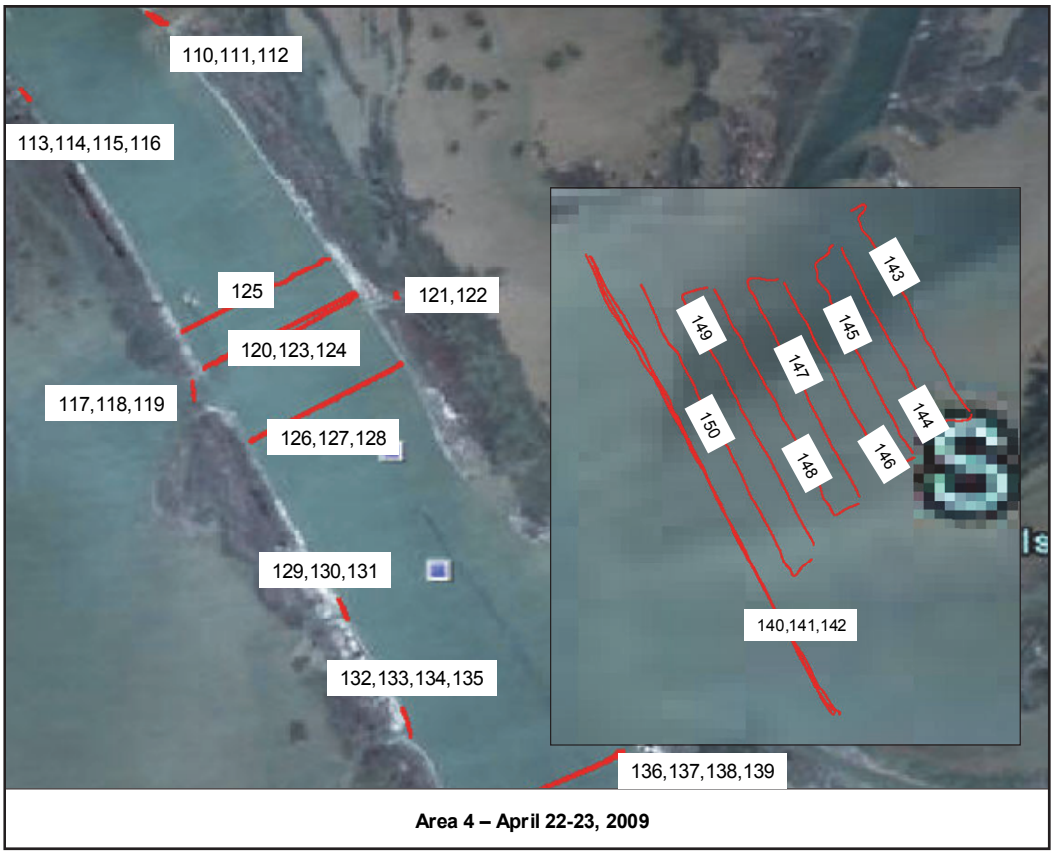

Figure 2.10. ADCP survey transects on May 5 and 6, 2009.

Figure 2.11. ADCP survey transects on May 30, 2009.

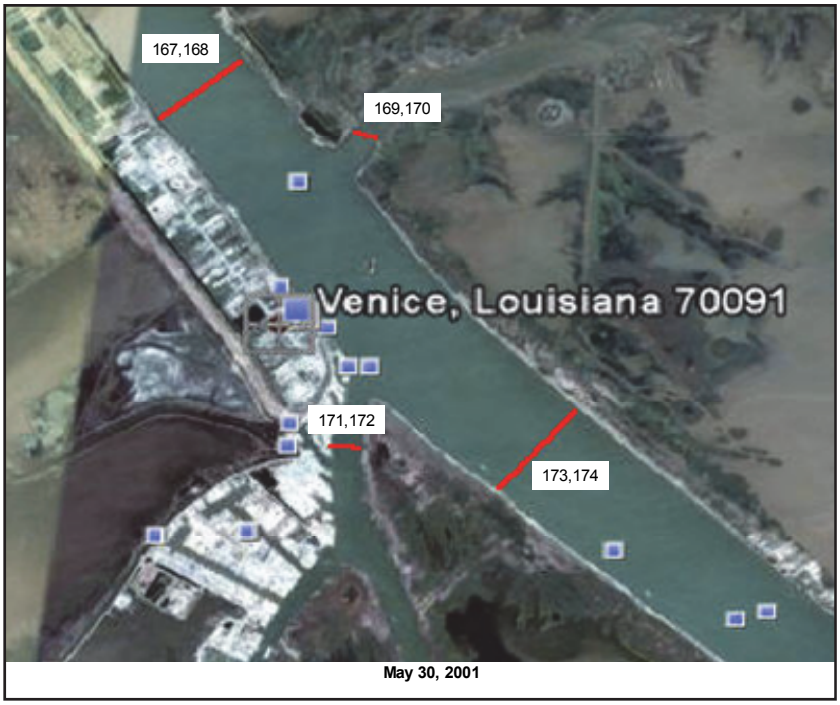

Figure 2.12. ADCP survey transects on May 29 and 30, 2009.

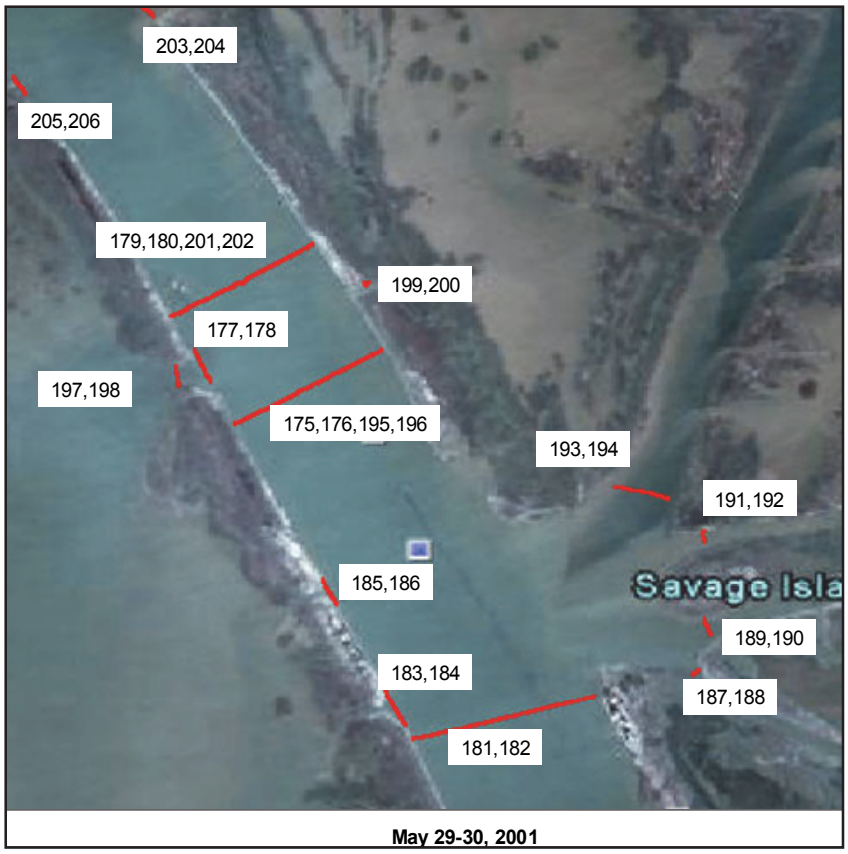

Figure 2.13. ADCP survey transects on June 16 and 17, 2009.

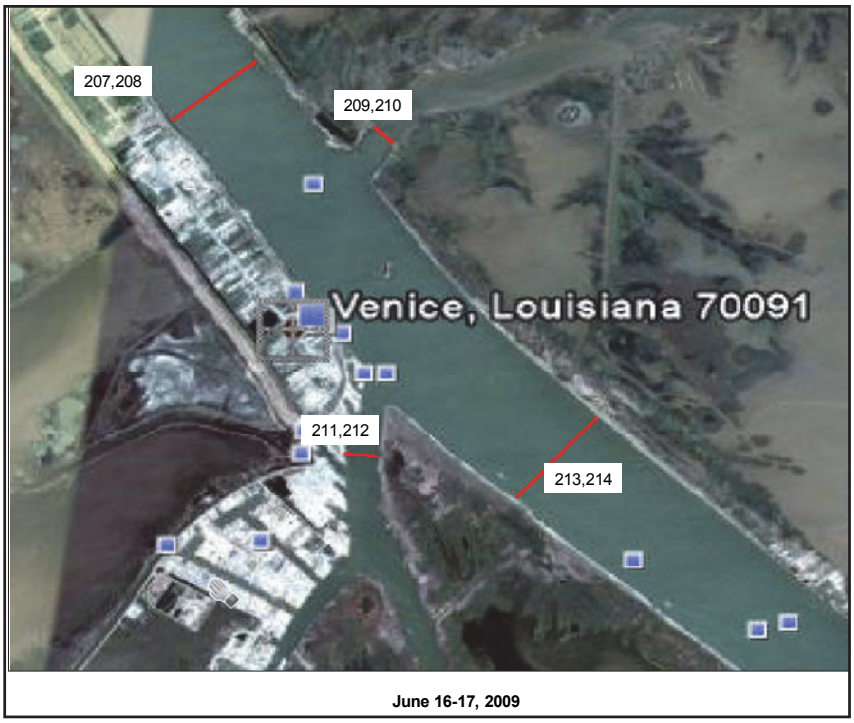

Figure 2.14. ADCP survey transects on June 16 and 17, 2009.

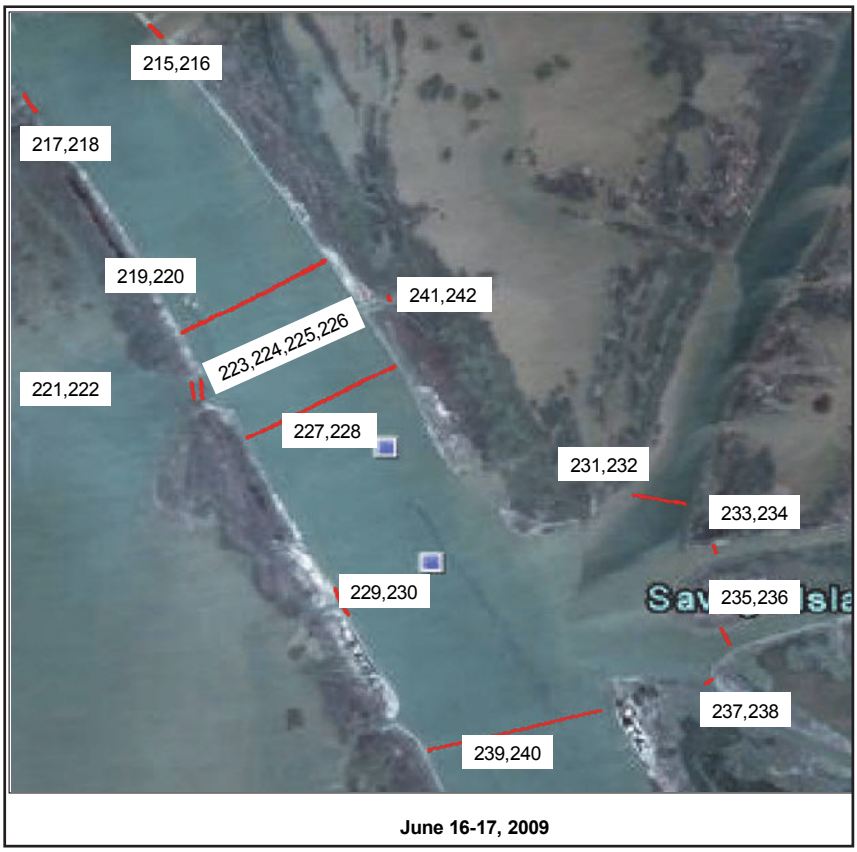

Figure 2.15. ADCP survey transects on July 21 and 22, 2009.

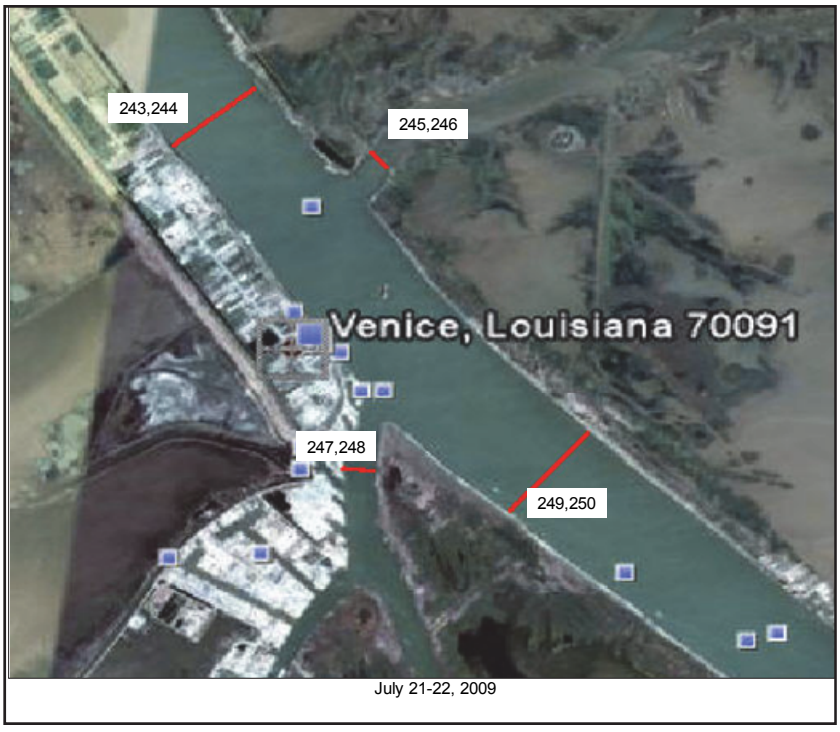

Figure 2.16. ADCP survey transects on July 21 and 22, 2009.

Figure 2.17. ADCP survey transects on September 24, 2009.

Figure 2.18. ADCP survey transects on September 23 and 24, 2009.

Figure 2.19. Locations of suspended sediment samples, OBS measurements, and salinity measurements near Venice, LA.

The locations of the suspended sediment samples, OBS measurements, and salinity measurements are shown in Figures 2.19 and 2.20. The locations of the push-cores and the bottom drag samples are shown in Figures 2.21-2.23. Examples of the suspended sediment samples are shown in Figures 2.25 and 2.26. Field activities began on March 9, 2009 and were ended on September 25, 2009. Locations of samples are shown in Figures 2.19-2.23.

Data Processing and Analysis

Processing Steps

OBS and salinity measurements

The OBS with salinity and pressure sensors was suspended approximately 0.5 ft above the P-61 suspended sediment sampler. When the suspended sediment sample was taken at 1 ft, the OBS was out of the water. For that reason, the time and OBS measurements near the 1-ft depth are for readings taken coincidently near 1-ft depth when the system was being lowered or raised from some deeper depth.

Laboratory analysis for suspended sediments:

Suspended sediment concentrations (SSC): Each sample for SSC was shaken to re-suspend particles and then poured into a 1 L graduated cylinder to record the volume. The samples were then transferred into a ground glass vacuum filtration system (8-lb vacuum maximum) and drawn through pre-weighed, 90 cm diameter, glass-fiber filter with 0.7 μm particle retention. The sample bottles, graduated cylinders, and filter towers were rinsed several times with distilled water to make sure that all particles were introduced to the filter. The filters were then dried in a low temperature oven overnight at approximately 50˚C. The filters were then re-weighed and SSC was calculated for each sample.

Suspended sediment grain-size analysis: The laser diffraction technique was utilized to analyze suspended sediment samples. A Coulter LS100 particle size analyzer was used for samples collected prior to the July, 2009 sampling trip. Samples collected in July and September were analyzed for grain size with a Malvern Mastersizer 2000. Pre-treatments of samples prior to analysis by the laser were consistent throughout all sampling trips. Prior to analysis, a dispersant agent (sodium meta-phosphate) was added to each sample bottle to bring the concentration to approximately 1-2 g/L,

Figure 2.20. Locations of suspended sediment samples, OBS measurements, and salinity measurements.

sonicated for 60 seconds, and passed through a 850 μm (#20 ASTM) sieve to remove any debris from the sample. Each sample was cycled through the laser at least three times and an average-size distribution was reported.

Laboratory analysis of the bottom samples

Within West Bay and parts of Cubits Gap, bottom samples were collected via 1.5" push cores. Bottom samples for the main stem of the river were collected via bottom drag. All the push-cores were extruded and sectioned at 1 cm intervals, but only the top 1 cm was analyzed for this work. As with the suspended sediment samples, the bottom samples were analyzed for grain-size distribution through laser diffraction. Samples collected prior to July were analyzed with the Coulter LS100 and those collected after were analyzed with the Mastersizer 2000. Prior to introduction to the laser, all bed samples were introduced to and suspended in a solution of sodium

Figure 2.21. Locations of bottom drag samples north of Venice, LA.

meta-phosphate (1-2 g/L) for at least 5 hrs. Samples were then sonicated and passed through an 850 μm (#20 ASTM) sieve to remove any large debris from the sample. No sediment grains were ever observed to be retained in the sieve for all samples. Each sample was cycled through the laser at least three times and an average-size distribution was reported.

Data Return and Assessment of Data Quality

During the trip to West Bay on April 22 and 23, 2009, the orientation of the current meter mounted to the survey vessel changed. Figure 2.24 shows a comparison between the ship track using GPS and the ship track using bottom track in ADCP transect 52 (Figure 2.7), which was the forth

Figure 2.22. Locations of the bottom drag samples and push-cores between Venice, LA and the diversion channel. The push-core samples are denoted with the green pins while the bottom drags are noted with the blue pins.

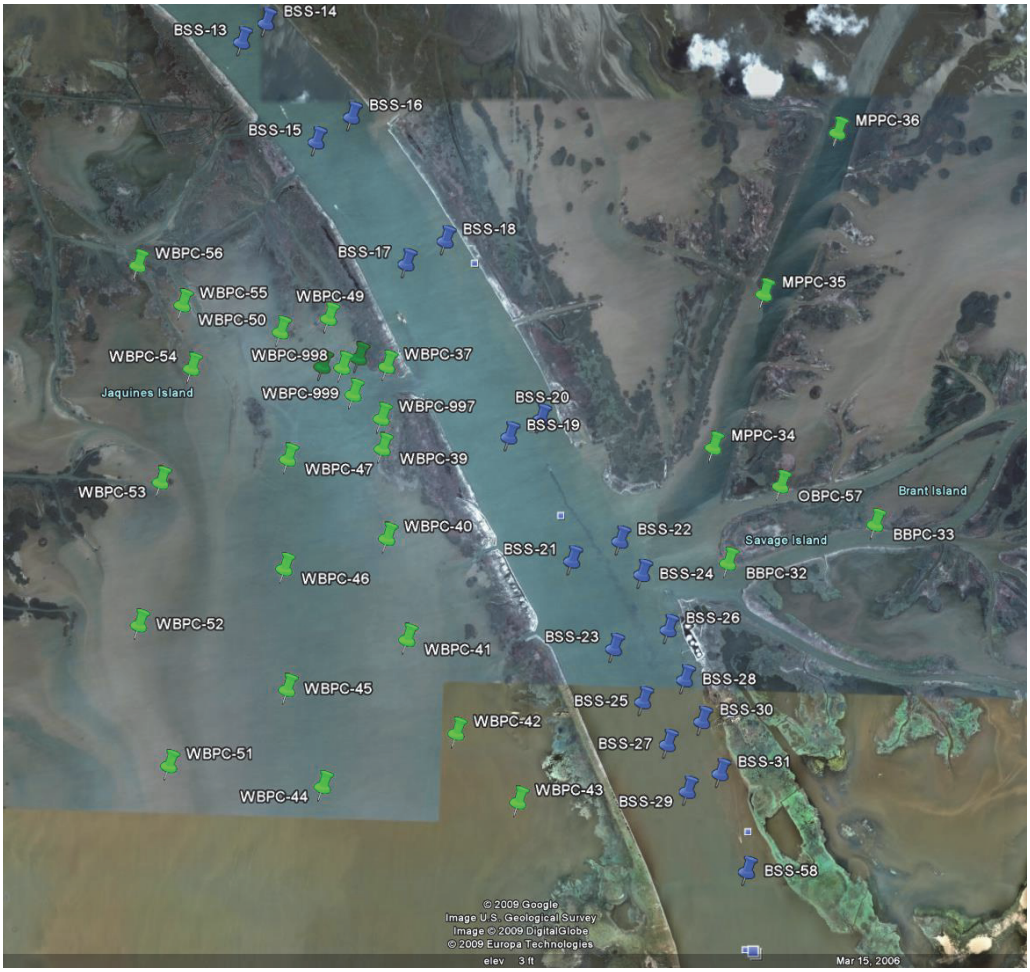

transect run on the first day of the survey (a total of 121 transects were run during the two days), and ADCP transect 84 (Figure 2.7), made along the same line the next day. In transect 52, the tracks are in close agreement and the Q's are 499,387 cfs using bottom track, and 526,705 cfs using GPS, a 5 percent difference. In transect 84, the tracks diverge widely, and the Q's are 484,719 cfs using bottom track, and 287,959 cfs using GPS, a 68 percent difference. This large discrepancy is the result of the current meter changing orientation in its mount. The value of the orientation can be changed during post processing of the ADCP data. This was done for all ADCP data obtained during this trip. After substituting new orientation values during post processing, the discharges using the GPS reference are 507,132 cfs for transect 52 and 517,015 cfs for transect 84, a 2 percent change from one day to the next. It is believed that following this post processing that the discharge measurements are as accurate as those taken on the other trips when there were no problems with the ADCP mount.

Figure 2.23. Locations of the bottom drag samples in Southwest Pass.

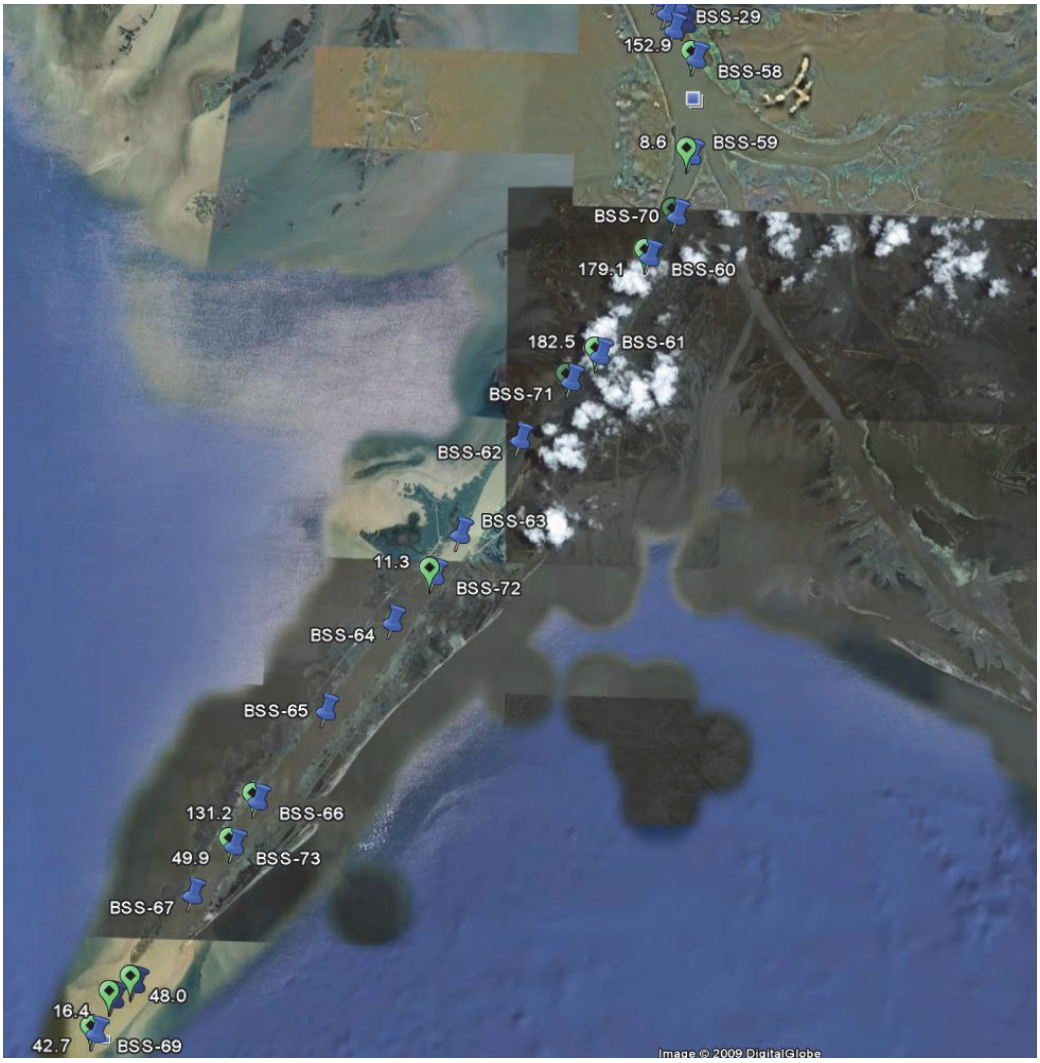

Not all transects were made with quality control suitable for the best-possible quality discharge measurements. When making discharge measurements, the survey vessel was held at the start of the transect line, at a position where the distance to the edge of the channel was known and there were at least two cells of valid data, for ten ensembles. The transect line was then crossed at the slowest possible speed, until a position at the end of the transect line was reached where the distance to the edge of the channel was known and there were at least two cells of valid data. The vessel was then held there for ten ensembles. The process was then immediately repeated going in the opposite direction (in most cases) across the transect line. Some transect lines were run only to measure the current velocities along the transect. For these lines, estimating the discharges in the un-surveyed sections of the channel between the ends of the transect lines and the edges of the channel was not important and no special steps were taken at the start and end of the lines.

Figure 2.24. Comparison of bottom-track ship track (red line) and GPS ship track (blue line) on April 23, 2009 (ADCP transects 52 and 84).

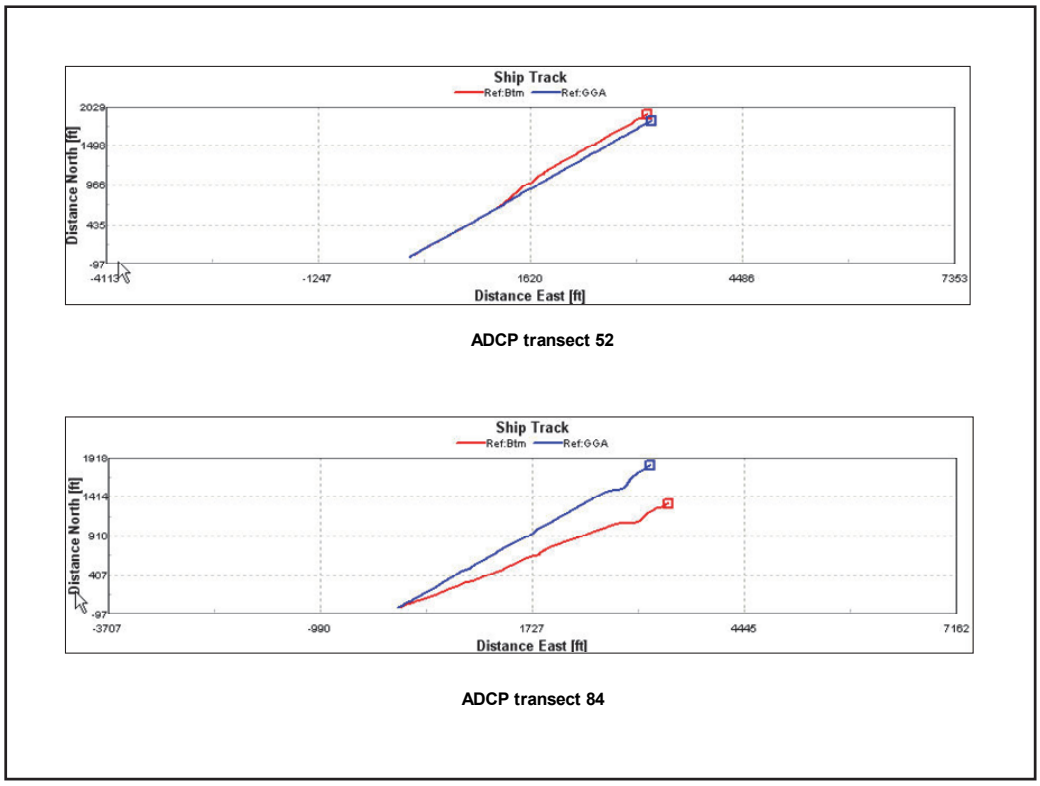

Figure 2.25. Suspended sediment concentrations sampled along Transect Line R-5.2 on June 16, 2009.

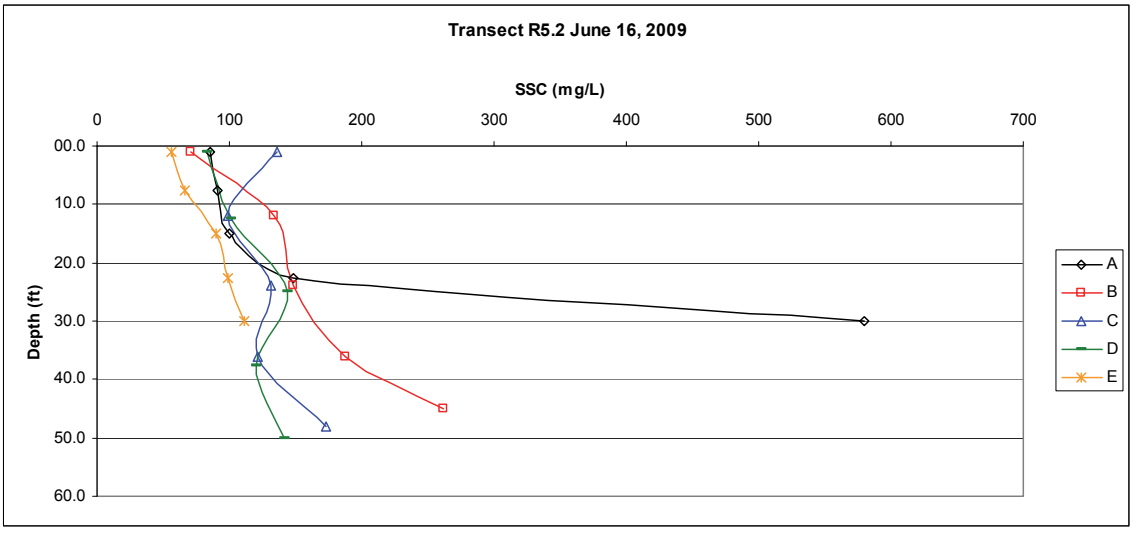

Figure 2.26. Suspended sediment concentrations sampled along Transect Line R-5.2 on May 6, 2009.

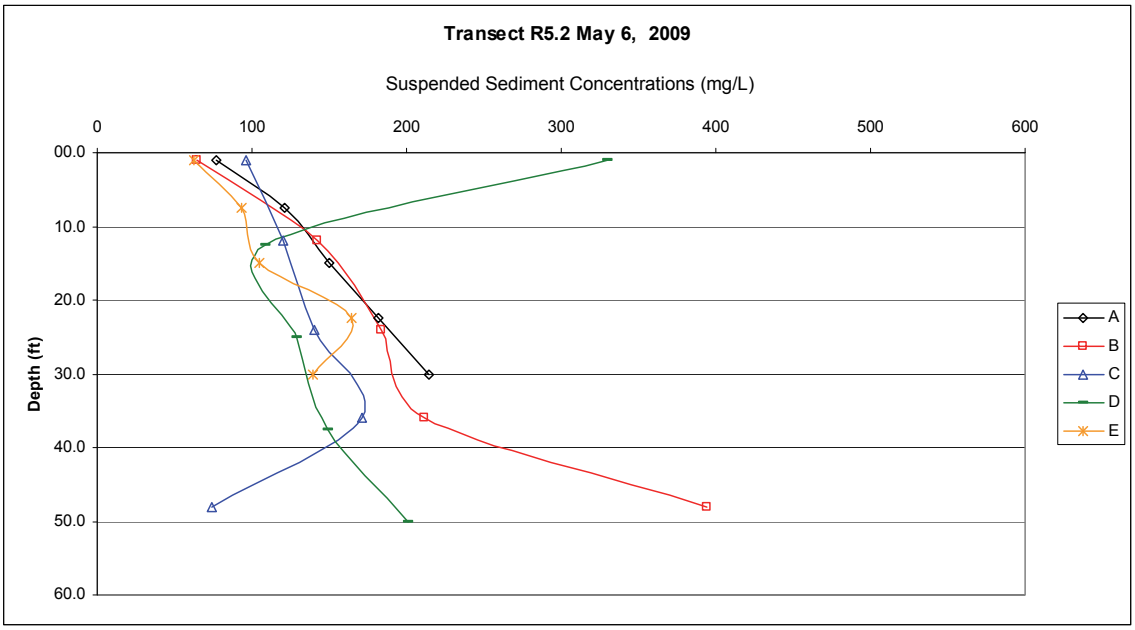

Measuring discharges into West Bay was particularly challenging because of the complexity of the discharge near the diversion channel. Lines that were too far out in the Mississippi River from the diversion channel were affected by current eddies in the region of the channel. Likewise lines too far into West Bay from the diversion channel were affected by the complexity of the discharge in the Bay.

Also very challenging were the discharge measurements into secondary channels off the Mississippi River. The discharge in these channels was low, the depths were shallow (meaning there were very few good velocity cells under the boat), and maneuvering in the channels was difficult. Based on the poor repeatability of discharge measurements, the accuracies are thought to be poor.

During the last trip, when ADCP surveys were conducted on September 23 and 24, 2009, there was a problem with the navigation. For an unknown reason, the position data had shifts in it during transects. The measured current directions are clearly incorrect because the heading information is inaccurate. However, when referenced to bottom track, the discharges appear to be correct. Whereas, all discharges before September are calculated from being referenced to GPS track to eliminate any possibility that movement of bottom sediments could affect discharge measurements, the discharges for September 23 and 24, 2009 are calculated from being

referenced to bottom track. The river discharge in September was very low and bottom movement may have also been very low during the trip.

There are a few suspended sediment samples that have abnormally high sediment concentrations that may be the result of the P-61 sampler hitting the bottom and causing bottom material to be suspended and sampled. Figure 2.25 shows suspended sediment concentrations along Transect Line R-5.2, just north of the diversion channel, where this obviously happened. With the exception of Station A, the near-bottom concentrations range from 111 to 261 mg/l, however, at Station A, the concentrations jump from 148 mg/l for the sample at 22.5 ft depth, to 580 mg/l for the bottom sample at 30 ft of depth. However, other cases are suspect, but not clearly incorrect. Figure 2.26 shows a case where the same thing may or may not have happened at Station B.

Analysis

Discharges across survey lines in the Mississippi River immediately north of the diversion channel, discharges into the diversion channel, and discharges across survey lines in the Mississippi River immediately south of the diversion channel were analyzed and results are in Table 2.1. The discharges into West Bay through the diversion channel are given as percentages of the discharges in the river across the survey lines immediately north of the diversion channel. The amounts of unaccounted for discharges (i.e., the failures to achieve perfect mass balance in the control volume that includes the diversion channel) are also given as percentages of the discharges in the river across the survey lines immediately north of the diversion channel. The flows through the secondary channel immediately across the river from the diversion channel are not taken into account because they were measured as having negligible effects on the overall mass balance. Due to the fact that the required discharge measurements are not all at the same time, and in a couple cases acquired over two days, tidal elevation changes and temporal discharge differences could affect the mass balances. The inability to achieve mass balance is an indicator of the reliability of the discharge measurements into West Bay through the diversion channel.

The same analyses of discharges through a control volume that includes Cubits Gap were performed. The results are in Table 2.2. During the April 22 and 23, 2009 survey, ADCP transects were made all the way across Cubits Gap west of the secondary channels. In Table 2.2 the discharge shown as being through Cubits Gap during this survey is the average of the

Table 2.1. Discharges through the control volume that includes the diversion channel.

Survey Dates	April 22 and 23, 2009	May 5 and 6, 2009	May 29 and 30, 2009	June 16 and 17, 2009	July 21 and 22, 2009	September 23 and 24, 2009	February 20 and 21, 2010	March 31 and April 1, 2011
Discharge north of the channel	550,738 cfs	500,448 cfs	740,062 cfs	568,041 cfs	311,852 cfs	331,732 cfs	650,297 cfs ec	651,019 cfs ec
Discharge into the channel	46,514 cfs	42,011 f t^3/s	68,373 cfs	52,252 cfs	28,724 cfs	31,357 cfs	66,470 cfs ec	60,403 cfs ec
Discharge south of the channel	509,966 cfs	454,715 cfs	675,834 cfs	485,332 cfs	256,360 cfs	279,250 cfs	588,435 cfs ec	589,968 cfs ec
Percentage discharge into the channel	8.4%	8.4%	9.2%	9.2%	9.2%	9.5%	9.5%	9.3%

Table 2.2. Discharges through the control volume that includes Cubits Gap.

Survey Dates	April 22 and 23, 2009	May 29 and 30, 2009	June 16 and 17, 2009	July 22 and 23, 2009	September 23 and 24, 2009	Feb 20 and 21 2010	March 31 and April 1, 2011
Discharge north of Cubits Gap	509,966 cfs	675,834 cfs	485,332 cfs	237,569 cfs	279,518 cfs	588,435 cfs ec	589,968 cfs ec
Discharge through Cubits Gap	80,945 cfs	131,320 f t^3/s	87,884 cfs	41,209 cfs	28,274 cfs	112,820 cfs ec	106,296 cfs ec
Discharge south of Cubits Gap	443,033 cfs	560,997 cfs	378,873 cfs	273,710 cfs	229,120 cfs	488,687 cfs ec	490,334 cfs ec
Percentage discharge into the channel	15.9%	19.4%	18.1%	17.3%	10.1%	19.1%	18.1%

measured discharges for the survey line that went across the Gap. During the May 29 and 30, and the June 16 and 17 2009 surveys, transects across Cubits Gap were not made. However, during the April 22 and 23, 2009 survey, transects across each of the secondary channels off Cubits Gap were made. In Table 2.2, the discharges through Cubits Gap for these surveys are the sum of the average discharges through the secondary channels. During the July 22 and 23, 2009 and the September 23 and 24, 2009 surveys, ADCP transects across Cubits Gap, and across each of the secondary channels off Cubits Gap were made. In July, the total measured discharge going through the secondary channels is 19.7 percent lower than that measured going through Cubits Gap. In September, it is 7.4 percent lower. These results for July and September indicate that there is significant discharge in Cubits Gap that is across areas too shallow to survey, and that

the percentages of discharge through Cubits Gap in May and June, which are based on the flows through the secondary channels, are low. However, the percents of discharge unaccounted for in May and June (2 and -4 percent) don't support this conclusion. It may be that in May and June, when the river flows were much greater than in July and September, the deeper depths allowed greater survey coverage in the secondary channels in Cubits Gap. A careful review of the measurements during July 23 and 23, 2009, did not reveal a reason for the large percentage of unaccounted for discharge (33 percent).

Analyses of the discharges through a control volume that surrounds Venice, LA, are given in Table 2.3. The control volume is seen in Figure 2.11 as defined by the four transect lines in Figure 2.11. The lines are across the Mississippi River north of Venice, across the River south of Venice, and in the channels that lead away from Venice to the east and west. The discharges for July 21 have an unusually large unaccounted for percentage. It is believed that a significant amount of discharge through the channel to the west was missed because the survey transect line was short.

Table 2.3. Discharges through the control volume that includes the south part of Venice, LA.

Date	Discharge from the north	Discharge to the east	Discharge to the west	Discharge to the south
May 30, 2009	986,538 cfs	241,952 cfs	170,924 cfs	560,996 cfs
April 22-23, 2009	687,920 cfs ec	155,288 cfs ec	127,723 cfs ec	443,035 cfs ec
June 17, 2009	699,118 cfs	160,110 cfs	126,243 cfs	378,883 cfs
July 21, 2009	234,775 cfs	38,175 cfs	59,620 cfs	269686 cfs
September 23, 2009	388,628 cfs	47,229 cfs	79,439 cfs	229,120 cfs
February 20—21, 2010	832,634 cfs ec	211,512 cfs ec	153,018 cfs ec	384,689 cfs ec
March 31-April 1, 2011	830,536 cfs ec	186,801 cfs ec	149,034 cfs ec	490,334 cfs ec

Plots of the median grain size (D50) for the push-cores taken in West Bay and Cubits Gap are shown in Figures 2.27 and 2.28. They show two distinctly different mixture types of materials in both areas. A mixture of fine material with mean D50 values of 26.4 microns in both West Bay and Cubits Gap, and a mixture of fine sand-size material with a mean D50 value of 158.3 microns in West Bay.

Figure 2.27. D50 values for the push-cores taken from West Bay.

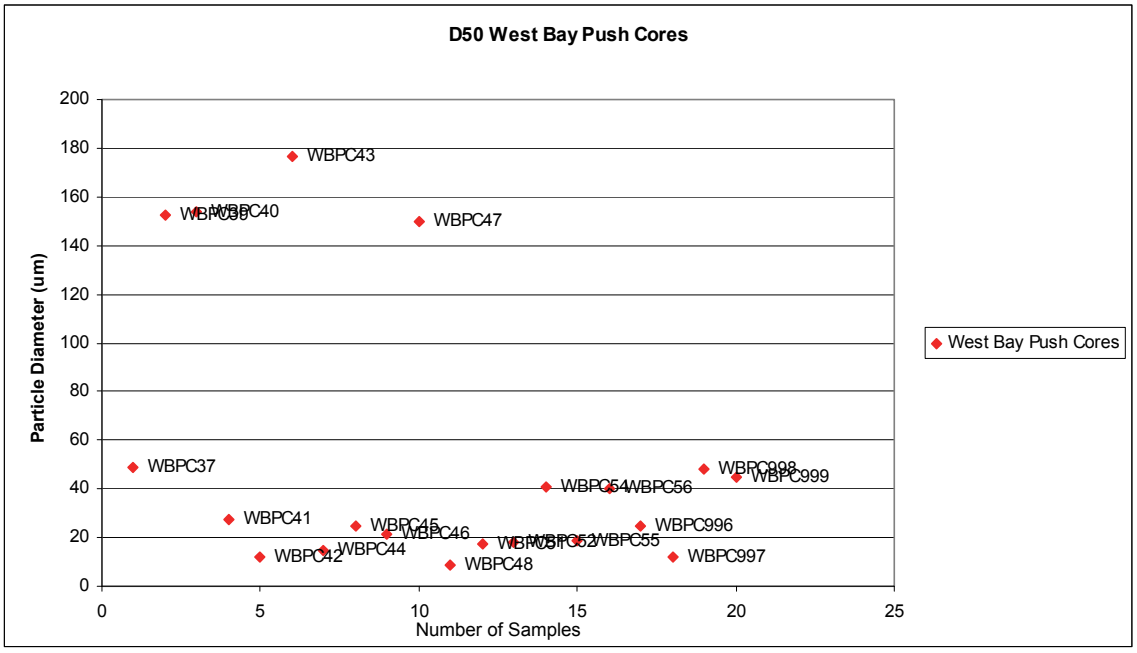

Figure 2.28. D50 values for the push-cores taken from Cubits Gap.

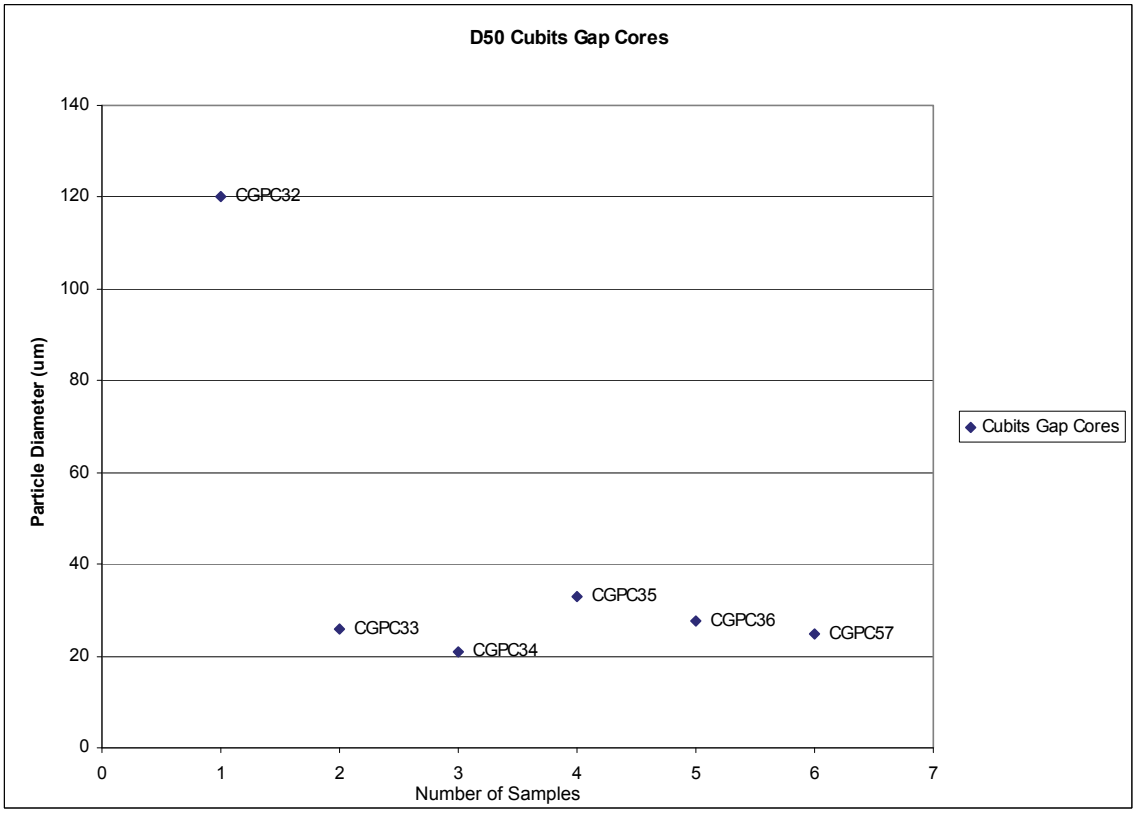

In Cubits Gap, there is only one sample with a mixture of fine sand-size material (D50 value of 120.3 microns) while there are four locations with

sand-size material in West Bay. Two of the four push-core locations having sand-size material are near the diversion channel. However, the other two are roughly a half mile south of the channel on the eastern side of the bay nearest the Mississippi River and may be primarily dredged material from the river placed in West Bay.

Going down-river, the sediment samples from the west side of the Mississippi River are more fine-grained than the samples from the east side of the river, until the sample line across the river just north of Cubits Gap (samples 19 and 20, Figure 2.22). Figure 2.29 shows an example of this, where the grain-size distribution for the finer sample 15, on the west side of the river, is plotted with the grain-size distribution of the coarser sample 16, directly across the river on the east side the 3 different series are the analysis checks for each sample(Figure 2.22). Starting with samples 19 and 20 just north of Cubits Gap and going down-river to Southwest Pass, the trend is reversed. In this region the samples from the west side of the river are coarser than those from the east side of the river. Overall, as is the case in West Bay, the D50 values show two distinct types of bottom material in the Mississippi River, sand-size material, with a mean D50 value of 185.0 microns, a little coarser than the mean value of 158.3 microns found in West Bay, and fine material about the same size as that found in West Bay with a mean D50 value of 22.3 microns. Figure 2.30 shows the D50 values throughout West Bay and Cubits Gap.

Figure 2.31 shows a cross section of vertical current velocities measured along three consecutive ADCP transects across the same survey line done on April 23, 2009 in the throat of the diversion channel. The transect numbers are 117, 118, and 119 (Figure 2.9). The cross sections are displayed from south (right side) to north (left side) across the channel, so that they are viewed as looking from the Mississippi River into West Bay. The figure shows an area of downward (negative – blue to purple colors) current speeds from 120 to about 180 ft across the channel, and an area of upward (positive-yellow to red) current speeds at about 270 ft across the channel. Figure 2.32-2.34 shows the 3D discharge patterns inside the WBSD cut. Figure 2.32 is a depth average velocity plot of all the 3D velocity lines collected during the April survey. Notice the discharge patterns in the cut itself. By depth averaging the entire water column the eddy pattern is diminished. That pattern is more evident when you look at the surface currents and bed currents in Figures 2.33 and 2.34. There is an eddy in the discharge in the shallow water on the north side of the diversion channel.

Figure 2.29. Grain-size distributions for bottom drag samples 15 and 16.

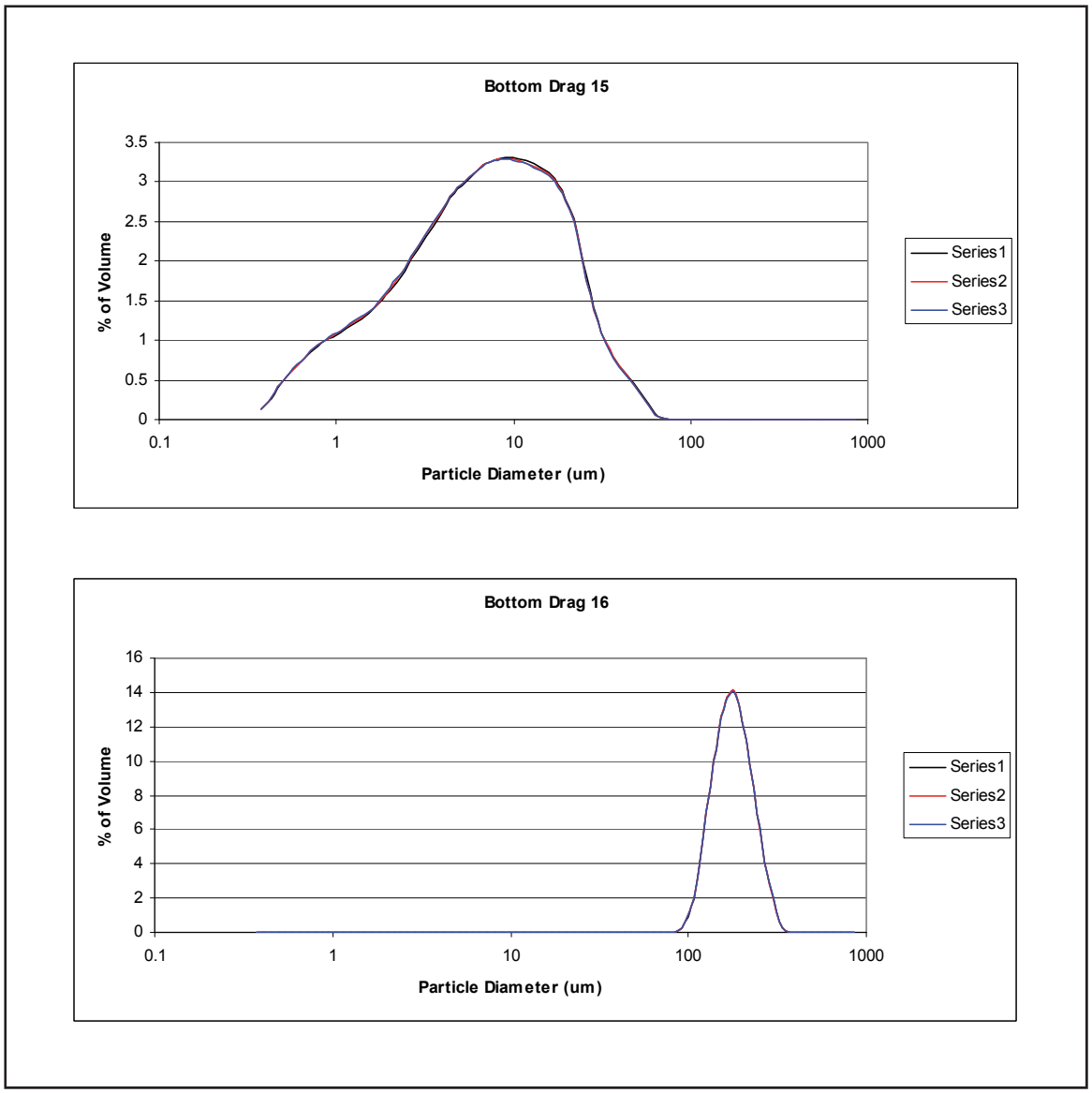

The CTD casts made on May 29 and 30, 2009, when the discharge north of the diversion channel was 740,062 cfs, shows no indication of a salt wedge. On July 21, 2009, when the discharge is 311,852 cfs, it is present at 46.74 ft depth with a salinity of 28.71 PSU, at survey transect line R-5.2 (the one immediately north of the diversion channel). No CTD casts were made further upstream from R-5.2 on July 21. On September 23 and 24, when the discharge is 331,732 cfs , it is present as far north as survey transect line R-12.1 (north of Venice) at 52.12 ft depth with a salinity of 2.56 PSU. During this survey it was measured at R-5.2 with a salinity of 5.49 PSU at a depth of 33.79 ft and 22.68 PSU at a depth of 46.33 ft.

Figure 2.30. Map of D50 values in West Bay and Cubits Gap.

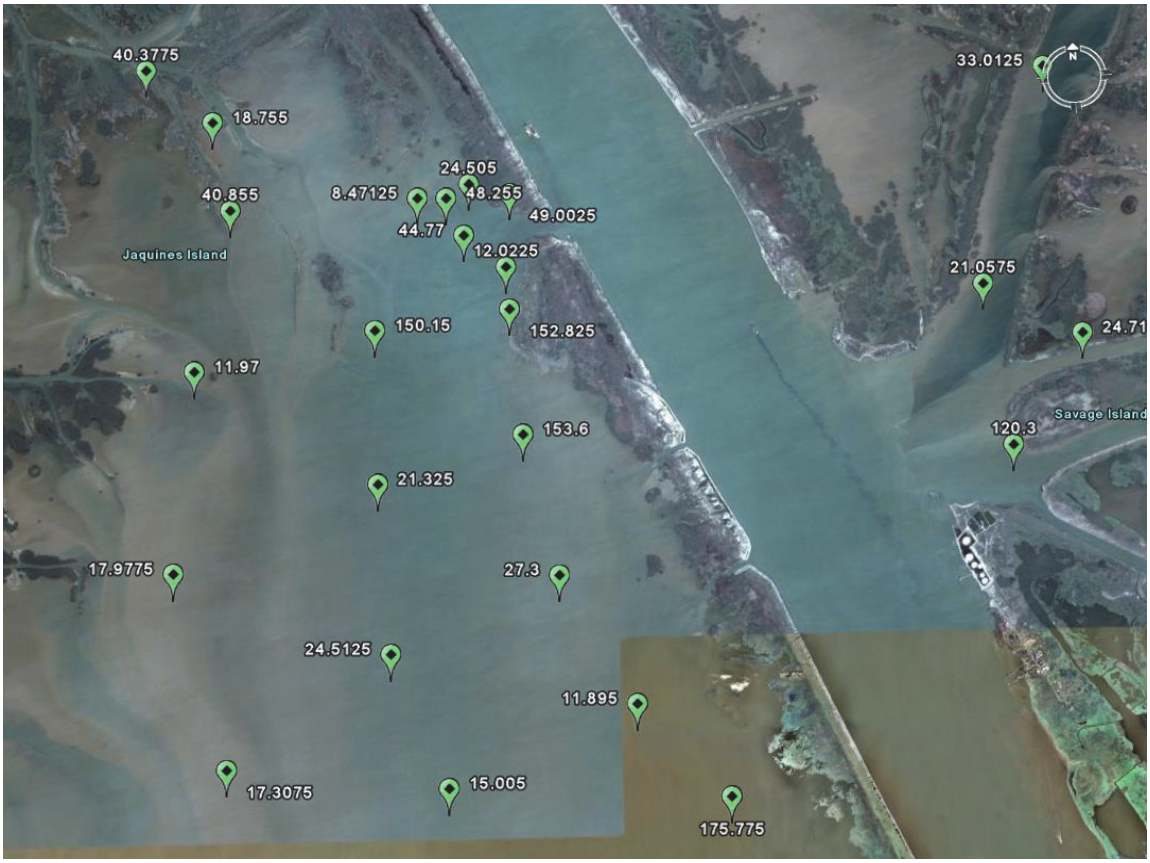

ADCP backscatter calibration to suspended sediment concentration data are the means by which sediment flux calculations were made to determine the suspended sediment transport rates out the various diversions along the main Mississippi River from RM 12.1 to RM 2.6. The method of calibration has been developed over several years of application. It involves the relationship between the distribution function of the acoustic backscatter energy values and the calibration Total Suspended Sediment Concentration (TSM) distribution function. The ideal calibration TSM data set needs to be collected across the cross-sections where ADCP transects are collected. The range of acoustic backscatter energy values is from 0 to 256. Several representative ADCP transects are read and the energy values are counted over the range of 0 to 256 to create the distribution function for the acoustic backscatter. The same process is done for all of the TSM samples, each time a concentration value occurs then a count value is added to a distribution function. The whole premise for the calibration is that the two distribution functions are related for that particular stage. After the two distribution functions are populated, then the value for each function in one percent increments are paired. These paired values are regressed against each other

Figure 2.31. Vertical current velocities across the diversion channel on April 23, 2009.

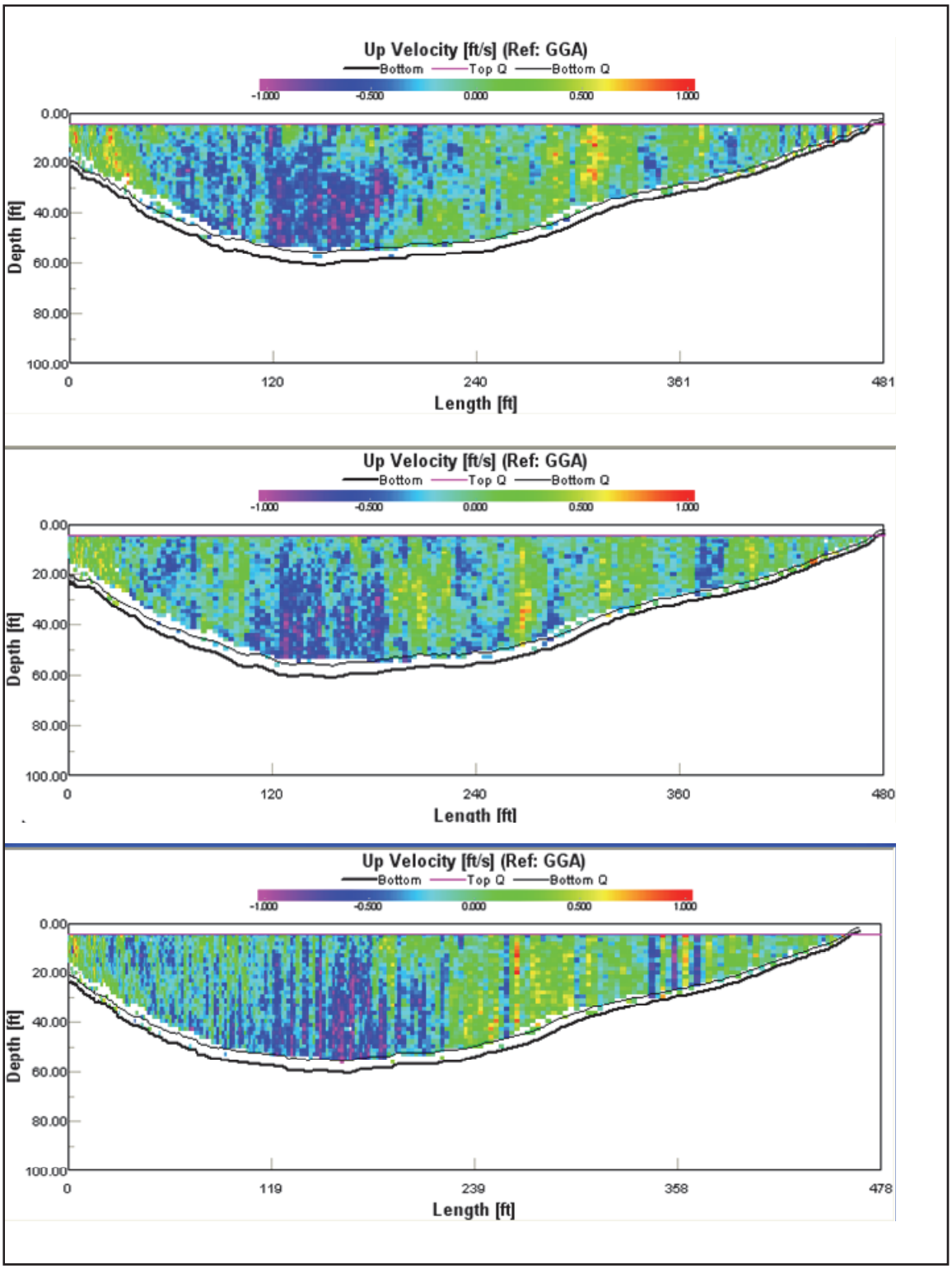

Figure 2.32. Depth Averaged 3D discharge measurements from the April 23, 2009 trip.

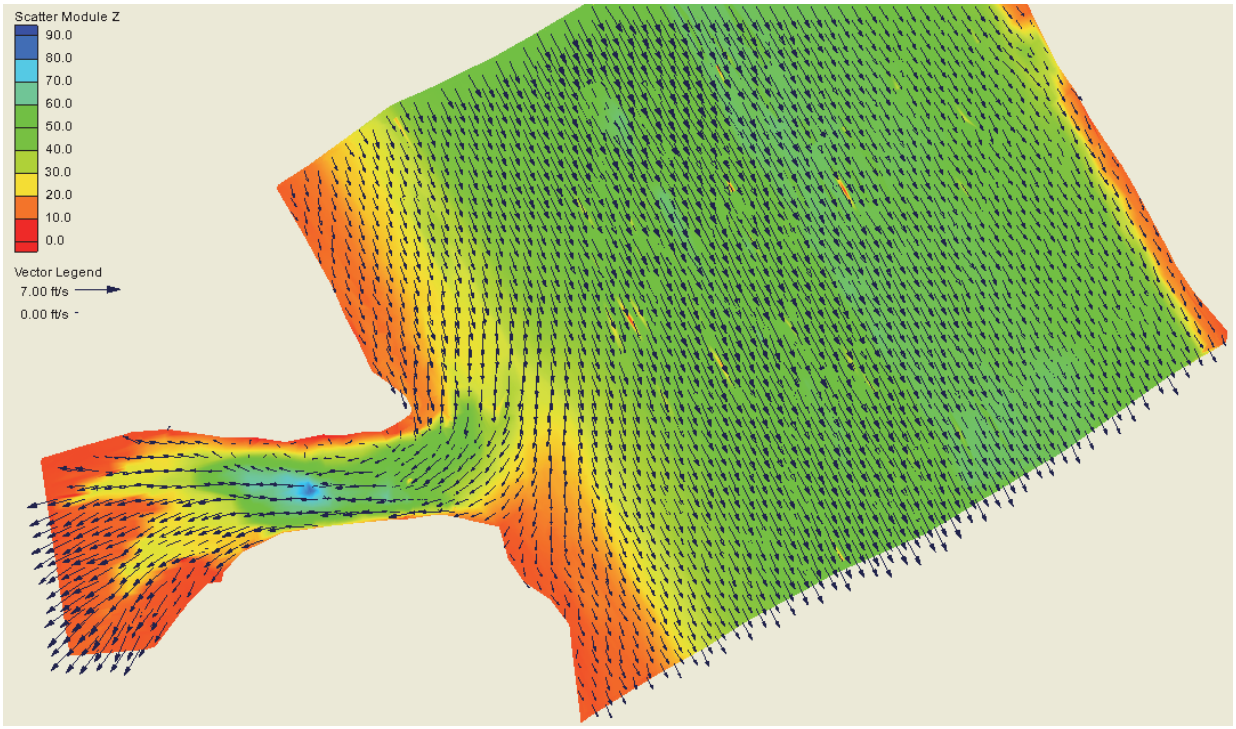

Figure 2.33. Surface Velocities of the 3D discharge measurements during April 23, 2009 trip.

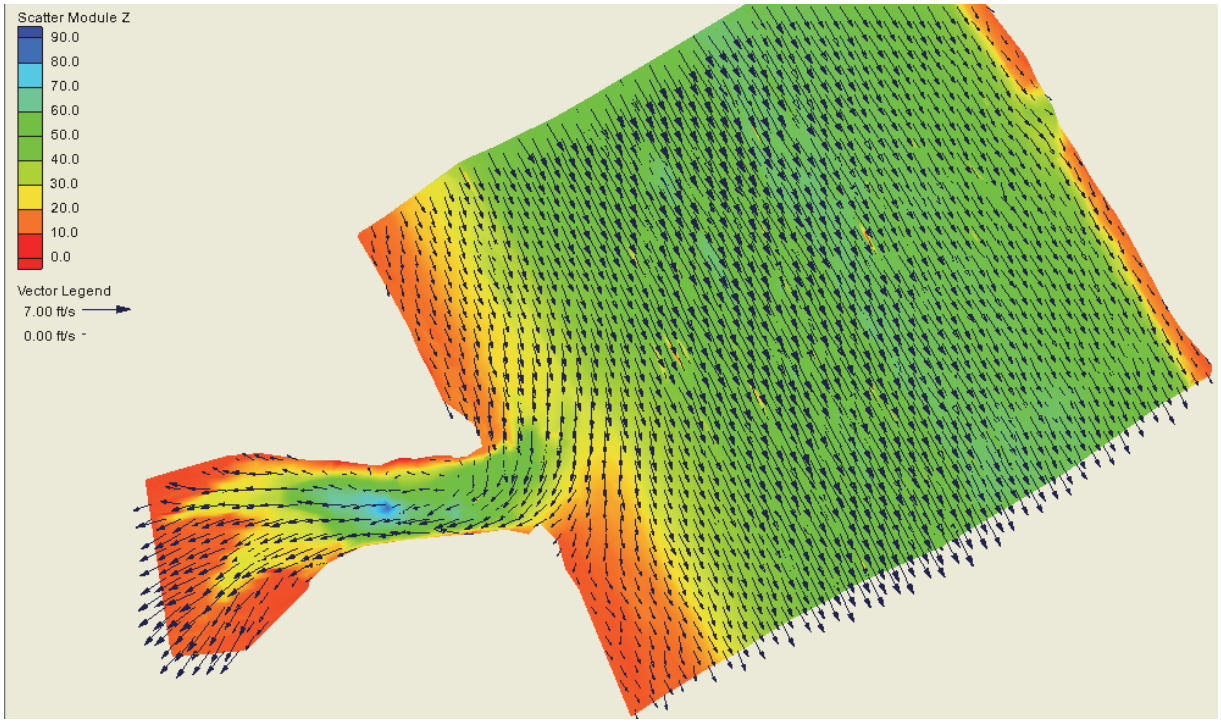

Figure 2.34. Bottom Velocities of the 3D discharge measurements during April 23, 2009 trip.

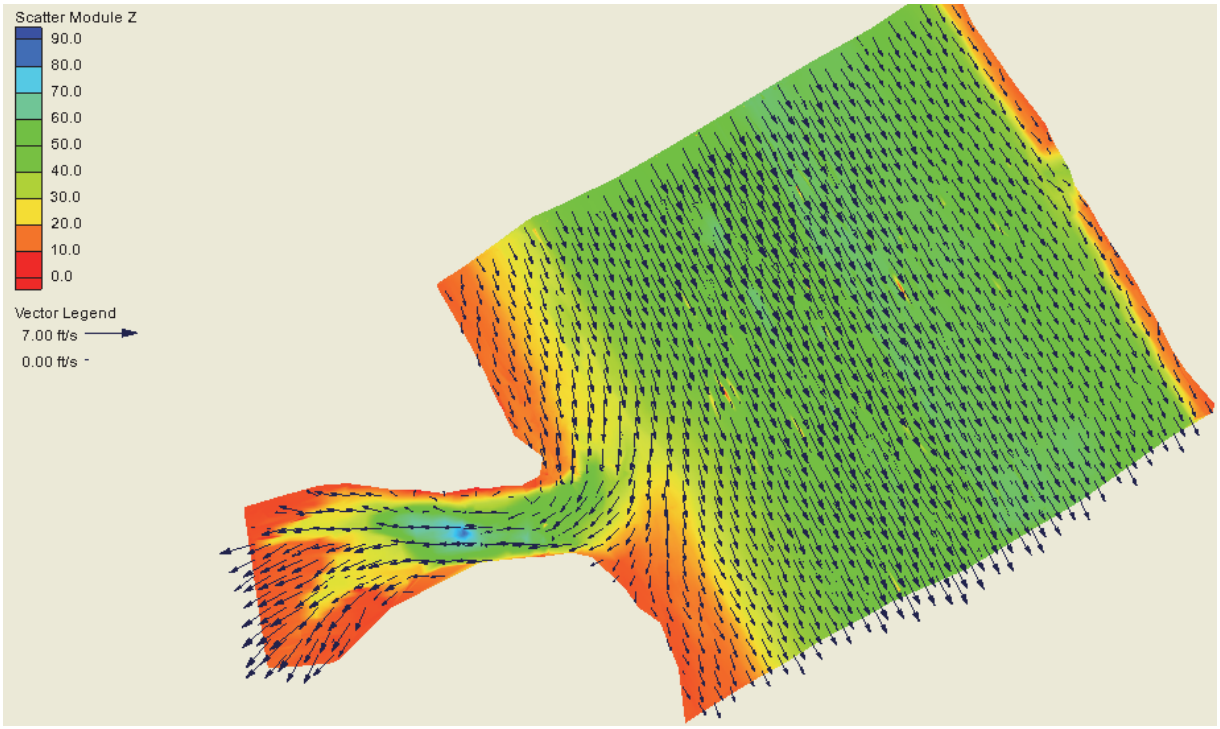

to define a calibration curve between the two data sets. Usually a second order polynomial fit gives *r* squared values greater than 0.96. That calibration curve is only good for the stage in which it was collected because the relationship of the acoustic backscatter energy to TSM is a function of the material characteristics in suspension. As the source, size distribution, and concentration change with the hydrograph then the backscatter distribution function will change and take a slightly different shape.

The next step in the calibration process is the conversion of the acoustic backscatter data to TSM values. The calibration equation is applied to the ASCII ADCP data to convert backscatter to TSM values. The conversion of backscatter data closer to the bed often does not match well. It tends to overestimate the profile as it approaches the bottom. The converted ASCII file concentration data are fit to a Rouse profile near the bed. A maximum concentration value has to be supplied by the user to determine where to start applying the Rouse profile algorithm to the concentration profile. This value is derived from the actual sample data. The choice of this value is an iterative process to achieve the closest fit to the actual field samples.

During the samples collection operation two physical samples were collected at each point in the water column. One sample was analyzed for TSM while the other sample was analyzed for grain-size distribution. In

addition to the sample data, ADCP velocity and backscatter data were collected during the entire sampling operation. These backscatter data were converted to TSM values for the entire sampling period. The converted TSM values at the specific depth elevation were extracted to compare to the actual physical samples. This comparison showed how well the calibration process worked. If the converted data near the bed was too high as compared to the sample data then the value of the pick point is increased in applying the Rouse profile in the conversion process. The process might be repeated several times until the best fit was achieved.

Once the backscatter data are converted, the next step in the flux calculation process begins. The ADCP collects velocity data as the boat is driven across the channel. The collection rate of the instrument is fixed and the vertical spacing of data in the profile is fixed but the speed of the vessel as it moves across the channel can vary slightly as different discharge conditions arise. Therefore, the cells or bins can vary in length as the boat moves across the cross section. In addition to the velocity data for each cell, TSM values are obtained for each cell through the calibration process. The dot product of the water flux with the concentration at each cell is computed to determine the sediment flux through that cell. This process is done throughout the entire profile at which time the values are summed for the entire cross section. The resultant value is in mg/sec which is then converted to tons/day for the cross section.

In response to peer review comments, an additional calculation of suspended flux using a method called the moving boat method was created. This method does not use the converted acoustic backscatter to make the flux calculation but instead a mean concentration from the suspended sediment samples taken at each cross section. This concentration is used with the individual *q*-values calculated throughout the water column. The fluxes for each bin are summed as you move across the cross-section to give a total flux for the cross-section. The percentages of the different size classes for the suspended sediment are then used to determine fluxes by size class for each cross section. The moving boat method gave slightly larger suspended flux values as expected since the whole cross section is treated with one mean concentration value. This method does not capture the cross sectional variability that exists. This exercise confirmed the validation of the original flux calculation approach.

Suspended Sediment Concentration Method Comparison

The concentration values calculated from the ADCP backscatter data were very similar to the actual measured values for each trip. They tend to be slightly lower than the mean measured values. That could account for the slightly lower backscatter flux calculations when comparing to the flux measurements from the moving boat method. Figure 2.35 shows the relationship between the measured and the calculated TSM values which gives confidence to the further analysis.

Figure 2.35. Average TSM values compared to average TSM from backscatter data

	Depth Averaged Suspended Sediments Concentration (SSC) of all Transects (mg/L)							
	April 22-23, 2009	May 5-6, 2009	May 29-30, 2009	June 16-17, 2009	July 20-23, 2009	Sept 22-24, 2009	Feb 20-21, 2010	March 31 to April 1 2011
Measured SSC	224.0	151.0	237.4	122.5	34.9	30.0	182.43	204.4
ADCP SSC	208.6	159.1	208.0	131.1	31.9	26.9	192.3	213.9

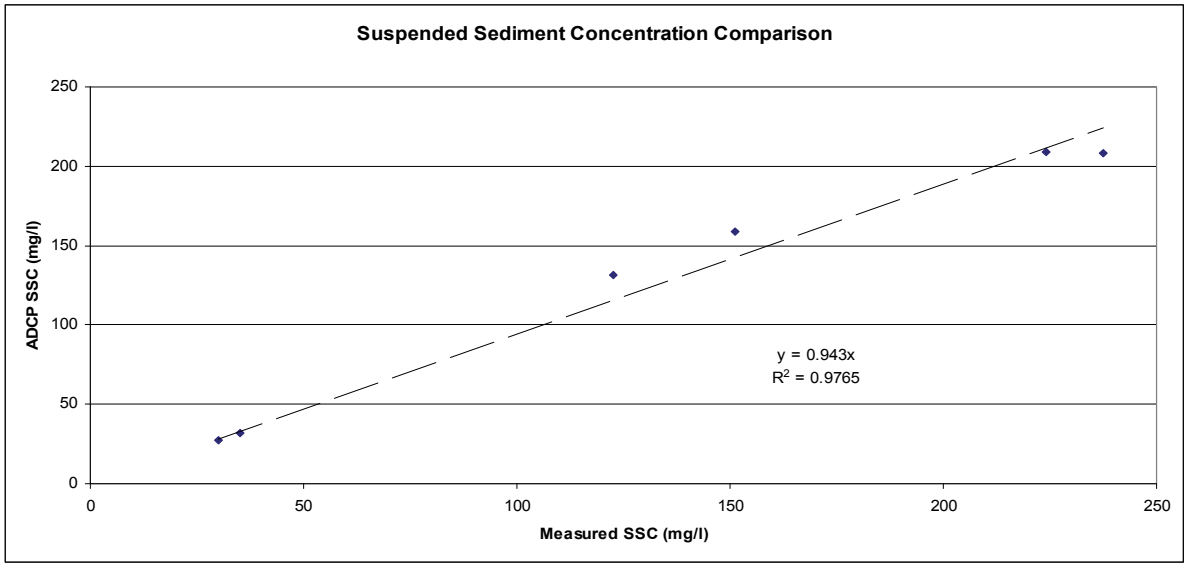

These two multi-beam surveys of the WBSD before and after the high water event in late May show that the Cut is eroding more in the vicinity of lines 7—14 (Figures 2.36 and 2.37). The red erosion area has increased in size and the green area has split to form a y-pattern. The cross section lines cut through the two surveys show this erosion and deposition along the north side of the cut (Figures 2.38 and 2.39). These results are very similar to the patterns shown in the 2D and 3D model. (The orientation of the cross section graphs is the north bank on the left side of the plot looking out the diversion cut.)

Figure 2.36. April multi-beam survey of the Diversion Cut.

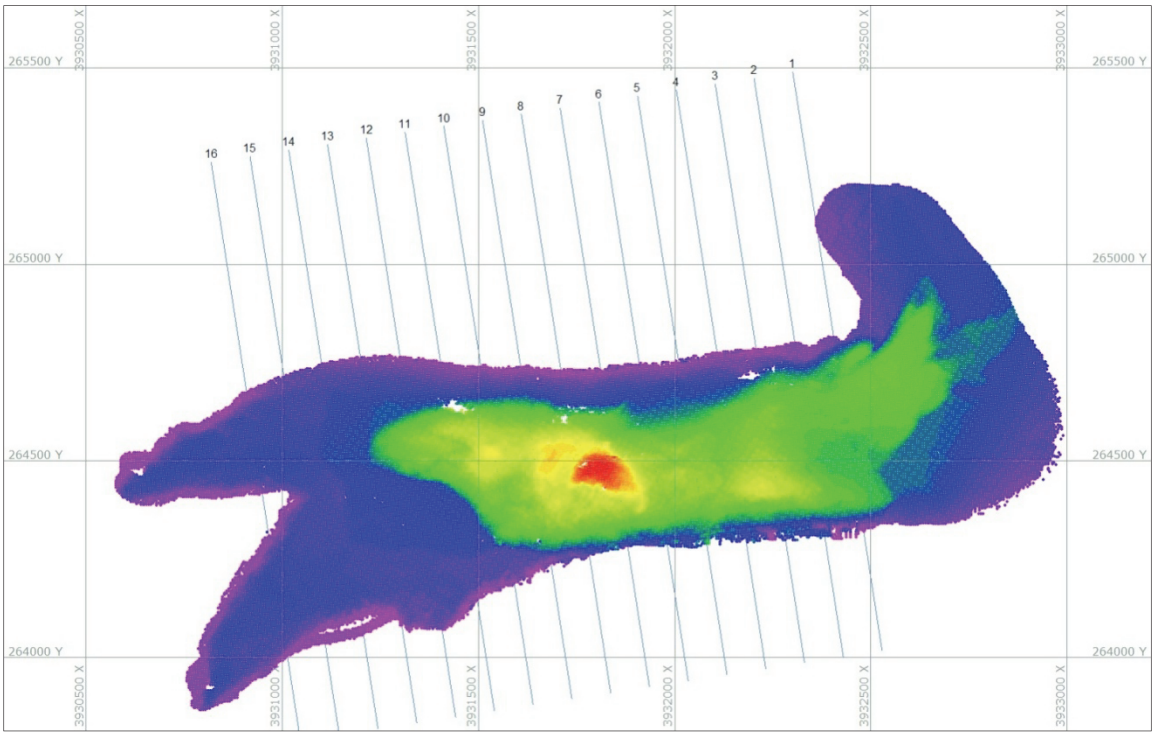

Figure 2.37. August multi-beam survey of the Diversion Cut.

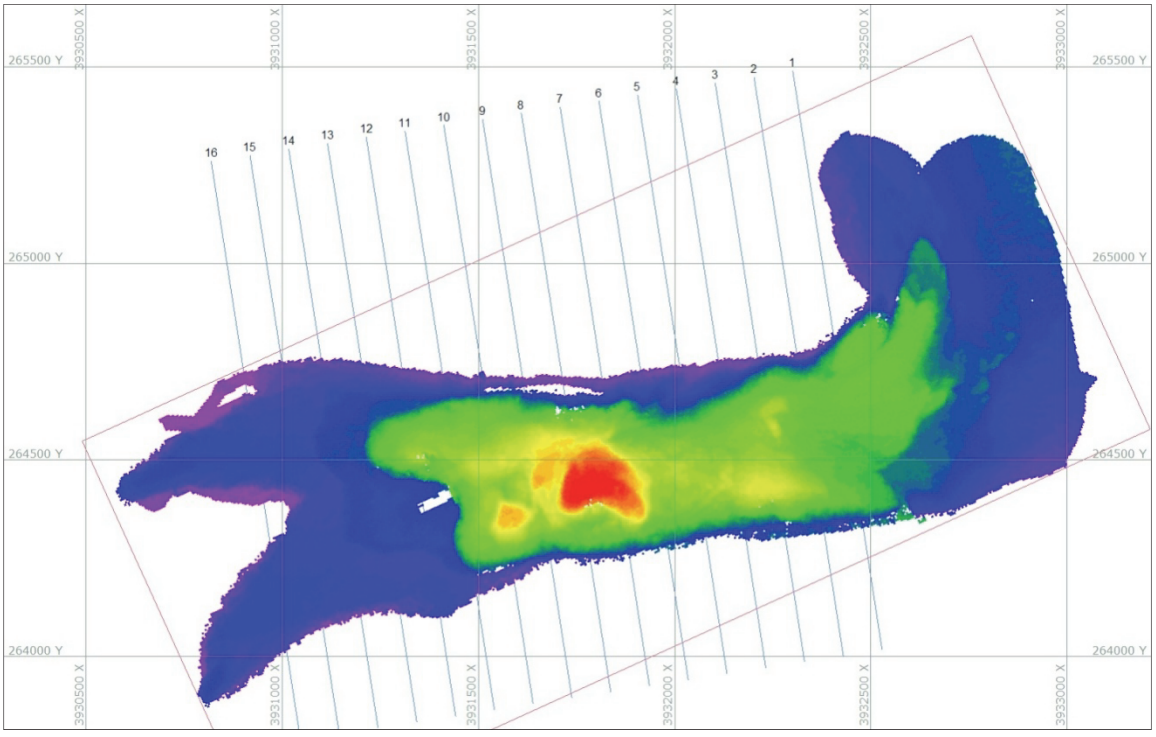

Figure 2.38. Cross section plots of the multi-beam survey lines 1-8.

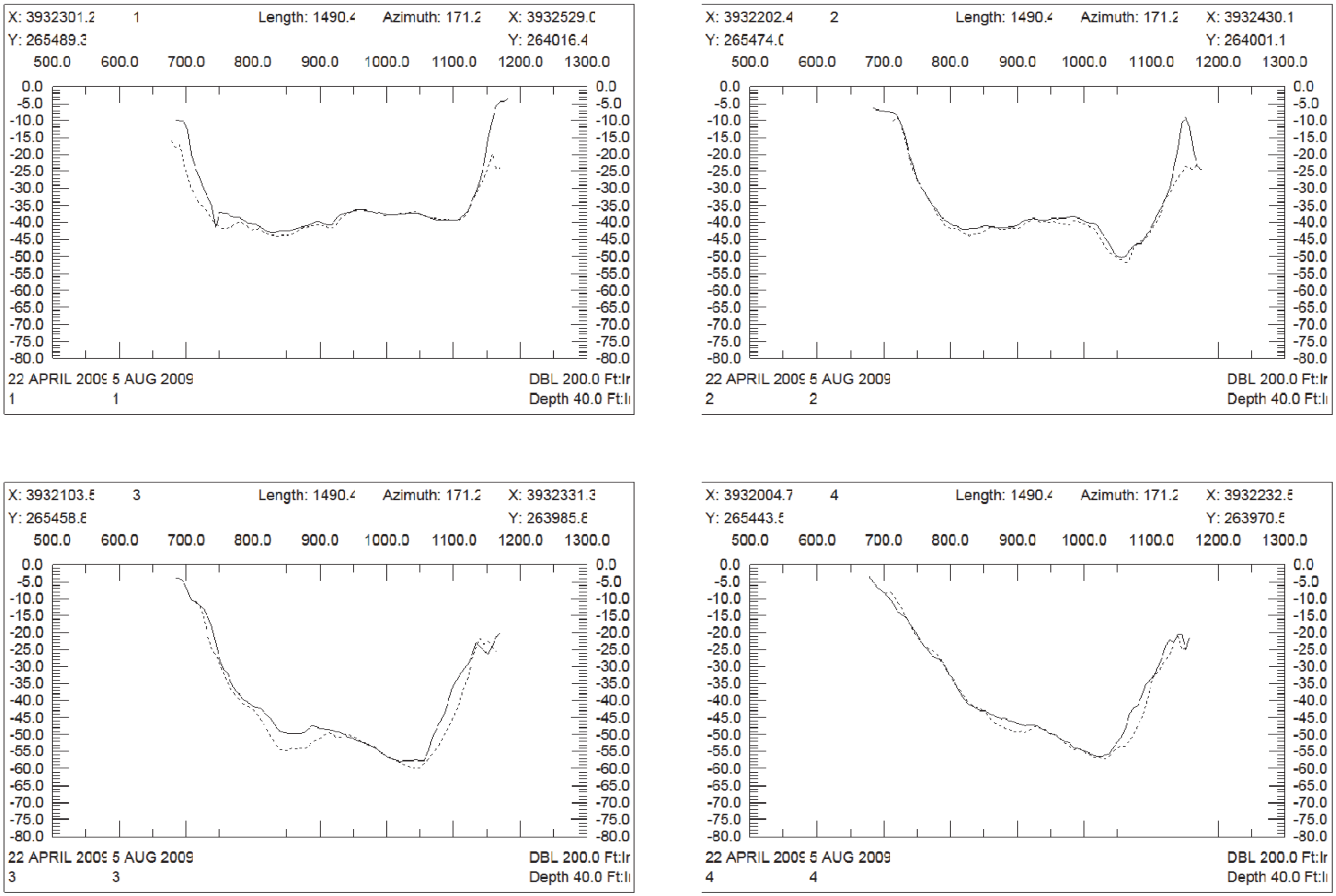

Figure 2.38. (concluded).

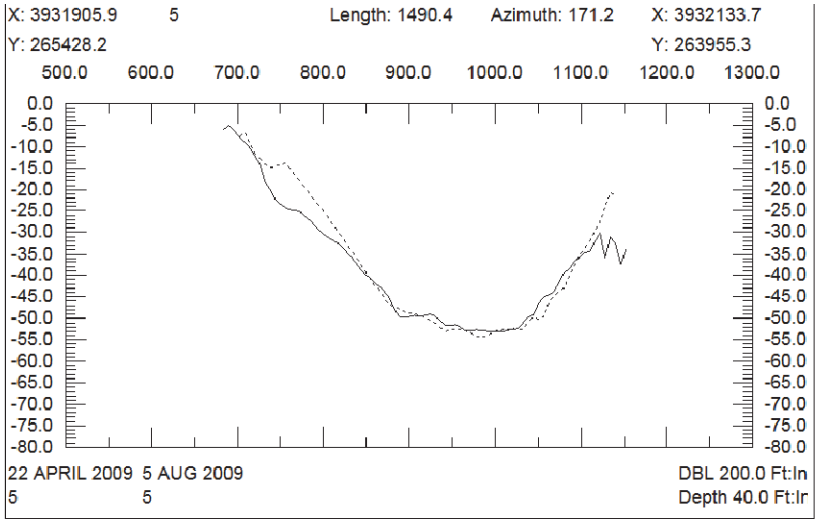

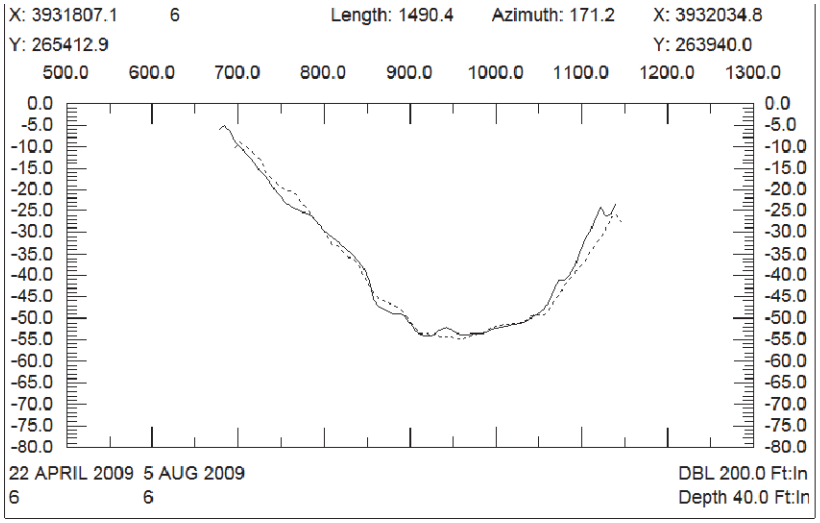

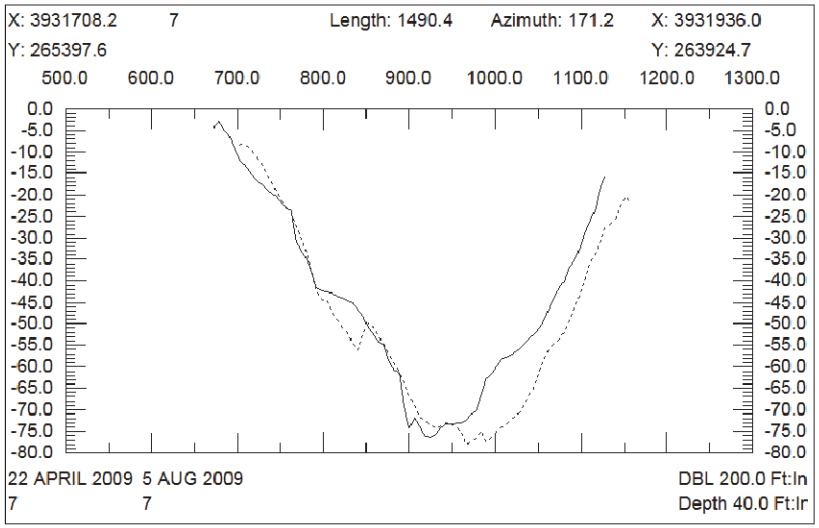

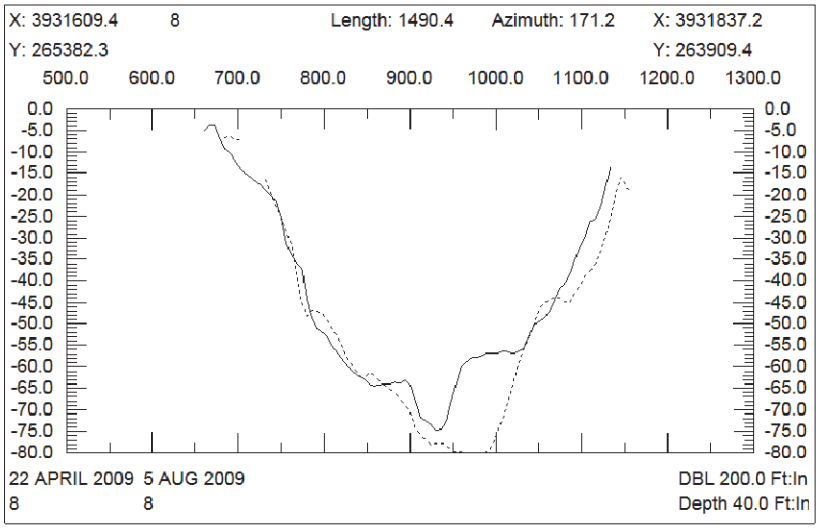

Figure 2.39. Cross sections of the multi-beam survey lines 9-15.

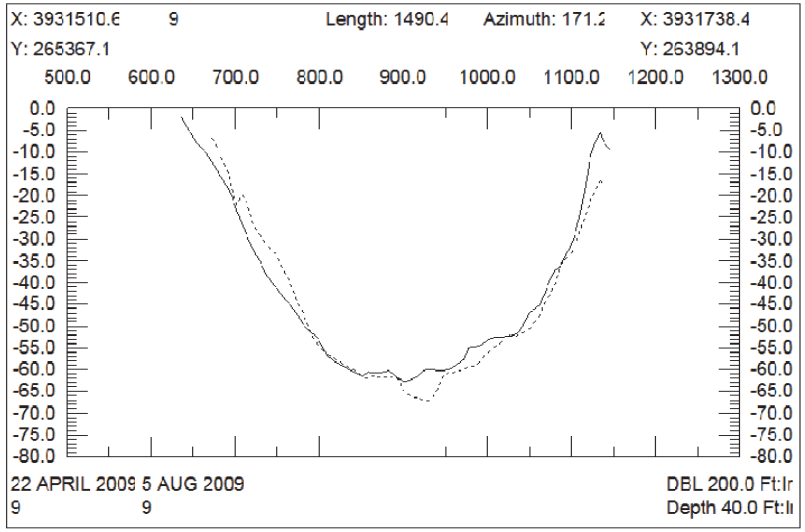

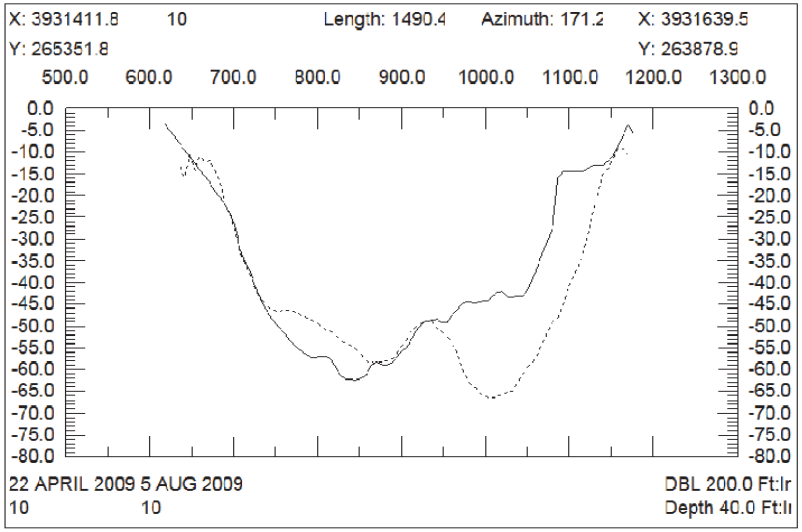

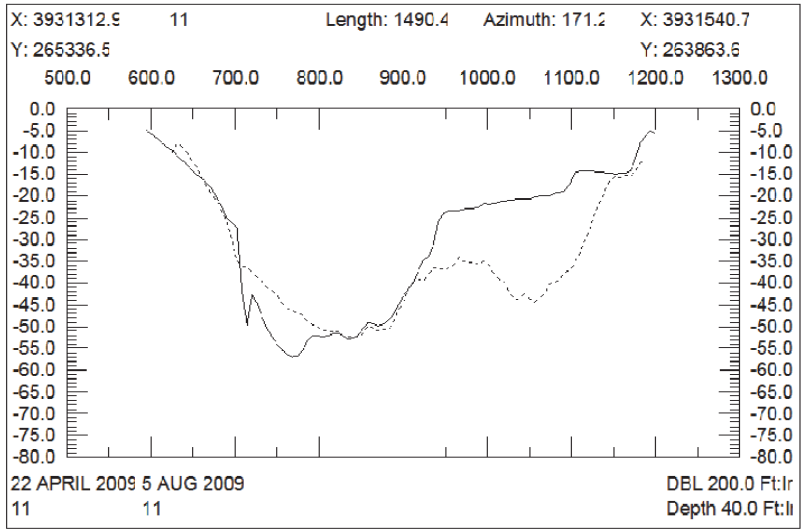

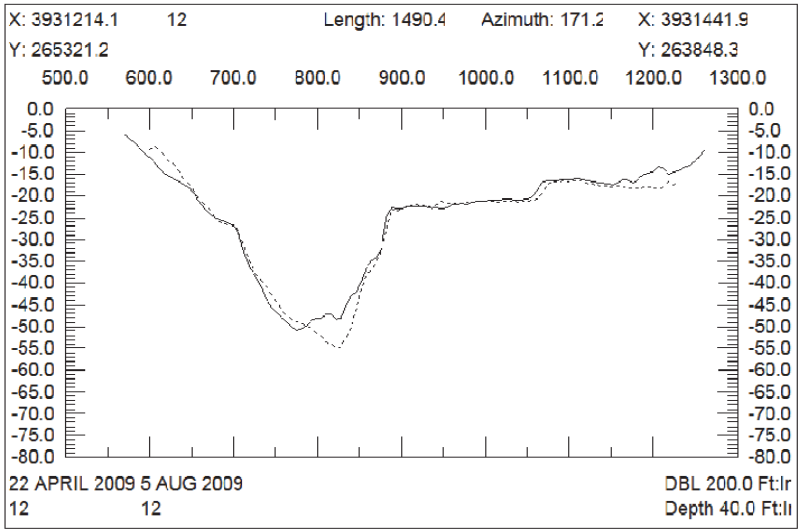

Figure 2.39. (concluded).

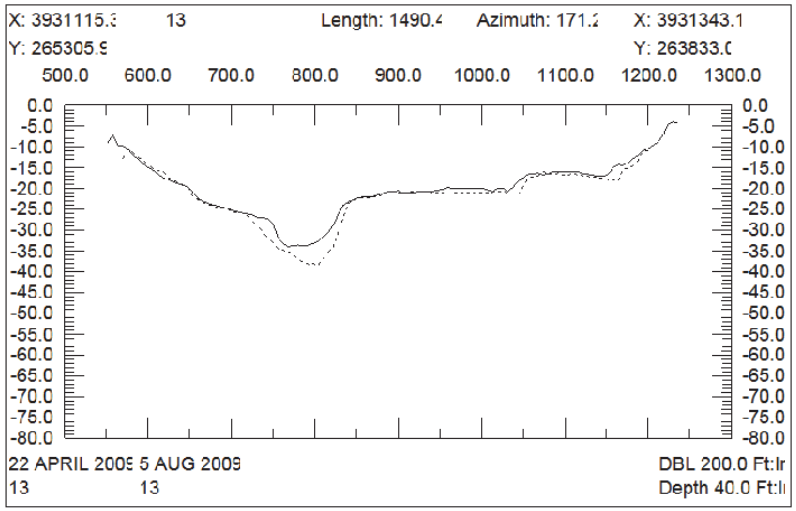

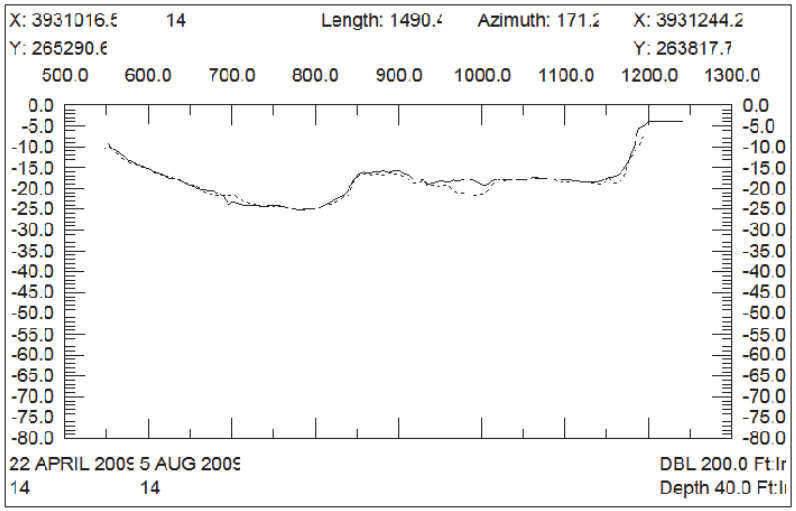

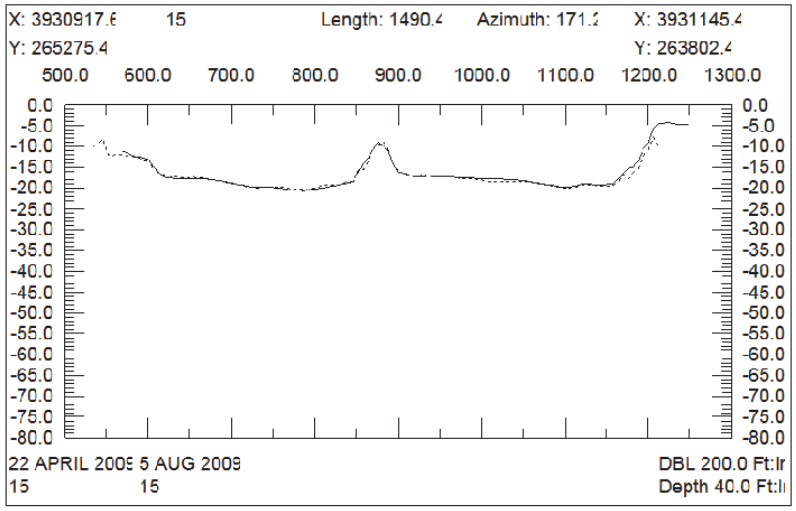

Figures 2.40—2.48 show the different size transport rating curves for the different cross-sections moving downstream from Venice. The suspended sediment data was analyzed through a Laser Diffraction Particle Sizer to give the complete breakdown by size class for suspended sediment. We plotted the data against the corresponding discharge and fit the curve though the resulting points. We did this analysis for each cross-section that was measured during the study.

Figure 2.40. Babtiste Colette transport by grain size.

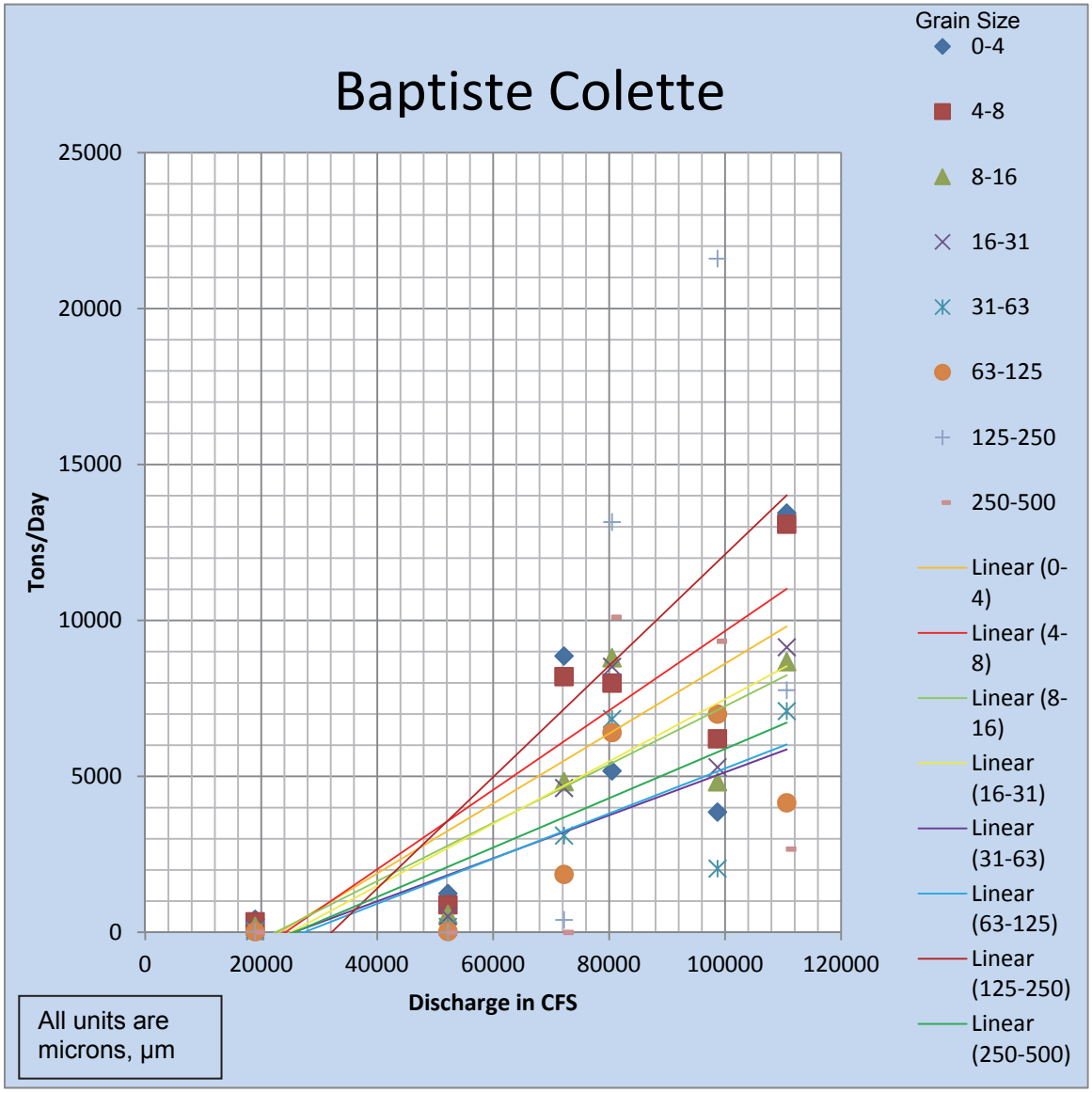

Figure 2.41. Grand Pass transport rating curves by grain size, µm.

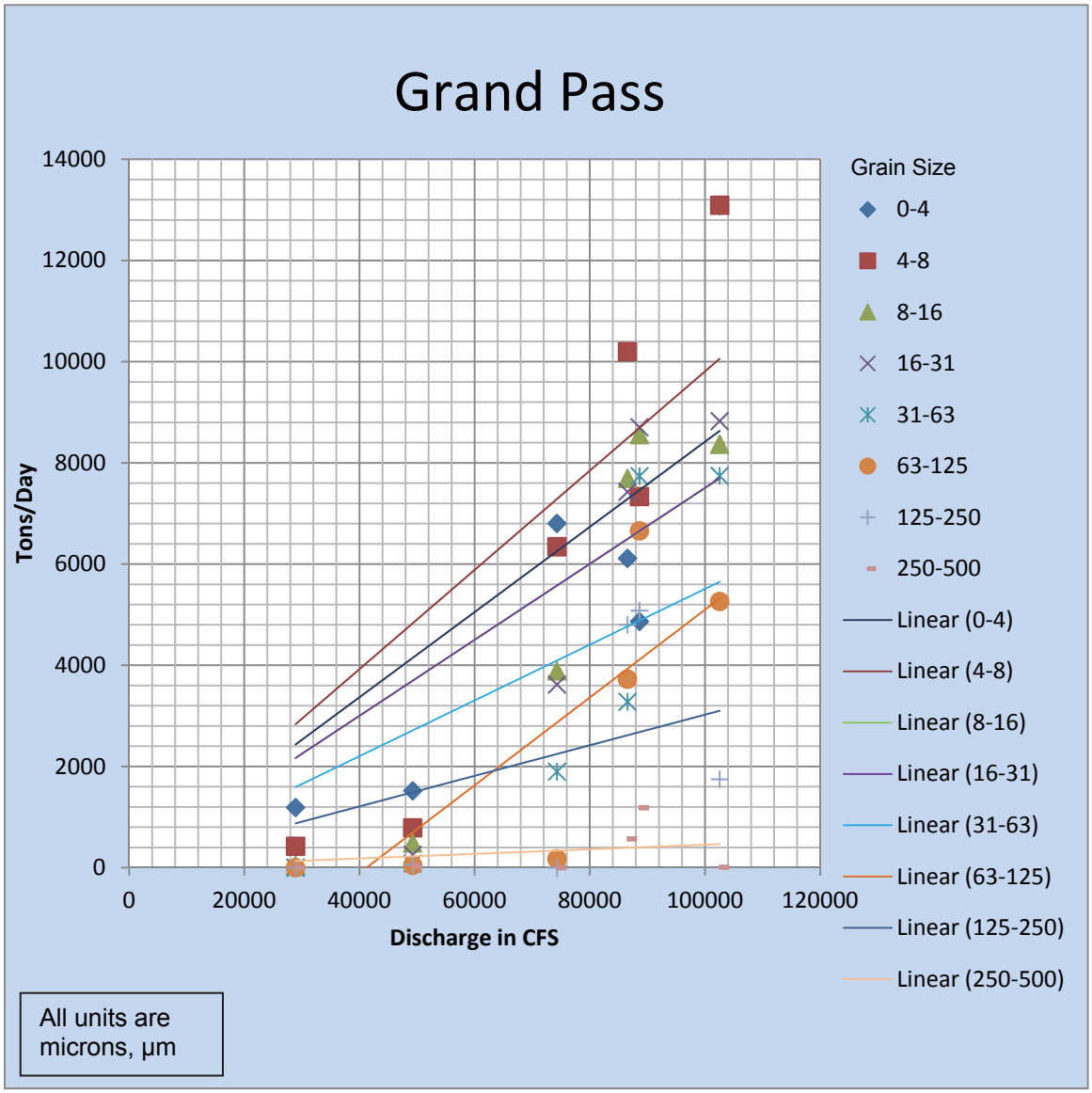

Figure 2.42. RM 5.2 transport rating curves by grain size, µm.

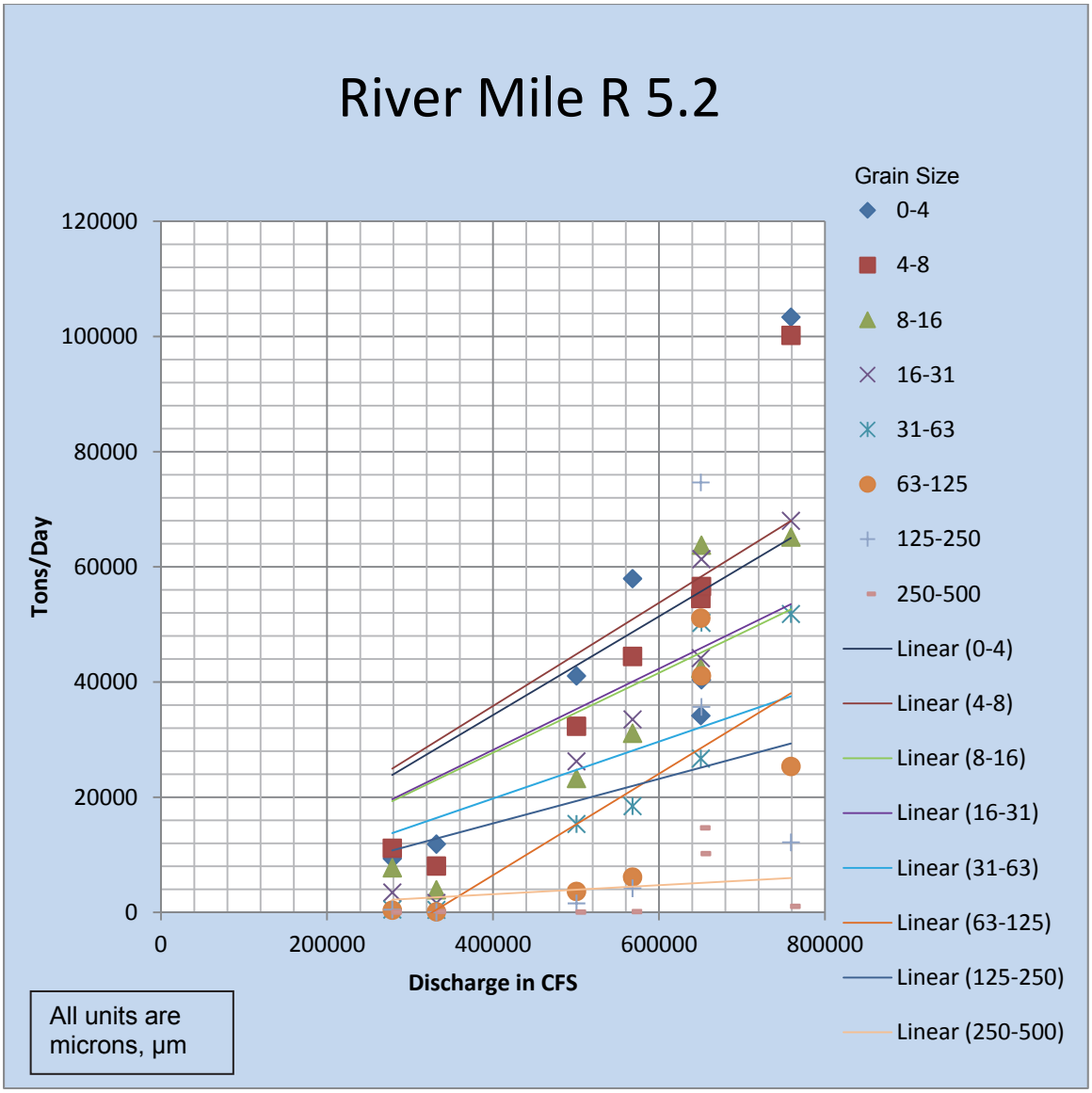

Figure 2.43 WBSD transport rating curves by grain size, µm.

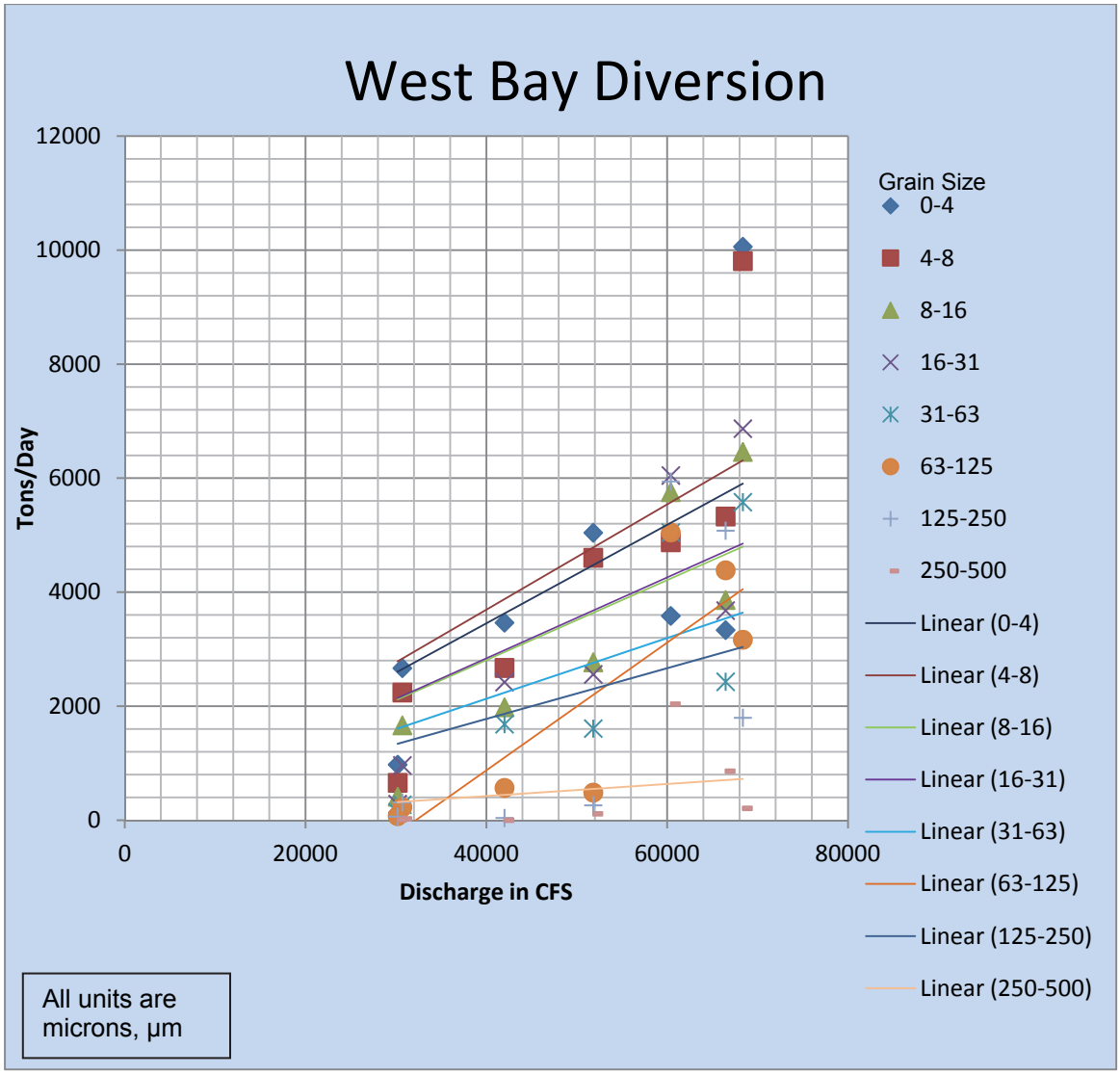

Figure 2.44 RM 4.5 transport rating curves by grain size, µm.

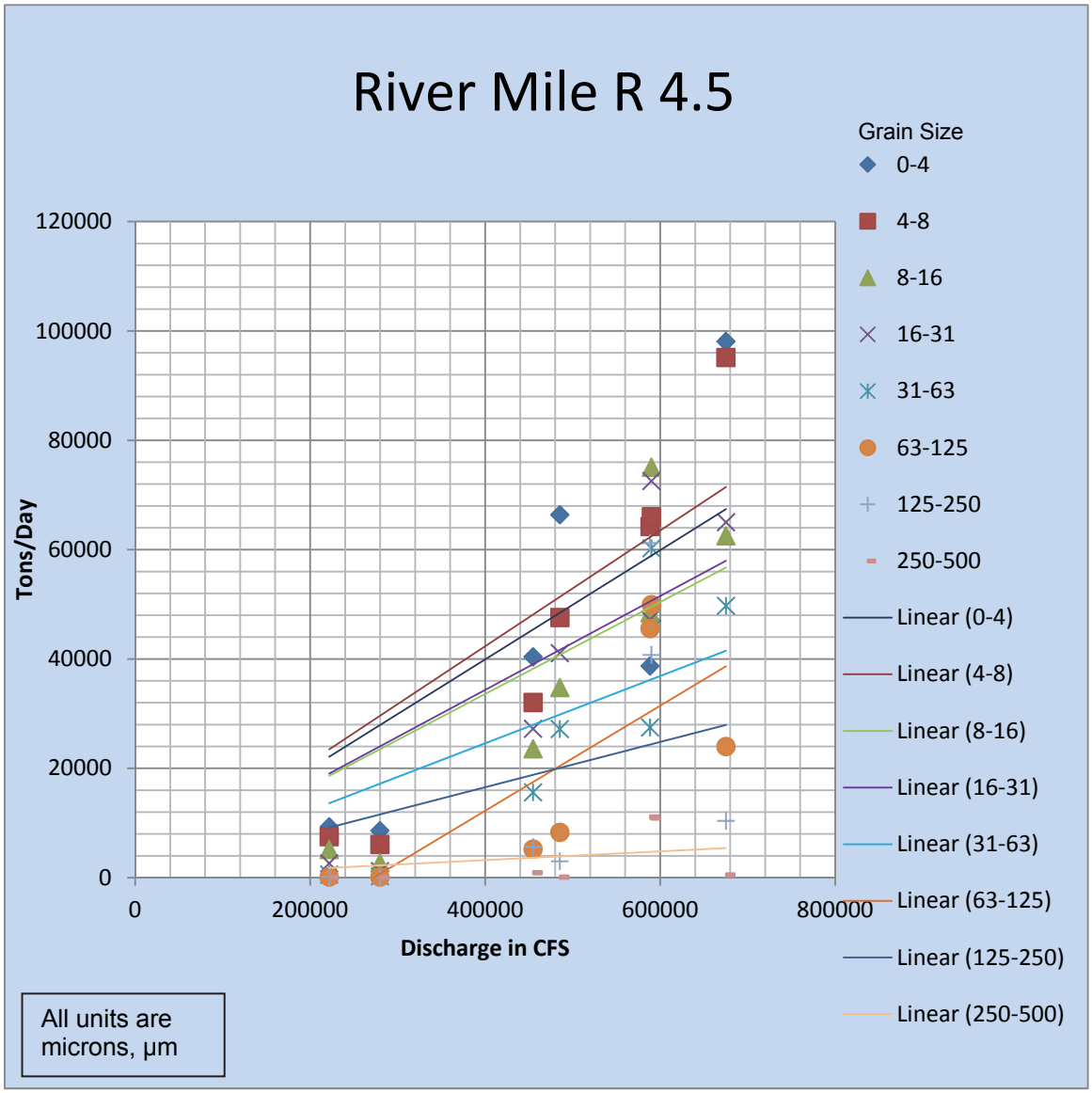

Figure 2.45. Cubits Gap Main Pass transport rating curves by grain size, µm.

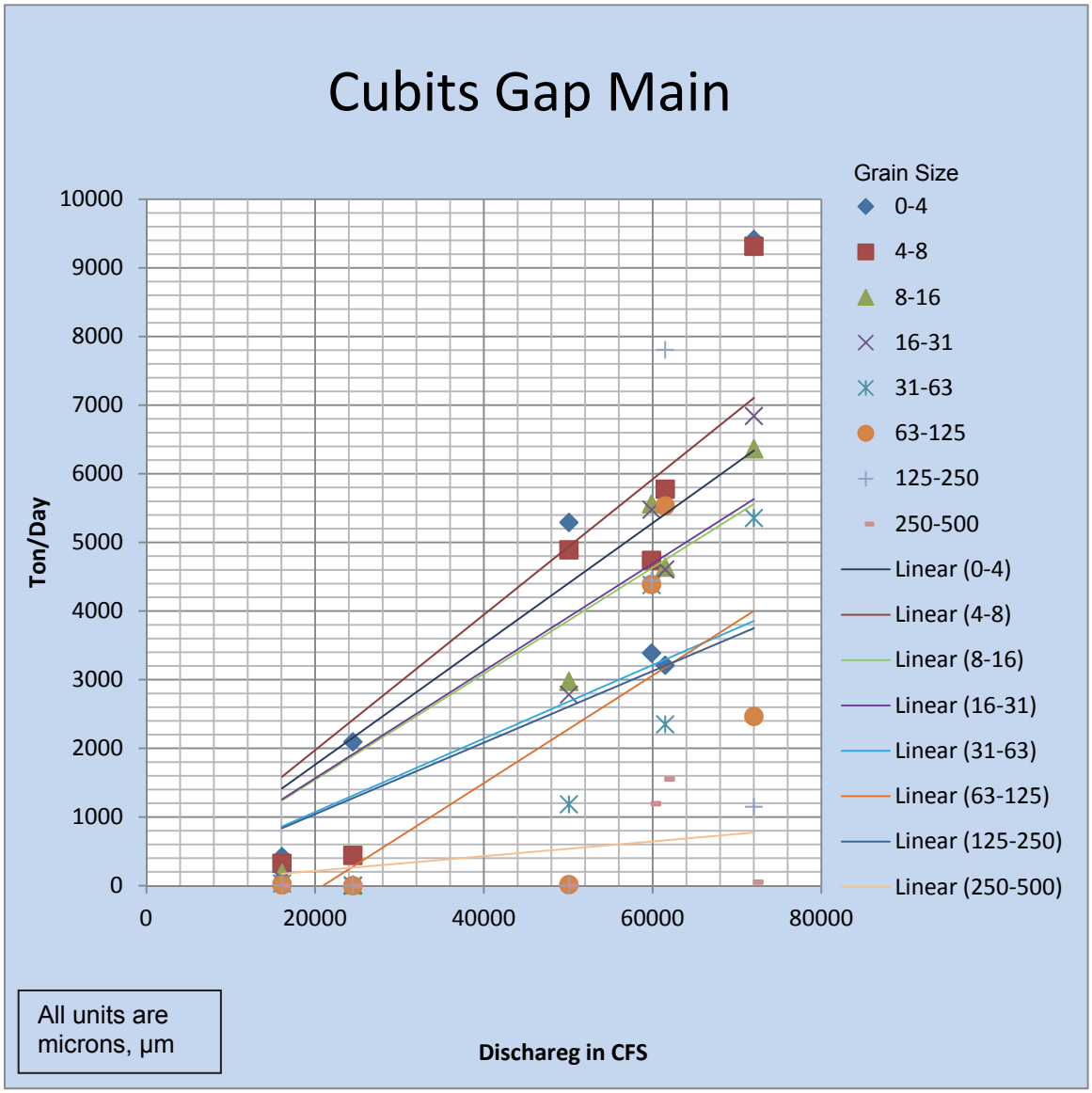

Figure 2.46. Cubits Gap BB Pass transport rating curves by grain size, µm.

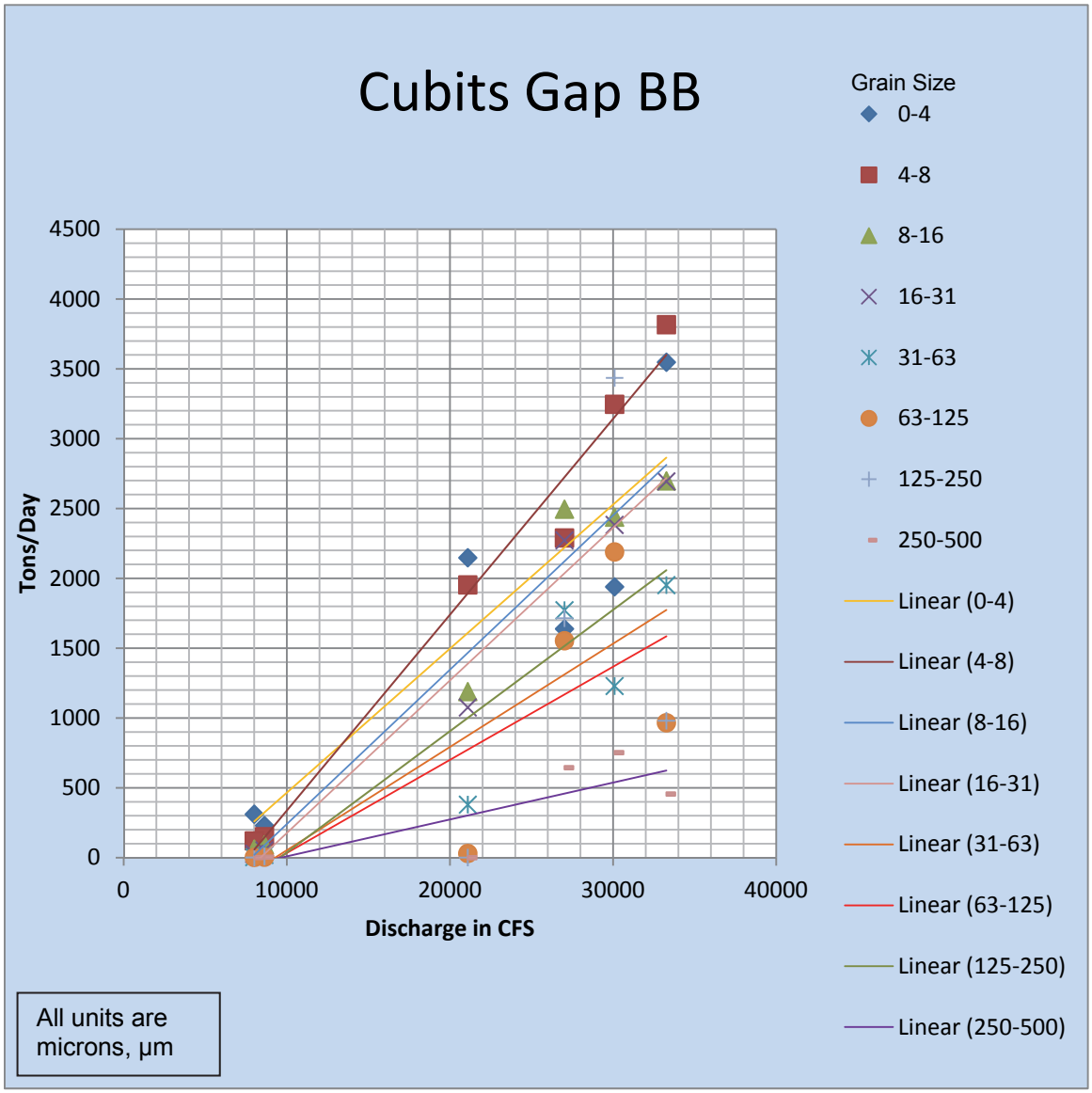

Figure 2.47. Cubits Gap OP Pass transport rating curves by grain size, µm.

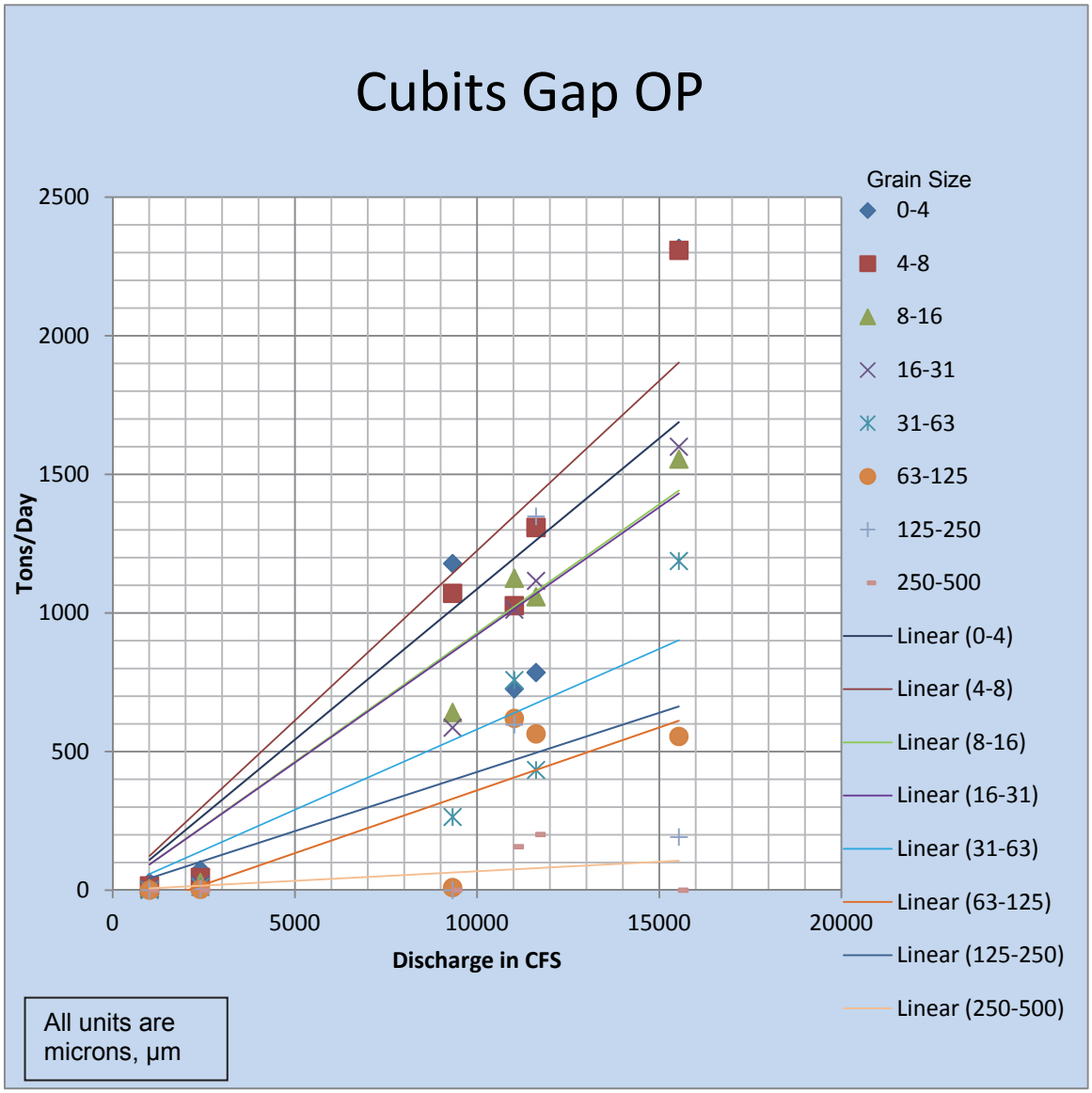

Figure 2.48. Cubits Gap RP Pass transport rating curves by grain size, µm.

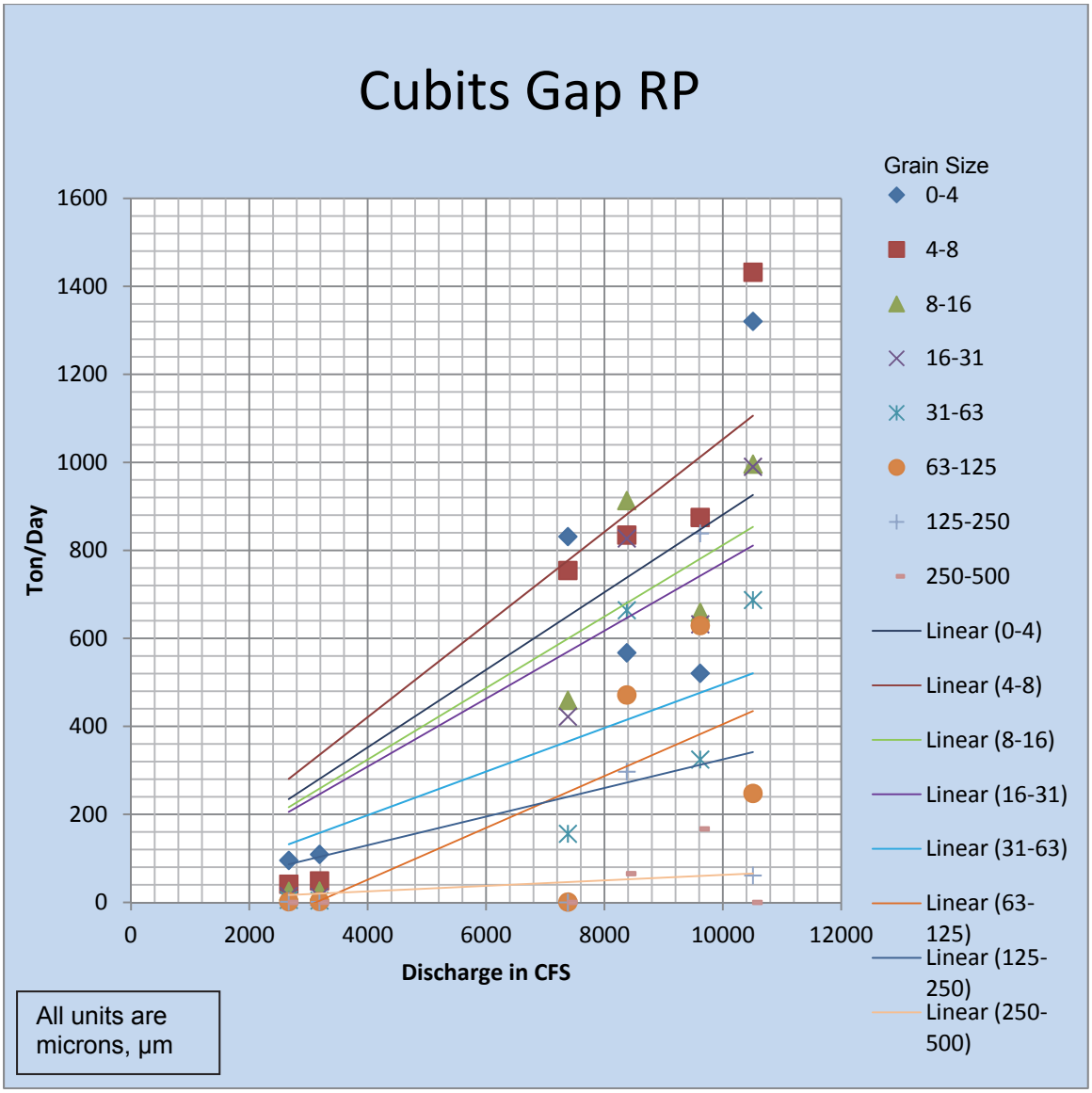

Bed Load Transport Measurements

Two measurement efforts were tried during the study period. During the first attempt the sand waves were not evident in the data so no conclusive results could be drawn. The second effort was attempted during the March 31-April 1 2011 survey period. Computations were completed by the end of July 2011. There were sufficient data within the selection criteria to produce meaningful computations using the ISSDOTV2 method. Figures 2.49-2.51 are for West Bay 'Cubits Gap', called site 7 in this study.

Figure 2.49. Difference Plot of Sand Waves for Site 7 Cubits Gap

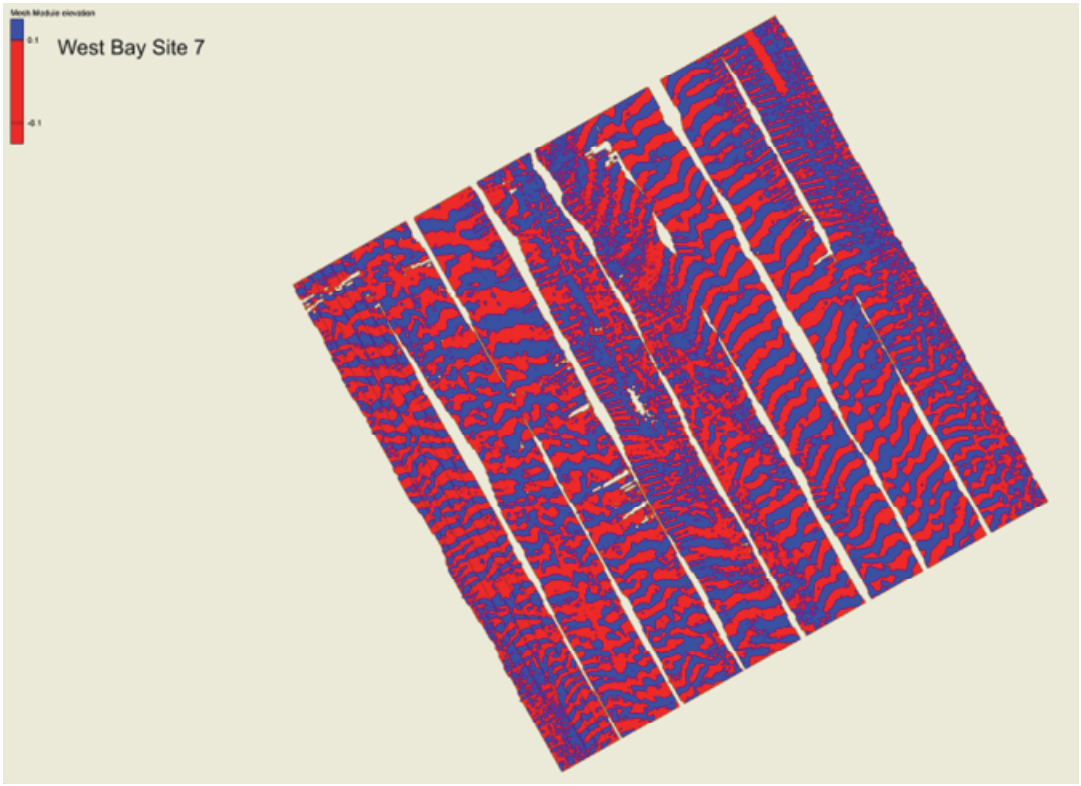

Figure 2.50 Site 7 Cubits Gap XYZ Bed Elevations

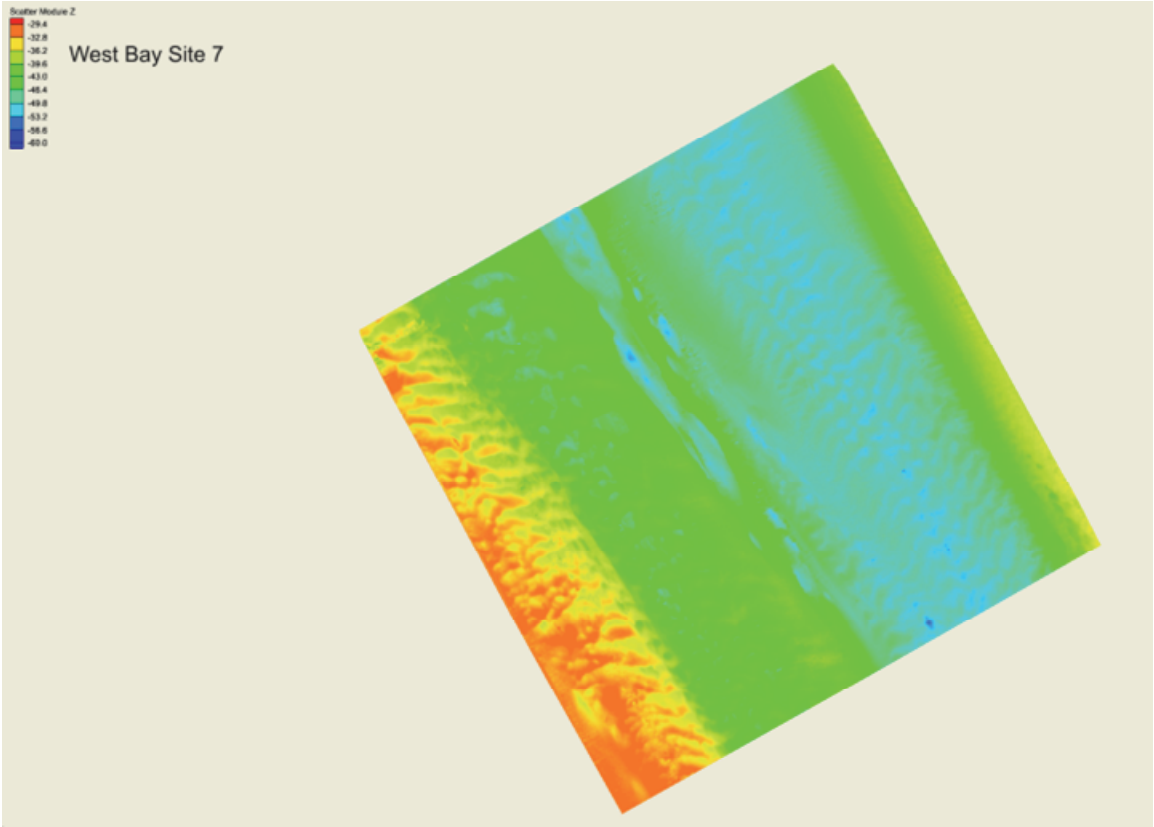

Figure 2.51 Difference Plot of Sand Waves for Site 2 RM 8.5

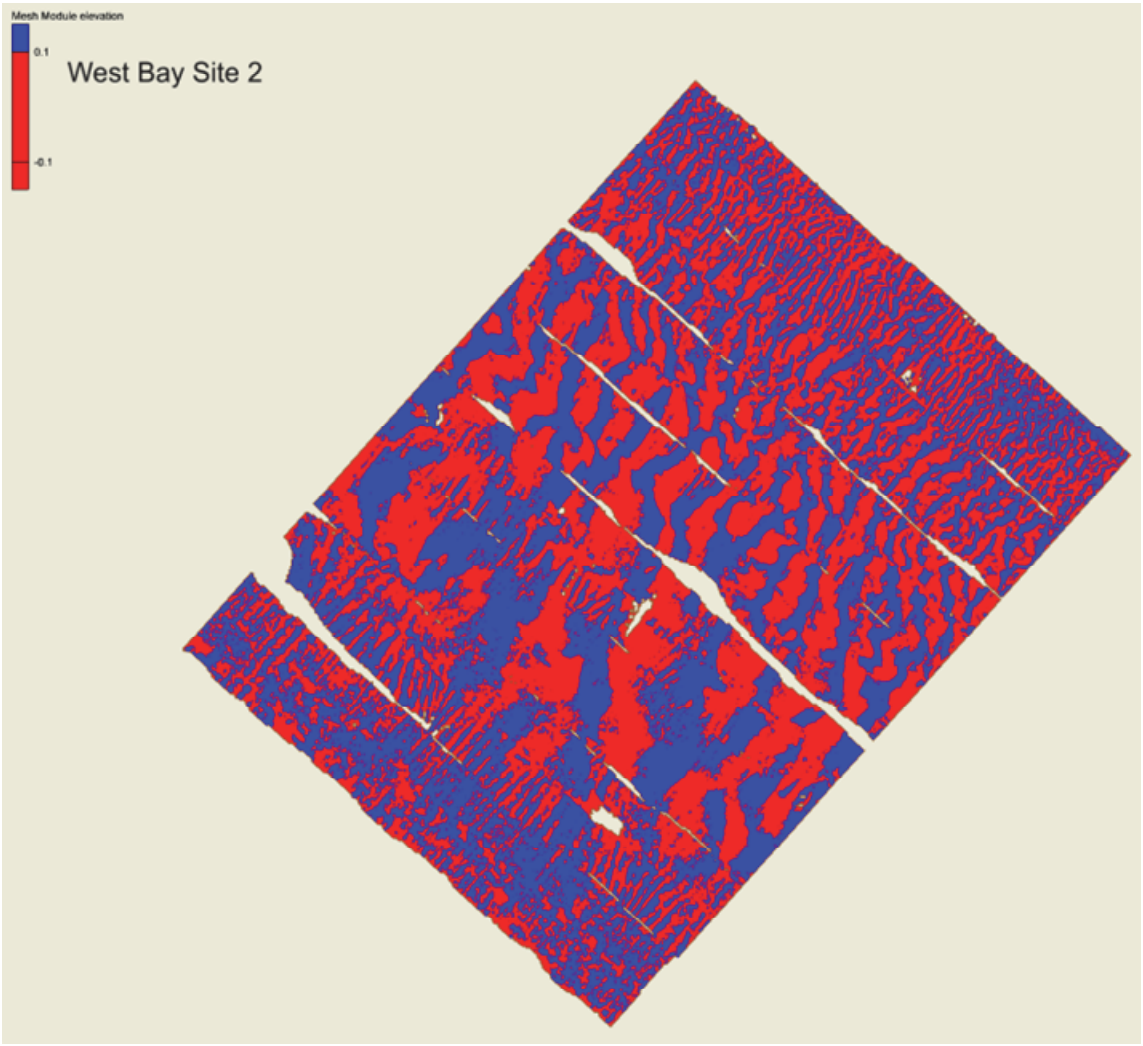

The total width of the measured swaths was 1,988 feet. Using the ISSDOTV2 method bed load was computed as 9,617 tons per day from data collected on 1 Apr 2011 over this section of the river. On a per ft basis, this equates to a rate of about 4.8 tons per day per foot of channel width for the measured section.

Site 2 was upstream from the WBSD approximately RM 8.5. The total width of the measured swaths was 2014 feet. Bed load was computed as 15,121 tons per day from data collected on 31 Mar 2011 over this section of the river. On a per ft basis, this equates of a rate of about 7.5 tons per day per foot of channel width for the measured section. These data show that the region from RM 8.5 to RM 4.0 are net depositional for this particular discharge condition. The suspended flux measurements show a small increase at RM 2.6 so some of the material off the bed is getting back into

suspension. Over an annual basis this will support the building of the point bar as shown through the geomorphic analysis.

Summary and Conclusions

A field data collection program was conducted in the lower Mississippi River from Venice to HOP, in Southwest Pass, in WBSD and in Cubits Gap form March 9, 2009 to April 1, 2011. It produced the following data to improve definition of boundary conditions for 1D and multi-dimensional models, and for calibrating and verifying model results:

1. A bathymetric base map of the Mississippi River channel in the vicinity of the diversion entrance channel and through the diversion entrance channel into West Bay to the extent that water depths in the Bay allow.
2. Current speeds and directions across transects of the Mississippi River in the vicinity of the diversion and across the diversion entrance, as well as acoustic backscatter intensity measurements across the same transects.
3. Suspended sediment concentrations and suspended sediment types (percent sand and fines) at horizontal and vertical sample locations along the ADCP transects.
4. Optical backscatter and salinity measurements along the ADCP transects.
5. Bottom-sediment types and grain-size distributions at selected locations in the Mississippi River and West Bay.

An iterferometric (phase measuring) swath sonar survey conducted prior to the start of the field measurement program produced a bathymetric map determined to be adequate for the purposes of this study. It extends from about 2 miles north of the diversion channel to about 2.25 miles south of the diversion channel, and into West Bay to the extent allowed by the water depths in the Bay.

The diversion channel diverted 8.4 to 9.5 percent of the discharge in the Mississippi River into WBSD. Cubits Gap diverts 13.0-18.7 percent of the discharge in the river for the measurement periods. There are significant vertical current velocities in the diversion channel. An eddy in the discharge was observed in the shallow water on the north side of the diversion channel. The concentration profiles shown in Figure 2.52 show that there is difference of approximately 150mg/l in the maximum concentration from the main river to the West Bay Cut. This observation is for only one event but similar trends exist for different stages of the hydrograph.

Figure 2.52 Concentration profiles for north of the diversion cut RM 5.2 and the diversion cut.

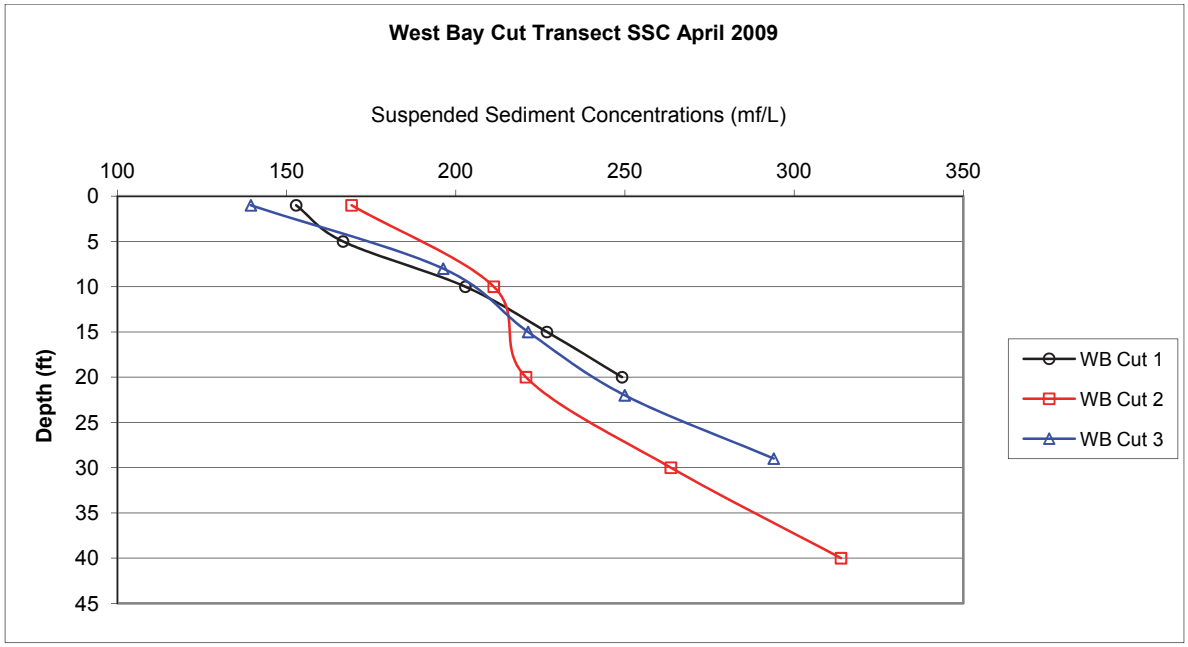

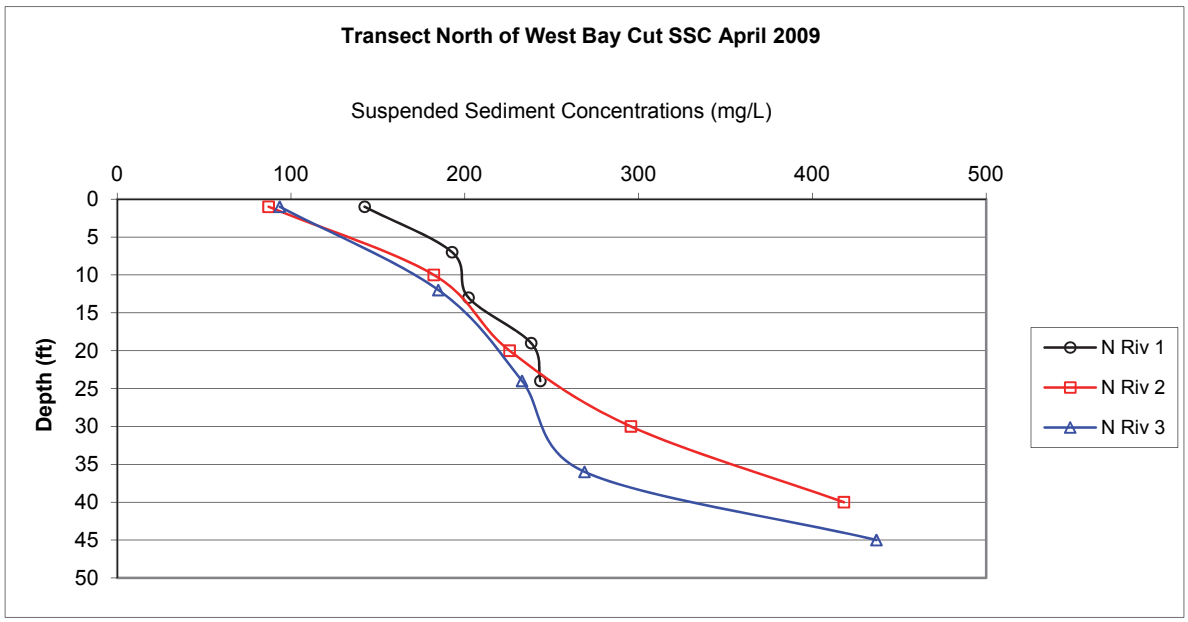

3 Geomorphic Assessment

Purpose

The dominant morphological processes at work in the lower Mississippi River and delta system can operate over very large spatial and temporal scales. There are many factors, both natural and man induced, that can contribute to these processes. The effects of large floods and storms, changing sediment loads and characteristics, channel maintenance activities, dredging practices, diversions (natural and man-made), subsidence, and relative sea level rise are just a few such factors. In terms of temporal scales that are typically associated with river morphology, the diversion at West Bay has been operating for a very short time period. The determination must be made as to what degree the observed shoaling at the PAA is a result of large-scale, long term river adjustments, or a direct result of the impacts of the West Bay diversion. It is therefore important to identify the long term morphological trends that are occurring in this reach of the river and to evaluate the observed shoaling at the PAA with regard to these trends. These morphological trends are determined by means of a geomorphic assessment.

The geomorphic assessment brings together all the known information and data about the river reach, and provides a description and understanding of if/how the lower Mississippi River has changed in a historical perspective. Methods and tools used in the geomorphic assessment include analysis of channel geometry data stage and discharge data, dredging records, sediment data, and natural events and anthropogenic influences. Each section of the geomorphic assessment provides an incremental contribution to the overall understanding of the dominant processes that have shaped and formed the system.

The results of the analyses are integrated with the overall objectives of documenting the historic trends and changes in hydrology, sedimentation, and channel geometry for the lower Mississippi River, summarizing the local changes observed in the Pilottown anchorage since construction of West Bay diversion, and evaluating the impacts of the diversion with regard to the historic trends.

Often times the results of a particular analysis may conflict with the results of other analyses. Therefore, it is important to interpret results of all analyses in an integrated manner in order to achieve the most accurate description of the dominant processes that have influenced channel development in the study area. It is also important to remember that a geometric analysis of this nature focuses on observed data, which gives a description of specific channel conditions representative of a given point in time. Any observed change from one time period to another is a cumulative response resulting from all influencing forces acting on the system during that span of time. Careful engineering judgment must be exercised when attributing an observed system response to a specific cause or event, because the response may be due to multiple factors with varying degrees of influence.

In addition, the geomorphic assessment can provide information of baseline conditions necessary for development, application, and accurate interpretation of numerical model results.

Task Description

The detailed geomorphic assessment was conducted for the lower Mississippi River from Belle Chase (RM 75.0 Above Head of Passes (AHP)) to East Jetty in Southwest Pass (RM 18.5 Below Head of Passes (BHP)). The assessment focused on the time period from 1960 to the present. The specific tasks of the geomorphic assessment include the following:

- Geometric Data Analysis
- Gauge/Discharge/Sediment Data Analysis
- Dredge Records Analysis
- Historic Events Timeline Analysis
- Integration of Results

Geometric Data Analysis

The purpose of the geometric data analysis is to document the changes in channel dimension, pattern and profile of the lower Mississippi River within the study reach. A comprehensive database of channel geometry data were compiled from historic comprehensive hydrographic surveys of the lower Mississippi River as well as channel condition surveys collected by MVN in support of the annual channel maintenance program for the lower Mississippi River. The comprehensive hydrographic surveys

generally provide full coverage of the study area, whereas the channel condition surveys generally cover from the upper limit of the PAA to East Jetty in Southwest Pass. These surveys will be the basis of the geometric data analysis for the Mississippi River channel, with emphasis on the vicinity of WBSD and the PAA.

The types of analyses conducted as part of the geometric data analysis were as follows:

- Cross-section comparisons. Channel cross sections were compared at selected locations for sequential hydrographic surveys to determine scour and shoaling trends. These comparisons include a qualitative evaluation along the full extent of the cross section for all cross section locations in the study area, and a quantitative evaluation of a 250 foot section westward of the PAA line for cross sections located within the anchorage area limits. Locations of the selected cross sections are presented in a later section that presents the procedures and results of the geometric data analysis in detail.
- Volumetric computations. The study area was partitioned into reaches, and each reach was defined by a specific area over which volumetric changes between sequential hydrographic surveys were computed. These reach areas vary in length, with the more detailed reaches located within the PAA. Average bed elevation changes were computed for each reach from the computed volumetric changes and the surface area of each reach. Details of the reach locations are presented later in the geometric data analysis section.
- Channel pattern analysis. Contours of the -40 and -30 foot North American Vertical Datum 1988 (NAVD88) channel bed elevations were computed for each hydrographic survey and used to determine changes in channel location with time. Colored contour maps of each survey were developed and used to qualitatively assess changes in the location of the deep water channel with time.

Gauge/Discharge/Sediment Data Analysis

The purpose of the gauge, discharge and sediment data analysis is to evaluate existing data to determine how the distribution of discharge in the diversions within the study area has changed over time, and how these trends have impacted the morphology of the lower Mississippi River. Historic discharge data published by MVN and non-published post-construction data at the WBSD collected by MVN were obtained to form a

discharge database for this analysis. Discharge data were collected for Baptiste Collette, Grand Pass, West Bay diversion, Cubits Gap, Southwest Pass, South Pass, and Pass a Loutre. In addition, discharge data were collected for Tarbert Landing and Venice on the Mississippi River. Sediment data obtained include bed material and suspended sediment data at Tarbert Landing and Belle Chase on the Mississippi River. Suspended sediment data were collected as part of this overall study at WBSD and other distributaries in the vicinity. However, there are no earlier data for determining historic trends in sediment transport in the diversions. The data collected for this study were used primarily for the numerical model investigations.

Dredge Record Analysis

Dredge records were obtained from MVN and analyzed to determine trends in dredging requirements in the lower Mississippi River and Southwest Pass. Total dredge volumes were available by year, and are representative of the total dredging requirements for the reach from Venice, LA to the outlet of Southwest Pass. Daily dredge records for each dredge contract could not be obtained; therefore no information on the location, amount and time of specific dredge quantities could be determined. In addition to the dredge records, grain size analyses of dredge material grab samples were available for many of the dredge contracts.

Historic Events Timeline Analysis

A tabulation of historic events pertaining to the lower Mississippi River was compiled by MVN and provided as part of the geomorphic assessment. The document provided information on river engineering activities that have occurred in the study area since 1960, including changes to navigation channel maintenance, enlargement of passes and diversion construction. This information, along with information on significant flood and storm events, was used to improve the interpretation of results of the other analyses and to gain a better understanding of the geomorphology of the lower Mississippi River.

Integration of Results

This task integrated the results from all of the analyses conducted as part of the geomorphic assessment, and was the basis for formulating study conclusions. The results from each analysis were evaluated with respect to the results of the other analyses to establish the trends in river morphology

and sedimentation from a historic perspective as well as for the post-West Bay construction time period. The integrated results were evaluated to determine if observed shoaling trends in the PAA were within the influence of large-scale, long term morphological changes occurring within the study reach, or a specific result of the impact of West Bay diversion. It should be noted that conflicting results are a possibility; therefore, all results are evaluated in an integrated manner to arrive at the most accurate and complete assessment.

Review and Discussion of Data

The analyses of the geomorphic assessment were conducted with historic data from the study area, and the accuracy and value of the results is largely dependent on the quality and availability of the data. Data obtained for this geomorphic assessment include comprehensive hydrographic surveys encompassing the entire study area, channel condition surveys covering the reach from Venice downstream to East Jetty, discharge measurements for the main river and the passes, dredge records and dredge material grab sample gradations, and suspended and bed material sediment data. Due to the breadth of the study time period (approximately 50 years), the format of the data ranges from hard copy maps and published data tables to digital maps and XYZ data sets. All data were evaluated for quality assurance, and obvious errors were corrected when sufficient justification existed.

Comprehensive Hydrographic Surveys

Comprehensive hydrographic surveys of the Mississippi River have been collected by MVN, approximately one survey per decade. The surveys cover the Mississippi River for the entire MVN district area from Black Hawk, LA to HOP, and include survey data for Southwest Pass, South Pass and Pass a Loutre. The surveys generally cover from waters edge to waters edge, and are collected along survey ranges at approximately two-tenths of a mile interval. Bathymetry data were expressed as elevation relative to a specified vertical datum.

The 5 comprehensive surveys used in the geomorphic assessment were 1961-1963, 1973-1975, 1983-1985, 1991-1992 and 2003-2004. It should be noted that each survey period spans several years, and the survey data may have been collected at any point within that time span.

The data for the comprehensive surveys were obtained from MVN. The data for all surveys except the 2003-2004 survey were provided in DGN files, and the 2003-2004 survey was provided in XYZ digital format. All survey data were brought into a GIS database and a triangulated irregular network (TIN) was developed for each survey. Typically, TINs are best developed from data points that were uniformly distributed over the area. In the case of the comprehensive surveys, the data exist in a straight line along each survey transect. This is less than ideal for TIN development; however, the survey ranges were close enough together that the TIN surface was considered satisfactory for all areas except the extreme edges of the survey. Contours were developed from each TIN and were compared to the contours on the hard copy maps of the survey. Data value errors were quickly identified based on obvious contour disagreement, and corrections to the survey data were made based on the published hard copy map values.

Channel Condition Surveys

Channel condition surveys are collected by MVN on a regular basis for the area from Venice to East Jetty. These surveys are collected to evaluate the condition of the navigation channel and to determine maintenance dredging requirements. For the geomorphic assessment an annual channel condition survey was selected for October of each year from 1990 to 2001, and quarterly channel condition surveys were selected from 2001 to 2008. The October period was selected because it corresponds to the start of a water year, and conditions are generally representative of a complete annual hydrologic cycle. The more frequent quarterly surveys were selected beginning in 2001 to provide more detail in the time period prior to and subsequent to construction of the West Bay Diversion. The spatial coverage of the channel condition surveys varies, and the surveys that provided the broadest coverage were selected. In addition, the upstream extent of the channel condition survey coverage is variable from survey to survey, ranging typically from the upstream limit of the PAA to near Venice. These surveys were provided by MVN in DGN files and XYZ format. The survey data were brought into the GIS database, TINs were developed, contoured, and checked for errors. In addition to these surveys, post-flood surveys for the 1997 and 2008 floods were also obtained, as well as pre-storm and post-storm surveys for Hurricane Katrina in 2005.

Horizontal and Vertical Datum

The horizontal datum for the comprehensive surveys is NAD27 and NAD83, and the vertical datum includes Mean Sea Level Datum, NGVD29 and NAVD88. For the channel condition surveys, the horizontal datum is NAD83 and the vertical datum is Mean Low Gulf (MLG). In order to compare data from surveys of different datum, all survey data were projected to the NAD83 horizontal datum. The State Plane Coordinate System for the survey data were Louisiana South.

Vertical control in the study area is a very complex issue due to such factors as subsidence and sea level rise. Complicating the matter is the fact that 3 different vertical datum are present in the survey data. Considering the significant time span of the survey data used in this study, it is expected that vertical controls and gauges in the area have most likely been adjusted several times. In the case of the comprehensive survey data, the gauges used to reduce the raw survey data were not known, and temporal adjustment of the data were not attempted. The channel condition surveys are tied to known gauges, and the vertical consistency for these surveys is believed to be reasonable. A 2002 survey of various monuments in the Mississippi River delta area was provided by MVN. This survey provided elevation references in NGVD29, NAVD88 and MLG for the tidal benchmark at Venice (087 0849A). These elevations were used to determine a relationship between the vertical datum, and corrections were applied to correct all survey elevations where required to NAVD88. The corrections to convert NGVD29 and MLG to NAVD88 were -1.19 feet and -1.90 feet, respectively.

Survey Data Uncertainty

Hydrographic survey data collected over a time span of over 40 years and referenced to multiple datum are likely subject to potential error and uncertainty, originating from both equipment accuracy and collection methodology. The hydrographic surveys conducted in the early years of the study period were taken with single beam fathometers and without GPS position control, whereas the more recent surveys, although still collected with a single beam fathometer, utilize GPS positioning for more horizontal accuracy. Single beam fathometers typically have accuracy within 0.5 feet for depths encountered within the study area. In addition, the earlier survey data points were digitized from hard copy maps, thus potentially introducing digitizing and data entry error in both horizontal position and elevation. Also, the vertical datum correction relationship

used to convert survey data to NAVD88 was determined from a single tidal bench mark, and may not be representative of the entire study area. All data were carefully checked to ensure their accuracy and viability for use in this study. Regardless, it is understood that potential inaccuracies and uncertainty are still present within the data set. This uncertainty is likely more prevalent in the earlier comprehensive hydrographic surveys of the 1960s through 1980s. Data from the channel condition surveys, being more recently collected with more modern equipment and referenced to a single horizontal and vertical datum, should contain less uncertainty and error in comparison. Although no formal attempt was made to quantify the uncertainty of the hydrographic survey data, the vertically adjusted data were thought to be within +/- 1 foot and are sufficient for the types of trend analyses conducted as part of the geomorphic assessment.

Discharge Measurements

Discharge measurements collected at irregular time intervals by MVN and published annually in the *Stages and Discharges of the Mississippi River and Tributaries in the New Orleans District* from 1960 until 1998 were obtained for use in this study. Discharge measurements were obtained for the main river as well as all distributaries within the study reach, although yearly data were not always available. Additional data were obtained from MVN that included substantial measurements collected since the construction of the WBSD for purposes of monitoring the development of the diversion. Discharge measurements made prior to approximately 1995 were conducted using a current meter for point velocities along verticals. More recent discharge measurements were collected using acoustic doppler current profiler (ADCP) technology.

Geometric Data Analysis and Results

The geometric data analyses were conducted with the comprehensive and channel condition hydrographic survey data adjusted to horizontal NAD83 State Plane Louisiana South and vertical NAVD88. All computations and results presented are in English units unless specifically stated otherwise.

Cross-section Analysis. The cross section analysis was conducted with two areas of focus; 1) a broad focus of the entire study reach using the comprehensive surveys and the annual (October) channel condition surveys, and 2) a detailed focus of the PAA using the quarterly channel condition surveys from 2001 to 2008. The locations of the cross sections used in the broad

focus analysis are shown in Figures 3.1 through 3.4, and the locations of the cross sections used in the detailed focus analysis are shown in Figure 3.5. All cross sections are orientated from left to right looking downstream. The cross sections were generated in the GIS system and used to extract the bathymetry data for each hydrographic survey. It should be noted that cross sections RM 75.0 AHP to RM 15.0 AHP are available only for the comprehensive hydrographic surveys, since the channel condition surveys do not cover that area. The extracted bathymetric data for all surveys available at each cross section were plotted for comparison and to determine any trends in channel dimension change.

The comparison plots of the broad focus analysis for cross sections RM 75.0 AHP through RM 12.8 AHP indicate variability across the channel, both at the thalweg and along the point bar, of sometimes 5 to 10 feet, but channel shape in general is fairly consistent. For example, Figure 3.6 shows the cross section comparisons for RM 75.0 AHP, which is at the upstream limit of the study area near Belle Chasse. There is variability in the elevation of the thalweg channel over the survey period of approximately 8 feet and a deepening of the upper half of the point bar on the right side of the channel of approximately 15 feet.

The deepening of the thalweg channel seems to occur over the 1970s and 1980s surveys which cover a time period of generally higher discharge on the river (floods of 1973, 1975, 1979, and 1983), but depths recover such that the more recent channel of 2003-2004 is little different than the 1961-1963 channel. The same pattern can be seen on the point bar side of the channel, but the channel remains overall deeper in this area. The same trend is observed for RM 69.0 AHP.

The comparison plot for RM 64.0 AHP shown in Figure 3.7 indicates a case where a change in cross section shape occurs. In general, the thalweg channel deepens over time, the lower portion of the point bar becomes shallow over time, and the upper portion of the point bar deepens over time. The thalweg channel deepens after the 1960s survey, most likely in response to construction of the Belair revetment subsequent to that survey.

Figure 3.8 indicates an example of significant shift in the channel dimension as observed at RM 43.8 AHP. This plot shows a significant shift of the channel towards the right descending bank, along with significant filling

Figure 3.1. Cross section locations for broad focus analysis, RM 75.0 AHP to RM 28.0 AHP.

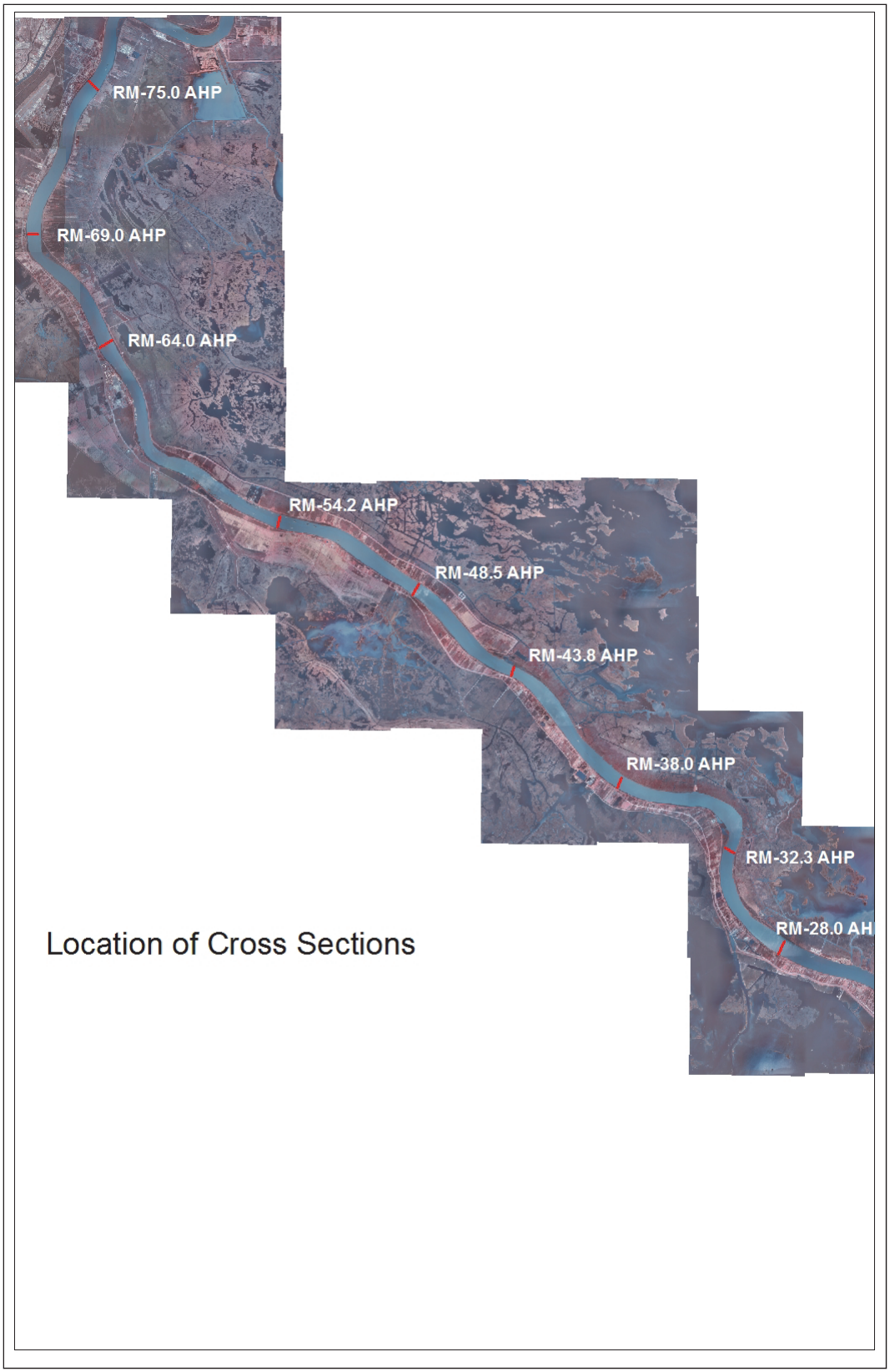

Figure 3.2. Cross section locations for broad focus analysis, RM 28.0 AHP to RM 8.3 AHP.

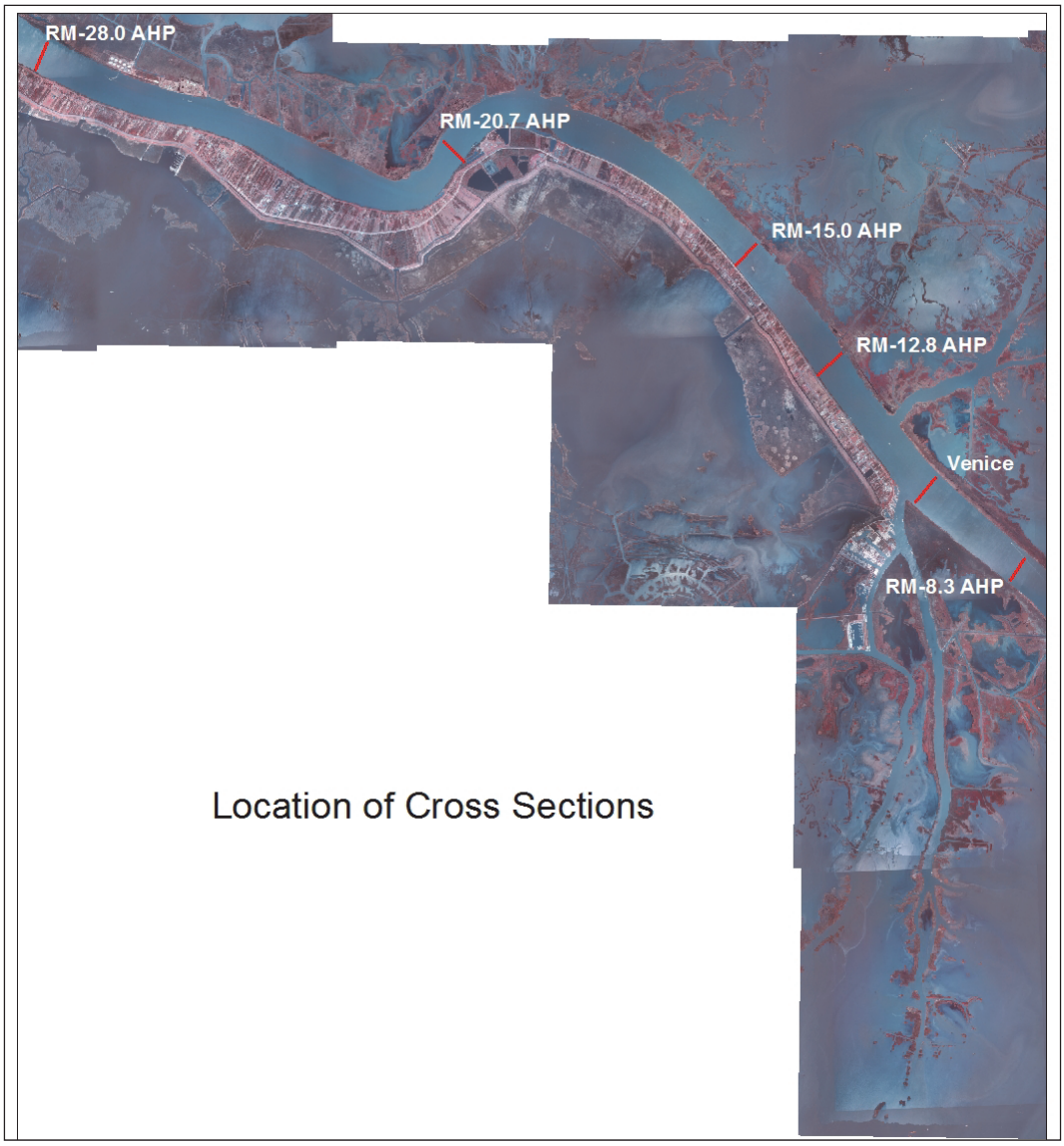

along the point bar area on the left side of the channel. The high degree of variability in this comparison suggested potential data inaccuracy. However, inspection of the hard copy maps of the surveys revealed that this section is at the location of the Point Michael revetment, and prior to the construction of the revetment approximately 200-300 feet of foreshore was present along the right descending bank. Through erosion of this foreshore, the channel shifted toward the right bank until the revetment was constructed. As the channel shifted to the right the point bar along the left side of the channel responded by filling. Note that there is a slight overall reduction in thalweg depth over the survey time period.

Figure 3.3. Cross section locations for broad focus analysis, RM 8.3 AHP to RM 12.5 BHP.

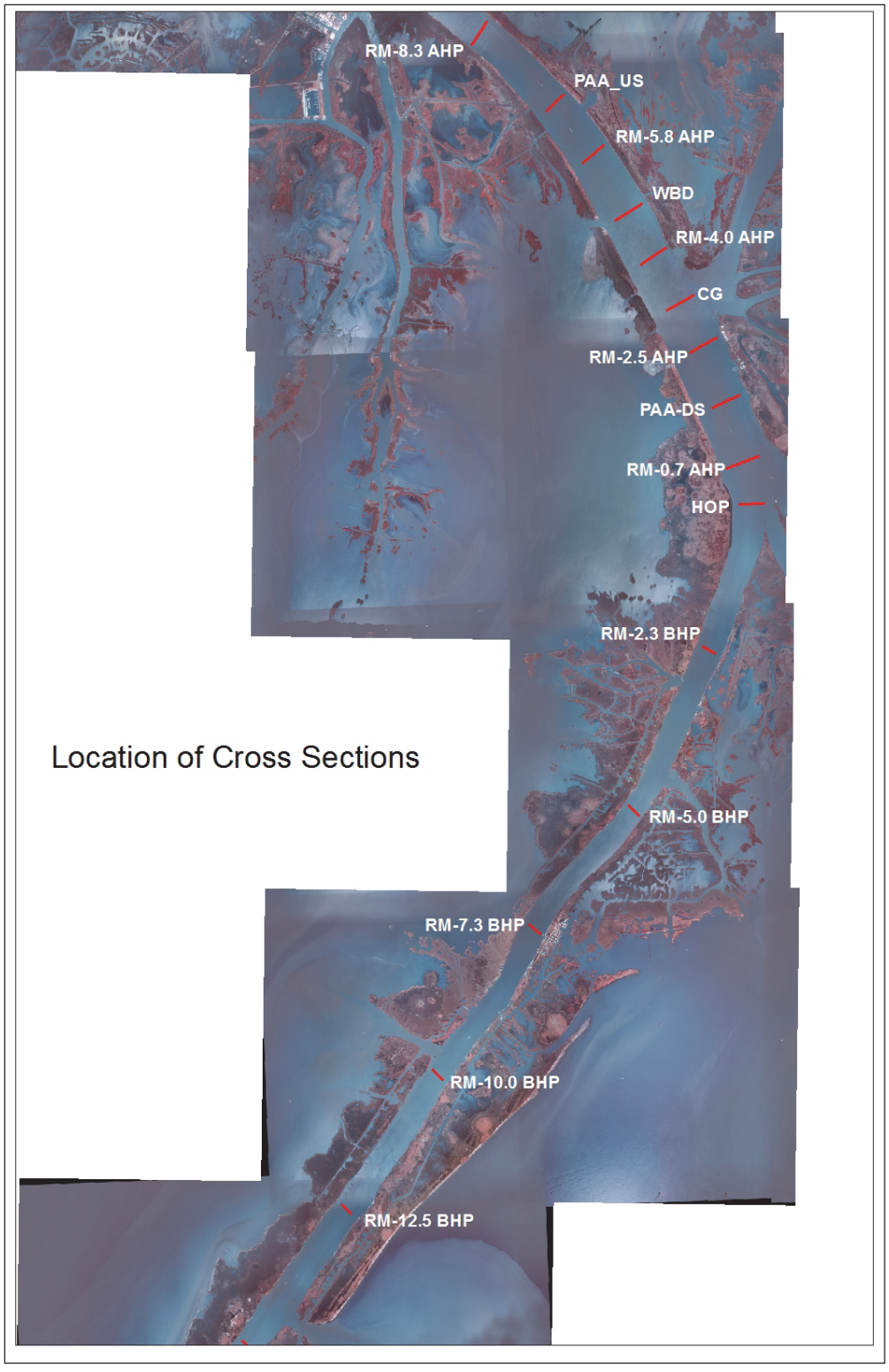

Figure 3.4. Cross section locations for broad focus analysis, RM 12.5 BHP to RM 18.6 BHP.

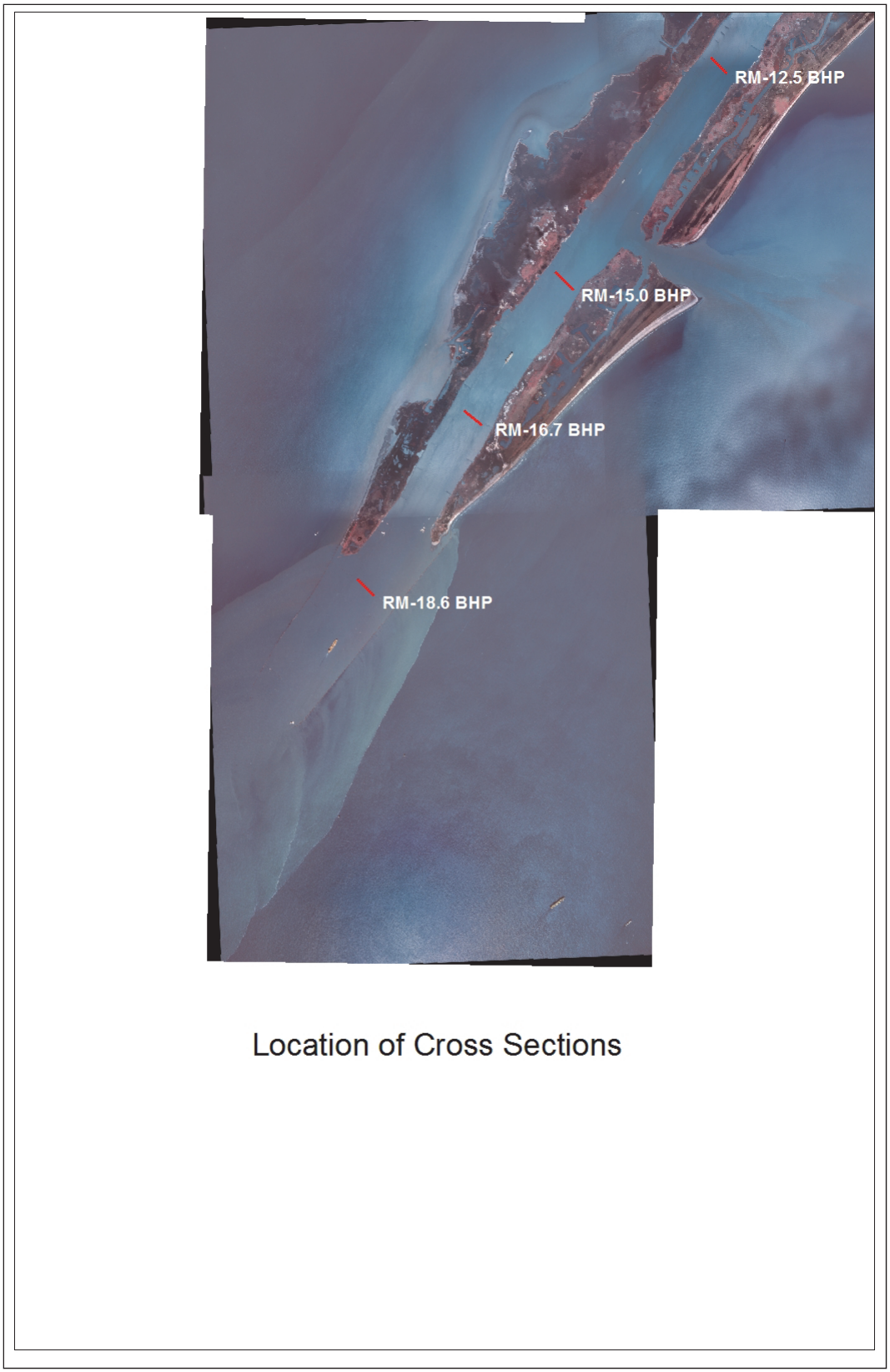

Figure 3.5. Cross section locations for detailed focus analysis, PAA.

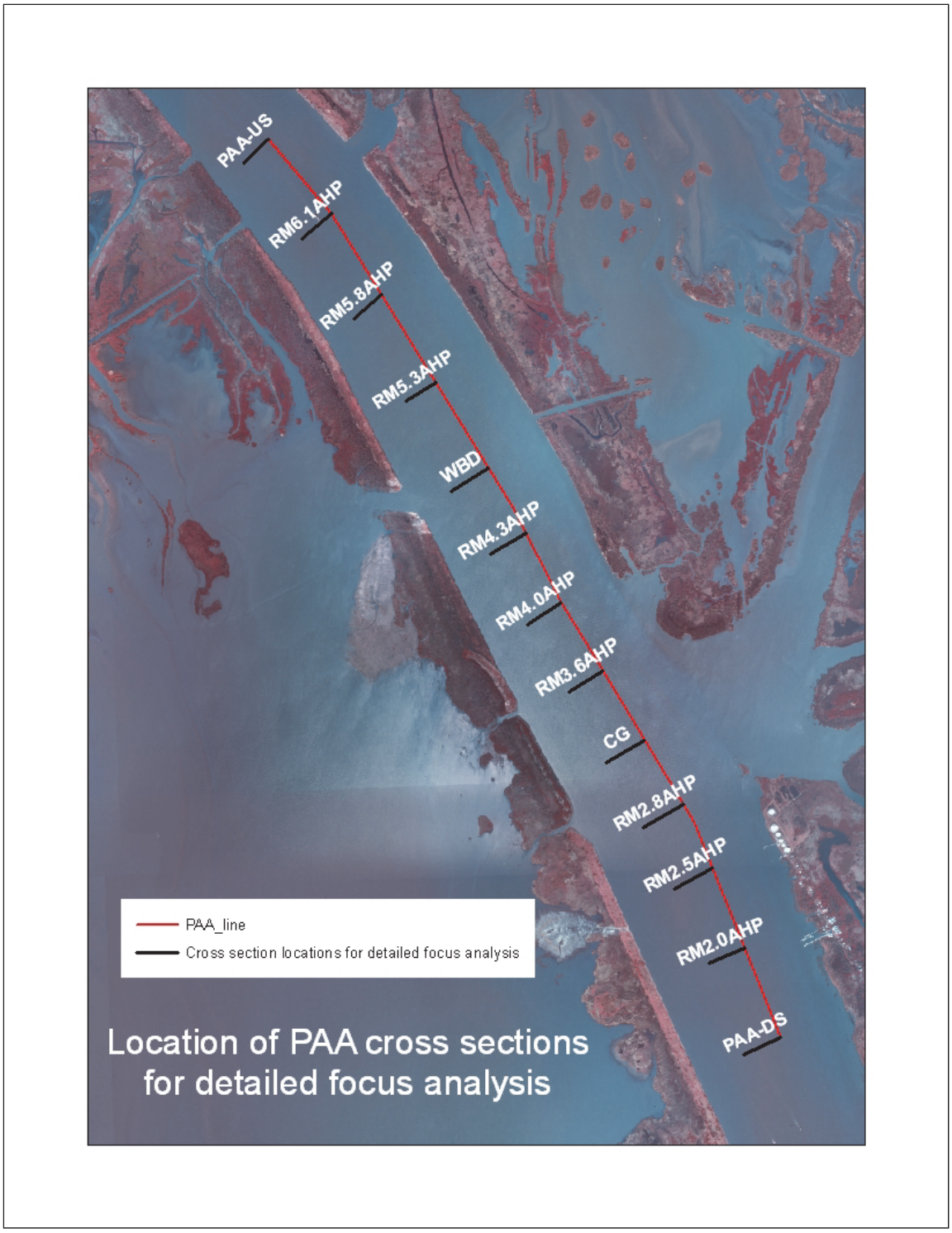

Figure 3.6. Cross-section comparison plot for RM 75.0 AHP.

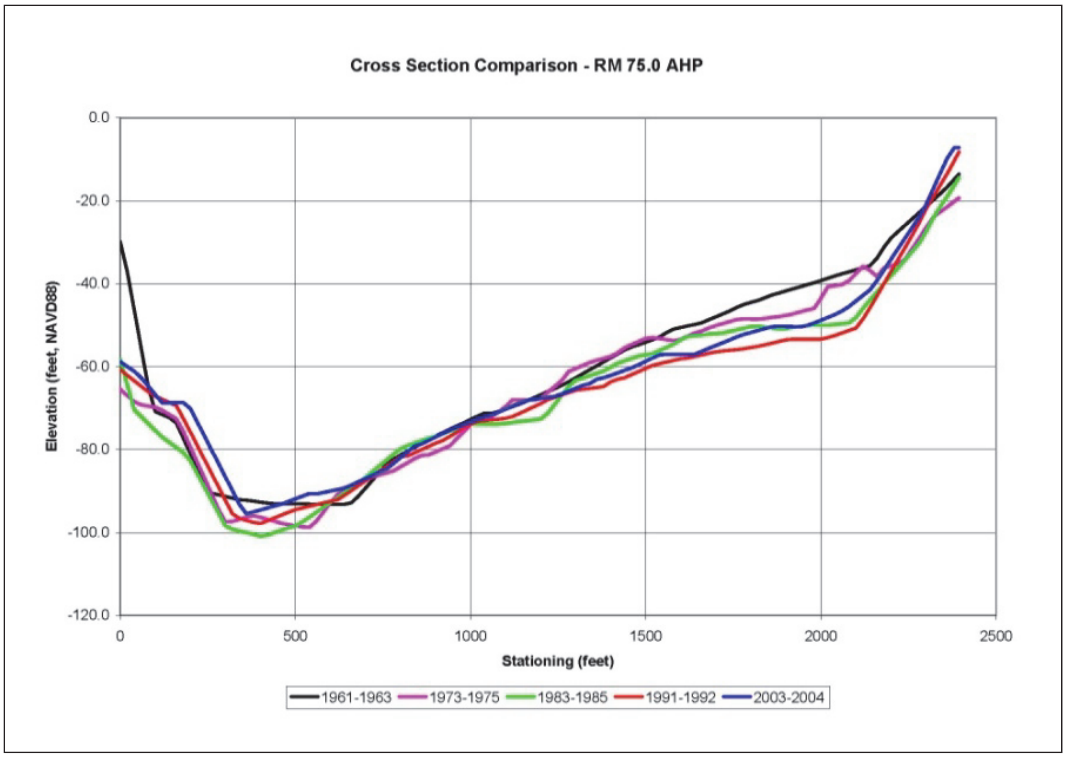

Figure 3.7. Cross-section comparison for RM 64.0 AHP.

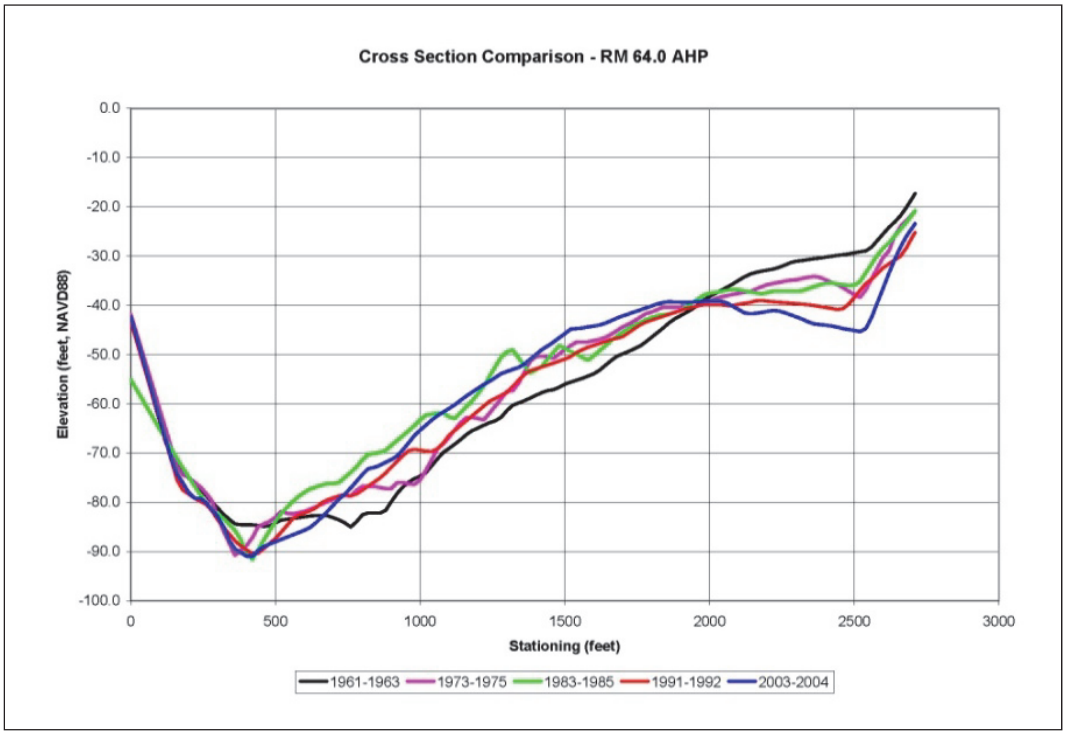

Figure 3.8. Cross-section comparison for RM 43.8 AHP.

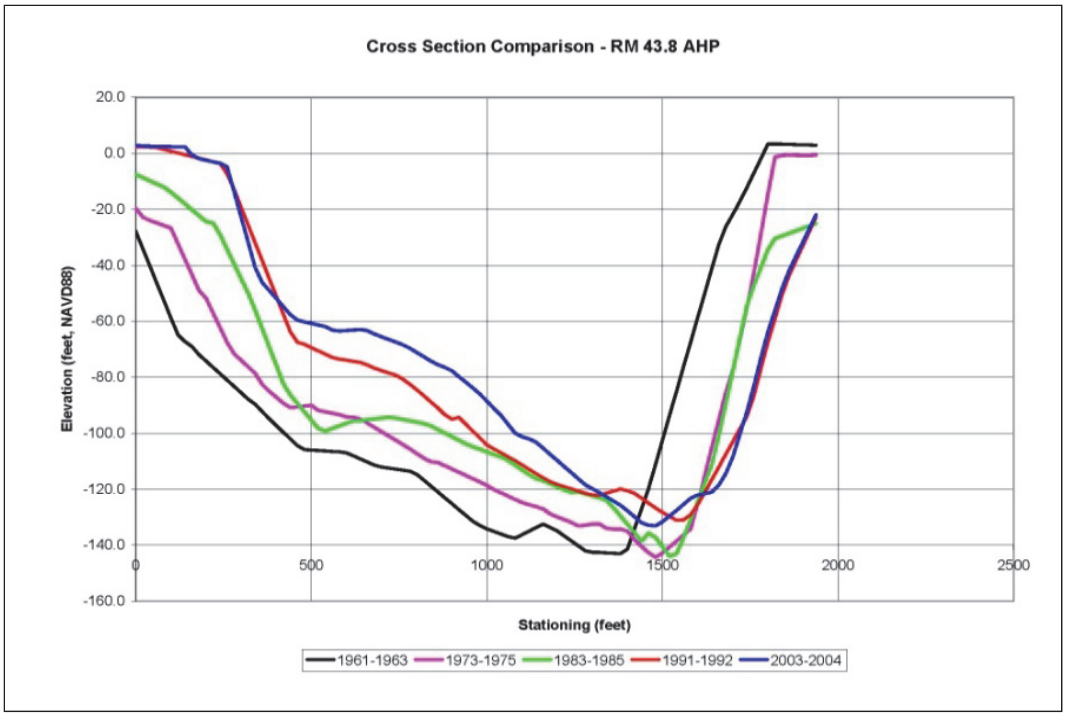

Cross section comparisons at RM 28.0 AHP through RM 12.8 AHP indicate a general deepening of the thalweg channel occurred after the 1960s survey. However, for all the other surveys there is a noted consistency and very little observed changes or trends between successive surveys. Outside of the 1960s survey, there has been little appreciable change from the 1970s to the present. Figure 3.9 shows the cross section comparison for RM 12.8 AHP, which is located in a crossing just upstream of Baptiste Collette. This section also contained data from a few channel conditions surveys which extended that far upstream. Overall, the channel has deepened from the 1960s through the 1980s, but depths were generally reduced in subsequent surveys.

Analysis of the cross sections from RM 75.0 AHP to RM 12.8 AHP reveals that the general trend in channel dimension has been a slight deepening to no significant change in the depth of the thalweg channel. Changes in channel shape due to point bar shifting and possible response to revetment construction were noted, but overall the shape of the channel cross section has been fairly consistent.

However, the trend observed from RM 75.0 AHP to RM 12.8 AHP changes from Venice downstream to approximately Cubits Gap, shifting to a trend where the depth of the Mississippi River channel has decreased over the

Figure 3.9. Cross-section comparison for RM 12.8 AHP, just upstream of Baptiste Collette.

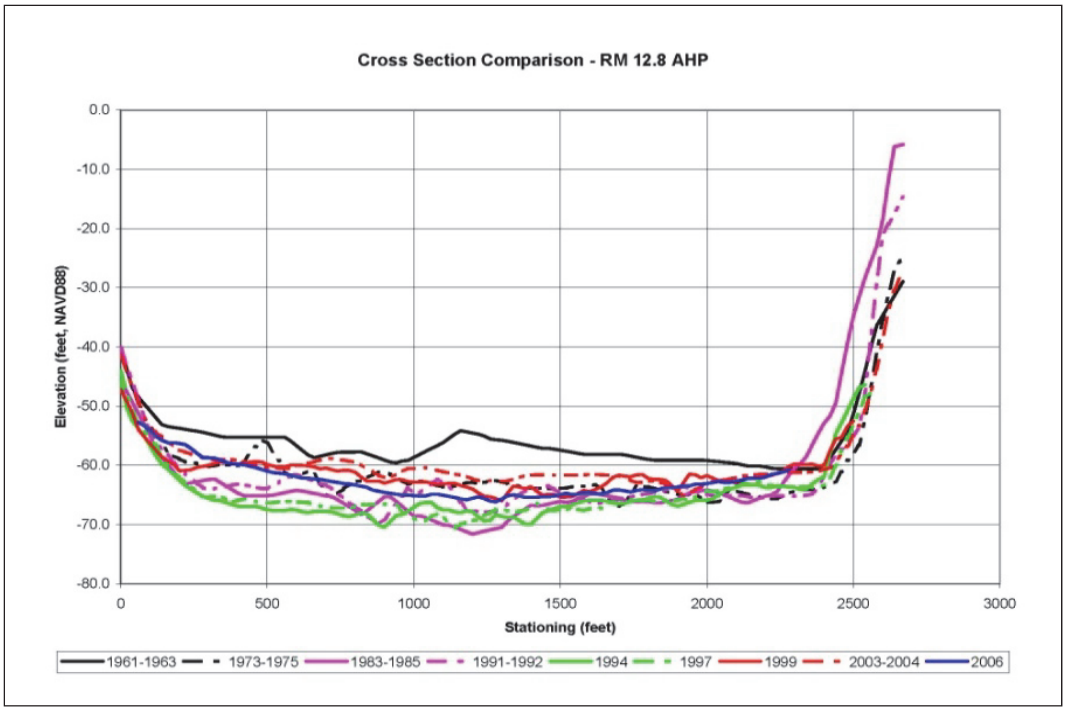

study time period. Figure 3.10 illustrates the observed changes in channel dimension for the cross section at Venice, which is just downstream from Grand Pass. There is a dual shift observed here, with a general decrease in thalweg depth and a shift in thalweg location toward the right descending bank (toward Grand Pass). The overall decrease in depth is approximately 18-20 feet, and the shift in channel location is approximately 500 feet toward the right descending bank. These changes result in a channel with a more uniform depth and shape. The thalweg channel location and depth for the 1961-1963 and 1973-1975 surveys is fairly consistent, and the shift begins prior to the 1980s survey.

Cross-section comparisons for RM 8.3 AHP to RM 5.8 HP indicate a general decrease in thalweg channel depth of 15 to 20 feet over the time range of the surveys. A slight shift in thalweg channel location can also be detected, as illustrated in Figure 3.11 for the cross section at the upstream limit of the anchorage area. The cross section comparison shows that in addition to the decrease in depth there has been a slight shift in thalweg location of approximately 400-500 feet toward the right descending bank. This occurs in an area where the river channel is crossing from the right descending bank below Venice to the left bank upstream of Cubits Gap. It can be seen that the thalweg channel for current conditions is actually located within the upstream portion of the anchorage area. A similar trend is observed for RM

Figure 3.10. Cross-section comparison at Venice, just downstream of Grand Pass.

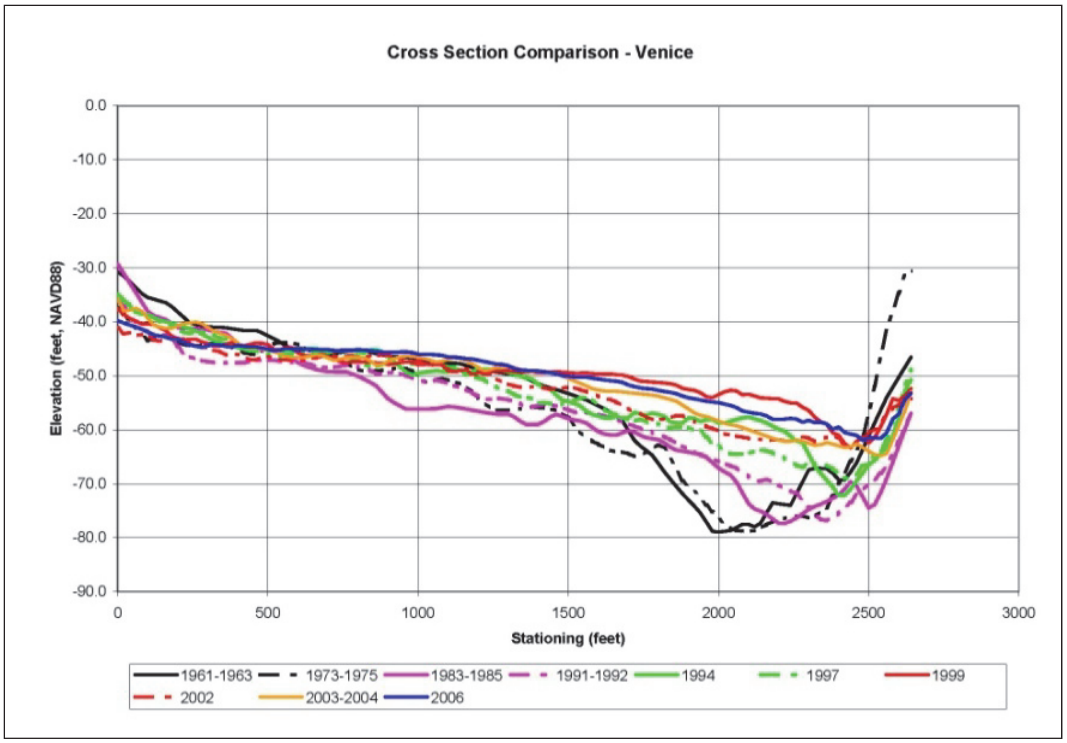

Figure 3.11. Cross-section comparison for cross section located at the upstream limit of the PAA.

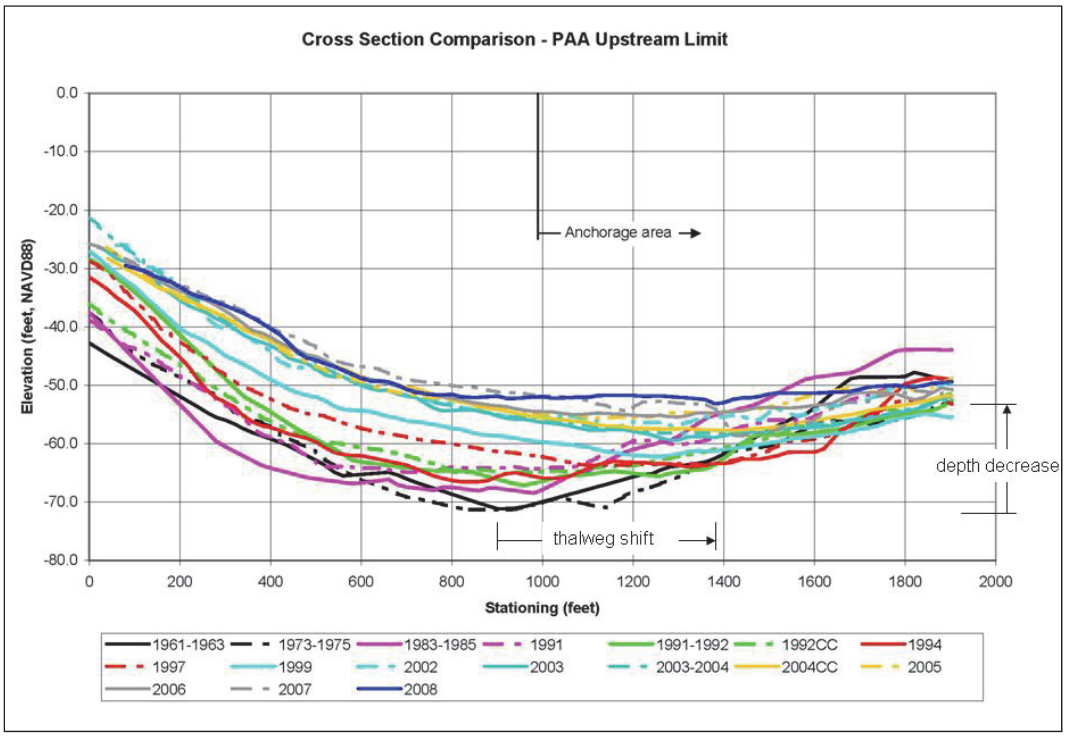

5.8 AHP. Note that the location of the PAA line between the anchorage and the navigation channel is shown on this and all plots for cross sections located within the anchorage area. This line was determined from MVN plan drawings for the current PAA dredging contract which indicated the horizontal coordinates of the line. The coordinates were entered into the GIS system, and the intersections of the anchorage area line and the cross sections were determined.

The cross section comparison shown in Figure 3.12 for the section located at West Bay Diversion (WBD) shows that a deeper thalweg channel existed along the left descending bank in the 1960s survey timeframe, and the elevation on the lateral bar along the right descending bank was actually as high or higher than current elevations. The cross section from the 1970s survey indicates that the channel had changed significantly, most likely in response to the 1973 flood. The deep portion of the channel had filled, and the lateral bar slope had been degraded by approximately 10 feet. Since the 1970s survey time there has been a general decrease in thalweg channel depth of approximately 20 feet and a filling along the lateral bar area of 10 to 15 feet. A similar pattern is observed at RM 4.0 AHP.

Figure 3.12. Cross-section comparison for section located at West Bay Diversion.

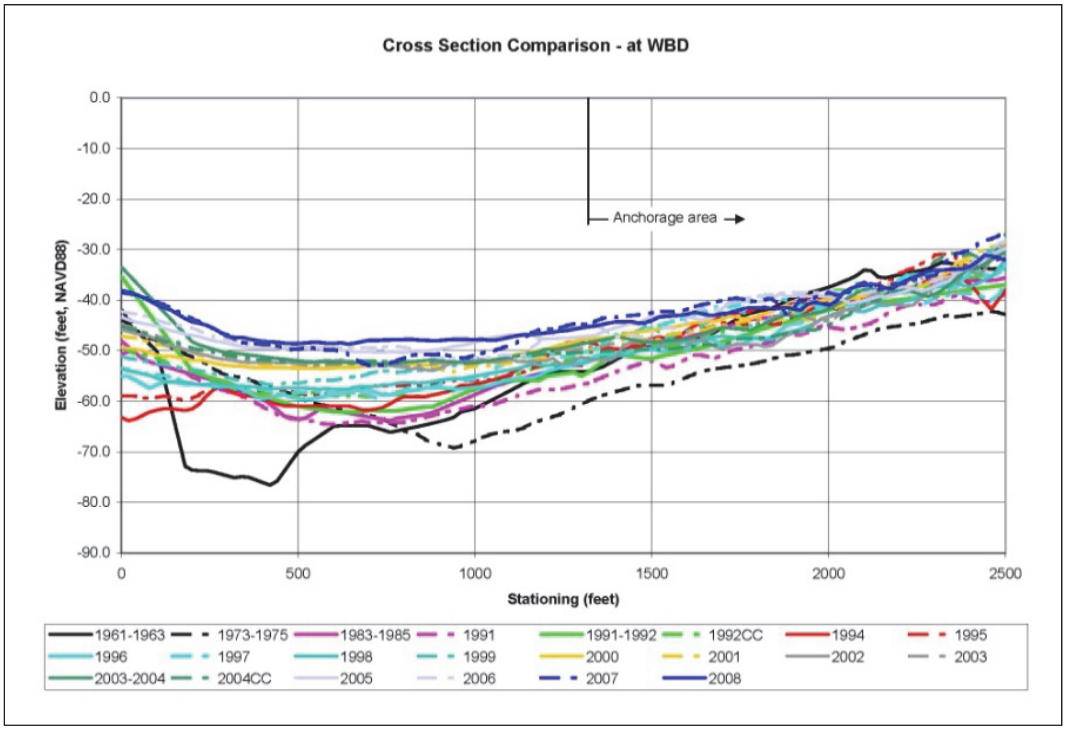

Beginning at the cross section located at Cubits Gap, a channel that is significantly influenced by dredging for navigation can be seen. Figure 3.13 illustrates the information for the cross section located at Cubits Gap. Observed change between the 1960s survey and the 1970s survey once again indicates scour along the right side of the channel within the anchorage area of 5 to 8 feet, resulting in a channel that has significantly more depth than for current conditions. The 1970s survey indicates a more uniform depth across the section. This was also true for the 1980s survey, which indicated significant filling in the thalweg channel to approximately elevation -44 feet NAVD88. At first this was believed to be erroneous data; however, examination of the hard copy survey maps revealed that the data were accurate. Maintenance of the navigation channel to -45 feet MLG began in the late 1980s. All surveys subsequent to that time indicate that the channel dimension and shape is shifting from a fairly uniform depth to more of a bendway-type section with an entrenched channel along the left descending bank and a developing lateral bar along the right side of the channel.

Figure 3.13. Cross-section comparison for section located at Cubits Gap.

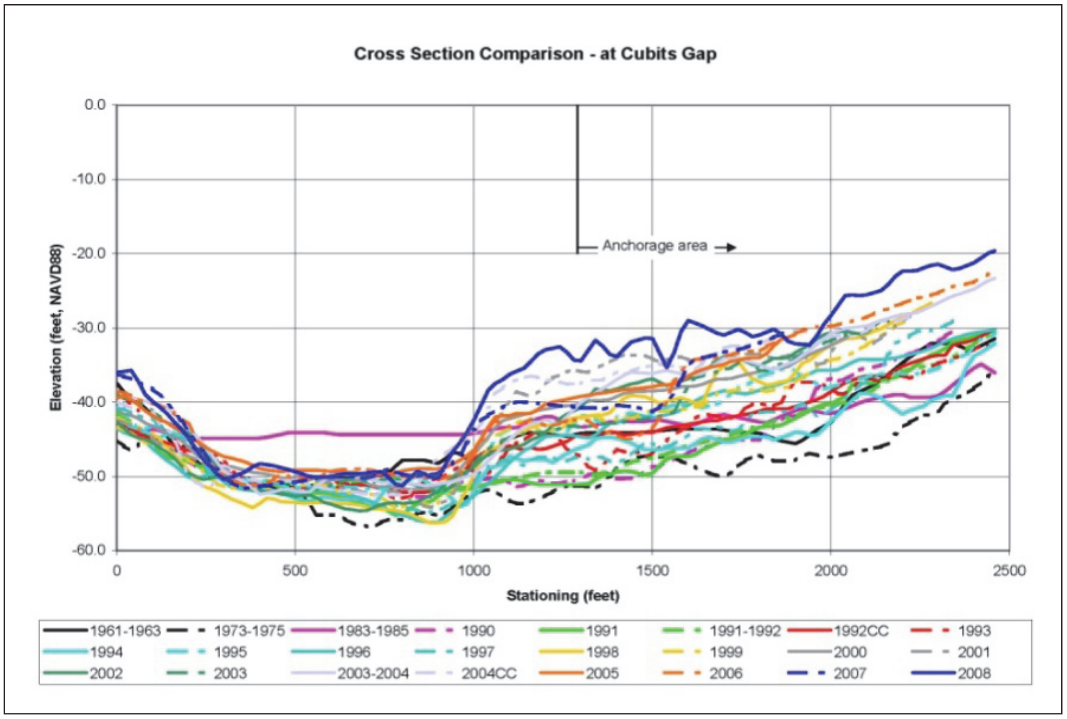

The plot indicates there is fluctuation in the riverbed elevation within the anchorage area, but that the trend has been a decrease in depth for the period prior to and after WBSD construction. As much as 12 to 15 feet of filling occurred in the anchorage area from the 1970s survey to the time of diversion construction. Since the time of construction, as much as 10 feet of

filling has occurred. The thalweg channel is obviously strongly influenced by dredging, and depths tend to fluctuate within a 5 foot range. No real trends can be determined within the thalweg portion of the channel.

Figure 3.14, which shows the cross-section comparisons for RM 2.5 AHP, illustrates the degree of channel change that has occurred at this location during the study time period. In fact, the 1960s survey shows that the thalweg of the channel was actually westward of the anchorage area line, and depths were uniform across the section for the 1970s and 1980s surveys. From the 1960s survey until the construction of WBSD approximately 12 to 15 feet of deposition occurred within the anchorage area. Since construction of the diversion approximately 3 to 5 feet of deposition has occurred in this area. Similar trends are observed for the cross section at the downstream limit of the anchorage area.

Figure 3.14. Cross-section comparison for RM 2.5 AHP.

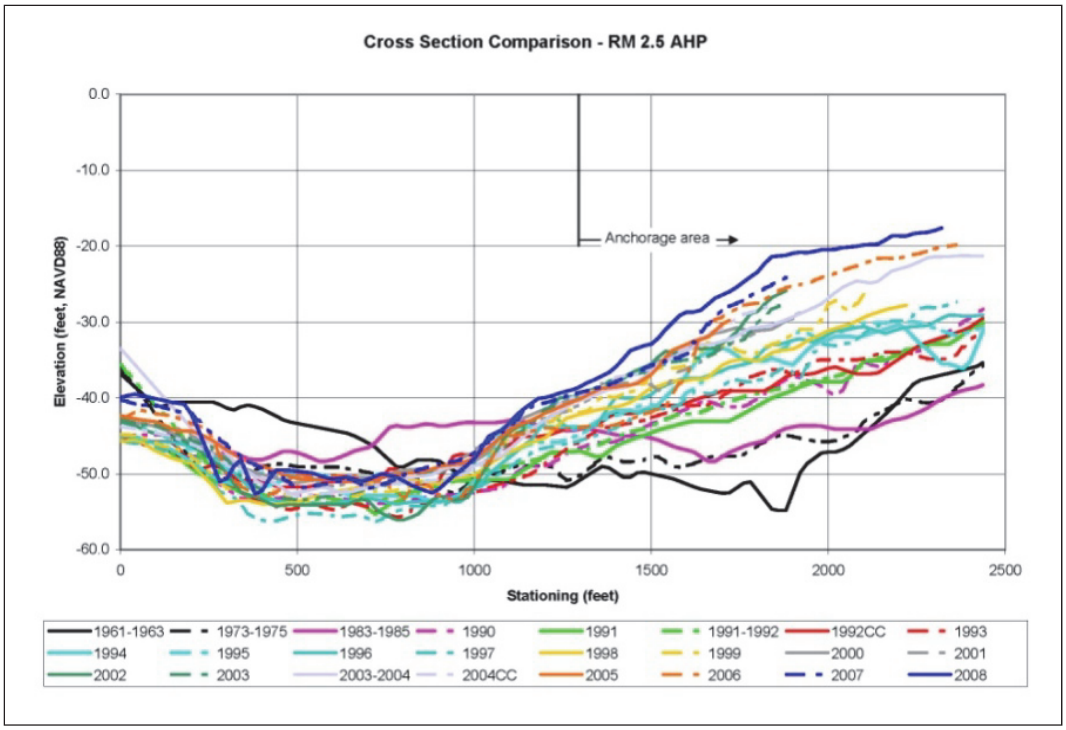

For the Mississippi River channel from the downstream limit of the anchorage area to HOP, dredging associated with maintenance of the -45 foot navigation channel dominates. This is seen in Figure 3.15 for the cross-section comparison at RM 0.7 AHP. For surveys prior to the -45 foot navigation channel the thalweg channel is shallower and the channel at the lateral bar along the right descending bank is approximately 10 feet deeper.

It can be seen that the lateral bar is almost fully developed to the current conditions by the 2003-2004 comprehensive survey. Very little additional filling has occurred in this area since the construction of the diversion. It should be noted that few of the channel condition surveys extend far enough toward the right descending bank to capture the full lateral bar. Similar conditions are observed for the section at HOP, with the exception that the channel location changes as the dredged navigation channel shifts westward to enter Southwest Pass.

Figure 3.15. Cross-section comparison for RM 0.7 AHP.

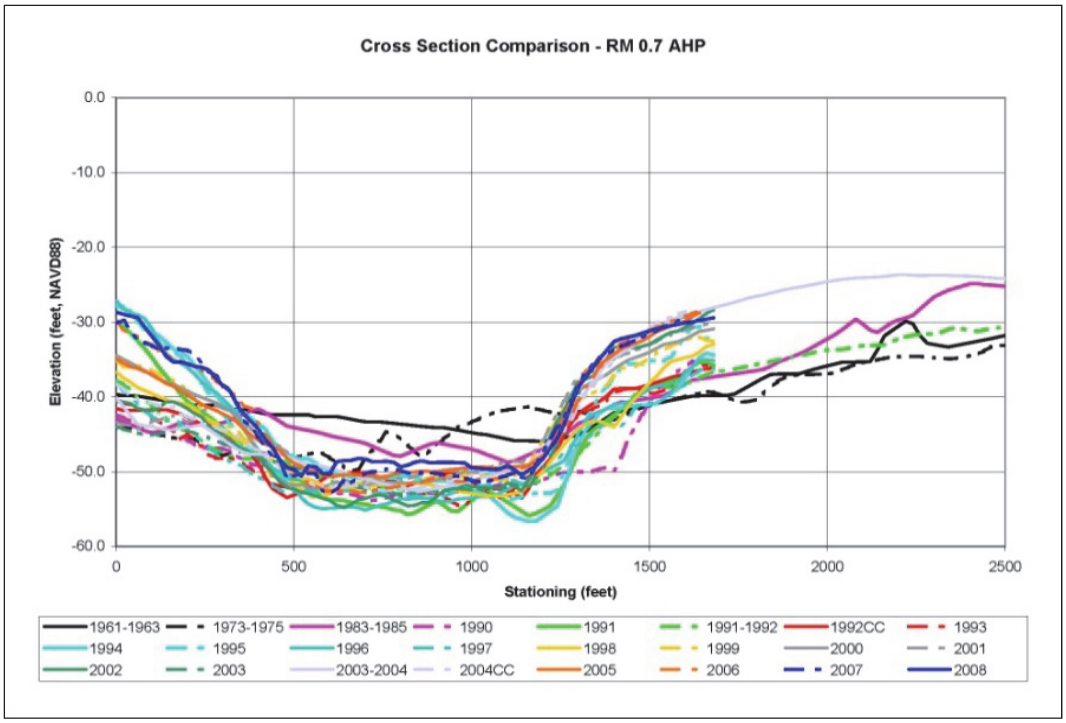

For the cross-sections within Southwest Pass, the channel is completely dominated by dredging associated with the navigation project. No trends can be discerned, other than the existence of a shallower channel prior to the -45 foot navigation project. Cross section comparisons for RM 10.0 BHP and RM 18.6 BHP are shown in Figure 3.16 as an example. Note that the 1980s comprehensive survey data were not available in digital format for Southwest Pass.

To gain a better perspective of the channel geometry changes in the vicinity of the PAA in relation to the construction of the West Bay Diversion, an analysis of the survey data were conducted with a detailed focus on the anchorage area. This detailed focus analysis utilized channel condition

Figure 3.16. Cross-section comparison for RM 10.0 BHP.

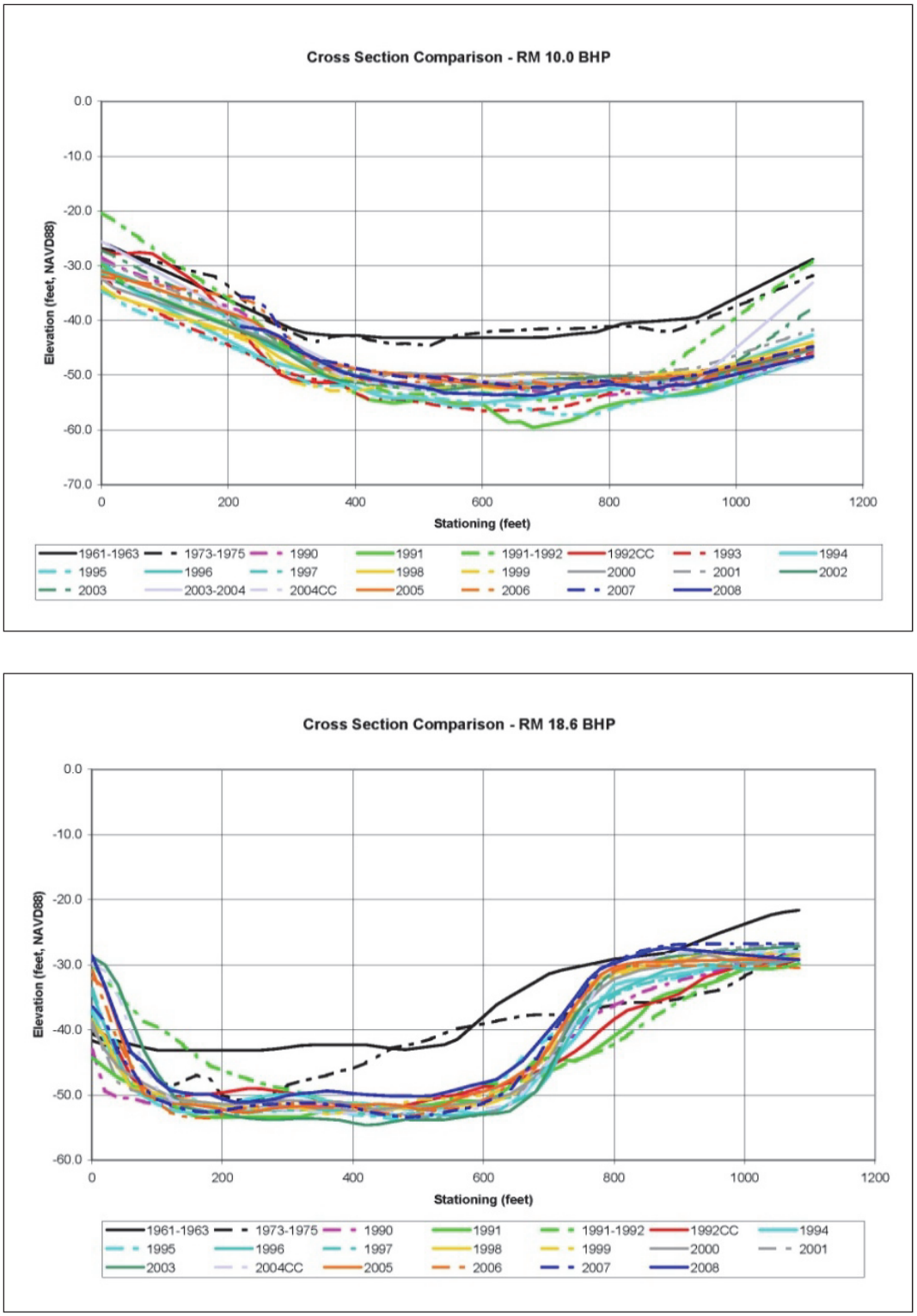

surveys approximately every quarter year from 2001 to 2008. The density of cross sections used in this analysis was greater than the broad focus analysis. The portion of the cross section that is plotted is 500 feet westward

from the PAA line, so that dredge cuts in the anchorage area will be fully captured. The symbology for the plots show the surveys prior to diversion construction as solid lines, the surveys between diversion construction in 2003 and the first maintenance dredging event in 2006 as dashed lines, and the surveys subsequent to the 2006 dredge event as dotted lines. The purpose of the detailed focus analysis was to determine geometry changes within the PAA that occurred in the immediate time before and after the construction of the diversion and the 2006 PAA dredge event.

The detailed focus cross section comparison plots for the portion of the PAA upstream of the WBSD generally indicate that depths have decreased between 5 to 10 feet since 2001. There is a significant degree of variability in the surveys, and determining what change is related to the diversion construction is difficult. The cross section comparisons for the broad focus analysis indicate a similar trend. The changes are most likely associated with the general decrease in depths occurring as a system response, since it would be unlikely for diversion induced effects to occur upstream of the diversion of water. The cross-section comparison plot for RM 5.8 AHP is shown as an example in Figure 3.17. This section is located halfway between the diversion and the upstream end of the anchorage area. The plot illustrates that the surveys prior to and immediately following diversion construction show variability in the riverbed elevation but no discernible trends. The riverbed elevations indicated by the post-2006 PAA dredge event surveys show a fairly consistent elevation of approximately -50 feet NAVD88.

For the portion of the anchorage area between the diversion and Cubits Gap, the comparative cross sections again indicate significant variability, and trends related to diversion construction are difficult to distinguish. The comparative cross-section plot for RM 4.3 AHP, just downstream of the diversion, is shown in Figure 3.18 as an example. The plot indicates there have been approximately 10 feet of variation in riverbed elevation between 2001 and the 2006 PAA dredge event. The curve for the 01 April 2001 survey indicates that depths were actually the least during that time, but depths had increased to the deepest by the 23 July 2002 survey. All of this variability was prior to construction of the diversion. The surveys subsequent to the 2006 dredge event generally indicate the shallowest conditions for the period of 2001 to 2008.

Figure 3.17. Cross-section comparison for RM 5.8 AHP, detailed focus analysis.

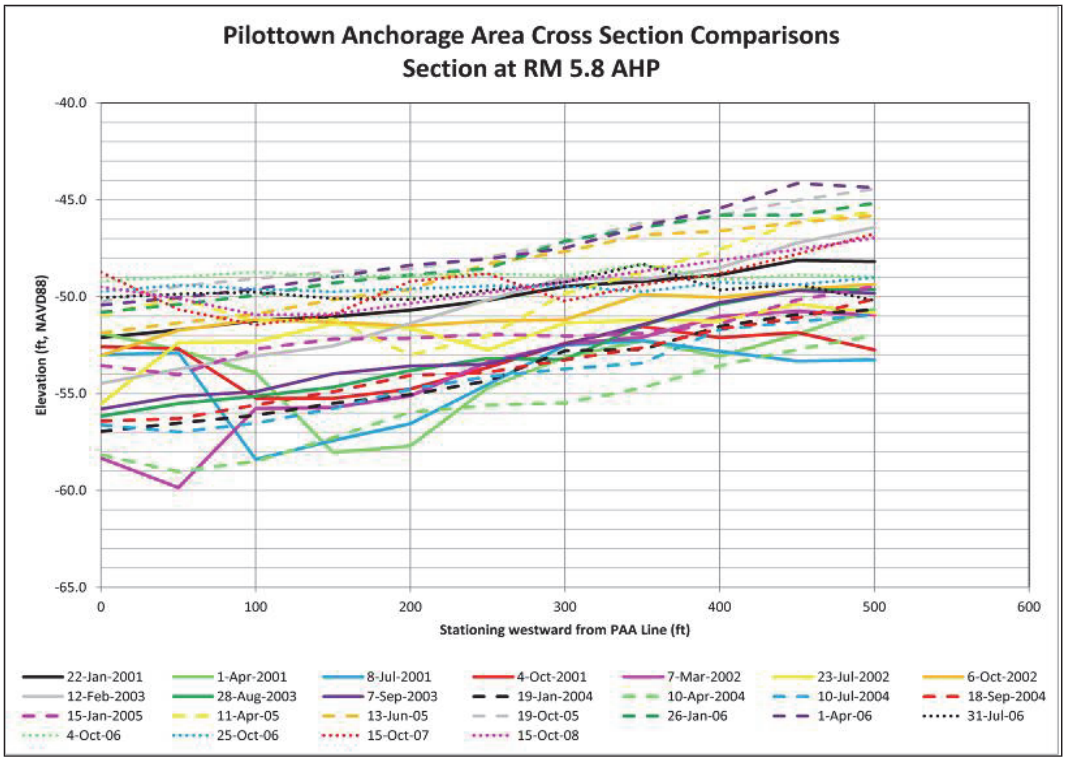

Figure 3.18. Cross-section comparison for RM 4.3 AHP, detailed focus analysis.

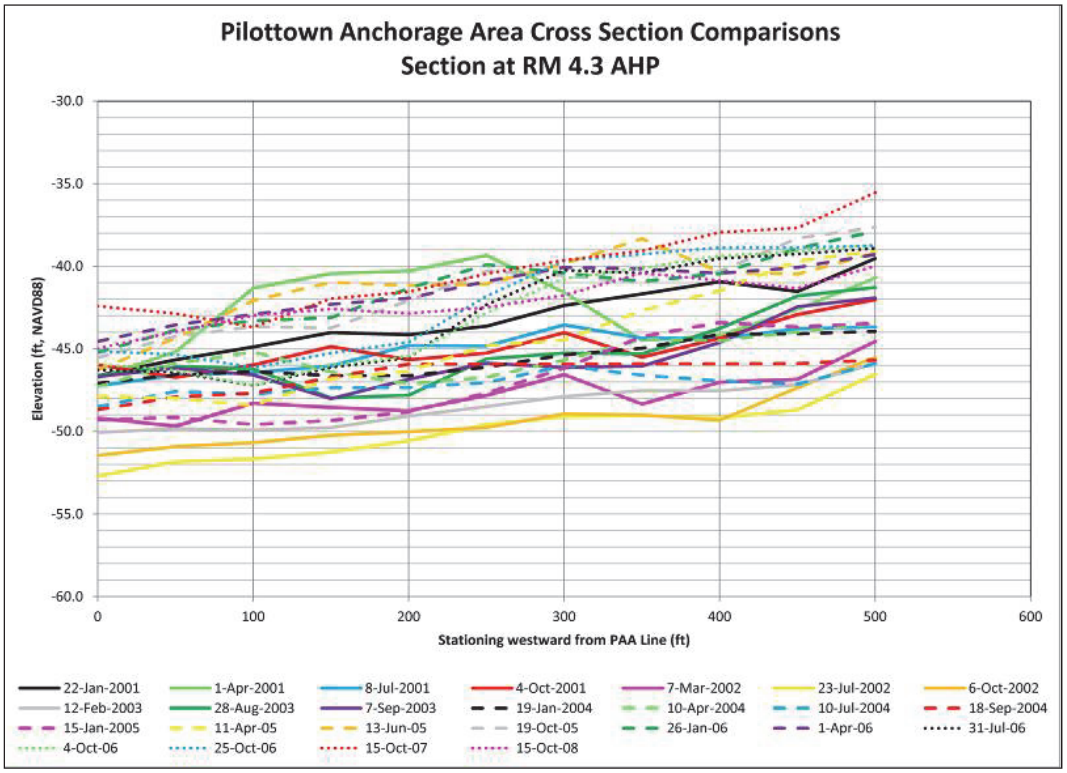

Within the portion of the anchorage area located downstream of Cubits Gap, the detailed focus cross-section comparisons indicate that for the 500 foot section westward of the PAA line the riverbed was very shallow prior to diversion construction. It is also very evident that the dredge cuts associated with diversion construction in 2003 and the 2006 PAA dredge event are very short lived due to rapid shoaling following the dredge events. This can be best illustrated by the cross section comparison plot for RM 2.8 AHP, shown in Figure 3.19. The surveys prior to construction of the diversion (solid lines) indicate that the riverbed was consistent, with riverbed elevations less than -40 feet NAVD88. The survey of 07 March 2002 shows a temporary shoaling and bed elevations less than -35 feet NAVD88, but this deposition had been scoured by the 23 July 2002 survey. The PAA dredge cut associated with construction of the diversion in 2003 can clearly be seen (dashed lines), and the surveys indicate that the cut filled rapidly, except for sour denoted by the 11 April 2005 survey. By the time of the last survey (01 April 2006) prior to the 2006 PAA dredge event, the dredge cut had completely shoaled to within approximately 1 foot of pre-diversion construction conditions. The surveys subsequent to the 2006 PAA dredge event (dotted lines) again clearly show the dredge cut and indicate the rapid

Figure 3.19. Cross-section comparison for RM 4.3 AHP, detailed focus analysis.

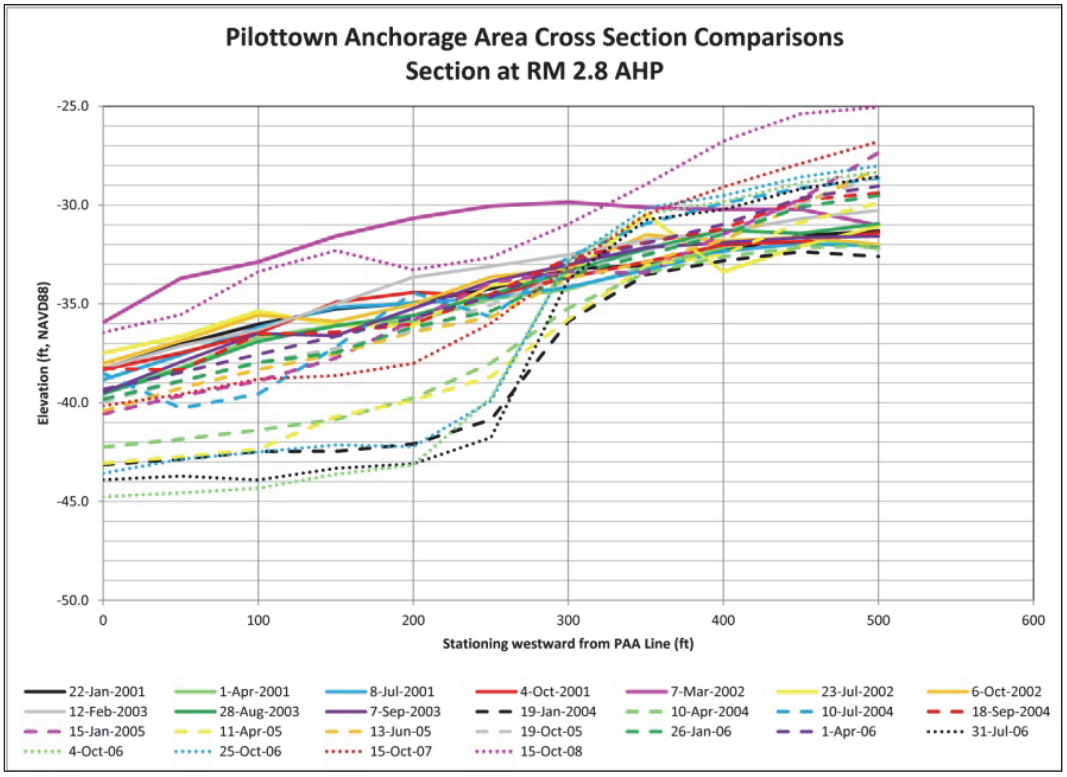

shoaling that took place after the dredge event. By the time of the 15 October 2008 survey (approximately 28 months after the dredge event) the dredge cut in the PAA had shoaled to its greatest extent since construction of the diversion. Overall, the survey comparisons for the cross sections located in the PAA downstream of Cubits Gap indicate that the riverbed had shoaled significantly prior to construction of the diversion. Dredge activities within the PAA in this location tend to be very short lived and shoal rapidly to near pre-dredge conditions.

The overall assessment based on the comparison of cross sections in the broad focus and detailed focus analyses is that the general trend for the Mississippi River upstream of Venice has been no appreciable change to a slight increase in channel depth over time. The river thalweg channel observed in the 1960s time period is generally shallower than the current river depths. A shift in this trend appears to occur in the reach from Venice to Cubits Gap. Beginning at Venice, the comparative cross sections indicate a trend of reduced depth over time. Depth reductions as much as approximately 20 feet have occurred in the reach over the study time period. The location of the channel crossing has also experienced a general shift toward the right descending bank during this time. The riverbed within the anchorage area between WBSD and Cubits Gap appears to have experienced shoaling both before and after construction of the diversion; however, how much of the shoaling, which is attributable to construction of the diversion, is unclear due to the variability in the survey data. For the reach from Cubits Gap to HOP the channel is heavily influenced by maintenance dredging for the navigation project. For survey periods after the change to the -45 foot navigation project, the channel in this reach is entrenched along the left descending bank, and the lateral bar along the right descending bank is actively developing. Surveys indicate the riverbed elevation in the PAA downstream of Cubits Gap had significantly shoaled prior to construction of the diversion. Dredge cuts in this portion of the PAA associated with diversion construction and maintenance in 2006 have been short lived and have rapidly shoaled to near pre-dredge conditions. There appears to be very little additional shoaling of the lateral bar in the downstream portion of the anchorage area that can be attributed to construction of the diversion; however, the most recent survey used in the analysis does indicate the most excessive shoaled conditions for some cross sections. From HOP to East Jetty the channel is dominated by navigation dredging, and no real trends can be determined other than the channel prior to the -45 foot project was more shallow than the current channel.

Average Bed Elevations

The comparison of cross sections from the comprehensive and channel condition surveys provides a means for a qualitative assessment of the observed trends in channel depths and dimension for the Mississippi River within the study reach. However, it is difficult to quantify the observed changes due to the variability at each cross section and from survey to survey. An average bed elevation investigation was conducted in an attempt to resolve the variability in the bed elevation data. The average bed elevation was computed for the portion of the detailed focus analysis cross sections extending 250 foot westward (towards the right descending bank) from the anchorage area line. A combination of the decadal hydrographic surveys and quarterly channel condition surveys were used in this analysis to provide a long time period yet sufficient detail for the period prior to and after diversion construction. The computed average bed elevations for each cross section were then plotted versus time to determine if any trends in riverbed elevation are present. For purposes of this discussion, a negative (-) bed elevation change refers to shoaling/reduction in depth, and a positive (+) bed elevation change refers to scour/increase in depth. This method provides better visualization of channel depth trends that are specific to the anchorage area.

The plot of average bed elevation for cross section PAA-US at the upstream limit of the anchorage area is shown in Figure 3.20. The plot indicates that the rate of negative bed elevation change before and after construction of the diversion is very similar. Note that there is no indication of a PAA dredge cut at this section since existing depths are more than sufficient for ship anchorage. Although the rate of negative bed elevation change is steady after diversion construction, the changes are thought to be related to a system wide adjustment rather than an impact of the diversion, since it is upstream of the withdrawal of water. The cross section at RM 6.1 AHP indicates a similar trend, as shown in Figure 3.21.

For the cross sections located at RM 5.8 AHP and RM 5.3 AHP, the average bed elevation plots indicate quite a bit of variability in the years prior to diversion construction. This could be due to the shifting of the channel crossing that occurs in this area. An example of this is shown in Figure 3.22 for the cross section at RM 5.3 AHP. Notice that there was a fairly rapid rate of negative bed elevation change after diversion construction, but the bed elevation is not less than what existed during the 1980s survey. The impact of the 2006 PAA dredge event can be seen in this plot, and once again the rate of subsequent filling is fairly rapid. Note that there was no PAA dredge cut in this location associated with diversion construction in 2003.

Figure 3.20. Average bed elevation for cross section PAA-US located at the upstream limit of the PAA.

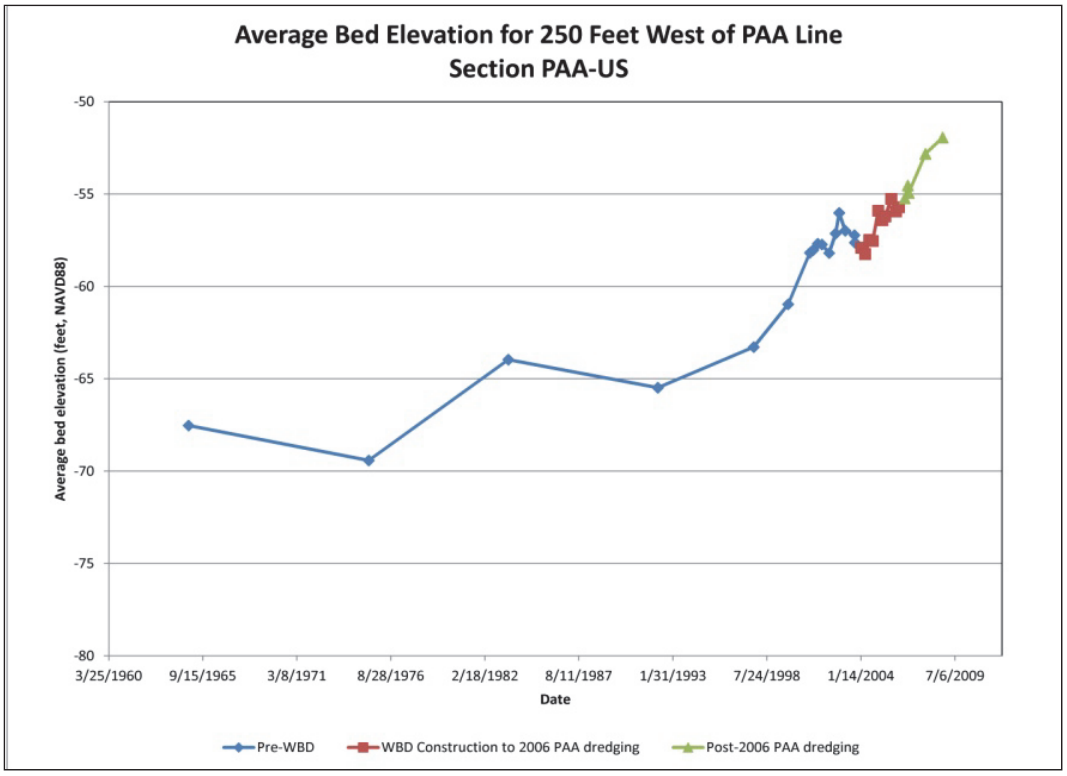

Figure 3.21. Average bed elevation for cross section RM 6.1 AHP.

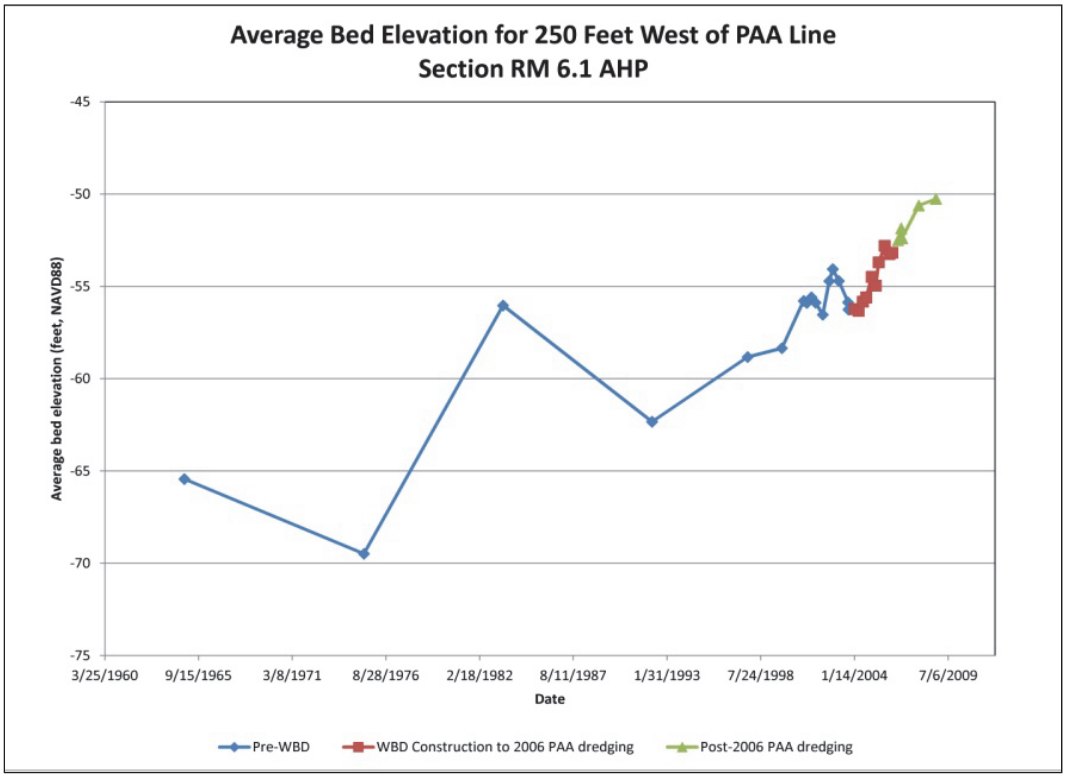

Figure 3.22. Average bed elevation for cross section RM 5.3 AHP.

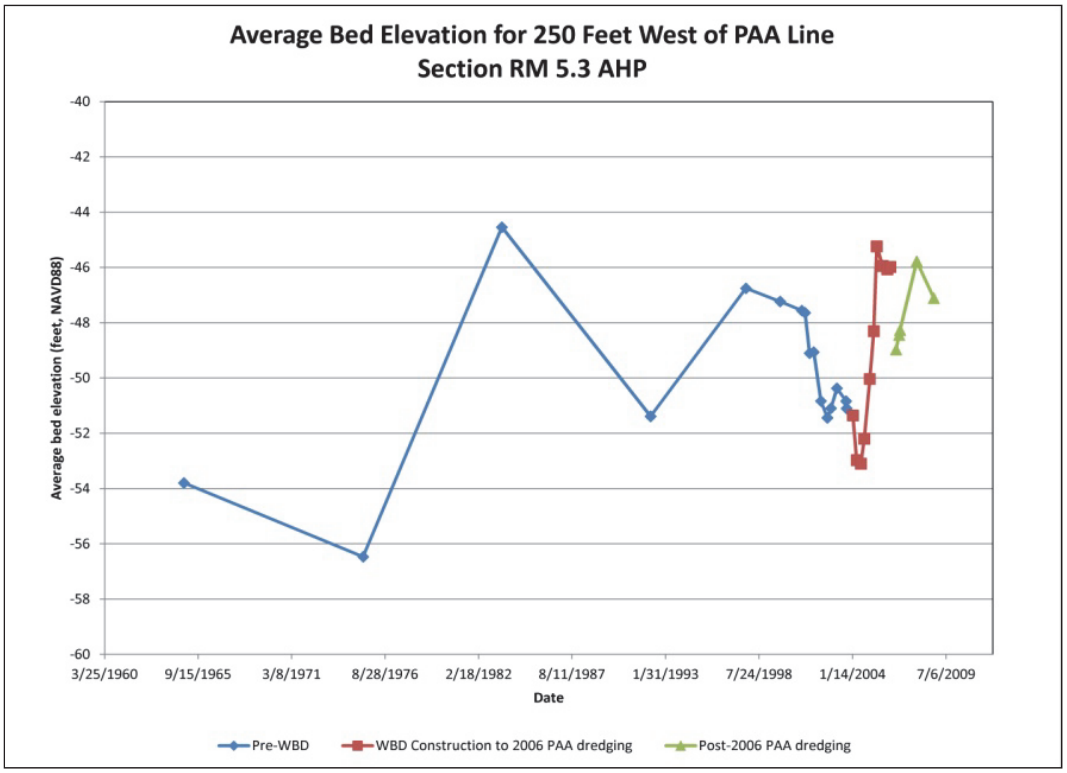

Average bed elevation plots for the cross section located between WBSD and Cubits Gap indicate considerable variability in be elevation prior to the construction of the diversion. The plots show the average bed elevation at several cross sections was higher at some point prior to diversion construction, while at other sections the average bed elevation has achieved its highest elevation after diversion construction. An example of this variability is shown in Figure 3.23 for the cross section located at RM 4.0 AHP. The plot indicates that the average bed elevation at this cross section was as high in the 1960s survey as it was at the time of diversion construction in 2003, but was lower during the years in between. The dredge cuts associated with the diversion construction and the PAA maintenance dredge event in 2006 can be seen, as well as the subsequent filling that occurred after those dredge events. The variability of the average bed elevation shown in this plot is fairly representative for the cross sections between WBSD and Cubits Gap.

Figure 3.23. Average bed elevation for cross section RM 4.0 AHP.

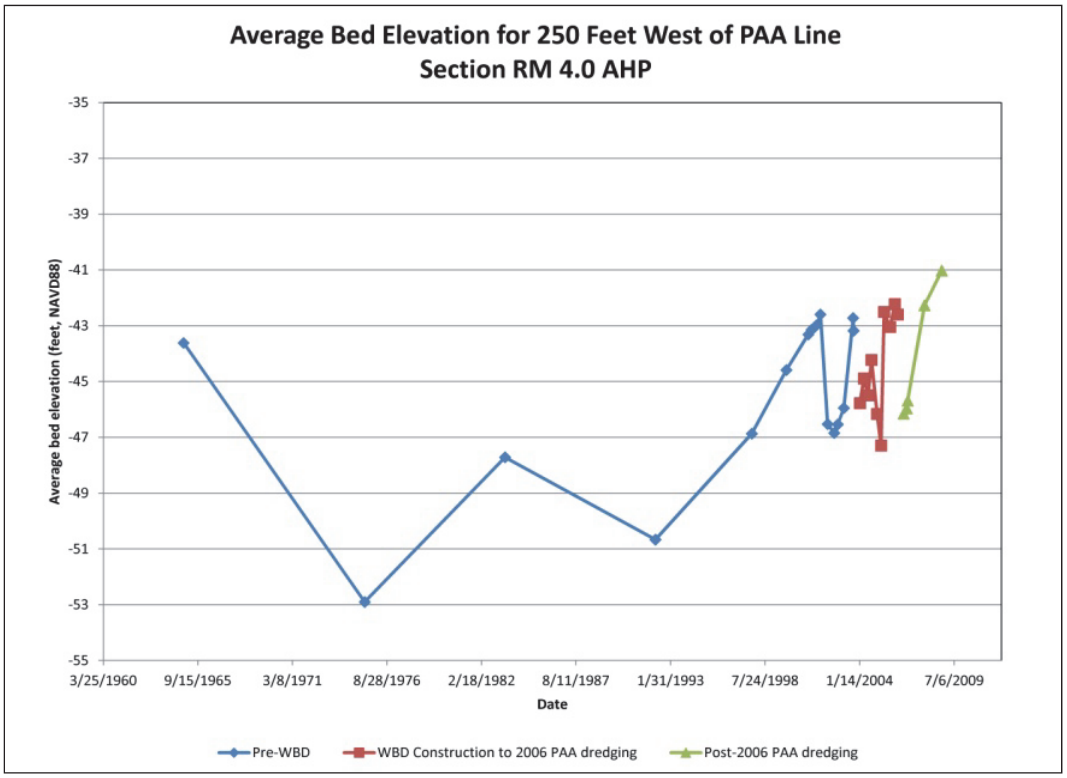

For the cross section in the portion of the PAA downstream of Cubits Gap, the average bed elevation plots indicate that bed elevations were decreasing prior to the construction of the diversion and that dredging efforts in this area are very short lived. The plot for the cross section at RM 2.5 AHP shown in Figure 3.24 is very representative of the trends in this area. The plot indicates that the average bed elevation was decreasing fairly uniformly until the late 1990s when the rate increased. The effects of the dredge cuts for the diversion construction and the 2006 PAA maintenance event can clearly be seen, and as is typical of other locations the dredged area fills rapidly in the years that follow. The extent of the average bed elevations before and after diversion construction is nearly equal.

Analysis of the average bed elevation trends for the detailed focus analysis cross sections within the PAA is complicated by the variability in the data. Trends in average bed change specifically related to diversion construction are difficult to quantify. Qualitatively, there are indications that the average bed elevation for the 250 foot section of the PAA cross sections was decreasing prior to diversion construction. Average bed elevations for the period after diversion construction are not significantly higher than pre-construction elevations for the cross sections downstream of Cubits Gap.

Figure 3.24. Average bed elevation for cross section RM 4.0 AHP.

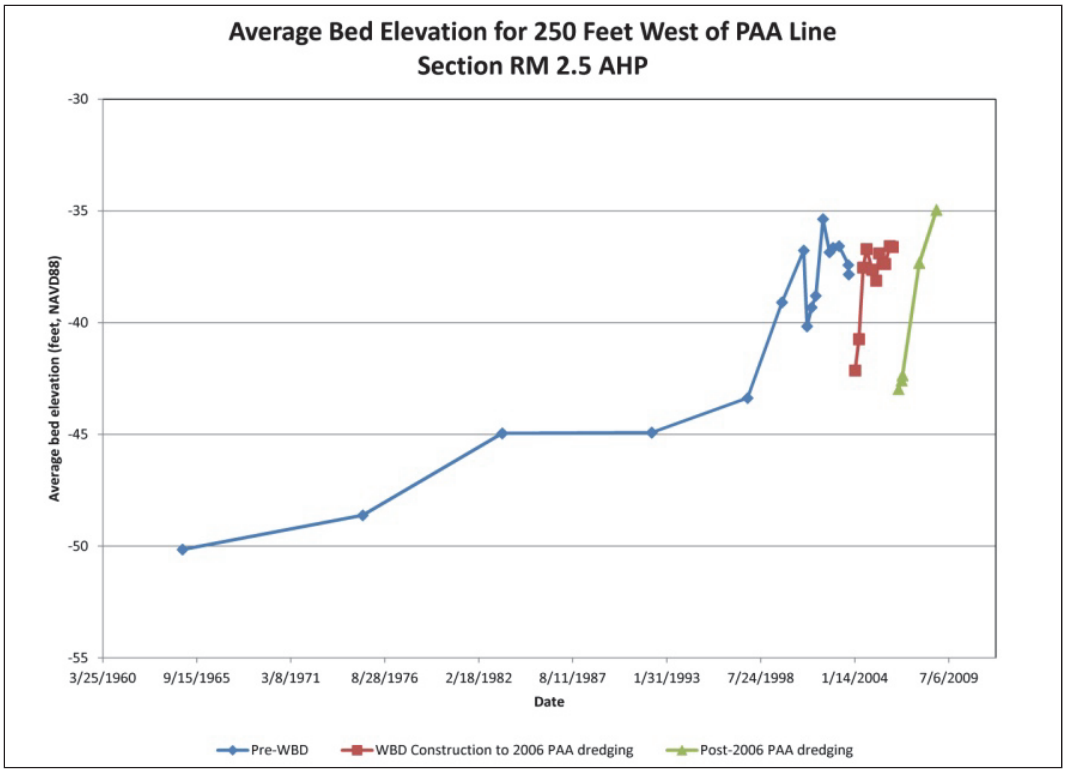

Of particular interest is the rapid rate in which deposition occurs after the 2006 PAA dredge event in the section of the PAA downstream of West Bay Diversion, and in particular downstream of Cubits Gap. Post-dredge shoaling occurs at a greater rate than was observed after the initial dredging associated with diversion construction. A linear trend line was applied to the post-2003 construction and the post-2006 PAA dredge event average bed elevations for the sections downstream of West Bay Diversion. The post-2003 construction period mean rate of deposition is approximately 1.6 feet/year with a range of 0.4 to 3.3 feet/year. The post-2006 PAA dredge event period mean rate of deposition is approximately 2.8 feet/year with a range of 0.8 to 4.6 feet/year. It is most probable that future maintenance dredge activities in this portion of the PAA will be subject to similar rates of post-dredge deposition and will be very short lived at best.

Analysis of Flood and Hurricane Impacts

Surveys following the floods of 1997 and 2008 and Hurricane Katrina in 2005 were analyzed to determine the degree of impact due to extreme hydro-meteorological events. For the floods of 1997 and 2008, surveys that were analyzed are the October survey preceding the spring flood

event, the survey collected 2 to 3 weeks after the flood peak, and the following October survey. For Hurricane Katrina, the surveys that were compared are the pre-storm survey of early August 2005, the mid-September 2005 survey, and the October 2005 survey. Channel condition surveys were used for all these comparisons.

Cross-section comparisons for the floods of 1997 and 2008 indicate that large magnitude floods of this nature result in substantial changes that are often irregular in pattern. The flood peaks produce sufficient stream power to move the bed sediments through the river channel in large waves, resulting in a noticeably remolded channel perimeter. Figures 3.25 and 3.26 illustrate the impact of the 1997 flood for the cross sections at RM 5.8 AHP and Cubits Gap. Figure 3.25 illustrates that at RM 5.8 AHP slight filling in the thalweg channel and considerable deposition on the point bar occurred due to the flood. Interestingly, approximately half of the flood deposits on the point bar had been eroded by the following October. Figure 3.26 shows that at Cubits Gap very little change in thalweg depth occurred, but significant erosion along the point bar in the anchorage area took place. It is interesting that deposition in the anchorage area occurred at one point, but erosion occurred at a location not much farther downstream. This may be indicative of the large sand waves that can be generated during large flood events. Figure 3.27 shows the changes that occurred at RM 10.0 BHP as a typical example for Southwest Pass. The plot indicates that both erosion and deposition occurred over as much as a 5 foot vertical range at this location.

Figures 3.28 and 3.29 illustrate the observed impacts on channel dimensions resulting from the flood of 2008. Figure 3.28 shows the cross-section comparisons for the section located at the West Bay diversion. The surveys indicate a slight filling within the thalweg channel, and 3 to 5 feet of erosion in the anchorage area adjacent to the navigation channel. Deposition of 2 to 3 feet occurred farther upslope on the point bar. The October 2008 survey indicates that the anchorage area adjacent to the channel had almost completely refilled with sediment by the following autumn. Figure 3.29 shows the observed changes at Cubits Gap for the 2008 flood. It can be seen that 6 to 8 feet of sediment deposition occurred along the edge of the navigation channel and the anchorage area. The shape and elevation of the channel within the anchorage area for the pre-flood survey (October 2007) is indicative of the effects of the 2006 anchorage area dredging effort. This suggests that deposition from the 2008 flood effectively negated the dredging effort in this location. The conditions in the

Figure 3.25. Cross-section comparisons for 1997 flood for cross section located at RM 5.8 AHP.

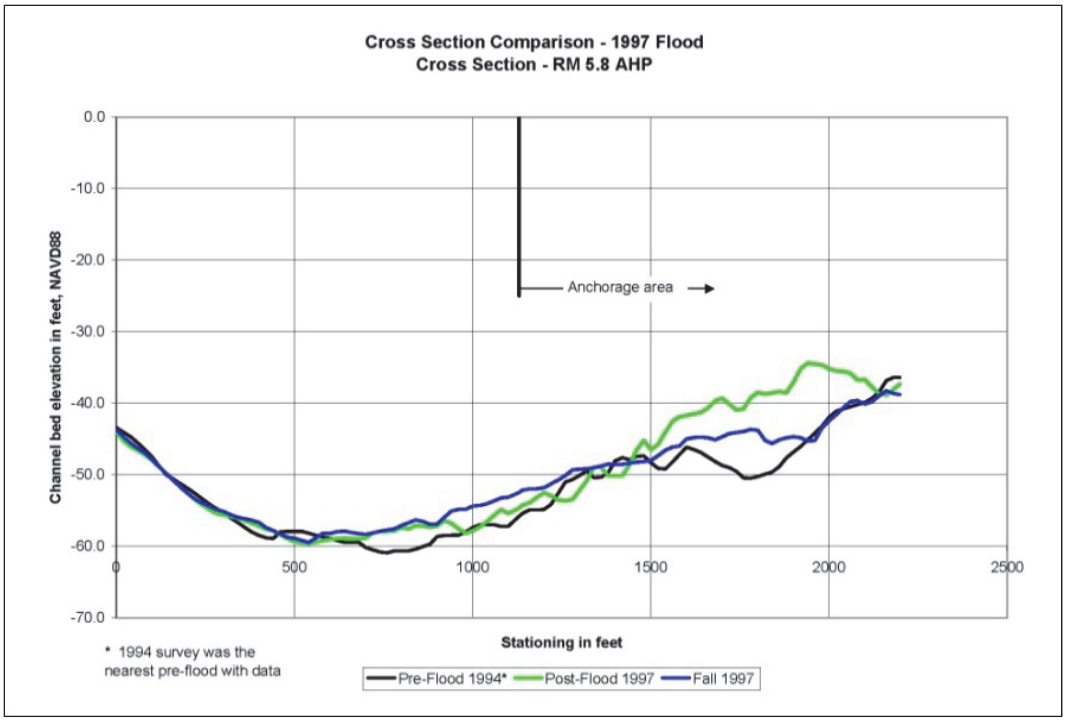

Figure 3.26. Cross-section comparisons for 1997 flood for cross section located at downstream limit of PAA.

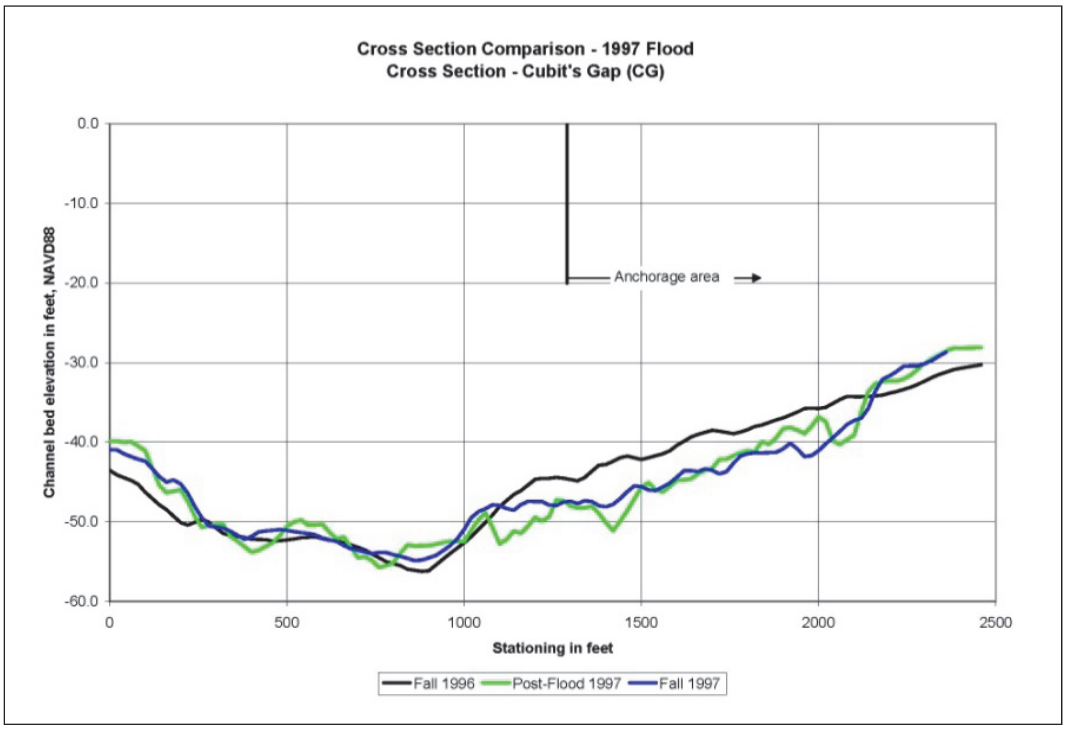

Figure 3.27. Cross-section comparisons for 1997 flood for cross section located at RM 10.0 BHP.

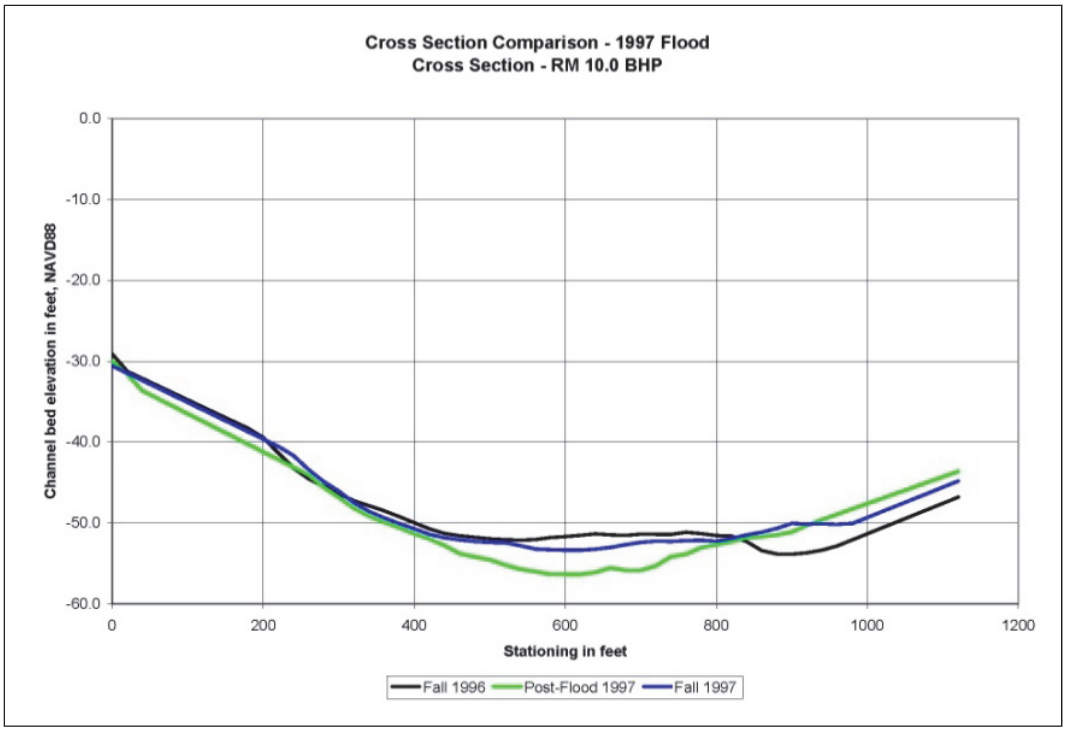

Figure 3.28. Cross-section comparison for 2008 flood for cross section located at West Bay diversion.

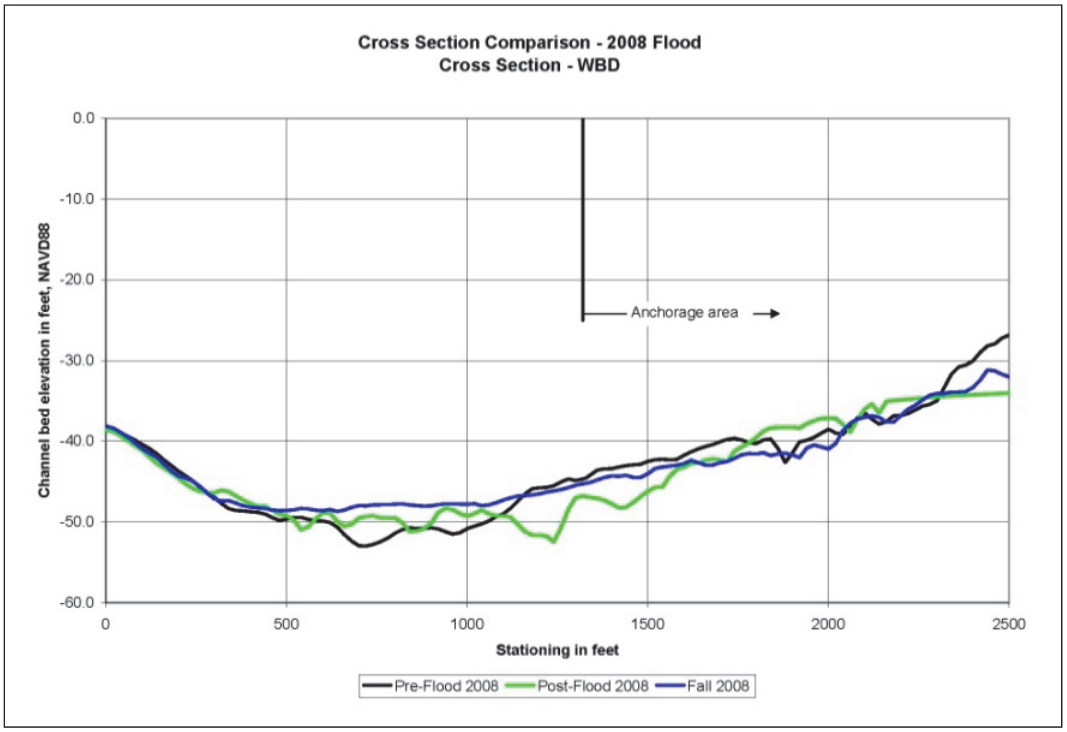

Figure 3.29. Cross-section comparison for 2008 flood for cross section located at Cubits Gap.

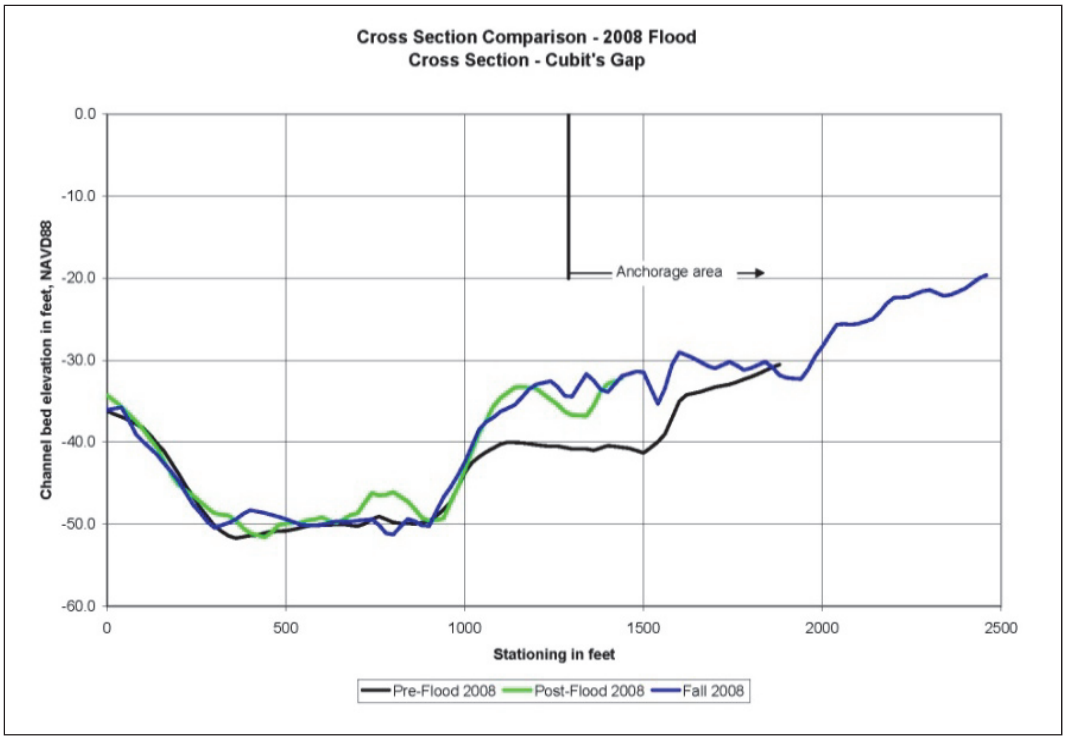

following October has not changed significantly since the post-flood survey, except for removal of flood deposited material from the channel. Figure 3.30 shows the changes that occurred at RM 5.0 BHP as an example of the typical changes observed within Southwest Pass for the 2008 flood. The plot indicates scour of the channel, as much as 10 feet, occurred during the flood, but most of the scoured area had refilled by the following autumn.

The cross-section comparisons for Hurricane Katrina in 2005 indicate that a general deposition of sediment occurred in the area. The deposition pattern was fairly uniform, with slightly more deposition observed in the channel than along the point bar within the anchorage area. Depths of deposition range from approximately 2 feet in the upstream anchorage area to approximately 5 feet in Southwest Pass near East Jetty. The survey comparisons also indicate a portion of the deposited material was either dredged or scoured away within a couple of months after the storm. Figure 3.31 shows the observed changes at the cross section at West Bay diversion. Approximately 2 feet of deposition occurred in the thalweg channel, but less in the anchorage area. The cross-section comparisons in Figure 3.32 indicate a similar deposition pattern at Cubits Gap, with 2 to 3 feet of filling in the channel and approximately 1 foot of deposition within the anchorage area. Figure 3.33 illustrates the typical changes observed at HOP. The

Figure 3.30. Cross-section comparison for 2008 flood for cross section located at RM 5.0 BHP.

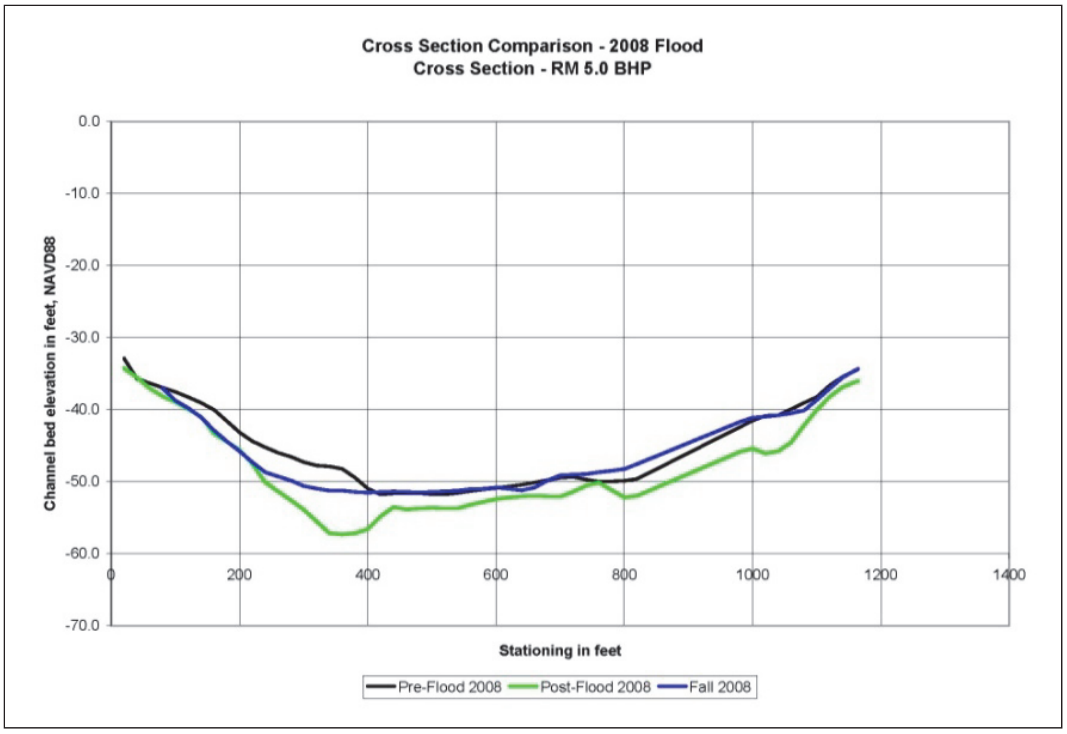

Figure 3.31. Cross-section comparison for Hurricane Katrina for cross section located at West Bay diversion.

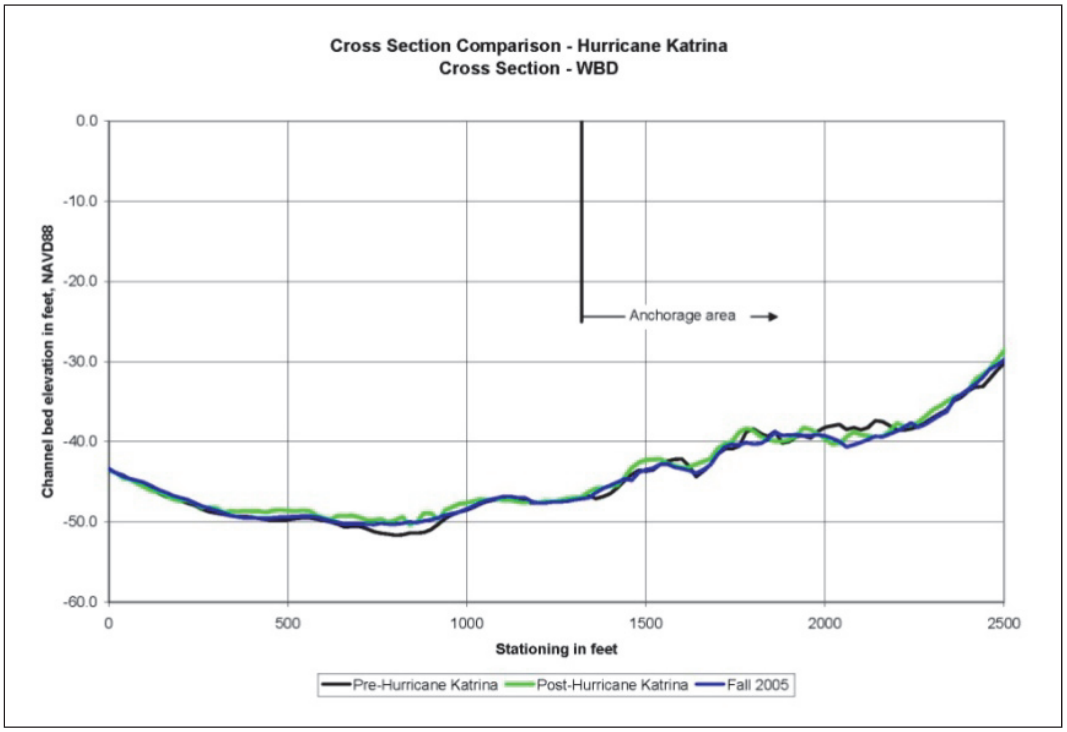

Figure 3.32. Cross-section comparison for Hurricane Katrina for cross section located at Cubits Gap.

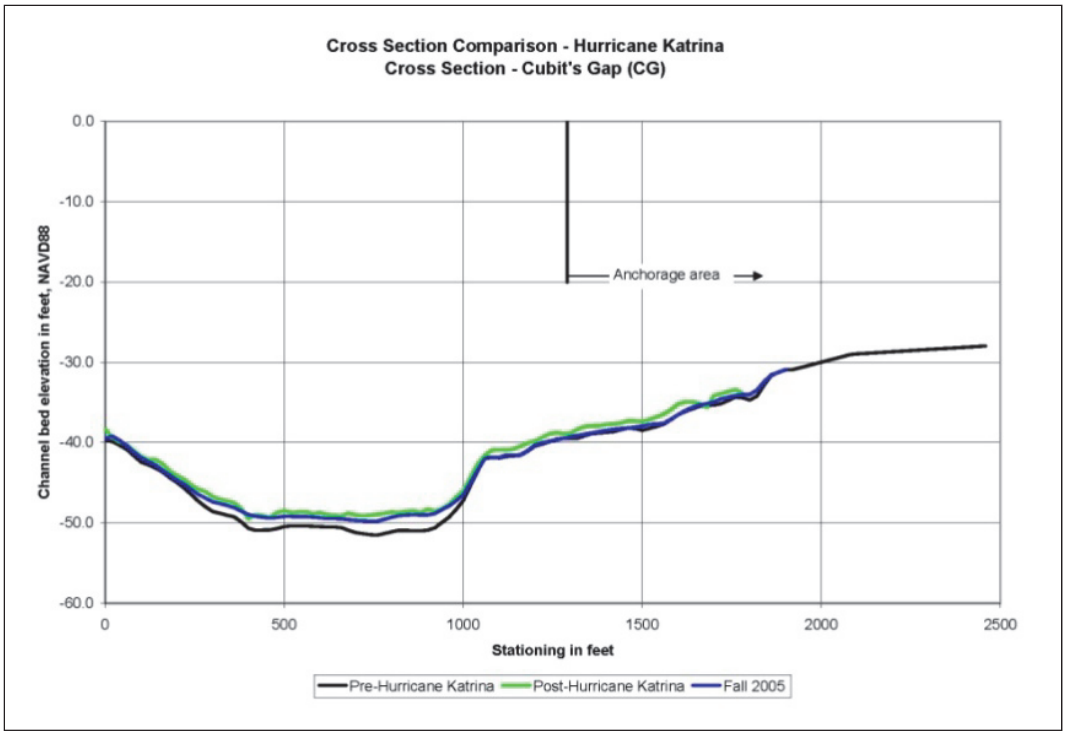

Figure 3.33. Cross-section comparison for Hurricane Katrina for cross section located at HOP.

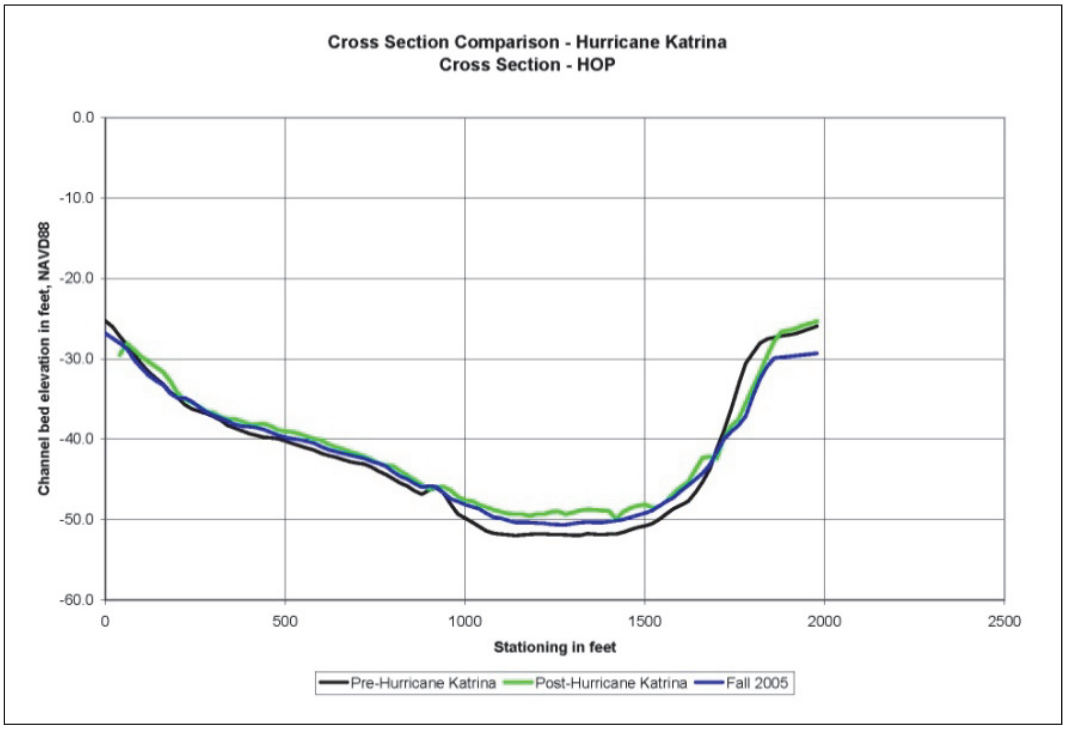

trends observed from HOP to East Jetty indicate deposition in the channel during the storm and scour of storm deposits during the ensuing few months. In general, approximately 3 to 5 feet of sediment deposition occurred during the storm in Southwest Pass, with the amounts increasing with proximity to the gulf. Deposition patterns were very uniform across the section. Removal of the deposited material in the months after the storm resulted in a restoration of 30 to 50 percent of the pre-storm channel geometry. Figure 3.34 shows the cross section comparisons for RM 18.6 BHP at East Jetty.

Figure 3.34. Cross-section comparison for Hurricane Katrina for cross section located at RM 18.6 BHP.

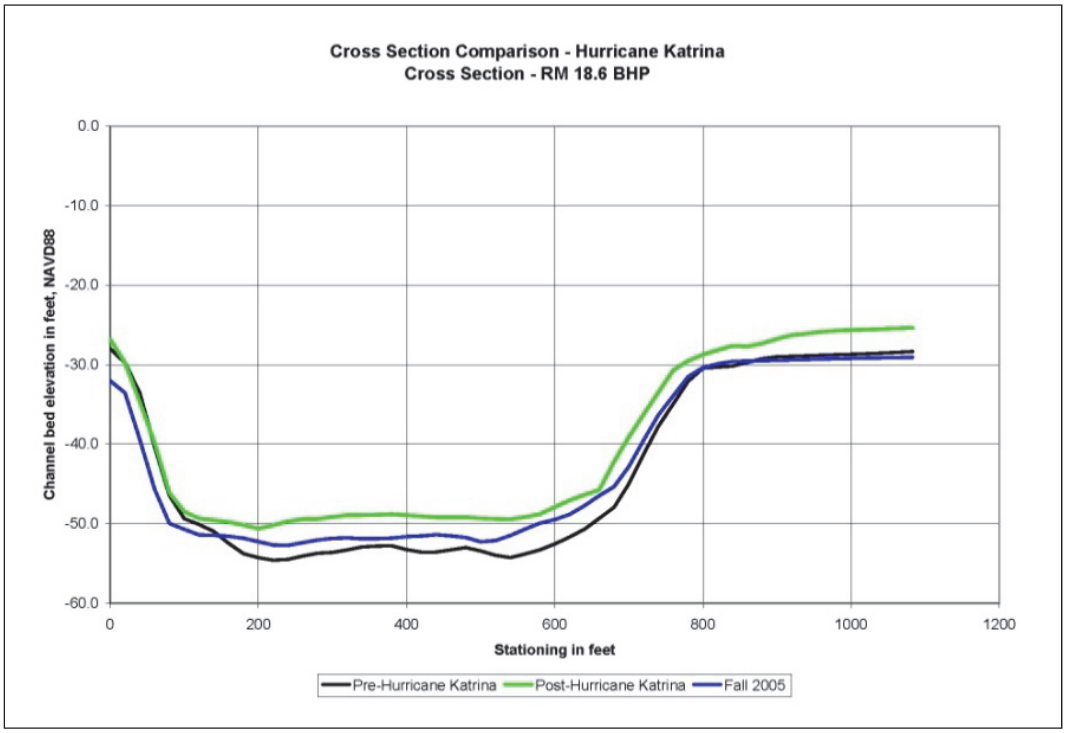

The analysis of the cross-section comparisons for the spring floods of 1997 and 2008, and for Hurricane Katrina in 2005 reveal that major flood events can significantly alter and remold the channel of the lower Mississippi River and Southwest Pass. Cross-section comparisons indicate the flood events can both scour and deposit sediments in both the thalweg channel and along the point bar. In general there is no discernable pattern or trend in the scour or deposition, although deposition in the thalweg channel typically occurs. The stream power associated with large floods mobilizes the channel bed material and moves it downstream in waves, resulting in a reworked channel perimeter. As was shown in Figure 3.29, approximately

6 to 8 feet of sediment deposition occurred in the anchorage area at Cubits Gap during the 2008 flood, effectively filling the area dredged in the 2006 anchorage area dredge work. In contrast to the effects of the major floods, the effects of Hurricane Katrina appear to be primarily depositional, and the pattern of deposition is generally uniform with greater deposition in the thalweg channel and less deposition along the point bar in the anchorage area. Depths of sediment deposition increase in the downstream direction and are greatest near the gulf. The cross-section comparisons indicate that the material deposited during the storm is removed in the weeks following the storm, either by dredging are natural erosion. It should be noted that these patterns and trends could be different for a storm that approaches the Mississippi River delta on a different track than that of Hurricane Katrina.

Volumetric Analysis

The cross section analysis of the preceding section was based on survey data extracted along a single cross-section line, and the data were assumed to be representative of the average channel bed conditions within that local area. However, irregularities and undulations certainly exist in the channel bed, and cross section data may sometimes be influenced by these irregularities and not be completely representative of the average channel bed in the area. For instance, cross-section data in an area where large sand waves or dunes have been formed by a recent flood event may reflect the crest of a sand wave or the trough of the wave. Analysis of survey data over a larger area will tend to average out these irregularities and will be perhaps more representative of the average channel bed from a spatial perspective.

The study area was divided into reaches for the volumetric analysis. These reaches range in length from as much as 15 miles in the upstream study area to less than 1 mile in the anchorage area. The reaches upstream and downstream of the anchorage area were constructed with the GIS system and were arranged to cover the channel area roughly within the -20 foot contours. Reaches within the limits of the anchorage area were constructed in parallel segments, with one segment covering the navigation channel portion and a parallel segment covering the anchorage area. The anchorage area segment covers a width of approximately 500 feet westward of the anchorage area line. The reach descriptions and limits are presented in Table 3.1 and the locations are shown in Figures 3.35 through 3.37.

Table 3.1. Limits and description of reaches for volumetric analysis.

Reach Name	RM Limits	Description
Reach1	75.0-64.0 AHP	Belle Chasse to near Alliance
Reach2	64.0-48.5 AHP	Near Alliance to West Point a la Hache
Reach3	48.5-38.0 AHP	West Point a la Hache to Port Sulphur
Reach 4	38.0-28.0 AHP	Port Sulphur to Sunrise
Reach 5	28.0-15.0 AHP	Sunrise to Duvic
Reach 6	15.0-10.3 AHP	Duvic to Grand Pass
Reach 7	10.3-6.7 AHP	Grand Pass to U/S Limit PAA
Reach 8	6.7-4.7 AHP	U/S Limit PAA to WBSD (channel)
PAA1a	6.7-5.8 AHP	U/S Limit PAA to RM 5.8 AHP (anchorage)
PAA1b	5.8 -4.7 AHP	RM 5.8 AHP to WBSD (anchorage)
Reach 9	4.7-3.2 AHP	WBSD to Cubits Gap (channel)
PAA2a	4.7-4.0 AHP	WBSD to RM 4.0 AHP (anchorage)
PAA2b	4.0 -3.2 AHP	RM 4.0 AHP to Cubits Gap (anchorage)
Reach 10	3.2-1.6 AHP	Cubits Gap to D/S Limit PAA (channel)
PAA3a	3.2-2.5 AHP	Cubits Gap to RM 2.5 AHP (anchorage)
PAA3b	2.5-1.6 AHP	RM 2.5 AHP to D/S Limit PAA (anchorage)
Reach 11	1.6-0.0 AHP	D/S Limit PAA to HOP
Reach 12	0.0-5.0 BHP	1st quarter Southwest Pass
Reach 13	5.0-10.0 BHP	2nd quarter Southwest Pass
Reach 14	10.0-15.0 BHP	3rd quarter Southwest Pass
Reach 15	15.0-18.5 BHP	4th quarter Southwest Pass (end at East Jetty)

GIS tools were used to calculate the volume from the survey TINs for each reach, and the volumes of successive surveys were subtracted from each other to determine volumetric changes from survey to survey. The volumetric change for each reach was converted to an average bed displacement by dividing the volumetric change by the surface area of the reach. The average bed displacement is proportional to and varies as the volumetric change since the surface area for each reach is a constant. The average channel bed displacements computed from the comprehensive surveys were converted to an annual average channel bed displacement by dividing by the number of years between successive surveys. The annual average channel bed displacements were then plotted to determine the trend of average channel bed change for the reach. The plots for Reaches 1 through 7 are based solely on the comprehensive hydrographic surveys because coverage for channel condition surveys did not extend that far

upstream. The plots for Reaches 11 through 15 and the anchorage area Reaches PAA1a through PAA3b are based on the yearly channel condition surveys. The plots for Reaches 8 through 10 are based on both surveys.

Figure 3.35. Location of Reaches 1-5.

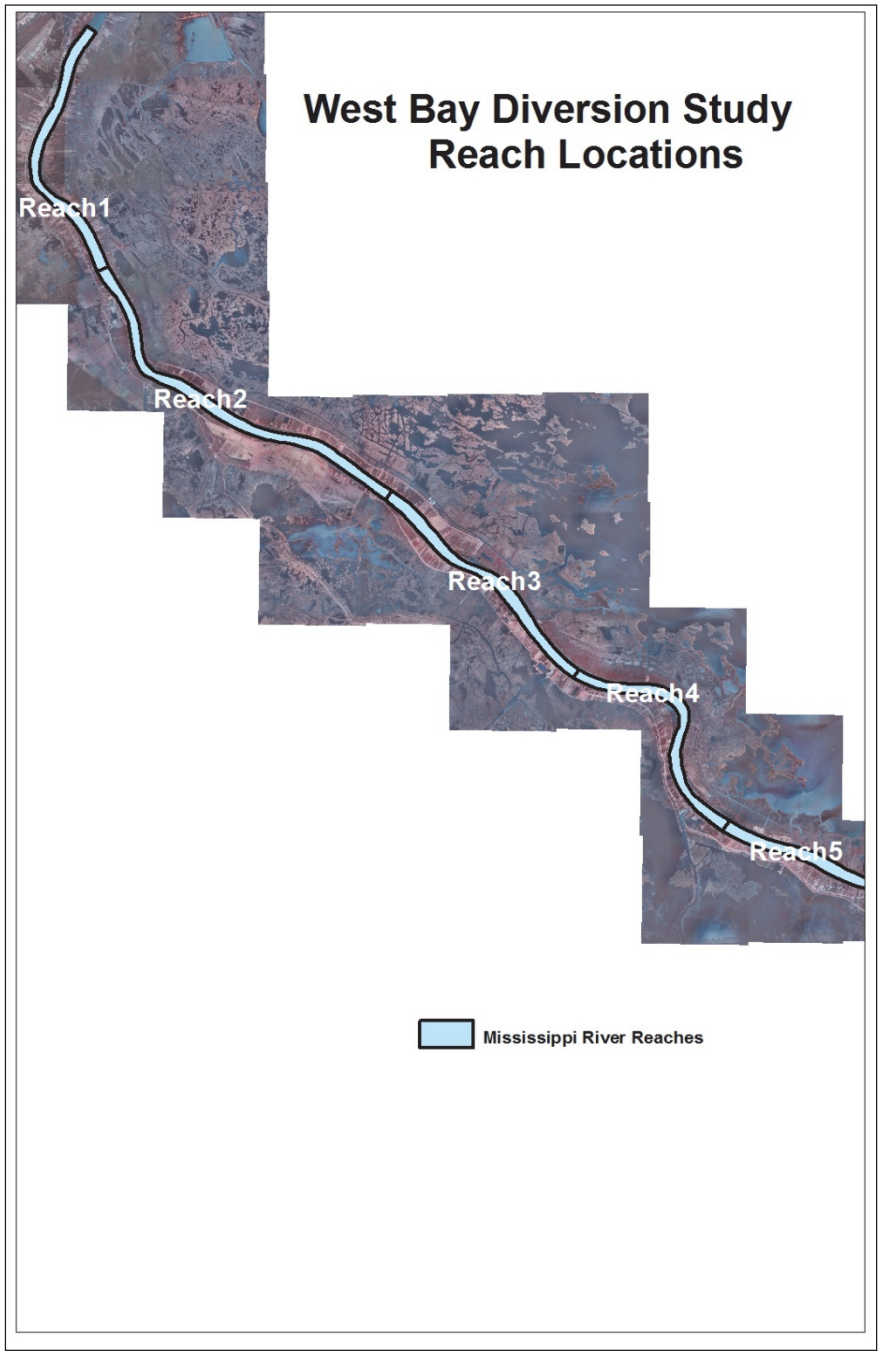

Figure 3.36. Location of Reaches 6-11 and anchorage area reaches.

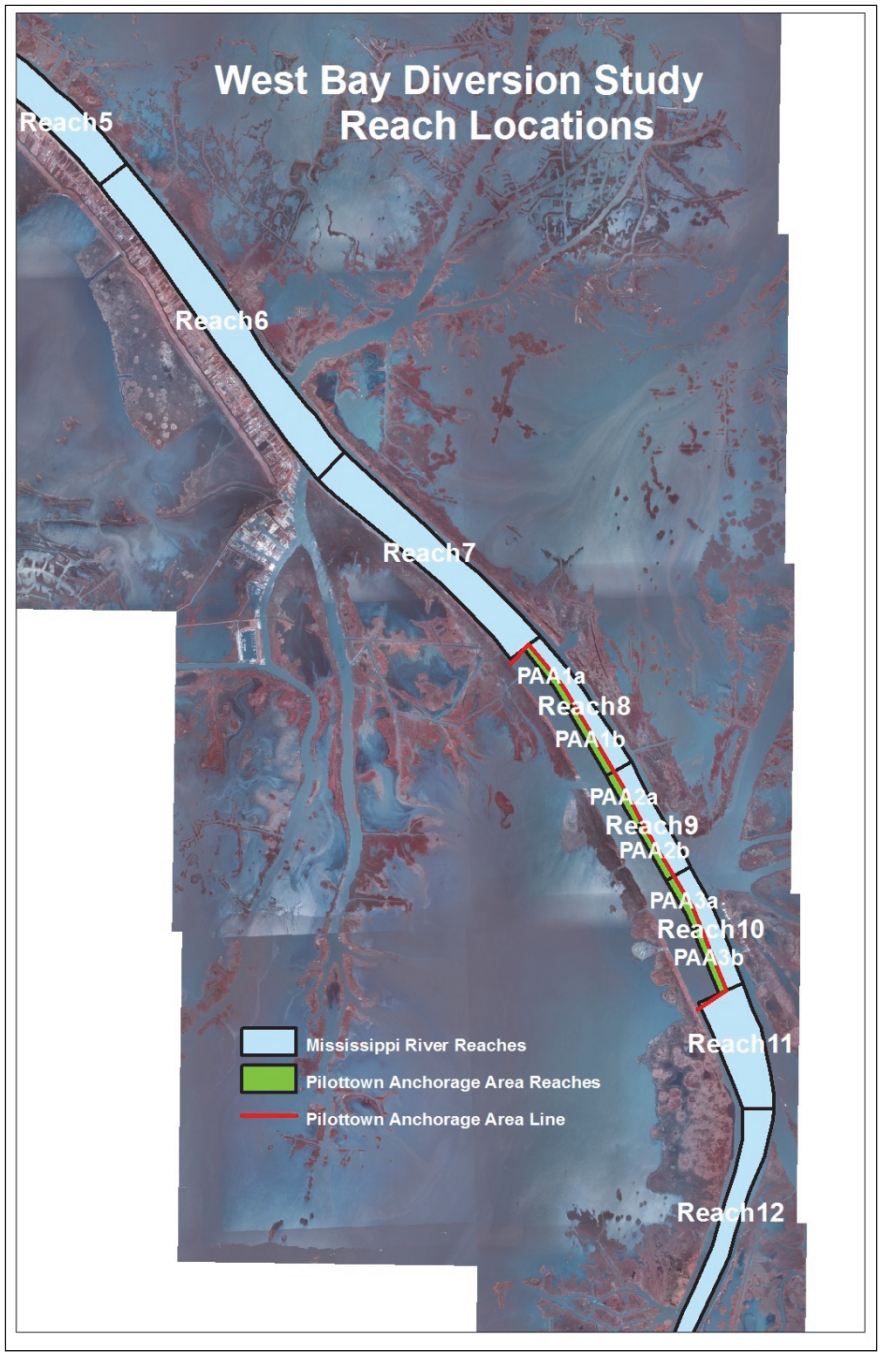

Figure 3.37. Location of Reaches 12-15.

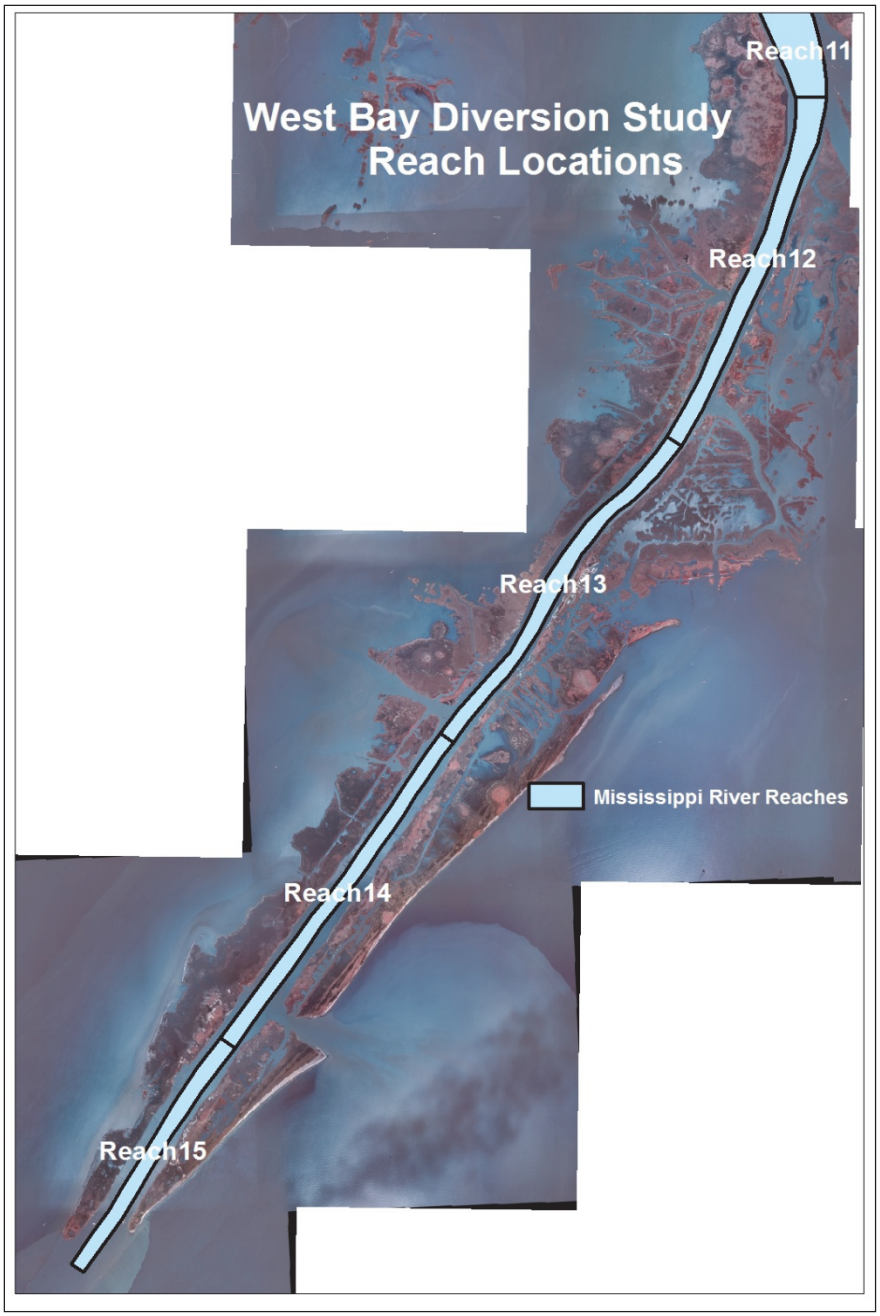

For Reaches 1 through 6, the reaches located upstream of Venice, the yearly average bed displacement between surveys ranges from 0 to almost 0.5 feet. In general, there is no discernable trend or pattern, with negative (scour) and positive (deposition) displacements occurring randomly between survey periods. The one except is Reach 3, which showed a consistent negative bed displacement from survey to survey. The annual average bed displacement plot for Reach 5 (RM 28.0-15.0 AHP) is shown in Figure 3.38 as an example for these reaches.

Figure 3.38. Annual average channel bed displacement between comprehensive survey periods for Reach 5.

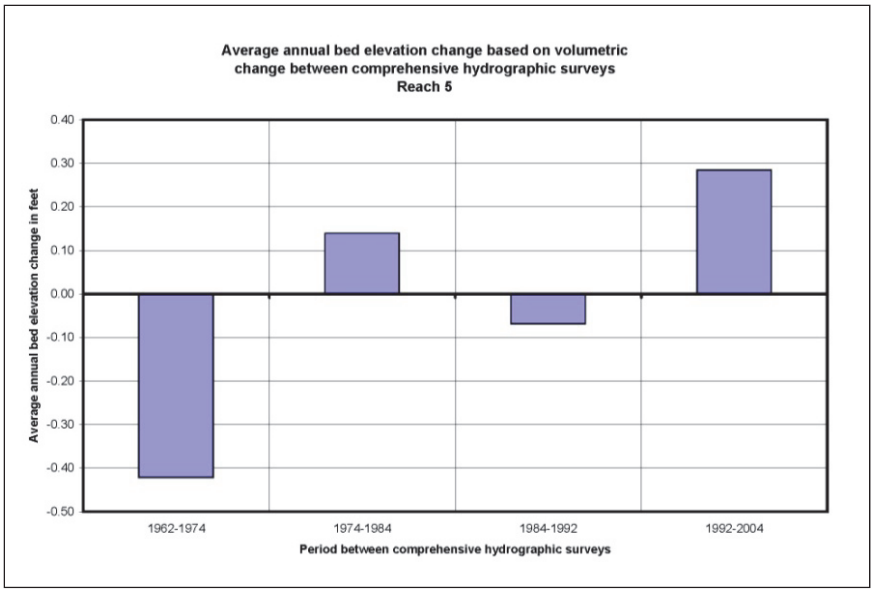

For Reaches 7 through 9, the reaches from Venice to Cubits Gap, the annual average channel bed displacement indicates a fairly consistent pattern of positive displacement (deposition) between survey periods. This is consistent with the trend observed in the cross section analysis for this area. The plots for Reaches 7 through 9 are shown in Figures 3.39 through 3.41, respectively. At Reach 7, a negative annual displacement occurred annually for the period between the 1960s and 1970s comprehensive surveys, but a positive annual displacement was observed for all successive survey periods. For Reaches 8 and 9, positive annual displacement of the average channel bed occurred for all survey periods, although the displacement for Reach 8 during the 1960s to 1970s survey period was essentially zero. These plots indicate a trend of channel deposition within these reaches. For Reaches 8 and 9 the annual average bed displacement rate for the period between the 1990s and 2000s surveys is several times greater than other survey periods.

Channel condition survey coverage also existed for Reaches 8 and 9. Yearly average channel bed displacements were computed based on these surveys and are shown in Figures 3.42 and 3.43, respectively. Although some yearly surveys are missing, the general trend in positive displacement (deposition) is similar to the trend observed from the comprehensive surveys.

Figure 3.39. Annual average channel bed displacement between comprehensive survey periods for Reach 7.

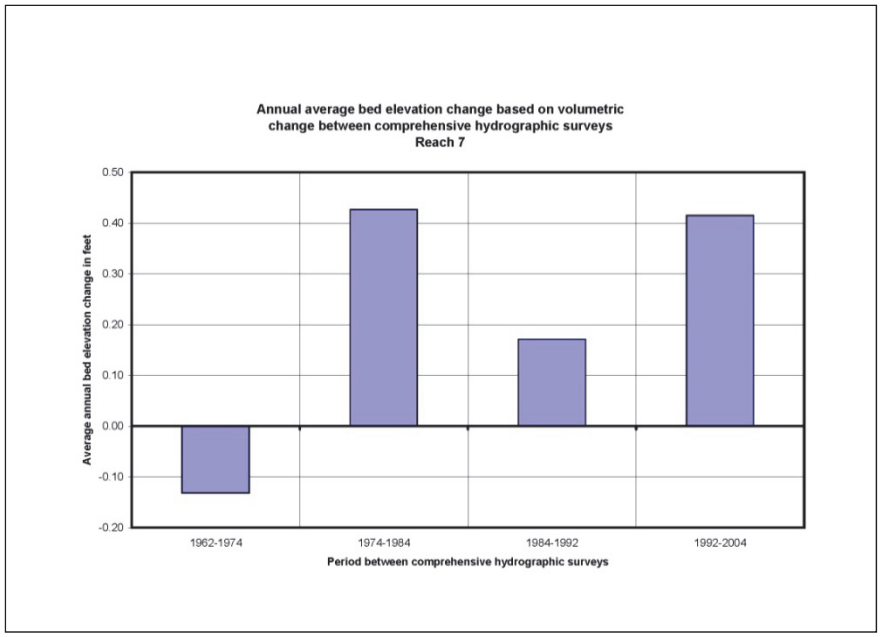

Figure 3.40. Annual average channel bed displacement between comprehensive survey periods for Reach 8.

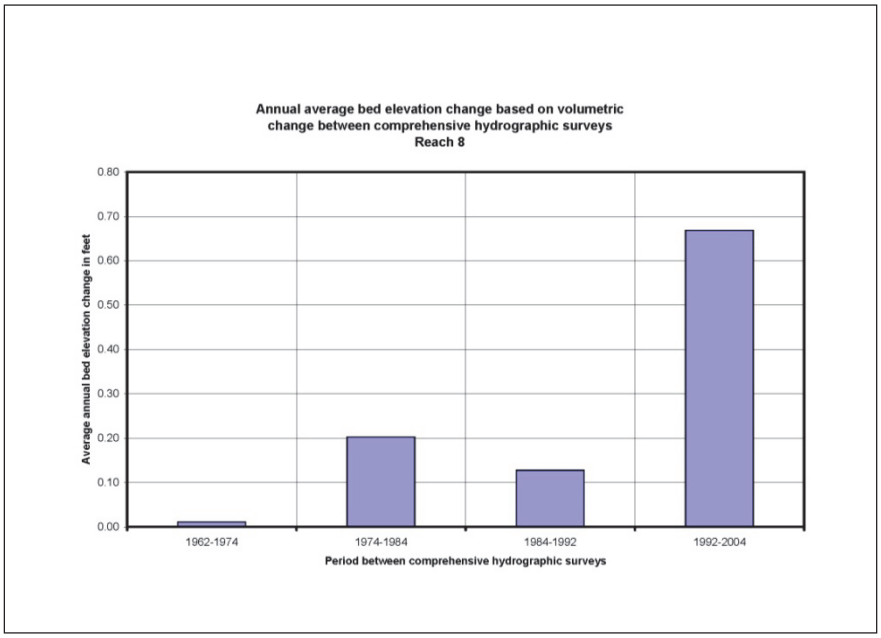

Figure 3.41. Annual average channel bed displacement between comprehensive survey periods for Reach 9.

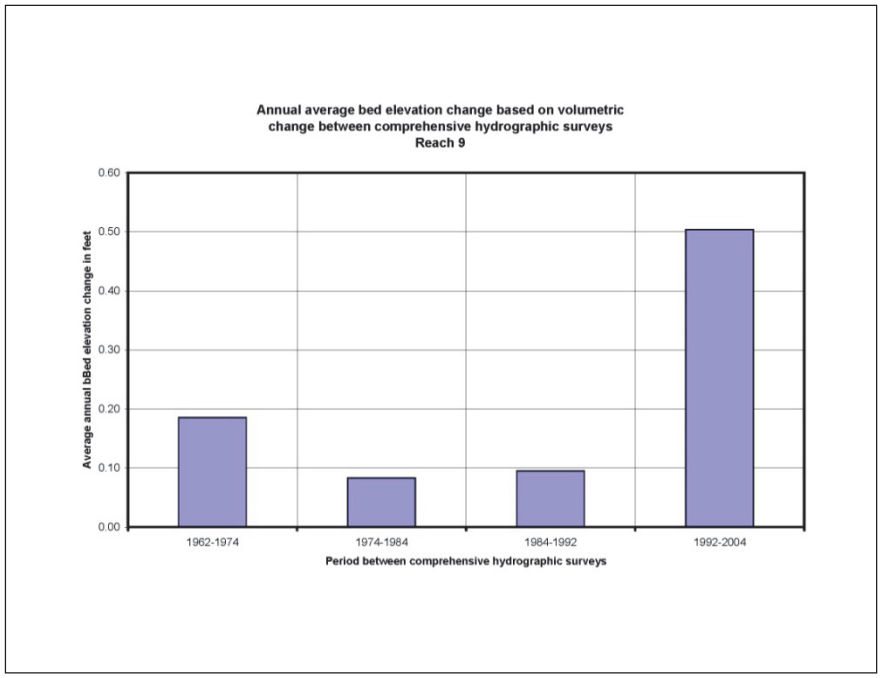

Figure 3.42. Annual average channel bed displacement between channel condition survey periods for Reach 8.

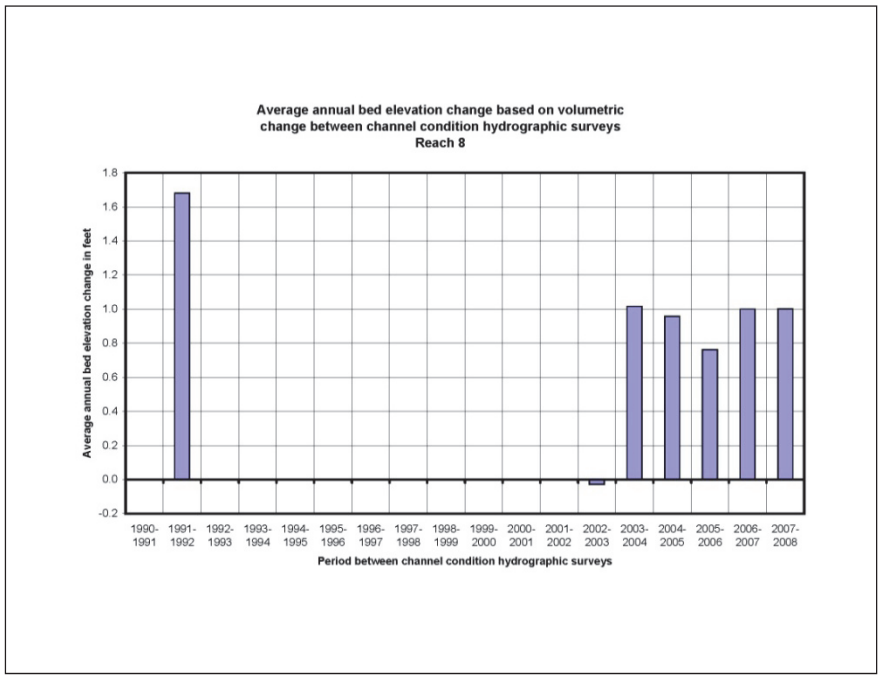

Figure 3.43. Annual average channel bed displacement between channel condition survey periods for Reach 9.

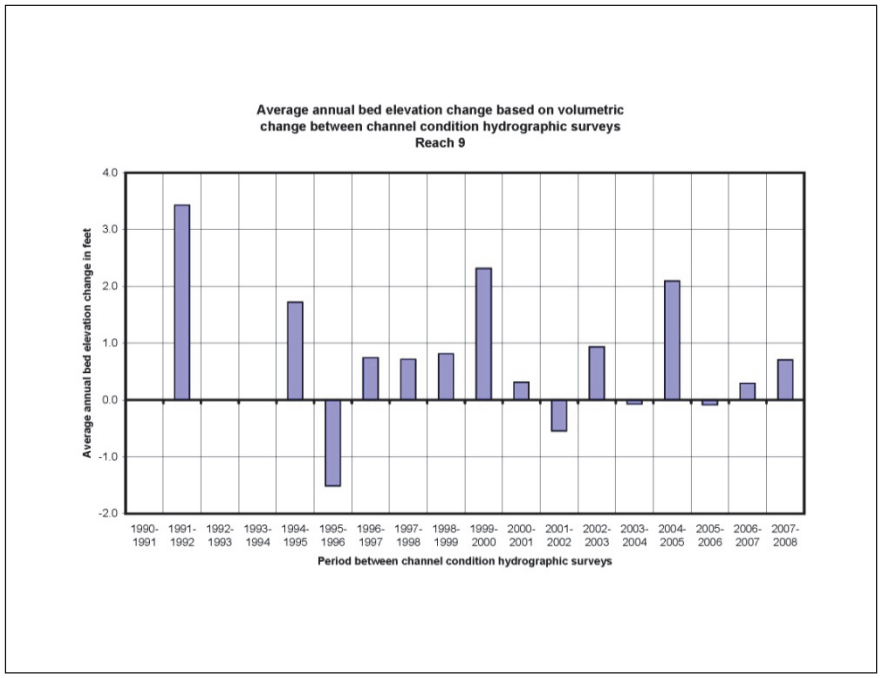

Beginning at Reach 10 and continuing through Southwest Pass to Reach 15, the river channel is dominated by dredging for navigation, and, thus, the annual average channel bed displacement data display a more random fluctuation between positive and negative displacement. No discernable trends can be identified for these reaches. The plot for Reach 12 in Southwest Pass is shown in Figure 3.44 to illustrate the random displacement values resulting from regular maintenance dredging.

The average channel bed displacements for the reaches upstream of Cubits Gap were summed to determine the cumulative bed displacement between the 1960s survey and the 2000s survey. Only reaches above Cubits Gap are presented since these reaches are not modified by navigation dredging. The cumulative average bed displacements are shown in Table 3.2.

Note that the trend for the reaches above Venice (Reaches 1-6) is for little change to some negative bed displacement up to 4.3 feet, whereas for the reaches below, Venice the trend is for significant positive bed displacement, as much as 11.2 feet. This agrees well with the findings from the analysis of cross-section data within this area.

Figure 3.44. Annual average channel bed displacement between channel condition survey periods for Reach 12.

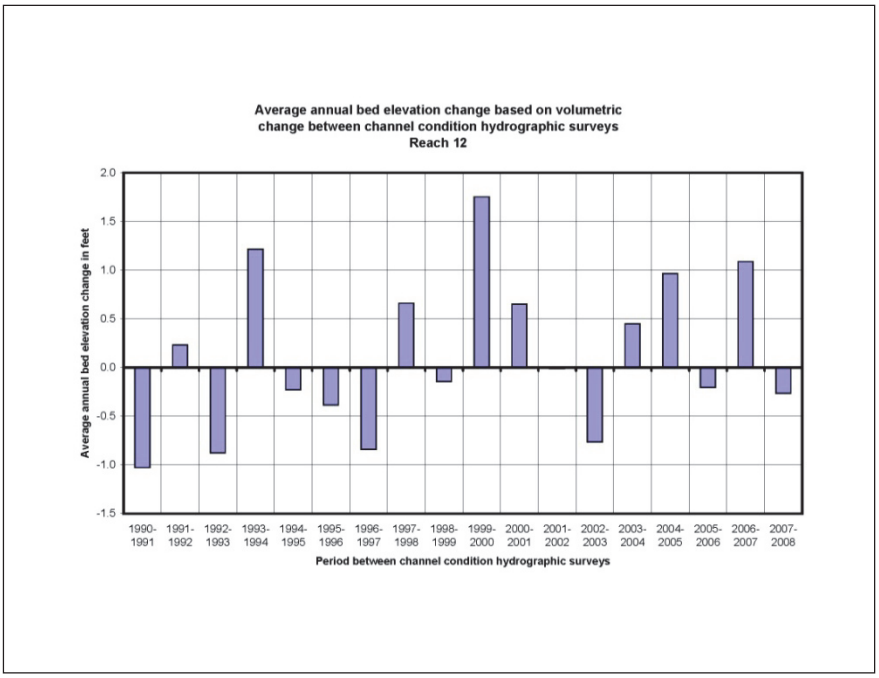

Table 3.2. Cumulative average channel bed displacement over 1960s to 2000s comprehensive survey periods for Reaches 1 through 9.

Reach	Average channel bed displacement (ft)
Reach 1	-2.8
Reach 2*	-4.1
Reach 3*	-4.3
Reach 4	0.6
Reach 5	-0.8
Reach 6	-3.4
Reach 7	9.0
Reach 8	11.2
Reach 9	9.9

* 2003-2004 survey data missing in these reaches. Cumulative displacement does not include average displacement from 1991-1992 survey to 2003-2004 survey

The reaches within the PAA were constructed with a width of approximately 500 feet, which extends from the anchorage area line westward towards the right descending bank. This results in narrower reaches than the other reaches of the analysis. A detailed map of the anchorage area reaches is shown in Figure 3.45.

Figure 3.45. Location of Pilottown Anchorage Area reaches.

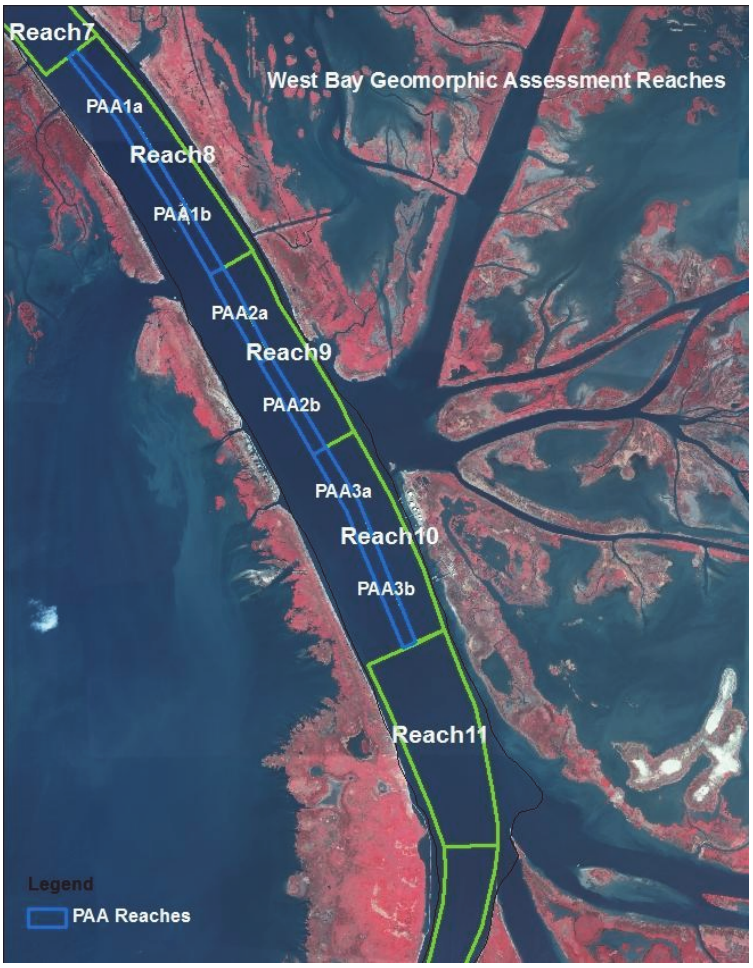

The volumetric change between comprehensive survey periods was computed for each anchorage area reach (PAA reach) and was converted to an average channel bed displacement by dividing the volume by the surface area of each reach. The displacements were converted to an annual displacement by dividing by the number of years between each survey. These annual average bed displacements for the PAA reaches are shown in Figure 3.46.

It is difficult from these results to discern any definitive trends in average channel bed displacement for the PAA reaches. For the 1960s through 1970s and 1980s through 1990s survey periods, the trend for Reaches PAA1a through PAA2b was negative displacement, but was basically no change for Reaches PAA3a and PAA3b. Also, the overall trend for Reaches PAA3a and PAA3b, the most downstream reaches, indicates from little change to positive displacement for all survey periods. No other discernable trends can be detected.

Figure 3.46. Annual average channel bed displacement based on comprehensive hydrographic surveys for the Pilottown Anchorage Area reaches.

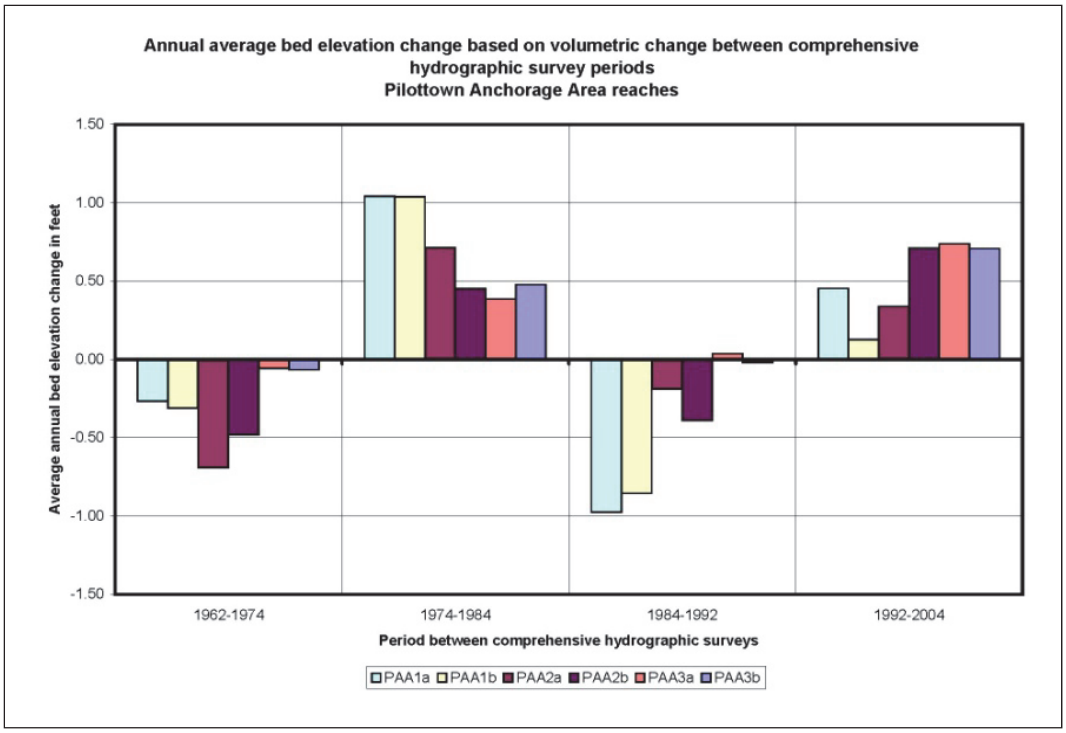

The average channel bed displacements for each reach were summed to determine the cumulative displacement over the entire period of comprehensive surveys. The results are presented in Table 3.3. The results indicate that the overall trend was for positive (deposition) displacement over the entire survey period. In addition, there appears to be a spatial trend as well, as the displacements for Reaches PAA3a and PAA3b (reaches downstream of Cubits Gap) are much greater than the other reaches.

The average channel bed displacements determined from the channel condition surveys for the periods before and after construction of WBSD are shown in Figures 3.47 and 3.48, respectively. For the pre-construction time period shown in Figure 3.47, no real trends can be determined. Similar to the results from the comprehensive surveys, the trend for Reaches PAA3a and PAA3b is from little change to positive bed displacement. For the post-construction time period shown in Figure 3.48, the data for the years 2002-2003 and 2005-2006 seem to indicate the anchorage area dredging events that occurred in 2003 and 2006. For the other yearly periods, the results are variable but tend to indicate a general trend in positive average channel bed displacement.

As mentioned in the above discussion of the volumetric analysis, the volumes determined from each survey period were converted to an average channel bed elevation by dividing the volume by the surface area of each reach. These elevations represent the average channel bed surface over the entire reach area. Average channel bed elevations were determined from the comprehensive surveys and the channel condition surveys, and are presented in Figures 3.49 and 3.50.

Table 3.3. Cumulative average channel bed displacement over 1960s to 2000s comprehensive survey periods for Pilottown Anchorage Area reaches.

Reach	Average channel bed displacement (ft)
PAA1a	4.9
PAA1b	1.3
PAA2a	1.4
PAA2b	4.2
PAA3a	12.3
PAA3b	12.3

Figure 3.47. Average channel bed displacement based on pre-construction channel condition surveys for Pilottown Anchorage Area reaches.

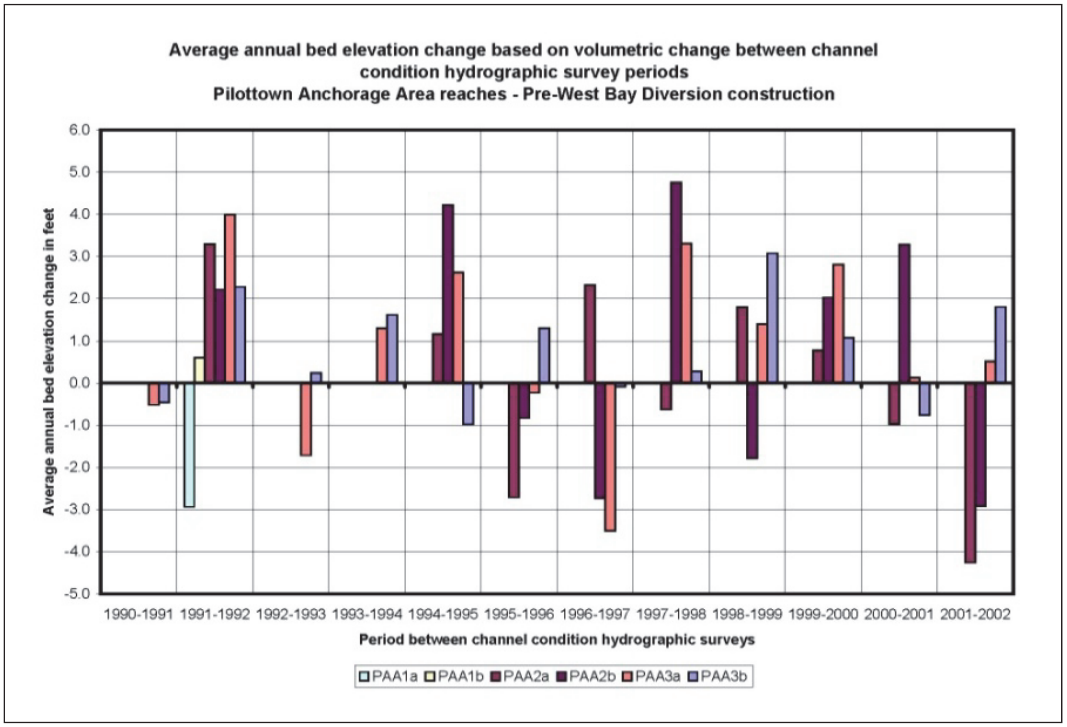

Figure 3.48. Average channel bed displacement based on post-construction channel condition surveys for Pilottown Anchorage Area reaches.

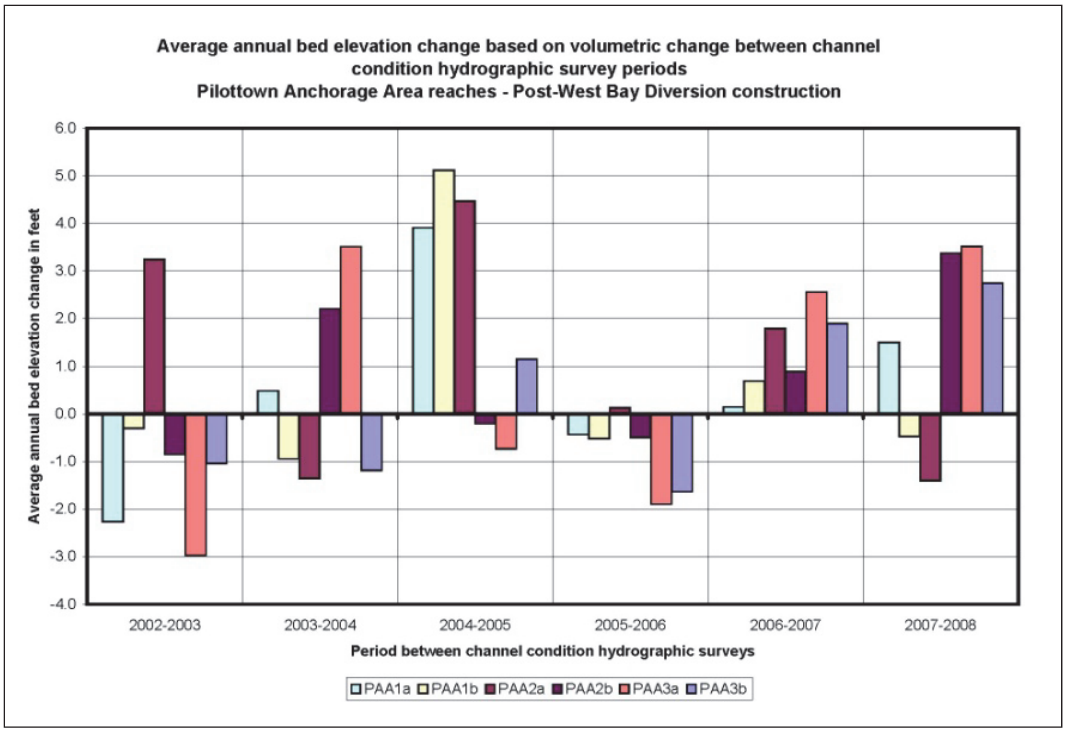

The plots of the average channel bed elevations for the comprehensive surveys shown in Figure 3.49 indicate some fluctuation from survey period to survey period, but display an overall general increase in channel bed elevation. Also, the plot illustrates how the average channel bed elevation increases from the upstream to the downstream reaches, indicating that the downstream portion of the anchorage area is significantly shallower than the upstream portion. Similar trends are observed from the plot of the channel condition surveys shown in Figure 3.50. In general, the overall trend has been an increase in average channel bed elevation over time and a deeper channel in the upstream portion of the anchorage area than in the downstream anchorage area. The curve for Reach PAA2a, the reach immediately downstream of West Bay diversion, does indicate a slight increase in the rate of bed elevation change observed after the construction of the diversion in 2003. A similar increase is noted for Reaches PAA1a and PAA1b in 2005. The plots for Reaches PAA3a and PAA3b indicate no discernable difference in the rate of average bed elevation before or after diversion construction.

Figure 3.49. Average channel bed elevation computed from volume based on comprehensive surveys for Pilottown Anchorage Area reaches.

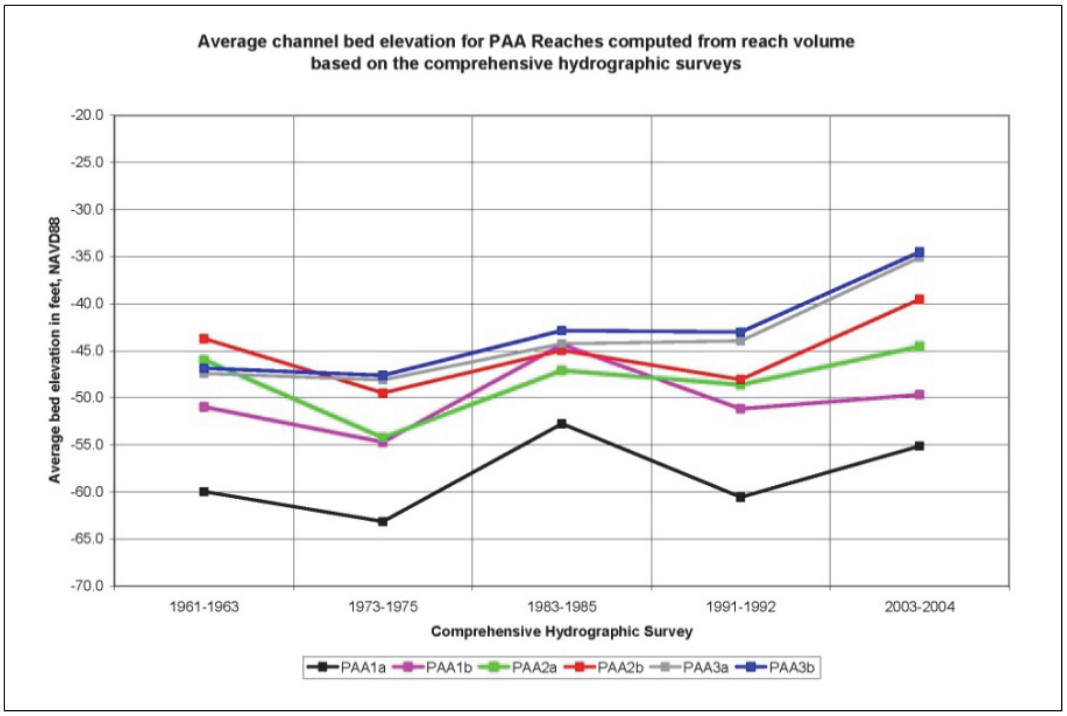

Figure 3.50. Average channel bed elevation computed from volume based on channel condition surveys for Pilottown Anchorage Area reaches.

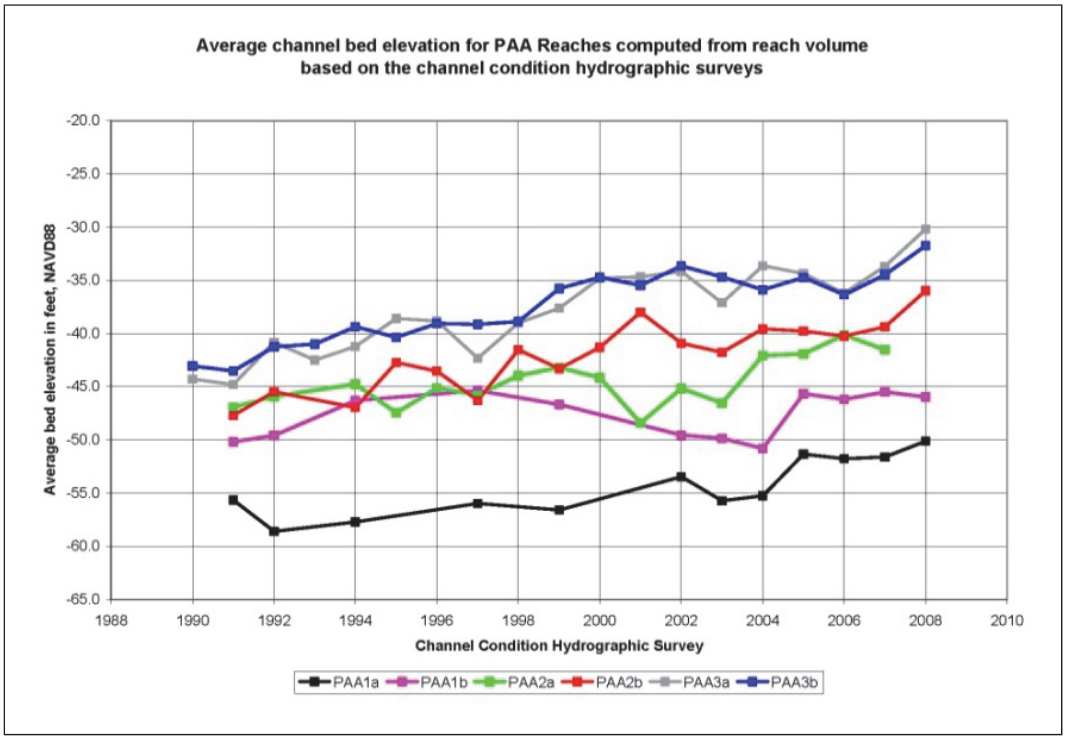

In summary, the results of the volumetric analysis indicate that the trend for the reaches upstream of Venice has been from little change to a slight decrease in the average channel bed elevation. A shift in this trend is observed for the reaches downstream of Venice to Cubits Gap, where the trend has been for a significant increase in channel bed elevation. This agrees well with the results from the cross-section analysis. For the reaches within the PAA, the results also indicate a general increase in channel bed elevation over time. The cumulative change in average channel bed elevation determined from the comprehensive surveys is shown to be approximately 3 times greater for reaches in the downstream portion of the anchorage than reaches in the upstream portion. Also, the results indicate that the channel is significantly deeper in the upstream portion of the anchorage area than in the downstream portion. A slight increase in the rate of change from the pre- to post-construction periods for Reach PAA2a downstream of the diversion was observed. The rate of change in average channel bed elevation for Reaches PAA3a and PAA3b in the downstream portion of the anchorage area appears unaffected by construction of the diversion.

Channel pattern analysis

The comprehensive survey TINs were contoured, and contour tracings for selected elevations were plotted to describe the general location of the river channel within the study area. The channel location tracings were analyzed to determine any trends in channel migration over time. Contours based on the comprehensive, decadal, hydrographic surveys were used for analysis of the entire study reach, and contours based on the quarterly, channel-condition, hydrographic surveys were used for analysis focused in detail on the PAA reach.

Contour tracings from the comprehensive surveys for elevation -45 feet were developed for the entire study reach and are shown in Figures 3.51 through 3.53. The contour tracings shown in Figures 3.51 and 3.52 indicate that the channel location upstream of Venice has been very consistent over time, and no major shifts in pattern are noted. This is not surprising, as the channel has been effectively locked in place with revetments. The sinuosity of the Mississippi River in the study area is very minor, and only slight variations in channel location are observed within the top banks. Channel widths at the -45 foot contour are 80 percent or more of overall top bank widths. Beginning downstream of Venice, a slight alternating point bar pattern can be observed. In addition, the channel downstream of Venice

Figure 3.51. Channel location tracings of the -45-ft contour based on the comprehensive surveys from Belle Chase to near Venice.

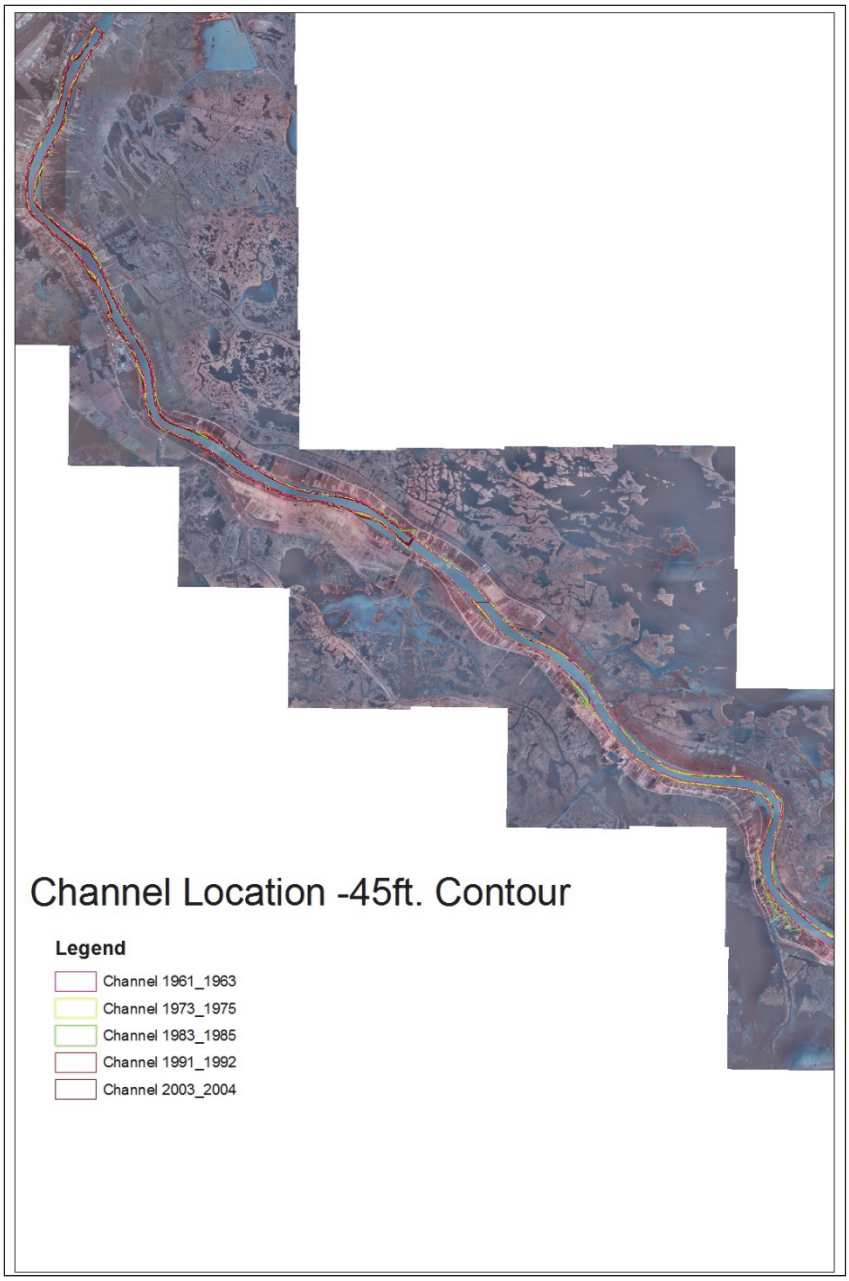

Figure 3.52. Channel location tracings of the -45-foot contour based on the comprehensive surveys from Venice to near Head of Passes.

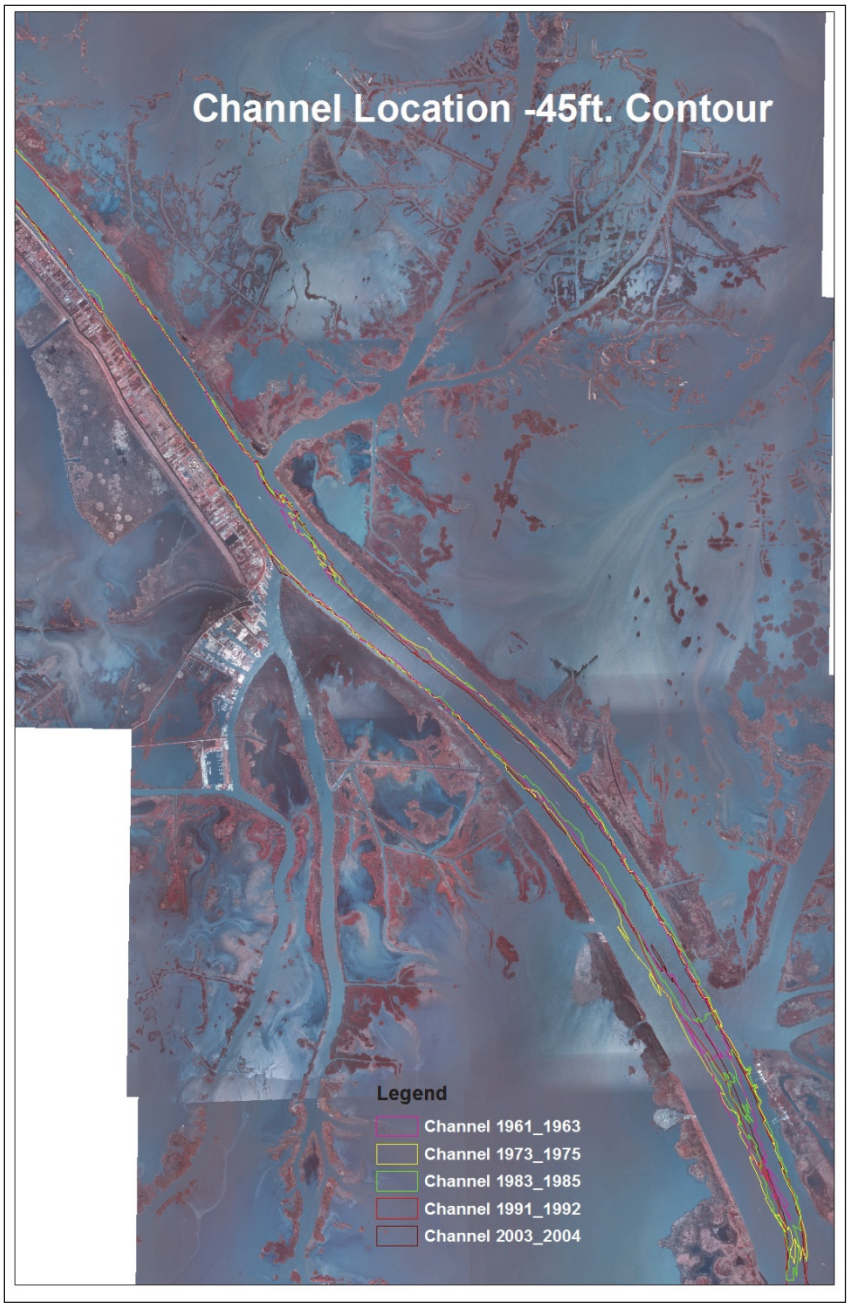

Figure 3.53. Channel location tracings of the -45-ft contour based on the comprehensive surveys from Head of Passes to East Jetty.

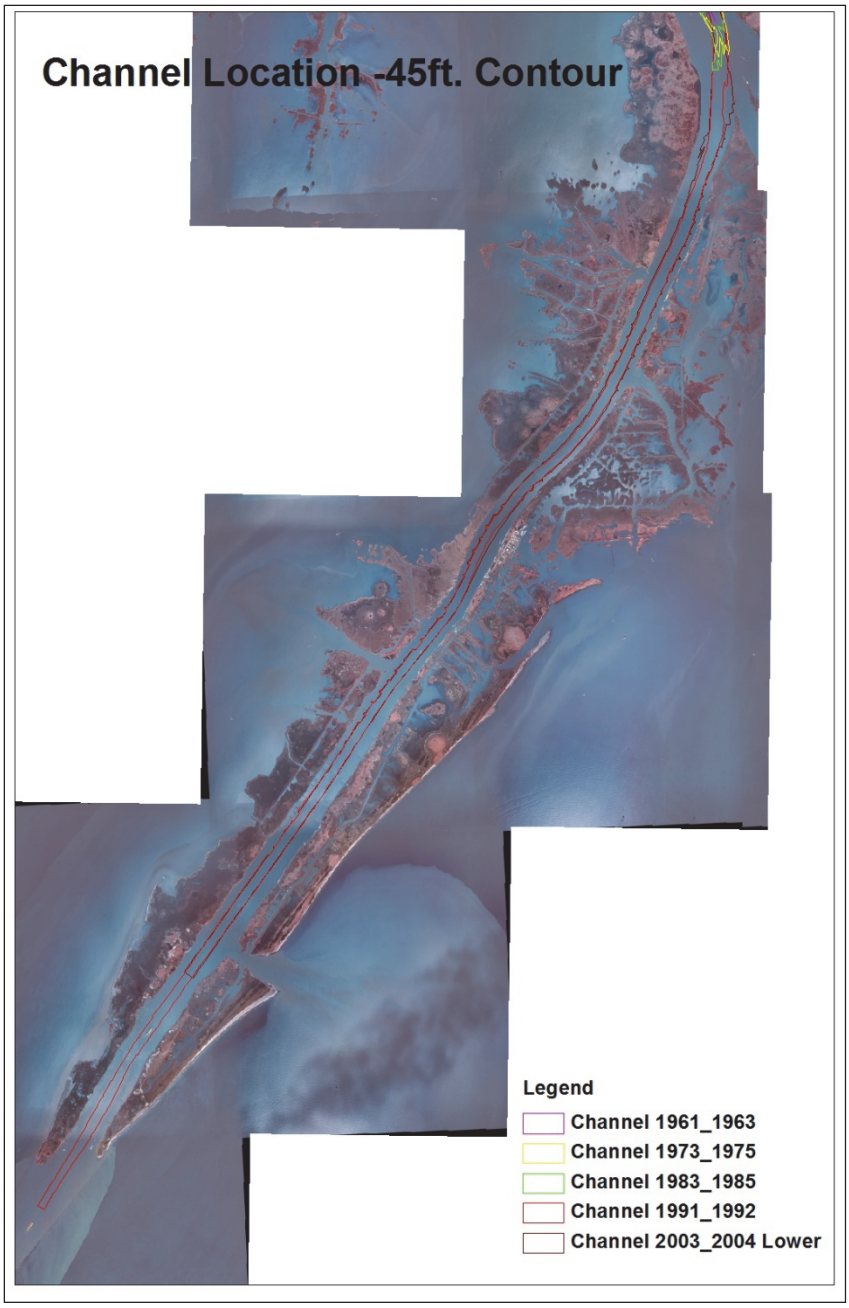

generally appears to be narrower than the channel upstream of Venice. Downstream of Venice, the channel is located along the right descending bank, and a lateral bar is present along the left descending bank. Cross sections in this area also indicate these features. Channel width at the -45 foot contour is approximately 50 percent of the top bank width at this location. The river channel continues along the right descending bank until a crossing begins in the vicinity near the upstream limit of the anchorage

area. The crossing occurs as the channel passes through the upstream portion of the anchorage area, and a lateral bar begins to develop along the right descending bank. The channel shifts to the left descending bank in the vicinity between WBSD and Cubits Gap, and remains along the left bank until it shifts westward to enter Southwest Pass. Contours at elevation -45 feet between Cubits Gap and HOP are fairly irregular because of depths less than -45 feet prior to the deepening of the navigation project. Within Southwest Pass the channel location varies little, indicative of the effects of regular navigation dredging in the pass.

Contour tracings for elevations of -40 feet and -30 feet were also developed from the quarterly channel condition surveys for the analysis that focused in detail on the PAA. These contours were selected to provide better visualization of the development of the lateral bar along the right descending bank within the PAA. Contours developed from the comprehensive surveys of 1964 and 1992 were also plotted to give some reference to historical depths within the PAA. The contour tracings focused on the PAA are shown in Figures 3.54 through 3.57. The contour tracings are shown in several plots rather than one plot for all years for clarity.

Analysis of the portion of the PAA upstream of WBSD indicates the location of the -40 foot and -30 foot contours has been fairly consistent. Contour locations along the right descending bank show slight variation for the -40 foot contour, but no real discernible trends. Location of the shallower -30 foot contour along the right descending bank has been very consistent, particularly from the late 1990s to present. Contours along the left descending bank in this portion of the PAA are very consistent for both specific elevations.

For the portion of the PAA from WBSD to Cubits Gap, the analysis indicates there is variability in the location of the contours for the specific elevations within the PAA. The plots indicate the contours in the vicinity immediately upstream of Cubits Gap shifted noticeably toward the left descending bank beginning with the October 1999 survey, indicating a reduction in depths for this area. This shift was observed to continue for surveys up until the time of West Bay construction (September 2003 survey). For surveys subsequent to construction of West Bay Diversion, the -30 foot contours in the area immediately upstream of Cubits Gap shift toward the left descending bank and remaining in that position fairly consistently. This indicates that the upper slope of the lateral bar along the right descending bank has shoaled

and reduced depths. The -40 foot contour in the area immediately downstream of WBSD also shifted toward the left descending bank after diversion construction, indicating potential depth reduction due to shoaling. The variability in the data makes it difficult to determine diversion related impacts with certainty, as the -40 foot contour shift back and forth in later surveys.

Figure 3.54. Channel location tracings of the -40 foot and -30 foot contours based on the channel condition surveys for the detailed focus on the Pilottown Anchorage Area (1964 to 1999).

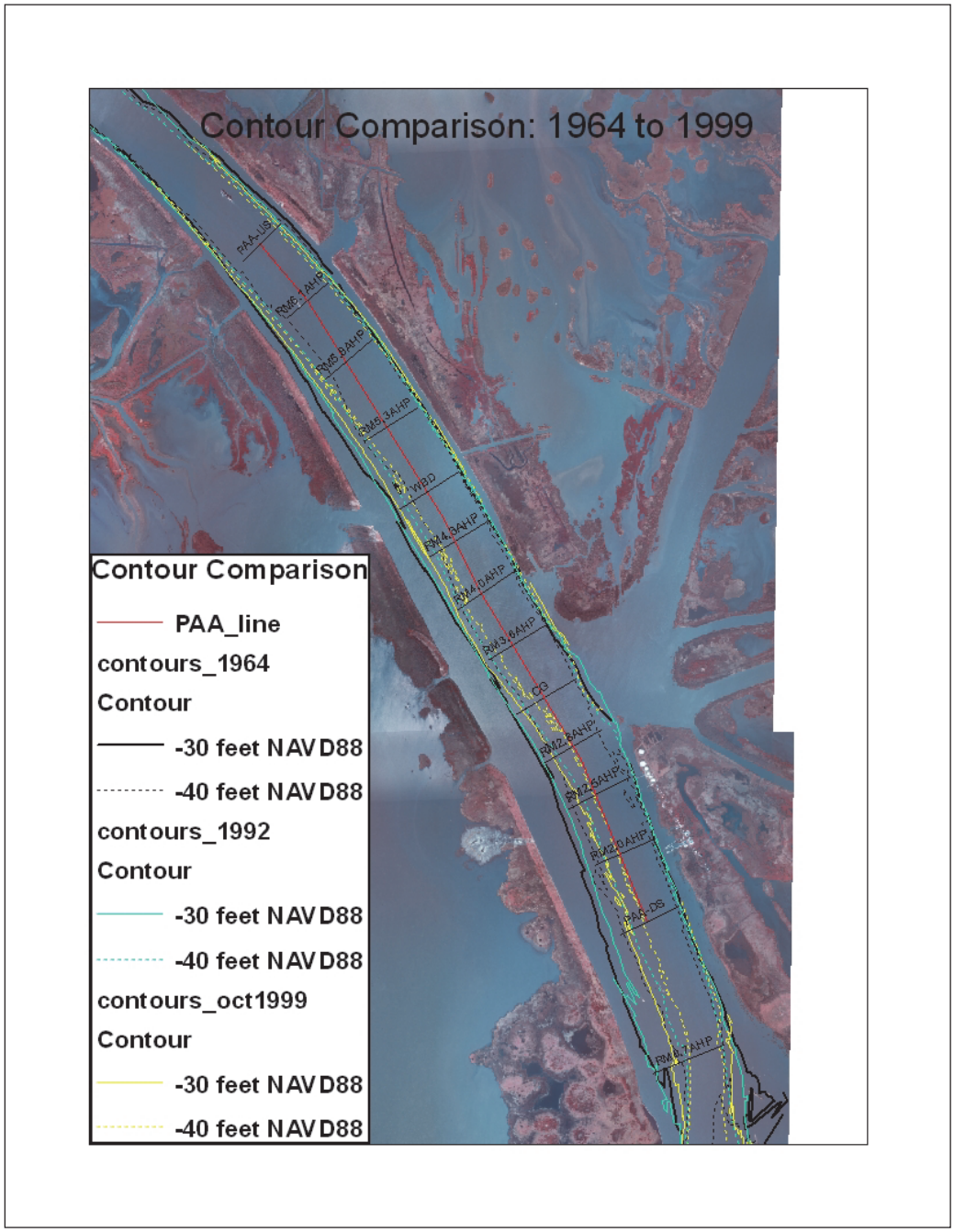

Figure 3.55. Channel location tracings of the -40 foot and -30 foot contours based on the channel condition surveys for the detailed focus on the Pilottown Anchorage Area (1999 to 2003).

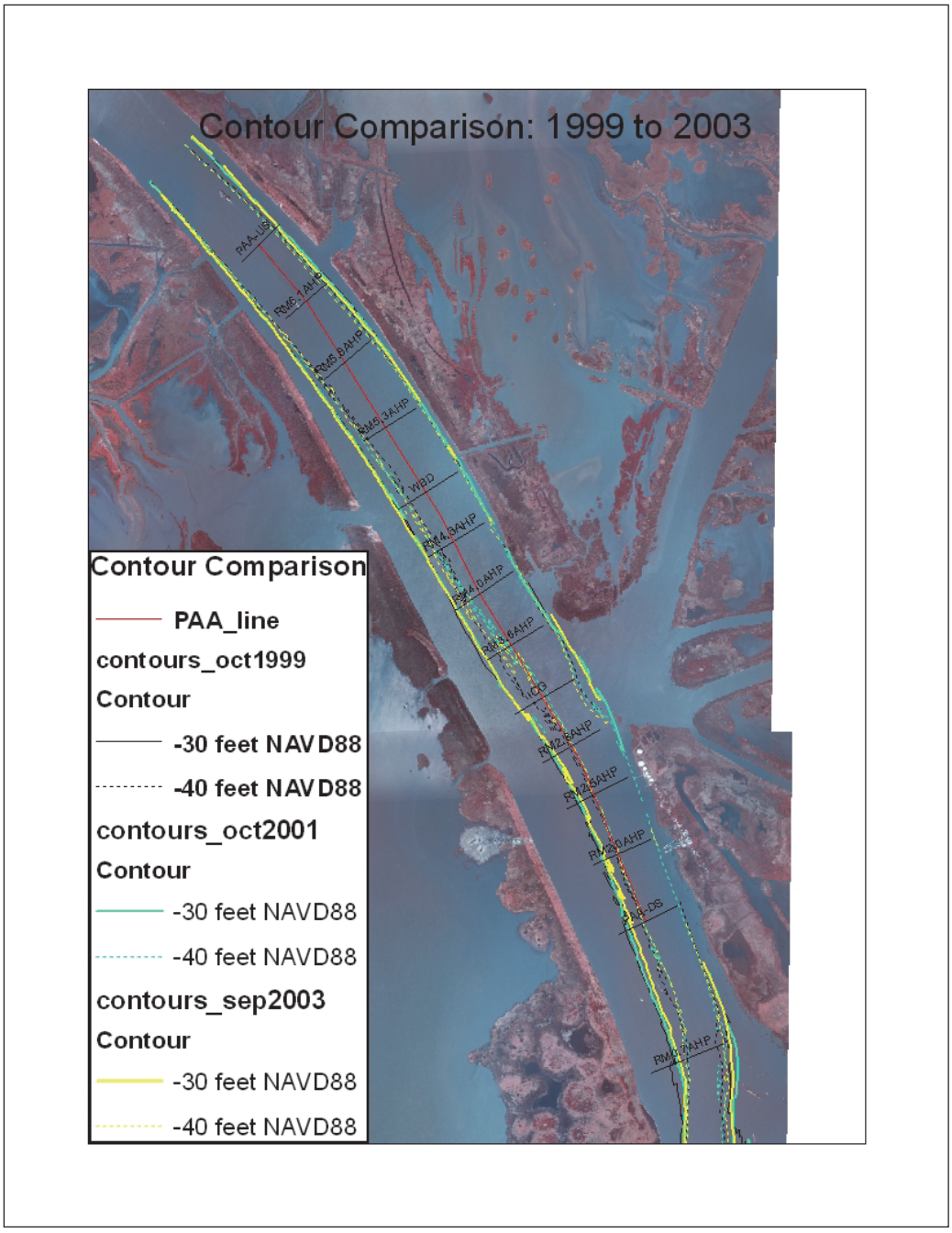

Figure 3.56. Channel location tracings of the -40 foot and -30 foot contours based on the channel condition surveys for the detailed focus on the Pilottown Anchorage Area (2004 to 2006).

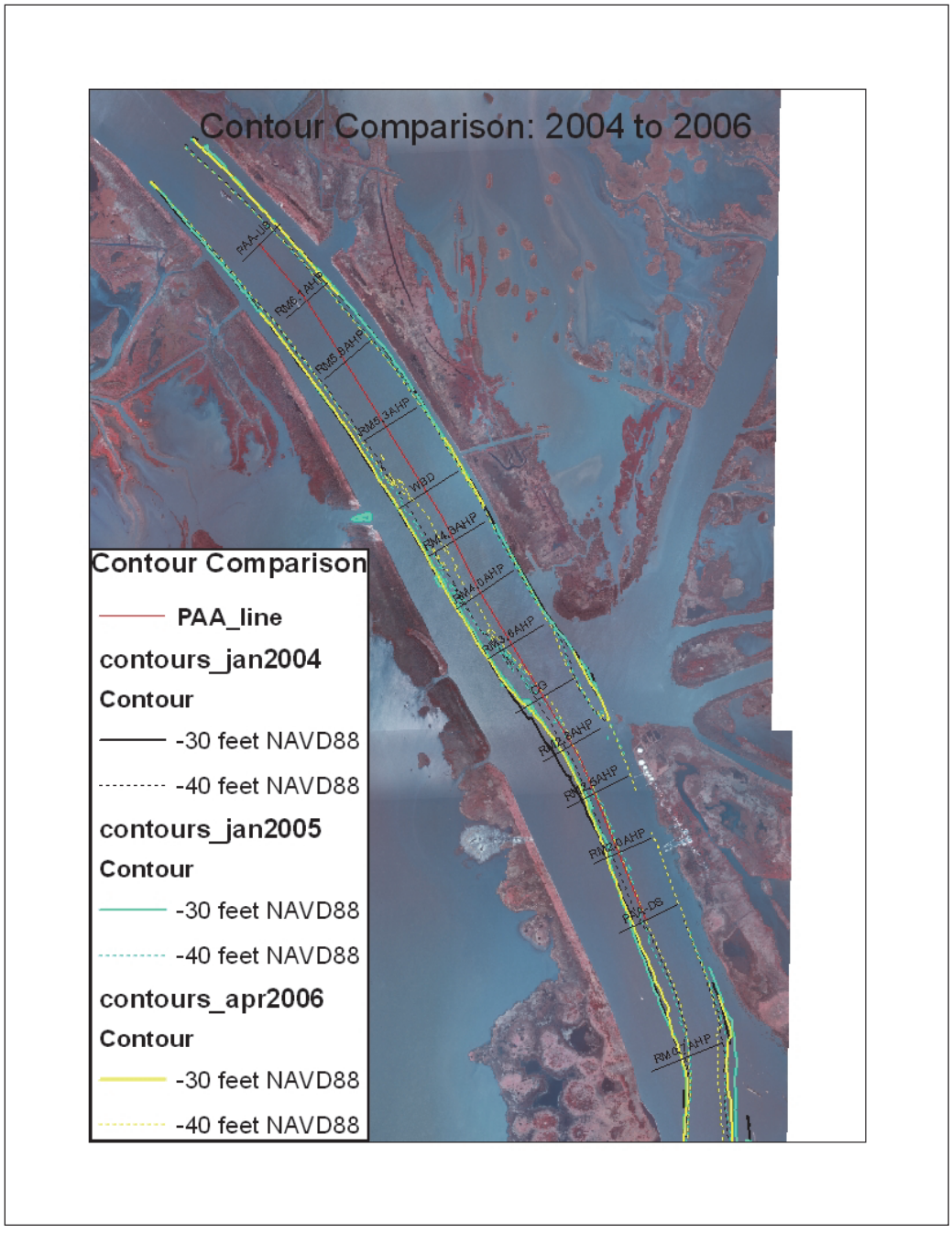

Figure 3.57. Channel location tracings of the -40-foot and -30-foot contours based on the channel condition surveys for the detailed focus on the Pilottown Anchorage Area (2006 to 2008).

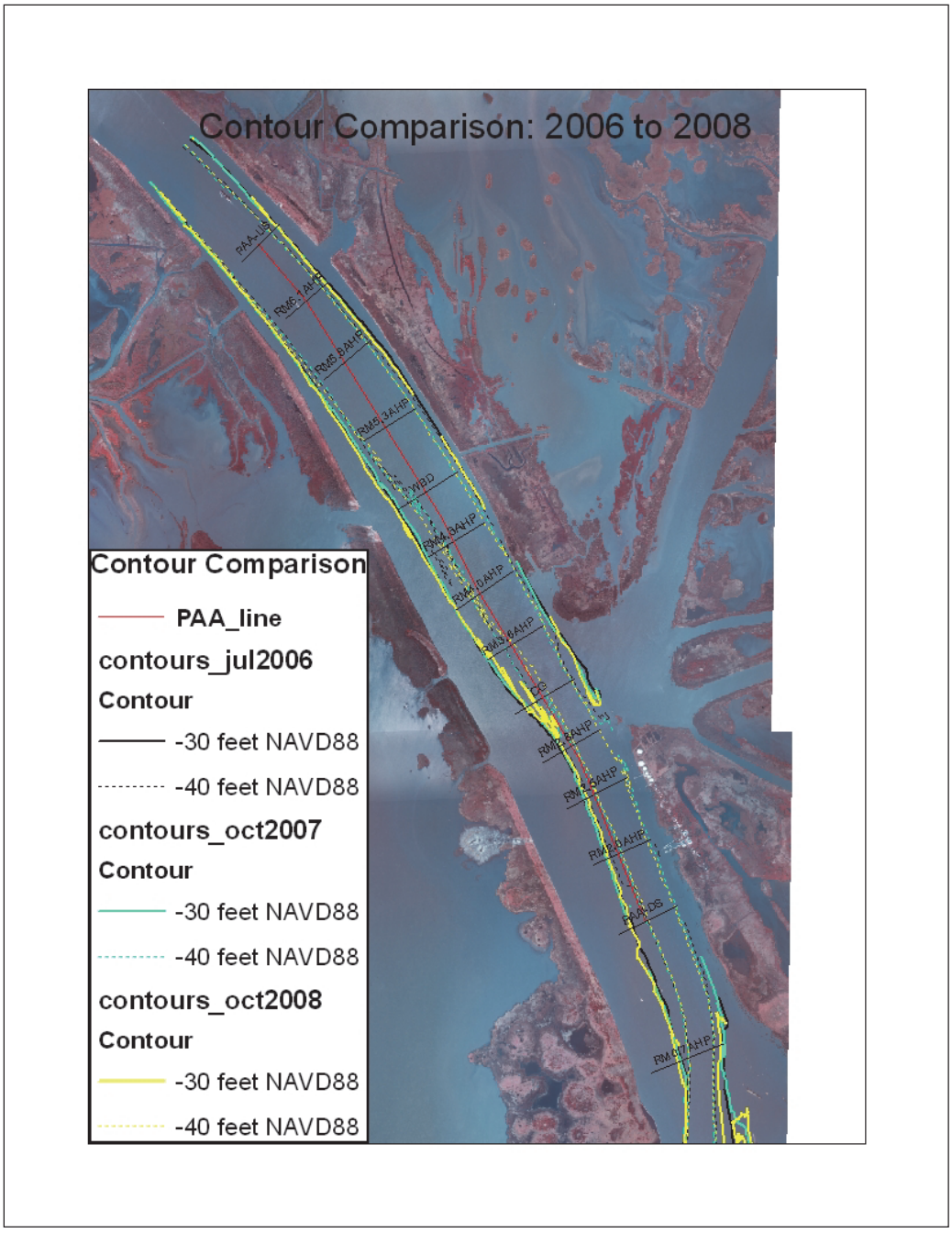

For the portion of the PAA downstream of Cubits Gap, the contour analysis indicates a very distinct and interesting trend. Compared to the 1964 survey, the contours for the 1992 and October 1999 surveys indicate a significant shift toward the left descending bank. Both the -40-foot and -30-foot contours exhibit this shift, indicated shoaling of the lateral bar and reduction of depths in the PAA. From the October 1999 survey to the September 2003

survey prior to diversion construction, the -40-foot contour has shifted all the way to the PAA line, indicating that depths no greater than -40 feet NAVD88 existed in this portion of the PAA prior to diversion construction. The -30-foot contour shift indicates that the entire lateral bar was building during this period. In Figure 3.56, the effect of the dredge event associated with diversion construction can readily be seen as the -40-foot contour for the Jan 2004 survey (dotted black line) shifts back toward the right descending bank. The impacts of the dredge cut are very short-lived, however, as the -40-foot contour shifts back to the PAA line for the January 2005 and April 2006 surveys. The 2006 PAA maintenance dredge event can be seen in Figure 3.57, with the -40-foot contour again is shifted toward the right descending bank. The benefits of the dredge cut are again very brief, as the -40 foot contour is shifted back to the PAA line by the October 2007 and October 2008 surveys. For the portion of the PAA downstream of Cubits Gap, it is clear that significant development of the lateral bar along the right descending bank occurred prior to construction of West Bay Diversion. It appears that this development may be more closely associated with the deepening of the navigation project in the late 1980s. Benefits from dredging efforts in this portion of the PAA have proved to be very short-lived, with rapid filling occurring immediately after the dredge events.

Since interpretation of the contour analysis results presented above is very qualitative in nature, a method was developed to provide a quantitative description of the contour analysis. The PAA was divided into three zones by creating polygons in the GIS system. The three polygon zones were from the downstream limit of the PAA to Cubits Gap, from Cubits Gap to West Bay Diversion, and from WBSD to the upstream limit of the PAA. The polygons were constructed to cover the area from the PAA line to near the right descending bank line. These polygons were then intersected with the contour lines for -40 feet and -30 feet, and the encompassed area within the polygons for each contour was computed. In effect, this exercise determined the portions of each polygon zone that correspond to minimum depths described by the location of the -40-foot and -30-foot contours. The computed surface areas were then plotted versus time to determine trends for each zone. Change in the computed areas with time can be interpreted as reduction in minimum depths because of shoaling within the PAA.

The result of this analysis for the -40-foot contour is shown in Figure 3.58. The plot indicates that for the zone from the downstream PAA to Cubits Gap, the area containing depths of at least -40 feet NAVD88 begin to diminish

Figure 3.58. Computed surface area for minimum depth based on the -40-foot contour for three zones of the PAA.

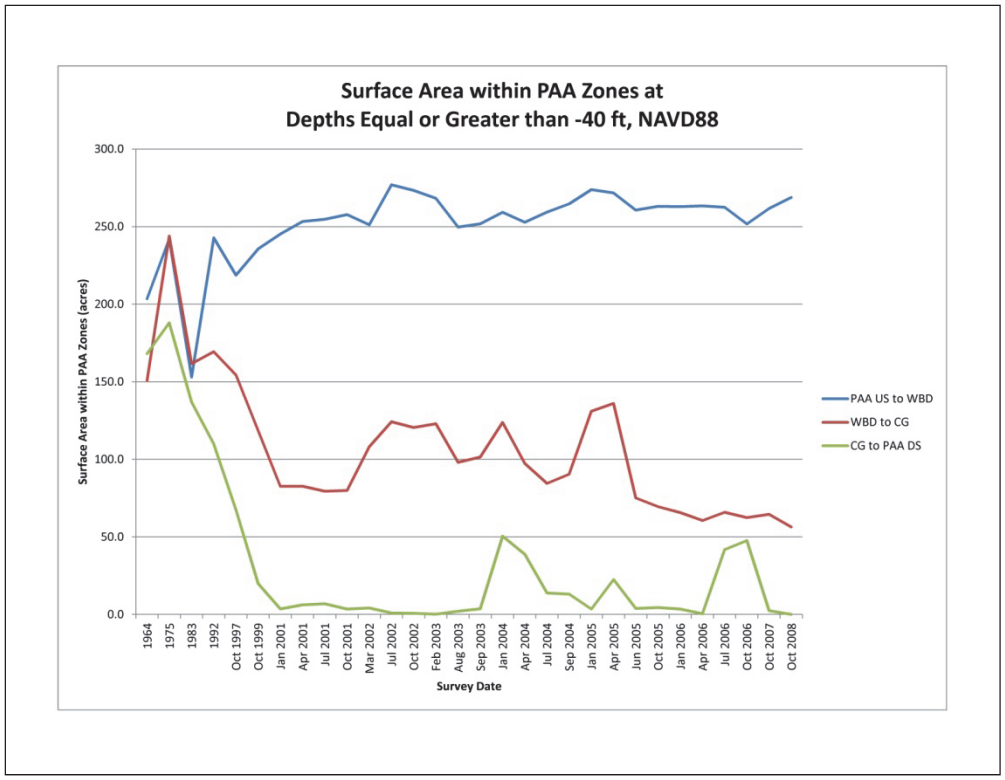

significantly in the 1990s. By the time of the January 2001 survey, there was practically no area within this zone of the PAA with a depth of -40 feet or greater. An increase in area for this elevation can be seen at the time of the January 2004 and July 2006 surveys that corresponds to the dredge events in the PAA. The area quickly diminishes because of shoaling after the dredge events, as has been demonstrated in other analyses. This plot supports the previously determined trend that shoaling and development of the lateral bar within the portion of the PAA downstream of Cubits Gap had occurred prior to construction of West Bay Diversion. In addition, the plot indicates that there is no observable change in this trend because of construction of the diversion. For the zone of the PAA from Cubits Gap to West Bay Diversion, reduction in surface area corresponding to minimum depths of -40 feet NAVD88 also occurred prior to diversion construction, although not to the degree as seen in the downstream zone. There is a slight indication of continued reduction of minimum depth area subsequent to diversion construction, particularly for the 2005 to 2008 time frame. This gives some indication that shoaling and depth reduction in this zone may have been increased because of diversion construction, but with a degree of uncertainty. Interestingly, the surface area for a minimum depth of -40 feet

within the portion of the PAA upstream of WBSD increased slightly over the same time period. The reasons for this are unclear, though the most likely reason is a slight shift in the channel crossing that occurs in this zone.

The result of the analysis for the -30-foot contour is shown in Figure 3.59. The -30 foot contour location gives an indication of how the slope of the lateral bar has developed closer to the right descending bank. As seen in Figure 3.59, the surface area at the -30-foot contour for all three zones declined during the 1990s after the deepening of the navigation project. Around 2001 this decline in surface area ceased for the zones from the upstream limit of the PAA to Cubits Gap. Since that time the surface area has been very stable. This indicates that there was shoaling and depth reduction possibly associated with the change in the navigation project but no discernible impacts due to diversion construction. For the PAA zone downstream of Cubits Gap, the rate of reduction in surface area at the -30-foot contour slowed noticeably around 2001 but continued to decline at a slower rate until 2008. This indicates that the upper slope of the lateral bar continues to build but at a much lower rate. There are no discernible changes in the rate of surface area reduction associated with diversion construction.

Figure 3.59. Computed surface area for minimum depth based on the -30-foot contour for three zones of the PAA.

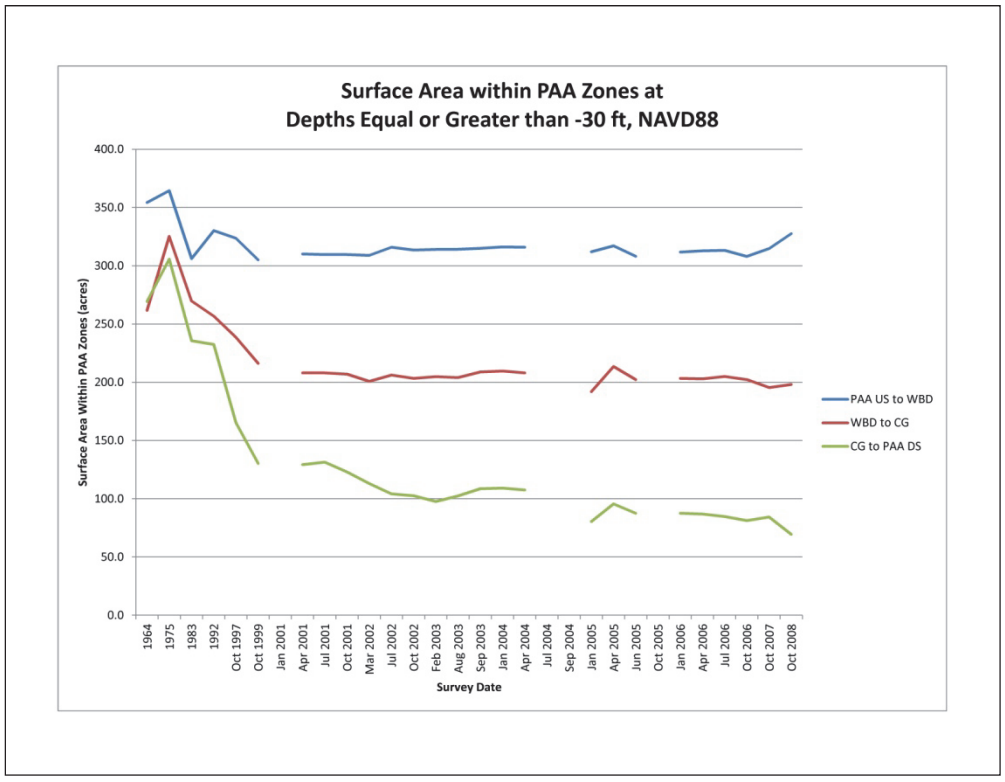

A summary of the results of the surface area for specific contours analysis is shown in Table 3.4. Using changes in surface area at a given contour elevation as an indication of deposition or scour, this analysis shows that the portion of the PAA immediately adjacent to the navigation channel has changed significantly over time. It appears that significant shoaling occurred in this area soon after the deepening of the navigation project, particularly for the PAA zone downstream of Cubits Gap. Based on this analysis, there was basically no area within the PAA zone downstream of Cubits Gap that had depths greater than -40 feet NAVD88 prior to construction of West Bay Diversion. Dredge activity within this zone is also shown to be very short-lived. Whether or not the rate of shoaling after PAA dredge events is impacted by WBSD is difficult to determine.

Table 3.4. Computed surface area at given elevations for Pilottown Anchorage Area zones.

	Computed Surface Area at a Given Elevation for Pilottown Anchorage Area Zones (Area in Acres)					
	-40-foot NAVD88 Contour			-30-foot NAVD88 Contour		
Survey Date	Upstream PAA to WBD	WBD to Cubits Gap	Cubits Gap to Downstream PAA	Upstream PAA to WBD	WBD to Cubits Gap	Cubits Gap to Downstream PAA
1964	203.6	150.7	168.1	354.3	261.7	269.4
1975	242.1	244	188.1	364.5	325.4	305.8
1983	153	161.7	136.9	306.1	269.8	235.7
1992	242.8	169.4	110	330.2	256.8	232.5
Oct 1997	218.8	154.4	67.6	323.6	238.5	165.2
Oct 1999	235.7	118.5	19.9	305.1	216.2	130.3
Jan 2001	245.2	82.6	3.6			
Apr 2001	253.4	82.7	6.2	310.2	208	129.3
Jul 2001	254.8	79.5	6.9	309.6	208	131.4
Oct 2001	257.8	80	3.5	309.7	207	123
Mar 2002	251.3	108.1	4.2	309	200.8	113.1
Jul 2002	277	124.2	0.9	316	206.2	104.2
Oct 2002	273.4	120.5	0.7	313.5	203.3	102.6
Feb 2003	268.3	122.9	0.1	314.1	204.8	97.6
Aug 2003	249.8	98.1	2.1	314.2	204	102.5
Sep 2003	251.9	101.5	3.7	315	208.9	108.6
Jan 2004	259.3	123.8	50.5	316.2	209.7	109.1
Apr 2004	252.9	97.4	38.8	315.9	208	107.6
Jul 2004	259.4	84.5	13.8			

Survey Date	Computed Surface Area at a Given Elevation for Pilottown Anchorage Area Zones (Area in Acres)					
	-40-foot NAVD88 Contour			-30-foot NAVD88 Contour		
	Upstream PAA to WBD	WBD to Cubits Gap	Cubits Gap to Downstream PAA	Upstream PAA to WBD	WBD to Cubits Gap	Cubits Gap to Downstream PAA
Sep 2004	264.7	90.4	13.1			
Jan 2005	273.9	131	3.5	312.1	191.9	80.5
Apr 2005	271.8	136	22.5	317.2	213.6	95.6
Jun 2005	260.7	75.1	3.9	308.2	202.3	87.6
Oct 2005	263.1	69.5	4.5			
Jan 2006	262.9	65.7	3.5	311.8	203.3	87.6
Apr 2006	263.4	60.5	0.4	312.9	203	86.9
Jul 2006	262.5	65.9	41.8	313.3	205	84.8
Oct 2006	251.8	62.4	47.6	308	202.3	81.3
Oct 2007	261.7	64.6	2.5	314.8	195.5	84.3
Oct 2008	268.9	56.4	0.0	327.7	198.2	69.4

As a final part of the Channel Pattern Analysis, color contour plots of all hydrographic surveys were plotted for the PAA reach. The plots were used to visualize the overall changes in the channel depths over time. Impacts attributable to WBSD are difficult to determine from this type of analysis. However, the general trend of reduction in overall channel depth for the reach can clearly be detected as well as the development of the lateral bar along the right descending bank. The contours for the 1964 survey shown in Figure 3.60 show that deep water in the -60- to -70-foot range extends from Venice to Cubits Gap. The lateral bar on the right bank exists, but is not very prominent in the downstream portion of the PAA. Figure 3.61 shows the conditions for the 1992 after deepening of the navigation project. Deep water in the -60- to -70-foot range still extends to Cubits Gap, but the lateral bar is beginning to build. By the October 1997 survey shown in Figure 3.62, a significant reduction in overall channel depth had occurred, with the extent of deep water in the -60- to -70-foot range retreating well upstream near the upstream limit of the PAA. Figure 3.63 shows conditions in September 2003 prior to diversion construction. The deep water has retreated upstream of PAA, and overall channel depths are in the -50- to -60-foot NAVD88 range. The development of the right bank lateral bar can also be seen. The contours for the survey in July 2006 as shown in Figure 3.64 indicate even more depth reduction in the river channel upstream of Cubits Gap as well as continued development of the

right bank bar. Finally, the contours for the survey in October 2008 shown in Figure 3.65 indicate channel depths have decreased such that there are very intermittent locations of -50- to -60-foot water upstream of Cubits Gap. The trend of overall channel depth reduction shown in this analysis is thought to be a long term system change. Observations made as part of the cross section analysis also indicate this trend.

Figure 3.60. Contour map of PAA, 1964 survey.

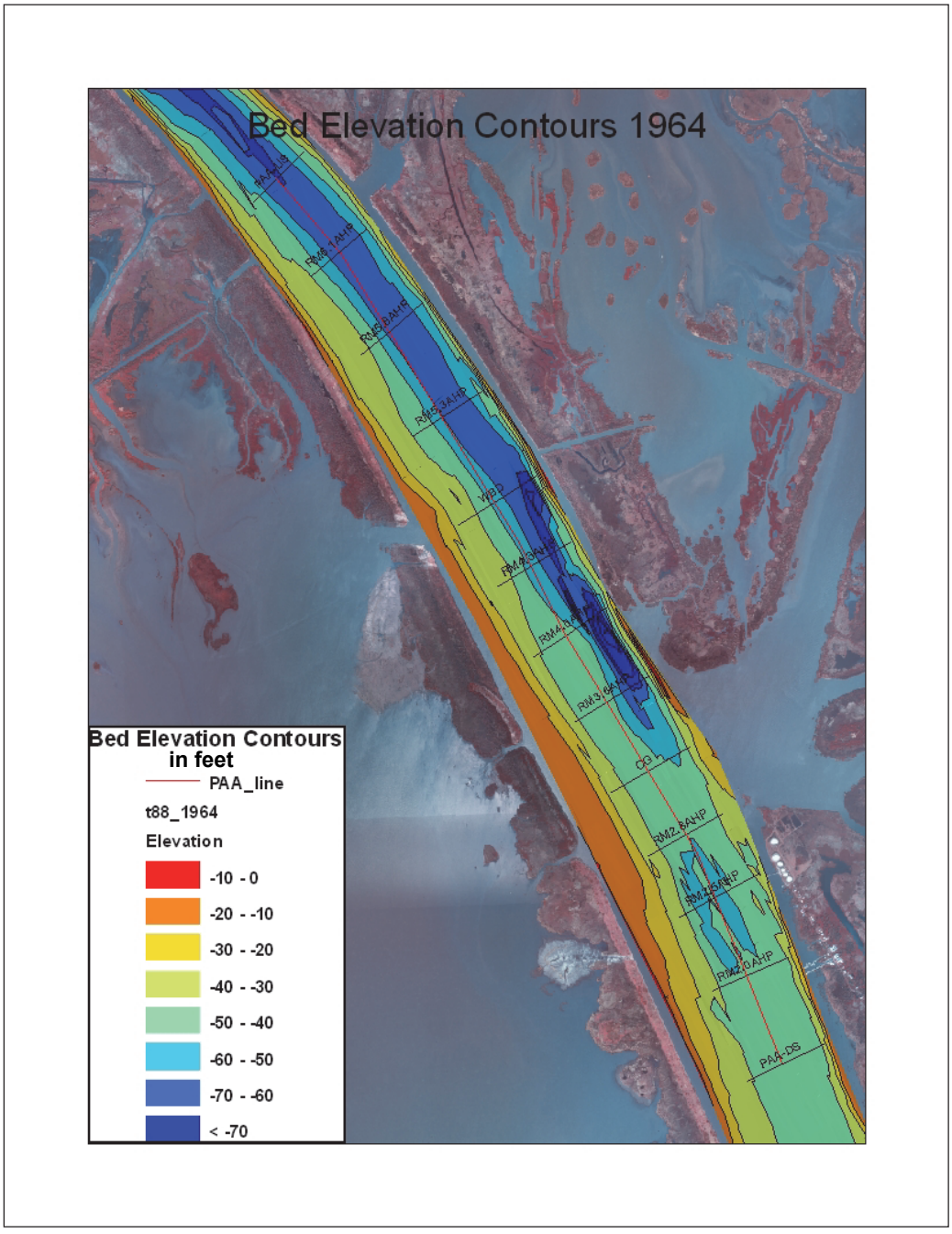

Figure 3.61. Contour map of PAA, 1992 survey.

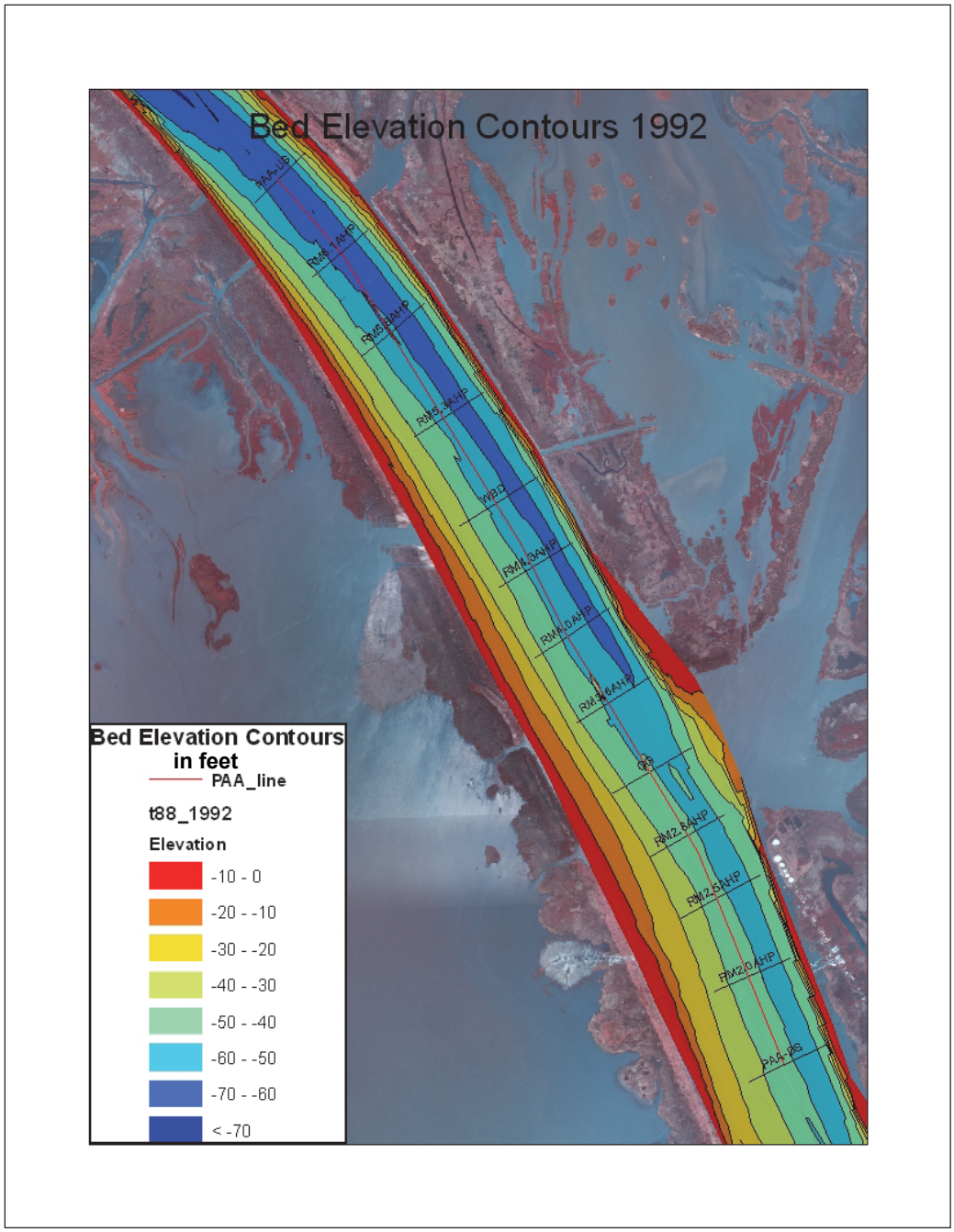

Figure 3.62. Contour map of PAA, October 1997 survey.

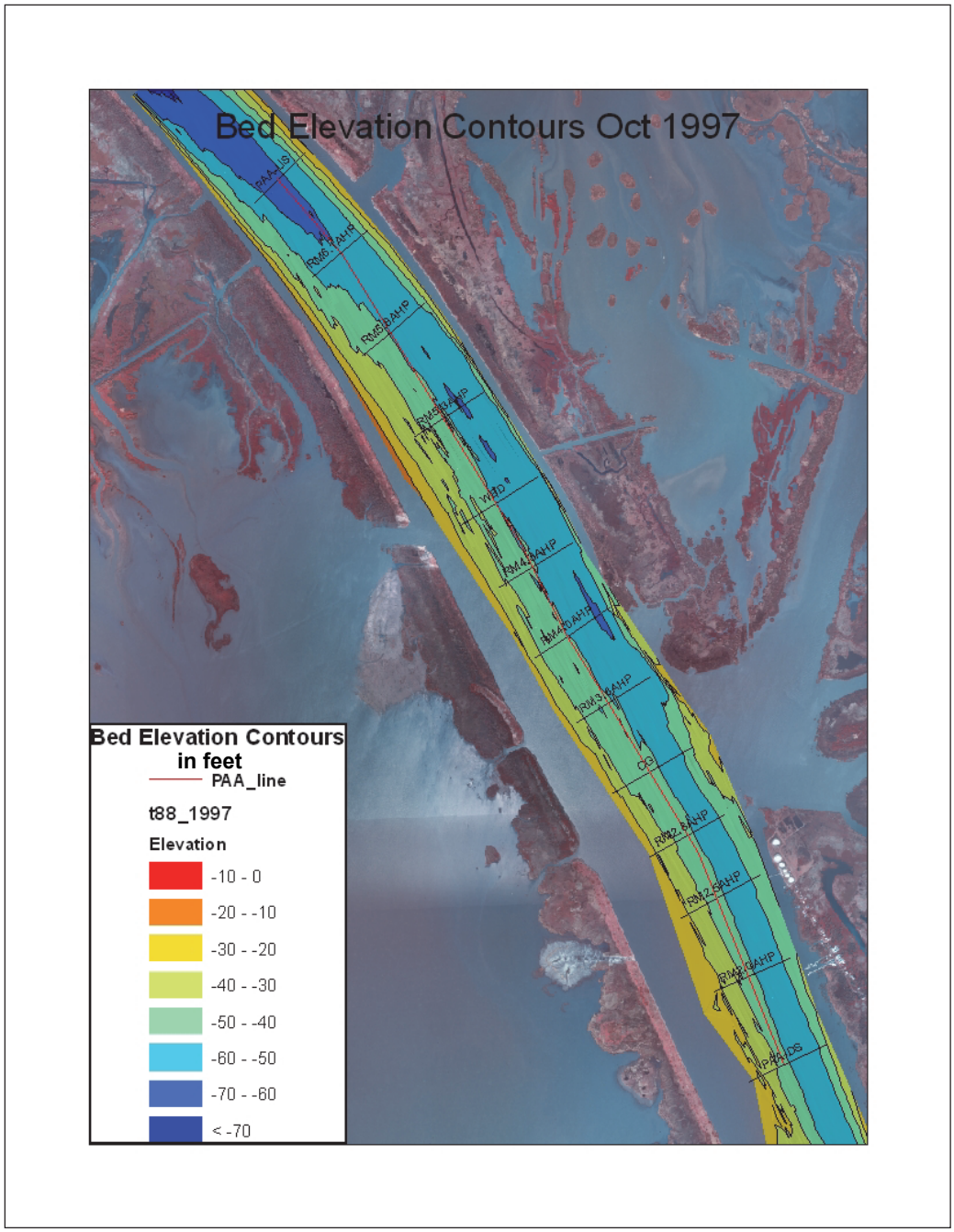

Figure 3.63. Contour map of PAA, September 2003 survey.

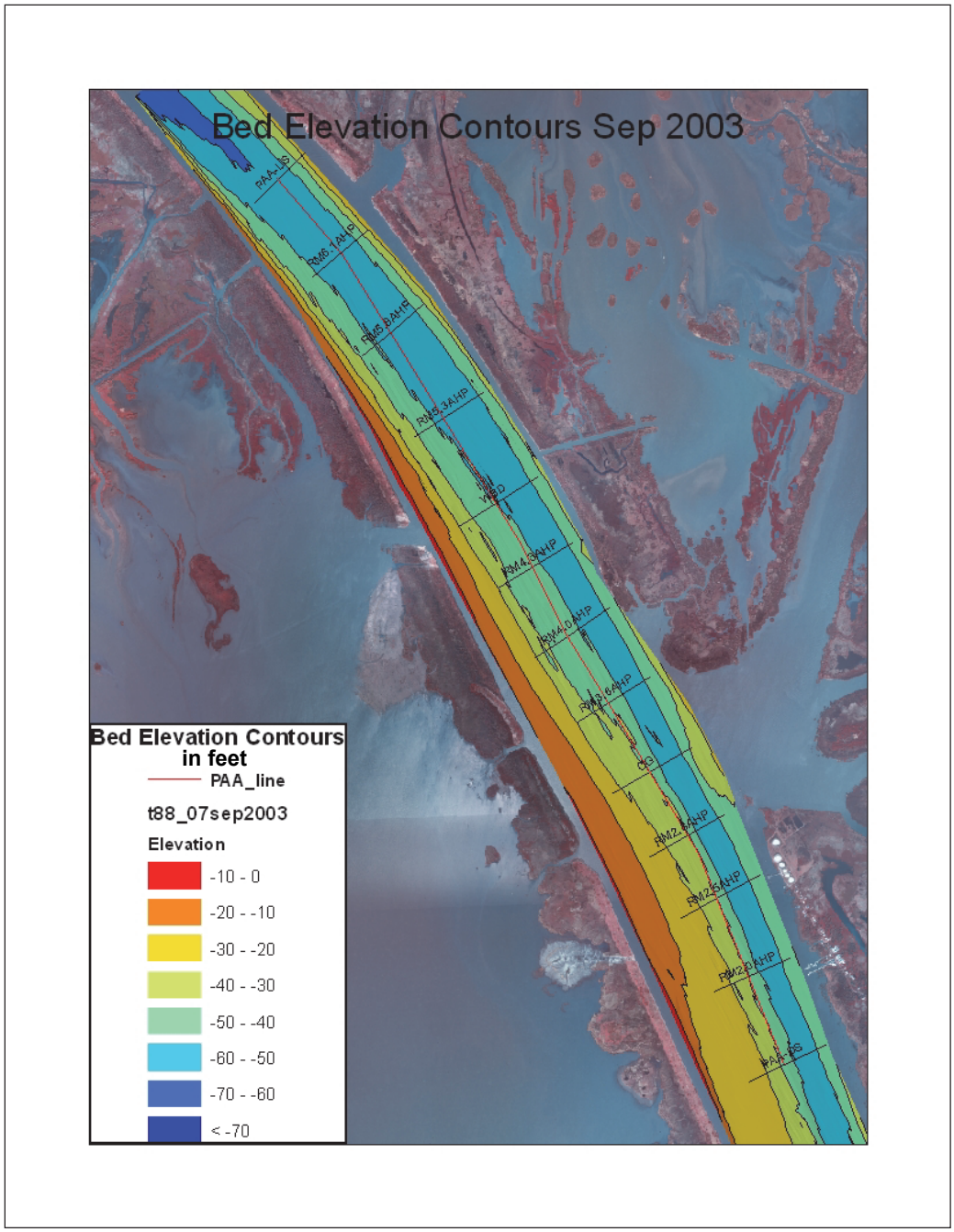

Figure 3.64. Contour map of PAA, July 2006 survey.

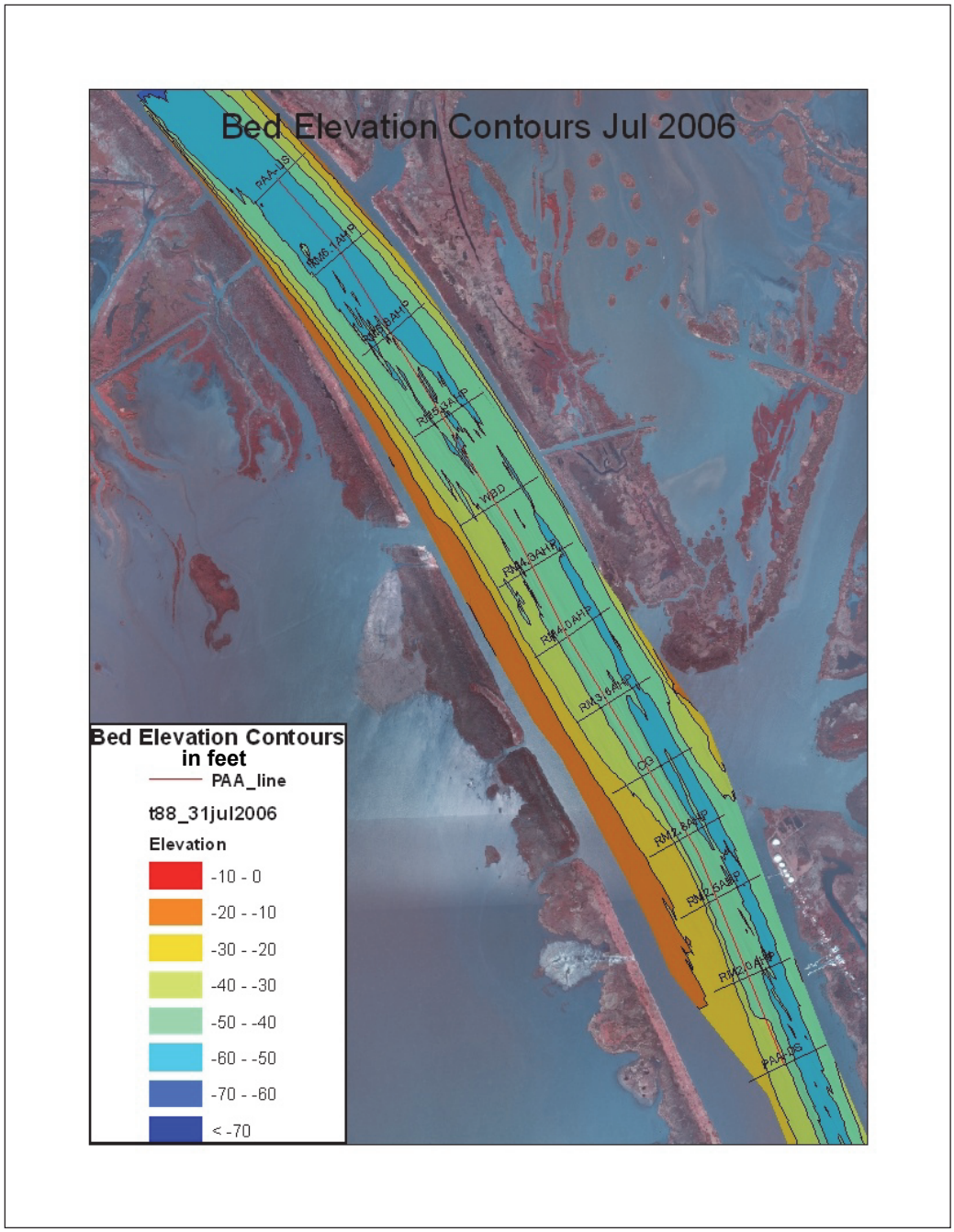

Figure 3.65. Contour map of PAA, October 2008 survey.

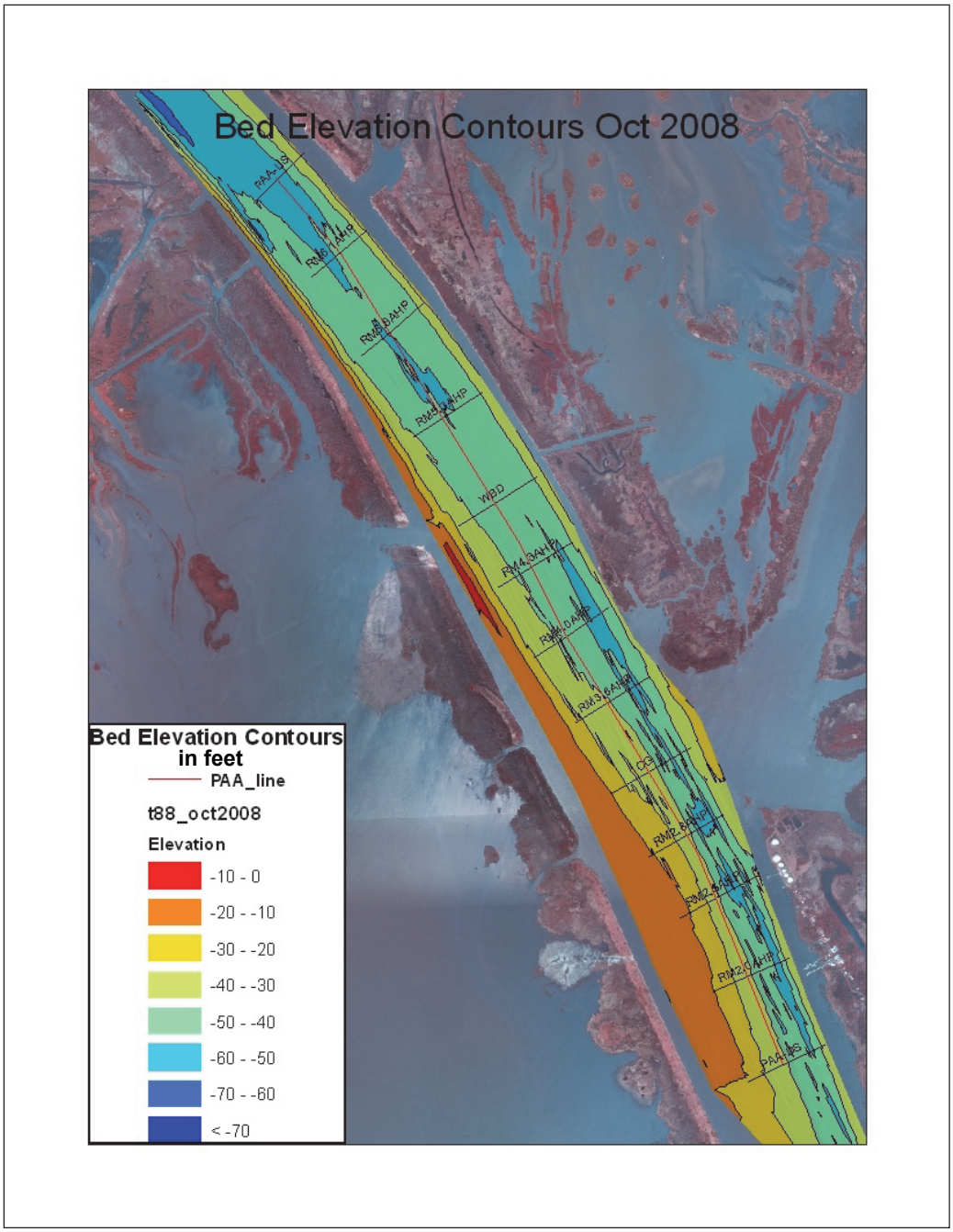

Gauge/Discharge/Sediment Data Analysis and Results

Discharge Data Analysis

Discharge observation data for the Mississippi River, distributaries and passes in the study reach were obtained from MVN published reports and databases. The historic discharge data in the published reports contained miscellaneous measurements at various stations for the years 1960 through

1998. Published measurements were obtained for the Mississippi River at Venice, Baptiste Collette, Grand Pass, Cubits Gap, Southwest Pass, South Pass, and Pass a Loutre. From the MVN databases, discharge measures at the above mentioned stations plus WBSD were obtained. Computed daily discharge at Tarbert Landing was also obtained. These discharge data were analyzed to determine the distribution of discharge for the passes, distributaries, and diversions in the lower Mississippi River, and to determine if any trends or changes in discharge distribution can be observed.

Computations were made for the discharge of the passes and distributaries as a fraction of the discharge at Venice and at Tarbert Landing. Tarbert Landing discharge was used because daily discharge was available that more readily corresponded to the dates of the discharge measurements of the distributaries. The discharge fraction values were plotted to determine if any changes to the capacities of the distributaries has occurred over the study period.

The discharge for Baptiste Collette and Grand Pass as a fraction of discharge at Venice and Tarbert Landing is shown in Figures 3.66 and 3.67, respectively. As seen in Figure 3.66, the percentage of the Mississippi River discharge carried by Baptist Collette and Grand Pass is very similar throughout the study time period. The percent of discharge in the 1960s was approximately 3 to 4 percent of Venice discharge, and the percentage began increasing in the 1970s to approximately 10 to 12 percent at the present time. Figure 3.67 indicates a similar trend of percentages for Tarbert Landing ranging from 3 to 4 percent at the beginning of the study period and now 8 to 10 percent for current conditions.

From the plots it appears that the change in discharge percentage was minimal until the mid-1980s, when the rate of change seemed to increase. This most likely correlates with the enlargement projects for Baptiste Collette and Grand Pass that occurred in the mid to late 1970s. In addition, data from a 1939 study of the Mississippi River passes indicate that the percent of discharge for these diversions in the 1930s was similar to the percentage at the beginning of the study period. The report (USACE 1939) stated that as a percentage of the mean discharge at New Orleans, Baptist Collette was carrying approximately 2 percent, and Grand Pass (referred to as The Jump) was carrying approximately 3 percent. Although stated as a percentage of New Orleans discharge rather than Venice discharge, this historic data indicate that there had been little change in the discharge distribution for these diversions from the 1930s until the 1960s.

Figure 3.66.Discharge at Baptiste Collette and Grand Pass as a fraction of Venice discharge.

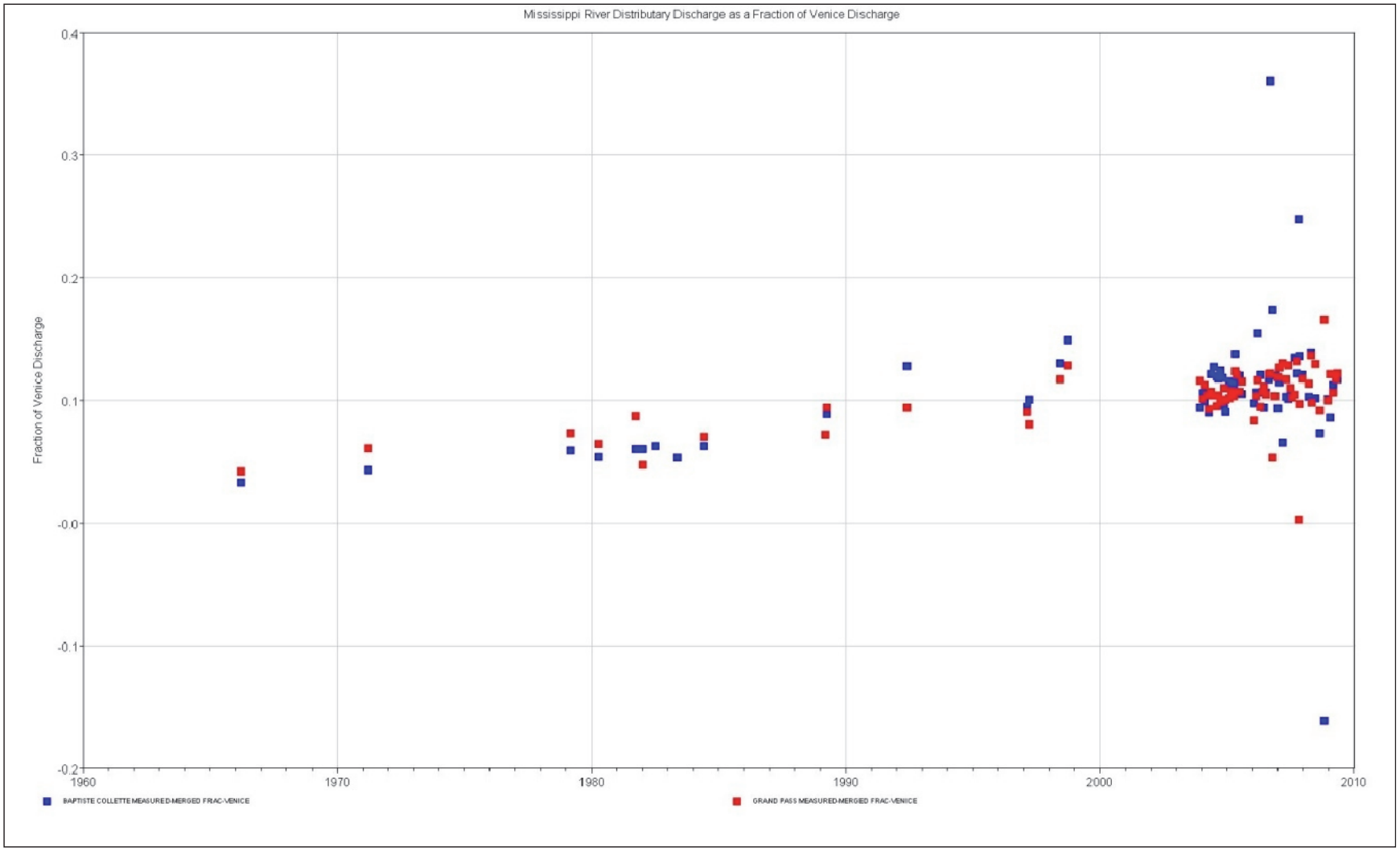

Figure 3.67. Discharge at Baptiste Collette and Grand Pass as a fraction of Tarbert Landing discharge.

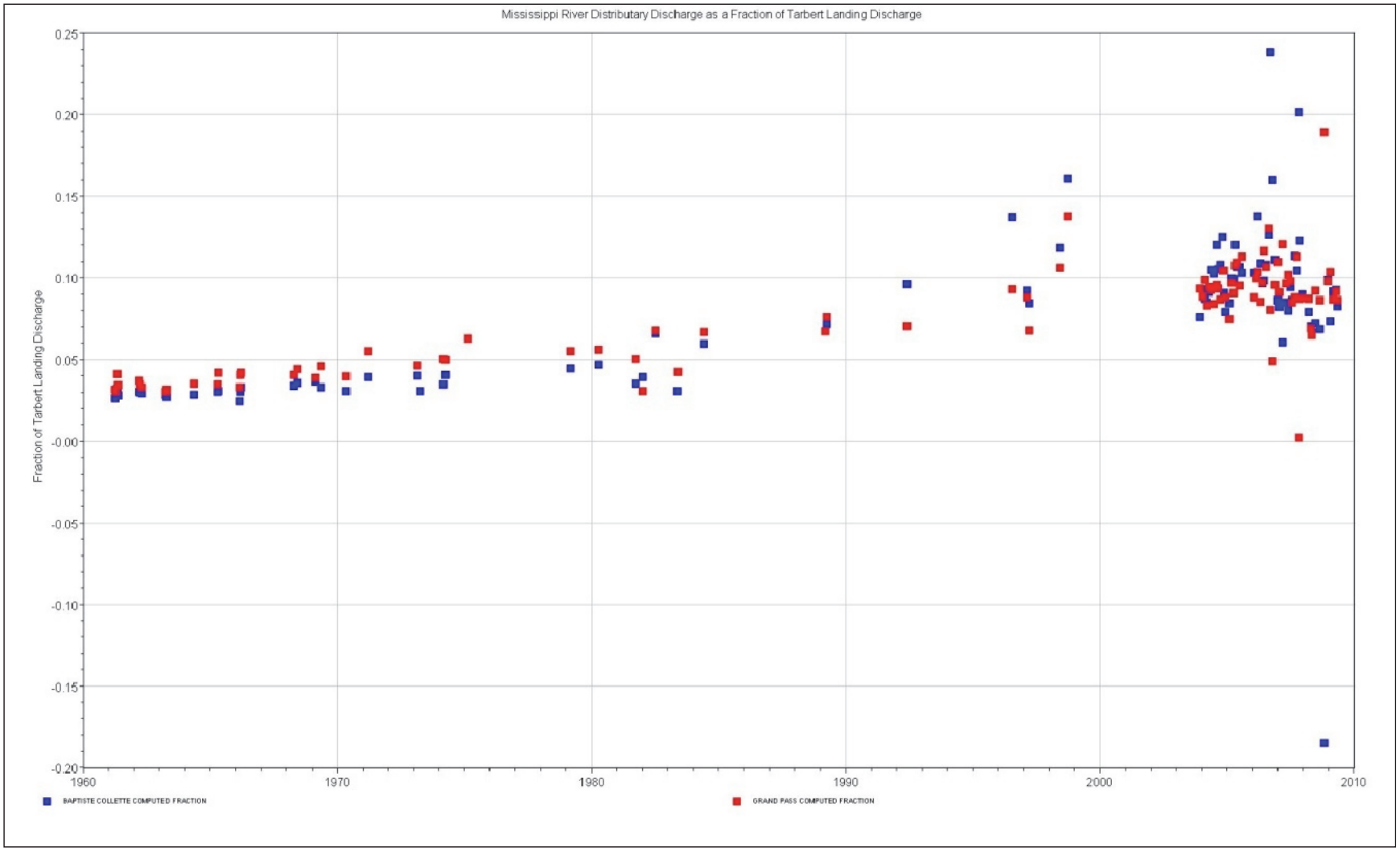

The discharge for Cubits Gap and WBSD as a percentage of discharge at Venice and Tarbert Landing is shown in Figures 3.68 and 3.69. As a percentage of Venice discharge, Cubits Gap has carried approximately 15 percent of the Mississippi River discharge until the construction of the diversion in 2003. At that time, there appears to be a steady decrease to approximately 10 to 12 percent for current conditions. The data for WBSD indicate that the diversion was carrying approximately 2 percent of the discharge immediately after construction, and has increased to approximately 7 to 8 percent for current conditions. It is logical that the percentage at Cubits Gap, or other diversions located downstream of West Bay, would adjust to offset the increase in percent for West Bay as the diversion developed. As a percentage of Tarbert Landing discharge, the discharge at Cubits Gap was approximately 10 to 12 percent with perhaps a slight increase to 13 to 14 percent prior to construction of WBSD. Since then, a reduction of approximately 10 percent has occurred.

The capacity of Cubits Gap as a percentage of New Orleans mean discharge reported by MVN (1939) is approximately 13 percent, indicating little change in the capacity of this outlet prior to the study period.

The capacity of Southwest Pass, South Pass, and Pass a Loutre as a percentage of discharge at Venice and Tarbert Landing is shown in Figures 3.70 and 3.71. These plots indicate that the greatest change in discharge capacity of all the diversions in the Mississippi River delta vicinity occurred at Pass a Loutre. The plots indicate that the outlet capacity as a percentage of Mississippi River discharge for Southwest Pass and Pass a Loutre was very similar at the beginning of the study period, approximately 30 percent. The percent for South Pass was approximately 14 to 16 percent. Beginning in the 1970s until the mid-1990s, a decreasing trend in distribution percentage for Pass a Loutre occurred. Distribution percentage for this outlet decreased to approximately 12 percent. The percentage for South Pass also decreased slightly during this time, and at present, the percentage for South Pass and Pass a Loutre is very similar. The data for Soutwest Pass indicate that the percentage for this outlet was fairly constant over the study period, although there is considerable scatter in the data. The capacity of Southwest Pass as a percentage of Mississippi River discharge is approximately 28 to 30 percent in the beginning of the study period and increases to approximately 35 to 40 percent for current conditions. This increase is most likely associated with the increase in the navigation project depth from -40 to -45 feet MLG that occurred in the late 1980s.

Figure 3.68. Discharge at Cubits Gap and WBSD as a fraction of Venice discharge.

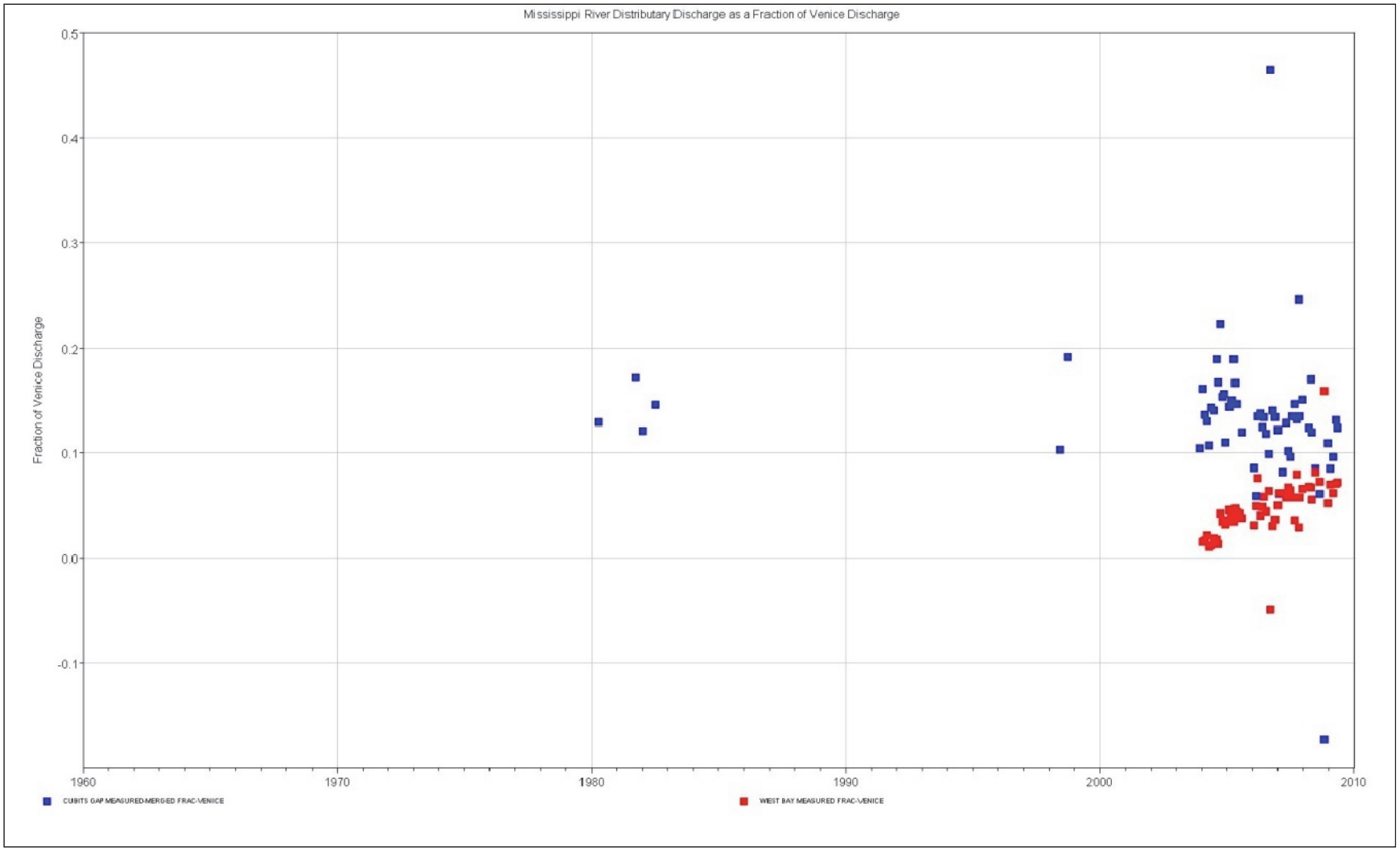

Figure 3.69. Discharge at Cubits Gap and WBSD as a fraction of Tarbert Landing discharge.

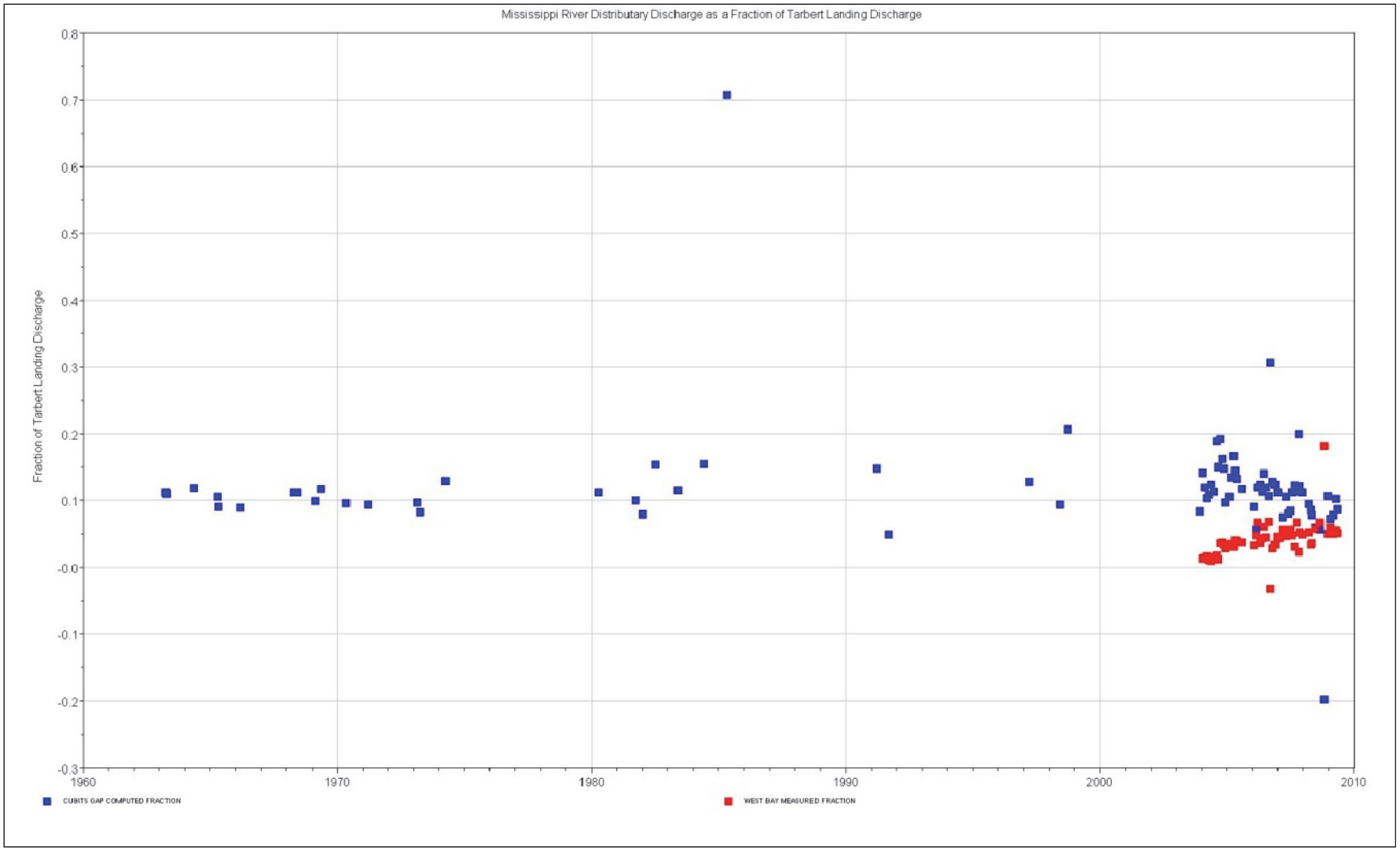

Figure 3.70. Discharge at Southwest Pass, South Pass, and Pass a Loutre as a fraction of Venice discharge.

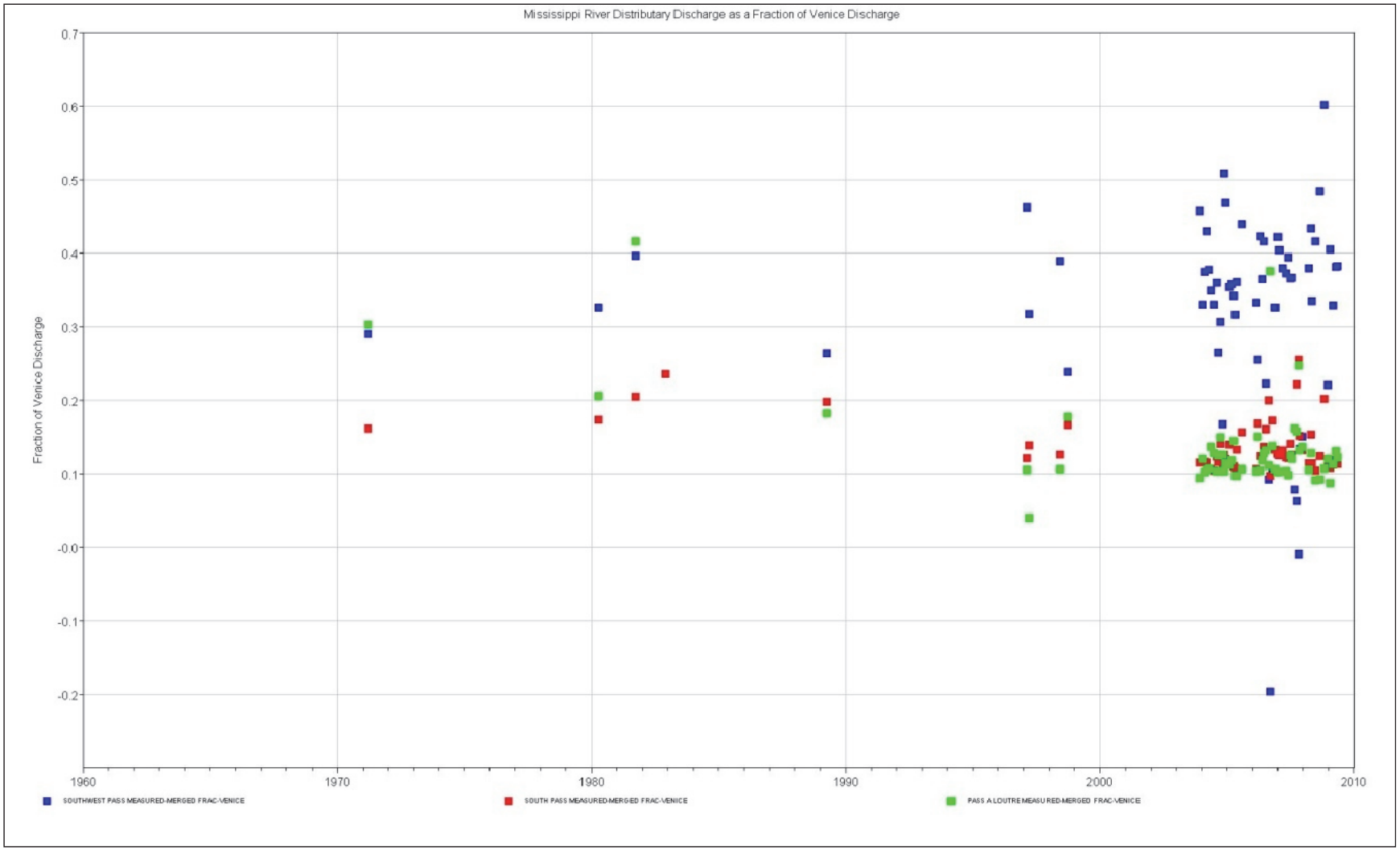

Figure 3.71. Discharge at Southwest Pass, South Pass, and Pass a Loutre as a fraction of Tarbert Landing discharge.

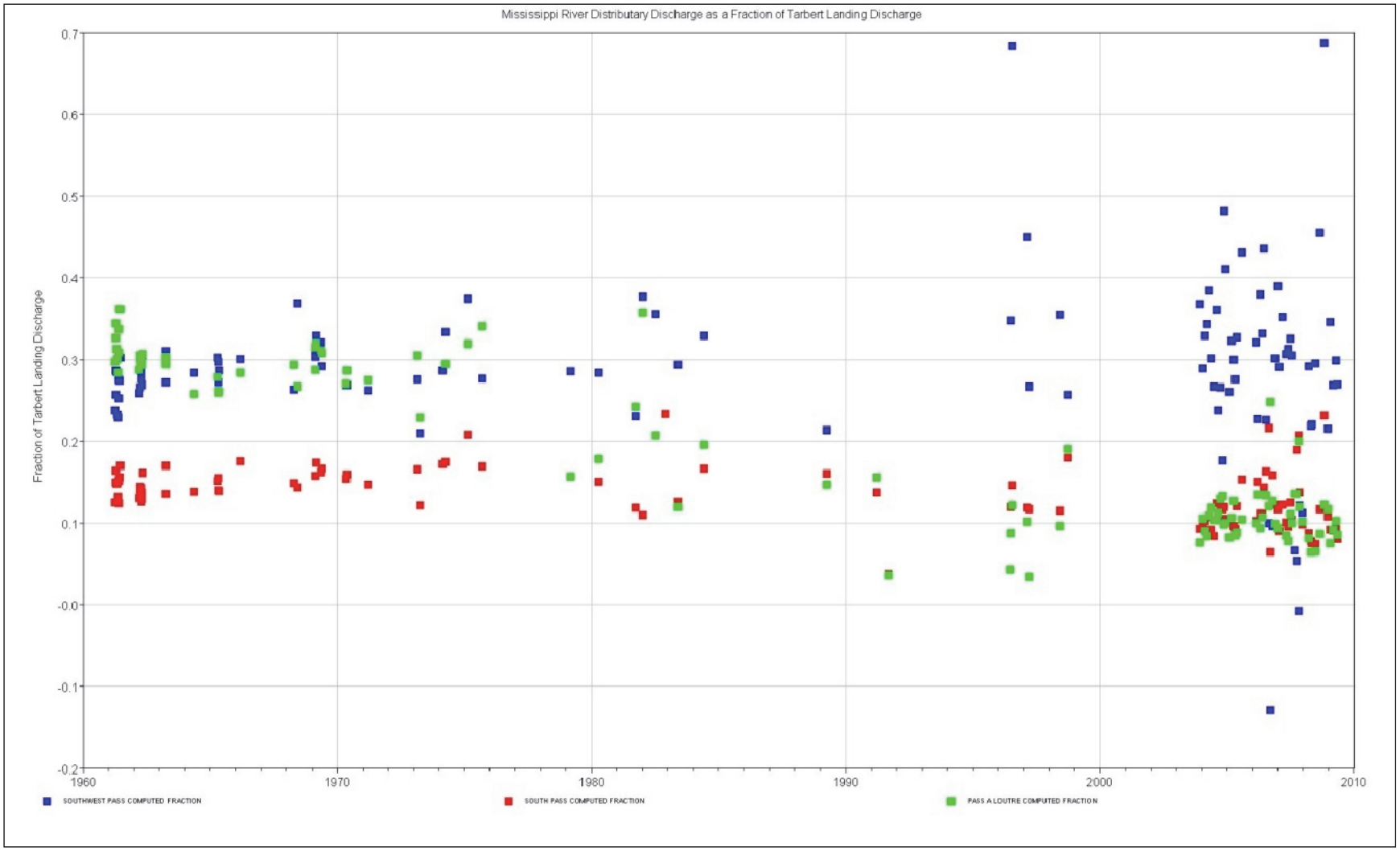

MVN (1939) states that the capacity of Southwest Pass, South Pass, and Pass a Loutre as a percentage of New Orleans mean discharge was 31, 14 and 36 percent, respectively. This indicates that the percentage of Pass a Loutre may have decreased slightly from the 1930s until the 1960s, while the percentage for Southwest Pass and South Pass was fairly consistent over that time period.

Capacity as a percentage of Venice discharge for WBSD and diversions downstream were plotted for the post-West Bay construction time period to determine how the capacity of the diversions has changed as the diversion has developed. The percentages of the diversions downstream of the WBSD must adjust as WBSD develops and capacity increases. The plot is shown in Figure 3.72. A linear trend line was applied to the data for each outlet to discern the trend in percentage. The trend line for West Bay indicates that the capacity of the outlet as a percentage of river discharge has increased from 2 to approximately 7 to 8 percent since the outlet was opened. The percentage for Cubits Gap appears to decrease over the same period by a similar amount. The percentage of South Pass and Pass a Loutre indicates essentially no change over that time period. The percentage for Southwest Pass appears to slightly decrease since diversion construction as well, although the degree of data scatter may bias the trend. From this data, it appears that the increase in capacity of WBSD since construction has been offset by a decrease in capacity of Cubits Gap and to some degree, Southwest Pass.

Sediment Data Assessment

Sediment data available for the study reach includes historic bed material data and suspended sediment data for the Mississippi River. In addition, suspended sediment measurements were collected as part of this study at West Bay diversion, Baptiste Collette, Grand Pass, and Cubits Gap, as well as points on the Mississippi River. Since sediment discharge data for the diversions was limited to the recent measurements collected, no trend analysis or assessment for the diversions was attempted. Rather, the trends in annual suspended sediment and water discharge and the distribution of bed sediments for the Mississippi River are presented to provide a general description of the nature of sediments within the study area. This subject has been investigated by many researchers, therefore reference is made to their work rather than conducting a duplicate effort for this study.

Figure 3.72. Capacity as a percentage of Venice discharge for the diversions downstream of WBSD for the post-construction time period.

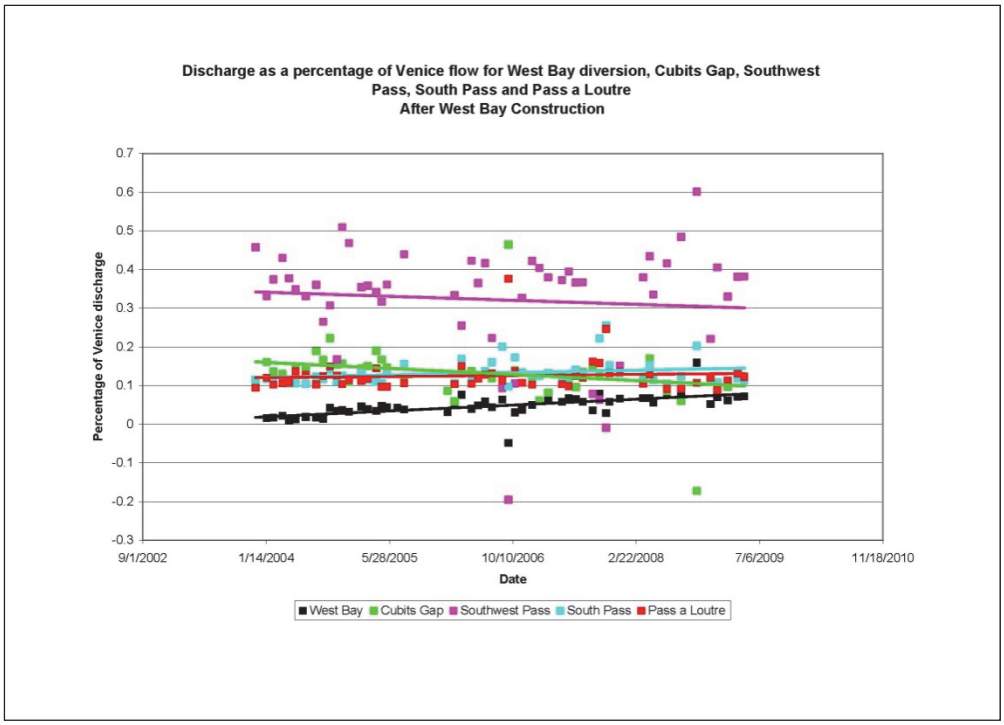

Bed material data for the Mississippi River were collected and analyzed in 1989 by Nordin and Queen (1992). The grain-size distribution for the bed material samples by RM is shown in Table 3.5. The data indicate that the channel bed of the Mississippi River in the study area above HOP is primarily composed of fine sand, with very fine sand and silt also present. Grain size analyses of dredge material grab samples conducted by MVN indicate a similar composition and will be presented later in this chapter. Bed material samples collected by ERDC in 2009 as part of this study near RM 5.5 AHP and RM 2.5 AHP agree reasonably well with the Nordin data in percentage of medium and fine sand, but generally contain a higher percentage of very fine sand and silt than the Nordin samples. These bed material samples are further discussed in the 1-dimensional model chapter of this report.

- Samples that contain a significant amount of clay and silt
- Legend: FSilt = Fine Silt; MSilt = Medium Silt; VFS = Very Fine Sand; FS = Fine Sand; MS = Medium Sand; CS = Coarse Sand

Table 3.5. Mississippi Riverbed material gradations (Nordin and Queen 1992).

Sample Location (1989 RM AHP)	D_{16} (mm)	D_{50} (mm)	D_{84} (mm)
75.2	0.13 FS	0.16 FS	0.20 FS
73.1	0.17 FS	0.23 FS	0.34 MS
65.8	0.18 FS	0.22 FS	0.29 MS
63.0	0.34 MS	0.45 MS	0.60 CS
59.0*		0.00	0.02 MSilt
57.0	0.14 FS	0.18 FS	0.23 FS
55.4	0.15 FS	0.19 FS	0.25 FS
52.8	0.17 FS	0.21 FS	0.26 MS
51.2	0.11 VFS	0.14 FS	0.18 FS
47.3	0.15 FS	0.23 FS	0.33 MS
44.8	0.14 FS	0.17 FS	0.20 FS
42.8	0.17 FS	0.23 FS	0.32 MS
40.0	0.12 VFS	0.16 FS	0.20 FS
37.0	0.17 FS	0.21 FS	0.25 FS
35.2	0.18 FS	0.24 FS	0.32 MS
33.0	0.26 MS	0.30 MS	0.36 MS
30.4*	0.01 FSilt	0.14 FS	0.19 FS
26.0	0.17 FS	0.20 FS	0.23 FS
23.9*	0.00	0.02 MSilt	0.07 VFS
21.9	0.15 FS	0.18 FS	0.23 FS
18.0*	0.00	0.00	0.01 FSilt
13.5	0.11 VFS	0.14 FS	0.18 FS
11.9*	0.08 VFS	0.11 VFS	0.15 FS
5.5*	0.13 FS	0.15 FS	0.18 FS
2.8	0.13 FS	0.16 FS	0.20 FS

Suspended sediment discharge data observed at Tarbert Landing indicate that an overall trend of decreasing suspended sediment discharge has occurred throughout the study period. Demas and Allison (2009) presented that the annual suspended sediment load at Tarbert Landing has decreased by 17 to 20 percent from 1975 to 2006 (Figure 3.73). However, the trend in annual water discharge has experienced little change over the same period (Figure 3.74). Similar trends in decreasing suspended sediment load have been reported by Horowitz (2010) and Thorne et al. (2008).

Figure 3.73. Annual suspended sediment load for Mississippi River at Tarbert Landing (after Demas and Allison 2009).

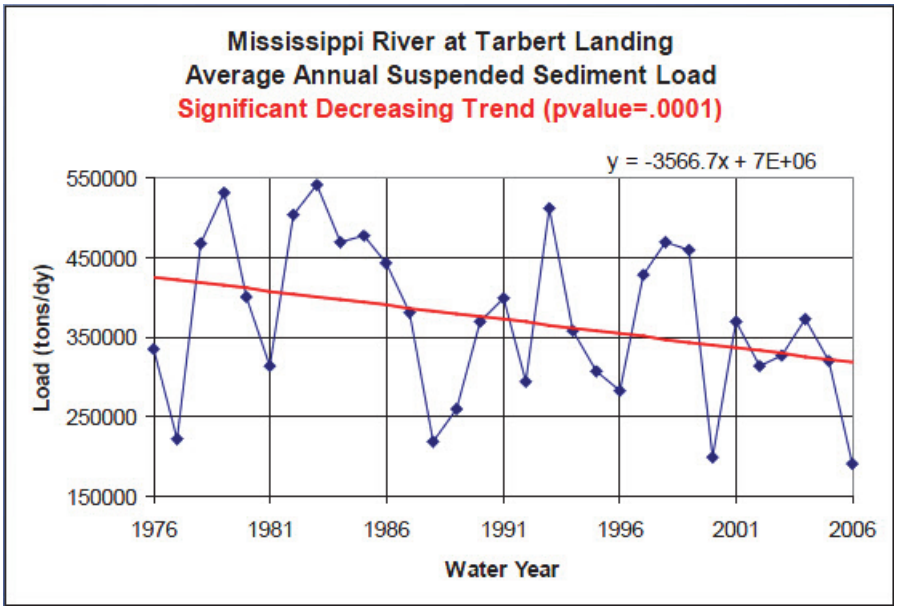

Figure 3.74. Annual water discharge for Mississippi River at Tarbert Landing (after Demas and Allison 2009).

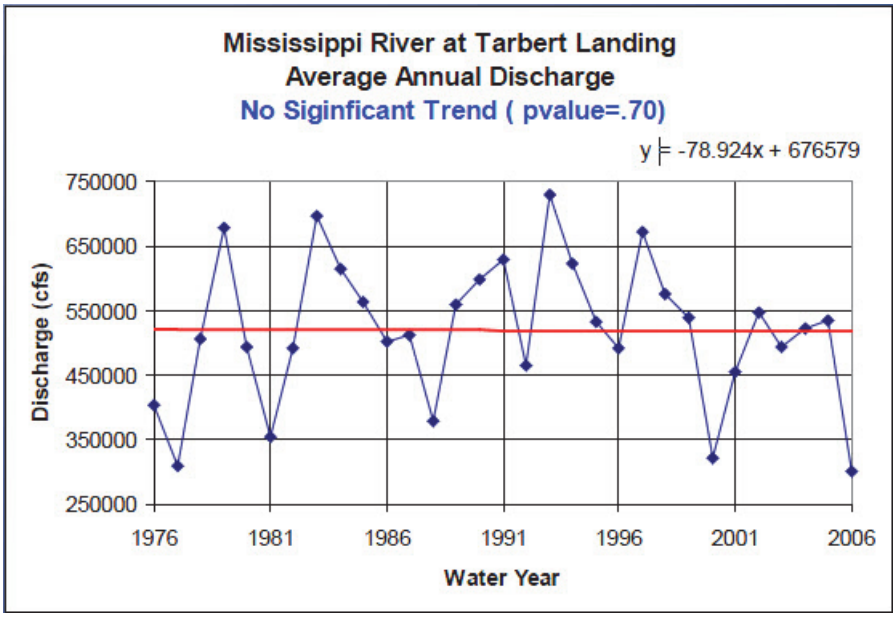

Dredge Data Analysis and Results

Dredge records from the 1970s to the present were obtained from MVN for the purpose of investigating the trends in dredging requirements for the study area. The data include the total maintenance dredge volumes by year for the Southwest Pass reach. MVN defines the Southwest Pass reach as extending from Venice through the entire Southwest Pass. It was originally

intended to determine dredge volumes by specific RM; however, this could not be accomplished for all dredge contracts. Therefore, only a summary of the total dredge volume is presented. Historically, the vast majority of maintenance dredging on the lower Mississippi River has occurred from approximately RM 3.5 AHP to HOP and throughout the entire Southwest Pass. Minimal dredging has been required in the past between RM 3.5 AHP and Venice.

Total dredge volume by fiscal year dredging contracts for the Southwest Pass reach is shown in Figure 3.75. The plot indicates the probable effects of the floods of the 1970s on maintenance dredging requirements. It is also noted that the dredge volumes since the late 1990s are much less than the long-term yearly average for the period. This decrease could possibly be a result of the Mississippi River-bank line restoration project of the late 1980s and early 1990s. During this project, the deteriorated bank lines of the Mississippi River and Southwest Pass were restored via foreshore dike construction and hydraulic fill dredged from the channel.

Figure 3.75. Total yearly dredge volumes for Southwest Pass.

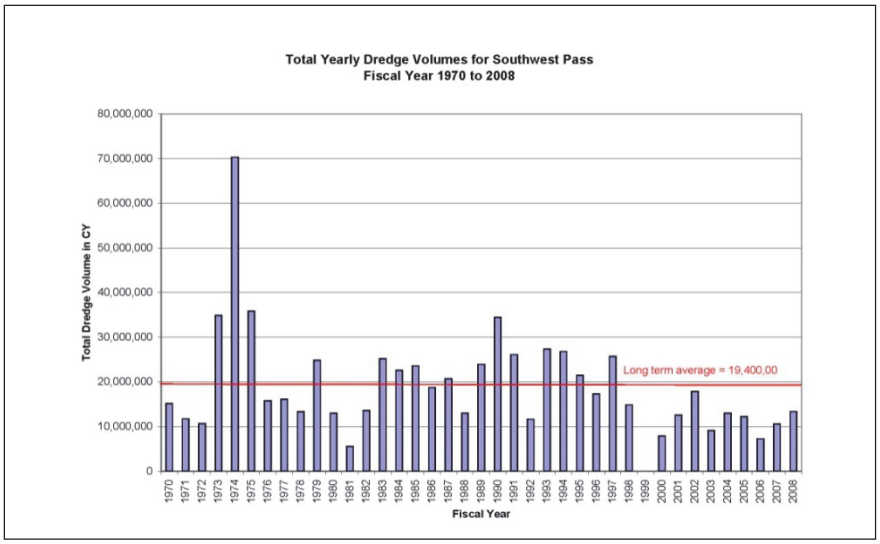

Dredge material grab samples from various dredge contracts from 1996 to 2008 were collected and grain size analyses conducted by MVN. This data included grain-size distribution and XY coordinates for sample location; however, not all sample data contained location coordinates. The data with location coordinates were entered into the GIS system and plotted. The spatial distribution of the D_{50} of the grab samples is shown in Figure 3.76. In general, the D_{50} of the dredge grab samples is fine sand in the vicinity of Cubits Gap and transitions to very fine sand and some silt between Cubits

Gap and HOP. There are some instances of D_{50} in the silt class at and upstream of Cubits Gap. Throughout Southwest Pass, the D_{50} of the dredge material grab samples is primarily very fine sand and silt/clay. No grab samples with a D_{50} of medium sand were observed. These grab sample data included samples collected as part of the initial dredging of the PAA in 2003. These samples all indicate a D_{50} of fine sand.

Figure 3.76. Dredge material grab sample location and D_{50} grain size.

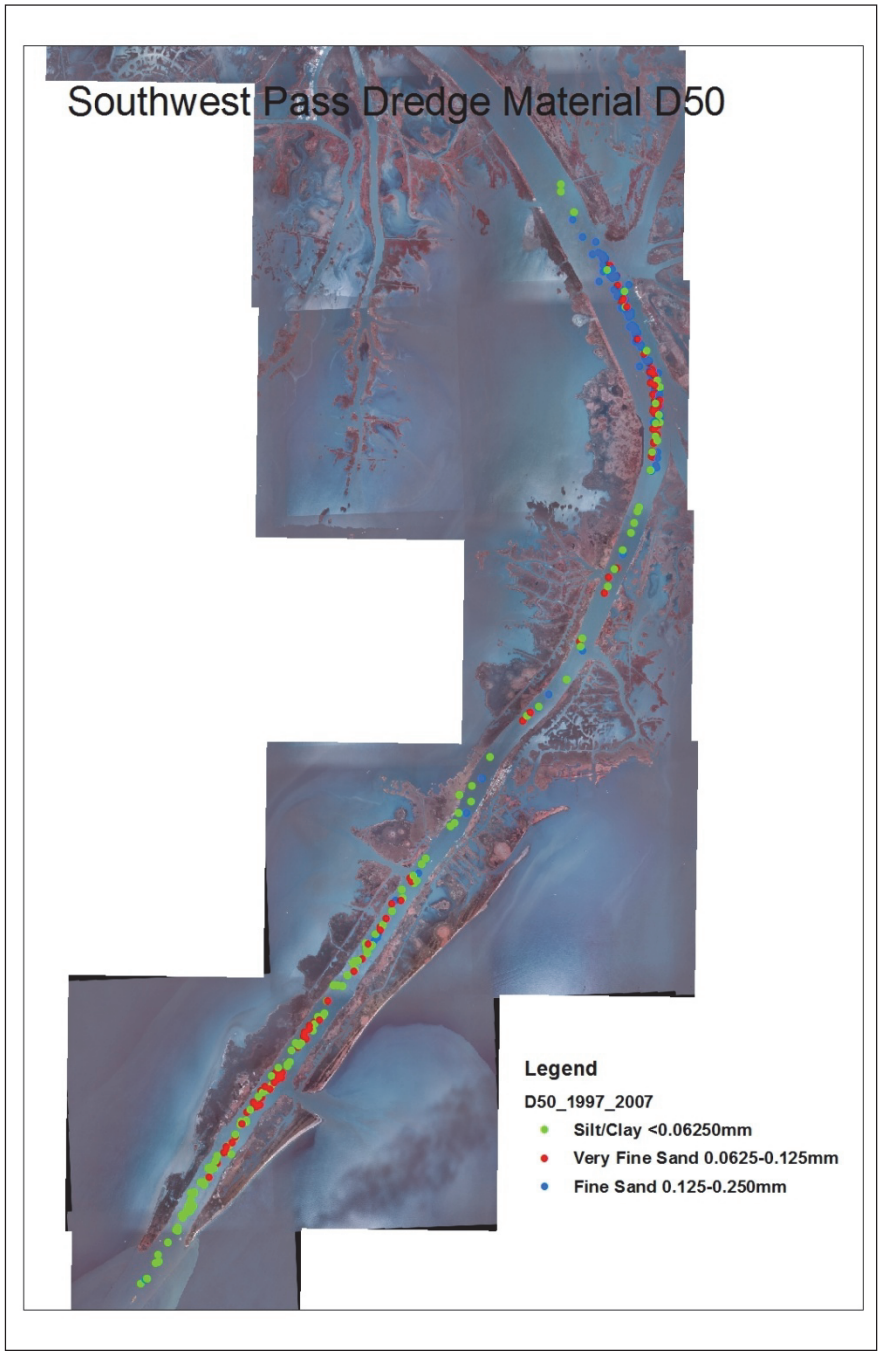

Historic Events Timeline

A comprehensive report of the events that have transpired in terms of river engineering, channel maintenance, and other man-induced activities for the study area was compiled by MVN. The information in this summary provides background information that is essential for an accurate interpretation of the results of the various analyses conducted in the geomorphic assessment. The report covers the principal river engineering activities that have occurred from 1960 to the present. Four significant events are detailed in the report that are believed to at least contribute in some degree to the river channel morphology observed over the study period: 1) deepening of the navigation project from -40 feet MLG to -45 feet MLG, 2) enlargement projects on Baptiste Collette and Grand Pass, 3) river-bank line restoration projects, and 4) construction of West Bay diversion.

Deepening of Navigation Project

As stated in the events summary, the navigation project as authorized in 1960 provided a channel to a depth of -40 feet MLG and 1000 feet wide from New Orleans to HOP. The authorized channel for Southwest Pass was for the same depth but at a width of 800 feet. Deepening of the navigation project to -45 feet MLG was authorized by PL 99-88 (Aug 1985) and WRDA 1986. In addition to deepening the navigation channel, the width of the channel from New Orleans to RM 17.5 BHP was reduced from 1000 feet to 750 feet. Dredging to achieve the new depth was conducted in 1987 and occurred from RM 3.5 AHP to the gulf.

Possible effects of the deeper and narrower navigation channel were observed in the geometric data analysis, primarily from Cubits Gap downstream. In this reach of the river that is heavily modified by regular maintenance dredging, the channel is firmly entrenched along the left descending bank of the river. In this reach, the point bar along the right descending bank appears to have developed significantly. This has resulted in a channel cross-section shape typically observed in a bend of a river, with a narrow, deep thalweg channel and a well-defined point bar. Comprehensive hydrographic surveys prior to the deepening project indicate that the channel section in this reach was wider than the present-day channel.

Enlargement of Baptiste Collette and Grand Pass

Projects to enlarge the diversions of Baptiste Collette and Grand Pass were constructed in 1978-1979. These projects included dredging of the channel and construction of jetties.

The possible effects of these projects can be noted in the increase in discharge capacity as a percentage of Mississippi River discharge for the diversions. Capacity percentages for the diversions were approximately 3 to 4 percent each in 1960 and have increased to approximately 8 to 10 percent each at current conditions. This increase in capacity seems to correspond in time to the enlargement project construction. This change has resulted in an increase in the combined distribution percentage for these diversions from 6 to 8 percent to 16 to 20 percent. Although the effects of this change are difficult to determine without numerical modeling, the increase in discharge percentage is likely to increase deposition potential in the river downstream of the diversions.

River Bank Line Restoration

Restoration of deteriorated river bank lines was approved in 1985 and project construction conducted from 1986 to 1991. The purpose of the restoration project was to construct a foreshore dike along the deteriorating bank line and replenish the area behind the dikes with hydraulic fill borrowed from the river channel.

The effect of the bank-line restoration was to prevent river discharge over the banks and to confine the discharge within a well defined channel. This resulted in increased velocities in the river channel. Dredge records indicate a general reduction in maintenance dredging has occurred from the late 1990s to the present. The restoration project was possibly a contributor to this observed reduction in maintenance dredging.

Construction of West Bay Diversion

Construction of WBSD was completed in 2003 at RM 4.7 AHP. The initial diversion channel was constructed to a capacity of 20,000 cfs, requiring the dredging of approximately 655,000 CY (gross). In addition, the anchorage area was dredged as part of the construction of the diversion. Approximately 735,000 CY (gross) was removed from the anchorage area downstream of the diversion channel in the shallow draft portion of the

anchorage area. In 2006, a second dredging event for the anchorage area was conducted, resulting in the removal of approximately 1.88 million CY (gross). Of this total, 640,000 CY (gross) were removed from the deep draft portion of the anchorage area upstream of the diversion, and 1.24 million CY (gross) were removed from the shallow draft portion of the anchorage area downstream of the diversion.

Results from the gauge/discharge data analysis indicate that the percentage of Mississippi River discharge distribution for WBSD at time of construction was approximately 2 percent but has increased to approximately 7 to 8 percent. It is probable that the diversion has had an impact on the morphology of the river in a manner similar to that resulting from the enlargement of Baptiste Collette and Grand Pass. As the diversion capacity has increased, capacity of diversions downstream from the diversion must likewise decrease based on continuity of flow. This cumulative change in discharge distribution has most likely had an impact on deposition trends in the river downstream of the diversion. Geometric data analyses indicate that the point bar was developing and had significantly developed prior to WBSD construction. The fact that dredging was required in the anchorage area at the time of diversion construction indicates that the point bar had developed sufficiently prior to construction. However, determining if and/or how the development of the point bar has been affected specifically by the diversion is difficult with this type of analysis. Numerical model investigations conducted as part of this study aid in identifying potential impacts specific to the diversion.

Integration of Results and Conclusions

Integration of Results

Results from the various analyses conducted as part of the geomorphic assessment were integrated in order to formulate conclusions that best describe and explain the cause and effect of the overall morphological trends observed in the study area. The integration process takes the results from a given analysis and interprets the results in relation to the results of all analyses. In doing so, definitive trends can be established, and areas of conflicting results can be identified. In addition, the results of the geomorphic assessment will be integrated with the results of the other aspects of this overall study to determine a comprehensive assessment of the anchorage area and the potential impacts of WBSD on induced shoaling.

The geometric data analyses indicate that, in general, there has been little change to a slight lowering of the river channel bed upstream of Venice. Results from cross-section comparisons and reach average channel bed displacement and elevation comparisons agree reasonably and verify this trend. It should be noted that the geometric analyses for this reach of the river are based solely on comprehensive surveys collected approximately every decade. Observed changes in channel dimension for this reach can reasonably be correlated with revetment construction.

A distinct change in the trend of channel dimension occurs in the vicinity of Venice. Several things occur at this location. First, the main distribution of discharge for the lower Mississippi River begins at Baptiste Collette and Grand Pass. The combined distribution of discharge as a percentage of Mississippi River discharge for these two diversions has increased from approximately 5 percent to 16 to 20 percent over the study period.

Second, an alternating lateral bar channel pattern is observed. A lateral bar is located on the left descending bank immediately downstream of Grand Pass. The thalweg channel continues along the right descending bank until approximately the upstream limit of the anchorage area, where a crossing occurs. The thalweg channel shifts toward the left bank as it crosses through the upstream portion of the anchorage area and is located closely along the left bank at Cubits Gap. A corresponding lateral bar begins along the right descending bank in the upper portion of the anchorage area and extends throughout the anchorage area to near HOP.

Third, a trend in reduced river channel depths is observed. Beginning at Venice and continuing to Cubits Gap, a general reduction in channel thalweg depths by as much as 20 feet has occurred over the study period. This trend is identified at individual cross sections and over reach average areas. There is a degree of variability in the data, particularly associated with the occurrence of large floods; however, the overall trend is one of general depth reduction. The effect of regular maintenance dredging is evident beginning at Cubits Gap and proceeding downstream to HOP and throughout Southwest Pass. Because of the continual modification of the channel from maintenance dredging in this area, no definitive trends can be determined other than changes in depth that transpired as a result of the navigation channel deepening project.

The lateral bar that is located on the right descending bank within the anchorage area limits is very extensive, and the development of the bar has had a major impact on conditions within the anchorage area. From a qualitative assessment of cross-section and contour plots, the lateral bar had been actively developing for years prior to construction of WBSD. Survey data indicate that there has been a degree of fluctuation in the vertical extent of the point bar. Some cross sections show that conditions in the anchorage area were actually higher in 1997 than at the time of WBSD construction. Also, survey data indicate that the 1973 flood caused significant erosion of the point bar in the upper portion of the anchorage area. The combination of the deep, narrow channel and the well developed lateral bar in this area produces a channel shape that is typically observed in sharp river bends. Reach average channel bed displacement determined from the hydrographic surveys indicates the lower portion of the lateral bar within the anchorage area has increased in elevation 3 times as much as the upper portion of the anchorage area.

The development of the lateral bar in relation to the construction of WBSD is difficult to accurately determine. Analysis of average channel bed elevations along a 250-foot section landward (westward) of the PAA line for detailed cross sections within the anchorage area indicates a potential increase in post-construction deposition rates for locations between the diversion and Cubits Gap. For locations downstream of Cubits Gap, no significant change in the rate of deposition relative to diversion construction is observed. Reach average channel bed elevations indicate a similar trend, with an increase in post-construction elevations observed for the reaches in the vicinity of the diversion and downstream to Cubits Gap, but little change in rates for reaches downstream of Cubits Gap. Dredge cuts for PAA construction and maintenance events have been shown to be very short-lived in the PAA area downstream of Cubits Gap because of rapid post-dredge shoaling.

Indication of the development of the lateral bars can be seen in the analysis of channel pattern. The channel pattern analysis for the hydrographic surveys indicates that channel widths become narrower downstream of Venice. Since the deepening of the navigation project, the channel width and location downstream of Cubits Gap have been very consistent along the left descending bank, and the lateral bar on the right descending bank has developed significantly in response.

The channel pattern analysis also indicates that the channel width at the -45-foot contour for the river reach immediately above Venice accounts for approximately 80 percent or more of the total top bank width. In the vicinity of the lateral bar on the left descending bank downstream of Venice, the channel width at the -45-foot contour is approximately 50 percent of the top bank width. Contours developed for elevations of -40 and -30 feet NAVD88 indicate the right bank lateral bar had significantly developed prior to WBSD construction, perhaps more in response to deepening of the navigation project in the late 1980s. Analysis of the surface area for depths of -40 and -30 feet within the PAA zones indicates that growth of the right bank lateral bar had reduced depths to less than -40 feet NAVD88 in the PAA downstream of Cubits Gap prior to diversion construction. This agrees well with the results of the cross-section analysis. Color contour plots for all surveys indicate a long-term trend of overall channel depth reduction in the reach downstream of Venice. Cross-section analyses also support this observation. This trend is believed to be more of a system-scale response to discharge distribution changes rather than a result of WBSD.

Distribution of Mississippi River discharge through some of the diversions located in the lower river and delta has changed over time. The combined percentage of river discharge distributed by Baptiste Collette and Grand Pass has increased from approximately 5 percent to 16 to 20 percent, with the time frame of the increase corresponding to the enlargement of those diversions in the late 1970s. Discharge distribution at Pass a Loutre has significantly decreased by as much as 20 to 25 percent beginning in the mid 1970s. The primary cause of this reduction at Pass a Loutre is unclear but may be associated with the aforementioned changes at Baptiste Collette and Grand Pass, as well as the deepening of the navigation project in Southwest Pass. Discharge distribution percentage for WBSD has increased fairly uniformly since construction from approximately 2 percent to 7 to 8 percent of river flow. The distribution percentage at Cubits Gap has decreased correspondingly as has possibly the distribution percentage at Southwest Pass. In consideration of the geometric changes in depth and width that occur with the beginning of discharge distribution near Venice, it appears that discharge distribution through the diversions may be the primary reason for the observed morphological change in the study area.

Major floods result in noticeable change to the channel perimeter, and changes are often without a discernible pattern. The flood of 1973

produced significant erosion in the point bar within the upper portion of the anchorage area. Patterns of scour and deposition are often observed for the same cross section. In the case of tropical storms, the effects seem to be more general. Sediment deposition observed during Hurricane Katrina appeared more uniform over the river channel, and deposit depths tended to increase with increasing proximity to the gulf. The track of the storm relative to the river delta most likely affects deposition trends.

Conclusions

The results of the various analyses of the geomorphic assessment were integrated and evaluated using best engineering judgment with regard to long-term morphological trends in the study area, construction of WBSD, and the potential impacts of the diversion on induced shoaling in the PAA. The following conclusions are presented as follows:

- The lower Mississippi River and delta region is a dynamic system that has experienced significant morphologic adjustment over the study period.
- The river channel upstream of Venice has been generally stable in dimension and pattern over the study period, with essentially no change to a slight increase in channel depth.
- A definitive change in channel trends occurs at Venice. In general, channel depths from Venice to Cubits Gap decrease consistently over the study period. Downstream of Cubits Gap and throughout Southwest Pass the channel is heavily influenced by navigation maintenance dredging. Depth-change trends are basically indistinguishable except for increases due to deepening of the navigation project.
- The lateral bar along the right descending bank that extends throughout the PAA was developing prior to the construction of WBSD, and would have continued to develop to some degree without construction of the diversion. Development of the lateral bar downstream of Cubits Gap appears to correspond to deepening of the navigation project.
- Construction of the WBSD has potentially resulted in increases in deposition rates in the anchorage area between the diversion and Cubits Gap. Deposition rates in the anchorage area downstream of Cubits Gap indicate little influence because of construction of the diversion.
- The distribution of Mississippi River discharge via diversions in the study area is believed to be a major factor in observed channel morphology and deposition trends. It is reasonable to assume that the WBSD likewise affects these trends by contributing to the overall

distribution of river discharge in the area; however, determination of the percentage increase that is attributable to WBSD is difficult based on observed data.

- Identifying and quantifying impacts that are attributable to WBSD is difficult using these types of assessments. Changes observed in the geometric data were cumulative results of all processes and influences such as river hydrology, floods, storms, dredging activities, and river engineering projects. Impacts specifically attributable to the construction of WBSD are best determined through numerical modeling. Modeling results should be evaluated along with the geomorphic assessment results to achieve the most comprehensive and accurate interpretation of diversion impacts on anchorage area shoaling.

4 1-Dimensional Modeling Analyses

Purpose of 1-Dimensional Analysis

The HEC-6T numerical model software package (MBH 2009) is utilized as a part of a multi-task evaluation to determine the effects of the WBSD on sedimentation rates and dredging requirements in the PAA. The 1-dimensional (1D) model estimates the long-term river responses to the diversion and the upstream sediment boundary conditions for the multi-dimensional models. Fifty year simulations were run with the 1D model, with the results integrated with the geomorphic assessment and the multi-dimensional models to provide an evaluation of the effect of the WBSD.

1-Dimensional Modeling Background

The Engineering Research and Development Center (ERDC) conducted a two-phased investigation with the 1D model. First, ERDC Phase I was a preliminary effort to establish the usability and potential impact of the WBSD on dredging above Head of Passes (HOP). Second, ERDC Phase II refined the ERDC Phase I and evaluated the sensitivity of the model to key input parameters. The ERDC Phase I model is based on the validated USACE, Vicksburg District, MVK HEC-6T model, regional scale model. Changes to the ERDC Phase I model which were made for the construction of ERDC Phase II model are discussed along with key aspects critical for the model description. For a complete account of the MVK HEC-6T model, see Copeland and Lombard (2009), and for the ERDC Phase I model, see Heathet et al. (2010).

HEC-6T Model

The HEC-6T software, an enhanced version of HEC-6, is applied in this effort. HEC-6 is “a 1D movable boundary open channel discharge numerical model designed to simulate and predict changes in river profiles resulting from scour and/or deposition over moderate time periods, typically years” (HEC 1993). Model input requirements for this study include channel geometry, subsidence rates by cross section, boundary conditions, bed material gradations, distributary out discharge and sediment concentration, water temperature, and user-specified sediment transport functions.

HEC-6T is an ideal 1D model for reservoirs and other relatively low energy environments such as the lower Mississippi River. The discharge conditions in the model are specified by a series of sequential steady state discharges where water surface elevations at each cross section are calculated with the standard step method, Method II (USACE 1959). Thus, from the user-defined hydrograph, HEC-6T calculates velocity and depths. Then, in a decoupled manner at each time-step, the calculated parameters (depth, velocity, and discharge) are applied to determine sediment transport potential. The computed transport potential is compared to the available sediment supply in the water column and riverbed to determine bed erosion or deposition. Finally, these bathymetric changes are applied within the movable bed limits, and the next discharge condition is calculated, repeating the process.

Implementing HEC-6T has both advantages and disadvantages for the WBSD. Understanding these are pivotal in correctly interpreting and understanding model output and usability.

HEC-6T offers four capabilities needed for the evaluation of WBSD. First, HEC-6T allows for long-term simulations. For the WBSD evaluation, 50-year simulations were conducted to describe a broad range of potential discharge events. Second, the model has the ability to simulate dredging activities. Dredging in both the navigation channel and in the PAA is required for the WBSD study. For the ERDC Phase II model, modifications were made to the code by the engineering firm Mobile Boundary Hydraulics (MBH) to allow multiple dredging templates at any cross section, so adjacent sites could be dredged concurrently or at different times for varying widths and depths at the same cross section. Additionally, HEC-6T allows for the diversion of both water and sediment and calculates the downstream impacts of the diverted flux. Finally, it directly accounts for subsidence and sea level rise, an important factor in the Gulf region for a long term simulation.

The primary disadvantage of HEC-6T is that it is a 1D model and uses average hydraulic and sediment parameters to simulate 3-dimensional processes. Also, HEC-6T includes no provision for specifying either a lateral distribution of sediment load or a bed material gradation across a section. HEC-6T does not consider salinity or the impacts of organics on fine sediment transport. In HEC-6T the standard procedure for deposition and scour is to move each cross-section point, within the movable bed

limits, an equal distance. For the ERDC Phase II model, an option in HEC-6T was selected that preferentially deposits sediment within the dredging template before distributing deposition over the rest of the moveable bed portion of the cross section. This prevents the artificial build up of sediment along the dredged channel.

Modeling Approach

The ERDC Phase II model provides a method to evaluate, on a regional scale, the long-term channel changes and delivery of sediments along the lower reach of the Mississippi River. It also provides boundary condition inputs for the multi-dimensional modeling effort. In addition to providing regional scale evaluation, the model is used to simulate long-term sediment deposition rates on a local scale within the navigation channel and PAA. Two 50-year scenarios were conducted representing conditions with and without the WBSD. Comparisons of the two scenarios identified both temporal and spatial changes in the sedimentation rates with and without WBSD alternatives.

The ERDC Phase II model WBSD evaluation was conducted with a HEC-6T model previously developed by the MVK. The MVK HEC-6T model is part of a regional model being developed by the Mississippi River and Tributaries (MR&T) Project to identify long-term channel maintenance sites within the Lower Mississippi River. Since the MVK model was developed for regional use, modifications were made for the ERDC WBSD evaluation and are as follows:

- Additional cross sections downstream of Belle Chase were used to adequately define the channel geometry within the study reach, with the highest density of cross sections required within the PAA (RM, RM, 1.5 to RM 6.7).
- The 2D model study was implemented along with field data collection effort to refine sediment diversion ratios, discharge diversion, sediment concentration, and bed material gradation. If needed, MVK model values were modified.
- Code modifications for multiple dredging templates were made to represent dredging in the Navigation channel and the PAA.
- Subsidence and sea level rise rates were estimated and incorporated into the model.

- A typical discharge hydrograph which provides a plausible range of future flows was selected and duplicated as needed to create a projected 50 year hydrograph.
- Fifty-year downstream water surface elevations were developed that matched the time period used in the 50 year discharge hydrograph.

The ERDC Phase II effort provided a chance for code modifications, quasi-validation, and sensitivity tests. For the validation portion of the ERDC Phase II model effort, a 1991 – 2002 hydrograph was simulated. This was the same hydrograph used for validation of the MVK HEC-6T model. The MVK HEC-6T model was validated, so for every change in the ERDC Phase II, model comparisons were made between the ERDC Phase II and MVK HEC-6T model to verify validation. The checks were primarily in the form of water surface elevations, dredging comparisons, and sediment load. The sensitivity testing evaluated the impacts of varying sediment diversion ratios, sea level rise, subsidence, and sediment-transport functions.

ERDC HEC-6T Model Input

The Vicksburg to the Gulf portion of the MVK HEC-6t model was used for the ERDC Phase II model investigation, even though the primary focus was on the Belle Chasse, LA RM (RM) 75 to HOP RM 0 reach. The additional upstream reach in the model from Belle Chase to Vicksburg allows the sediment load to adjust varying inflow boundary conditions prior to entering the study area, thus reducing bias from the input sediment load at Vicksburg. Cross sections were added to the MVK model for the refinement of the ERDC model to provide more resolution in the study area. Also, sediment data both from the field collection effort and the multi-dimensional modeling effort were implemented. All new model inputs were compared to the original data and the MVK HEC-6T model such that a congruent model validation was maintained.

Cross-sections

The model provided by MVK extends about 455 miles from Vicksburg, Mississippi RM 437 .3 to Pilots' Station in Southwest Pass at RM -18.0. Model cross sections were derived from the 1992 Mississippi River comprehensive hydrographic survey. The MVK HEC-6T model originally contained 201 cross sections, but the ERDC modifications added 28 cross sections between Belle Chasse and HOP to define better the channel geometry within the study reach. The greatest increase in cross-section

density occurred from Venice at RM 10.6 to HOP RM 0, which includes the PAA, the primary reach of interest for this study. The average cross-section spacing through the PAA reach is 0.42 mi (0.68 km). The spatial distribution of the cross sections for both models is provided in Table 4.1.

Table 4.1. Spatial Distribution of MVK and ERDC HEC-6T Model Cross Sections.

Reach	MVK No. Cross Sections	ERDC No. Cross Sections
Southwest Pass (RM -18 – RM 0 At HOP)	13	13
HOP (RM 0) to Venice (RM 10.6)	8	19
PAA (RM 1.5 – RM 6.7)	5	12
Venice (RM 10.6) to Belle Chasse (RM 76)	21	38
Belle Chasse (RM 76) to Vicksburg (RM 437.28)	159	159
Total	201	229

Table 4.2 provides a comparison of the MVK HEC-6t model and the ERDC Phase II model cross-section locations between HOP (RM 0) and Belle Chasse (RM 76). Within the HOP (RM 0) to Venice (RM 10.6) reach, the ERDC model contains 19 cross sections which provide an average cross-section spacing of 0.56 miles. The PAA extends from RM 1.5 to RM 6.7. Through that reach, the ERDC models contain 12 cross sections. Eight of those sections are located downstream of the WBSD. The average cross-section spacing through the PAA reach is 0.43 miles. The data for all cross sections added to the model were obtained directly from the 1992 comprehensive hydrographic survey.

Table 4.2. Comparison of Model Cross-Section Locations (HOP (RM 0) to Belle Chasse (RM 76)).

Reach	MVK Model Sections (RM)	ERDC Model Sections (RM)
HOP (RM 0) to Downstream End of PAA (RM 1.5)	0.72	0.72
		0.98
PAA (RM 1.5 to RM 6.7)	1.6	1.6
		1.7
	2.46	2.46
		2.75
		3.36
	3.83	3.83

Reach	MVK Model Sections (RM)	ERDC Model Sections (RM)
		4.26
		4.46
		4.9
	5.5	5.5
		6.0
	6.7	6.7
Upstream End of PAA (RM 6.7) to Venice (RM 10.6)	8.1	7.5
		8.1
		8.8
	9.5	9.5
		10.3
Venice (RM 10.6) to Belle Chasse (RM 76)	11.05	11.05
		11.8
	12.5	12.5
		13.4
	14.1	14.1
	15.4	15.4
	17.0	17.0
		18.0
		19.1
		20.0
		21.0
	22.4	22.4
		23.2
	24.0	24.0
		25.0
	26.1	26.1
	24.0	24.0
		25.0
	26.1	26.1
		28.0
		30.0
	32.0	32.0
		33.6
	35.1	35.1
	39.3	39.3

Reach	MVK Model Sections (RM)	ERDC Model Sections (RM)
	43.2	43.2
	45.2	45.2
	49.0	49.0
	53.0	51.1
		53.0
	55.0	55.0
	57.0	57.0
		59.0
		60.9
	62.9	62.9
		65.0
		67.0
	69.0	69.0
		71.0
	73.0	73.0
	75.0	75.0

Overbanks for the MVK model were obtained from various sources including hydrographic survey contours, US Geological Survey (USGS) Quad Maps, available Louisiana Digital Orthophoto Quarter Quadrangle (DOQQ) and Light Detection and Ranging (LiDAR), and a previous 1D model developed in 1983. This provides a complete floodway representation of the river.

Boundary Conditions

Boundary conditions include water discharge, water surface elevations, subsidence, sea level rise, and sediment loads. Simulated sediment loads, deposition and erosion locations, and trends can vary if larger floods or drier periods occur more frequently than contained in the typical hydrograph. For water discharge, a typical average daily discharge hydrograph is constructed. This hydrograph includes the 25-year period from 1 January 1984 to 31 December 2008. This period contains several higher discharge years (1984, 1991, 1997, 2005, and 2008) as well as several lower water years (1988, 2000, and 2007). The highest discharge in the hydrograph occurred during 2008, which approached the 50-year frequency flow. The 25-year hydrograph is simply repeated to create the 50-year typical hydrograph used for the simulations (Figure 4.1).

Figure 4.1 Typical 50-Year Hydrograph

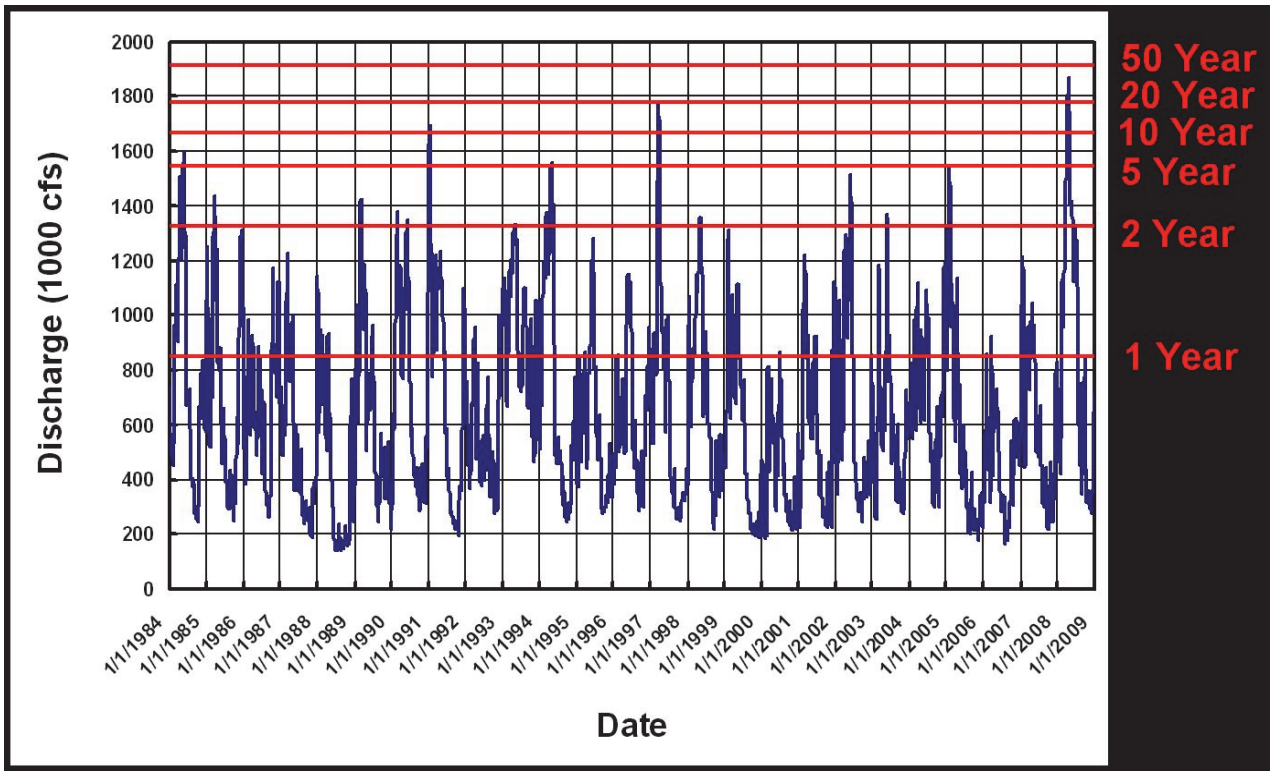

The 50-year downstream water surface elevations were developed from daily data and match the time period used in the 50-year discharge typical hydrograph. For the ERDC Phase II model, the 8:00 a.m. daily stages recorded at the NOAA tidal gauge at Grand Isle East Point were used. As reported by NOAA, the average difference between high and low tides at Grand Isle was approximately 1.05 feet (0.32 m) 1/1/1984 – 1/1/2009. Daily stages, over the period of record, vary throughout the daily tidal cycle, capturing the full range of tidal conditions. Tides provide the greatest impact during periods of low discharge when the river's sediment transport capacity is reduced. Additionally, the monthly average temperature was used in the ERDC Phase II model.

In south Louisiana, both subsidence and sea level rise are significant and can alter sediment transport rates. Subsidence rates are a direct input into HEC-6T. Reported subsidence rates along the lower Mississippi River vary from different sources. The ERDC model subsidence rates were derived from the National Oceanic and Atmospheric Association (NOAA) Technical Report NOS/NGS 50 (Shinkle and Dokka 2004). Subsidence rates vary from 0.87 in/year (22 mm/year) at RM 22.0 to 0.12 in/year (3.0 mm/year) at RM 306.00. The adopted subsidence rate from RM 16.0 (upstream of

Venice, Louisiana) to the downstream end of the model is 0.63 in/year (16 mm/year). This rate equates to approximately 2.6 feet (0.8 meter (m)) of subsidence over the 50-year simulations. Subsidence rates in NOAA Technical Report NOS/NGS 50 were computed with a eustatic sea level rise of 0.05 in/year (1.25 mm/year) at Grand Isle. The daily stages at the downstream boundary are increased at this rate for the 50-year simulations. The adopted subsidence rates for the ERDC Model are listed in Table 4.3

Table 4.3 Subsidence Rates ERDC Model.

Location	RM	Subsidence Rate (mm/year)
Southwest Pass Outlet	-20	16
Venice	10.6	
	11	16
	16	16
	20	20
	22	22
	27	15
	32	12
	35	10
	38	14
	45	13
	49	10
	60	8
	68	7
Belle Chasse	76	
	78	8
New Orleans	102	
	135	9
	216	8
Baton Rouge	230	9
	237	6
	240	4
	266	4
	306	3
Vicksburg	435	
	440	6

Incoming sediment loads were specified at the Vicksburg, MS, gauge. The incoming load was divided into sands and fine material. The silt and clay sediment inflow at the upstream boundary of the MVK HEC-6T model was determined from the 1991 – 2002 measured sediment concentrations at Union Point (RM 326.6) and Coochie (RM 317.3) (Copeland and Lombard 2009). These sampling locations were used instead of Vicksburg and Natchez for the following reasons:

- The 1992-2002 measured fine sediment concentrations at Vicksburg and Natchez were found to be an order of magnitude less than those fine concentrations reported between 1984 and 1989 at the same gauges.
- The 1992-2002 fine sediment concentrations at Vicksburg and Natchez were inconsistent with downstream measurements for the same time period at Union Point, Coochie, and Tarbert Landing.
- The Vicksburg and Natchez fine sediment measurements do not include particle-size class distributions.

These sediment loads were assumed to be the same at Vicksburg as those at Union Point and Coochie since the size classes (clay, very fine silt, fine silt, medium silt, and coarse silt) are typically wash load.

The sand flux curves were determined from a combination of calculated and measured sand transport at Coochie (RM 317.3) and Union Point (RM 326.6) (Copeland and Lombard 2009). This was necessary since the size-class percentages of the measured suspended load at Vicksburg were not available. When the calculated load at Vicksburg for a specific size class was greater than the measured load at Coochie and Union Point for that size class, then the greater portion of the calculated load at Vicksburg was considered to be bed material load and was used to develop the boundary sediment rating curve. When the measured load for a specific size class at Coochie and Union Point was greater than the calculated load at Vicksburg, then that size class was considered to be wash load at Vicksburg. The sediment discharge was increased by 10 percent to account for unmeasured load and was used to develop the sediment inflow at Vicksburg. Using both the calculated load at Vicksburg and the measured load at Coochie and Union Point, sediment inflow values for a range of discharges were developed for each size class (Copeland and Lombard 2009).

Both the model channel geometry and the downstream boundary water surface elevation are referenced to NGVD, the downstream, boundary-water surface elevations must also be referenced to NGVD. NOAA does not report the gauge readings at Grand Isle, and East Point is not referenced to any geodetic datum, only to a tidal datum. Thus, a conversion to NGVD is required, but NOAA does not provide a conversion for this site. However, previous work has indicated that NGVD at the Grand Isle, East Point gauge is equal to the gauge reading in mean sea level (MSL) plus 0.8 feet. This corresponds with the conversion utilized for the MVK HEC-6T Model.

Figure 4.2 is a conversion furnished by NOAA for a previous ERDC study. Information on Figure 4.2 indicates that NGVD = Mean Tide Level (MTL) + 0.78 feet. According to the Elevation on Station Datum on the NOAA Tides and Currents web site, the difference between MSL and MTL at this gauge is 0.01 feet. Adding this difference would be insignificant in a 1D model, especially given the additional uncertainties in relative sea level rise and subsidence in this area. Therefore, for the ERDC model, 0.8 feet is added to the Grand Isle East Point MSL gauge readings to determine the daily downstream water surface elevations.

Figure 4.2. Datum Conversions for the NOAA Gauge at Grand Isle East Point, Louisiana.

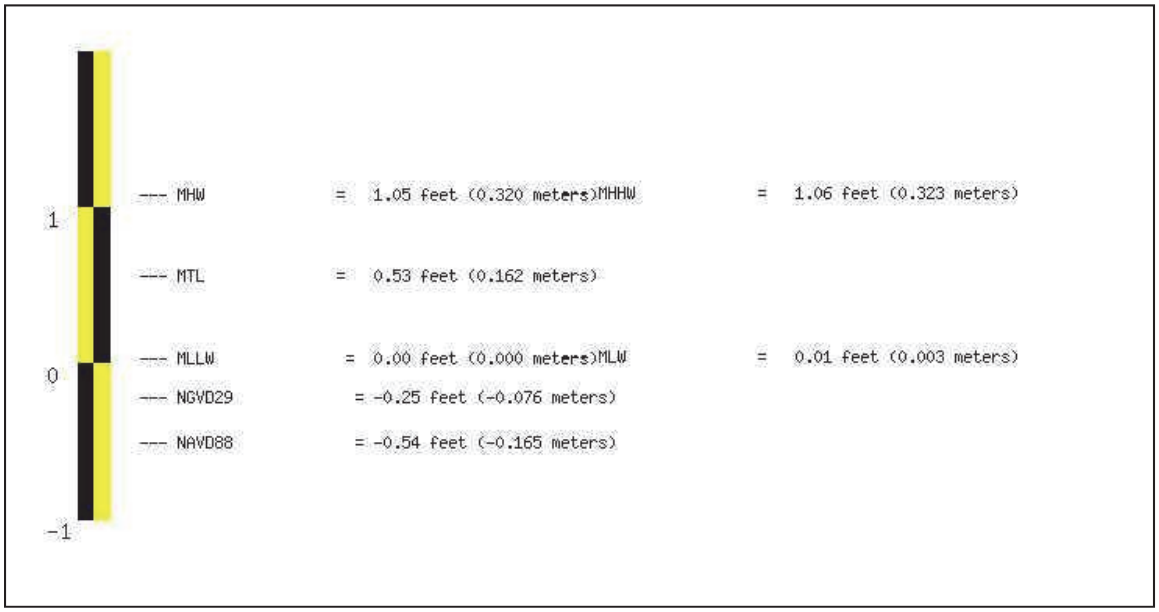

Transport Function

The evaluation of transport capacity is calculated with a specified transport function. For the MVK model and ERDC Phase II modeling efforts, the

Toffaleti-Meyer-Peter Muller function was applied. With this function, bed load is calculated using the Toffaleti and the Meyer-Peter Muller methods and with the larger of the two used. The Toffaleti equation was derived based on field data from the Lower Mississippi at Talbert Landing, Atchafalaya Rivers, five other river locations, and flume data from four data sets were used (Vanoni 1975). Data were collected over a broad range of flows for 12 years on the Mississippi River (Toffaleti 1963, 1968, and 1969). Other river data included the Mississippi River at St. Louis (Jordan 1956), Rio Grande at Bernalillo (Nordin 1964), Middle Loup (Hubbell and Matejka 1959), Niobrara (Colby and Hembree 1955). The data included depths ranging from 0.98 ft – 49.2 ft (0.3 m – 15 m) with fine to medium sands (Vanoni 1975). The flume data were taken by Kennedy (1961), Vanoni and Brooks (1957), Einstein and Chien (1953), Guy et al. (1966), and USACE, Waterways Experiment Station. Flume data were collected in flume widths ranging from 0.25 m – 2.4 m, discharge depths ranging from 0.16 ft – 1.97 ft (0.05 m – 0.6 m), and sediment sizes of 0.01 in – 0.04 in (0.3 mm – 0.93 mm) (Vanoni 1975). The Toffaleti function was applied in this study because it was developed for large rivers. The Meyer-Peter Muller equation was developed for gravel transport and is important in the MVK HEC-6T model to facilitate the transport of gravel size classes.

While HEC-6T does not provide for the direct impact of salinity in the sediment transport functions, this impact can be approximated by varying the silt and clay shear threshold deposition coefficients. For the MVK HEC-6T model, the critical shear stress for deposition for both silt and clay were increased downstream of Venice and the coefficient for clay was further increased in Southwest Pass to account for the effects of salinity on sediment deposition, salinity encourages flocculation and higher fall velocities. The model allows for varying the threshold coefficients by reach but does not allow for varying the coefficients with discharge or stage. The salinity throughout the PAA varies greatly with discharge. During low flow, the salinity is much higher than during high discharge periods. The variance is deemed reasonable since the deposition coefficients were determined during the MVK HEC-6T model validation by comparing computed dredge volumes to those reported in Southwest Pass and between HOP and Venice.

Bed Gradation

Initial bed material gradations in the MVK HEC-6T model were derived from particle size distribution of bed sediments collected along the

thalweg of the Mississippi River by Nordin and Queen in 1989 (Copeland and Lombard 2009). One hundred seventy-six samples were collected between Vicksburg, MS, and HOP. Of those samples, 25 were collected between Belle Chasse and HOP. Nordin did not collect any samples in Southwest Pass. The location, along with the D_{16}, D_{50}, and D_{84} of each of the Nordin samples within the Belle Chasse to HOP reach, is provided in Table 4.4.

Table 4.4. Bed Material Sample Locations and Sizes (As Collected By Nordin and Queen in 1989).

Sample Location (1989 RM)	D_{16} (mm)	D_{50} (mm)	D_{84} (mm)
75.2	0.13 FS	0.16 FS	0.20 FS
73.1	0.17 FS	0.23 FS	0.34 MS
65.8	0.18 FS	0.22 FS	0.29 MS
63.0	0.34 MS	0.45 MS	0.60 CS
59.0*		0.00	0.02 MSilt
57.0	0.14 FS	0.18 FS	0.23 FS
55.4	0.15 FS	0.19 FS	0.25 FS
52.8	0.17 FS	0.21 FS	0.26 MS
51.2	0.11 VFS	0.14 FS	0.18 FS
47.3	0.15 FS	0.23 FS	0.33 MS
44.8	0.14 FS	0.17 FS	0.20 FS
42.8	0.17 FS	0.23 FS	0.32 MS
40.0	0.12 VFS	0.16 FS	0.20 FS
37.0	0.17 FS	0.21 FS	0.25 FS
35.2	0.18 FS	0.24 FS	0.32 MS
33.0	0.26 MS	0.30 MS	0.36 MS
30.4*	0.01 FSilt	0.14 FS	0.19 FS
26.0	0.17 FS	0.20 FS	0.23 FS
23.9*	0.00	0.02 MSilt	0.07 VFS
21.9	0.15 FS	0.18 FS	0.23 FS
18.0*	0.00	0.00	0.01 FSilt
13.5	0.11 VFS	0.14 FS	0.18 FS
11.9*	0.08 VFS	0.11 VFS	0.15 FS
5.5*	0.13 FS	0.15 FS	0.18 FS
2.8	0.13 FS	0.16 FS	0.20 FS

* Samples that Contain a Significant Amount of Clay and Silt Legend: FSilt = Fine Silt MSilt = Medium Silt VFS = Very Fine Sand FS = Fine Sand MS = Medium Sand CS = Coarse Sand

Once the Nordin bed material gradations were input into the model, a 2-year discharge of 1,289,000 cfs was run for 30 days (Copeland and Lombard 2009). This channel-forming discharge allows the model to rework the bed material gradations to those that best represent the channel conditions. These new bed material gradations are then used as the initial gradations for the MVK and ERDC Phase I and II model. As part of the ERDC field data collection program, bed material samples were collected from RM 19.6 through Southwest Pass, and comparisons made to the MVK model.

The grain-size distributions for 4 of the 17 ERDC sampling sites are presented below. Those sites include BSS-17, BSS- 18, BSS-23, and BSS-26. BSS-17 and BSS-18 are located at RM 5.5, upstream of the WBSD. BSS-23 and BSS-26 are located at RM 2.5, downstream of the WBSD. These sites were selected because a sample was taken by Nordin at these locations. Furthermore, the ERDC models include a cross section at these locations, and both locations are within the PAA reach. Bed material samples were collected at these sites in March, July, and September 2009. At RM 5.5, BSS-17 is located toward the right descending bank, and BSS-18 is located toward the left descending bank. The approximate locations of these sample sites are shown on Figure 4.3. The cross section at RM 5.5 is beginning to resemble a typical channel cross section with a flatter shape and the thalweg located toward the center of the channel. BSS-17 is located in the PAA. Figure 4.4 provides the grain-size distribution at Site BSS-17. Figure 4.4 provides the grain-size distribution at Site BSS-18. For BSS-17, all three bed material samples collected in 2009 are significantly finer than the sample collected by Nordin. However, the Nordin sample was collected from the channel thalweg, and BSS-17 is located more on the adjacent bar. The Nordin sample is 95 percent sand while all three samples collected during 2009 have a much higher concentration of finer material (silt and clay). The sample collected during March is just over 70 percent fine material. Both the sample collected during July and the sample collected in September are approximately 47 percent fine material.

For BSS-18, the sampled collected in March 2009 replicates the Nordin sample well. As stated, the Nordin sample was 95 percent sand while the BSS-18 sample collected in March 2009 was 98 percent sand. The samples collected in July and September 2009 were much finer. The sample collected in July was 68 percent fine material while the sample collected in September was 82 percent fine material. The data on Figure 4.5 for BSS-18 indicates a possible seasonal or discharge variation in the grain-size distribution.

Figure 4.3. Approximate Bed Sample Locations at RM 5.5.

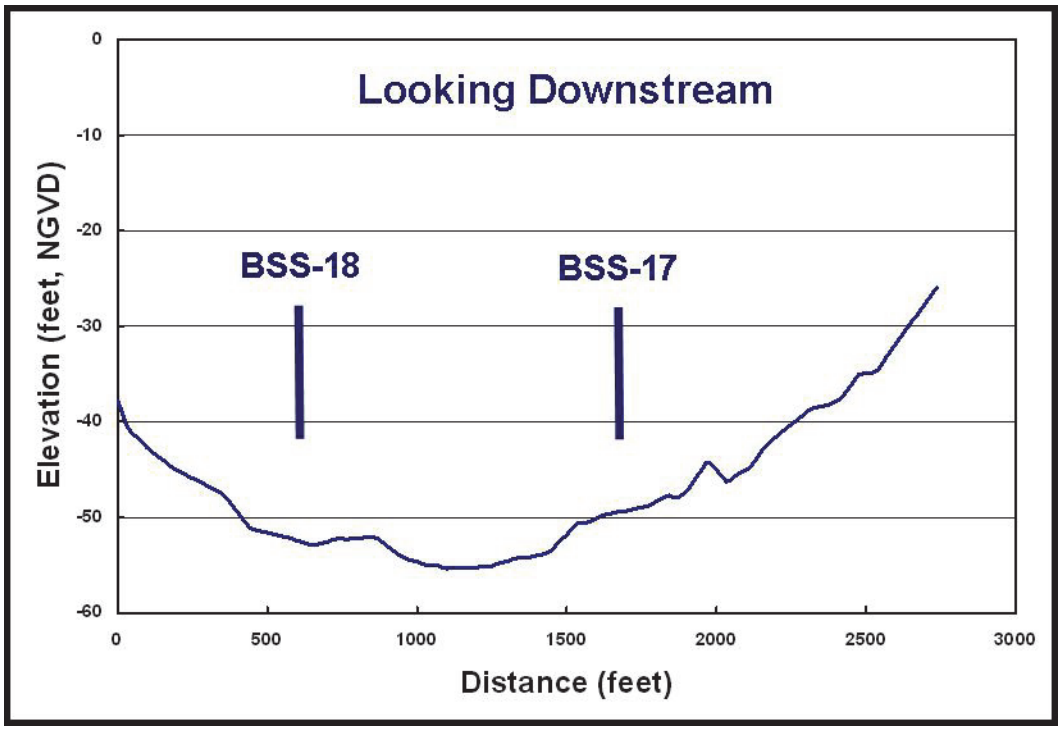

Figure 4.4. Bed Material Gradations at Site BSS-17.

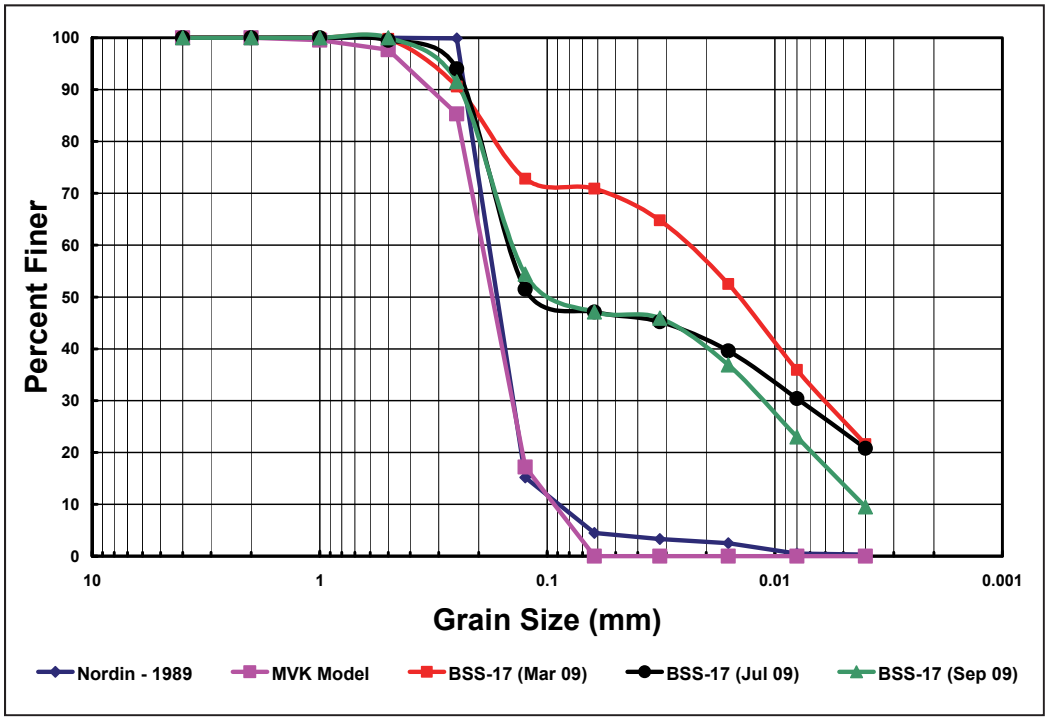

Figure 4.5. Bed Material Gradations at Site BSS-18.

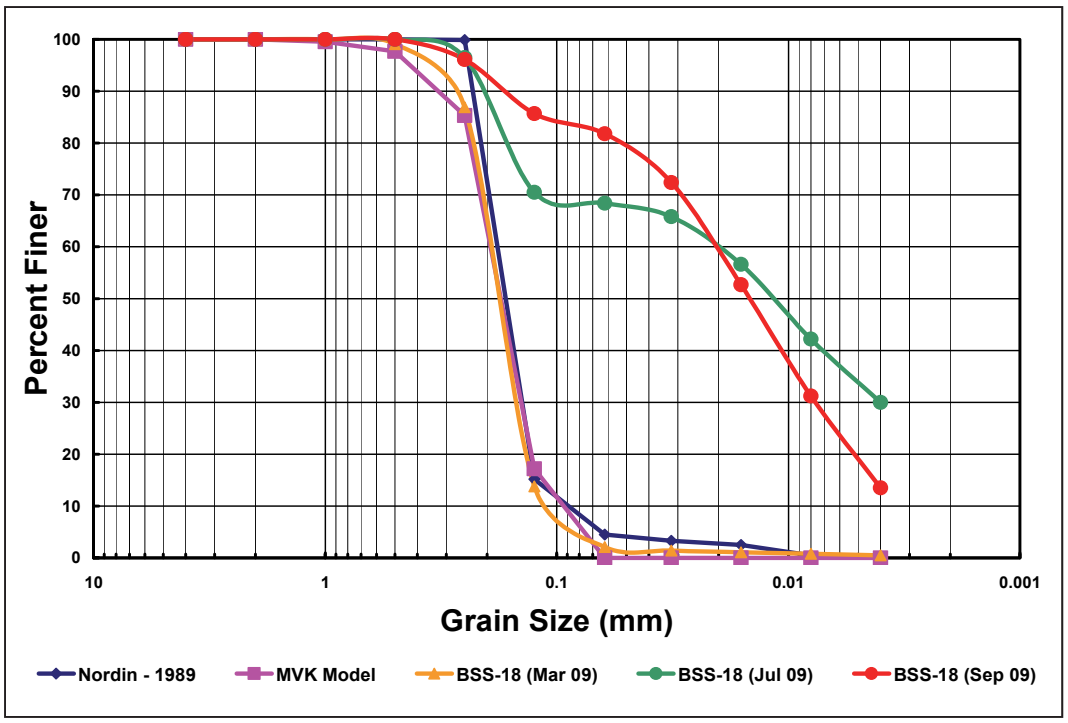

At RM 2.5, BSS-23 is located toward the right descending bank, and BSS-26 is located toward the left descending bank. The approximate locations of these sample sites are shown on Figure 4.6. The cross section at RM 2.5 has a typical bendway section shape with the thalweg along the outside of the bend and a point bar formation on the inside of the bend. BSS-23 is located in the anchorage area. Figure 4.7 provides the grain-size distribution at Site BSS-23. Figure 4.7 provides the grain-size distribution at Site BSS-26. For BSS-23, all three bed material samples collected in 2009 were similar to the sample collected by Nordin even though the Nordin sample was collected from the channel thalweg and BSS-23 is located on the adjacent bar. All samples were between 96 and 99 percent sand.

For BSS-26, samples were only collected during March and July 2009. The grain-size distribution for both of these samples was much finer than the Nordin sample. The March sample was 65 percent fine material, and the July sample was 60 percent fine material while the Nordin sample was approximately 97 percent sand. The data in Figures 4.7 and 4.8 indicate a lateral variation in the grain-size distribution across the channel at RM 2.5. Because of the variation in the bed material samples bed, material gradations in the model were not modified for the ERDC effort.

Figure 4.6. Approximate Bed Sample Locations at RM 2.5.

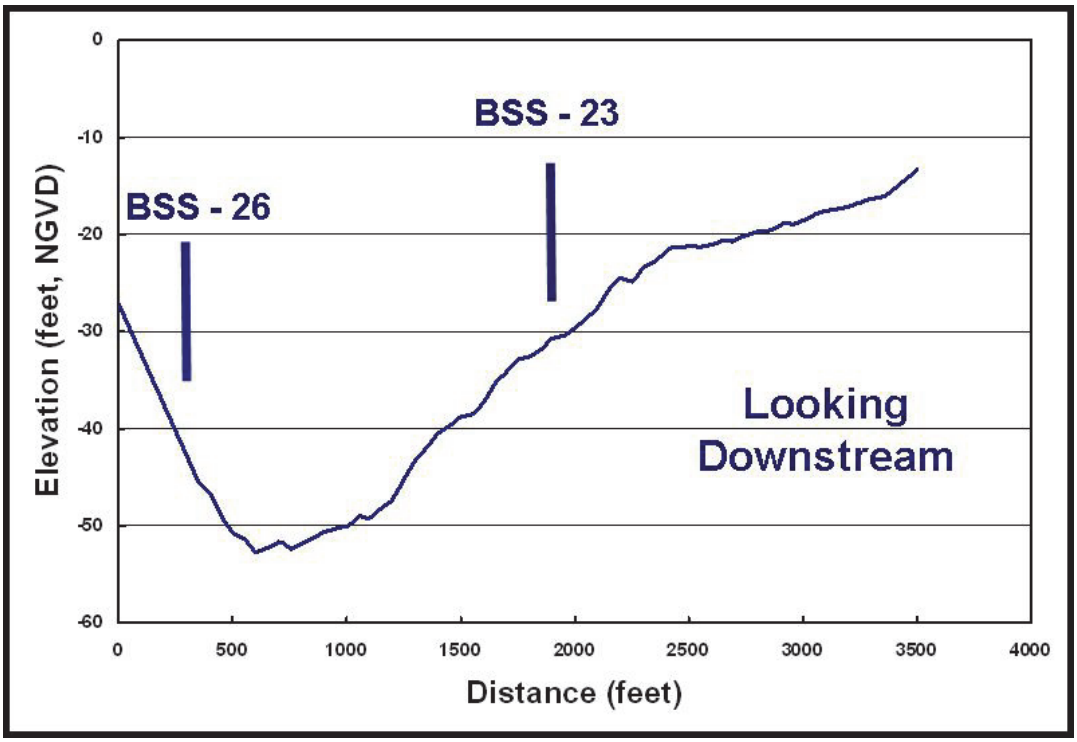

Figure 4.7. Bed Material Gradations at Site BSS-23.

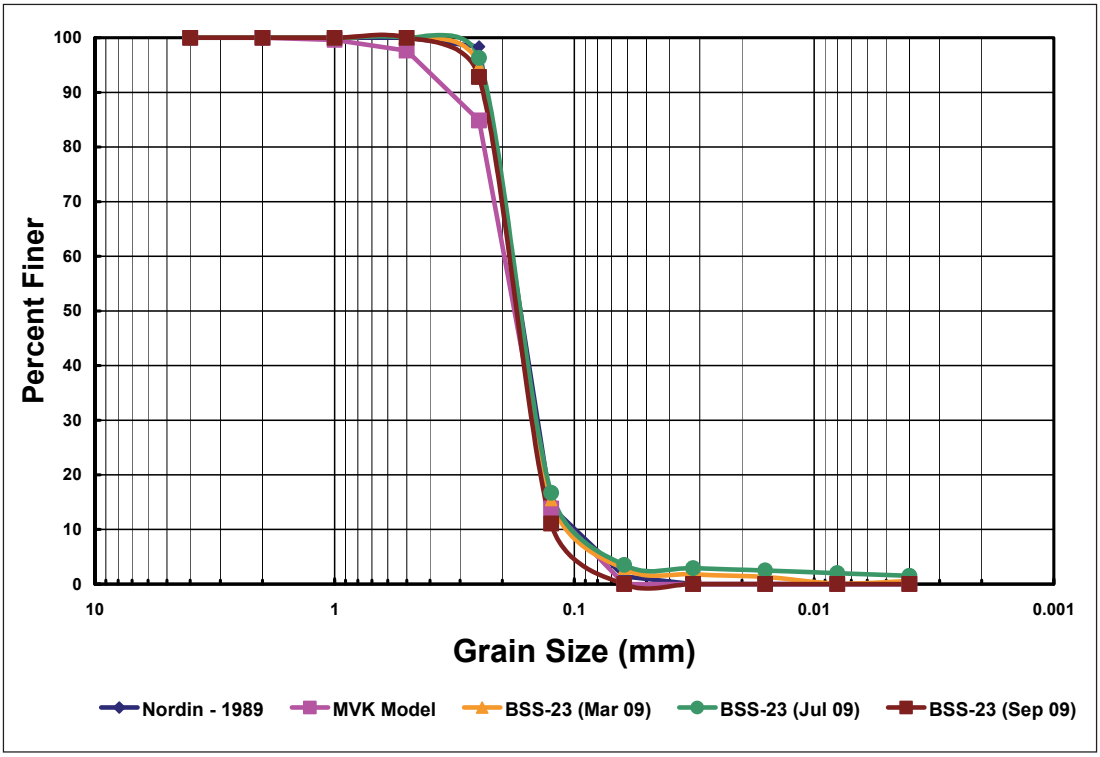

Figure 4.8. Bed Material Gradations at Site BSS-26.

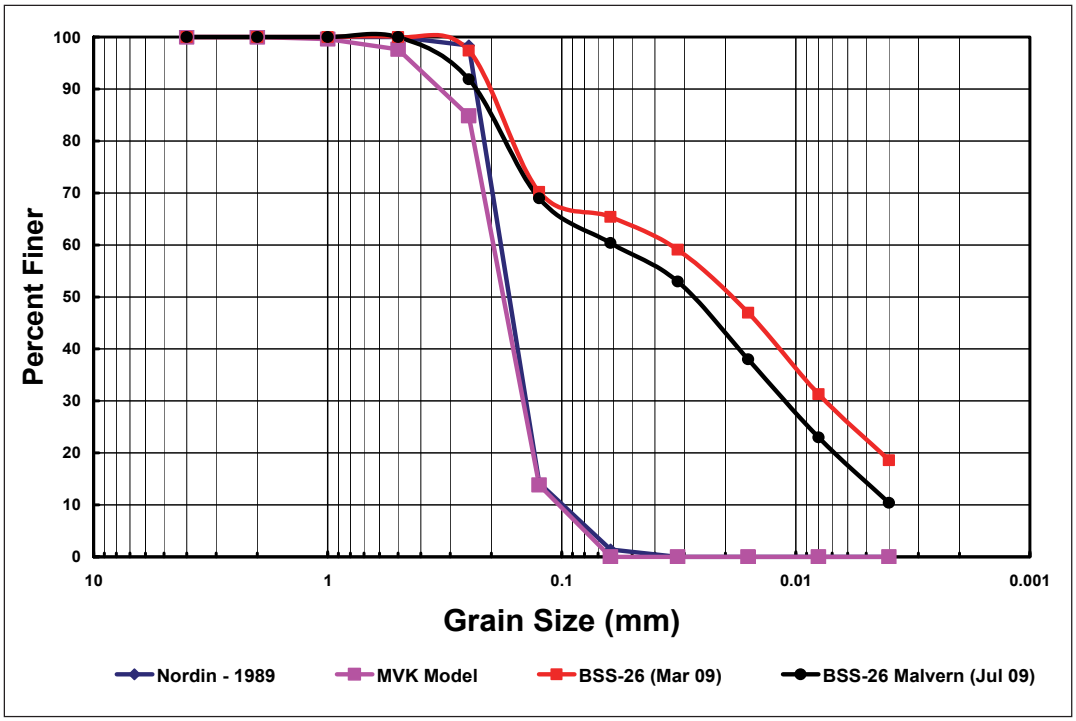

Diversions

In the HEC-6T model, the percentage of discharge leaving the river through diversions compared to the discharge in the river immediately upstream of that diversion is an input parameter. Discharge distribution measurements were taken by ERDC at Baptiste Collette Bayou, Grand Pass, WBSD, Cubits Gap, Mississippi River upstream of Baptiste Collette Bayou, Mississippi River immediately upstream of WBSD, Mississippi River immediately downstream of WBSD, and in various small diversions in the bank of the Mississippi River between Venice and HOP. Figure 4.9 is a plot of the discharge distributions at Baptiste Collette Bayou, Grand Pass, WBSD, and Cubits Gap for the 2003 through 2009 time period as compared to the discharge in the Mississippi River at Venice. The plot includes the data collected by the ERDC along with previous measurements obtained by the New Orleans District (MVN). Review of this data indicates that for most discharge conditions, Baptiste Collette and Grand Pass each divert approximately 10 to 13 percent of the Mississippi River discharge at Venice. Cubits Gap diverts approximately 13 to 18 percent of the discharge, and WBSD diverts approximately 5 percent of the flow. Figure 4.10 shows the discharge distribution at WBSD by year. This plot shows the increase in discharge over time as the WBSD has enlarged. For the ERDC model evaluation, the discharge distribution at WBSD was set at the current rate of approximately 7 percent of the Mississippi River discharge at Venice.

Figure 4.9 Measured Discharge Distributions for Baptiste Collette Bayou, Grand Pass, West Bay Diversion, and Cubits Gap (2003 – 2009).

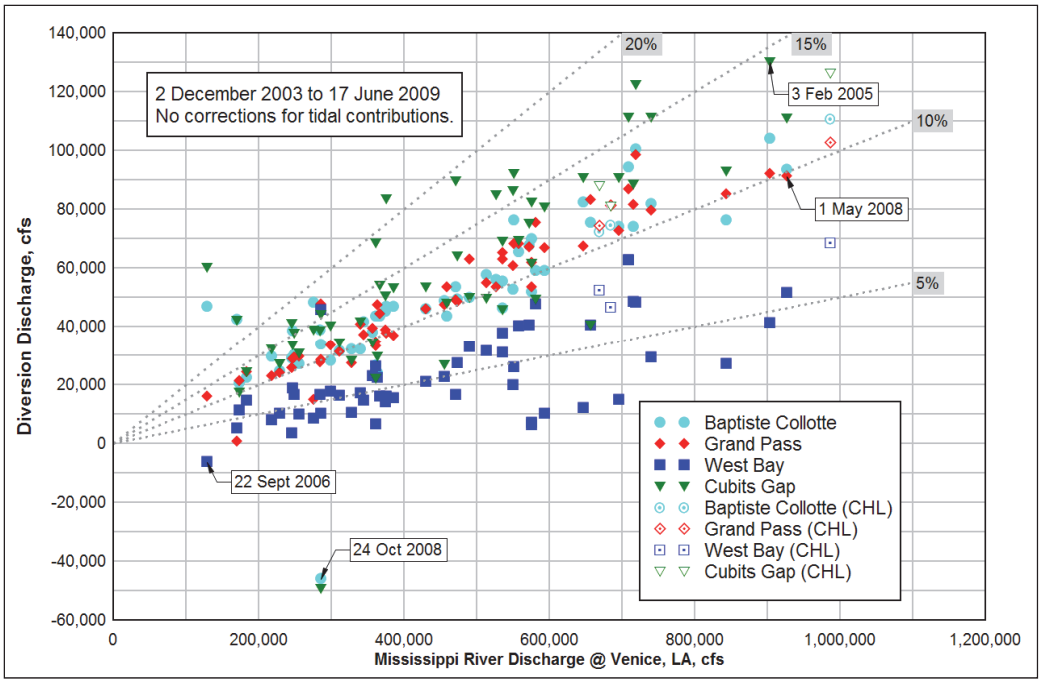

Figure 4.10. Measured Discharge Distributions at WBSD (2004 – 2009).

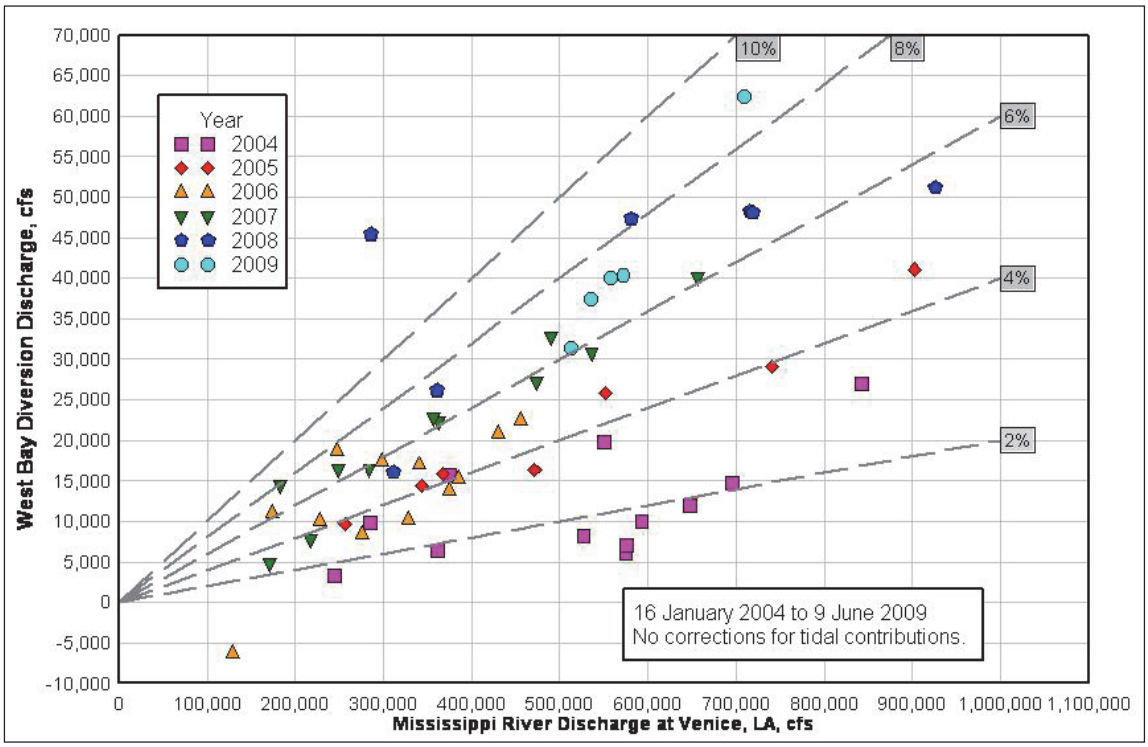

Table 4.5 provides the locations of the diversions contained in the ERDC Phase II model. The Davis Pond Diversion, WBSD, and Fort St. Philip Diversion were added to the ERDC Phase II model. For the diversions that were included, discharge through each diversion was modeled as a percentage of the discharge in the Mississippi River upstream from that diversion. When available, the percentages were estimated from measured data. When no measured data were available, the percentage of discharge in the diversions was calculated (Copeland and Lombard 2009). For diversions added in the ERDC Phase II model, the diversion ratios were estimated from a combination of ERDC field data and multi-dimensional model data.

Table 4.5. Diversion / Distributary Locations.

Reach	Diversion / Distributary	RM
Southwest Pass	Burrwood Bayou	-14.4
	Outlet W-2 and Overbank Flow	-9.8
	Joseph Bayou	-4.5
	Soutwest Pass At Mile 3.0 West	-3.0
HOP to Above Venice	South Pass and Pass a Loutre	0.0
	Cubits Gap and Overbank Flow	3.0
	West Bay *(ERDC model only)*	
	Grand Pass (The Jump)	10.5
	Baptiste Collette Bayou	11.5
	Fort St. Philip *(ERDC model only)*	18
Above Venice to Tarbert Landing	Bohemia Spillway	33 - 45
	Caernarvon Diversion	81.4
	Davis Pond *(ERDC model only)*	118.4
	Bonnet Carre' Floodway	127 – 129
	Morganza Floodway	280
Above Tarbert Landing	Old River Complex	311.5 – 316.5

For the diversions in Southwest Pass, the diverted discharge percentages were directly related to the widths of the diversions. For the previously mentioned Venice to HOP reach, the outflow through the diversions was estimated from measured data. For those diversions / distributaries whose discharge percentage changed with time, an average percentage for the 1992 – 2002 time period was adopted for the MVK validation simulations.

Discharge over the Bohemia Spillway and through the Bonnet Carre' and Morganza Floodways only occurs during flood flows. The diversion percentage of discharge over the Bohemia Spillway was calculated. Diversion percentages at Bonnet Carre' and Morganza were assigned in the model to match the operation schedules.

The Caernarvon Diversion structure is controlled, and its operation is not a direct function of Mississippi River flows. Discharge through this diversion was calculated based on the assumption that the gates would remain open during the entire simulation. For the Old River Complex that includes the Auxiliary Structure, Low Sill Structure, Overbank Spillway, and Hydropower Structure, percentages of discharge distribution are average discharges for the 1991 – 2002 period of record.

Sediment Diversion Ratios

The ratio of the sediment concentration by grain-size class in the diverted discharge to that in the river at an upstream reference section is a model input requirement. An unprecedented advantage of the WBSD evaluation is that multi-dimensional modeling was being conducted concurrent with the 1D modeling effort and was validated to field data. Multi-dimensional models have the ability to compute diverted sediment concentrations. For the WBSD, Grand Pass, and Baptiste Collette (Figures 4.11 -4.13), the sediment diversion concentration ratios used in the ERDC Phase II model differ from Phase I or MVK models and were derived from the Adaptive Hydraulics Model (AdH), a 2D depth-averaged model. Cubits Gap sediment diversion ratios were determined from the ERDC field data collection effort. For all other diversions in the model, the sediment concentration diversion ratios used were determined by MVK.

The lack of available accurate sediment concentrations for diverted discharge is a weakness of previous 1D modeling on the Lower Mississippi River. For the Barbe et al. (2002) HEC-6 model, a sediment diversion ratio of 1 was used for silts and clays, and 0.5 was used for sands. In the MVK

Figure 4.11 West Bay sediment diversion ratios for ERDC Phase II vs Phase I.

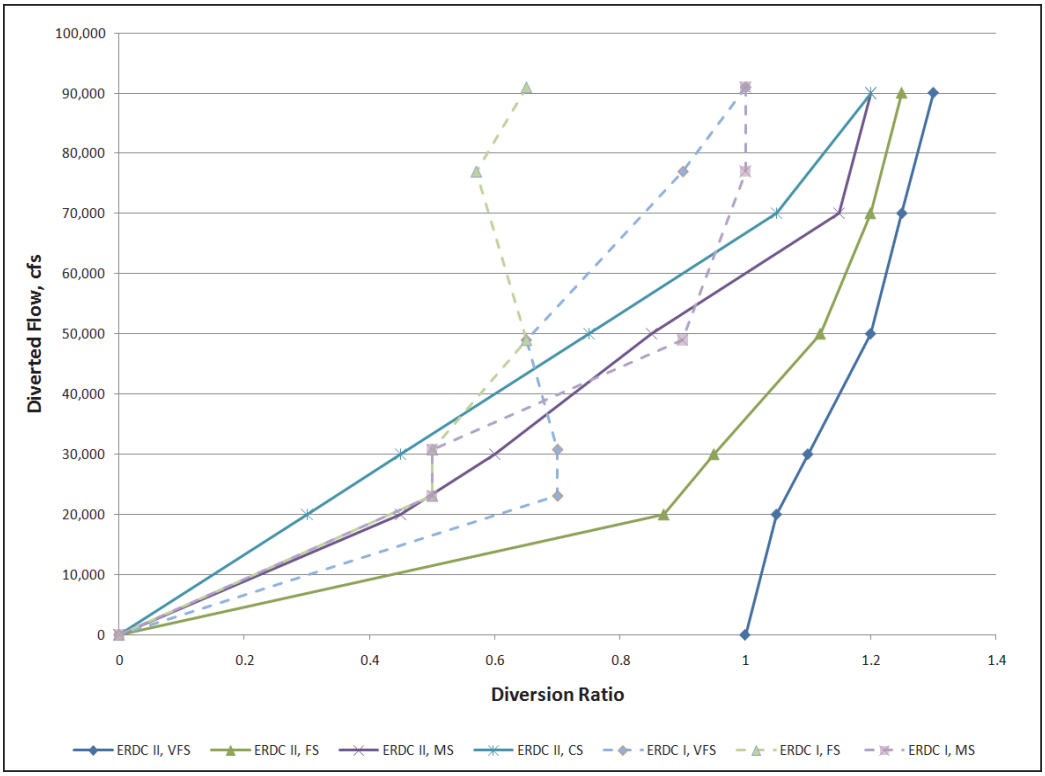

Figure 4.12 Grand Pass sediment diversion ratios for ERDC Phase II vs MVK Model.

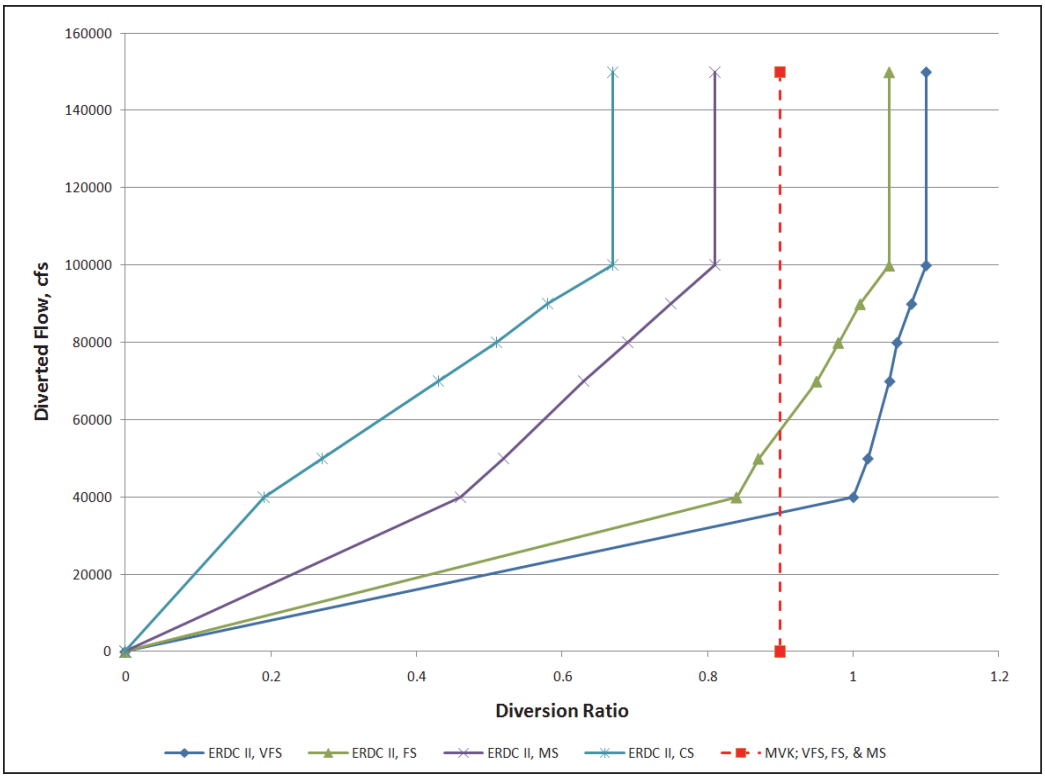

Figure 4.13 Baptiste Collette sediment diversion ratio Phase II vs MVK.

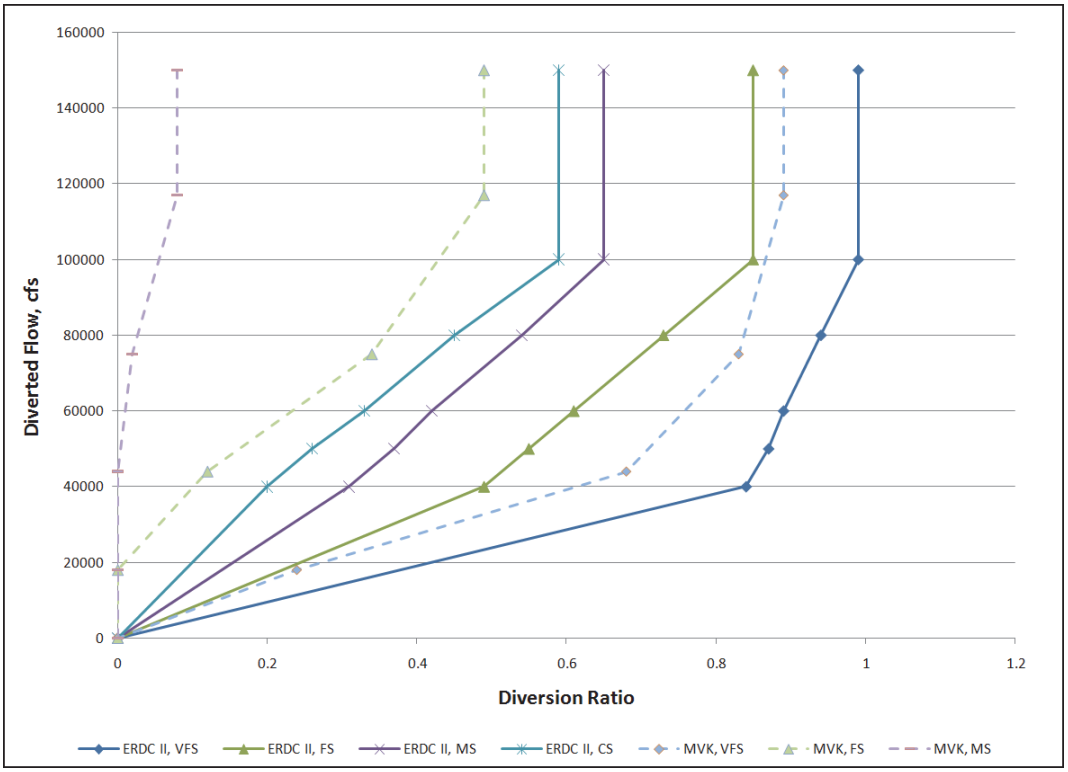

HEC-6T model, the Rouse equation was used to determine the sediment concentration of the diverted flow. This method estimates diverted sediment concentrations based on the sediment concentration profile in the river and the depth of the diversion inlet verses the average depth of the river. Current analysis of the collected field data indicates the true sediment diversion ratios might be greater than 1. Sensitivity analyses are usually conducted with sediment diversion concentration ratios varying from 0 to 1. A ratio of 0 means no sediment is diverted while a ratio of 1 means the concentration in the diverted discharge is equal to that in the river. The magnitudes, 0.1 – 2.5, of the ratios estimated from field data illustrate the complex relationship between diverted sediment concentration, flow, and sediment grain size. The magnitudes and considerable variability of the ratio was an unexpected result at the diversions and requires a more comprehensive study of river diversion dynamics.

Dredging

Dredging is an additional model parameter that is utilized for the MVK HEC-T and ERDC Phase II models. HEC-6T allows for dredging of the channel by specifying the bottom elevation and lateral extent of the dredge template. Dredging operations are conducted throughout the model

simulation during user-defined dredging windows; however, individual sections are dredged only when the bed elevation within the template exceeds the template bottom elevation plus a user-specified depth of over dredging and advance maintenance. The reach of the Mississippi River through the PAA is unique with respect to typical dredging requirements. Currently, the USACE, New Orleans District maintains a 750-foot-wide navigation channel adjacent to the 250-ft-wide PAA. The navigation channel is dredged to an elevation of -51 feet to accommodate the -45-foot channel plus 6 feet of advance maintenance. Parts of the navigation channel, especially the reach from Cubits Gap to HOP, require dredging annually or more frequently. A 250-foot-wide section of the PAA along with its access area is dredged to various depths (-48, -44, and -41 feet located at upstream, mid, and downstream respectively) along its length.

Dredging in the PAA is conducted once every 3 years. During the ERDC Phase I effort, HEC-6T did not allow for separate dredging templates or for a complex template with varying depths in the same template. Therefore, for the ERDC Phase I evaluation, a composite template was developed. This template attempts to simulate the combined navigation channel and anchorage area dredging as one. Developed by combining the areas of the navigation channel and anchorage area, the dredging template uses a composite width. The bottom elevation of the composite template is -50 feet with a bottom width between 940 and 970 feet dependent on the depth of dredging in the anchorage-area. This template is used for both simulations where dredging in the PAA scenarios are turned on. For the ERDC Phase I model, both the navigation channel and PAA are dredged twice a year, on January 1 and July 1. However, in actuality the PAA is dredged on a 3-year cycle. Thus, this results in an over estimation of the required dredging in PAA since the model fills the dredge channel before deposition is allowed in the remainder of the channel. For ERDC Phase II model, as previously stated, modifications were made to the code such that multiple templates can be dredged in the same cross section. This allows the PAA to be dredged on a 3- year cycle and the navigation channel on a 6-month cycle.

Implementation of multiple dredging templates in ERDC Phase II model allowed computation of cross-section shapes that were more realistic than the composite template used in ERDC Phase I. However, there are no simple algorithmic methods currently available in HEC-6T for distributing sediment deposition between the navigation and PAA dredging templates. After experimentation with a limited set of options, the following scheme was adopted:

1. After each 3-year dredging cycle (in which both the navigation channel and the PAA were dredged), deposition was distributed uniformly within both dredging templates. (All other factors being equal, cross-sectional area will be at a maximum immediately after a 3-year dredging cycle, and therefore deposition rates should be maximized. Actual model behavior is more complex since other factors, such as boundary forcings, are being varied throughout the simulation.)
2. After all other dredging cycles (in which only the navigation channel was dredged at 6-month intervals), deposition was distributed uniformly within the navigation dredging template.
3. Any deposition in excess of the volume required to fill the dredging template was distributed uniformly within the moveable bed limits, generally the entire river channel, including both dredging templates.

This scheme was successful in reproducing the relative quantities of dredging observed in the navigation channel and the PAA since creation of the WBSD 2003. However, the historical record of dredging within the PAA is limited to events in 2003, 2006, and 2009.

Validation

A two-phase validation was conducted for the ERDC Phase II model. The first phase was a comparison of computed water surface profiles to observed profiles. This was accomplished by running the ERDC Phase II model in the fixed-bed mode for a range of steady-state discharges and adjusting Manning's roughness coefficients so calculated water surface profiles matched measured stages at available gauge locations. Water surface elevations were validated to observed data from four gauge stations: Venice, Empire, West Pointe a la Hache, and New Orleans. At each gauge, stages versus discharge curves were generated from 1991 – 2011 data. Then a best fit function (see Figures 4.14 – 4.17), a forth-degree polynomial which generated the largest r^2 value, was fitted to the data.

For comparison to the best fit function, four steady-state discharges were simulated before and after a 1991 – 2002 simulation (Figure 4.18). Each best fit point, observation, for the four steady state flows was taken from the fourth-order polynomial. Then, a range in discharge was visually estimated from the stage versus discharge graphs and is denoted in Figure 4.18 as the whisker bars at each observation point. Reasonable validation was achieved with the calculated water surfaces from the ERDC Phase II model with all flows falling within the scatter of the observed data.

Figure 4.14 Stage vs. discharge curve at Venice.

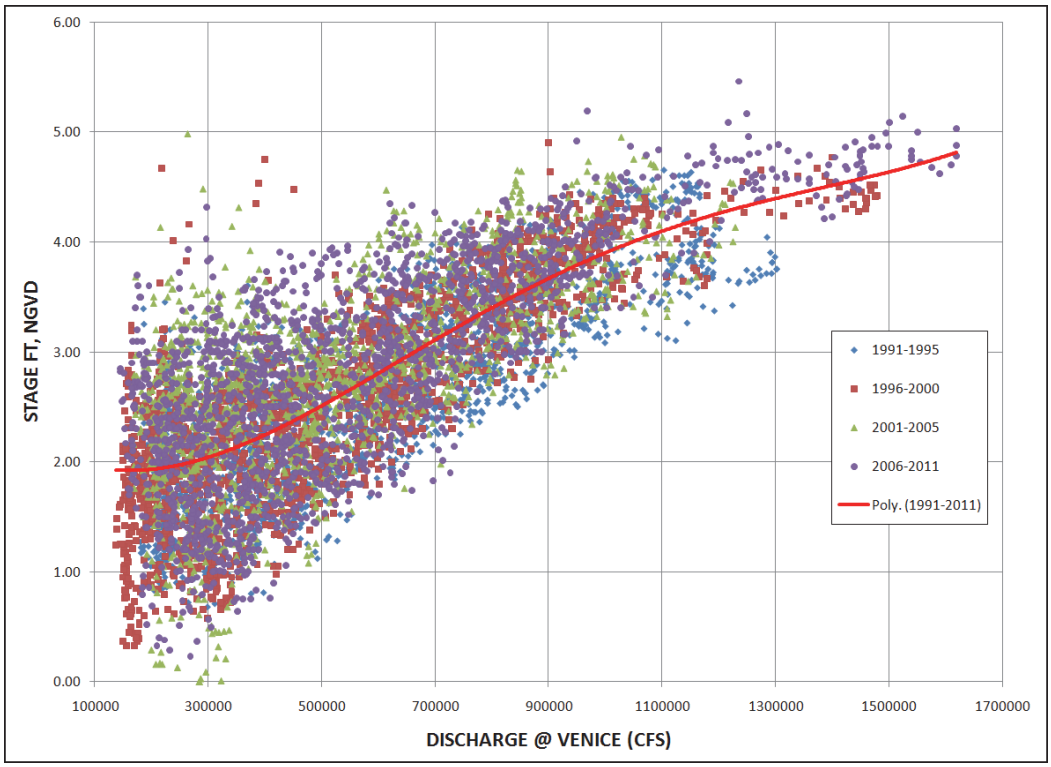

Figure 4.15 Stage vs. discharge curve at Empire.

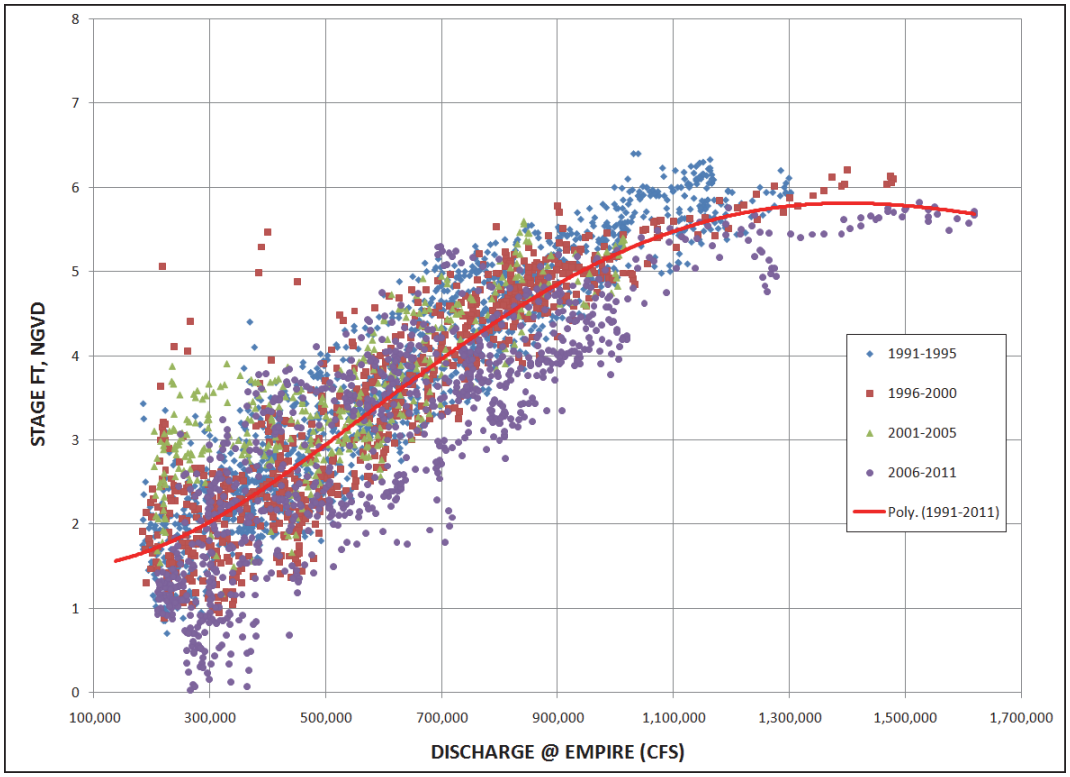

Figure 4.16 Stage vs. discharge curve at West Point.

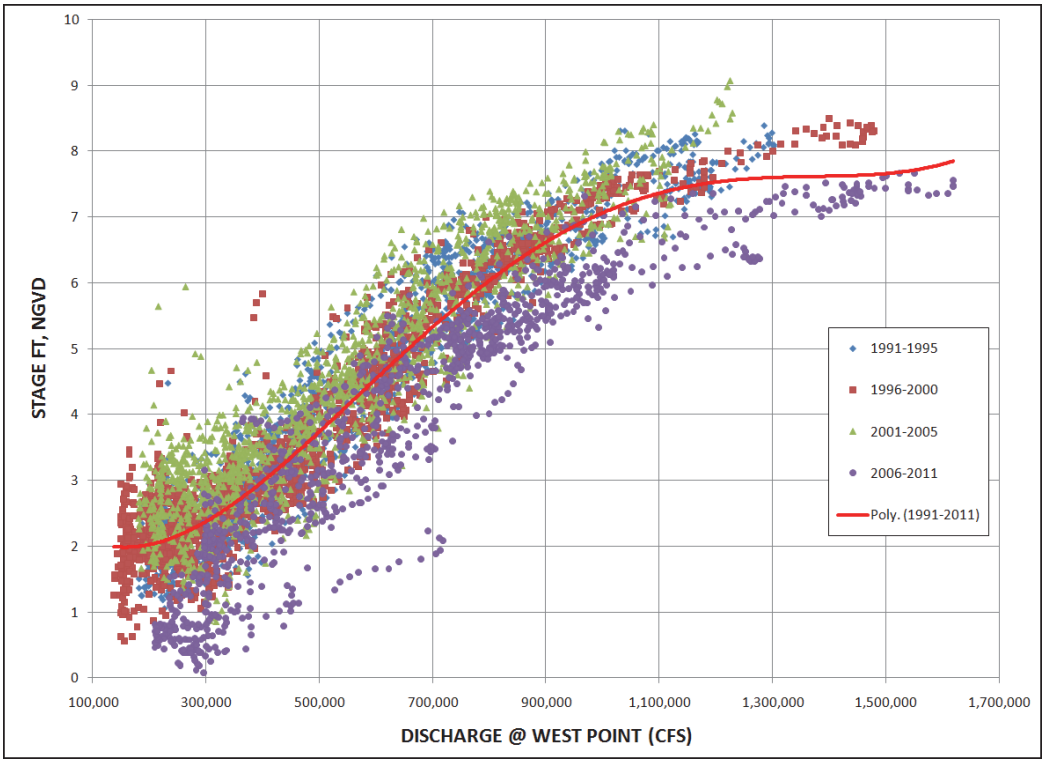

Figure 4.17 Stage vs. discharge curve at New Orleans.

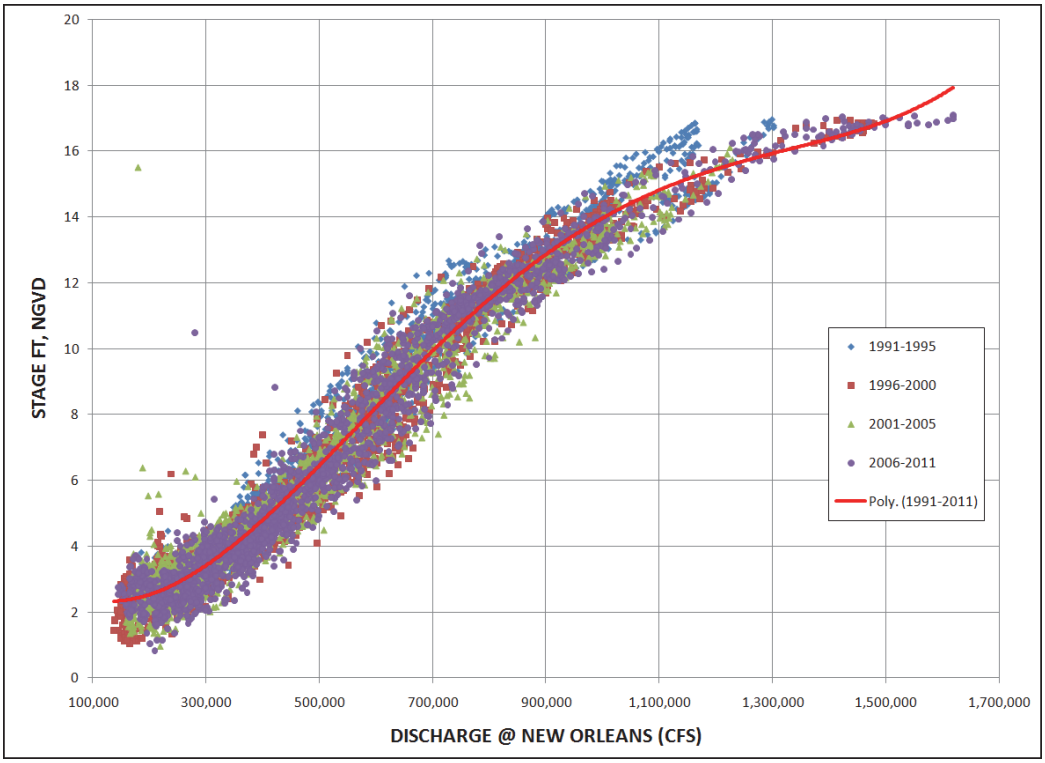

Figure 4.18 Water surface profile validation.

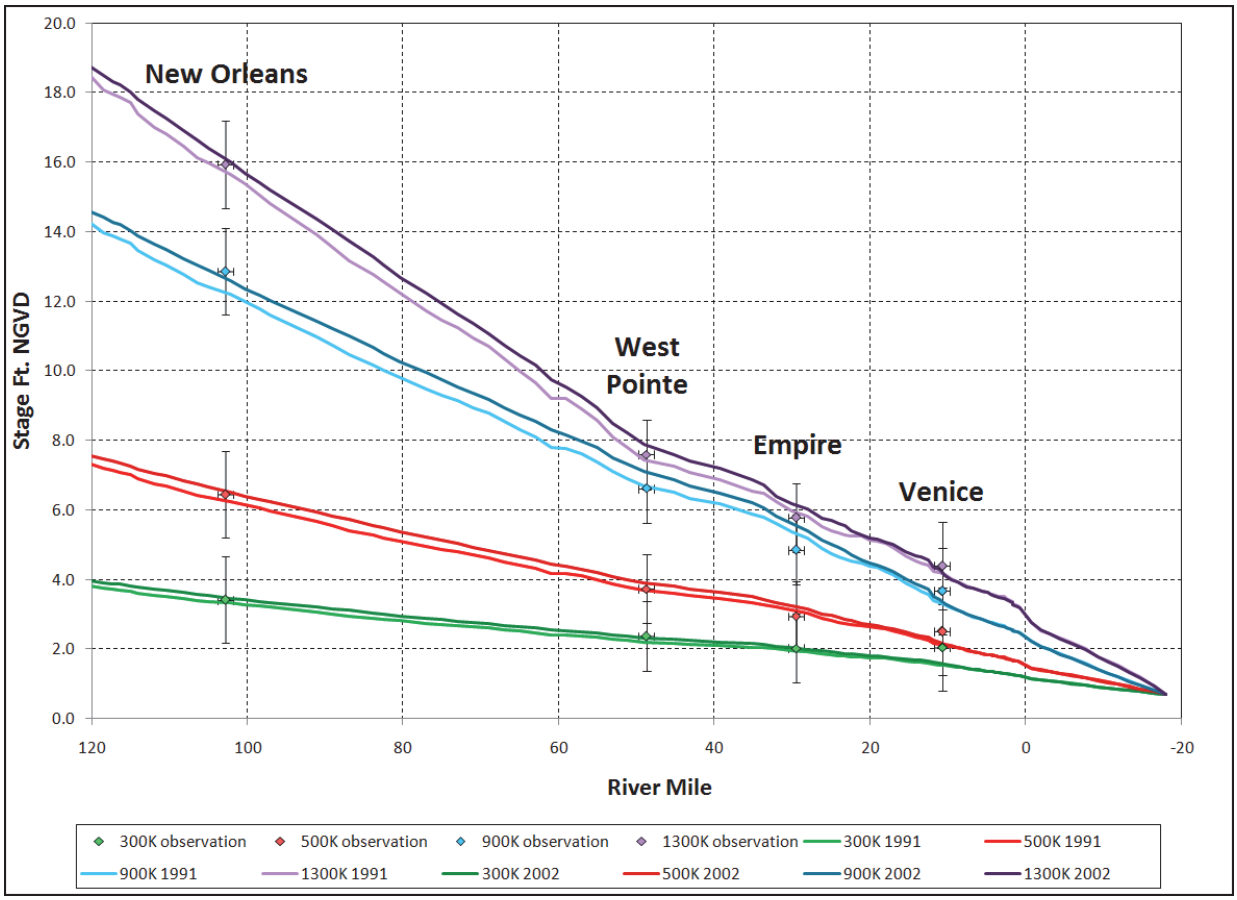

Sediment validation is accomplished in the MVK HEC-6T model by simulating observed erosion, deposition, and sediment transport. For the ERDC model, these validated parameters were rechecked for verification. The MVK HEC-6T model is validated to observed deposition downstream of the Old River Control Complex and to observed erosion at Smithland Crossing. The MVK HEC-6T model is also validated to measured sediment transport at Tarbert Landing (RM 306.0, RK 492.46) and Belle Chasse (RM 76.0, RK122.31) gauges. Validation also includes the simulation of reported dredging volumes in Southwest Pass and above HOP.

With the significant effort of the MVK HEC-6T model validation, simple comparisons between the ERDC Phase II model were conducted. Figure 4.19 shows the total sediment load passing comparisons between the two models. The variations between the two are primarily because of Ft. St. Philip and WBSD, thus the load passing does vary between the two models as would be expected.

Figure 4.19 Sediment passing comparison for 50-yr period, ERDC Phase II and MVK HEC-6T models.

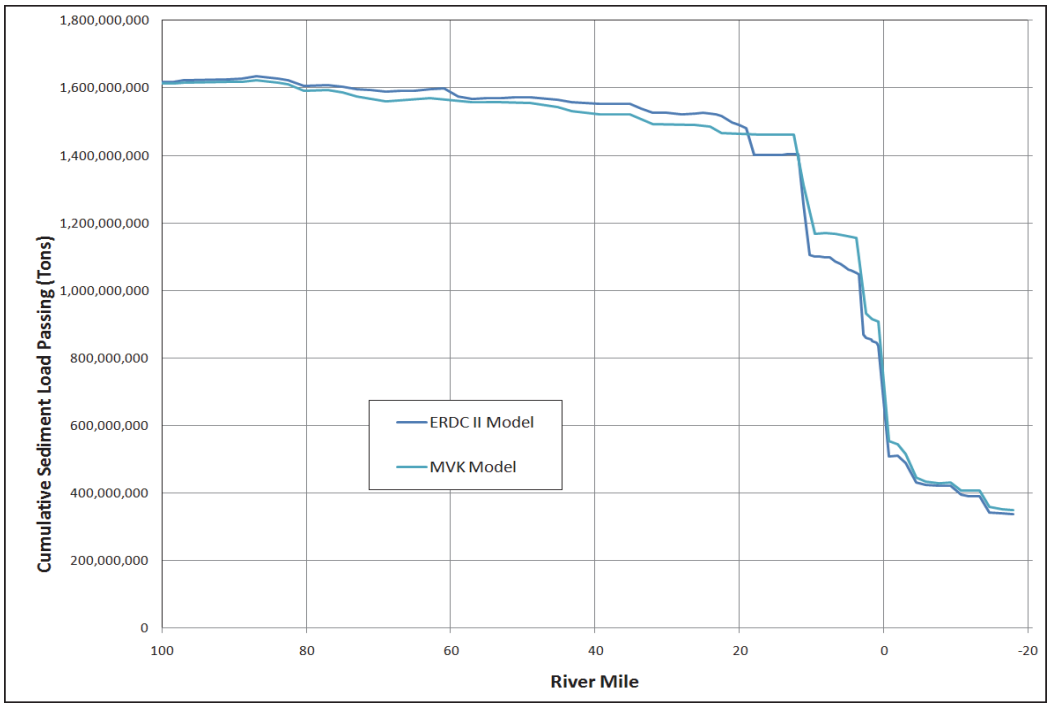

For the ERDC Phase II model, a recheck of the suspended sediment passing Belle Chase was done (Figure 4.20). Reasonable agreement exists in the model versus the observed suspended sediment data at the 700,000 cfs flows and above. This is beneficial since the majority of the sediment transport occurs in the higher flows. Less agreement is achieved in the lower flows, 600,000 cfs and less. Here the tidal influences are a factor changing the behavior of the system; therefore, it is expected that less agreement would exist.

Modeling results

For the ERDC Phase II Model, two scenarios were modeled:

- WBSD open and dredging in the Navigation and PAA template
- WBSD closed and dredging in the Navigation and PAA template.

Modifying the code for multiple dredge templates, as discussed previously, resulted in fewer necessary simulations for the ERDC Phase II model. Currently the model behaves appropriately in the area of interest, since dredging volumes calculated above HOP are close to reported values.

Figure 4.20 Suspended sediment concentration vs. ERDC Phase II model at Belle Chase.

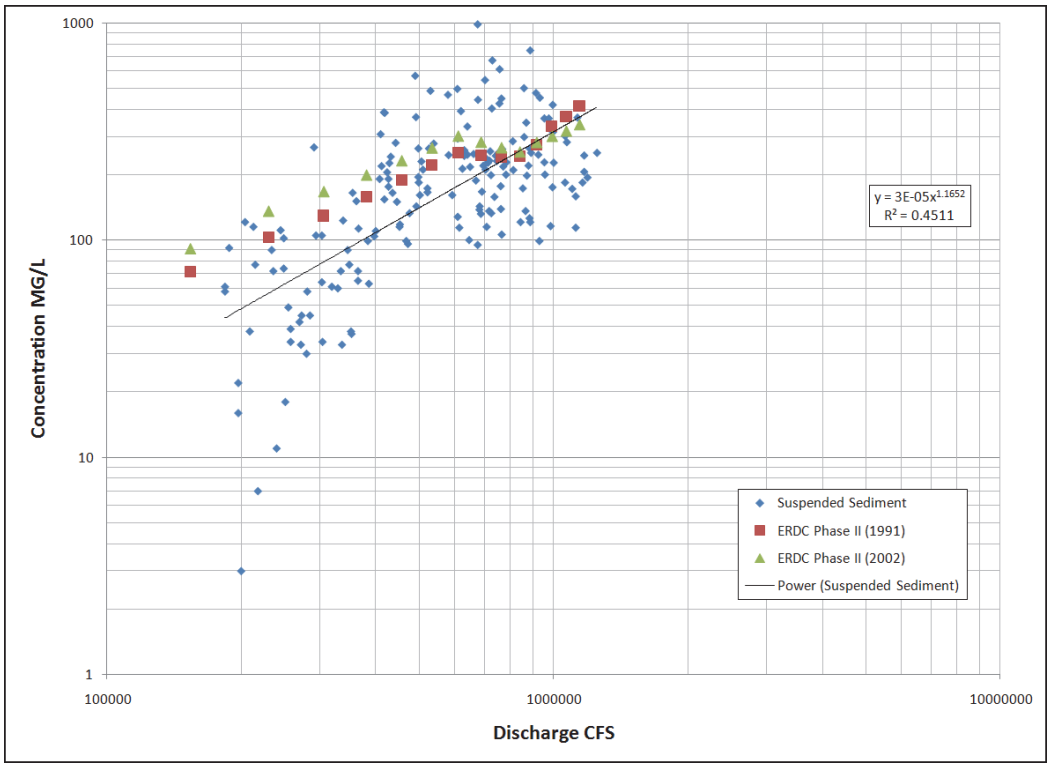

Based on the ERDC Phase II HEC-6T Model, the attributable dredging in the navigation channel and PAA due to WBSD being open for 50-yr simulation is 14 percent and 26 percent, respectively. Analyzing by decade over the 50-year hydrograph (Figure 4.21) shows the variability of these numbers. The navigation channel behavior is relatively consistent with 10 – 20 percent of dredging attributable to the WBSD. The PAA has a broader scale, ranging from -5 – 40 percent of dredging attributable due to WBSD being open.

While a net increase in PAA dredging of 36 percent was computed over the entire 50-year simulation, variations between individual 3-year dredging events were relatively large, and for a few 3-year cycles, dredging in the PAA decreased. Changes in the first decade, and to a lesser extent during the second decade, include the influence of relatively rapid adjustments in cross-section shape that may not be representative of long-term channel responses.

As compared to the ERDC Phase I model simulation of navigation channel dredging, the ERDC Phase II model showed a significant reduction in the quantity of dredging attributable to the WBSD. Since navigation channel dredging is approximately an order of magnitude greater than PAA

dredging, the portion of the total dredging (navigation channel and PAA) attributable to the WBSD, Figure 4.22, tends to mirror the response of the navigation channel.

Figure 4.21 Percentage of Current Dredging Due to Opening West Bay, based on 1D model.

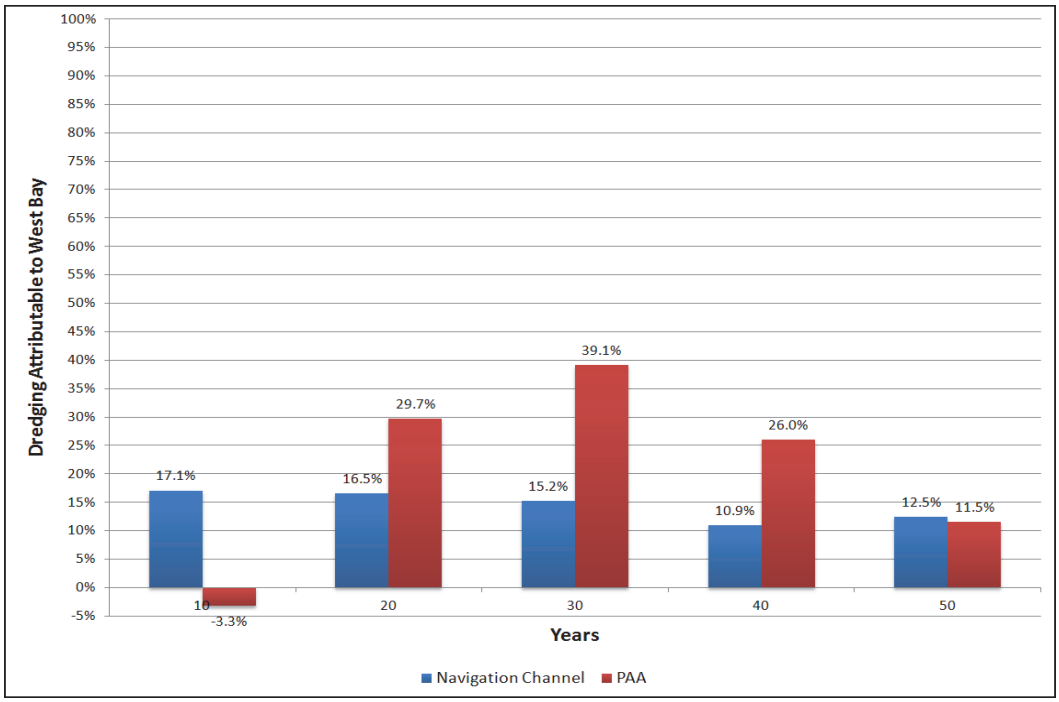

Figure 4.22 Combined Templates.

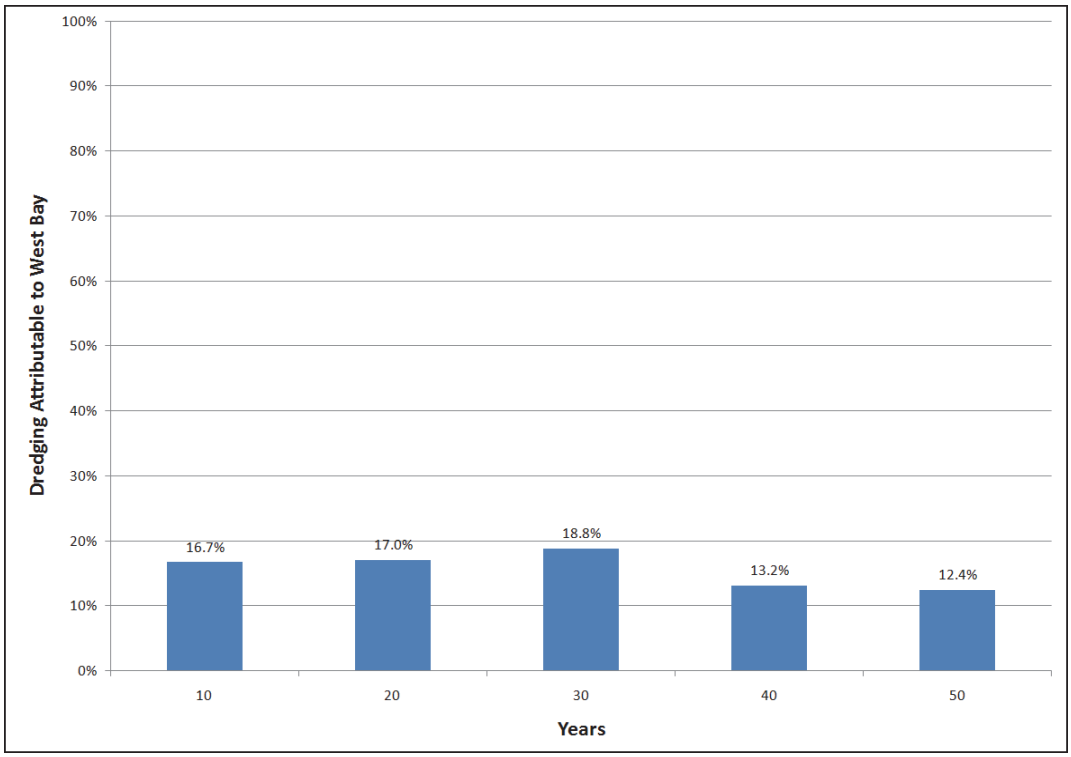

Figure 4.23 shows the total sediment load passing at each cross section normalized to RM 12.5. Fort St. Philip diversion was included and generates approximately a 5-percent reduction in sediment passing. Baptiste Collette and Grand Pass combine to generate a 20-percent reduction in sediment passing. WBSD indicated a 7-percent decrease in sediment load passing, and Cubits Gap yields a 13 percent reduction in sediment passing. These diversions, with WBSD open, total an approximate reduction of 54 percent in sediment load from RM 18 to RM 0 (Table 4.6).

Figure 4.23 Total Sediment Load in the Mississippi River from RM 80 to the Gulf Computed by the ERDC Phase II Model Relative to the Total Sediment Load at the Venice Discharge Range (RM 12.5).

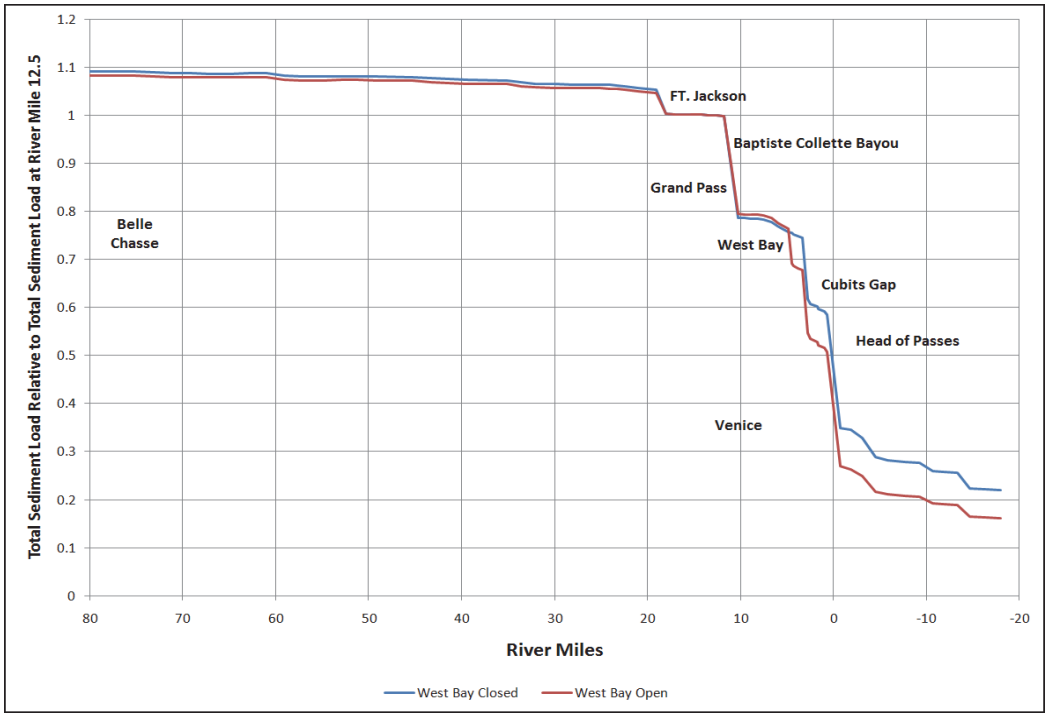

Table 4.6 Changes in Total Sediment Load in the Mississippi River Computed by the ERDC Phase II Model.

Diversion	RM	Changes in Sediment Passing			
		By Reach		Accumulated	
		Closed	Open	Closed	Open
Ft. St. Philip	18	5.02%	4.26%	5.02%	4.26%
	17	0.13%	0.13%	5.15%	4.39%
	15.4	0.05%	0.05%	5.20%	4.44%
	14.1	0.04%	0.05%	5.24%	4.49%
	13.4	0.04%	0.04%	5.28%	4.53%
	12.5	0.06%	0.07%	5.34%	4.60%

Diversion	RM	Changes in Sediment Passing			
		By Reach		Accumulated	
		Closed	Open	Closed	Open
	11.8	0.12%	0.12%	5.46%	4.72%
Baptiste Collete	11.05	10.61%	10.13%	16.07%	14.85%
Grand Pass	10.3	10.62%	10.24%	26.69%	25.10%
	9.5	0.10%	0.10%	26.79%	25.19%
	8.8	0.08%	0.08%	26.87%	25.27%
	8.1	0.05%	0.05%	26.91%	25.32%
	7.5	0.06%	0.06%	26.97%	25.38%
	6.7	0.53%	0.58%	27.50%	25.96%
	6	0.85%	0.97%	28.35%	26.93%
	5.5	0.60%	0.63%	28.96%	27.56%
	4.9	0.60%	0.59%	29.56%	28.14%
West Bay	4.46	0.31%	7.36%	29.87%	35.50%
	4.26	0.26%	0.40%	30.13%	35.91%
	3.83	0.34%	0.48%	30.47%	36.38%
	3.36	0.34%	0.44%	30.81%	36.82%
Cubits Gap	2.75	12.75%	13.02%	43.56%	49.84%
	2.46	1.00%	1.23%	44.56%	51.08%
	1.7	0.64%	0.80%	45.20%	51.88%
	1.6	0.51%	0.60%	45.71%	52.48%
	0.98	0.48%	0.60%	46.19%	53.08%
	0.72	0.71%	0.83%	46.90%	53.91%

Three cross-sections (RM 0.98, 3.83, and 5.5; Figures 4.32 -4.37) were selected to illustrate the behavior of the model in PAA reach while the WBSD is both open and closed. There are four key features that are central to all the plots. First, the plots clearly illustrate the impact of dredging the Navigation Channel and PAA separately. Second, once the dredging template fills, uniform deposition occurs at every point in the cross section that is within the moveable bed limits. Again, this is a 1-dimensional model and does not have the ability to distribute sediment laterally. Third, subsidence in the overbank area is clearly shown. Subsidence also reduces bed elevations within the channel, partially counteracting computed deposition. Finally, there is an increase in deposition downstream of the diversion when the WBSD is open that is also indicated in the AdH modeling effort (Figures 4.24 -4.29).

Figure 4.24 Channel Cross Section at RM 0.98, WBSD Closed.

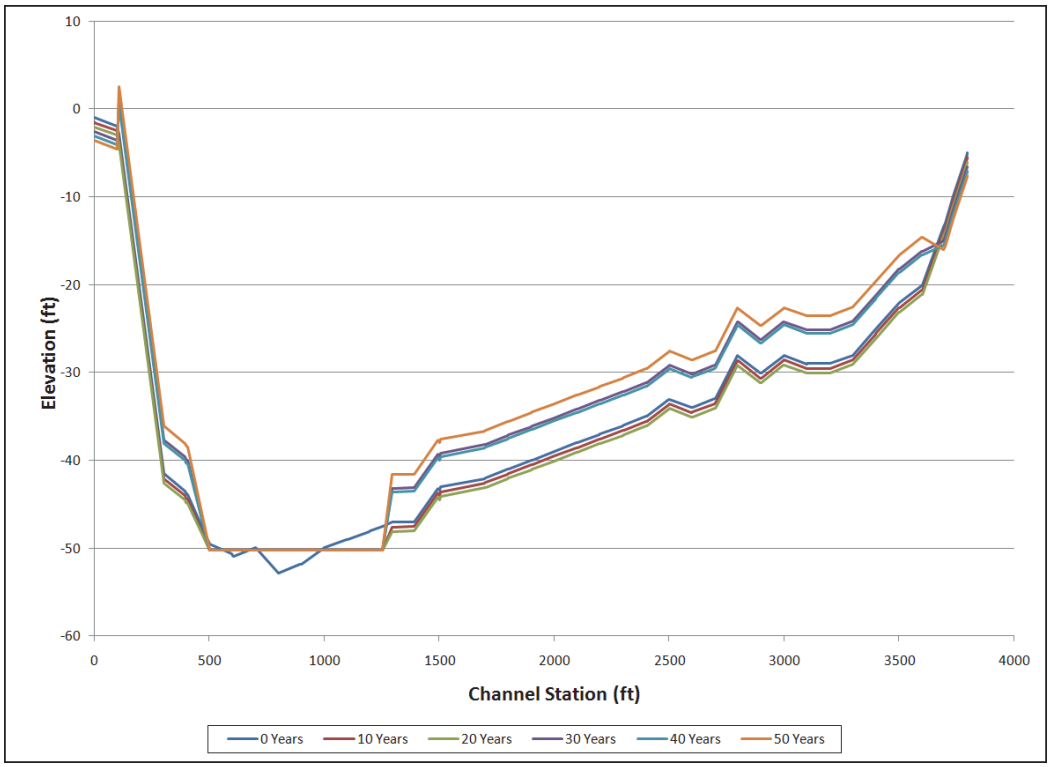

Figure 4.25 Channel Cross Section at RM 0.98, WBSD Open.

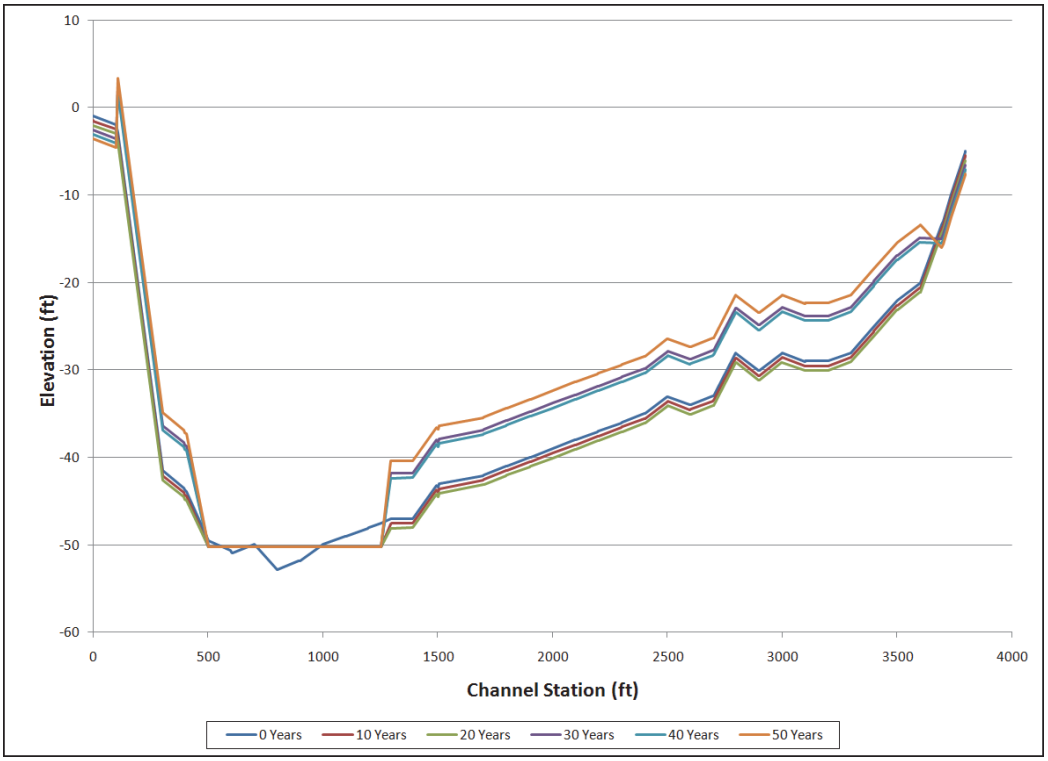

Figure 4.26 Channel Cross Section at RM 3.83, WBSD Closed.

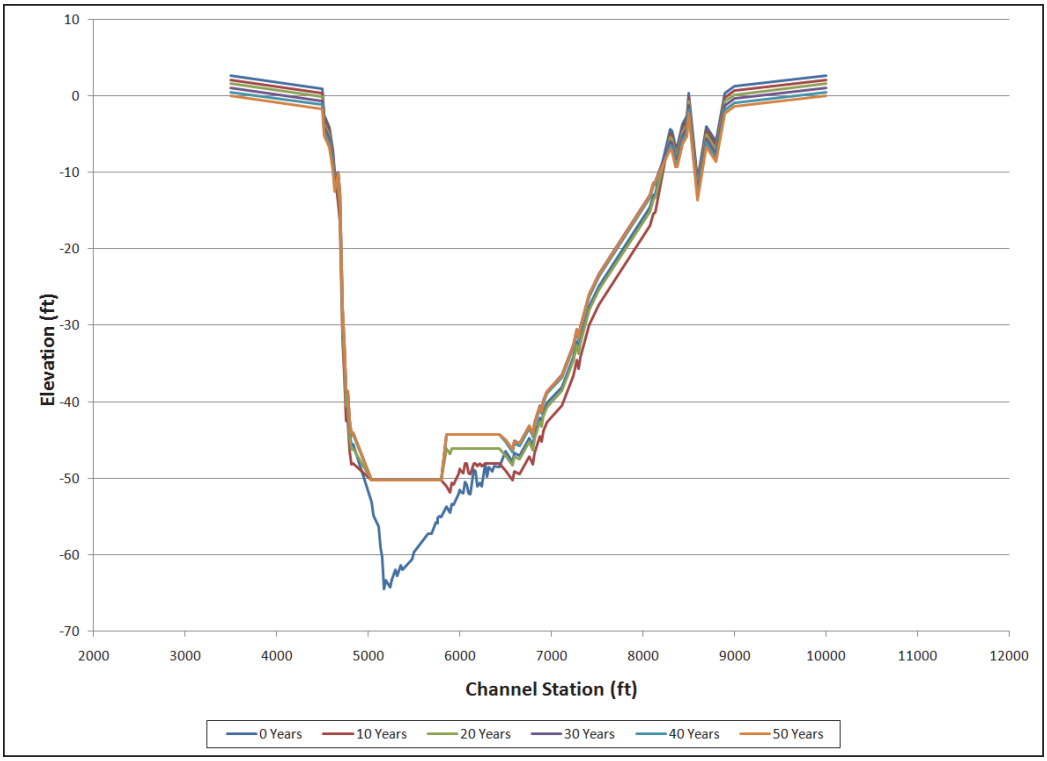

Figure 4.27 Channel Cross Section at RM 3.83, WBSD Open.

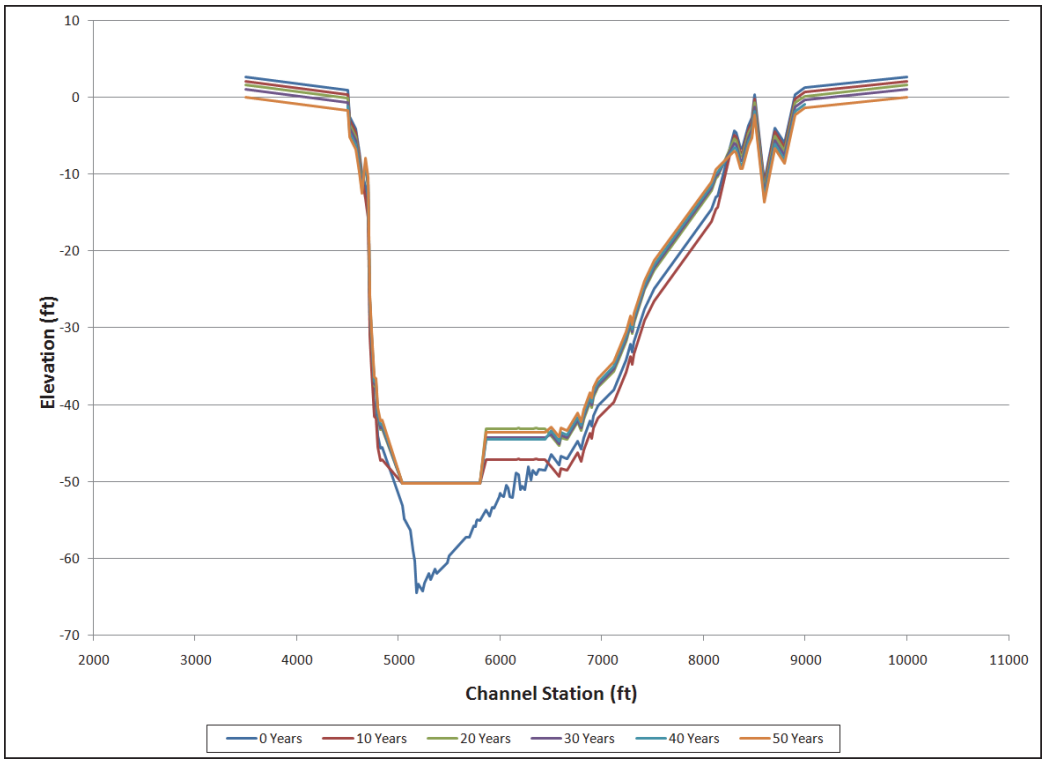

Figure 4.28 Channel Cross Section at RM 5.5, WBSD Closed.

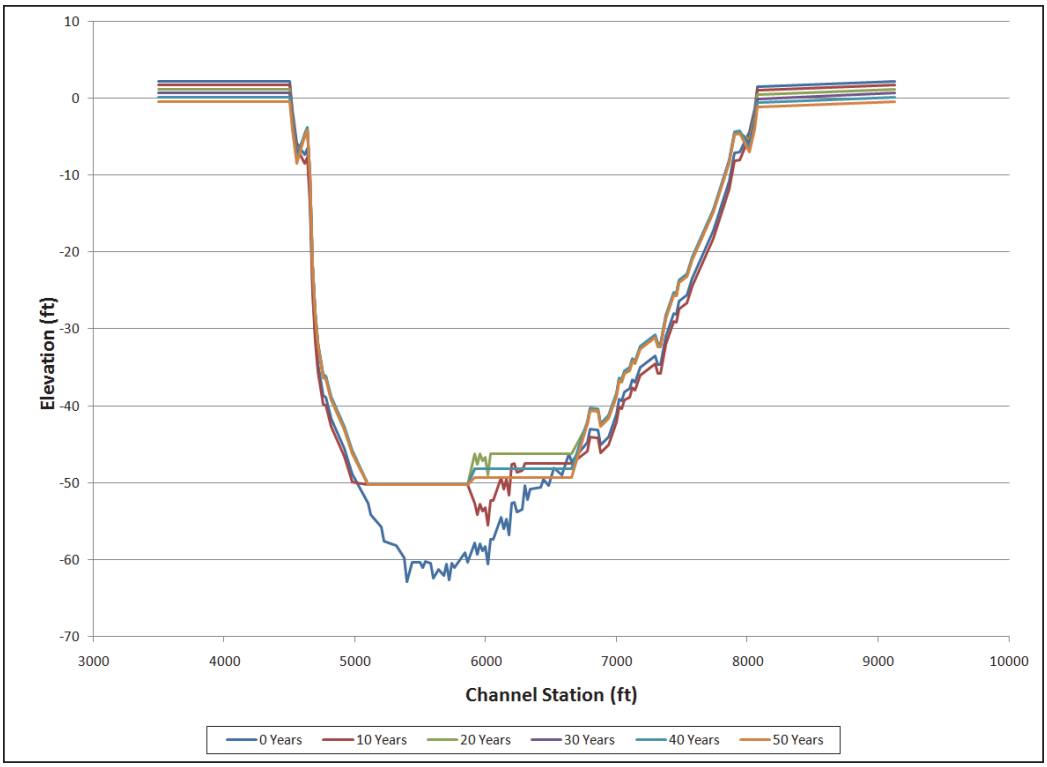

Figure 4.29 Channel Cross Section at RM 5.5, WBSD Open.

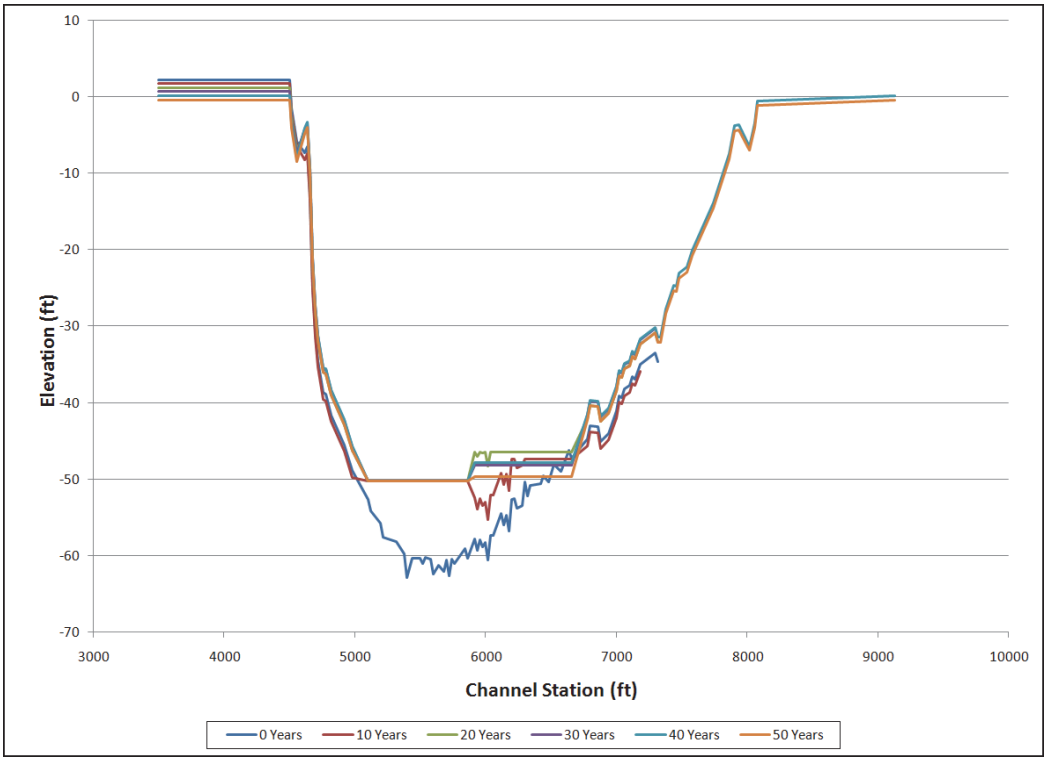

Sensitivity Analyses

Five sensitivity tests were conducted by varying key input parameters to determine the impact of attributable dredging due to WBSD being open.

- WBSD diversion ratios were varied +/-50 percent.
- Two sea level rise scenarios were run.
- Baptist Collette Bayou diversion ratios were varied +/- 50 percent.
- Both high and low subsidence rates were evaluated.
- Implemented Yang and Ackers White transport function.

Results of the five sensitivity tests are shown in Table 4.7.

Table 4.7 Sensitivity Test Results.

	Dredging Attributable to WBSD	
	Navigation Channel	PAA
WBSD Open	14.0%	26.4%
WBSD Open +50	11.9%	21.6%
WBSD Open -50	15.8%	29.5%
WBSD Open Sea Level Rise Scenario 1	12.9%	47.6%
WBSD Open Sea Level Rise Scenario 3	11.0%	53.0%
WBSD Open Baptist +50	11.7%	16.5%
WBSD Open Baptist -50	16.7%	31.9%
WBSD Open High Subsidence	14.5%	26.8%
WBSD Open Low Subsidence	13.2%	25.7%
WBSD Yang	13.4%	10.6%
WBSD Ackers White	16.2%	17.4%

With variations in sediment diversion ratios, it was imperative to quantify the potential impacts of changing them. Thus, both increases and decreases in the diversion ratios were applied at WBSD while all other model parameters were held constant. The changes in sediment diversion ratios are shown in Figure 4.30. One simulation increased the sand class diversion ratios by 1.5, and the other decreased it by 0.5, thereby creating a plus and minus 50 percent sand diverted test at WBSD. For the smaller grain sizes, (silts and clays) the ratios were held constant at 1. Decreasing the amount of diverted sand resulted in an attributable rate of 15.8 percent and 29.5 percent in the Navigation Channel and PAA respectively. Increasing the same values by 1.5 resulted in a decrease of the attributable rate of 11.9 percent and 21.6 percent in the Navigation Channel and PAA, respectively. These ranges represent the variations because of changes in the diversion ratios at WBSD.

Figure 4.30 Sediment Ratio for WBSD Sensitivity Test.

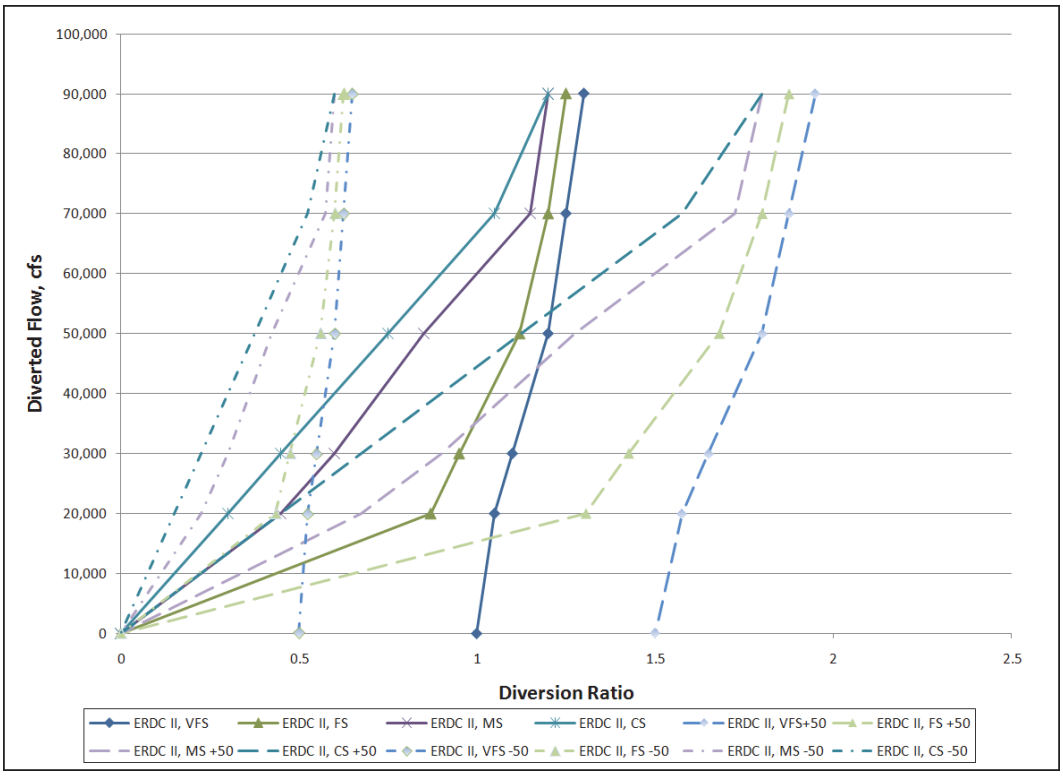

If the sediment diversion ratio is viewed as a measure of sediment diversion efficiency, this sensitivity test demonstrates that increasing efficiency reduces dredging by reducing the sediment supply downstream of the diversion. However, diverting water from the river also decreases the energy available to transport bed material sediments. In this case, where the downstream reach is already an efficient sediment trap, a ±50-percent change in efficiency produces less than a 3-percent change in the total computed dredging above the HOP.

Eustatic sea level rise appears to have the greatest impact on attributable dredging in the PAA. The applied rates are based on the USACE guidelines. Scenario 1 acceleration rate is 0.0000271 m/yr, and Scenario 3 acceleration rate is 0.000113 m/yr. Shown in Table 4.7, Scenario 1 results indicate that 12.9 and 47.6 percent of dredging is attributable to WBSD in the navigation channel and PAA, respectively. Scenario 3 results indicate 11 and 53 percent for the navigation channel and PAA, respectively.

Diversion impacts extend downstream and have the potential to change characteristics of other diversion. Baptiste Collette sediment ratios were also varied similarly to the WBSD increase and decrease of the sediment

diversion ratios in the first sensitivity test. Baptiste Collette was selected since it is upstream of WBSD. All other parameters were held constant with a 50-percent increase and decrease in the sediment diversion ratios at Baptiste Collette. This range of sediment diversion ratios represents the potential variation that WBSD might experience if diversions upstream were to change. For the navigation channel, the attributable amount due to WBSD ranged from 11 – 17 percent, while the PAA range was from 16 – 32 percent. The higher end in both ranges was from the reduction in sediment diversion ratios at Baptiste Collette.

Subsidence is counterproductive for land formation but beneficial for navigation. Here, two rates were evaluated, 8.0 mm/yr and 24 mm/yr. The production runs for the ERDC Phase I and II models used the rate of 16 mm/yr. These two new rates provided a 50-percent increase and decrease in subsidence. The low subsidence rate produced the least amount of dredging attributable to WBSD being open while the higher rate produced the most (Table 4.7).

The final sensitivity test was varying the sediment transport functions. In the MVK HEC-6T and ERDC Phase II model, the same function was implemented as previously discussed. For this test, two additional functions were applied, Yang and Ackers White, which are both standard functions used on the Mississippi River. The robustness of the model was tested by running different functions while holding all else constant, while both the attributable amounts of impact in the navigation channel did not change, and PAA attributable decreased.

Conclusions

The WBSD cannot be analyzed in isolation. It is a part of a complex system of diversions that influence the morphology of the Mississippi River and passes. An understanding of the response of the system to changes at any one diversion requires an understanding of the response of the system to each significant diversion.

Approximately 40-50 percent of the total discharge and sediment passing the Venice discharge range at RM 12.5 is diverted from the river upstream of HOP at RM 0. This reach is aggradational with deposition increasing in the downstream direction and concentrated below Cubits Gap. Deposition and subsequent maintenance dredging in this reach constitute a relatively

small fraction of the difference in total sediment load entering and exiting this reach.

The 1D model performs well in reproduction of deposition and dredging locations but underestimates the best available estimates of dredging quantities in Southwest Pass. Average computed annual dredging rates during the 50-year model simulation, including the reach above HOP, agree reasonably well with reported dredging rates over the last decade; however, these rates are considerably lower than the long-term average annual dredging rate.

From Cubits Gap downstream to HOP, the navigation channel functions as an efficient sediment trap. An action such as dredging, which increases the width of the sediment trap, increases the volumetric rate of deposition within this reach.

Although the WBSD diverts only 7 percent (as modeled) of the total flow, the computed impact on dredging is disproportionably large. The ERDC Phase II model consistently indicates that the WBSD accounts for 10-15 percent of the dredging required in the navigation channel reach above HOP. The WBSD accounts for 20 – 30 percent of the dredging in the PAA with a combined total rate of 10 – 20 percent for both the PAA and Navigation Channel.

Sedimentation processes in Southwest Pass, particularly those describing the behavior of cohesive sediments, are strongly influenced by tides and salinity intrusion. While these processes may be simulated to a limited extent by adjustment of model coefficients affecting cohesive sedimentation, a 3D or laterally averaged hydrodynamic/salinity/sedimentation model may be required to resolve the processes producing this deposition.

The left descending bank diversion immediately downstream of Fort St. Philip may be comparable in discharge capacity to the WBSD. However, the Fort St. Philip diversion is located on the outside of a reveted bend where maximum river depths are 3 to 4 times greater than at the WBSD. Additional field investigations are needed to characterize the sediment diversion efficiency of the Fort St. Philip diversion.

5 Multi-Dimensional Modeling Analysis

Multi-Dimensional Modeling Approach

In general, sediment diversions are multi-dimensional phenomenas. Horizontal and vertical variations in both velocities and sediment concentrations are important when considering the impacts associated with diversions. Erosion and deposition patterns in the main stem also tend to be spatially variable.

Observations of velocities and suspended sediment profiles conducted by ERDC for this study confirm the spatial variability of the velocity and suspended sediment concentration for the West Bay Diversion. In addition, the need to identify the impacts of the WBSD on specific footprints within the main channel (the Pilottown Anchorage Area (PAA) and Navigation Channel (NC) dredging footprints) implies the need for a tool that can isolate the impacts spatially.

For this study, two separate multi-dimensional modeling tools were used to analyze the impact of the WBSD on the dredging requirements in the PAA and adjacent navigation channel. Each tool is equipped with unique capabilities that are needed to fully analyze the diversion impacts.

The CH3D model is a 3D, multiple-grain size, noncohesive sediment transport model. The 3D capability makes the model ideal for analyzing the influence of 3D effects in the vicinity of the diversion. The CH3D model has been used for several studies in the lower Mississippi River, including earlier studies of West Bay.

The AdH (Adaptive Hydraulics) model, linked to the SEDLIB sediment model, is a 2D depth-averaged model. This model contributes several capabilities to the analysis, including the following:

- Quasi-3D discharge and transport formulations, which use analytical and semi-empirical methods, approximate the effects of 3D character of the discharge and sediment transport phenomena.
- The unstructured model mesh permits very high resolution in areas of interest and high fidelity resolution of shoreline geometry.

- The ability to extend the boundaries sufficiently far from the project area so as not to prescribe the answer will ensure that the results are not biased by the boundary conditions.
- Some improvements in the sand sediment model are available in the AdH model that are not in the CH3D model, including the ability to effectively armor the bed without having to pack many thin bed layers into the model, and also including the influence of gravity on both the critical shear stress and the bed load magnitude and direction.
- The model is equipped to handle cohesive and mixed sediments as well as cohesionless sediments. This capability is utilized to a limited extent in this study.

The use of both the AdH and CH3D models yields the most complete assessment of the multi-dimensional character of the WBSD and any associated downstream depositional impacts.

- The CH3D model can be used to assess the 3D character of the discharge and transport at the diversion, and to what degree this capability is required to assess the impacts of the diversion on the downstream deposition.
- The AdH model can be used to provide more accurate boundary conditions to the Ch3D model (since the AdH boundary will extend far beyond the study area).
- The AdH model can be run for a full river hydrograph duration to investigate the behavior of the system throughout the hydrograph.
- Comparison of the results from both models will provide quantitative and qualitative insights into the need for 3D modeling at diversions by demonstrating what a 2D model (with quasi-3D capability) can and cannot provide.
- Both models can provide insight into the dominant processes governing sediment deposition in the PAA and NC.

Adaptive Hydraulics Modeling

Model Description

AdH is a finite element model that is capable of simulating three-dimensional Navier Stokes equations, 2D and 3D shallow water equations, and groundwater equations. It can be used in a serial or multiprocessor mode on personal computers, UNIX, Silicon Graphics, and CRAY operating systems. The uniqueness of AdH is its ability to dynamically refine the mesh

in areas where more resolution is needed because of temporary changes in the discharge conditions. AdH can simulate the transport of conservative constituents, such as dye clouds, as well as sediment transport that is coupled to bed and hydrodynamic changes. The ability of AdH to allow the domain to wet and dry within the marsh areas as the tide changes is important for simulating a shallow marsh environment. AdH is being developed at CHL and has been used to model sediment transport in sections of the Mississippi River, tidal conditions in southern California, and vessel traffic in the Houston Ship Channel.

More details about AdH and its computational philosophy and equations can be found at https://adh.usace.army.mil.

SEDLIB is a sediment transport library developed at ERDC. The fundamental architecture of the sediment transport algorithms in SEDLIB are taken from the Ch3D model. This architecture is extended in SEDLIB to a more generalized sediment computational engine. It is capable of solving problems consisting of multiple grain sizes, cohesive and cohesionless sediment types, and multiple layers. It calculates erosion and deposition processes simultaneously and simulates such bed processes as armoring, consolidation, and discrete depositional strata evolution.

The SEDLIB library system is designed to link to any appropriate hydrodynamic code. The hydrodynamic code must be capable of performing advection diffusion calculations for a constituent. SEDLIB interacts with the parent code by providing sources and sinks to the advection diffusion solver in the parent code. The solver is then used to calculate both bedload and suspended load transport, for each grain class. The sources and sinks are passed to the parent code via a fractional step modification of the time derivative term.

Mesh Development

The mesh was developed using the Surface-water Modeling System (SMS), a graphical user interface developed by ERDC for increasing the modeling productivity for a variety of Corps numerical models, including AdH. The entire model domain is shown in Figures 5.1 and 5.2 and an inset of the model showing the study area is shown in Figure 5.3. The upstream boundary is at approximately RM 42.3 of the Mississippi River, and the downstream water surface boundary extends approximately 55 miles beyond the end of Southwest Pass into the Gulf of Mexico.

Figure 5.1. AdH 2-D Model Domain of the lower Mississippi River.

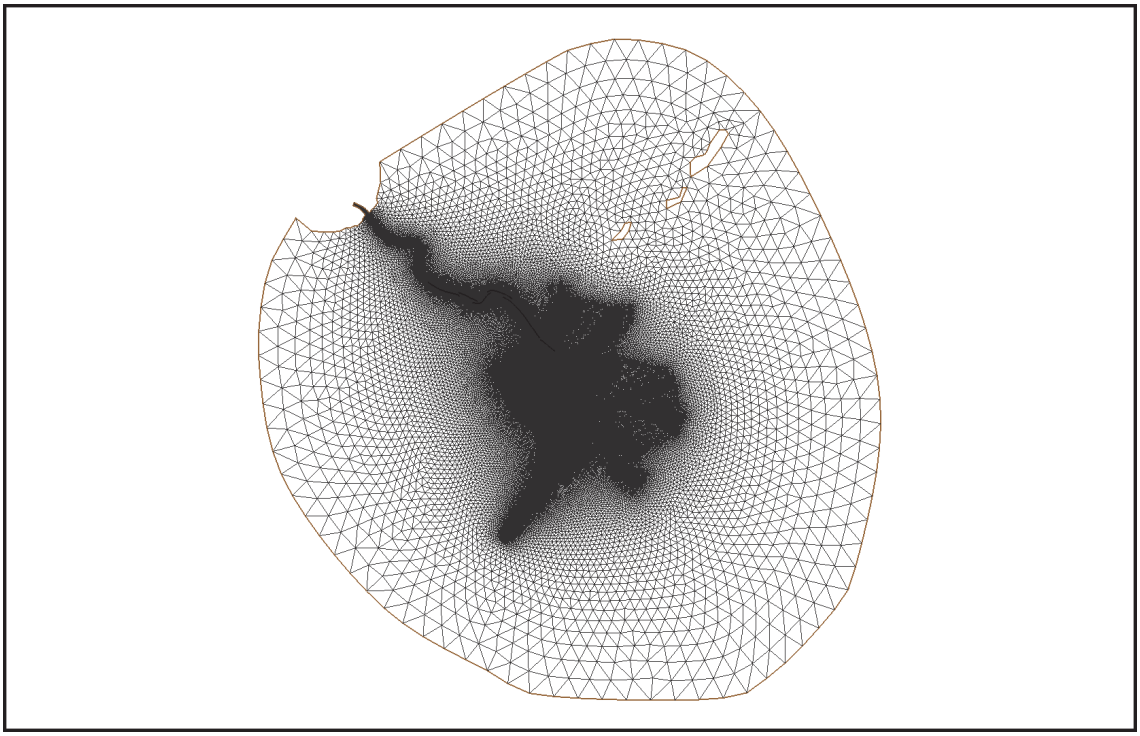

Figure 5.2. Model Domain with Contours.

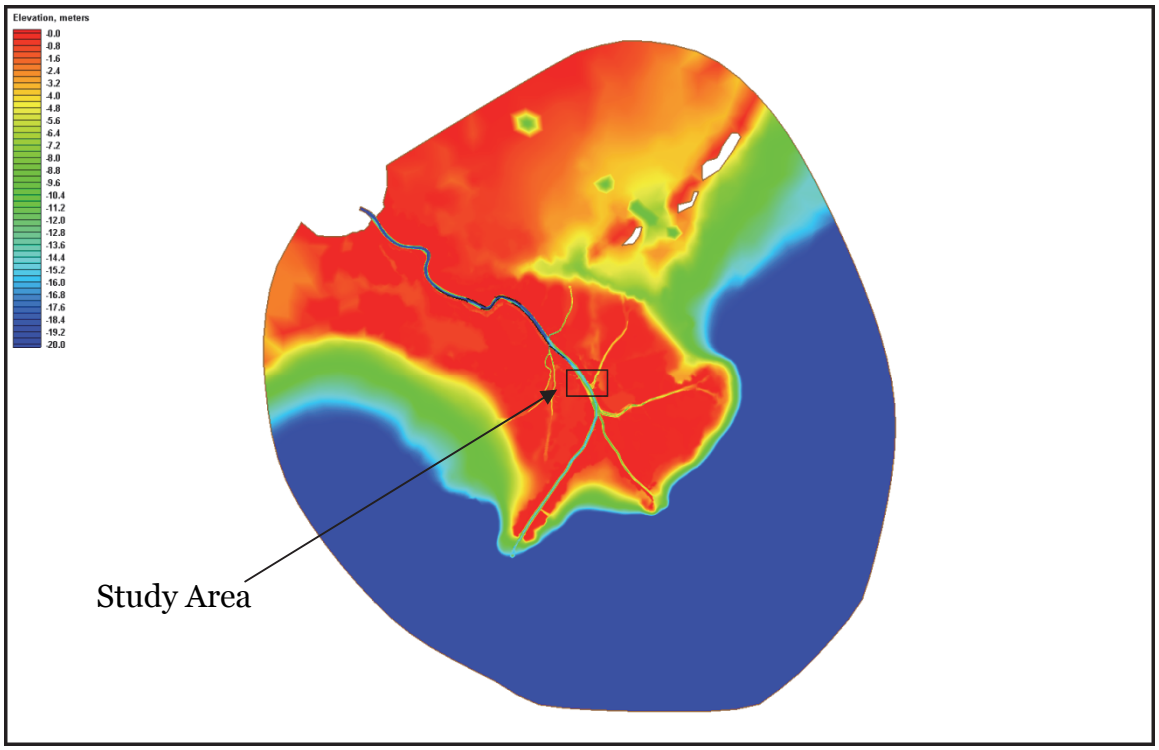

Figure 5.3. Inset Showing Study Area.

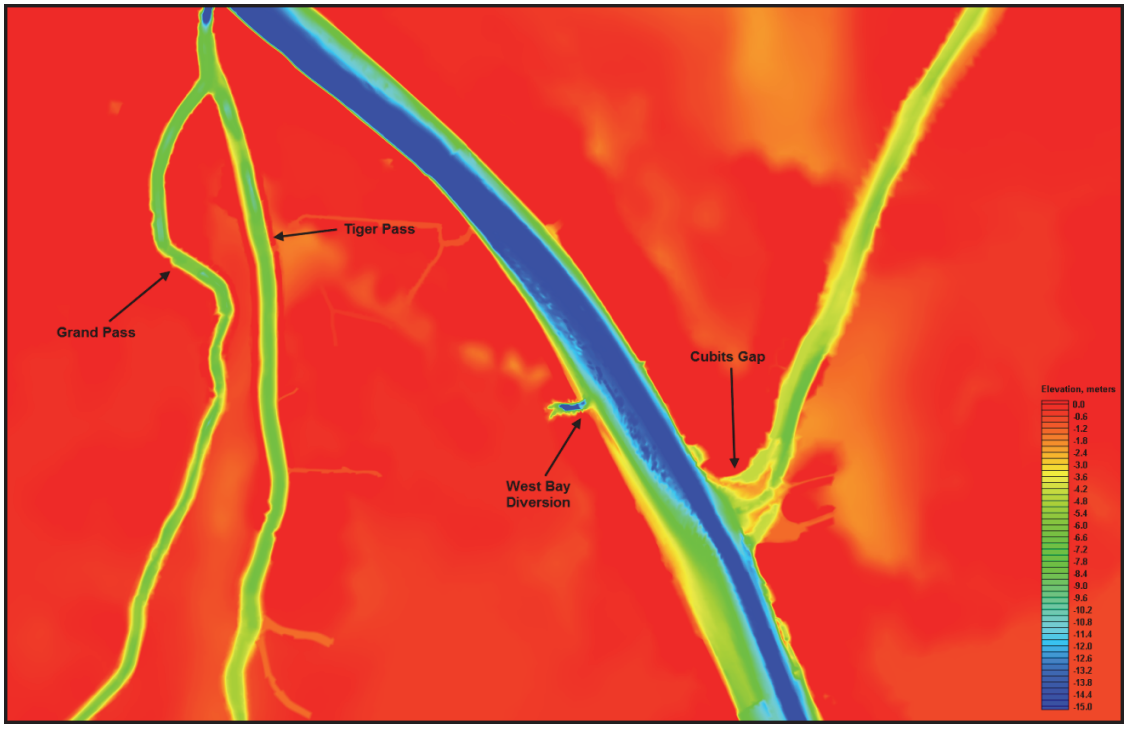

The bathymetry for the mesh was taken from three sources: the SL-15 bathymetry for the ADCIRC model of the Gulf of Mexico, USACE Condition Surveys for the Mississippi River, and multi-beam bathymetry data gathered by ERDC. The multi-beam bathymetry data were gathered as part of the present study and included bathymetry for the Mississippi River from 2 miles upstream of the WBSD to 2 miles downstream of the WBSD. Multi-beam data were also gathered in the diversion and in several other passes including Grand Pass, Baptiste Collette, and Cubits Gap.

The horizontal datum for the mesh is State Plane NAD83, Louisiana South. The vertical datum is NAVD88, m.

Hydrodynamic Boundary Condition Development

For the AdH model, the 2009 hydrograph from February to August was simulated.

The upstream boundary was specified using an inflow boundary based upon discharge measurements made at the USGS gauging station at Tarbert Landing. The inflows were adjusted so that they matched the inflows recorded by the ERDC data collection team at RM 12.1. The Tarbert Landing inflows and the adjusted and applied boundary inflows are given in Figure 5.4.

Figure 5.4. Mississippi River Discharge at Tarbert Landing and at the AdH Model Boundary for 2009.

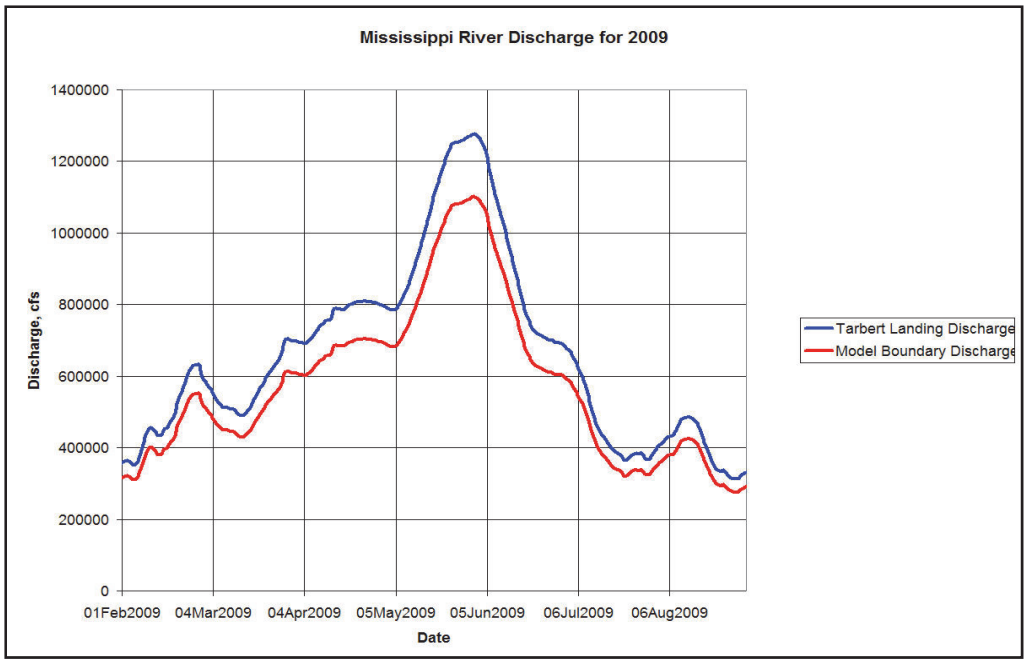

The downstream water surface boundary at the Gulf of Mexico was taken from the NOAA observation station at Southwest Pass. The data were adjusted so that the water surface elevation is referenced to NAVD88. The water surface elevation boundary is given in Figure 5.5.

Sediment Boundary Condition Development

The character and distribution of the bed sediment in the study area is very complex. Analysis of the bed samples collected in the field data collection effort show a wide range of sediment classes ranging from clay to coarse sand. For the March ERDC data collection event, an average sand/silt/clay breakdown was calculated for samples BSS 5-18. The average values are as follows: 64 percent sand, 25 percent silt, 11 percent clay. According to several sources (e.g. Le Hir et al, 2005) these values are near the threshold of the clay and silt content necessary for cohesive behavior to control the erosion characteristics of the bed material.

Galler and Allison (2008) note that significant deposition of fine sediment occurs throughout the lower river at low water, when the intrusion of the saline wedge induces flocculation and settling. They assert that most or all of these fines are remobilized and removed from the bed when the river rises. However, there is some evidence that some of this material may mix with sandy sediments in the river to form a stiff substrate.

Figure 5.5. Downstream Water Surface Elevation Boundary for 2009.

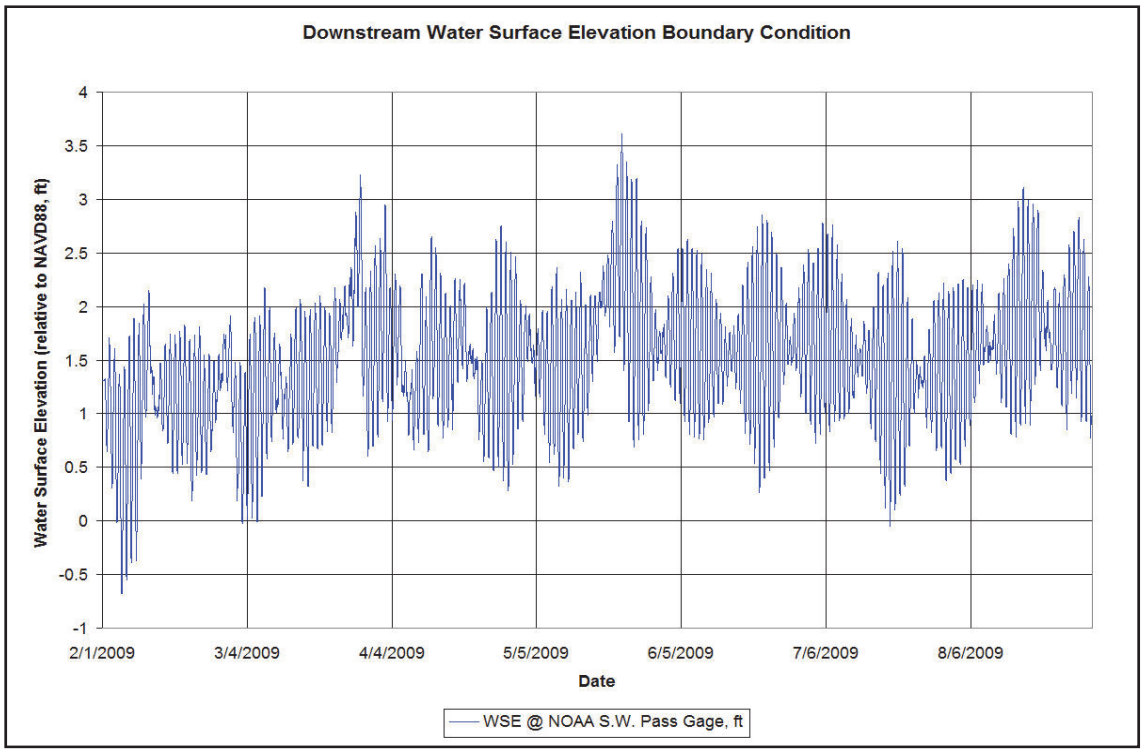

A CHIRP seismic study by Allison and Nittrouer (2004) indicates that the sand supply in the lower river is limited, with an active sand sheet thickness of 0 – 1.5 m. The study notes that the river thalweg can be scoured free of sand at high flows. The study also remarks that the active sand sheet is found atop a relict pavement of very stiff cohesive material. However, the geomorphological analysis conducted for this report indicates a long term trend of aggradation in cross sections between Venice and West Bay. This implies that some of the cohesive material beneath the sand sheet is not relict material but recently deposited sand that has mixed with cohesive sediment deposited during low flows. This cohesive behavior can limit the supply of sandy sediment available for transport by slowing the rate of erosion of the mud/sand mixture.

An examination of the suspended sand concentrations collected by ERDC for this study implies the strong possibility that both the limited sand supply and the slower rate of erosion for the underlying material are important processes operating in the lower river. Consider that the cross-sectionally averaged suspended sand concentration at RM 4.5 for the May 5-6 data collection event and the May 29-30 data collection event were both approximately 27 ppm, even though the discharge is 60 percent larger for the May 29-30 data collection event. This implies that the supply of sand in the active sand sheet has been exhausted in the intervening time

period, and the erosion of sand at the May 29-30 event is controlled by the cohesive material in the bed.

These observations indicate that the behavior of sediment in the system is very complicated; therefore, modeling the system properly requires a significant investment of time and resources to secure sufficient data to understand the behavior of the system. However, in order to construct a model adequate to address the specific question at hand (i.e. the impact of WBSD on downstream shoaling), some simplifying assumptions can be made to the conceptual model of the governing processes. These can be implemented into the model if the results are interpreted with consideration of the potential impact of these simplifications.

The model was constructed with the following assumptions:

- The active sand sheet consists of a uniform layer of sand 0.3 m thick. The sand sheet is comprised of 3 discrete sand classes: Very Fine Sand, Fine Sand, and Medium Sand.
- Beneath the active sand sheet is an armored layer of mixed cohesive/sandy material. The cohesive material is not fully included as a separate grain class; rather, it serves to control the rate of erosion of the sand classes in this layer.
- The thickness of the armored layer is variable. The thickness is initialized by starting with a uniform thickness, removing the cohesive material, and allowing the model to run through a hydrograph. This results in an initial thickness that is zero in much of the channel thalweg and 2.0 -3.0 m thick in lower energy regions.
- The armor layer is underlain by nonerodable material, which simulates the relict substrate.
- The inflowing boundary condition is controlled by the erosion rate of the armored bed at the boundary. This allows the active sheet to erode away and the rate of erosion associated with the armored bed to achieve equilibrium with the bed in the model.

Model Verification

Hydrodynamic verification

Figures 5.6 and 5.7 show the comparison of the observed and computed discharges through each of the diversions in the study. These comparisons show that the model represents the observed distribution of discharge to an acceptable degree of accuracy.

Figure 5.6. Hydrodynamic verification for April 22-23.

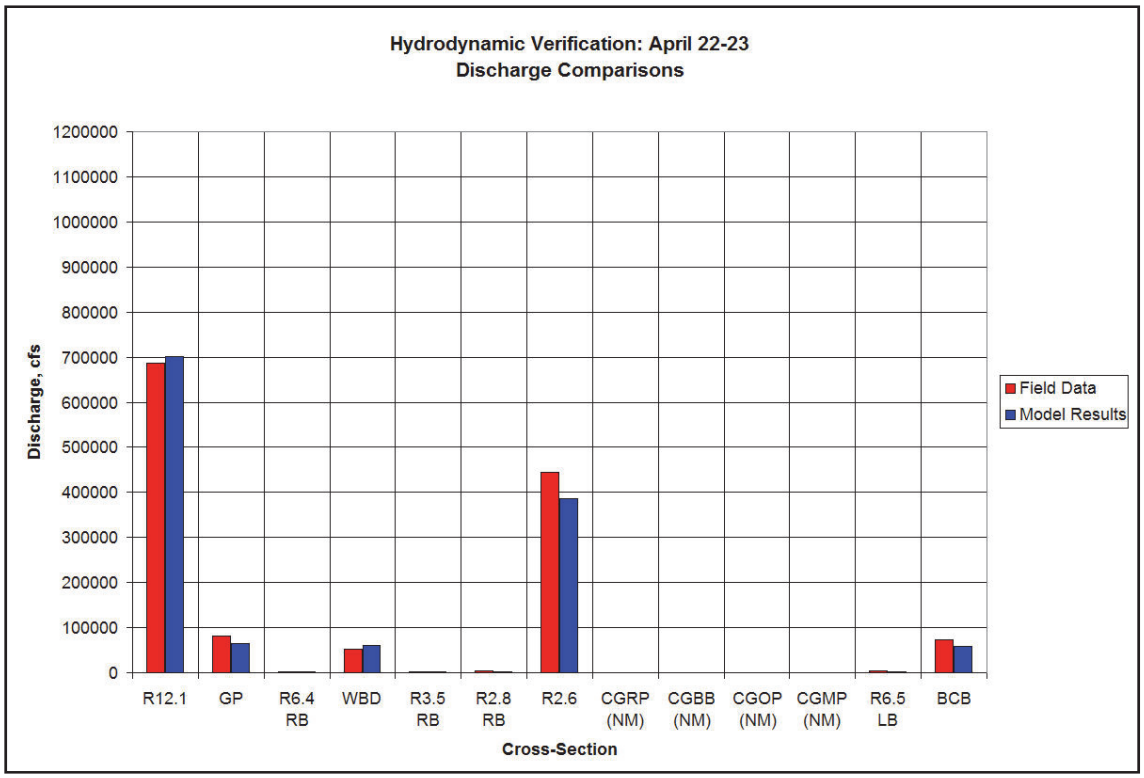

Figure 5.7. Hydrodynamic verification for May 29-30.

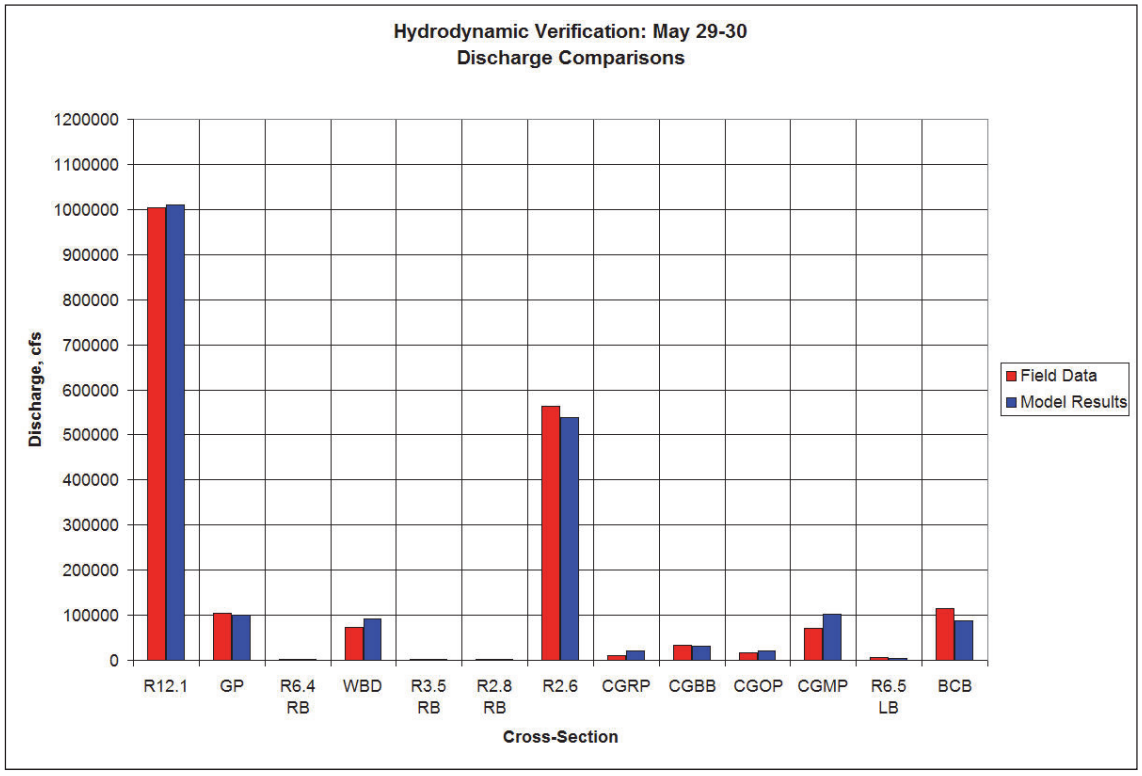

The discharge distribution is primarily governed by the shape and bathymetry of the cuts themselves. Under high and median discharge conditions, the stage in the river is significantly higher than the stage on the downstream side of each of the cuts; therefore, the discharge through the cuts is essentially a local loss problem, with the magnitude of the discharge governed by the geometry of the cuts themselves. Tidal signals and bed friction losses are of less significance. A significant wind set-up could have some influence but was not examined for this study.

The Manning's (n) value for the main stem was chosen to approximate the roughness height of the bedforms. It was set equal to 0.028. AdH is equipped with a friction algorithm that automatically adjusts the friction for variations in water depth.

Although the AdH model is a depth averaged model, it is equipped with several semi-analytical features designed to mimic 3D behavior. One of these is the implementation of streamwise vorticity transport (Bernard 1992). This is an adjustment to the momentum of the discharge designed to simulate the helical discharge resulting from the differential radial acceleration of the discharge velocity over the vertical velocity profile. This differential acceleration is the mechanism whereby rivers develop meanders; hence, this mechanism is sometimes called the *bendway* effect.

The vorticity transport allows the AdH to approximate the 3D character of the discharge through the West Bay diversion. Figures 5.8 and 5.9 show the observed and computed surface velocities in the cut on April 22-23. Figures 5.10 and 5.11 show the observed and computed bottom velocities at the same location.

Figure 5.8. Observed surface velocities at WBSD on April 22-23.

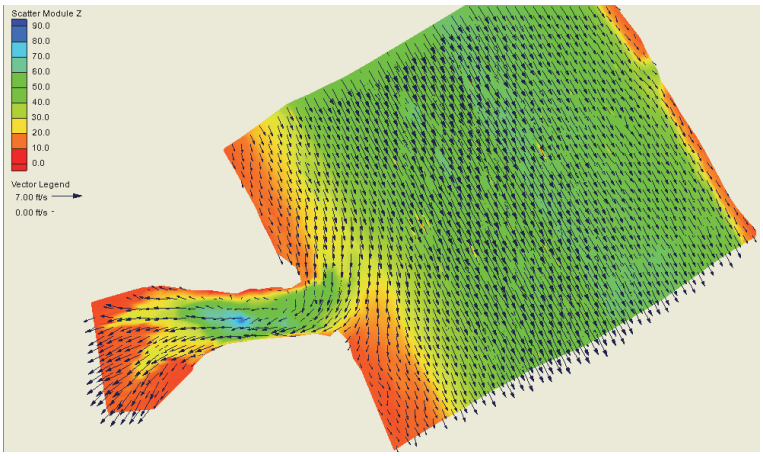

Figure 5.9. Computed surface velocities at WBSD on April 22-23.

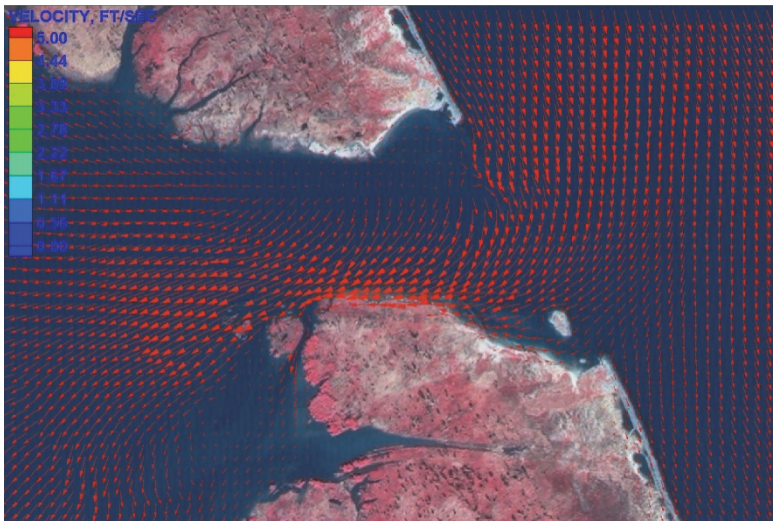

Figure 5.10. Observed bottom velocities at WBSD on April 22-23.

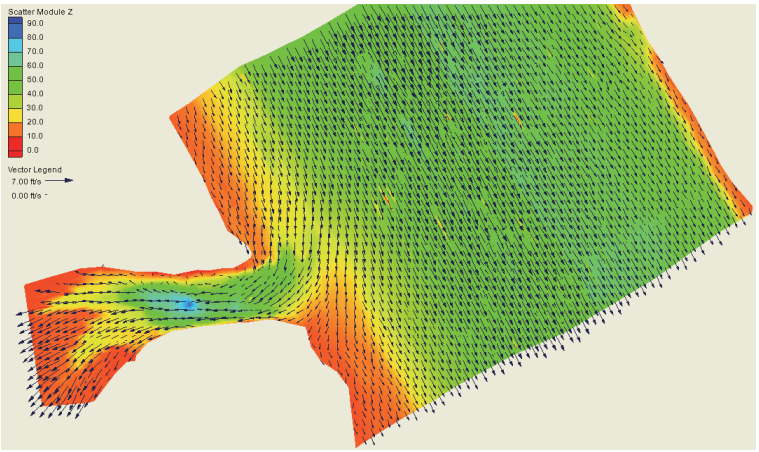

Figure 5.11. Computed bottom velocities at WBSD on April 22-23.

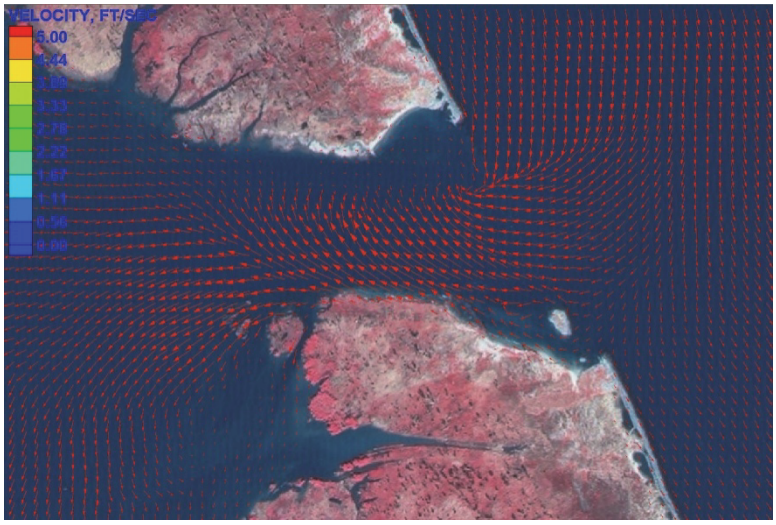

Suspended sediment verification

Figure 5.12 shows the observation locations for the suspended sediment samples in the vicinity of West Bay Diversion. Figures 5.13 – 5.15 show observed and computed values of total suspended sand concentration for the May 5-6 observation period (medium flow). Figures 5.16 – 5.20 show the same comparisons for the May 29-30 observation period (high flow). Note that these sand *profiles* result from a semi-analytic expression within AdH that produces a nonequilibrium sediment profile on the form of the Rouse equation (Brown 2008). This quasi-3D profile is used within the code for all sediment calculations.

The model consistently overpredicts the sand concentrations. There are several potential reasons for this. The dominant reason is likely the fact that the exact composition of the grain class distribution of the bed, and the relative influence of the cohesive behavior and the limited sand supply on the erosion rate of the sediments, is not known. Each factor can have a significant influence on the suspended sediment concentration in the river.

Figure 5.12. Suspended sediment verification at RM 5.2 for May 5-6.

Figure 5.13. Suspended sediment verification at RM 5.2 for May 5-6, 2009.

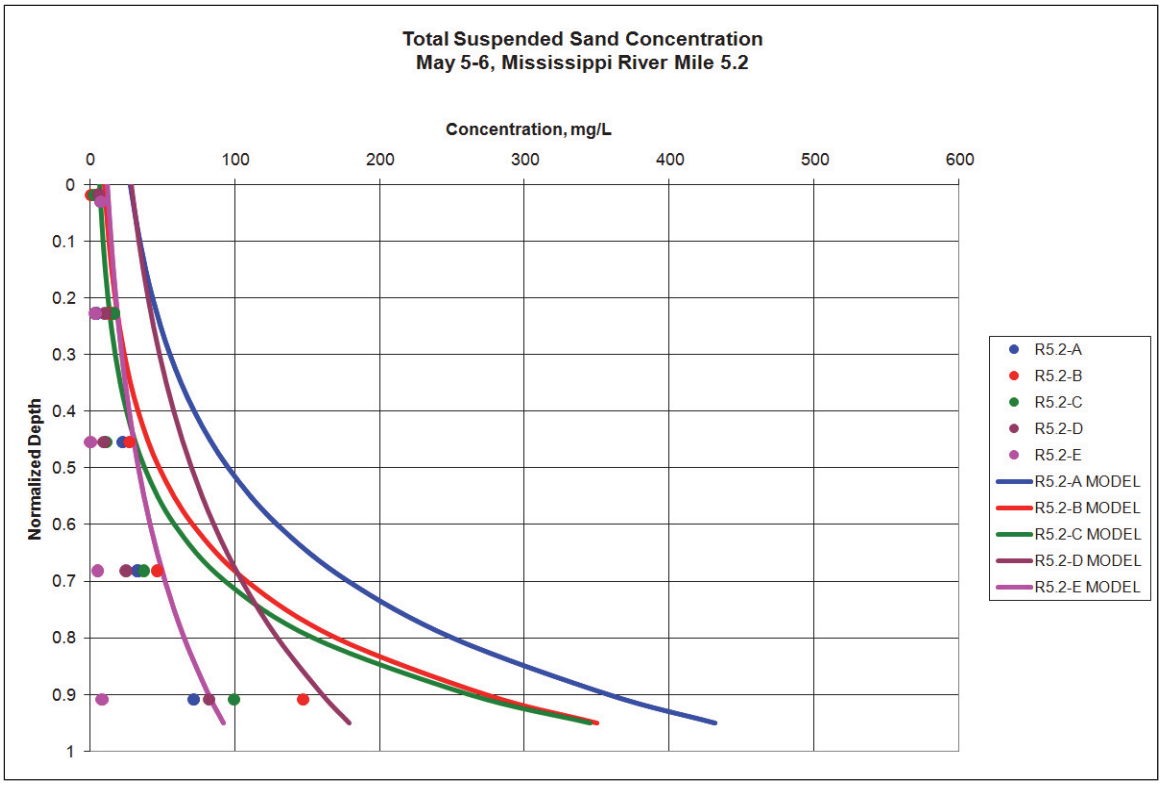

Figure 5.14. Suspended sediment verification at WBD for May 5-6, 2009.

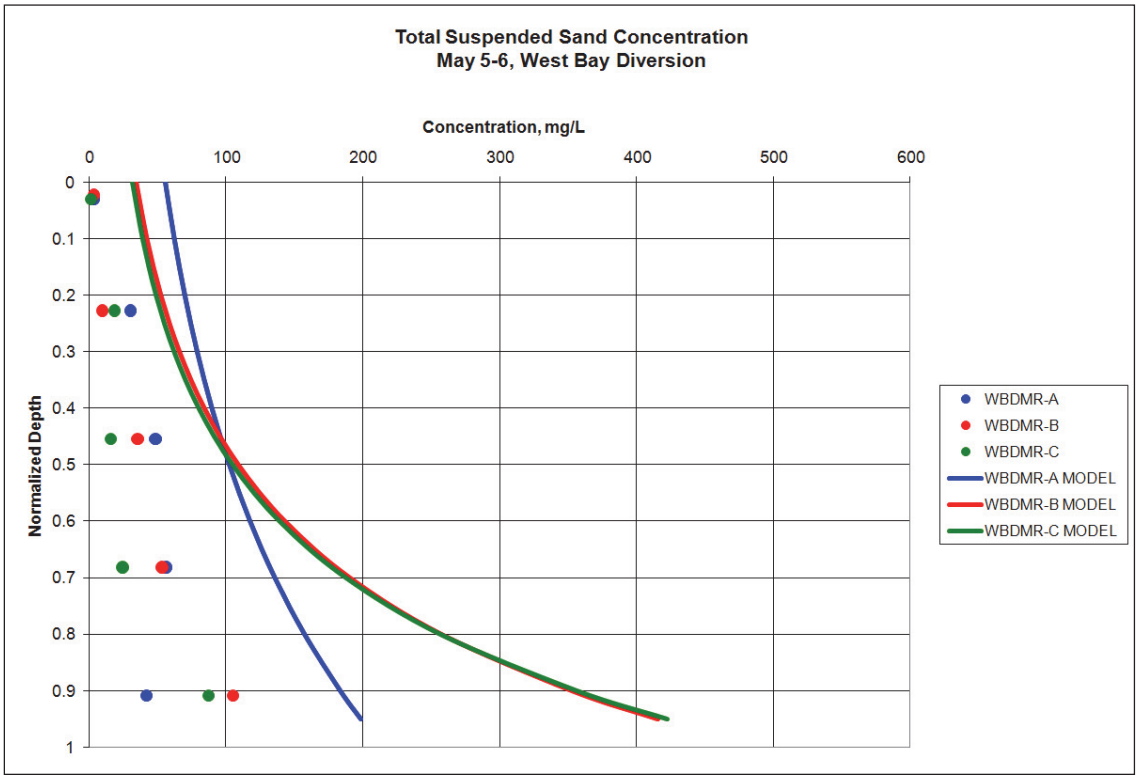

Figure 5.15. Suspended sediment verification for May 5-6, 2009.

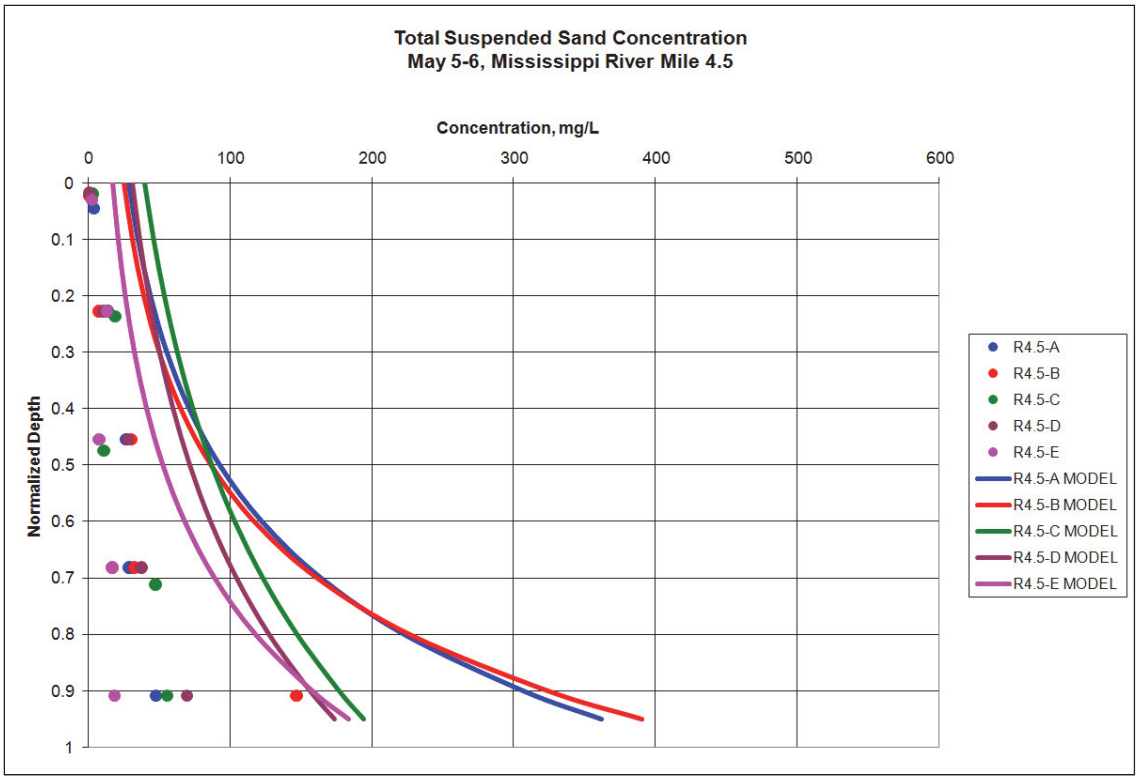

Figure 5.16. Suspended sediment verification at RM 5.2 for May 29-30, 2009.

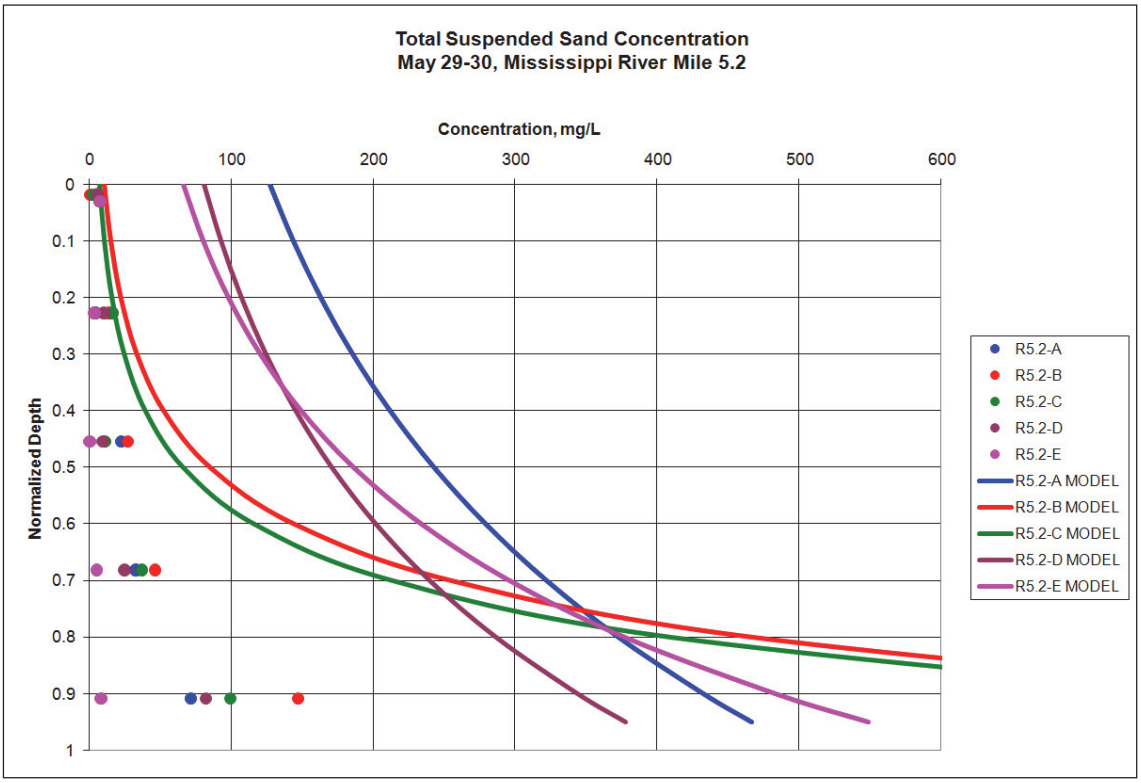

Figure 5.17. Suspended sediment verification at WBD for May 29-30, 2009.

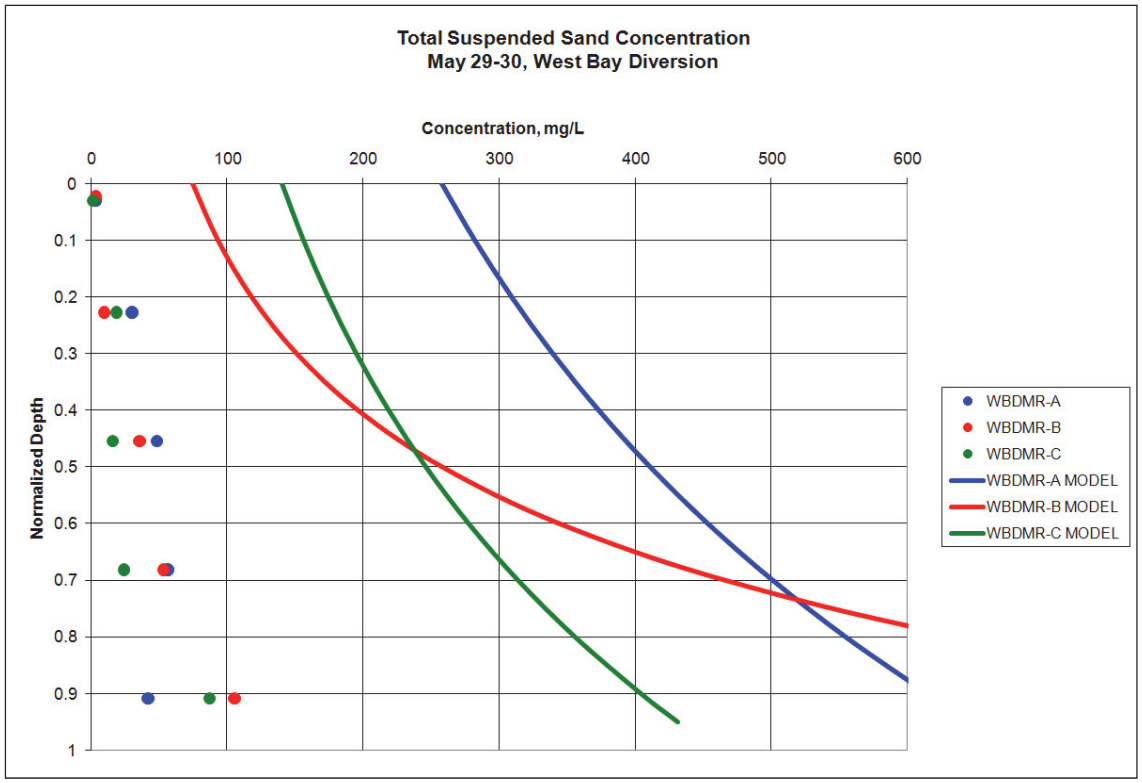

Figure 5.18. Suspended sediment verification at RM 4.5 for May 29-30, 2009.

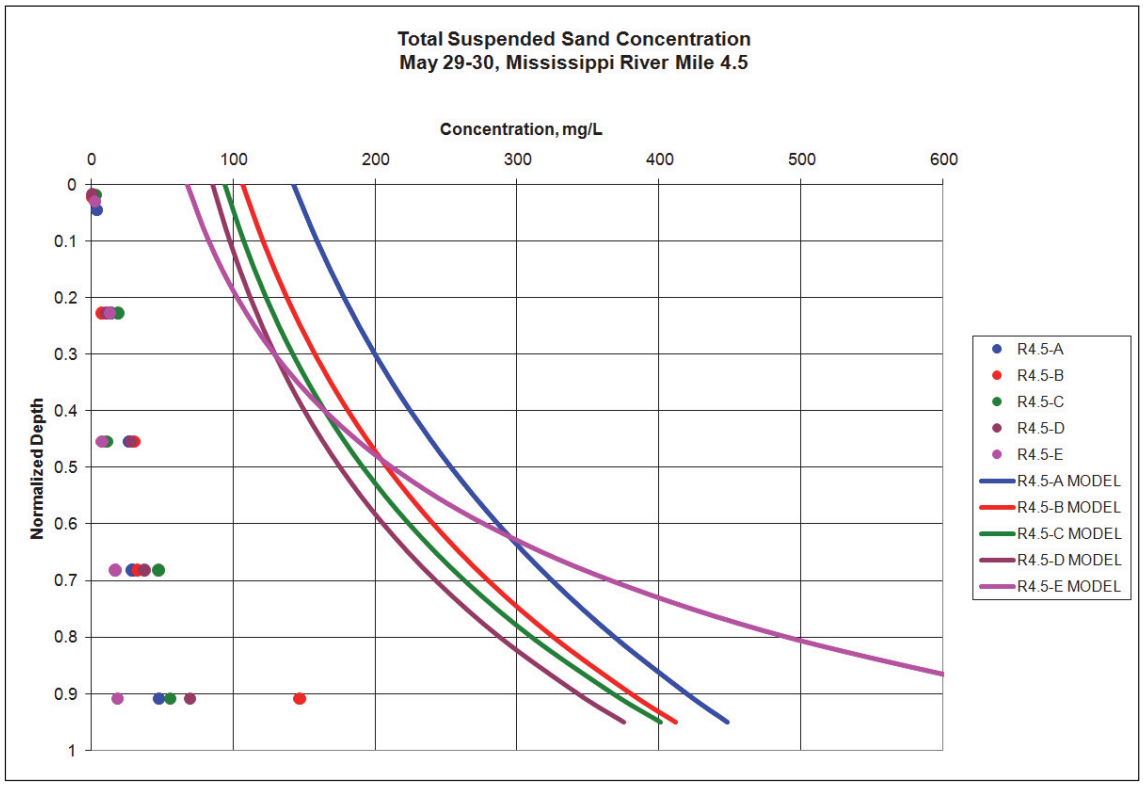

Figure 5.19. Suspended sediment verification at GP for May 29-30, 2009.

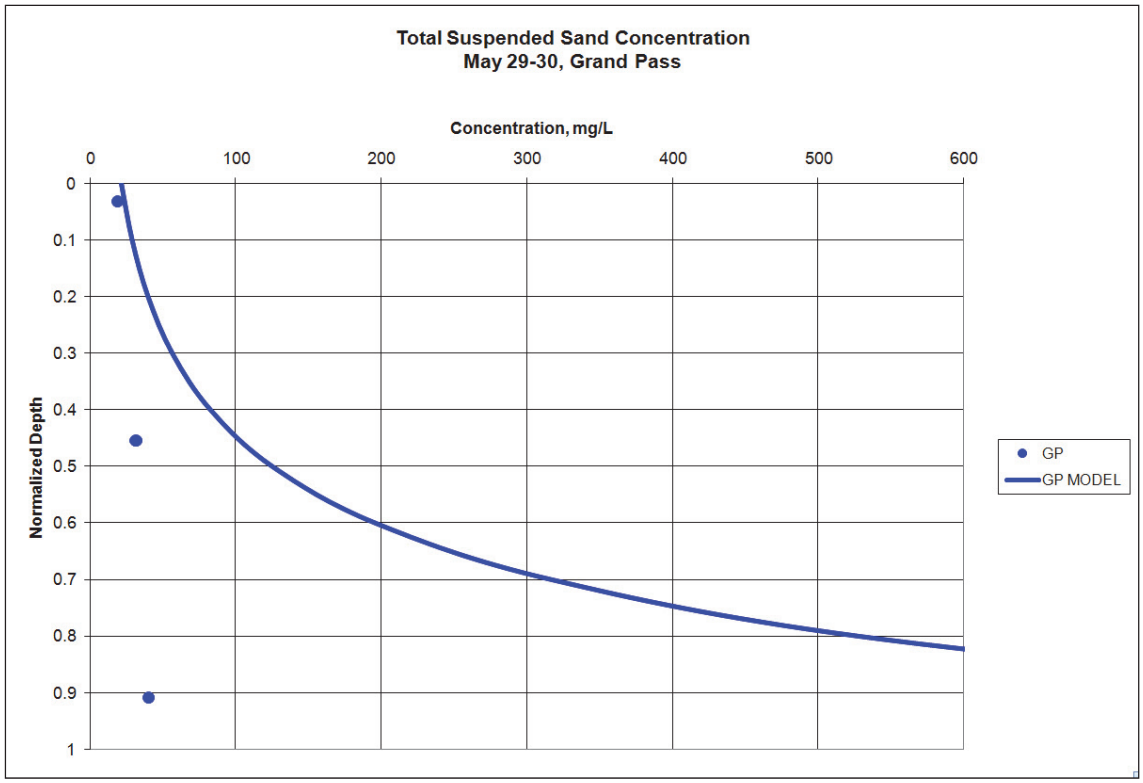

Figure 5.20. Suspended sediment verification at BCB for May 29-30, 2009.

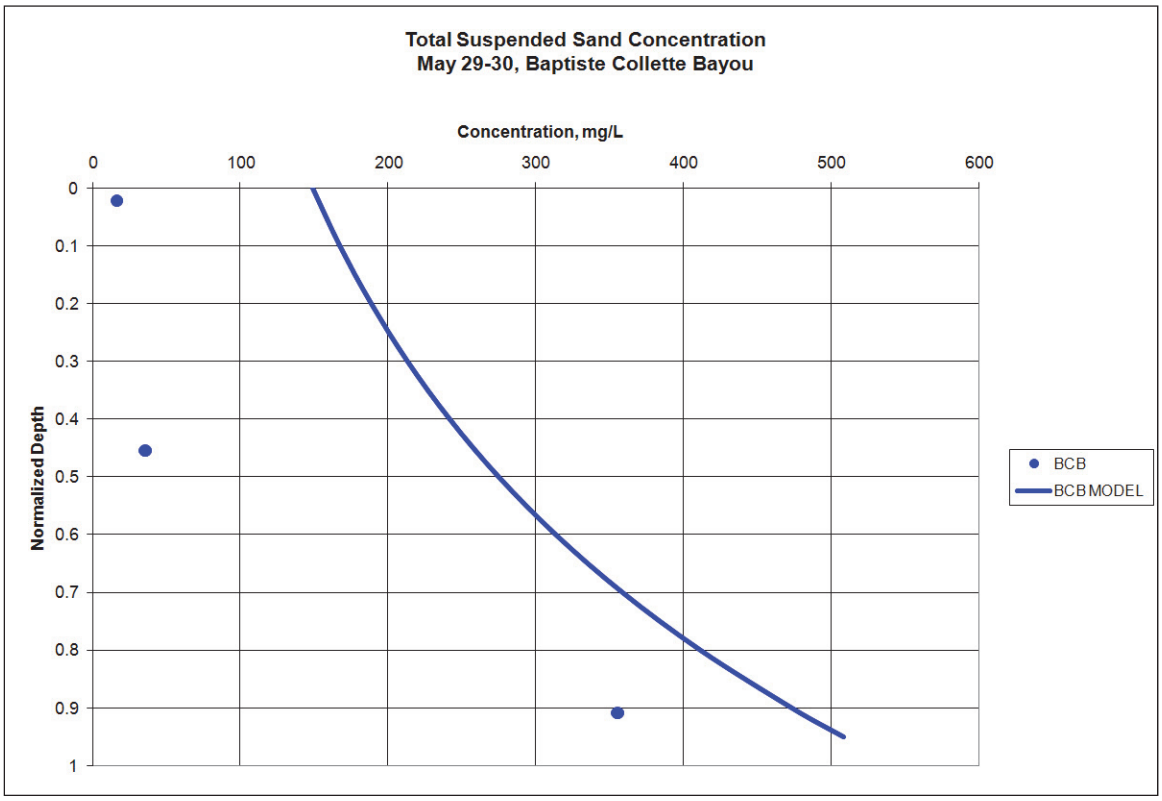

Several perturbations of these parameters were attempted in the model. The values selected were shown because they produced the best agreement with observed suspended sand concentrations while at the same time providing the best agreement with the observed bed change over the hydrograph (based on sequential channel condition surveys).

A different approach was taken for the Ch3D results where the sediment concentrations were essentially calibrated to the observed values. Hence, the Ch3D results yield a much better agreement with observations. These results are discussed later in this chapter.

Figures 5.21 and 5.22 show the calculated and observed bed elevation changes between March and August of 2009. The observed changes are taken from a difference plot of New Orleans District condition surveys. Note that the model (Figure 5.21) and the observed data (Figure 5.22) indicate scouring along the leading edge of the point bar in the Anchorage area. This lends credibility to the assumption of an eroded bed because of the large discharge year in 2008. The deposition patterns observed in the field are in general agreement with those observed in the model, but the field data indicates some significant deposition upstream of the WBSD that is not replicated in the model.

Results: Analysis of General Diversion Effects

In general, sediment diversions can affect river shoaling patterns by either of two different mechanisms:

- Disruption of sediment equilibrium – this results when the sediment diversion does not remove a sufficient amount of sediment to ensure that the river downstream of the diversion can return to sediment equilibrium without adjusting the bed. This is a global effect that impacts the entire length of the river downstream of the diversion. It is discussed in detail in Letter et al. (2010).
- Momentum loss through the diversion – the transport of momentum through the diversion represents a (nearly) discrete jump in the momentum of the main stem of the river. The hydraulic gradient cannot immediately respond to this jump and must adjust upstream and downstream of the diversion to accommodate this shock. These adjustments can result in increased scour upstream of the diversion and increased deposition downstream of the diversion. This effect is local as it only affects the river in the vicinity of the diversion.

Figure 5.21. Computed sediment bed change, March to August, 2009.

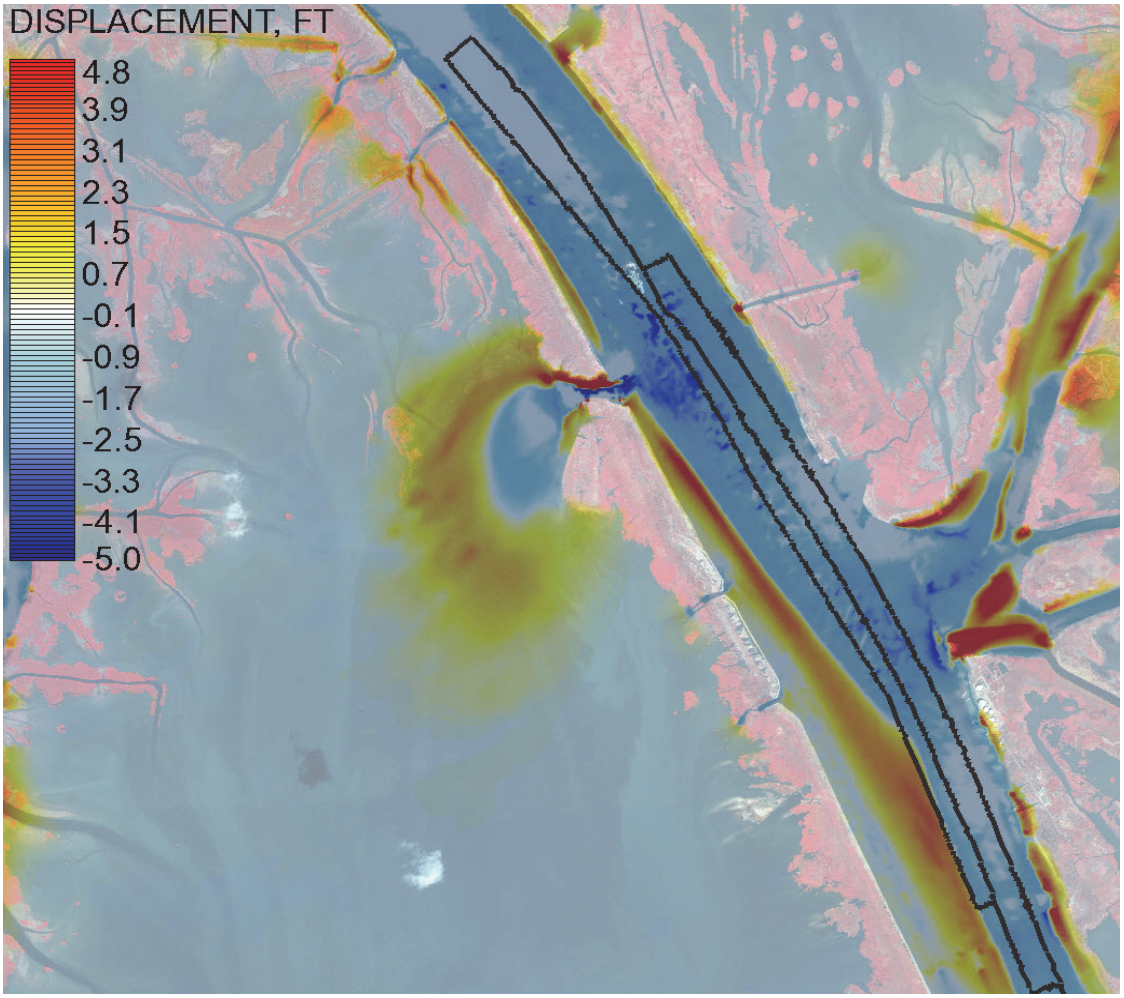

At WBSD, the momentum loss effect (the local effect) is likely the most significant factor with respect to downstream deposition. The global impacts of diversions associated with the disruption of sediment equilibrium are more significant for diversions that divert sediment-starved water (whether by design or by happenstance). Also, the river downstream of West Bay never achieves a true equilibrium state because it quickly diverges into several diversion channels and flows into the Gulf of Mexico. Therefore, the concept of an equilibrium downstream condition is not strictly applicable to the WBSD site.

Figure 5.23 depicts the effects of momentum loss through the diversion. It shows the difference in bed shear stress in the river channel associated with the WBSD. The modeled bed shear stress at high discharge with WBSD closed is subtracted from the modeled bed shear stress at high discharge with WBSD open. The results show that the opening of the diversion has impacts both upstream and downstream.

Figure 5.22. Observed sediment bed change, March to August, 2009.

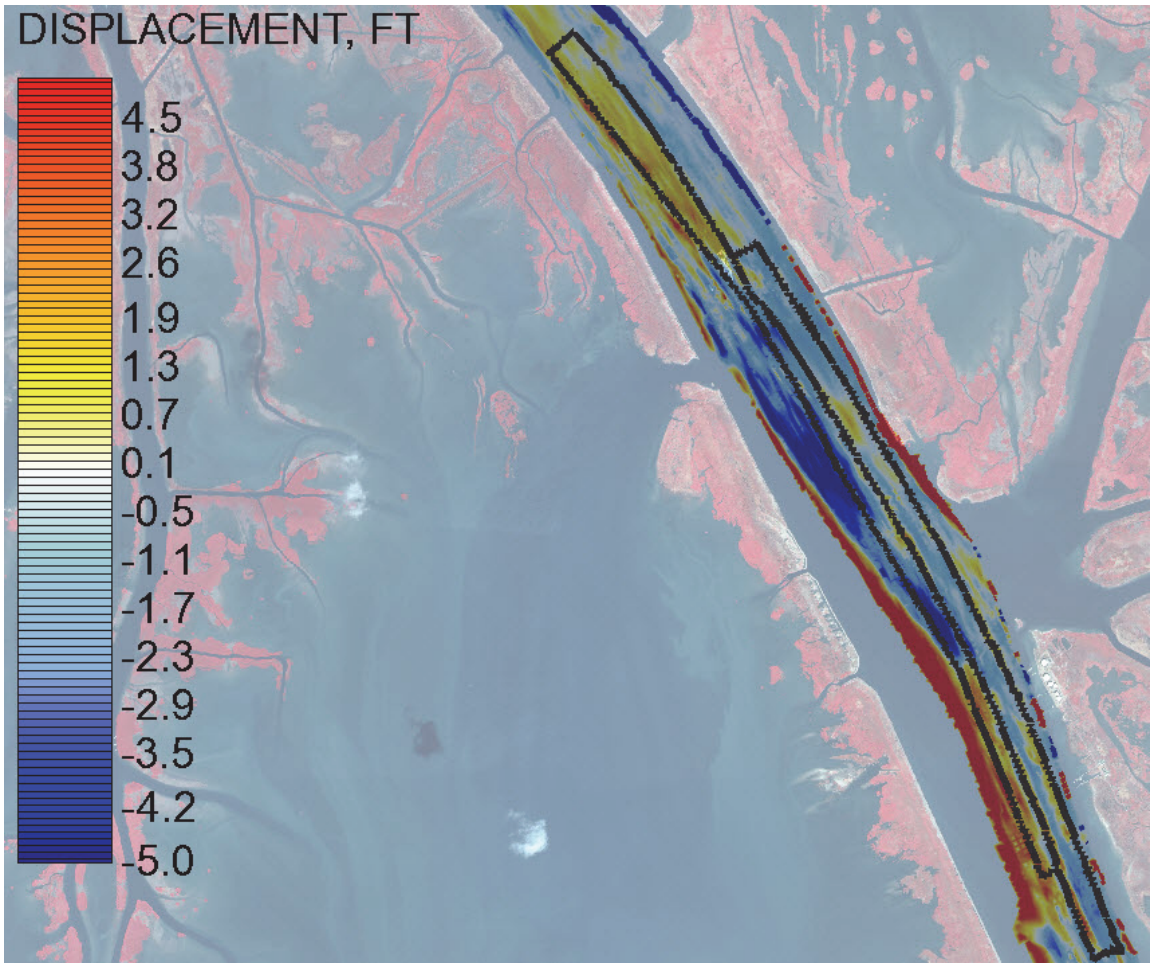

In the upstream direction, the bed shear stress increases by roughly 10 percent. This is because of a drawdown of the water surface associated with the opening of West Bay Diversion. The drawdown is arrested at Grand Pass. At this location, the drawdown results in a reduced volume of diversion though Grand Pass. Therefore, upstream of grand pass, the net result is that the river recovers nearly the same water surface profile as it has in the without WBSD condition.

Downstream of WBSD, the bed shear stress is reduced by roughly 10 percent. This is because the water surface profile cannot immediately recover from the sudden loss of momentum at the diversion. This impact is strongest just downstream of the diversion and dissipates in the downstream direction as the water surface profile begins to recover.

Figure 5.23. Bed Shear Stress Difference at High Discharge (w/ WBSD minus w/o WBSD).

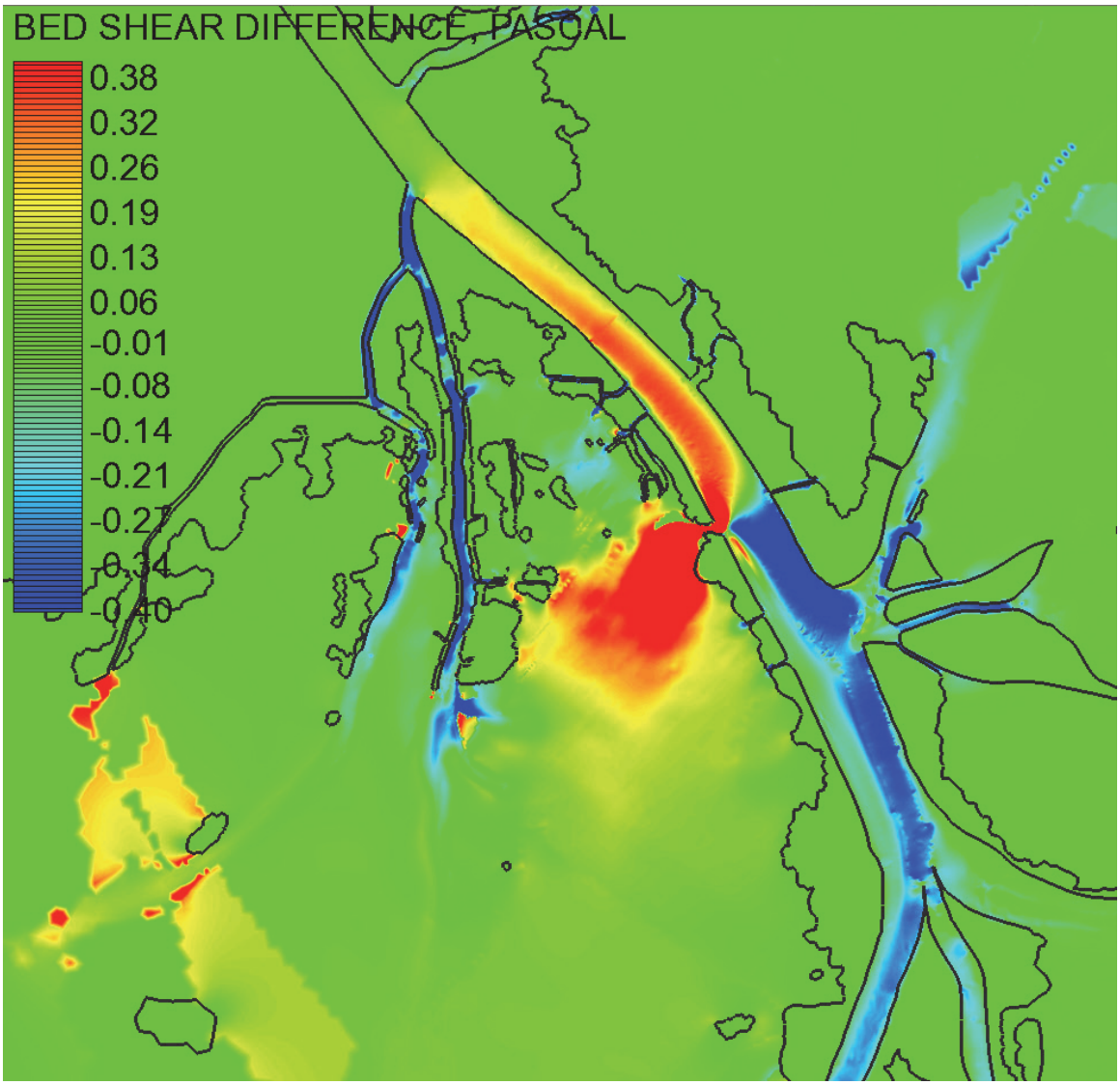

The shear stress analysis indicates that, if the study area is considered primarily a depositional zone, the primary impacts of WBSD on deposition should occur in the PAA and navigation channel just downstream of the diversion, and should dissipate in the downstream direction.

Results: Scenario Analysis

In order to determine the sensitivity of the results to the initial bathymetry, the model scenarios runs were conducted with two different starting bathymetries: an *undredged* condition (the 2009 bathymetry) and a *dredged* condition (the 2006 bathymetry). Figure 5.24 show these two bathymetries, and Figure 5.25 is a difference plot of the two bathymetries.

Figure 5.24 Undredged initial bathymetry.

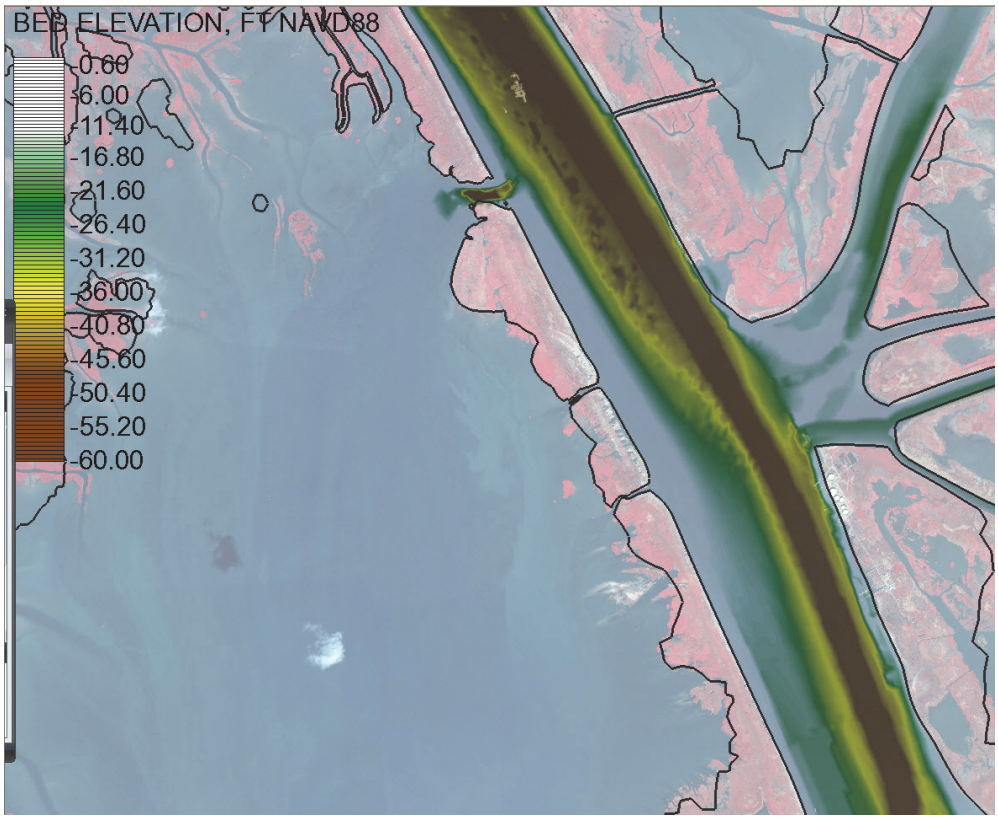

Dredged initial bathymetry.

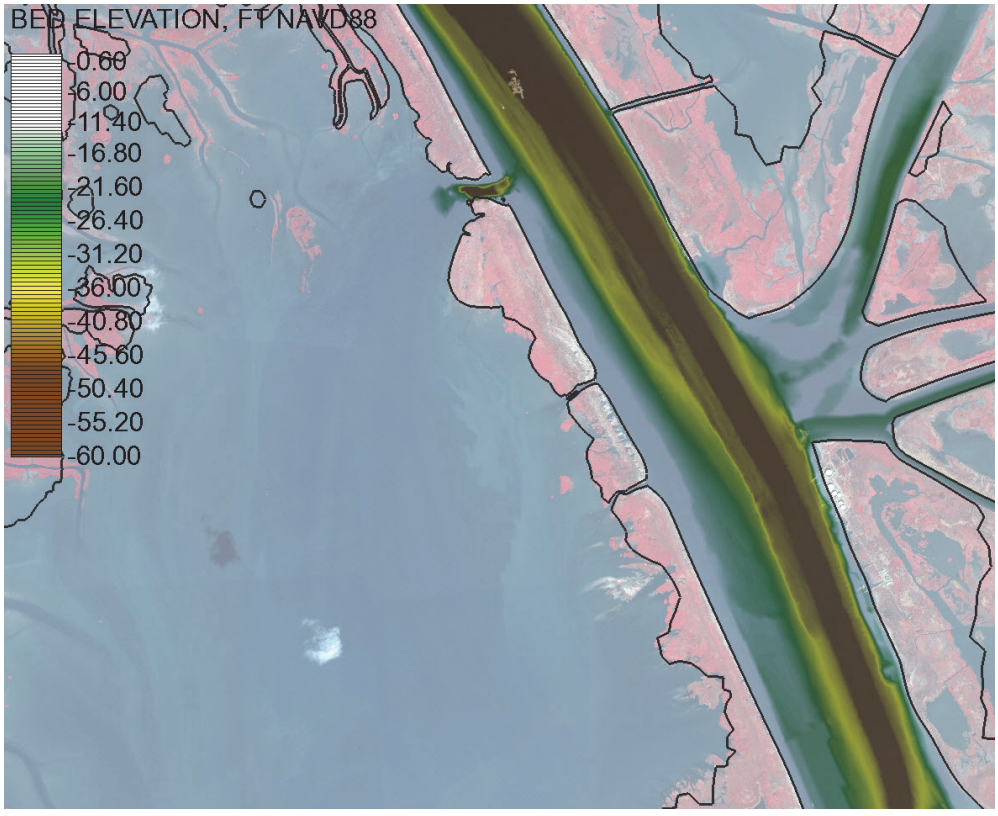

Figure 5.25 Difference in the bathymetries (Undredged minus dredged).

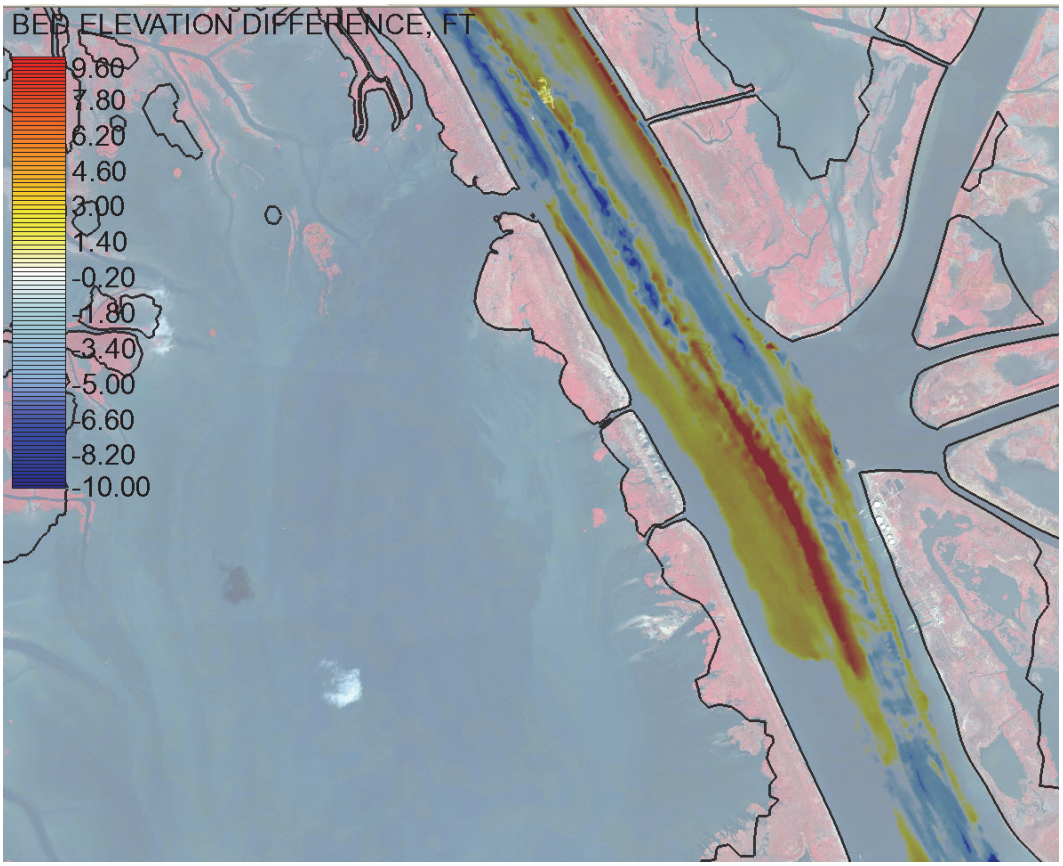

Using the same hydrograph, both bathymetries were run with and without the WBSD in place. The resulting sediment deposition was measured in each run to determine the impacts of the WBSD on deposition in terms of initial bathymetry conditions.

The model results indicate that the 2009 hydrographs resulted in some significant erosion in the study area due (evidently) to an exhaustion of the sediment supply. This result is corroborated by evidence from observations (Figure 5-22). This net erosion may not be typical, but for a system with limited supply, it is not unreasonable.

For these model results, the peak deposition in the study area occurred approximately 1 May 2009. Most of the results are presented for both 1 May 2009, and a post hydrograph date of 15 July 2009.

Figures 5.26 through 5.34 depict spatial distributions of modeled bed change. In each plot, a dredge template is shown. This template represents the dredge footprints used throughout this analysis for the PAA and NC.

Figure 5.26. Cumulative bed change with WBSD, Undredged Condition, 1 May 2009.

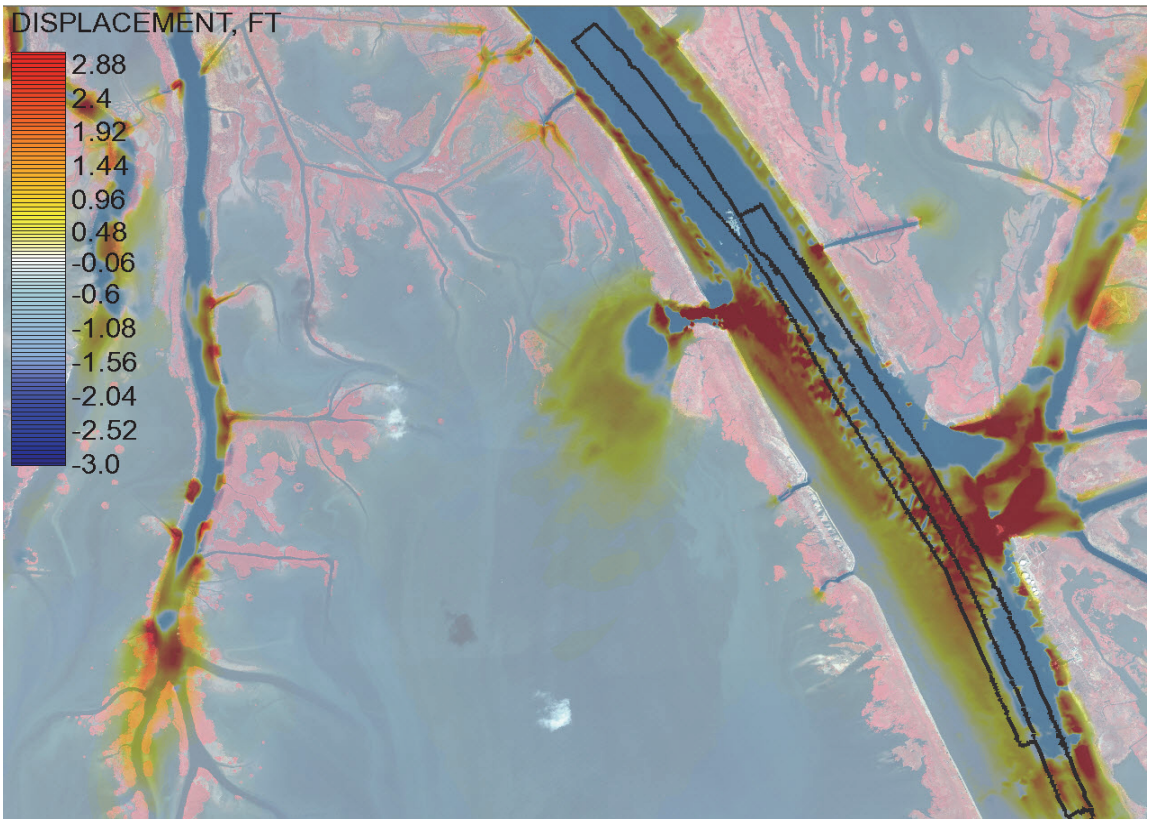

Figure 5.27. Cumulative bed change without WBSD, Undredged Condition, 1 May 2009.

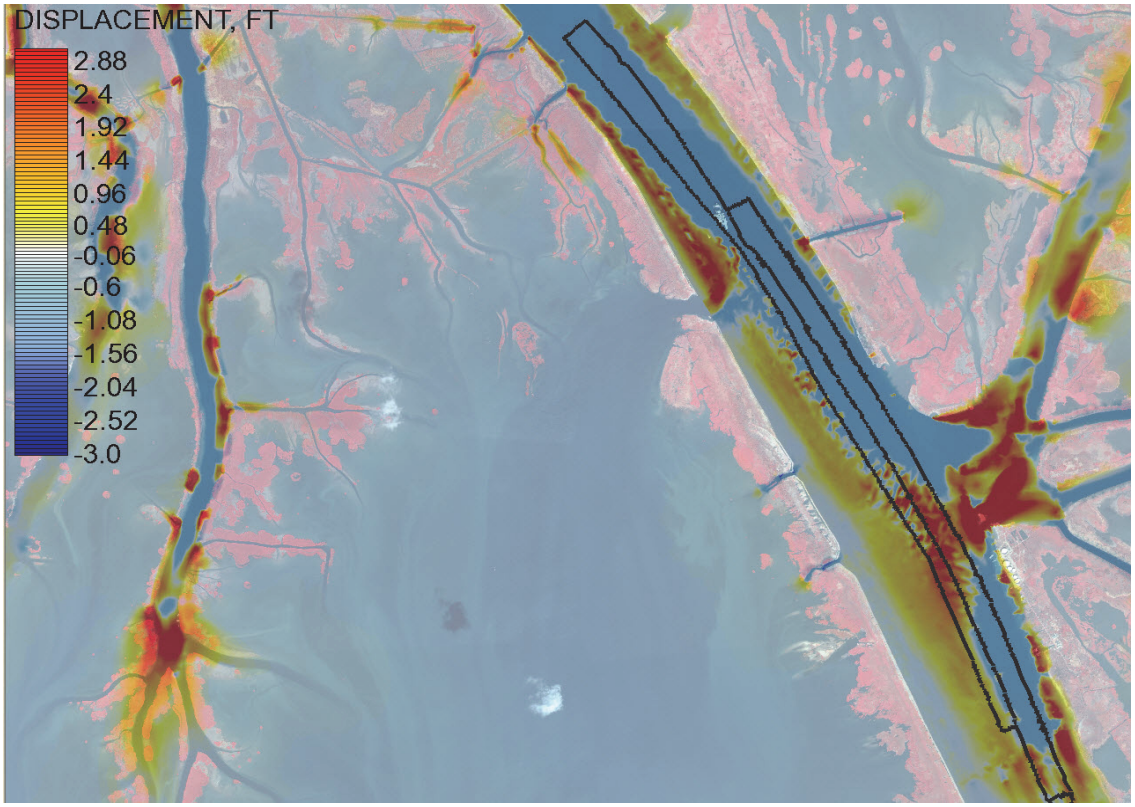

Figure 5.28. Bed change difference, w/ WBSD minus w/o WBSD, Undredged Condition, 1 May 2009

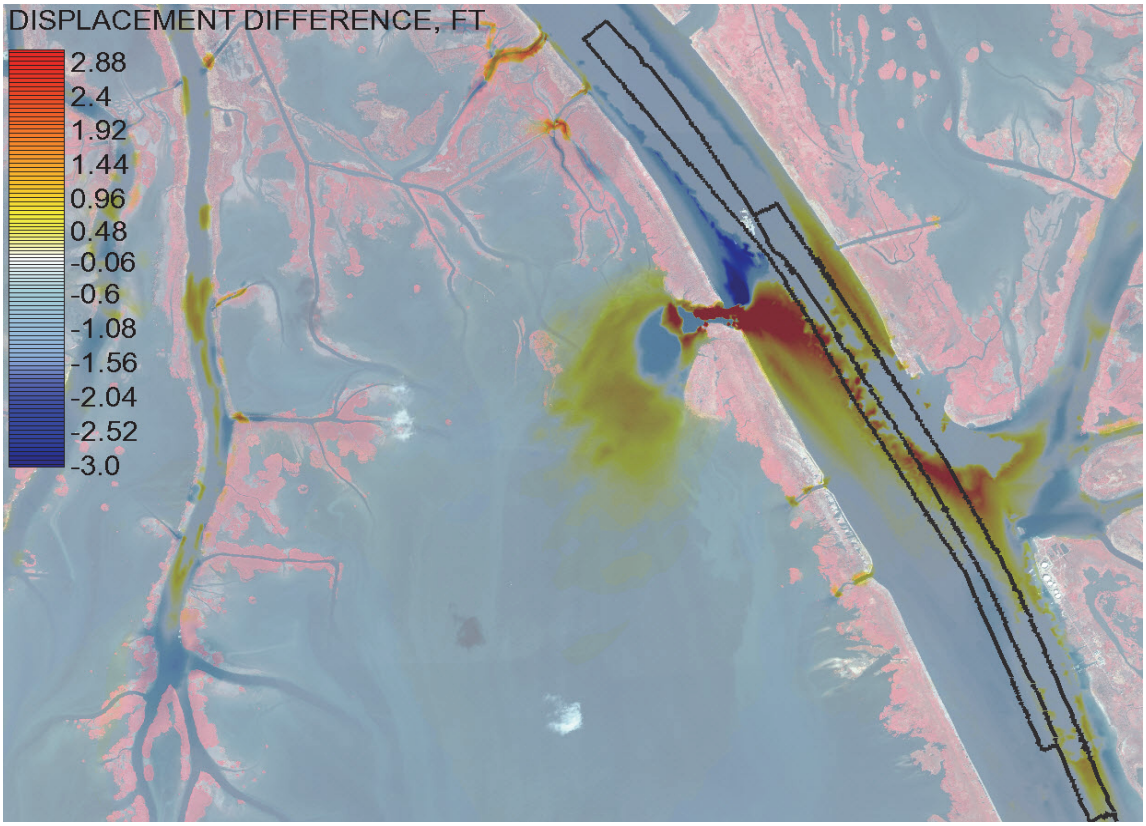

Figure 5.29. Cumulative bed change with WBSD, Dredged Condition, 1 May 2009

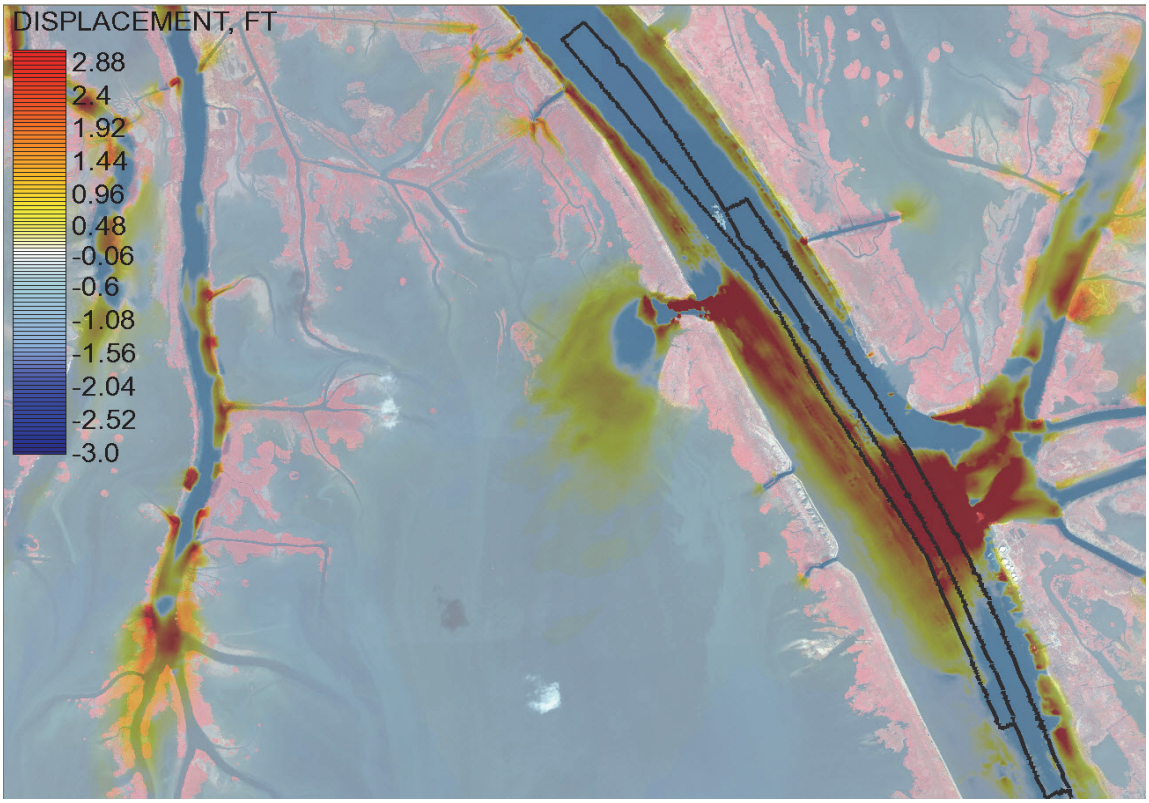

Figure 5.30. Cumulative bed change without WBSD, Dredged Condition, 1 May 2009

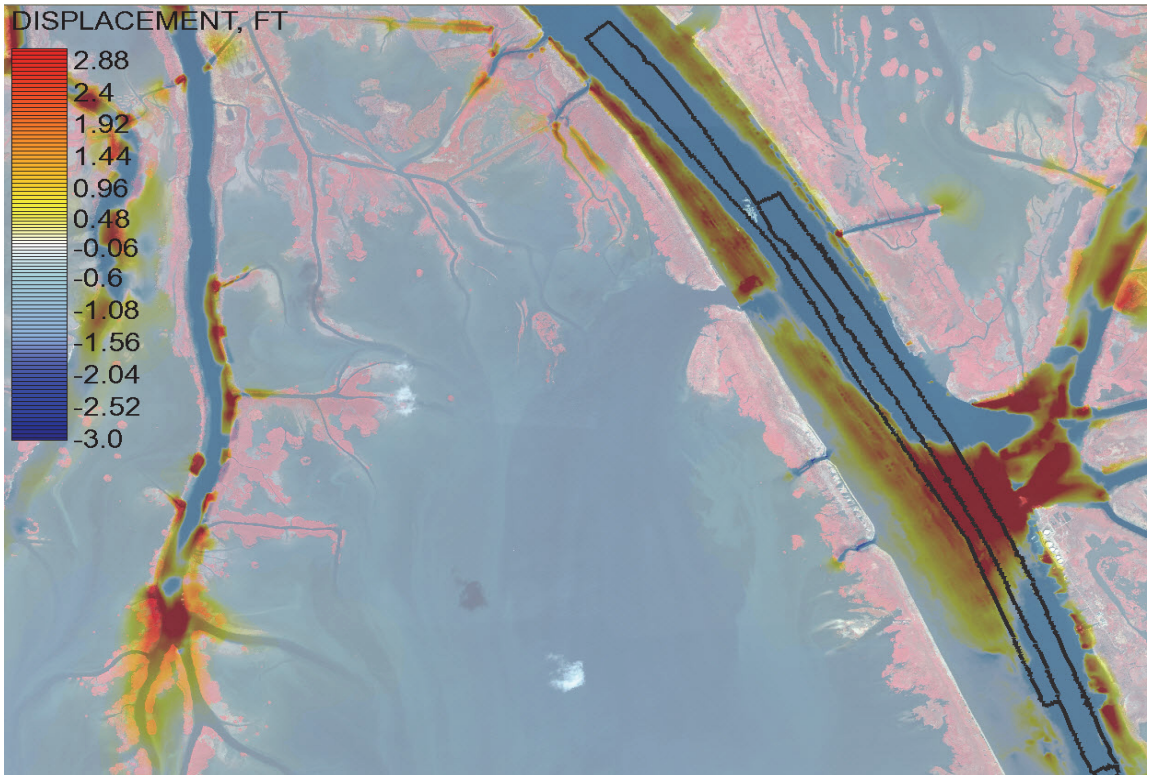

Figure 5.31. Bed change difference, w/ WBSD minus w/o WBSD, Dredged Condition, 1 May 2009.

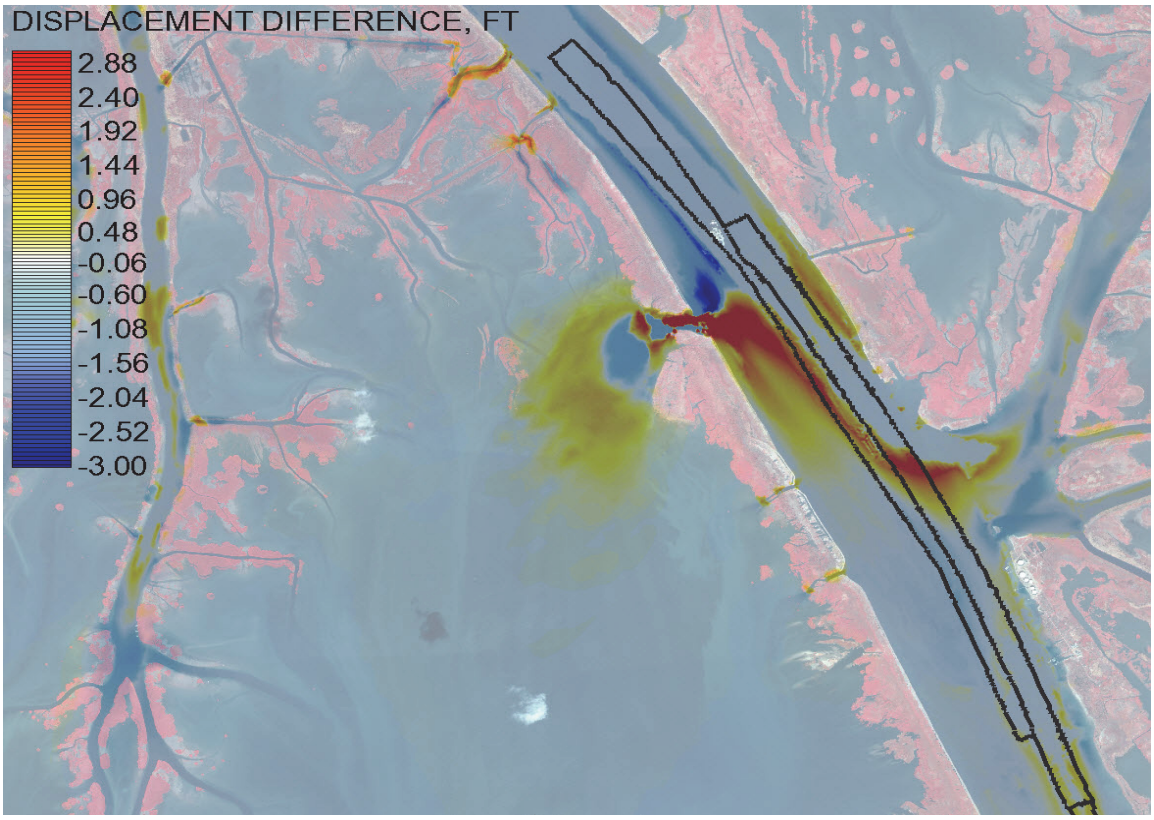

Figure 5.32. Cumulative bed change with WBSD, Undredged Condition, 15 July 2009.

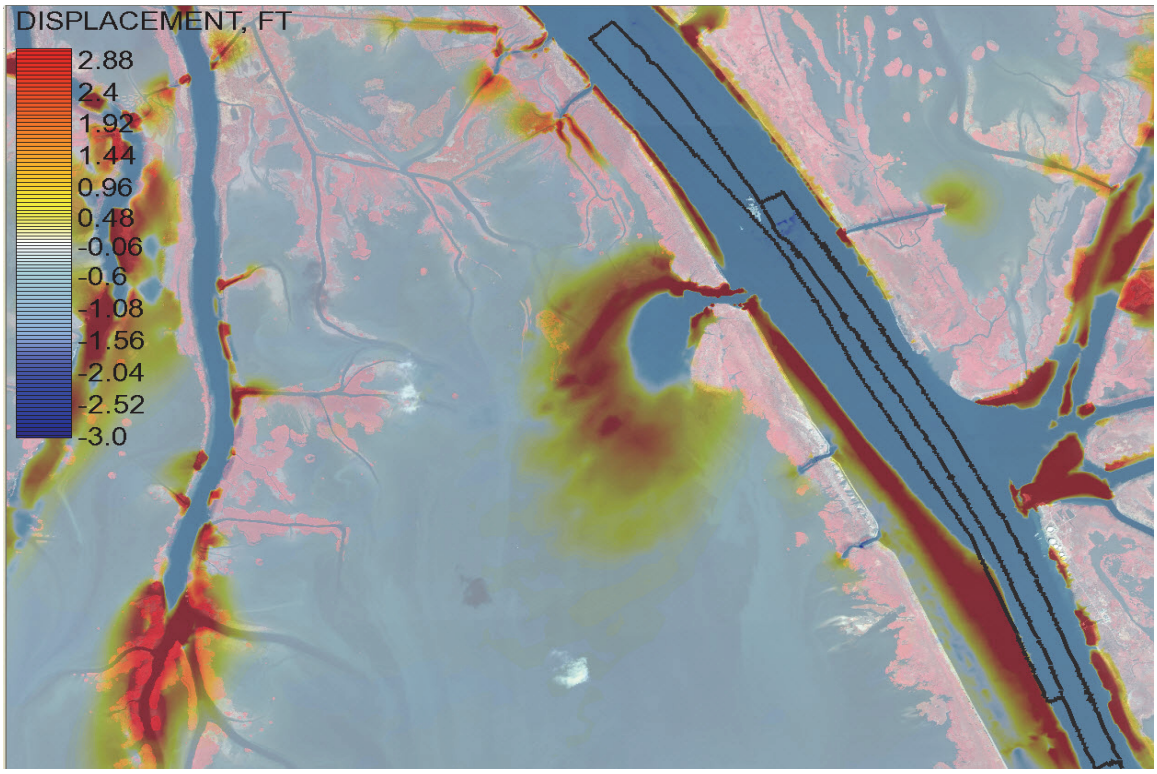

Figure 5.33. Bed change difference, w/ WBSD minus w/o WBSD, Undredged Condition, 15 July 2009.

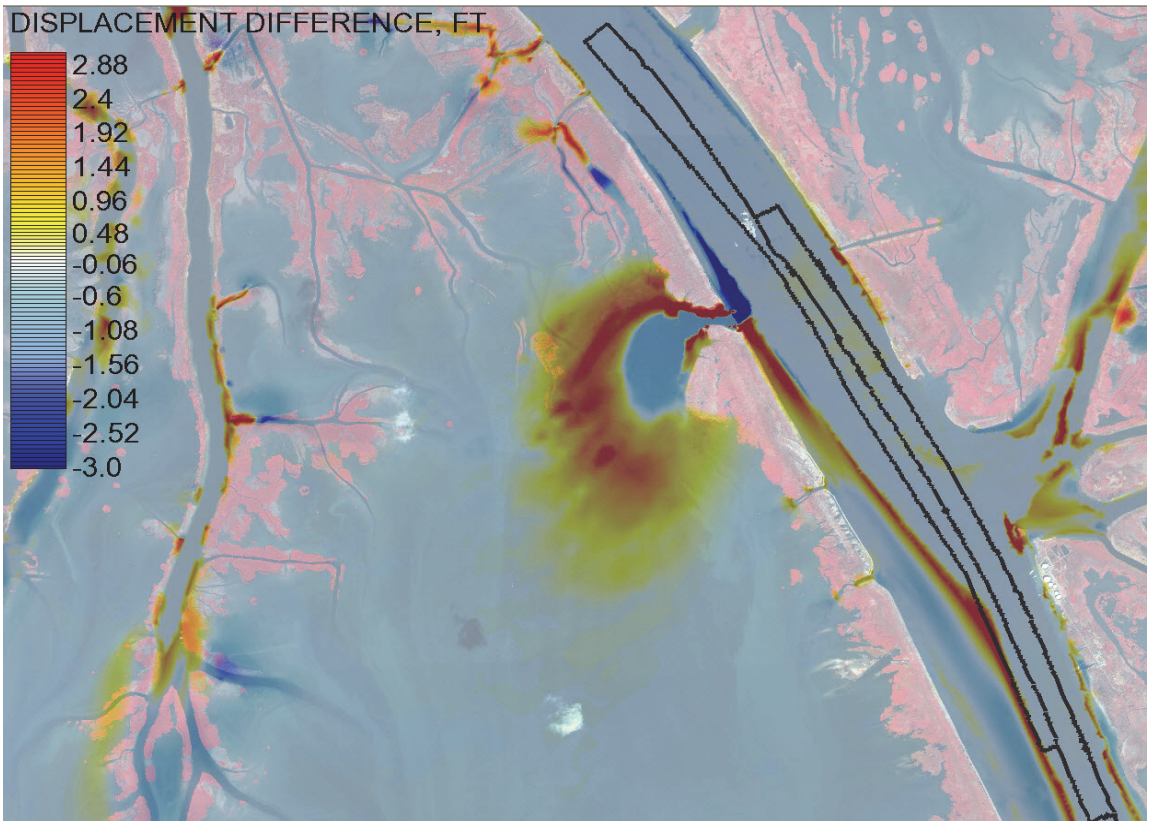

Figure 5.34. Bed change difference, w/ WBSD minus w/o WBSD, Dredged Condition, 15 July 2009.

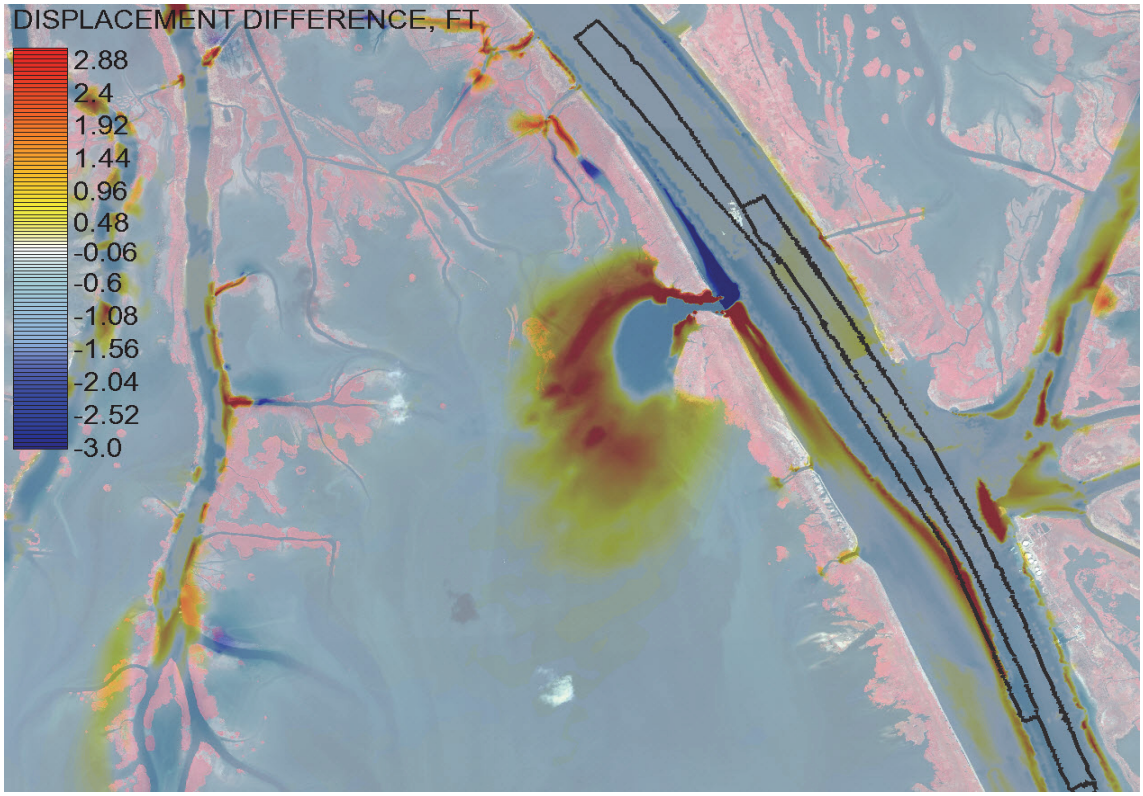

Figures 5.28 and 5.31 demonstrate that, during times when the system is locally depositional, the reduction in shear stress associated with the momentum loss though the diversion controls the change in deposition downstream of the diversion. The largest changes are observed just downstream of the diversion in the PAA and the NC. Figures 5.33 and 5.34 demonstrate that when the system is locally erosional (due to scouring of the upstream bed) the largest differences occur along the side slopes of the scouring channel. This is because, for the erosional condition, the transition to erosion begins sooner when WBSD is closed; hence, the channel has more time to expand.

A quantitative time history analysis of the volume of deposition in both the PAA and the navigation channel is given in Figures 5.35 though 5.41 (open West Bay (OWB) and closed West Bay (CWB)). Figure 5.35 depicts the footprints of both the anchorage area and the adjacent channel. These footprints are derived from coordinates provided by the New Orleans District for a specific dredged cycle. For the purposes of this study, however, it is necessary to have a specific definition of each footprint in order to perform a meaningful quantitative analysis.

Figure 5.35. The PAA and NC quantitative analysis footprints.

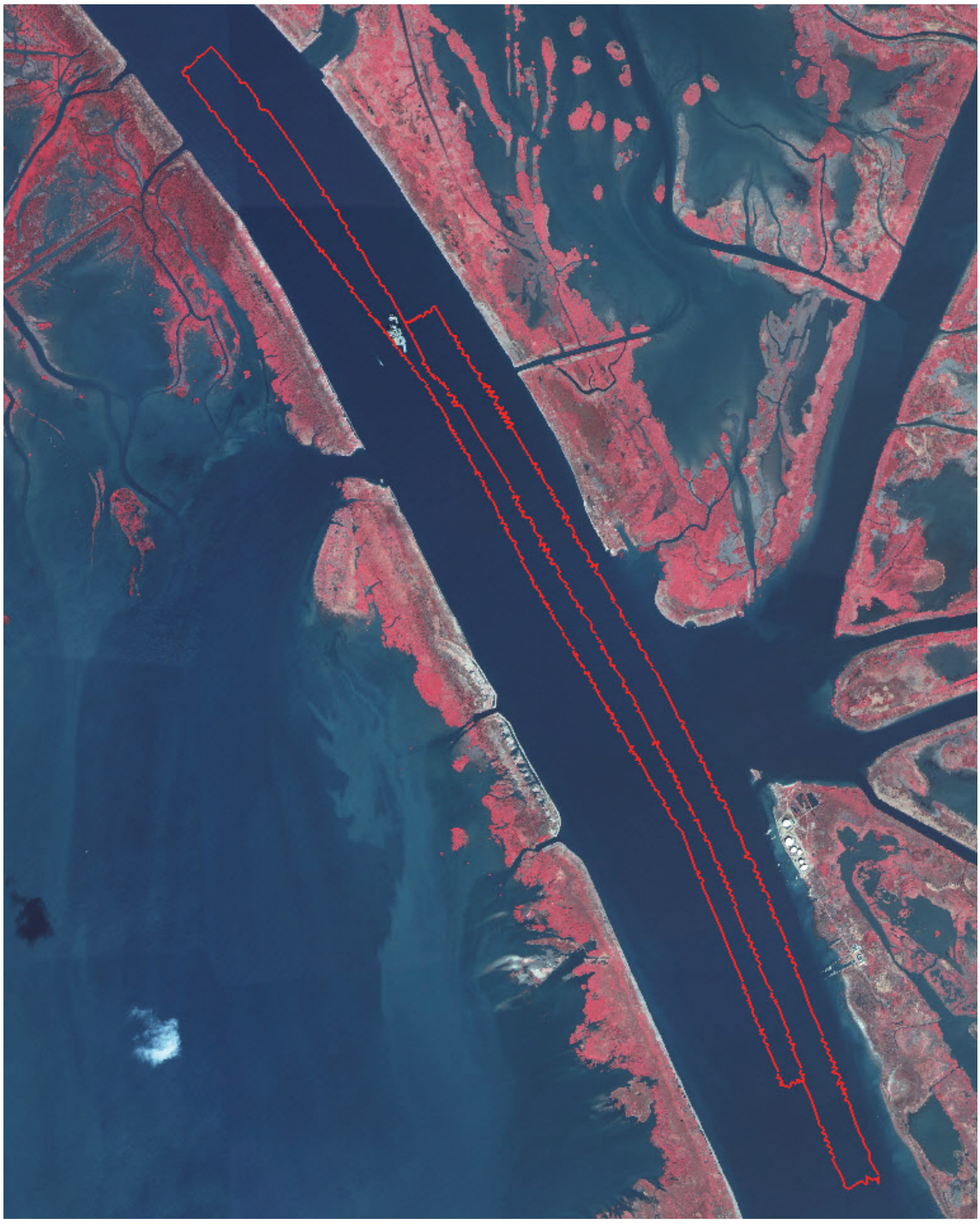

Figure 5.36. Deposition quantities for the PAA, Undredged condition.

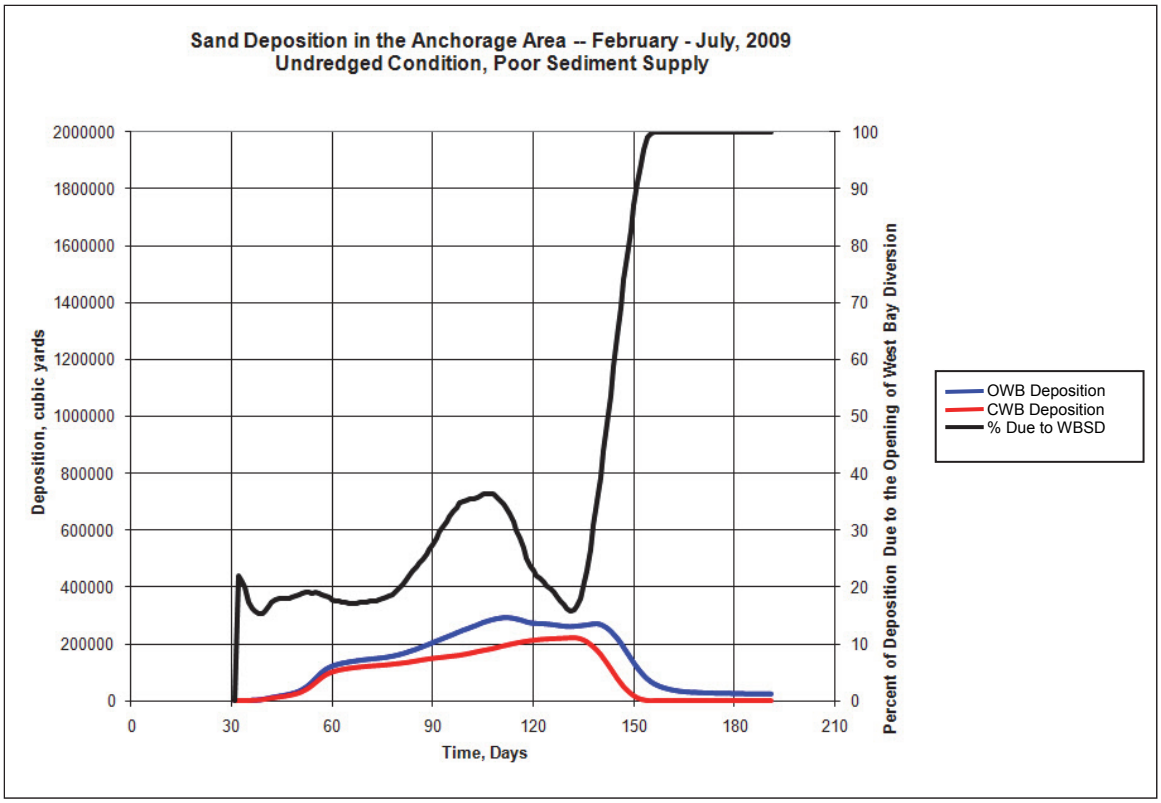

Figure 5.37. Deposition quantities for the NC, Undredged condition.

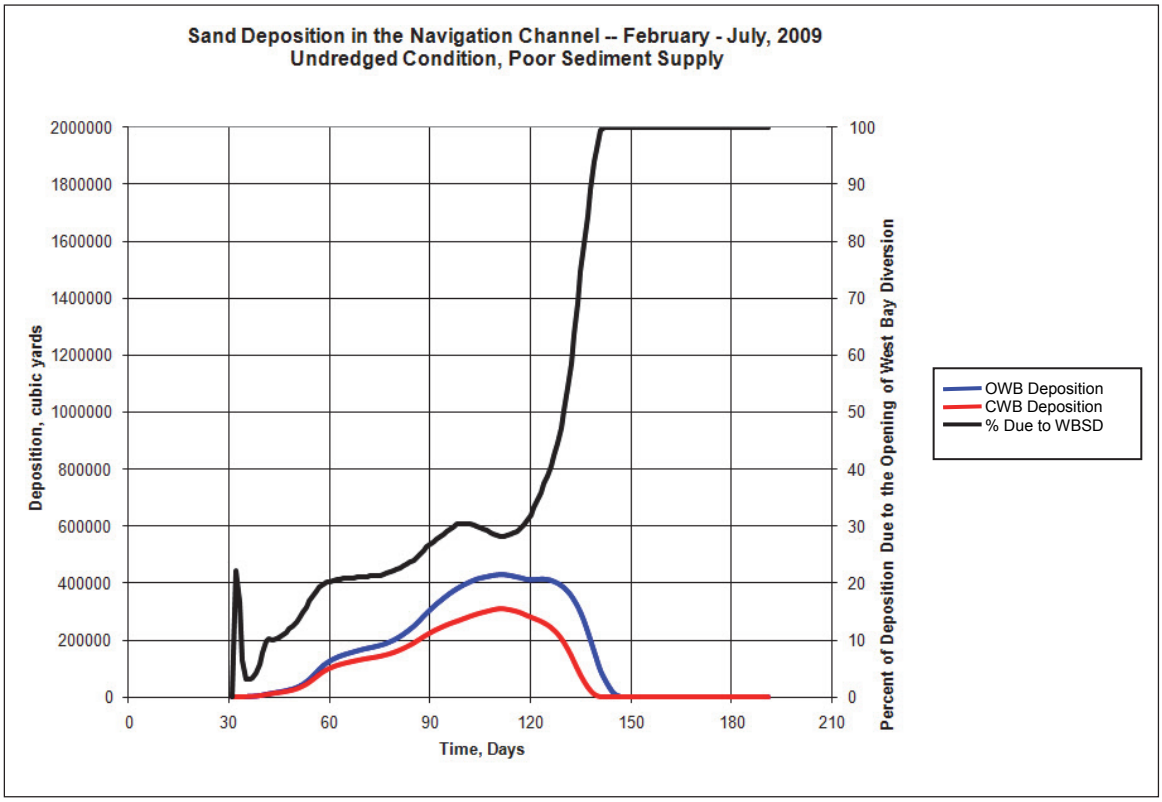

Figure 5.38. Deposition quantities for the PAA, Dredged condition.

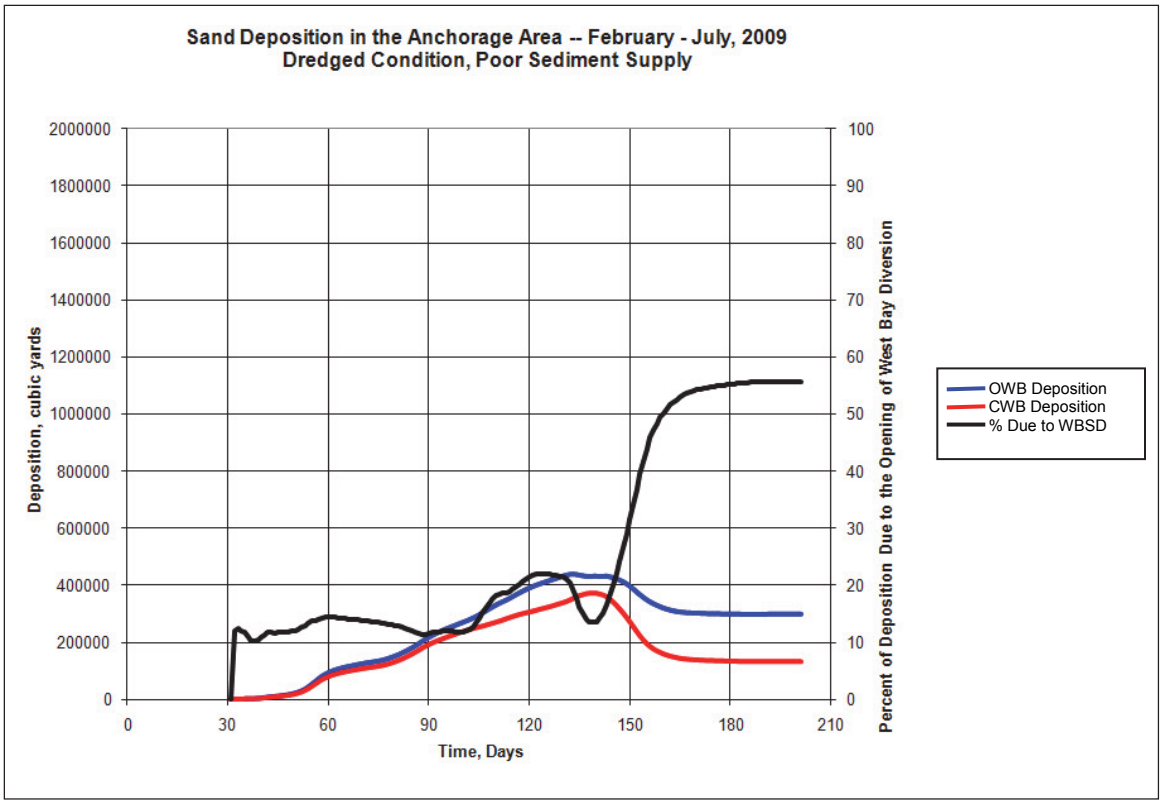

Figure 5.39. Deposition quantities for NC, Dredged condition

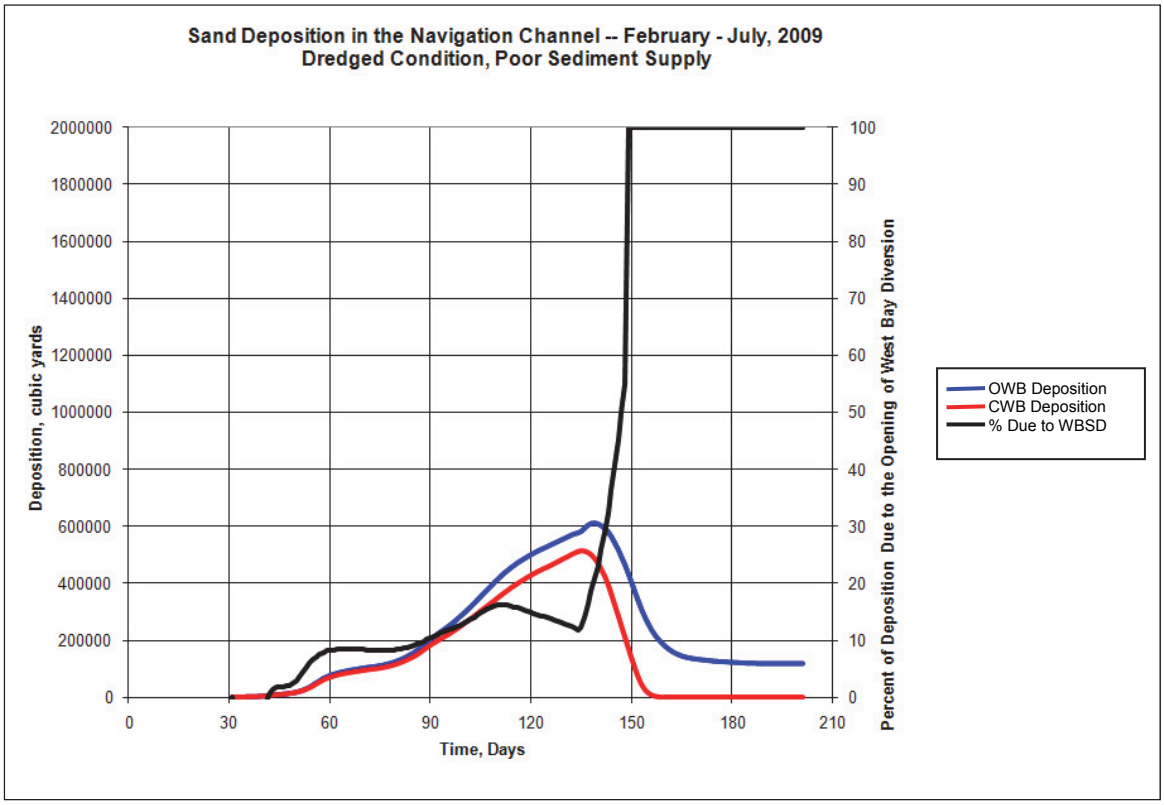

Figure 5.40. Deposition quantities for the combined PAA and NC, Undredged condition.

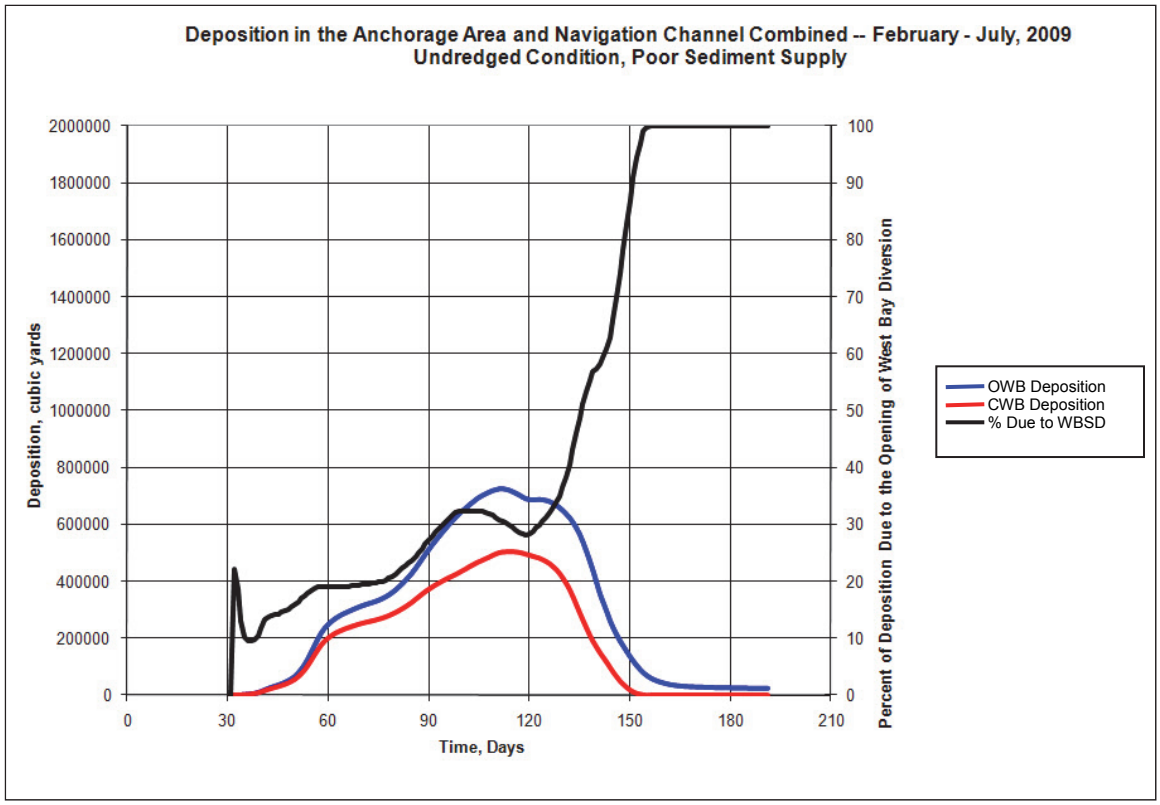

Figure 5.41. Deposition quantities for the combined PAA and NC, Dredged condition.

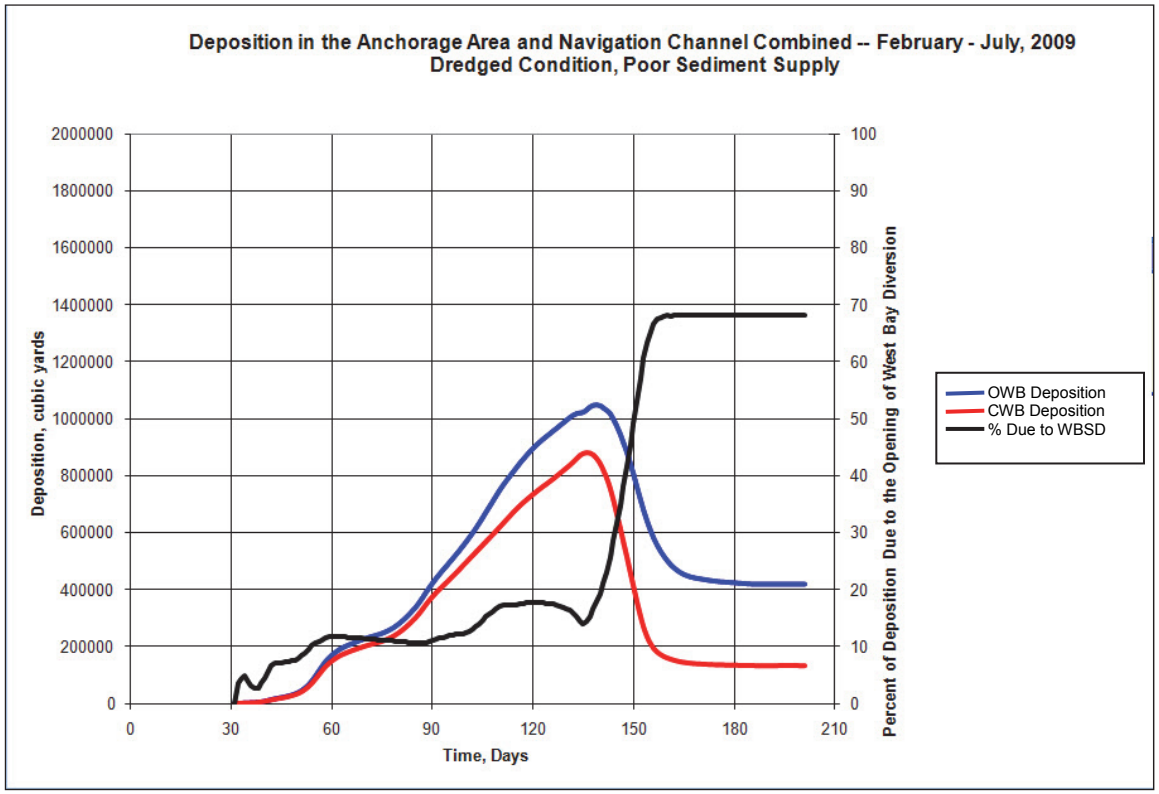

Therefore, these footprints are taken as the defined coordinates of the footprint boundaries. The PAA footprint is the western footprint, and the NC footprint is the eastern footprint. Note that the PAA is assumed to include any undefined area between the true PAA footprint and the NC footprint.

The time history plots in Figures 5.36-5.41 depict the volume of deposition in each footprint over time, for both with and without WBSD scenarios. The plots also depict the percent of deposition attributable to WBSD, expressed as the difference in deposited volume for each simulation divided by the deposited volume for the with WBSD simulation.

Each of these plots follow a similar pattern. During the depositional period, the percent of deposition attributable to WBSD is relatively consistent (about 20 percent). However, as the trend switches from depositional to erosional, the without WBSD simulations begin to erode sooner, resulting in a rapidly increasing percentage of the total deposited volume attributed to WBSD.

These plots can be used to generate a quantitative estimate of both the mean percentage of deposition attributable to the WBSD, and a quantitative estimate of the uncertainly of this mean. This can be done by computing volume weighted values of the mean and standard deviation of the time history plots. The volume weighting is appropriate, since the percentages associated with high rates of deposition are of more significance than quiescent or erosional periods, with respect to dredging.

The equations for the volume weighted mean and standard deviation are as follows:

$$\bar{\psi} = \frac{\sum_{i=1}^{nts} V_{WBO}\,\psi_i}{\sum_{i=1}^{nts} V_{WBO}} \tag{1}$$

$$\sigma = \left(\frac{\sum_{i=1}^{nts} V_{WBO}\left(\psi_i - \bar{\psi}\right)^2}{\sum_{i=1}^{nts} V_{WBO}} \right)^{1/2} \tag{2}$$

Where ψ_i is the percentage of deposition attributable to WBSD for time-step i

The data were analyzed though simulation day 150. The results of this analysis are given in Table 5.1.

Table 5.1. Weighted Mean and Standard Deviation of the Percent of Deposition Attributable to West Bay Diversion

	Pilottown Achoarge Area (PAA)	Navigation Channel (NC)	Combined PAA and NC Footprint
Volume Weighted Mean	23.7%	27.4%	25.7%
Volume Weighted Standard Deviation	12.7%	18.9%	13.9%

The results include both the dredged and undredged conditions; therefore, they implicitly include the uncertainty associated with these conditions. The standard deviation is largely associated with the divergence of the deposition curves during erosional conditions. However, these conditions can still result in a net increase in deposition over a hydrograph, and can contribute to dredging volumes over a multiyear cycle. Therefore, these net erosional periods must be included in the analysis.

Morphologic Trends Analysis

In order to gain insight into the general morphologic trends of the study area both with and without the WBSD, some additional AdH model simulations were conducted. These simulations were designed to mimic (in a qualitative sense) the long-term morphologic trends of the study area.

In each simulation, a steady supply of sediment was introduced to the system, such that the sediment concentration of the inflow was at maximum capacity for the given river discharge. Two steady river discharge rates are simulated: a medium discharge of 700,000 cfs and a high discharge of 1,000,000 cfs. For each discharge, simulations were conducted with and without the WBSD. Also, simulations were conducted for each of three separate dredging scenarios: no dredging, dredging the navigation channel only, and dredging the navigation channel and the PAA. These were conducted to investigate the impacts of dredging on the overall morphologic change in the study area. Table 5.2 is a matrix of all of the simulations conducted for this analysis.

Table 5.2. Morphologic Trends Analysis Simulations.

	No Dredging	Navigation Channel Dredging Only	Navigation Channel and PAA Dredging
Medium Discharge WBSD Open	X	X*	X
Medium Discharge WBSD Closed	X	X*	X
High Discharge WBSD Open	X	X*	X
High Discharge WBSD Closed	X	X*	X

* Navigation Channel Dredging Only

The morphologic changes associated with these simulations were compared to the long-term observations conducted in the morphologic analysis section of this report. It was determined that the medium discharge simulations yield results that are similar to the historic long-term morphologic changes associated with the PAA as well as the more recent depositional patterns (e.g., deposition is highest in the vicinity of Cubits Gap).

The matrix of initial runs demonstrated that the choice of dredging template did not have a significant qualitative impact on scour and deposition patterns. Therefore, the only runs that were carried forward were the runs associated with Navigation Channel dredging only. This was done in order to investigate the equilibrium morphology of the study area with and without the WBSD, assuming that the dredging of the PAA was discontinued.

The Navigation Channel Dredging Only runs (designated with an X* in Table 5.2) consist of the high and medium discharge runs. The high discharge runs were used to investigate the impacts of a large event (such as the 2011 Flood). The medium discharge runs were used to determine the long term morphologic equilibrium of the system. The medium discharge runs were run long enough so that the erosion and deposition patterns in the study area approached a steady state.

Because of the uncertainties in the river hydrograph, sediment supply, and other factors, the duration of these steady-state morphologic simulations can only be reconciled to equivalent prototype time periods in terms of orders of magnitude. The equivalent prototype time period for the high discharge run is on the order of months, and the equivalent prototype time

period for the medium discharge run is on the order of decades. Refinement of these estimates is not possible due to the simplifying assumptions inherent in this analysis.

The initial and final bed elevations in the study area are shown in Figures 5.42 – 5.44. The elevations are contoured such that any bed elevation below 40 feet is not color contoured. This delineates the 40-foot contour clearly.

The analysis indicates that more deposition occurs on the point bar along the right descending bank of the river when the WBSD is open. However, the spatial extent of the deposition is almost the same whether or not WBSD is open or closed. This is an important result; it implies that the 20-percent increase in deposition associated with the WBSD is associated with the shallower final equilibrium state of this shoal, but the spatial extent of the deposition is not impacted by the presence of the diversion. If the PAA is not maintained, the same footprint of the PAA will be affected by deposition whether WBSD is open or closed.

In order to understand this result, it is instructive to look at the progression of the cross-sectional morphology through time. Figures 5.45 -5.48 depict time-histories of the cross-sectional morphology at RM 3.6 AHP (just upstream of Cubits Gap) and RM 2.0 AHP (downstream of Cubits Gap). Since the morphological exercise is not associated with any specific prototype time scales (as indicated above), the time values are given simply as time 0 through time 5. The navigation channel template is located approximately between 1000 and 1700 feet on the abscissa and the PAA is located approximately between 1700 and 2200 feet. Note that for these runs, the navigation channel is continuously dredged; therefore, the bed elevation in the navigation channel never changes.

These cross sections show a definite pattern of change over time. In the short term, deposition continues to move north along the slope of the shoal (i.e., in the PAA footprint), and since deposition occurs more rapidly with the WBSD in place, the depositional front is further upstream with WBSD open.

However, in both simulations the migration of the shoal upstream eventually stops. As the shoal continues to shallow, the face of the shoal steepens toward the channel. This trend continues until the river cross section narrows to a stable condition. The stable cross section varies in width from the Navigation channel south of Cubits' Gap to nearly the width of the river cross section north of WBSD.

Figure 5.42. Initial Bed Elevations.

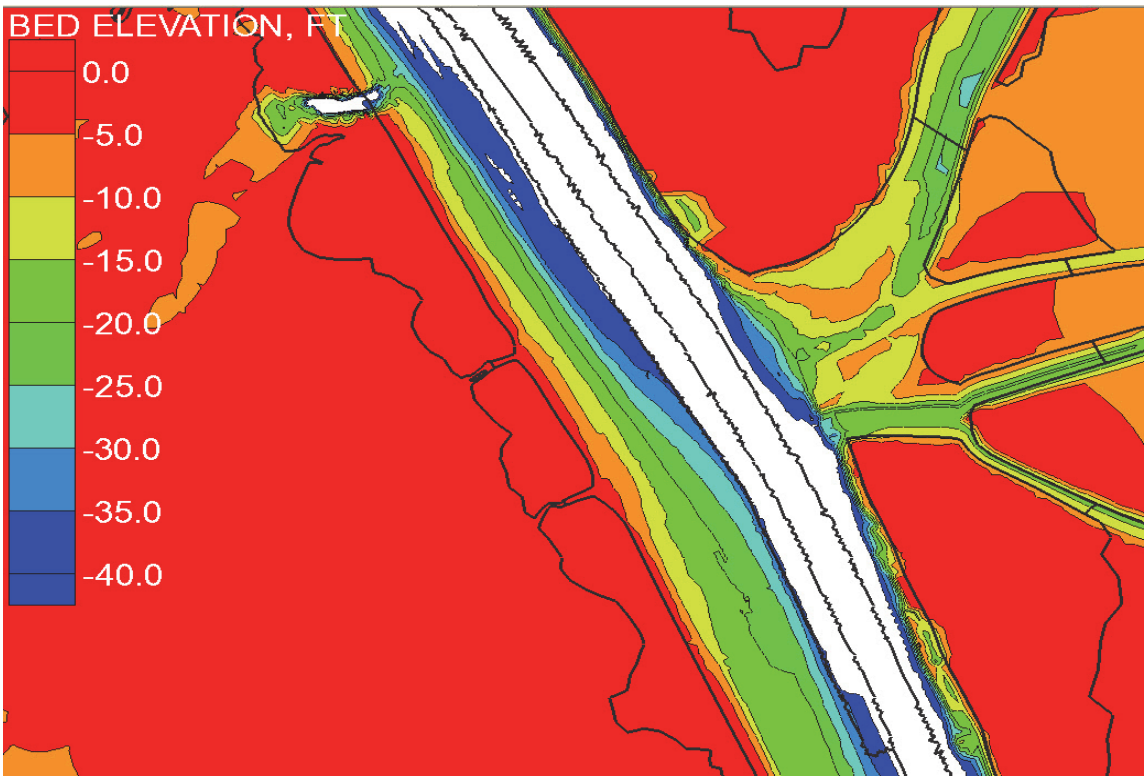

Figure 5.43. Final Bed Elevations, Medium Flow, Navigation Channel Dredging Only, WBSD Open.

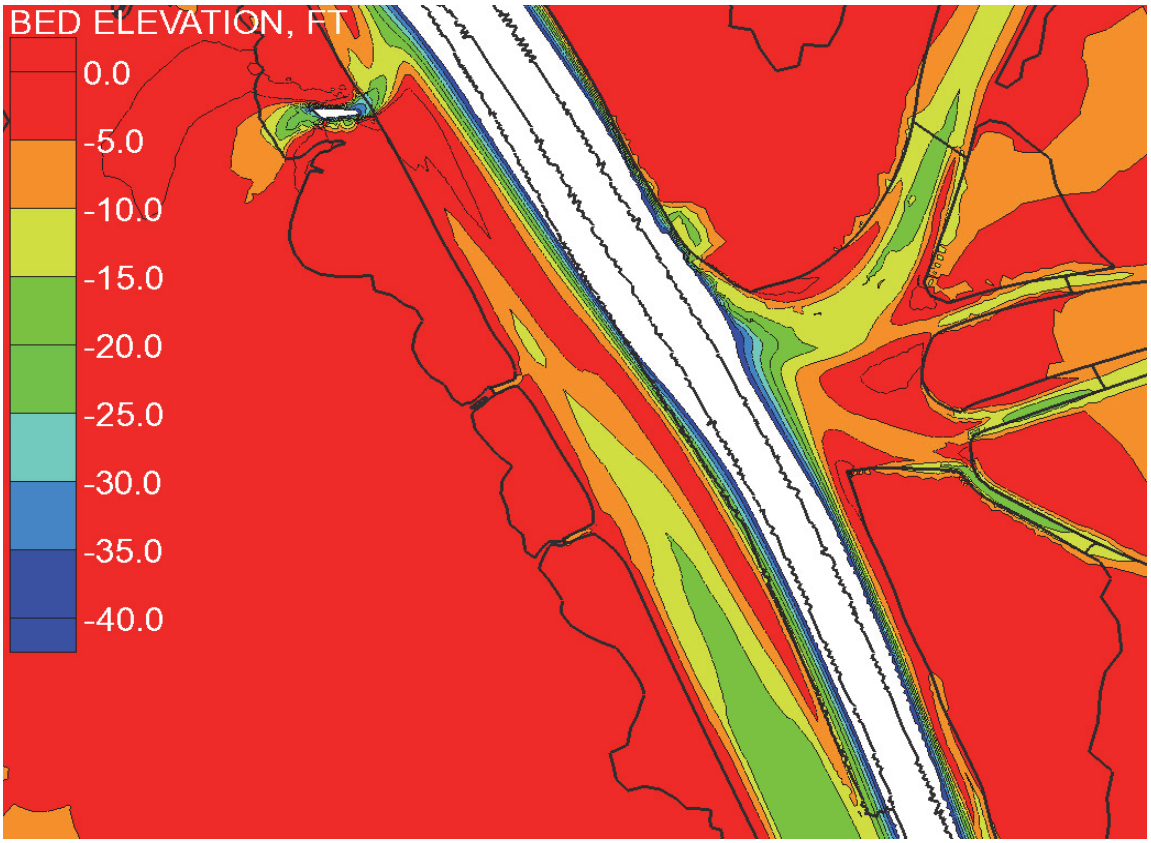

Figure 5.44. Final Bed Elevations, Medium Flow, Navigation Channel Dredging Only, WBSD Closed.

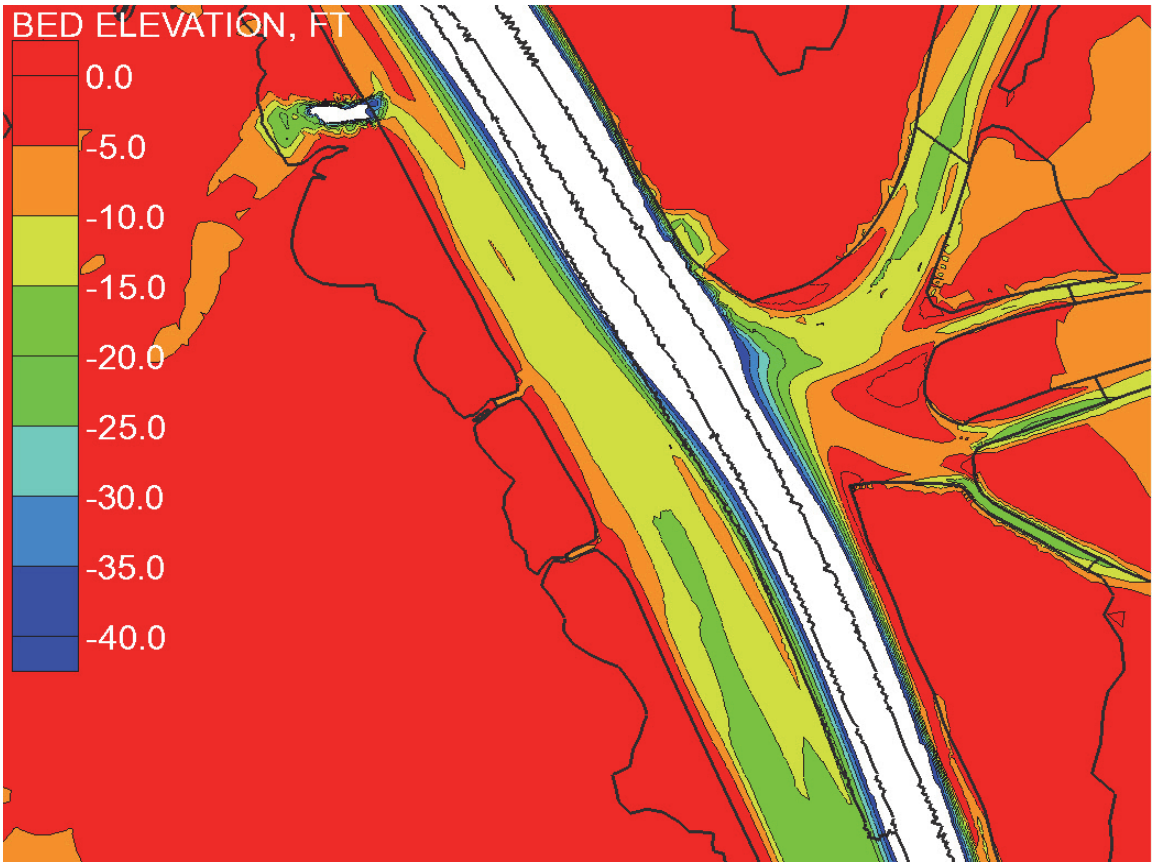

Figure 5.45. Progression of Cross section over Time (RM 3.6 AHP, Medium Flow, WBSD Open).

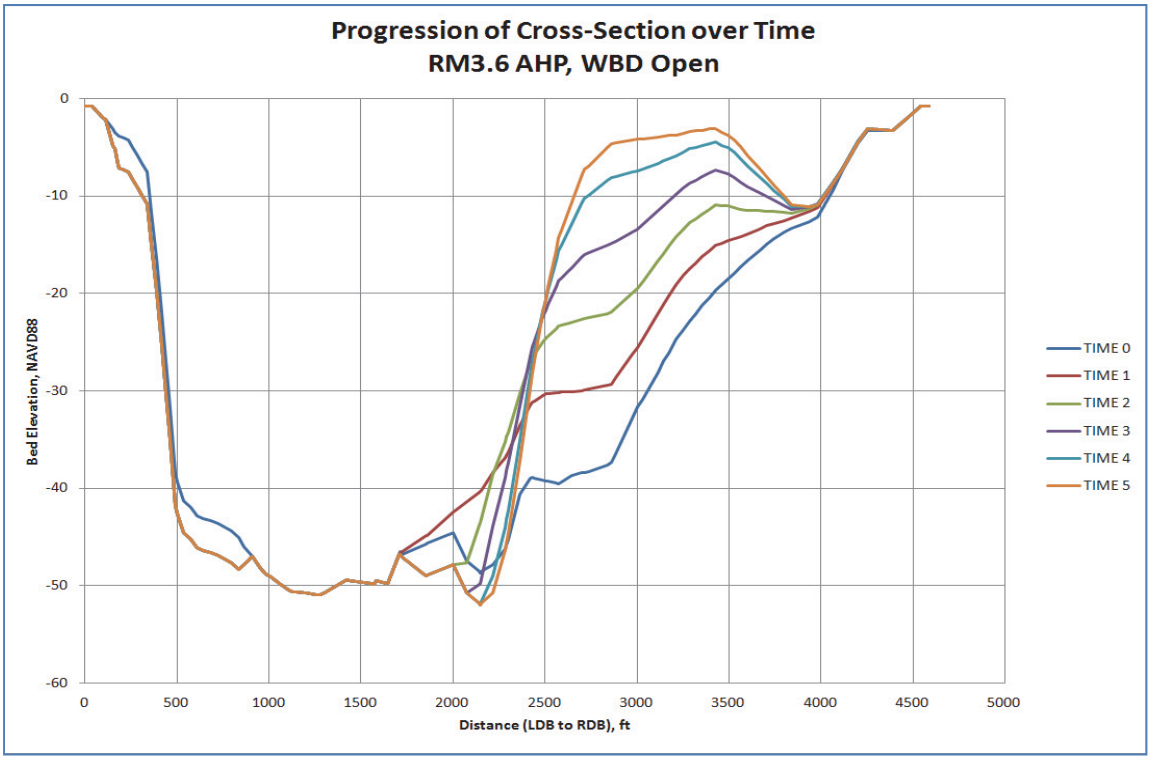

Figure 5.46. Progression of Cross section over Time (RM 3.6 AHP, Medium Flow, WBSD Open).

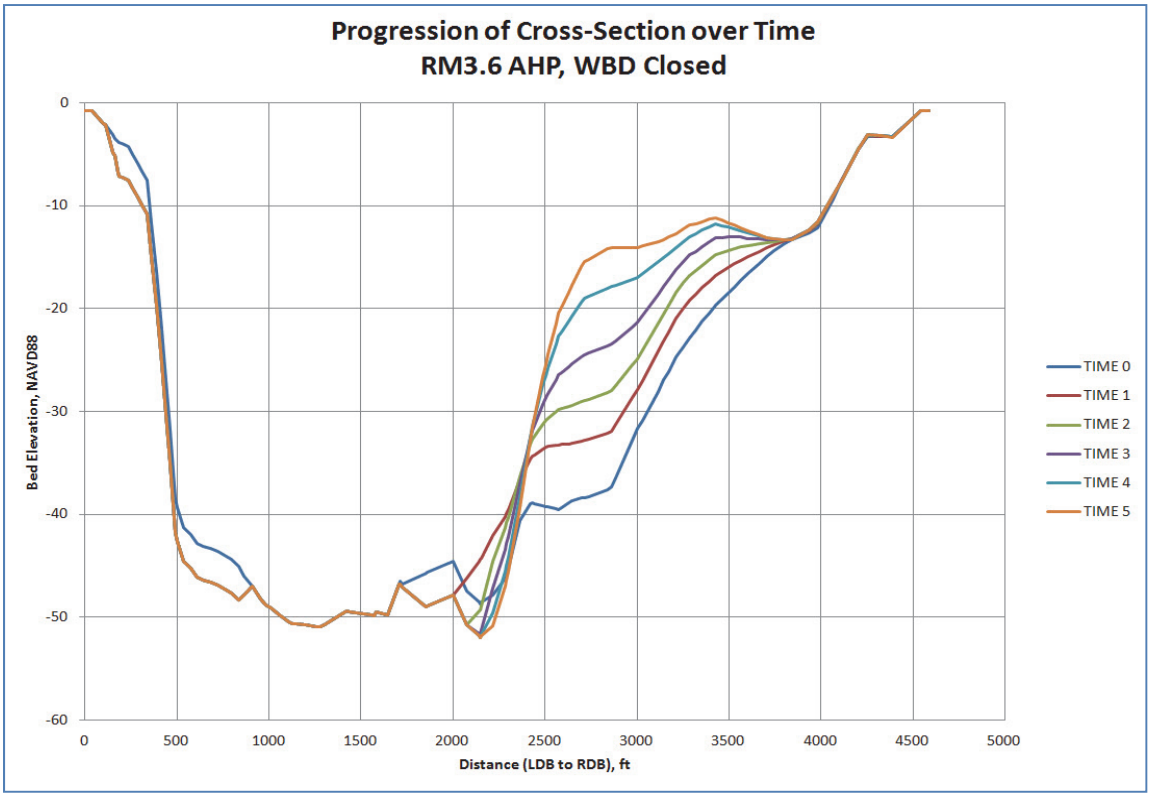

Figure 5.47. Progression of Cross section over Time (RM 2.0 AHP, Medium Flow, WBSD Open).

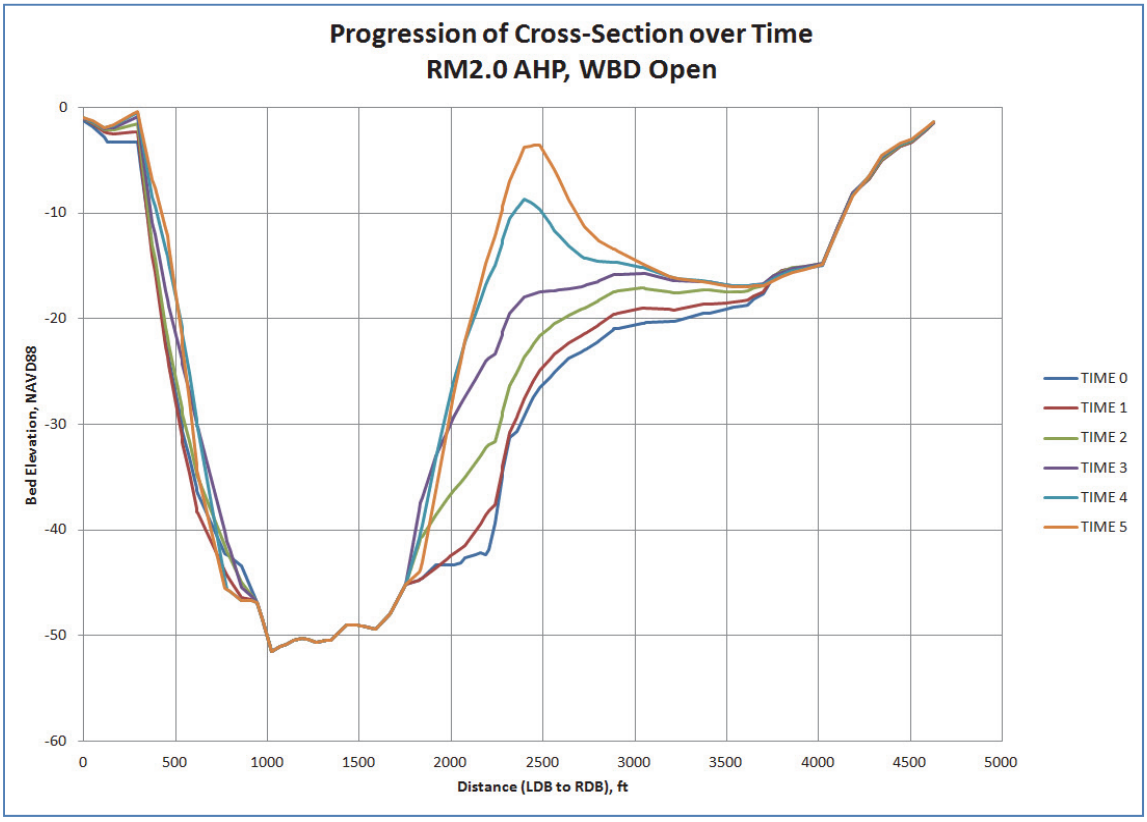

Figure 5.48. Progression of Cross section over Time (RM 2.0 AHP, Medium Flow, WBSD Open).

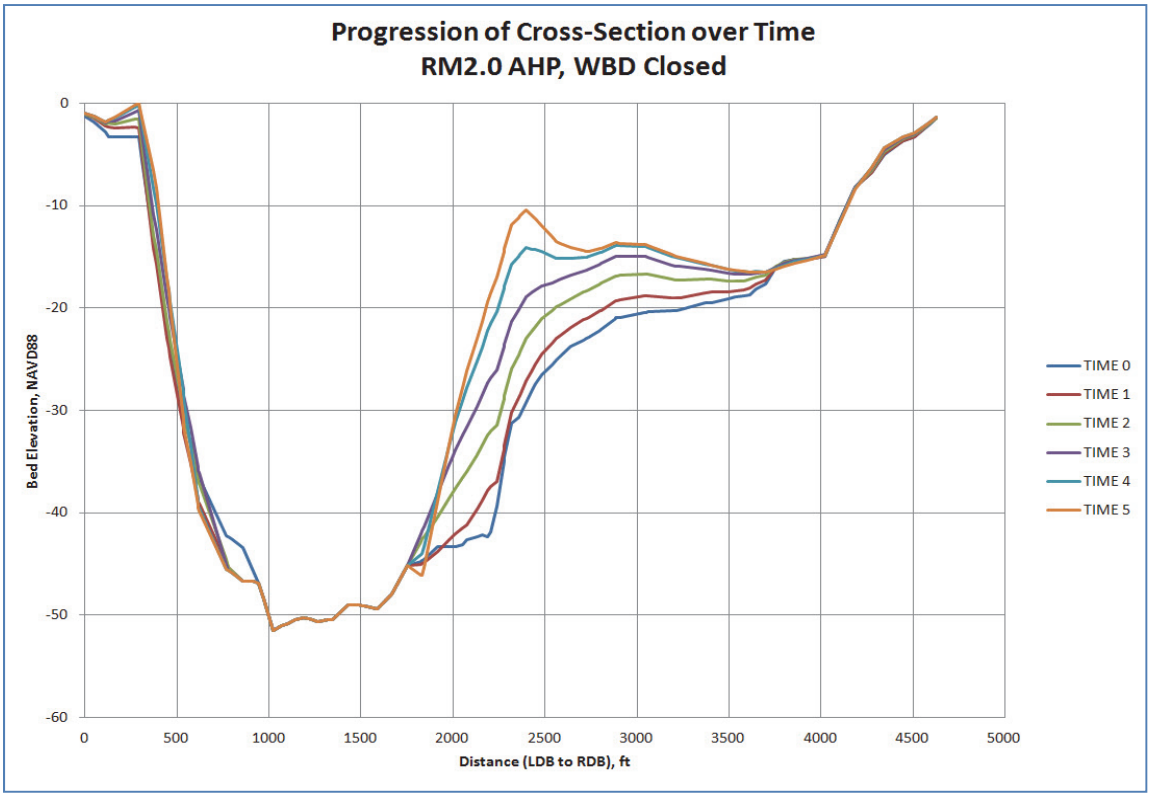

The impact of the WBSD on the navigation channel is illustrated in Figure 5.49 This shows a time-history of the total deposition in each dredge template over the course of the simulation. In addition to the PAA and Navigation Channel templates, a third Southwest Pass template is added to this analysis. This template starts at the southern extent of the Navigation Channel template and extends to the jetties. The deposition is expressed in terms of an average thickness of deposition.

The navigation channel shows a significant increase in total deposition with WBSD diversion open. This is because the morphology reaches equilibrium more quickly with the WBSD closed, and there is more time for material to accumulate (remember that the Navigation channel is continuously dredged in this analysis). However, that the deposition in Southwest Pass is decreased by the presence of the WBSD. This is due to the fact that the presence of the diversion effectively shifts the zone of deposition upstream. Figure 5.50 shows the normalized volume of the Navigation Channel increase, together with the normalized volume of the Southwest Pass deposition decrease (both volumes are normalized by the total volume of deposition in the Navigation Channel template with WBSD open). The volumes are almost the same as demonstrated by the plot of

Figure 5.49. Time History of Dredging Template Deposition Patterns.

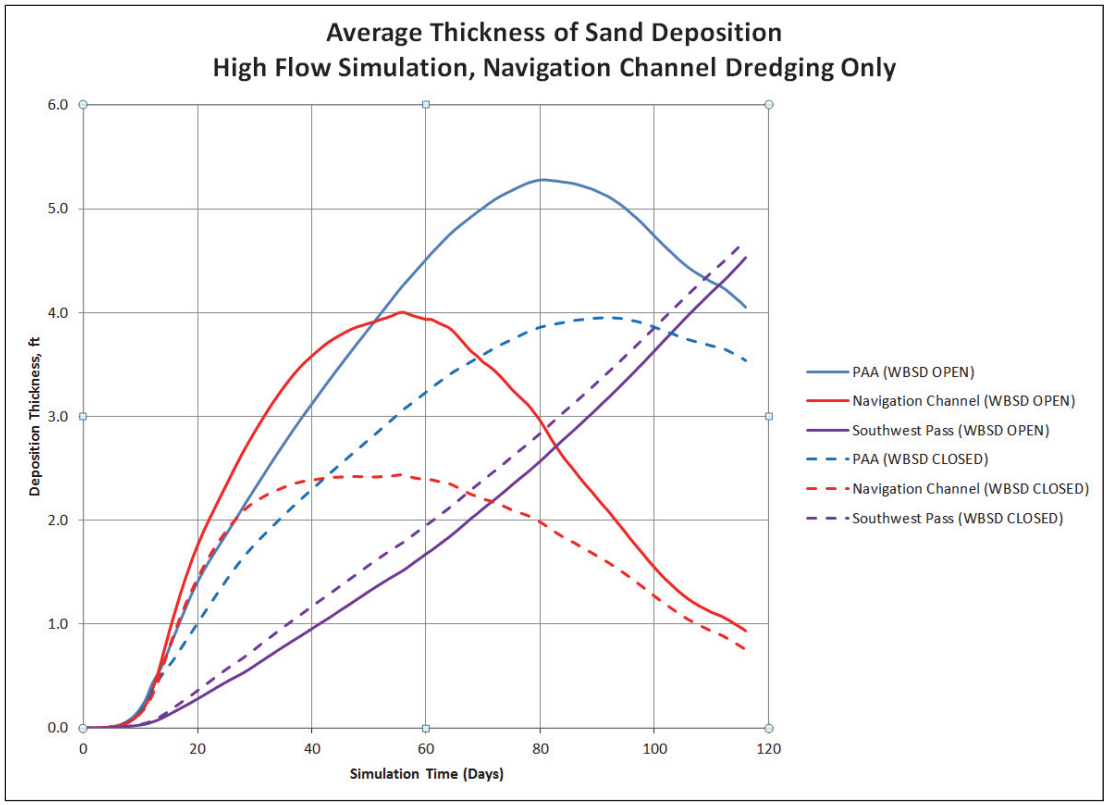

Figure 5.50. Normalized Volumetric Deposition Difference in the Navigation Channel and Southwest Pass Templates.

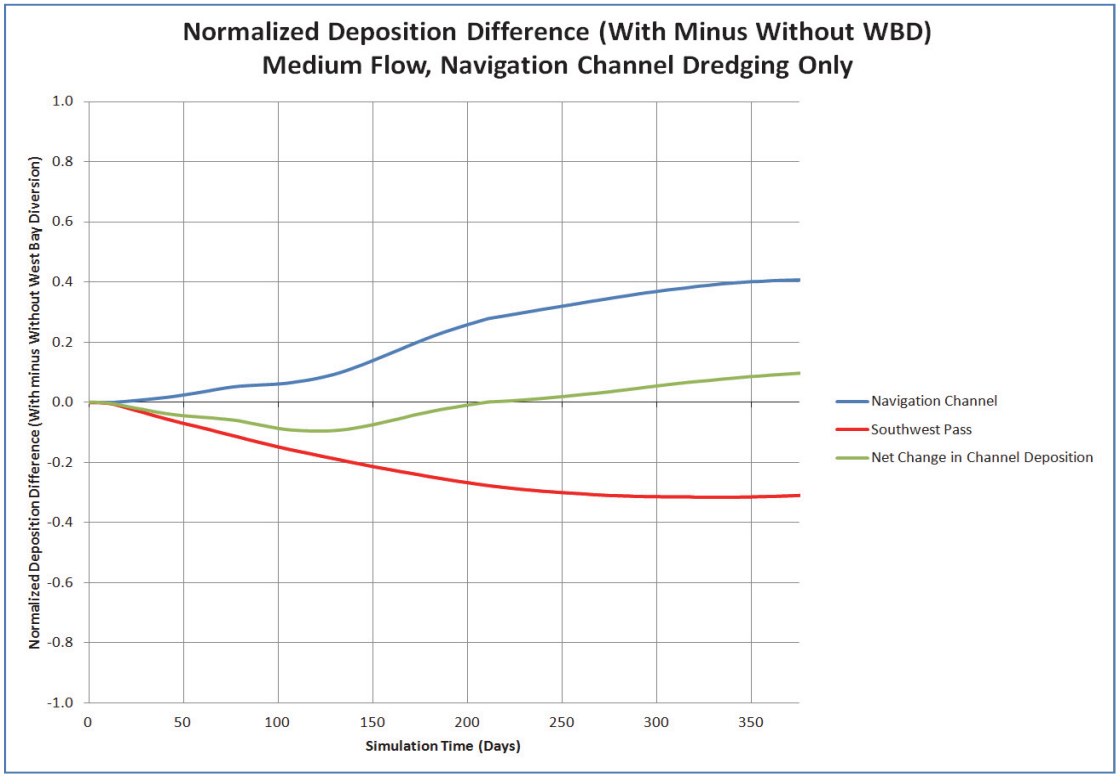

the difference between the two volumes (the green curve). This illustrates that the presence of the WBSD does not have much impact on increasing the total volume of deposition in the channel; it merely shifts that deposition upstream.

The high discharge results are shown in Figures 5.51 and 5.52. The morphology tends to the same patterns as the long-term medium discharge simulation, i.e., shallowing of the right descending bank shoal with the same footprint for the spatial extent of shoaling. The high discharge runs merely achieve this result faster and deposit material on the shoal further downstream. This indicates that the cross section the river is tending towards is robust, i.e., the same general cross section results for both medium and high discharge runs.

These analyses indicate that the long term trend of deposition in the PAA is likely to continue with or without the WBSD in place. The WBSD will induce more deposition in the right descending bank shoal, but the spatial extent of the deposition will be nearly identical with or without the diversion.

The presence of the WBSD also increases the deposition in the adjacent navigation channel; however, this increased deposition is almost entirely offset by a decrease in deposition in Southwest Pass, i.e., the WBSD shifts this quantity of sediment deposition upstream in the channel.

It must be emphasized that these long-term morphologic trends are not necessarily indicative of short term trends. The numerical and morphologic analyses suggest that the inter-annual morphologic change in the study area varies significantly depending on the discharge and sediment supply conditions. Under high discharge conditions, much of the deposition in the system is pushed downstream of Cubits Gap. Under lower discharge conditions, this deposition can shift to near Cubits Gap or upstream to Venice.

Also, the long-term morphologic trends in this reach are likely to be heavily influenced by other factors not included in this analysis. These include sea level rise and local subsidence, changes in sediment supply and sediment management in the system, and the impact of upstream diversions. Each of these factors is likely to impact the target equilibrium morphology toward which river is trending towards.

Figure 5.51. Final Bed Elevations, High Flow, Navigation Channel Dredging Only, WBSD Open.

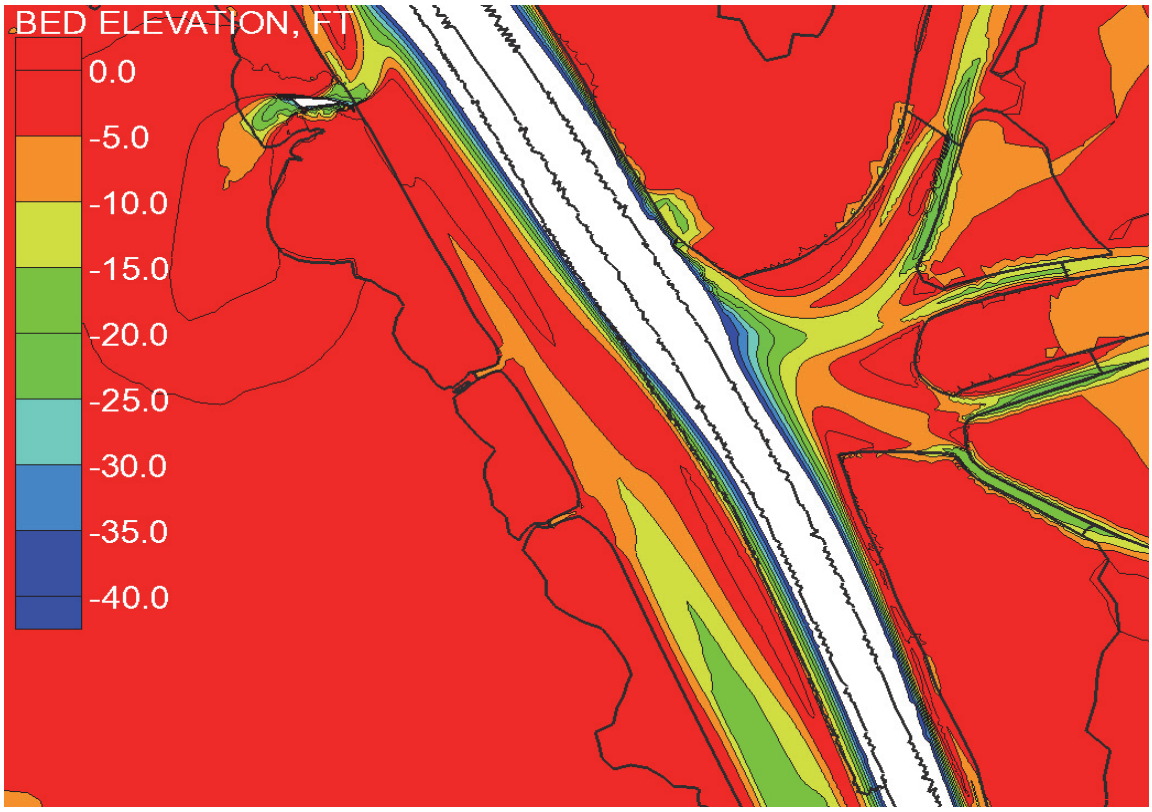

Figure 5.52. Final Bed Elevations, High Flow, Navigation Channel Dredging Only, WBSD Closed.

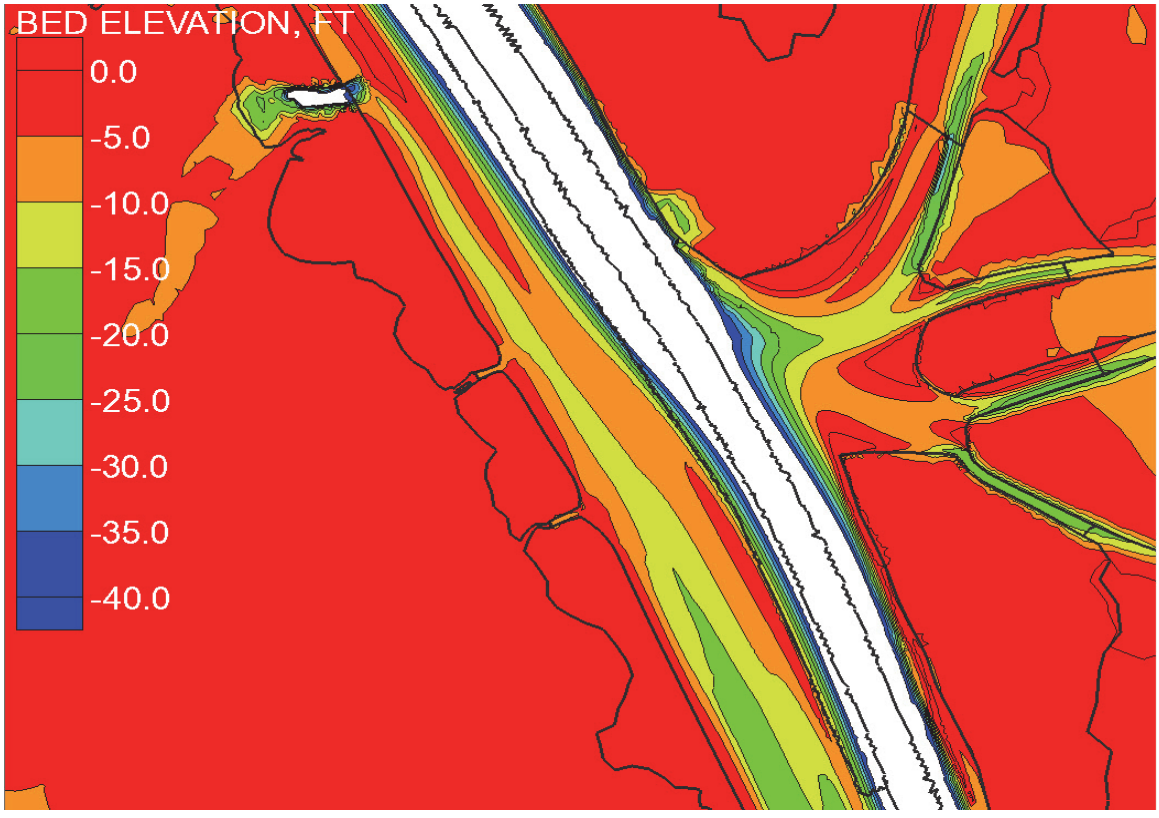

CH3D-SED

Model Description

CH3D stands for Curvilinear Hydrodynamics in 3 Dimensions. CH3D-SED is a 3D, finite-difference model suitable for simulating hydrodynamics and noncohesive sediment transport. The hydrodynamics in CH3D are based on work described in Sheng (1986), Johnson et al (1991), Chapman (1993, 1994), and Chapman et al. (1996). The governing sediment equations are based on a sediment modeling approach introduced by Spasojevic and Holly (1990). The original sediment modeling approach, developed for 2D shallow water situations, was extended by Spasojevic and Holly (1993) to fit the 3D, non-orthogonal, curvilinear framework of the CH3D code. The sediment modeling approach includes bed level changes (deposition and/or erosion), bedload transport, suspended-sediment transport, and interaction between the two. The approach allows for representing a sediment mixture in a natural watercourse through an unlimited number of size classes.

Mesh Development

The WBSD model domain has an upper inflow boundary located approximately at RM 7.5 (above Venice, LA) and extended to the south to approximately 3 miles below in HOP into Southwest Pass, South Pass, and Pass a Loutre. The CH3D-SED computational grid was generated with dimensions 61 ×322 m to accommodate high grid resolution at the WBSD. Figure 5.53 shows the CH3D-SED grid and Figure 5.54 shows the bathymetric contours of the mesh.

Grid resolution across the river is approximately 30 ×30 meters with the highest grid resolution located at the diversion with approximately 7 ×7 m resolution. Figure 5.55 shows grid resolution at the WBSD.

Boundary Condition Development

The model had an inflow boundary at the upstream end of the Mississippi River and outflow boundaries including Grand Pass, Baptiste Collette, West Bay Diversion, and Cubits Gap. The values used for these boundaries were taken from discharge measurements made by ERDC during the high discharge event in 29 – 30 May 2009.

Figure 5.53. CH3D-SED Model Domain.

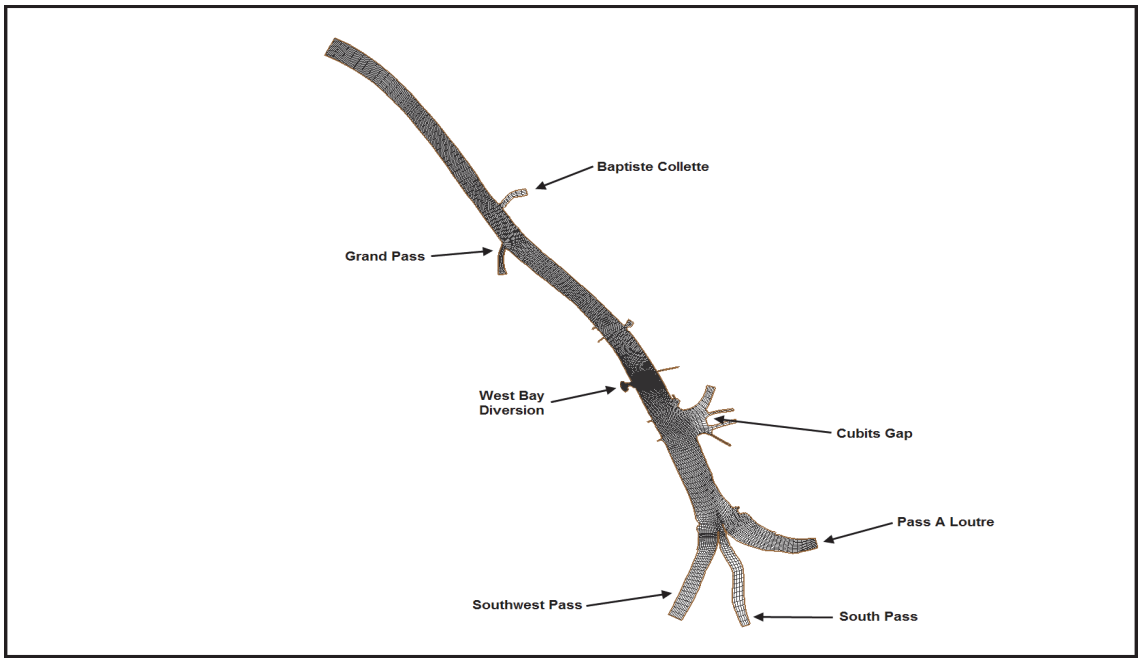

Figure 5.54. CH3D-SED Contours.

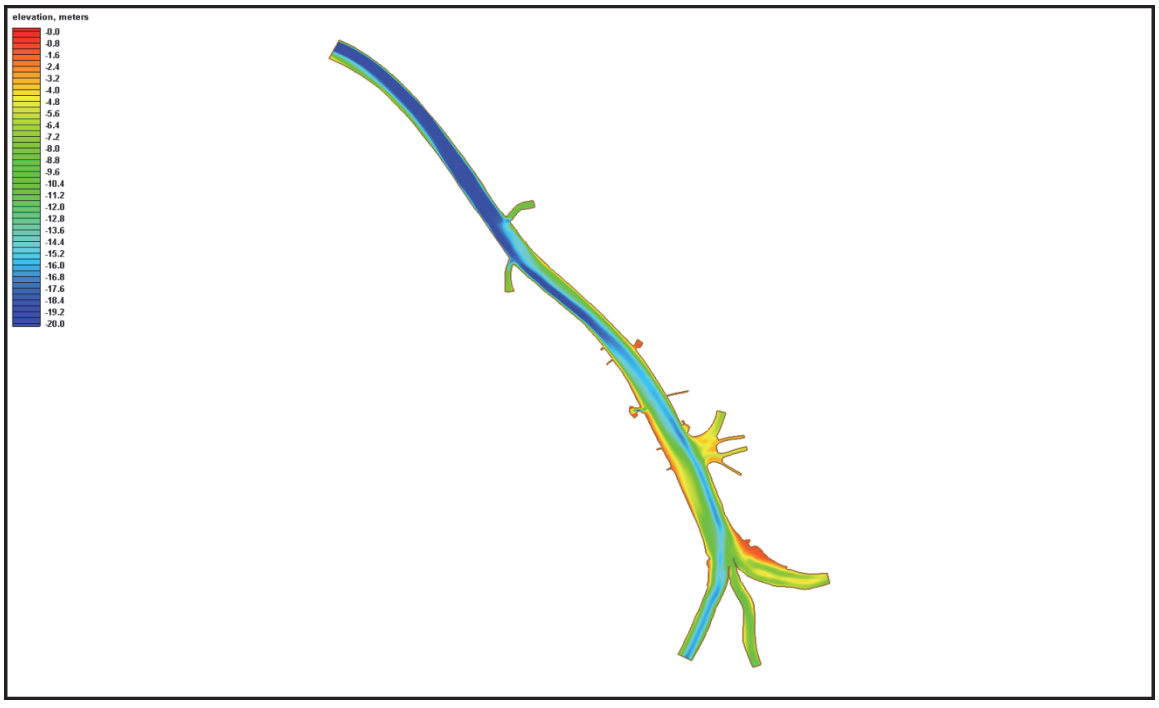

Figure 5.55. Grid Resolution at West Bay Diversion.

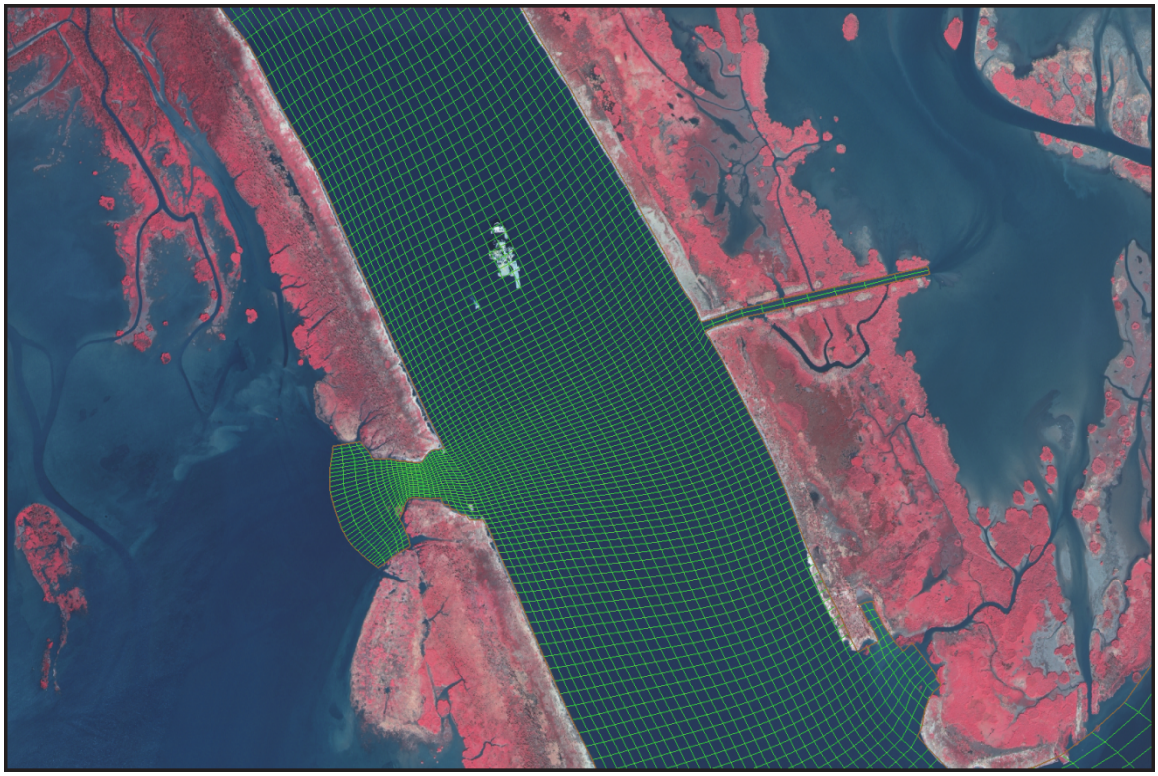

The water surface elevation boundaries at Southwest Pass, South Pass, and Pass a Loutre were developed using water surface elevation data from similarly located points in the AdH model.

CH3D-SED Verification

Sediment verification was obtained by comparing sediment concentrations from ERDC field data to those of the model for a 12 day simulation. The model was run for discharge conditions similar to those observed during ERDC data collection periods. This was done so that the results could be compared to observed data. Two flows were calculated, representing medium discharge (corresponding to the 5 – 6 May 2009 event) and a high discharge (corresponding to the 29 – 30 May 2009 event). These correspond to inflow values of 733,051 cfs and 898,726 cfs, respectively. The modeled erosion rate was calibrated such that the modeled suspended sand concentrations compared reasonably well to the observed field data. The same calibration coefficients were used for both the medium and high discharge conditions; they appear to be fairly robust. Comparisons were made at RM 5.2, just upstream of the WBSD, in the mouth of the WBSD, and at RM 4.5, just downstream of the WBSD. The results of these comparisons are seen in Figures 5.56 thru 5.61. The ERDC field data were

represented by the individual points and the CH3D-SED model results by the correspondingly colored curves. The model produced a favorable verification of suspended sediment (Figures 5.56 – 5.61).

CH3D Results

The velocity vectors at the surface and the bottom within the WBSD are shown in Figures 5.62 and 5.63. The flow patterns are representative of what was observed in the field. The eddy on the north side of the diversion shows favorable agreement with the pattern in the velocity data collected by ERDC. The strength of the eddy exceeds that observed in the ERDC field data collection effort, but these data were collected at a much lower discharge than what was simulated; this discrepancy is not unexpected.

The shoaling patterns are illustrated for the existing (undredged) condition with the WBSD (Figure 5.64) and without the WBSD (Figure 5.65). The difference (Figure 5.66) is that these patterns are for the high discharge condition used in the verification. The patterns compare extremely well to the patterns observed during the deposition period of the AdH simulations (Figures 5.26-5.28).

Figure 5.56. Sediment Concentration Comparison to Field Data, RM 5.2, Medium Flow.

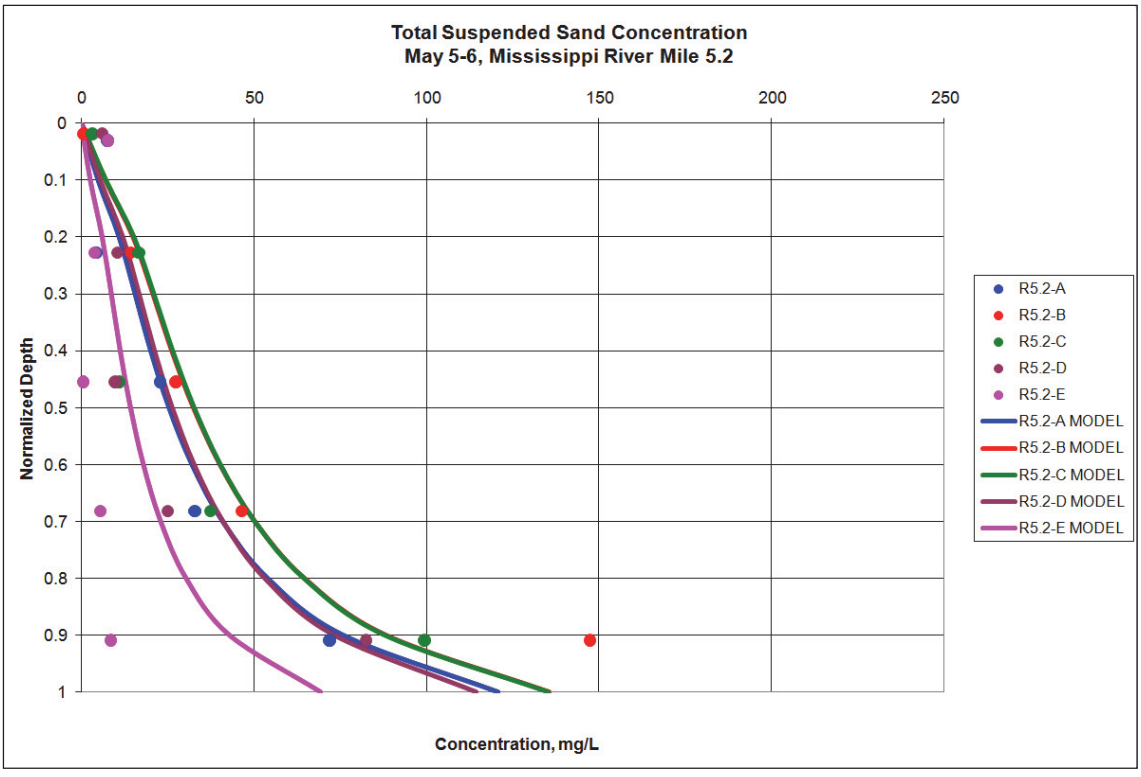

Figure 5.57. Sediment Concentration Comparison to Field Data, in Mouth of WBSD, Medium Flow.

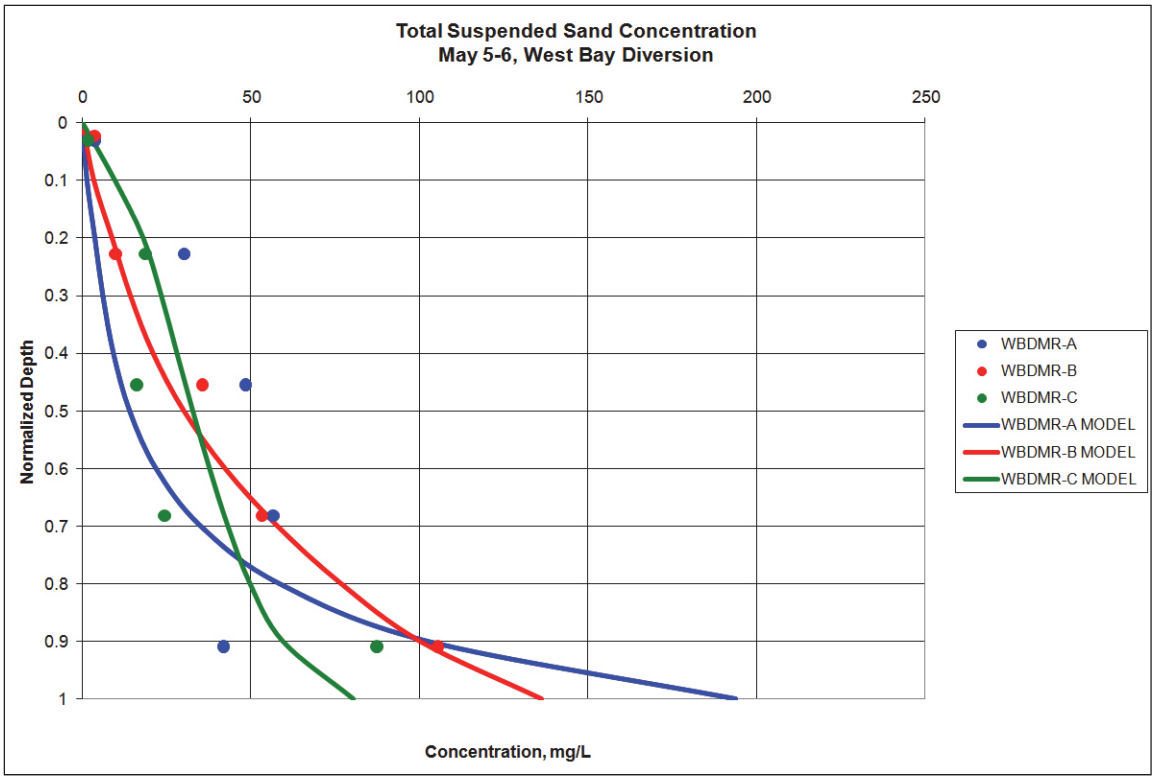

Figure 5.58. Sediment Concentration Comparison to Field Data, RM 4.5, Medium Flow.

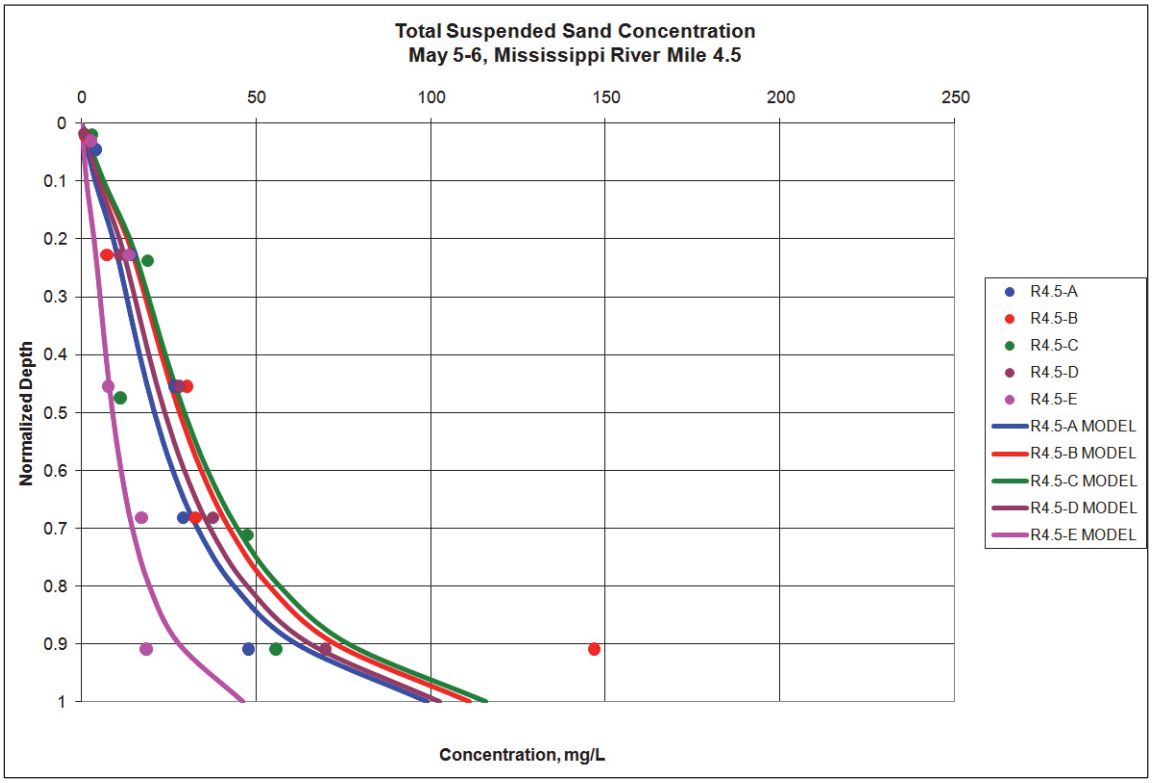

Figure 5.59. Sediment Concentration Comparison to Field Data, RM 5.2, High Flow.

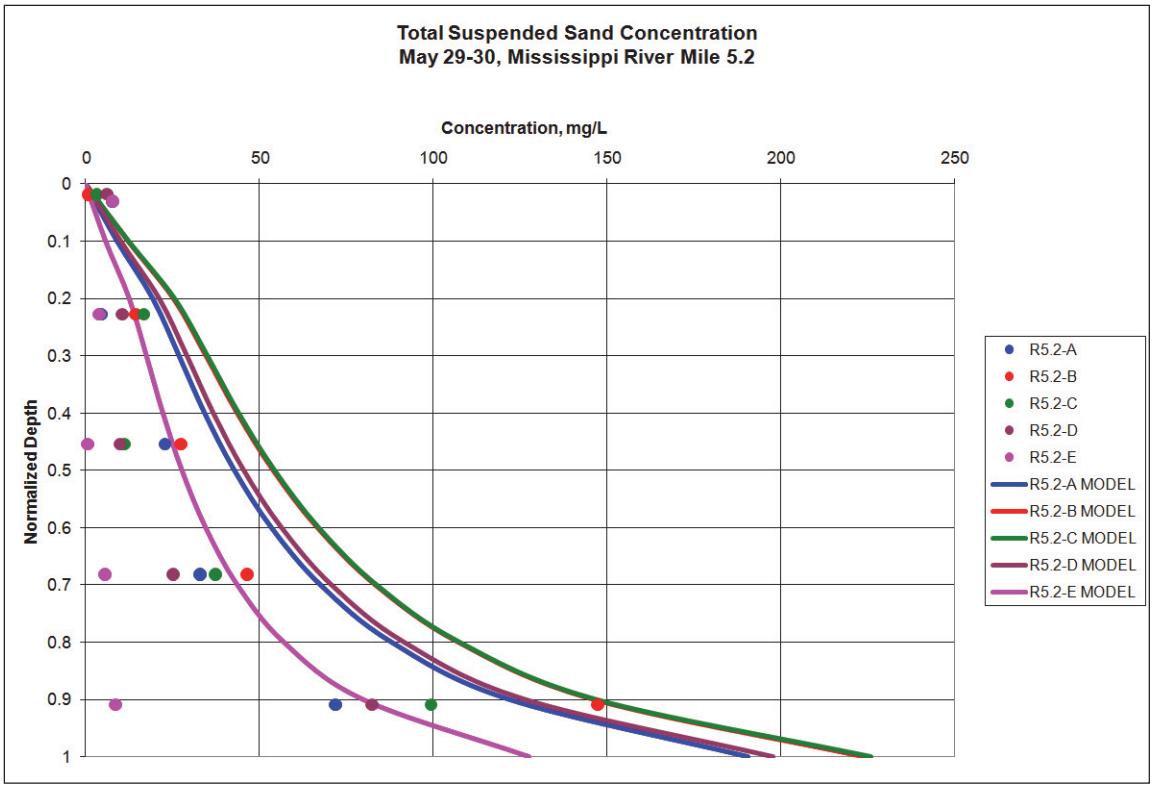

Figure 5.60. Sediment Concentration Comparison to Field Data, in Mouth of WBSD, High Flow.

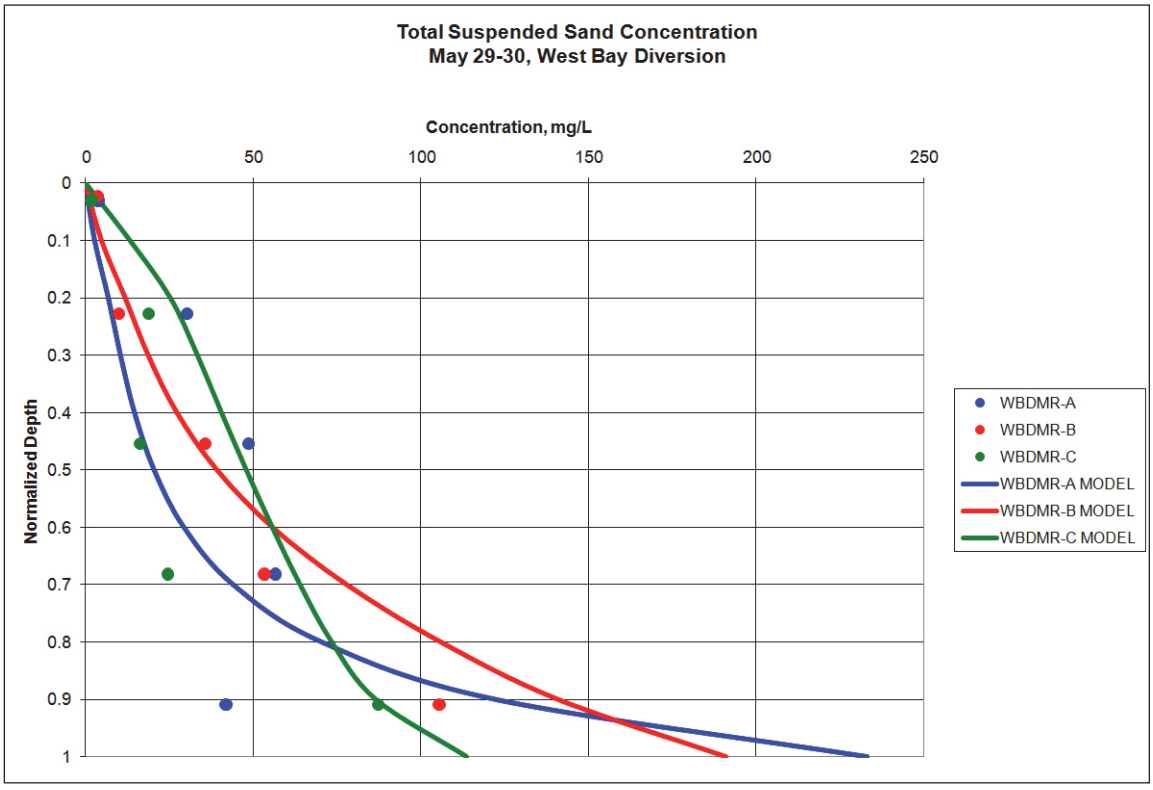

Figure 5.61. Sediment Concentration Comparison to Field Data, RM 4.5, High Flow.

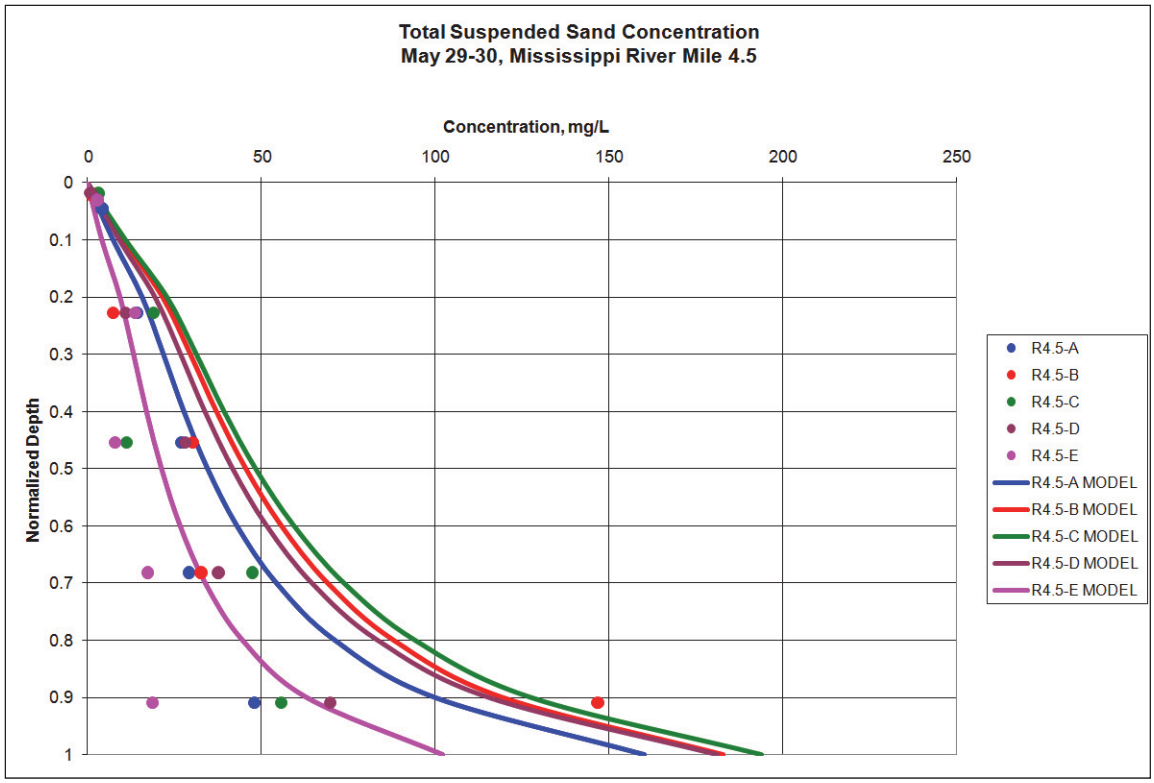

Figure 5.62. Surface Velocity Vectors from CH3D.

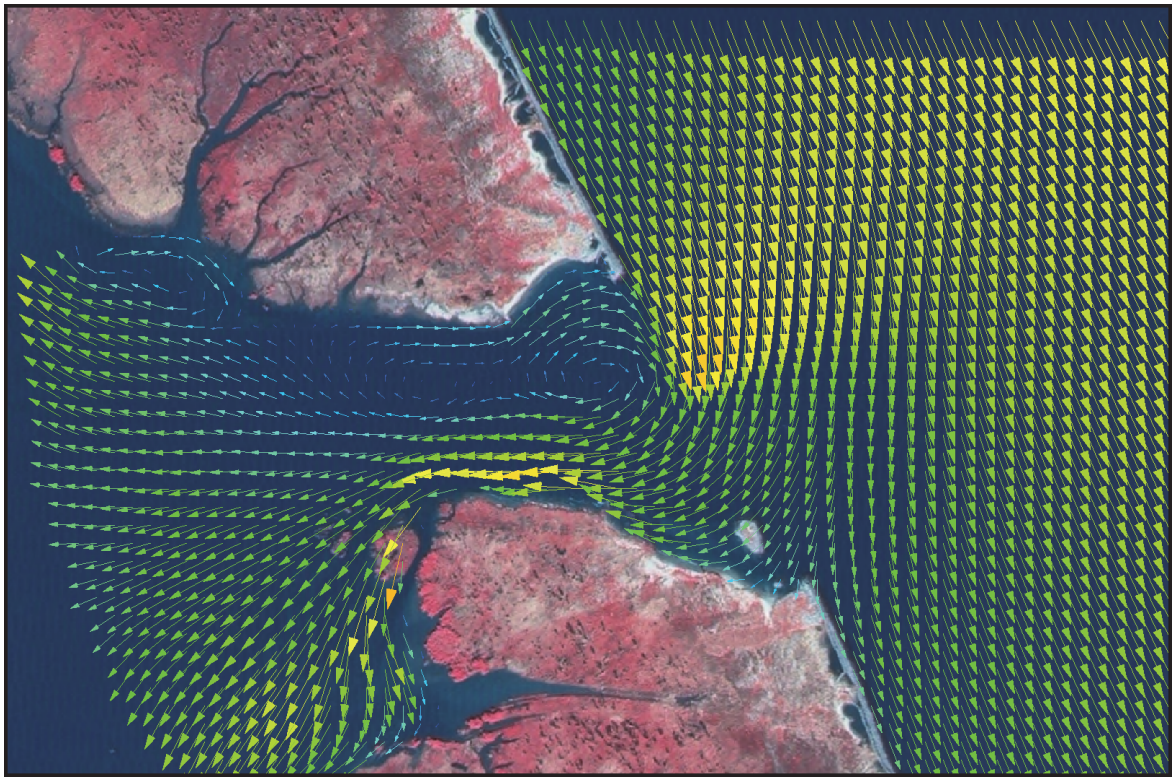

Figure 5.63. Bottom Velocity Vectors from CH3D.

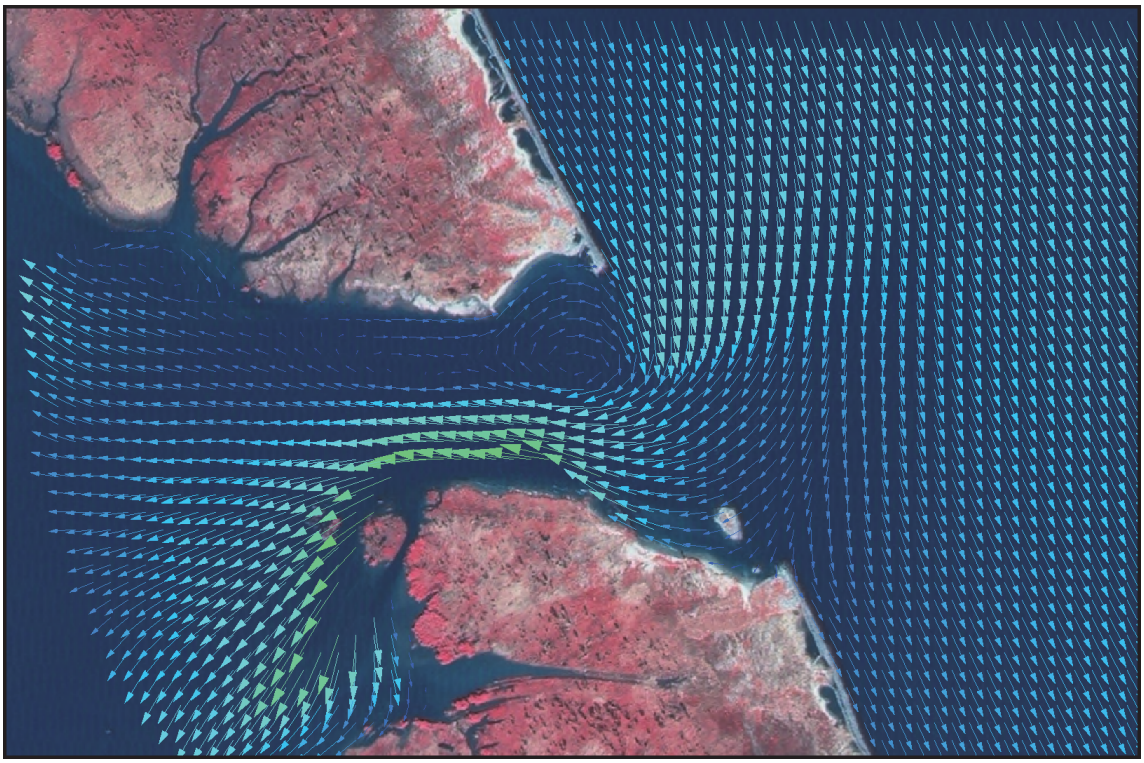

Figure 5.64. Bed Change over 10 Days – WBSD. Undredged Condition.

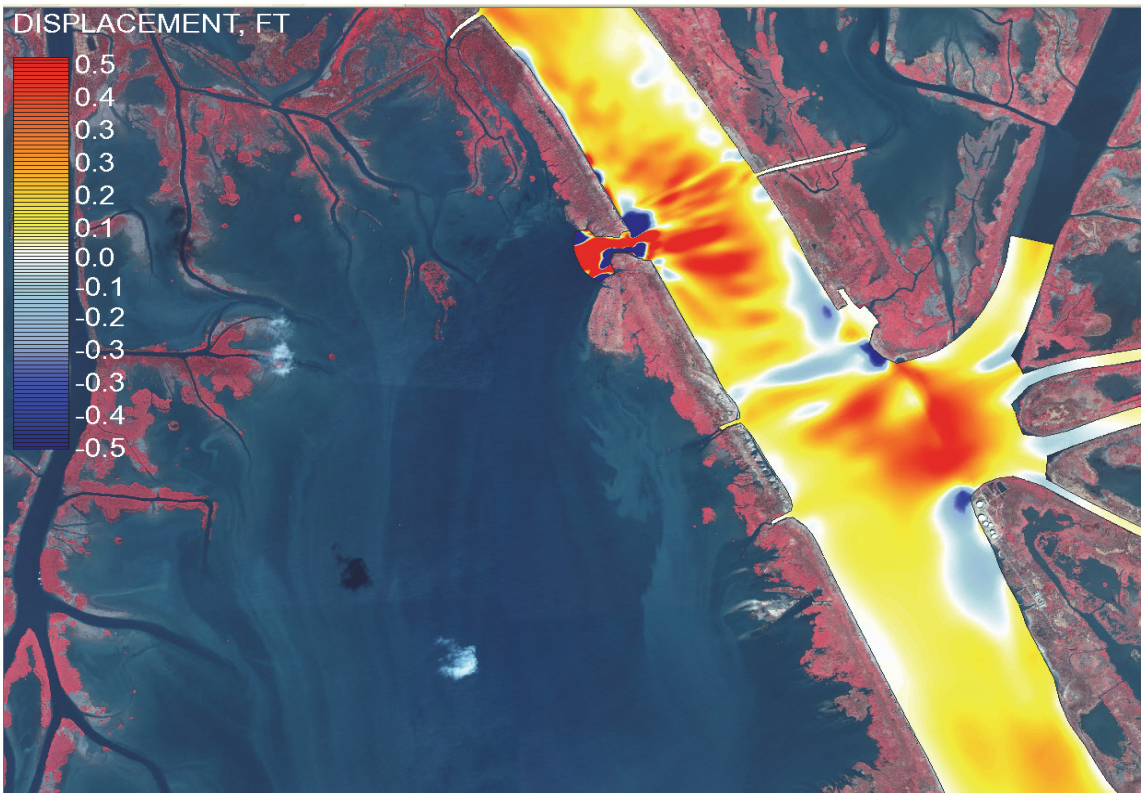

Figure 5.65. Bed Change over 12 days – Without WBSD, Undredged Condition.

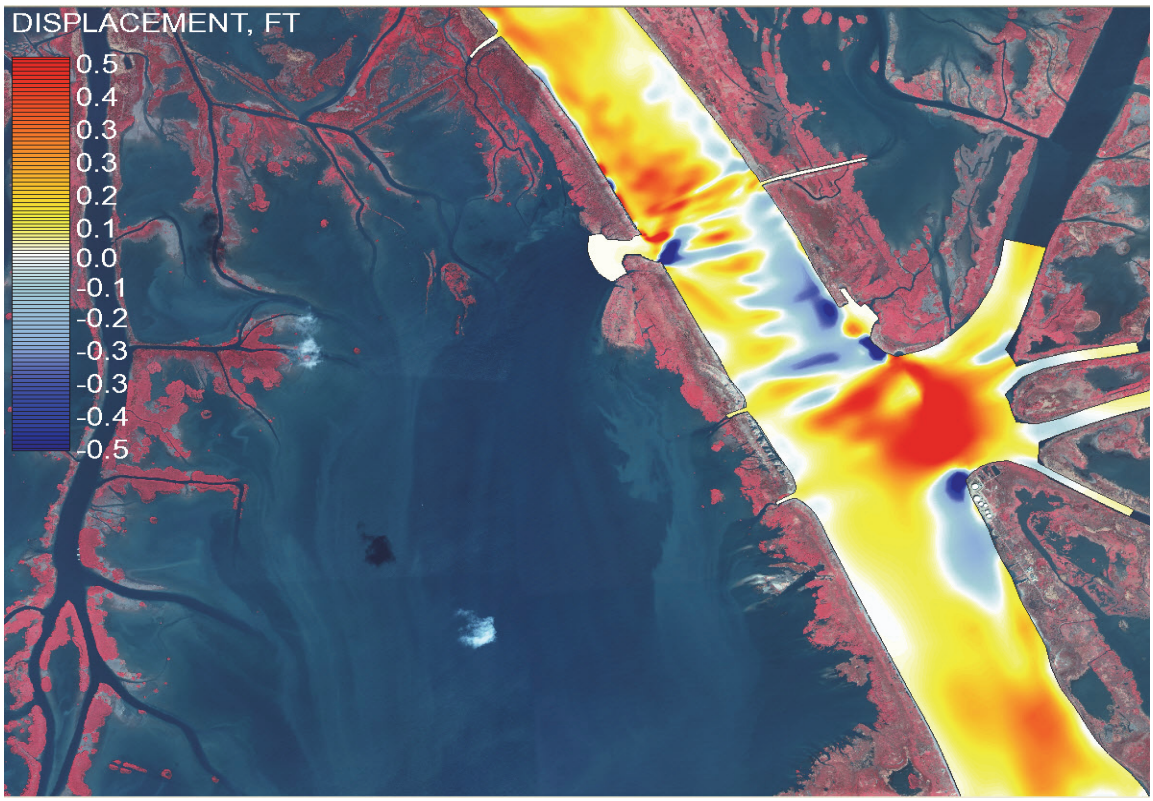

Figure 5.66. Bed change difference over 12 days, w/ WBSD minus w/o WBSD, Undredged Condition.

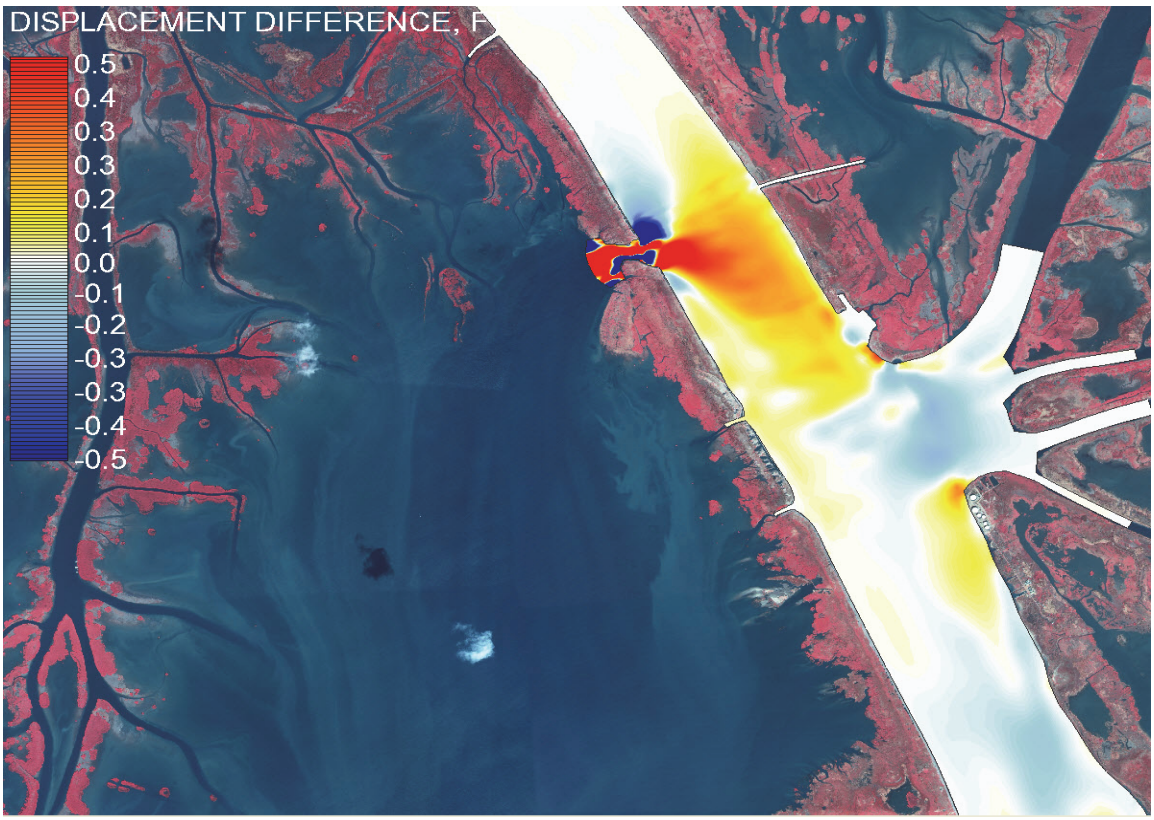

Figure 5-67. PAA and Access Area bounds.

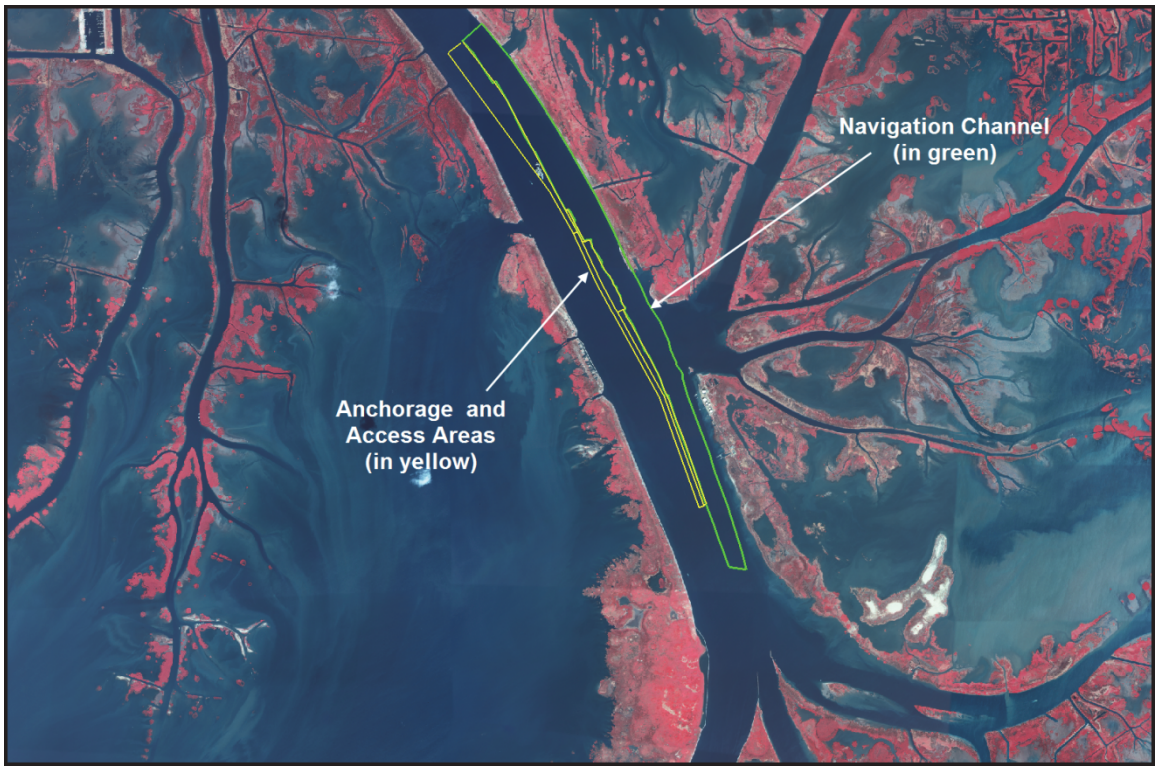

The results were analyzed for the percent of deposition attribuTable to WBSD. Four conditions were analyzed as high and medium flow, dredged, and undredged conditions (Table 5.3).

Table 5.3. Percent of Deposition Attributable to WBSD for the Ch3d Runs

	Pilottown Achorage Area (PAA)	Navigation Channel (NC)	Combined PAA and NC Footprint
High Flow, Undredged Condition	23.5%	23.3%	23.4%
High Flow, Dredged Condition	24.0%	18.0%	21.0%
Medium Flow, Undredged Condition	21.5%	24.9%	23.1%
Medium Flow, Dredged Condition	20.7%	18.8%	19.8%

The percent attributable is nearly 20 percent for all of the simulations. These results are consistent with the results obtained for the AdH runs (~20 percent). Since the Ch3D runs represent only a sediment-rich depositional condition, the variance of the results is much more limited than in the AdH results.

Conclusions

The momentum loss though the diversion and the consequent effect on the slope of the hydraulic grade line in the main stem of the river are the primary mechanisms for inducing deposition downstream of the WBSD. The shear stress analysis indicates that if the study area is considered mainly a depositional zone, the primary effect of the WBSD on deposition should occur in the PAA and navigation channel just downstream of the diversion and should dissipate in the downstream direction.

Both the AdH and Ch3D model results were analyzed using dredged and undredged bathymetry. This implicitly includes the uncertainty associated with the starting bathymetry into the analyses.

The AdH results indicate mean deposition of 23-27 percent attributable to the WBSD (standard deviation of 12-18 percent). The standard deviation is largely associated with the divergence of the deposition curves during erosional conditions/ high discharge conditions.

The shoaling patterns found in the Ch3D high discharge condition are similar to the patterns observed during the deposition period of the AdH simulations.

The percent of deposition attributable to the WBSD is nearly 20 percent for all of the simulations. These results are consistent with the results obtained for the AdH runs. However, since the Ch3d runs represent only a sediment rich, depositional condition, the variance of the results is much more limited than it is in the AdH results.

6 Discussion and Conclusions

Overview

Each of the methods of analysis employed in this study yielded insight into the central question this study was designed to address, i.e., what (if any) are the impacts of the WBSD on dredging requirements in the PAA and the adjacent navigation channel. The following chapter gives a discussion of how these results have been integrated into a coherent set of conclusions.

Synthesis of Results and General Conclusions

The field data collection effort has shown that as much as 45 percent of the measured water discharge at RM 12.1 is captured by Grand Pass, Baptiste Collette, WBSD, Cubits Gap, and various other small cuts. These cuts capture sediment loads that are approximately proportional to the water discharge volume. The sediment associated with both suspended sediment and bed sediment sampling consists of clay, silts, and sand up to the medium sand size class. The bed material gradations are variable, but the deposit in the PAA has been found to consist primarily of fine sand. Approximately 9 percent of the total discharge of the Mississippi River leaves through the cut at Fort St. Philips, which is upstream from Venice. This was measured for only one discharge condition of approximately 930,000 cfs on the main stem of the river. The percentage might be reduced with lower discharges, much like Cubits Gap because the cut has shallow areas that would not convey discharge during lower discharges. Cubits Gap drops to approximately 13 percent discharge during low discharge conditions from 19 percent during medium- to high-discharge conditions. The bed load measurement shows a net depositional region between RM 8.5 and RM 4.0 for the condition measured during the 31 March 2009 to 1 April 2009 measurement. This measurement supports the geomorphic analysis showing the growing point bar in that region of the river.

The field data collection effort shows the percentages of suspended sediment flux by size class for the various cuts. The tonnage should be sufficient to see some accretion in the various receiving areas. However, once sediment gets into the receiving areas, it does not have sufficient time to settle and consolidate before it is re-suspended during wind wave or storm events. If accretion is to be achieved in the receiving areas,

additional efforts must be made to allow for settling of the size classes in suspension. Protection of these recently deposited sediments must be provided until consolidation can occur naturally. Structures must be designed to accommodate the size classes available in suspension so that more deposition can occur in the desired locations.

Beginning in the vicinity of Venice, a significant percentage of the Mississippi River discharge is diverted through discharge and sediment diversions. Correspondingly, an alternate lateral bar pattern has developed in the reach between Venice and HOP. Growth of the lateral bars has been influenced by enlargement of existing diversions as well as deepening of the navigation project. Evaluation of historic survey data reveals that the lateral bar along the right descending bank located within the PAA, particularly downstream of Cubits Gap, was actively building prior to the construction of the WBSD.

The HEC-6T model indicates approximately 49 percent of the total sediment load is either diverted or deposited between just upstream of Baptiste Collette Bayou and HOP. This agrees with field data collected suggesting that approximately 50 percent of the measured suspended sediment load is diverted or deposited within that reach.

The HEC-6T model also indicates that the reach from about RM 7 downstream to the WBSD, the reach from WBSD to Cubits Gap, and the reach from Cubits Gap to HOP are all aggradational, with or without the WBSD open. This is supported with the geomorphic assessment that indicates these reaches were aggradational before the WBSD was opened and continues to be aggradational after the WBSD was opened.

Diversions in general can impact sediment deposition in the main channel by either of two general mechanisms: a disruption of sediment equilibrium associated with the diversion of too little sediment and the adjustment of the hydraulic grade line of the river to a sudden loss of momentum through the diversion. The model results indicate that the second effect (the hydraulic grade adjustment) is the dominant cause of main stem sediment deposition associated with the WBSD. An analysis of the shear stress differences induced by the presence of the diversion and resulting depositional patterns in the river were similar for both AdH and Ch3D. Also, sensitivity tests performed for the HEC-6T analysis indicate that the deposition patterns are relatively insensitive to the sediment diversion

ratio at WBSD, which indicates that the disruption of sediment equilibrium is not a significant factor.

The multi-dimensional modeling has shown that the addition of the WBSD results in an increase in sediment deposition just downstream of the diversion during depositional periods. During periods of prolonged high flow, where the supply of sand in the active sand sheet can be exhausted, the face of the lateral bar can experience some erosion. For this case, the erosion generally commences sooner in the model without the WBSD, resulting in a larger volume of residual sediment for the WBSD case. For the erosional condition, the presence of the WBSD permits less erosion, i.e., more net deposition over time. The multi-dimensional model indicates that this scouring is only evident when the sediment bed upstream of the study area is relatively sediment starved. This implies that the morphological changes in the study area are strongly dependent on both the current year's hydrographs and the antecedent conditions of the river from previous years.

In order to gain insight into the general morphologic trends of the study area both with and without the WBSD, some additional AdH model runs were conducted. These runs were designed to mimic (in a qualitative sense) the long-term morphologic trends of the study area. The runs indicated that the long-term trend of deposition in the PAA is likely to continue with or without the WBSD in place. The WBSD will induce more deposition in the right descending bank shoal, but the spatial extent of the deposition will be nearly identical with or without the diversion. The presence of the WBSD increases the deposition in the adjacent navigation channel, but this increased deposition is almost entirely offset by a decrease in deposition in Southwest Pass. In other words, the presence of the WBSD shifts this quantity of sediment deposition farther upstream in the channel.

The HEC-6T model consistently indicates that the WBSD accounts for a 15 +/- 12 percent of the increase in dredging required in the combined footprint of the PAA and the adjacent navigation channel. The 1D results represent 50 years of simulation time.

The Ch3D modeling indicates that approximately 20 +/- 2 percent of the deposition in the combined PAA and adjacent channel footprint are attributable to the WBSD. The Ch3D simulation represents 10 days of

steady flow, and four different scenarios such as high and medium flow, dredged, and undredged bathymetric conditions.

The AdH 2D modeling results indicate that 26 +/- 14 percent of the deposition in the combined PAA and adjacent channel footprint is attributable to the WBSD. The AdH results represent a single 6-month hydrograph, with two different bathymetric conditions: dredged and undredged.

The uncertainties in the results are not due primarily to differences in the models and modeling technique. The models tend to agree with one another in terms of qualitative trends and quantitative mean values. Rather, the uncertainties are associated with real uncertainties in the forcing mechanisms that cause deposition in the study area: i.e., the uncertainties represent the expected uncertainties in the real world.

Including insights from all aspects of the investigation, approximately 20 +/- 10 percent of deposition in the combined PAA and adjacent navigation channel footprint is due to the WBSD.

References

Allison. M. A., and J. A. Nittrouer. 2004. *Assessing Quantity and Quality of Sand Available in the Lower Mississippi River Channel for Coastal Marsh and Barrier Island Restoration in Louisiana* Final Technical Report for Governor's Applied Coastal research and Development Program.

Andrus, T. M. 2007. *Sediment flux and fate in the Mississippi River diversion at West Bay: Observation Study*. Master of Science Thesis, Louisiana State University, p. 229.

Barbe, D. E., K. Fagot, and J. A. McCorquodale. 2002. Effects on Dredging Due to Diversions from the Lower Mississippi River. *Journal of Waterway, Port, Coastal and Ocean Engineering*, ASCE, 126(3): 121-129, Paper 1743.

Bernard, B. 1992. *Depth-Average Numerical Modeling for Curved Channels*. Technical Report HL-92-9, Vickburg, MS: US Army Corps of Engineers, Engineering Research and Development Center.

Brown, Gary L.2008. *Approximate Profile for Nonequilibrium Suspended Sediment*. 134(7): 1010-1014.

Chapman, R. S. 1993. *Modification of the Momentum Diffusion Algorithm within CH3D*. Final Report to Coastal Engineering Research Center, Vicksburg, MS: US Army Waterways Experiment Station.

Chapman, R. S. 1994. *Implementation of a Vertical (k-ε) Turbulence Model Within the Z-grid and Sigma versions of CH3D*. Final Report to Coastal Engineering Research Center, Vicksburg, MS: US Army Waterways Experiment Station.

Colby, B. R., and C. H. Hembree. 1955. Computations of Total Sediment Discharge Niobrara River Near Cody, Nebraska. Water supply paper 1357, Washington, DC: US Geological Survey.

Chapman, R. S., B. H. Johnson, and S. R. Vemulakonda. 1996. *Users Guide for the Sigma Stretched Version of CH3D-WES; A Three-Dimensional Numerical Hydrodynamic, Salinity and Temperature Model*. Technical Report HL-96-21, Vicksburg, MS: US Army Engineer Waterways Experiment Station.

Coleman, J. M., and S. M. Gagliano. 1964 "Cyclic Sedimentation in the Mississippi River deltaic plain." Transactions – Gulf Coast Association of Geological Societies XIV:67-80.

Copeland, R. R., and L. Lombard. 2009 *Numerical Sedimentation Investigation, Mississippi River Vicksburg to Pilots Station* (DRAFT). Vicksburg, MS: US Army Corps of Engineers.Request Draft from Vickburg District.

Demas, C., and M. A. Allison. 2009. "Overview of Sediment Processes and Data Availability for the Lower River", presentation at Louisiana Coastal Area (LCA) Science & Technology Program Diversion Summit.

Einstein, H. A., and N. Chien. 1953. Transport of Sediment Mixtures with Large Range of Grain Size, MRD Sediment Series No. 2, Omaha, Neb.:United States Army Engineer Division, Missouri River, Corp of Engineers.

Galler, J. J. and M. A. Allison. 2008. "Estuarine Controls on Fine-Grained Sediment Storage in the Lower Mississippi and Atchafalaya Rivers" Geological Society of America Bulletin, 120(3-4): 386-398.

Guy, H. P., D. B. Simmons, and E. V. Richardson. 1966. Summary of Alluvial Channel Data Flume Experiments, 1956 – 61, Professional Paper 426-I, USGS.

Heath, R. E., J. A. Sharp, C. F. Pinkard, Jr. 2010. "1-Dimentional Modeling of Sedimetiaion Impacts for the Mississippi River at the West Bay Diversion." 9th Joint Federal Interagency Conference.

Horowitz, A. J. 2010. A quarter century of declining suspended sediment fluxes in the Mississippi River and the effect of the 1993 flood. Hydrol. Process.,24: 13-34. Doi:10.1002/hyp.7425.

Hydrologic Engineering Center (HEC). 1993. *HEC-6 scour and deposition in rivers and reservoirs, user manual.* Davis, CA: US Army Corps of Engineers.

Johnson, B. H., R. E. Heath, B. B. Hsieh, K. W. Kim, and H. L. Butler. 1991. "Users Guide for a Three-Dimensional Numerical Hydrodynamic, Salinity and Temperature Model of Chesapeake Bay," Technical Report HL-91-20, Vicksburg, MS: US Army Engineer Waterways Experiment Station, Vicksburg, MS.

Jordan, P. R. 1956. "Fluvial Sediment of the Mississippi River at St. Louis, Missouri," Water-Supply Paper 1802, Washington, D. C.: United States Geological Survey.

Kennedy, J. F. 1961. Stationary Waves and Antidunes in Alluvial Channels, Report KH-R-2, Pasadena, CA: W. M. Keck Laboratory of Hydraulics and Water Resources, California Institute of Technology.

Letter Jr., J. V. Pinkard Jr., C. Fred, and Nolan K. Raphelt. 2008. "River Diversions and Shoaling", ERDC/CHL CHETN-VII-9. http://chl.erdc.usace.army.mil/library/publications/chetn/pdf/chetn-vii-9.pdf

MBH Software, Inc. 2009. "Sedimentation in Stream Networks (HEC-6T) User Manual" Clinton, MS.

Nordin, C. F. 1964. "Aspects of Flow Resistance and Sediment Transport: Rio Grande near Bernalillo, New Mexico," Water Supply Paper 1498-H, Washington, D. C.: United States Geological Survey.

Nittrouer. J. A., M. A. Allison, and R. Campanella. 2008. "Bedform transport rates for the lowermost Mississippi River" *Journal of Geophysical Research*, Vol. 113.

Nordin, C. F. and B. S. Queen. 1992. "Particle Size Distributions of Bed Sediments Along the Thalweg of the Mississippi River, Cairo, Illinois, to HOP, September 1989, Potamology Program (P-1), Report 7". Vicksburg, MS: US Army Engineer Waterways Experiment Station.

Sheng, Y. P. 1986. "A Three-Dimensional Mathematical Model of Coastal Estuarine and Lake Currents Using Boundary Fitted Grid," Report No. 585, Princeton, NJ: A.R.A.P. Group of Titan Systems 22.

Shinkle, K. D. and R. K. Dokka. 2004"NOAA Technical Report NOS/NGS 50, Rates of Vertical Displacement at Benchmarks in the Lower Mississippi Valley and in the Northern Gulf Region". http://www.ngs.noaa.gov/heightmod/Tech50.shtml

Soileau, C.W., B. J. Garrett, and B. J. Thibodeaux. 1989."Drought induced saltwater intrusion on the Mississippi River", in Magoon, O.T., et al., eds., Proceedings of the sixth symposium in coastal and ocean management: New York, Proceedings, 6th Symposium on Coastal Zone Management, American Society of Civil Engineers, p. 2823–2836

"SMS version 8.0 Reference Manual for the Surface Water Modeling System," 2002, Brigham Young University, 1997, Provo, Utah: Engineering Graphics Laboratory, [http://chl.wes.army.mil/software/tabs/docs.htp].

Spasojevic, M. and F. M. Holly, Jr. 1990"2-D Bed Evolution in Natural Watercourses-New Simulation Approach," *J. of Waterway, Port, Coastal, and Ocean Engineering* 116:4, pp. 425-443.

Spasojevic, M. and F. M. Holly, Jr. 1993"Three-Dimensional numerical simulation of mobile-bed hydrodynamics," Technical Report No. 367, Iowa Institute of Hydraulic Research, The University of Iowa, USA.

Thorne, C., Harmar, O., Watson, C., Clifford, N., Biedenharn, D., and Measures, R. (2008) "Current and Historical Sediment Loads in the Lower Mississippi River", Final Report, London, England: European Research Office of the US Army.

Toffaleti, F.B. 1963. "Deep River Velocity and Sediment Profiles and the Suspended Sand Load," Paper no. 28, Federal Inter-Agency Sedimentation Conference, US Department of Agriculture.

Toffaleti, F.B. 1968. "A Procedure for Computation of the Total River Sand Discharge and Detailed Distribution, Bed to Surface," Technical Report No. 5, Committee on Channel Stabilization, Vicksburg, MS: US Army Corps of Engineers, United States Army.

Toffaleti, F.B. 1969. "Definitive Computations of Sand Discharge in Rivers," *Journal of the Hydraulics Division*, ASCE, Vol. 95, No. HY1, Proc. Paper 6350, pp. 225-248.

US Army Corps of Engineers (USACE). 1939. "The Passes of the Mississippi River" First New Orleans District. New Orleans, LA:US Army Corps of Engineers.

US Army Corps of Engineers (USACE). 1959. "Backwater Curves in River Channels," EM 1110-2-1409.

US Army Corps of Engineers (USACE).1992 "Guidelines for the Calibration and Application of Computer Program HEC-6, Training Document No. 13", Hydrologic Engineering Center, Davis, CA: US Army Corps of Engineers.

US Army Corps of Engineers (USACE).1993. "HEC-6 Scour and Deposition in Rivers and Reservoirs User's Manual", Hydrologic Engineering Center, Davis, CA.:US Army Corps of Engineers.http://www.hec.usace.army.mil/software/legacysoftware/hec6/hec6-documentation.htm

Vanoni, V. A. (Ed.).1975. *Sedimentation Engineering*, 745 pp., American Society of Civil Engineers, New York.

Vanoni, V. A., and N. H. Brooks. 1957. Laboratory Studies of Roughness and Suspended Load of Alluvial Streams, Sedimentation Laboratory Report No. E68, California Institute of Technology, Pasadena Calif. http://www.hec.usace.army.mil/software/legacysoftware/hec6/documents/td13man.pdf

REPORT DOCUMENTATION PAGE

Form Approved
OMB No. 0704-0188

1. REPORT DATE *(DD-MM-YYYY)*	2. REPORT TYPE	3. DATES COVERED *(From - To)*
November 2013	Final Report	

4. TITLE AND SUBTITLE

West Bay Sediment Diversion Effects

5a. CONTRACT NUMBER

5b. GRANT NUMBER

5c. PROGRAM ELEMENT NUMBER

6. AUTHOR(S)

Jeremy Sharp, Charlie Little, Gary Brown, Thad Pratt, Ronnie Heath, Lisa Hubbard, Freddie Pinkard, Keith Martin, Nathan Clifton, David Perkey, and Naveen Ganesh

5d. PROJECT NUMBER

5e. TASK NUMBER

5f. WORK UNIT NUMBER

7. PERFORMING ORGANIZATION NAME(S) AND ADDRESS(ES)

Coastal and Hydraulics Laboratory
US Army Engineer Research and Development Center
3909 Halls Ferry Road, Vicksburg, MS 39180-6199

8. PERFORMING ORGANIZATION REPORT NUMBER

ERDC/CHL TR-13-15

9. SPONSORING / MONITORING AGENCY NAME(S) AND ADDRESS(ES)

US Army Corps of Engineers New Orleans District,
New Orleans, LA

10. SPONSOR/MONITOR'S ACRONYM(S)

11. SPONSOR/MONITOR'S REPORT NUMBER(S)

12. DISTRIBUTION / AVAILABILITY STATEMENT

Approved for public release; distribution is unlimited.

13. SUPPLEMENTARY NOTES

14. ABSTRACT

An investigation is required to examine whether or not the West Bay Sediment Diversion (WBSD) is inducing shoaling in the Pilottown Anchorage Area (PAA) and in the navigation channel of the Mississippi River. Flow Diversions have the potential to induce shoaling (a sandbank or sand bar in the bed of a body of water) in the river channels from which water is being withdrawn (Letter et al. 2008). Thus, they can significantly reduce the sediment transport capacity of the main-stem river thereby inducing shoaling. The actual impact on shoaling is dependent upon a number of factors including the amount of water and sediment being diverted and the characteristics of the sediment being transported in the river. Diverting increasing amounts of water generally increases the potential for shoaling within the river, but the amount of water and sediment diverted is not necessarily linearly related. The objectives of this study are to understand the sediment transport processes in the Mississippi River in the vicinity of the WBSD and what, if any, impact the WBSD has on these processes.

15. SUBJECT TERMS

Sediment
Mississippi River
Diversions
Numerical Modeling
River
Dredging
Shoaling
Navigation

16. SECURITY CLASSIFICATION OF:			17. LIMITATION OF ABSTRACT	18. NUMBER OF PAGES	19a. NAME OF RESPONSIBLE PERSON
a. REPORT	b. ABSTRACT	c. THIS PAGE			19b. TELEPHONE NUMBER *(include area code)*
Unclassified	Unclassified	Unclassified		272	